CHEMICAL REVIEWS

pubs.acs.org/CR

Review

Visible-to-NIR-Light Activated Release: From Small Molecules to Nanomaterials

Roy Weinstain,* Tomáš Slanina, Dnyaneshwar Kand, and Petr Klán*

Cite This: *Chem. Rev.* 2020, 120, 13135−13272

Read Online

ACCESS | Metrics & More | Article Recommendations

ABSTRACT: Photoactivatable (alternatively, photoremovable, photoreleasable, or photocleavable) protecting groups (PPGs), also known as caged or photocaged compounds, are used to enable non-invasive spatiotemporal photochemical control over the release of species of interest. Recent years have seen the development of PPGs activatable by biologically and chemically benign visible and near-infrared (NIR) light. These long-wavelength-absorbing moieties expand the applicability of this powerful method and its accessibility to non-specialist users. This review comprehensively covers organic and transition metal-containing photoactivatable compounds (complexes) that absorb in the visible- and NIR-range to release various leaving groups and gasotransmitters (carbon monoxide, nitric oxide, and hydrogen sulfide). The text also covers visible- and NIR-light-induced photosensitized release using molecular sensitizers, quantum dots, and upconversion and second-harmonic nanoparticles, as well as release via photodynamic (photooxygenation by singlet oxygen) and photothermal effects. Release from photoactivatable polymers, micelles, vesicles, and photoswitches, along with the related emerging field of photopharmacology, is discussed at the end of the review.

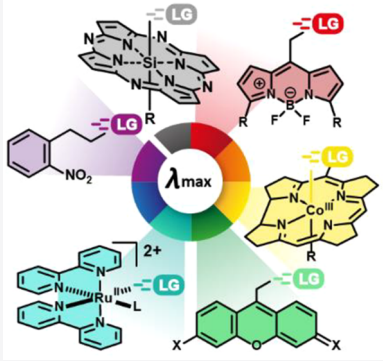

CONTENTS

Received: June 25, 2020
Published: October 30, 2020

https://dx.doi.org/10.1021/acs.chemrev.0c00663
Chem. Rev. 2020, 120, 13135−13272

1. INTRODUCTION

Photoactivatable (alternatively, photoremovable, photoreleasable, or photocleavable) protecting groups (PPGs) or caged compounds are used to achieve non-invasive spatiotemporal control over the release of molecules of interest including biologically active compounds, synthetic precursors, fluorescent probes, initiators of polymerization reactions, fragrances, and gasotransmitters. As such, they constitute one of the most important current applications of photochemistry in diverse research areas. The first PPGs were reported in the early works of Barltrop,[1] Barton,[2,3] Woodward,[4] and Sheehan,[5] and their first biological applications were presented by Engels and Schlaeger[6] and Kaplan[7] and co-workers. Since then, tens of photoactivatable molecules and systems have been developed. Several reviews and perspectives covering the applications of organic[8−55] and (transition) metal-containing[56−76] PPGs have been published in the past two decades. Special attention has been paid to compounds that release gasotransmitters such as nitric oxide (NO; photoactivatable NO-releasing moieties or photoNORMs), carbon monoxide (photoactivatable CO-releasing moieties or photoCORMs), and hydrogen sulfide (photoactivatable H_2S-releasing molecules).[77−114]

Key criteria for the design and use of PPGs, as discussed at length in previous works,[10,115−118] are often specific to individual applications. In general, however, a PPG (a) must exhibit sufficient absorption of the irradiated light, which must either not be absorbed by other molecules or not trigger unwanted photochemical transformations in the system of interest, (b) should release protected species within a timeframe compatible with the application, (c) must be soluble and stable in the targeted medium/environment (an aqueous solution in typical biological/medical applications), (d) should not produce reactive or toxic side-products upon irradiation, and (e) should be detectable in the medium, for example, by light emission. The overall efficiency of species release is evaluated using the quantity $\Phi_r\varepsilon(\lambda_{irr})$, sometimes called the uncaging cross section, which takes units of M^{-1} cm^{-1}, where Φ_r is the reaction quantum yield and ε is the decadic molar absorption coefficient.[10]

Short-wavelength UV photons have sufficient energy to induce bond cleavage, isomerization, or rearrangement reactions in many organic and inorganic molecules. For example, the energy of a photon with a wavelength of $\lambda \approx 300$ nm ($N_A h\nu = 95.6$ kcal mol^{-1}) is sufficient to induce homolytic cleavage of most single bonds in organic molecules. Most PPGs absorb light in the 300−400 nm region.[10] However, excitation in the UV region presents several challenges, especially in biological settings; high-energy UV light has very limited tissue penetration due to high optical scattering and strong absorbance by endogenous chromophores (e.g., hemoglobin or melanin),[119−121] can lead to sample overheating, and can cause phototoxic or photoallergic reactions resulting from its interactions with endogenous molecules such as DNA, RNA, and lipids.[122−124] Visible and especially NIR light can penetrate deeper into tissues[119,120,125−128] and is considerably less harmful to biological matter, opening the door to new applications in areas such as drug delivery.[20,103,129,130] Encouragingly, some photoresponsive approaches are already used routinely in clinical applications.[131−135] In addition, visible/NIR light sources, both coherent and non-coherent, are often cheaper, more common, and more accessible to non-specialist end-users than UV-light sources.

The desire to exploit these advantages has motivated several recent efforts to develop PPGs activated by visible/NIR light. Until recently, only a few PPGs activated directly by light of wavelengths above ∼600 nm were known, and the design of PPGs that undergo efficient photorelease upon irradiation at wavelengths above 500 nm was considered challenging.[10,11] According to the gap law,[136] nonradiative transition rate constants increase approximately exponentially as the associated energy gap contracts, which is one reason why π-extended organic PPGs absorbing visible or NIR light generally undergo inefficient photoreactions. However, while the quantum yields for release from such PPGs can be very small, their chromophores can have very large molar absorption coefficients, making their $\Phi_r\varepsilon(\lambda_{irr})$ values large enough for practical use.[11] Alternatively, PPG activation by one (1P)-photon direct excitation using short-wavelength radiation can be replaced by alternative methods using substantially less energetic photons such as two (2P)-photon excitation or sensitization via photoinduced energy- or electron-transfer.

The applications of PPGs are not restricted to the release of a single species of interest. Careful selection of complementary photoactivatable moieties that undergo specific phototransformations can enable wavelength-selective release, which is often called chromatic orthogonality. Photochemical reactions are also in principle orthogonal to reagent- or thermally-initiated chemical processes. A unique and elegant approach exploiting this orthogonality was introduced by Bochet and co-workers,[137,138] but the general concept remains somewhat underexplored. Multiple chromatically orthogonal systems including (among others) a monochromophoric system,[139] a single multichromophoric entity,[138] and mixtures of independent photoactivatable compounds[140−144] have been reported. The latter approach is uniquely well-placed to benefit from the expansion of the photoexcitation window resulting from the

https://dx.doi.org/10.1021/acs.chemrev.0c00663
Chem. Rev. 2020, 120, 13135−13272

Table 1. Organic and Metal-Containing PPGs Covered in This Review[ab]

Section 2.1.1. 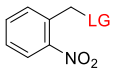 (<443 nm)	Section 2.1.2. 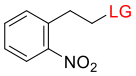 (<415 nm)	Section 2.2. 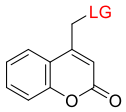 (<515 nm)	Section 2.3. 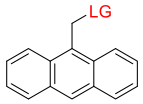 (<440 nm)
Section 2.4. 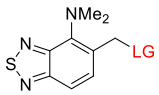 (<420 nm)	Section 2.5. 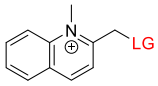 (<445 nm)	Section 2.6. 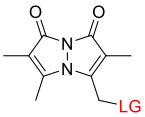 (<380 nm)	Section 2.7. 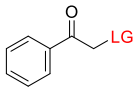 (<380 nm)
Section 2.8. 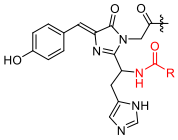 (<405 nm)	Section 2.9. 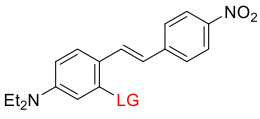 (<430 nm)	Section 2.10. 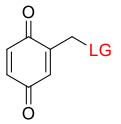 (<542 nm)	Section 2.10. 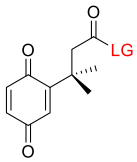 (<500 nm)
Section 2.10. 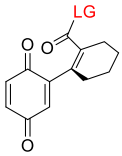 (<535 nm)	Section 2.11. 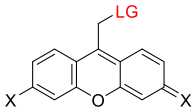 (<584 nm)	Section 2.12. 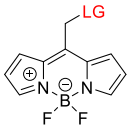 (<693 nm)	Section 2.12.  (<613 nm)
Section 3.1. 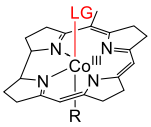 (<560 nm)	Section 3.2. 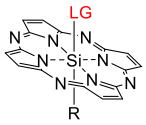 (<690 nm)	Section 3.2.  (<400 nm)	Section 3.3. 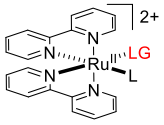 (<500 nm)
Section 3.4. 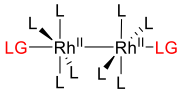 (<550 nm)	Section 3.5. 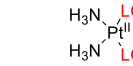 (<430 nm)	Section 3.5.  (<450 nm)	Section 3.5. 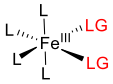 (<420 nm)

[a]Values in parentheses indicate the longest wavelength that can be used for PPG activation. [b]Leaving groups (LG) are depicted in red.

development of visible- and NIR-light excitable PPGs. We discuss several orthogonal systems here, and further examples can be found in recent reviews.[10,16,145−147]

This review follows up on an earlier article that provided a comprehensive overview of the photochemistry and applications of PPGs known and used before 2013.[10] We present a comprehensive list of PPGs absorbing in the visible and near-infrared (NIR) range including organic (section 2) and (transition) metal-containing molecular PPGs (section 3) that absorb photons directly (via 1P and (in several examples) 2P[30,31,148] excitation) to release various leaving groups (LG) (Table 1), organic and metal-containing photoCORMs, photoNORMs, and photoactivatable H_2S-releasing molecules (section 4, Table 2), and photoacids and photobases (section 5). These sections are followed by an overview of PPGs that use indirect methods of photoactivation, including photosensitization by molecular photosensitizers, quantum dots, upconversion, and second-harmonic nanoparticles, as well as photorelease by the photodynamic effect and photothermally-controlled release (section 6). The final sections discuss the chemistry of photoactivatable polymers, micelles, vesicles (section 7), and photoswitches (section 8), concluding with a brief discussion of the new concept of photopharmacology (section 9) (Table 3).

2. PHOTORELEASE FROM ORGANIC PHOTOACTIVATABLE COMPOUNDS

2.1. Nitroaryl Groups

The nitroaryl motif has proven to be a fertile scaffold for the development of photoremovable protecting groups (PPGs), leading to the emergence of several structural families, including the *o*-nitrobenzyl, *o*-nitro-2-phenethyl, and *o*-nitroanilide groups.[10] This section focuses on efforts to bathochromically shift the absorption spectra of *o*-nitrobenzyl and *o*-nitro-2-phenethyl PPGs toward the visible part of the spectrum. The absorption spectra of some representative nitroaryl PPGs are shown in Figure 1. A comprehensive review of UV-excitable nitroaryl derivatives covering their development and photochemical properties has been published.[10]

2.1.1. The *o*-Nitrobenzyl Group. *o*-Nitrobenzyl derivatives (oNB) make up a family of general-purpose PPGs that have been developed since the 1960s[4,154] and are still widely used.[10] Their photorelease mechanism has been studied

https://dx.doi.org/10.1021/acs.chemrev.0c00663
Chem. Rev. 2020, 120, 13135−13272

Table 2. Organic and Transition Metal-Containing CO-, NO-, and H_2S-Releasing Molecules Covered in This Review[ab]

Section 4.1.1. 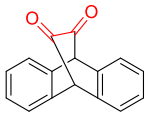 (<400 nm)	Section 4.1.1. 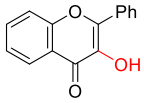 (<500 nm)	Section 4.1.1.  (<400 nm)	Section 4.1.1. 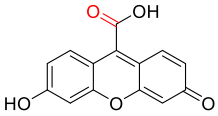 (<500 nm)
Section 4.1.1. 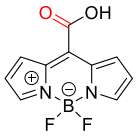 (<732 nm)	Section 4.1.2. 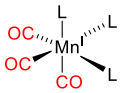 (vis/NIR)	Section 4.1.2  (<470 nm)	Section 4.1.2. 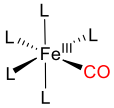 (<800 nm)
Section 4.1.2 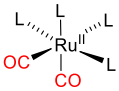 (<470 nm)	Section 4.1.2. 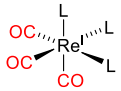 (<585 nm)	Section 4.2.1. 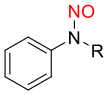 (<530 nm)	Section 4.2.1. 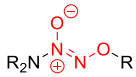 (<530 nm)
Section 4.2.1. 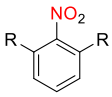 (<480 nm)	Sections 4.2.2 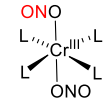 (<450 nm)	Section 4.2.2 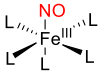 (<550 nm)	Section 4.2.2 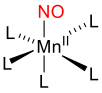 (<810 nm)
Section 4.2.2. 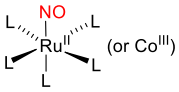 (<550 nm)	Section 4.3. (<410 nm)	Section 4.1. 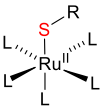 (<630 nm)	Section 4.3. 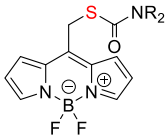 (<700 nm)

[a]Values in parentheses indicate the longest wavelength that can be used for PPG activation. [b]Leaving groups/moieties are depicted in red.

extensively.[155−160] Briefly, the excitation of the ground state of an oNB derivative **1** (Figure 1) is followed by intramolecular hydrogen abstraction by the nitro group to form an *aci*-nitro intermediate (**2**, Scheme 1; LG = leaving group). The decay rate constant of the *aci*-nitro intermediate (~10^2−10^4 s^{-1}) depends on the substitution of the oNB group, the solvent, and the pH. An irreversible cyclization of the *aci*-nitro intermediate leads to a 1,3-dihydrobenz[*c*]isoxazol-1-ol (**3**). Subsequent ring-opening gives a hemiacetal intermediate that hydrolyzes to release the leaving group (LG) and form an *o*-nitroso-benzaldehyde byproduct (**4**). The photorelease of many functional groups including carboxylic acids,[4] phosphates,[161] thiols,[162] alcohols,[163] and amines[164] has been demonstrated, although the latter two moieties are typically attached as carbonic acid derivatives.

Efforts to bathochromically shift the absorption maxima of the parental oNB **5a** (λ_{max}^{abs} ≈ 260 nm) have generally met with limited success because of an inverse correlation between the bathochromic shifts of absorption bands and photochemical parameters such as the release quantum yield (Φ_r) and rate constant.[137,163,165−167] For example, Jullien and co-workers examined a series of *p*-substituted nitrobenzyl derivatives **5b**−**5f** and found that bathochromic shifts of their absorption maxima were associated with a decrease in Φ_r (Table 4).[163] This loss of efficiency could be counteracted to some extent by substitution at the benzyl position,[4,163,166−168] leading to the development of the red-shifted α-methyl-6-nitroveratryl (**6**)[4] and α-methyl-(6-nitropiperonyloxymethyl) (**7**) PPGs (Figure 1).[169] However, due to the reduction in quantum efficiency, the uncaging cross section ($\Phi_r\varepsilon(\lambda_{irr})$) of the latter group tends to be comparable to that of the parent oNB **5a**.[4,170,171] Nitrodibenzofuran **8a** (NDBF; Figure 1), introduced by Ellis-Davies and co-workers, is an exceptional red-shifted oNB derivative that releases LGs efficiently.[172] The photolysis of ether,[172] thioether,[151] and phosphoester[173,174] LGs caged with this group reportedly proceeded with Φ_r values of 0.5−0.7, although lower quantum yields were obtained in some cases (0.04−0.2).[175−177] The tail absorption of **8a** in the visible range (398−440 nm) was sufficient to promote the photoreaction.[175,178] Introducing electron-donating groups (EDG) at the 7-position of NDBF (**8b** and **8c**) led to a bathochromic shift in λ_{max}^{abs} but also reduced its photouncaging quantum efficiency (Table 4).[151,174] The low quantum yield of **8c** was attributed to a charge-transfer transition following photoexcitation that competes with LG release.[174,179] Ball and co-workers recently reported that derivatives of **8a** and **8c** undergo efficient photocleavage of C(sp^2)−N bonds.[180] To explain this, a mechanism was proposed involving hydrogen-atom abstraction followed by selective nucleophilic attack of a solvent molecule on the resulting extended conjugated system. The absorption maximum of oNB-type PPGs can also be bathochromically shifted by extending the aromatic core,[181−183] as in the 7-methoxynaphthalene derivative **9**.[183]

Jullien and co-workers also found that a bathochromic shift in λ_{max}^{abs} relative to the parent PPG **5a** could be achieved by substitution to form a π-extended donor−acceptor system

https://dx.doi.org/10.1021/acs.chemrev.0c00663
Chem. Rev. 2020, 120, 13135−13272

Table 3. Other Photoactivatable Systems Covered in This Review

Section 6.1.	Section 6.2.	Section 6.3.
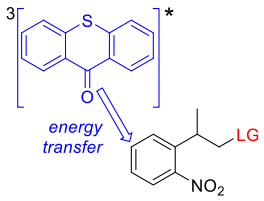	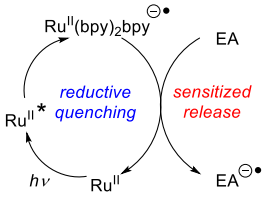	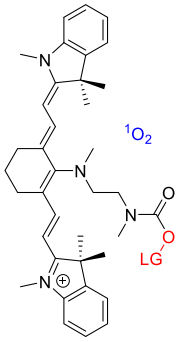
photosensitized release (energy transfer)	photosensitized release (electron transfer)	release via photodynamic effect
Section 6.4.1.	Section 6.4.2.	Section 6.4.3.
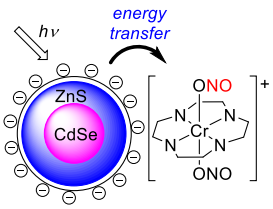	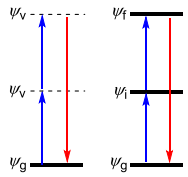	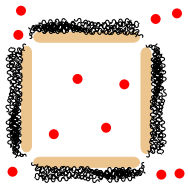
photorelease sensitized by quantum dots	photorelease sensitized by upconversion and SHG[d]	photothermally-controlled release
Section 7.	Section 8.	Section 9.
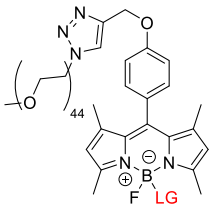	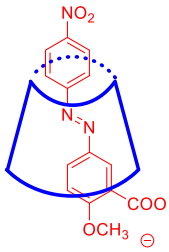	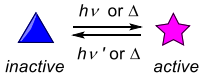
photorelease from materials (direct irradiation)	photorelease mediated by photoswitches	photopharmacology

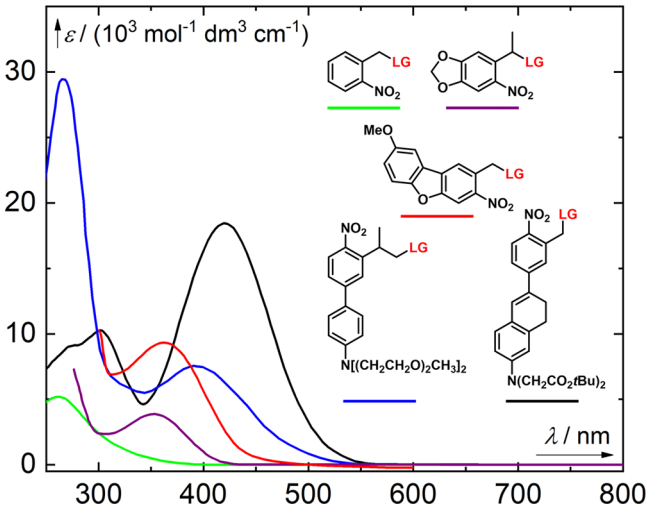

Figure 1. Absorption spectra of selected nitroaryl PPGs. Green line, a 2-nitrobenzyl derivative (LG = thymidine);[149] purple line, an α-methyl-(6-nitropiperonyloxymethyl) derivative (LG = thymidine);[150] red line, a nitrodibenzofuran derivative (LG = Fmoc-Cys-OH);[151] blue line, an *o*-nitro-2-phenethyl derivative (LG = Boc-glutamate);[152] black line, a π-extended 2-nitrobenzyl derivative (LG = GABA).[153]

Scheme 1. Proposed Photoreaction Mechanism of *o*-Nitrobenzyl PPGs[159]

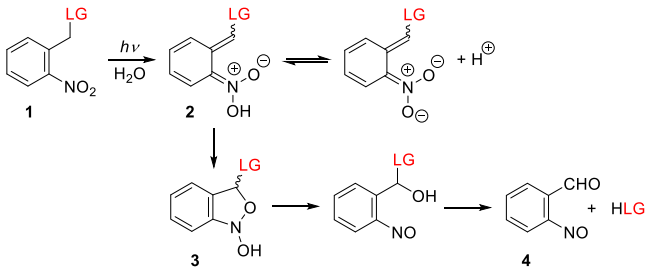

containing an electron-donating group (EDG) such as a methoxy group (**10**−**13**, Table 5).[163] These chromophores had λ_{max}^{abs} values of 336−371 nm but were photolyzed inefficiently to release a carboxylic acid (Φ_r = 0.001), in keeping with the previously mentioned inverse correlation between shifts in λ_{max}^{abs} and Φ_r.[163] Derivatives of biphenyl **10a** exhibited a bathochromic shift in λ_{max}^{abs} of ∼70 nm relative to **5a**,[163,185,186] and an additional ∼60 nm shift was achieved by using a dialkylamine EDG (**10b**; Figure 1).[187,188] The release of a carboxylic acid[187] and the fragmentation of the selective Ca^{2+}-chelator ethylene glycol tetraacetic acid[27] (EGTA) with subsequent Ca^{2+} release were achieved at λ_{irr} = 400−405 nm

https://dx.doi.org/10.1021/acs.chemrev.0c00663
Chem. Rev. 2020, 120, 13135−13272

Table 4. oNB Derivatives

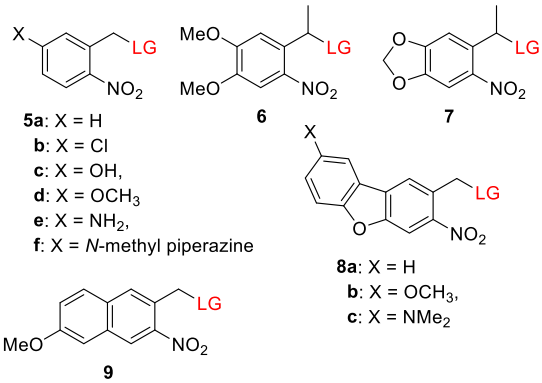

PPG	λ_{max}^{abs} (nm)	ε_{max} (M^{-1} cm^{-1})	leaving groups[a]	Φ_r (λ_{irr}/nm)	solvent[b]	ref
5a	262	5.2×10^3	thymidine (as carbonic acid)	0.033 (365)	CH_3OH/H_2O, 1:1	167−170
			pivalic acid	0.13 (254)	CH_3CN	149
5b	272	6.0×10^3	4-nitrophenol	0.1 (325)	CH_3CN	163
5c	310	9.0×10^3	4-nitrophenol	not reported	CH_3CN	163
5d	310	8.0×10^3	4-nitrophenol	0.007 (325)	CH_3CN	163
5e	367	1.6×10^4	4-nitrophenol	<0.001 (325)	CH_3CN	163
5f	394	1.6×10^4	4-nitrophenol	<0.001 (325)	CH_3CN	163
6	352	4.0×10^3	L-*threo*-β-benzyloxyaspartate	0.005 (355)	PBS buffer, pH 7.4	184
7	351	3.5×10^3 (ε_{365})	thymidine (as carbonic acid)	0.0075 (365)	CH_3OH/H_2O, 1:1	150
8a	325	18.4×10^3	EGTA (Ca^{2+}), IP_3	0.5−0.7 (350−400)	HEPES buffer, pH 7.2	172,173
8b	362	9.3×10^4	Fmoc-cysteine−OH	0.51 (350)	phosphate buffer, pH 7.4	151
8c	424	1.6×10^4	nucleobases	$0.5-11 \times 10^{-3}$ (420)	DMSO	174
9	339	1.1×10^4 (ε_{350})	hippuric acid	0.031 (420)	ethanol	183

[a]Only selected LGs are shown. [b]PBS = phosphate buffer saline. HEPES = 4-(2-hydroxyethyl)-1-piperazineethanesulfonic acid; DMSO = dimethyl sulfoxide; EGTA = ethylene glycol tetraacetic acid; IP_3 = inositol triphosphate.

Table 5. oNB Derivatives with Extended π-Systems

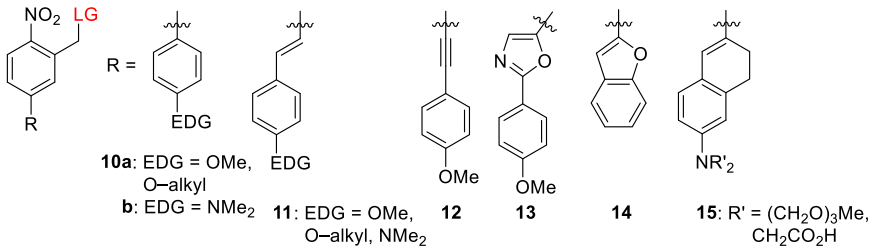

PPG	λ_{max}^{abs} (nm)	ε_{max} (M^{-1} cm^{-1})	leaving groups[a]	Φ_r (λ_{irr}/nm)	solvent[b]	ref
10a	335−342	$7.3-14.0 \times 10^3$	4-nitrophenol, chlorambucil, celecoxib	0.005−0.013 (325 or 355)	CH_3CN or CH_3CN/Tris pH 9.0, 1:1 or CH_3CN/phosphate buffer pH 7.2, 1:1	163, 185, 186
10b	403	8.8×10^3	EGTA (Ca^{2+})	0.05 (400)	C_6D_6	188
11	369−376	$1.9-2.5 \times 10^4$	coumarin, chlorambucil	$3.2-15.4 \times 10^{-4}$ (325 or 400)	CH_3CN or CH_3CN/Tris pH 9.0, 1:1	163, 189
12	348	1.9×10^4	4-nitrophenol, coumarin	0.001−0.005 (325)	CH_3CN/Tris pH 9.0, 1:1	163
13	371	1.9×10^4	coumarin	0.001 (325)	CH_3CN/Tris pH 9.0, 1:1	163
14	362−364	$1.2-1.8 \times 10^4$	benzoic acid, EGTA (Ca^{2+})	0.09−0.3 (360)	CH_3CN or DMSO	188, 195
15	420−443	$1.8-2.9 \times 10^4$	Boc-glutamate	0.01 (355)	CH_3OH	153

[a]Only selected LGs are shown. [b]Tris = tris(hydroxymethyl)aminomethane; DMSO = dimethyl sulfoxide; EGTA = ethylene glycol tetraacetic acid.

using PPGs of this type.[188] Stilbene-type derivatives **11**, which bear various alkoxy EDGs, had λ_{max}^{abs} values of 369−376 nm but released carboxylic acids with low quantum yields when irradiated above 400 nm.[163,189,190] Relatively similar quantum yields were reported for release from a derivative of **11** bearing the dimethylamino group as an EDG ($\Phi_r = 0.8-2 \times 10^{-4}$).[191] It was proposed that a photoinduced reversible *E*−*Z* isomerization[192−194] competes with photorelease in this case.[190] Accordingly, rigid derivatives **14** and **15** (Figure 1) were photolyzed more efficiently than **11** to liberate carboxylic acid LGs or to cleave an ether bond (causing EGTA bifurcation leading to Ca^{2+} release).[153,188,195,196] The π-extended 1,2-dihydronaphthalene **15**, which has a dialkylamino EDG, is the chromophore with the longest absorption wavelength in this series.[153] Visible-light uncaging from simple oNB derivatives has also been achieved through conjugation

https://dx.doi.org/10.1021/acs.chemrev.0c00663
Chem. Rev. 2020, 120, 13135−13272

with silicon quantum dots[197] or upconverting nanoparticles[198−203] (see also sections 6.4.1 and 6.4.2). It should be noted that many oNB derivatives with absorption maxima in the near UV-region have proven very useful in diverse applications[16,20,23,25,204−208] including *in vivo* experiments.[209−215] Several genetically encoded amino acids caged by oNB derivatives have also been reported.[216−218]

An outstanding 1-photon (1P)-absorbing oNB derivative is compound **16**, a dinitro-derivative of bisstyrylthiophene (BIST) coupled to two units of EGTA, which was recently reported by Ellis-Davies and co-workers and used for visible-light-induced (λ_{irr} = 473 nm) calcium uncaging (Scheme 2).[219]

Scheme 2. Photouncaging of Ca^{2+} with Visible Light[219]

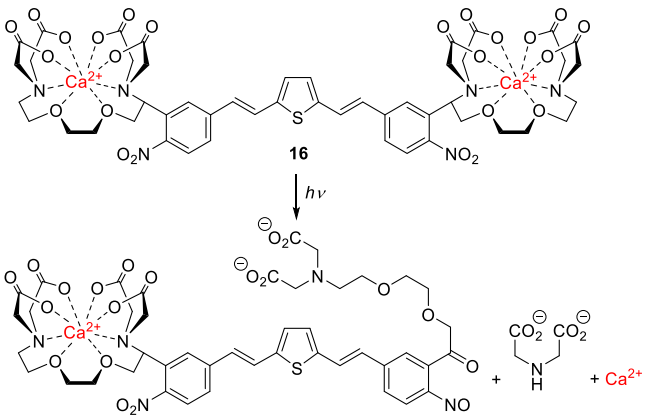

UV-excitable oNB derivatives are the PPGs most commonly used for photoscission of C−O or C−N bonds leading to the bifurcation of a chelator and the release of metal cations.[27,213,220,221] The π-extended electron-poor compound **16** exhibited strong absorption maxima in the blue light region (λ_{max}^{abs} = 440 nm, ε_{440} = 6.6 × 10^4 M^{-1} cm^{-1}) and a large two-photon (2P) absorption cross section (δ_{unc} of >250 GM) in the 720−830 nm range.[219] This compound is a strong Ca^{2+} chelator, but upon 1P (λ_{irr} = 473 nm, Φ_r = 0.23) or 2P excitation (λ_{irr} = 720 or 810 nm), its Ca^{2+} affinity falls markedly, leading to the release of free Ca^{2+}. A BIST scaffold masked with PEG dendrons was also used to cage γ-butyric acid (GABA), although this species was found to be resilient to 1P photolysis (λ_{irr} = 470 nm) and released GABA only upon 2P excitation.[222] Similar effects on uncaging have been reported previously.[174]

Simple oNB derivatives tend to have rather low 2P-uncaging cross sections (δ_{unc}), ranging from 0.01 to 0.035 GM.[163,165,223] Nevertheless, they have been used successfully in some biological applications.[224−226] NDBF derivative **8a** is an exception, with a reported δ_{unc} of 0.6 GM (at 720 nm).[172] The 2P-uncaging cross sections of derivatives of **6** were improved by incorporating the chromophore into dyads (δ_{unc} = 0.1−1.0 GM).[227,228] Jullien and co-workers observed that the δ_{unc} of derivatives **10**−**13** remained low for 2P uncaging of carboxylic acids (δ_{unc} = 0.02−0.05 GM, λ_{irr} = 730−800 nm).[163] The same authors reported that substitution at the benzyl position has similar effects on both δ_{unc} and Φ_r.[163] It was therefore suggested that the same excited state is involved in both 1P and 2P photolysis. Stilbene derivative **11** (OEt = EDG) exhibited 2P absorption of 20 GM and δ_{unc} = 0.014 GM for the release of chlorambucil,[189] whereas rigid stilbene derivatives of **15** and the biphenyl **10** were reported to be photolyzed more efficiently, with δ_{unc} = 5−21 and 7.8 GM at 740 and 800 nm, respectively.

2.1.2. The *o*-Nitro-2-phenethyl Group. The 1-(2-nitrophenyl)ethyloxycarbonyl (NPEOC) group[170] **17** and its α-methyl analog[170,229] **18** (NPPOC; the "OC" stands for the −OC(=O) group, which is typically a part of the LG) constitute a separate class of nitroaryl PPGs. Despite its close structural similarity to oNB (**5a**), the proposed photoreaction mechanism of *o*-nitro-2-phenethyl derivatives is markedly different, involving a photoinduced elimination step (Scheme 3)[170] reminiscent of that reported for (2-hydroxyethyl)-

Scheme 3. Photorelease from *o*-Nitro-2-phenethyl PPGs[170]

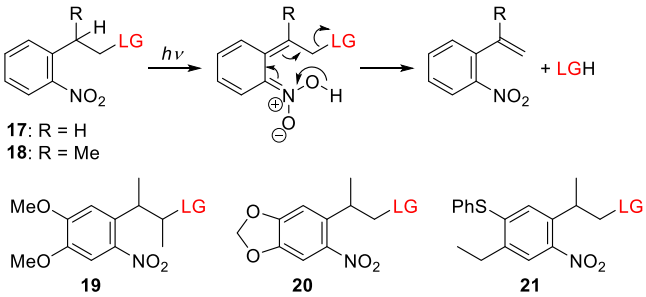

benzophenone-type PPGs.[118,230−235] The quantum yields obtained for *o*-nitro-2-phenethyl derivatives exceed those for their oNB analogs[150,170] (for example, Φ_r = 0.35 and 0.033 for 5′-*O*-nucleoside carbonate photorelease from **18** and **5a**, respectively), leading to their use in automated light-mediated oligonucleotide synthesis (DNA-chips),[236,237] the preparation of peptide[238−240] and RNA[241,242] microarrays, the synthesis of aptamers[243] and carbohydrates,[244] and gene assembly.[245]

The parent compounds **17** and **18** were further modified to enhance their absorption at longer wavelengths, as exemplified by the 3-(4,5-dimethoxy-2-nitrophenyl)-2-butyl group (DMNPB, **19**)[246−248] and the analogous 2-(3,4-methylenedioxy-6-nitrophenyl)-propoxycarbonyl group (MNPPOC, **20**).[150] Both these groups have a λ_{max}^{abs} at 350 nm but lack the associated decrease in Φ_r observed for oNB derivatives (Table 6). Bowman and co-workers showed that the tail absorption of **20** above 400 nm enables its use in visible-light photobase generation (see also section 5); the photorelease of tetramethylguanidine (TMG) at λ_{irr} = 405 and 455 nm proceeded with uncaging cross sections ($\Phi_r\varepsilon(\lambda_{irr})$) of 38.5 and 4.6 M^{-1} cm^{-1}, facilitating visible-light-mediated control over a thiol-Michael addition polymerization process.[249] The thiophenyl-2-(2-nitrophenyl)propoxycarbonyl derivative **21** was shown to have spectroscopic properties comparable to those of **20** (Table 6).[250,251] Additionally, Steiner and co-workers used intra- and intermolecular energy transfer from a triplet sensitizer (section 6.1) to initiate the release of LGs from NPPOC derivative **18** at λ_{irr} ≥ 400 nm.[171,252,253]

o-Nitro-2-phenethyl derivatives such as **17** and **18** typically have higher 2P δ_{unc} values than simple oNB derivatives such as **5** and **6** (δ_{unc} = 0.1−0.9[233,246] vs 0.01−0.35[163,165,223] GM, respectively).[246] NPPOC biphenyl systems **22** (Figure 2) have been studied to determine whether extending the π-system of *o*-nitro-2-phenethyl moieties could improve their 2P-absorption sensitivity. Goeldner and co-workers showed that *p*-methoxynitrobiphenyl platform **22** exhibits a ∼60 nm bathochromic shift in λ_{max}^{abs} relative to **18** while retaining a comparable 1P-photorelease quantum yield for glutamate

https://dx.doi.org/10.1021/acs.chemrev.0c00663
Chem. Rev. 2020, 120, 13135−13272

Table 6. Spectroscopic and Photochemical Properties of *o*-Nitro-2-phenethyl Derivatives

PPG	λ_{max}^{abs} (nm)	ε_{max} (M^{-1} cm^{-1})	leaving groups[a]	Φ_r (λ_{irr}/nm)	solvent	ref
17	~260	0.29×10^3 (ε_{365})	thymidine (as carbonic acid)	0.042 (365)	CH_3OH/H_2O, 1:1	170
18	~260	0.26×10^3 (ε_{365})	thymidine (as carbonic acid)	0.35 (365)	CH_3OH/H_2O, 1:1	170
19	350	3.5×10^3	GABA	0.26 (364)	phosphate buffer, pH 7.2	246
20	353	3.4×10^3 (ε_{365})	thymidine (as carbonic acid)	0.035–0.037 (365)	CH_3OH/H_2O, 1:1	150
21	~350	1.5×10^3 (ε_{365})	DNA phosphoramidites	0.68 (365)	CH_3OH	250
22	317	9.9×10^3	glutamate	0.09 (364)	phosphate buffer, pH 7.4	254, 255
23	296–302	$6.3–7.1 \times 10^3$	glutamate	n.d.	phosphate buffer, pH 7.4	254, 255
24	397	7.5×10^3	GABA	0.15 (405)	phosphate buffer, pH 7.4	152
25	415	6.4×10^4	glutamate	0.25 (354)	phosphate buffer, pH 7.4	267

[a]Only selected LGs are shown. GABA = γ-aminobutyric acid.

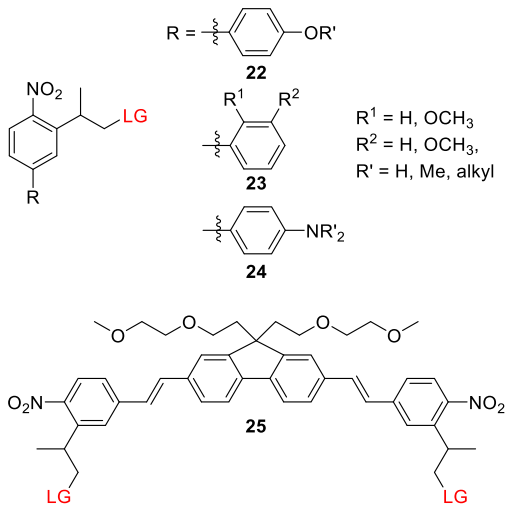

Figure 2. *o*-Nitro-2-phenethyl derivatives (LG = alkoxide, carboxylate, carbonate, carbamates, or phosphate).

(Table 6).[254] This stands in contrast to the previously mentioned inverse correlation between bathochromic shifts of λ_{max}^{abs} and Φ_r in oNB derivatives (see section 2.1.1). The 2P-uncaging cross sections of glutamate from **22** were 3.2 and 0.45 GM at 740 and 800 nm, respectively,[254,255] both of which are significantly higher than the corresponding values for **19** (δ_{unc} = 0.17 GM, 720 nm).[246] Moving the methoxy EDG to the *ortho* or *meta* positions (**23**) did not affect 1P photorelease yield but reduced the 2P uncaging cross section (δ_{unc} = 2.2 and 1.8 GM, respectively, 740 nm).[255] The introduction of a hydroxyl EDG was detrimental to the photouncaging of glutamate (reducing its chemical yield to <10%), presumably because it opened up photochemical pathways that compete with photorelease.[254] The impact of varying the *p*-alkoxy substituent of **22** on the photorelease of various LGs at λ_{irr} = 300–365 nm was investigated, but no appreciable effects on photoreaction properties were observed.[185,255–260] Specht, Goeldner, and co-workers further showed that dialkylamino substituents (**24**) caused an additional ~90 nm bathochromic shift with no significant detrimental effects on the quantum yield of 1P GABA photorelease (Table 6) and also substantially increased the 2P-uncaging cross section, giving δ_{unc} values of up to 11 GM at 800 nm.[152] The photorelease of carboxylates,[152,255,261] amines[260,262–264] (connected as carbamates), alcohols,[265] and phosphates[266] from various dialkylamino derivatives of **24** proceeded with Φ_r = 0.09–0.28 at λ_{irr} = 390–520 nm and with δ_{unc} values of up to 20.5 GM at 800 nm. To improve the water-solubility of these rather hydrophobic PPGs and enable their conjugation to (intra)cellular targeting groups, hydrophilic functional groups were attached to the amino[152,262,263,266] or alkoxy[256,260] moieties of **22** and **24**.[185,258]

The extension of the π-system of NPPOC with styrene and phenylacetylene substituents was also explored.[254,257,268] For example, Wombacher and co-workers synthesized **26** to cage the plant hormone gibberellic acid (GA_3) via an ester linkage (Scheme 4).[268] This conjugate had a λ_{max}^{abs} of 400 nm and

Scheme 4. Photouncaging of Plant Hormone GA_3 from π-Extended NPPOC Derivative[268]

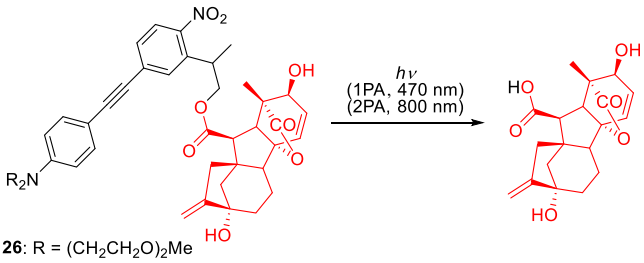

released GA_3 upon 1P (λ_{irr} = 470 nm) or 2P (λ_{irr} = 800 nm) excitation in cultured COS-7 cells, enabling light-mediated control over a chemically-induced dimerization system based on the gibberellin perception mechanism.[269,270] Symmetric biphenyl-substituted NPPOC structures such as **25** (Figure 2) exhibited significantly improved 1P- and 2P-absorption photorelease efficiencies (Φ_r = 0.25–0.30, δ_{unc} = 0.9–5.0 GM (at 840 nm),[267] but their size and poor solubility make them more suitable for applications where they are incorporated into larger structures.[271]

2.2. The (Coumarin-4-yl)methyl Group

Coumarin (2*H*-chromen-2-on) is a secondary metabolite found in many plants that was first isolated from the Tonka bean, known in French as coumarou, in 1820.[272–274] The development of coumarins as a new class of photoremovable protecting groups began with the discovery of Givens and Matuszewski that the (coumarin-4-yl)methyl group exhibits photoreactivity, enabling the release of phosphate esters (Scheme 5).[275]

The mechanism of the photorelease from (coumarin-4-yl)methyl derivatives has been extensively studied[276–278] and reviewed,[10,279] and it is summarized in Scheme 6.[276] Briefly, a heterolytic C–X bond cleavage takes place from the lowest $^1\pi,\pi^*$ singlet excited state, which competes with unproductive radiationless decay and fluorescence emission. A tight ion pair (TIP) was proposed to be the key intermediate in this process;

https://dx.doi.org/10.1021/acs.chemrev.0c00663
Chem. Rev. 2020, 120, 13135–13272

Scheme 5. Release of Phosphate from 7-Methoxycoumarin 27[275]

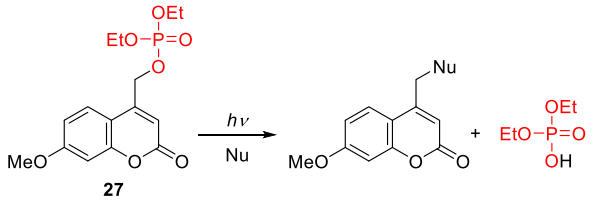

Nu = piperidine, cysteine, methanol, tyrosine, histamine *N*-methyltransferase, α-chymotrypsin

the (coumarin-4-yl)methyl cation in this pair could react directly with adventitious nucleophiles or solvents to form a new stable (coumarin-4-yl)methyl product. Recombination of the TIP to regenerate the ground-state caged derivative would be an unproductive competing radiationless pathway in this mechanism. It should however be noted that ultrafast time-resolved visible-pump-infrared-probe spectroscopy experiments yielded no evidence of TIP formation during the photorelease of a (coumarin-4-yl)methyl azide.[280] There are also evidences suggesting that some coumarin derivatives exhibit triplet-state reactivity.[165,281−284]

In general, coumarin-based PPGs offer several advantages: (1) high molar absorption coefficients at wavelengths above 350 nm, (2) high photorelease efficiencies, (3) acceptable stabilities in the dark, (4) fast photolysis kinetics, and (5) practically useful 2-photon excitation cross sections. Furthermore, their spectroscopic, photochemical, and other relevant properties (e.g., solubility and conjugation) can easily be tuned by varying the substituents on the coumarin ring. Given the high diversity of known coumarins, their synthesis is outside the scope of this review; interested readers are directed to reference works for extensive surveys.[10,285] Similarly, comprehensive reviews of the biological and other applications of (coumarin-4-yl)methyl PPGs can be found elsewhere.[16,19,21,22,26,50,285−289] The following section focuses on the evolution of coumarinyl PPGs that are excitable by light in the visible region of the spectrum. The absorption spectra of representative (coumarin-4-yl)methyl PPGs discussed in this section are shown in Figure 3.

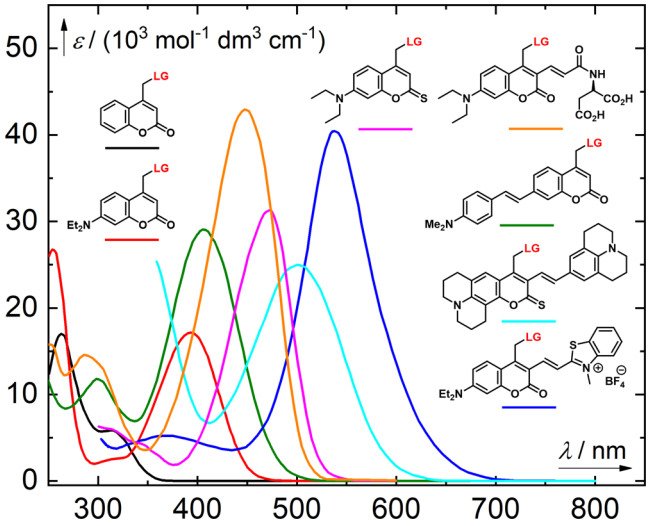

Figure 3. Absorption spectra of selected (coumarin-4-yl)methyl PPGs. Black line, a (coumarin-4-yl)methyl derivative (LG = cAMP);[290] red line, a [7-(diethylamino)coumarin-4-yl]methyl derivative (LG = benzoate);[290] magenta line, a thionated [7-(diethylamino)coumarin-4-yl]methyl derivative (LG = benzoate);[291] orange line, a 3-[3-(methylamino)-3-oxoprop-1-en-1-yl] derivative (LG = glutamate);[292] green line, a 7-styryl derivative (LG = 4-methoxybenzylcarbonate);[293] cyan line, a bis-julolidine derivative (LG = 4-methoxybenzoate);[294] blue line, a benzothiazolium derivative (LG = 3,5-dimethylbenzoate).[295]

The parent (coumarin-4-yl)methyl **28a** has an absorption maximum at 310 nm (Table 7; Figure 3) and was shown to photorelease cyclic adenosine monophosphate (cAMP) with $\Phi_r = 0.085$.[290] Introducing EDGs at the C7-position led to an increased intramolecular charge-transfer (ICT) character and a greater transition dipole moment, resulting in more intense and red-shifted absorption.[278,290,296−302] The weakly electron-donating 7-methyl substituent (**28b**) caused a ∼7 nm

Scheme 6. Photocleavage Mechanism of (Coumarin-4-yl)methyl-Caged Phosphates[276]

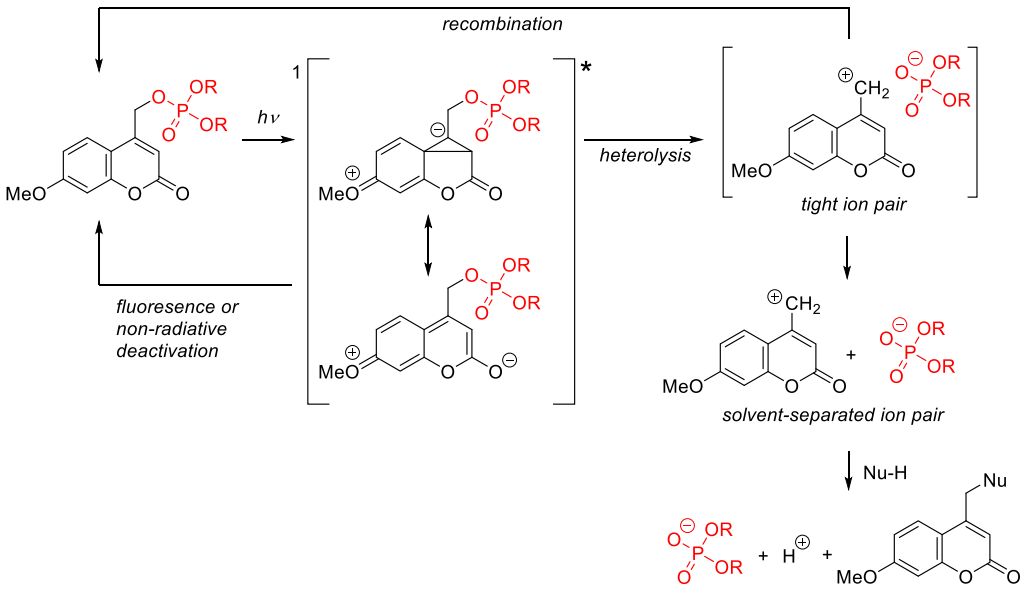

https://dx.doi.org/10.1021/acs.chemrev.0c00663
Chem. Rev. 2020, 120, 13135−13272

Table 7. Coumarin PPGs Substituted at the 7-Position[a]

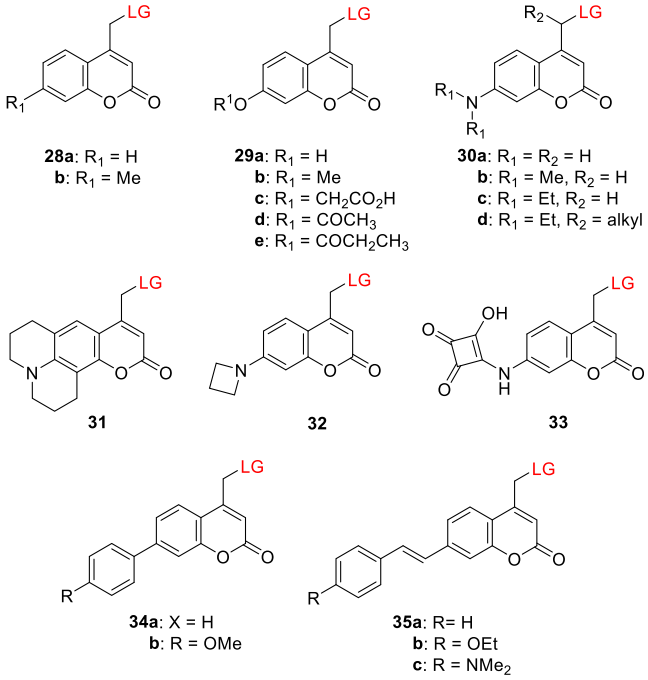

PPG	λ_{max}^{abs} (nm)	ε_{max} ($M^{-1}cm^{-1}$)	solvent[b]	ref
28a	310	5.1×10^3	CH_3OH/HEPES buffer pH 7.2, 1:1	290
28b	317	3.92×10^3	ethanol	303, 304
29a−e	314−328	$1.0–1.6 \times 10^4$	CH_3OH/HEPES buffer pH 7.2, 1:1 or MOPS buffer, pH 7.2	165, 290, 301, 308
30a	348	1.4×10^4	PBS buffer, pH 7.4	324
30b	378−398	$1.5–1.8 \times 10^4$	CH_3OH/HEPES buffer pH 7.2, 1:1	290, 332, 333
30c	387−406	$1.5–2.1 \times 10^4$	CH_3CN/HEPES buffer pH 7.2, 1:20 or HEPES buffer pH 7.2 or CH_3OH/HEPES buffer pH 7.2, 1:4	301, 334
31	399−403	$1.8–4.4 \times 10^4$	CH_3OH/H_2O, 9:1 or CH_3OH/HEPES buffer pH 7.2, 4:1	294, 335, 336
32	371	1.6×10^4	CH_3CN/PBS buffer pH 7.4, 7:3	337
33	450	not reported	CH_3CN	338
34a	323	4.1×10^4	CH_3OH/HEPES buffer pH 7.2, 4:1	339
34b	325−340	$3.9\text{-}4.1 \times 10^4$	CH_3OH/HEPES buffer pH 7.2, 4:1	339
35a	347−354	$3.5–5.8 \times 10^4$	CH_3OH/HEPES buffer pH 7.2, 4:1 or CH_3CN/H_2O, 9:1	293, 339
35b	366	2.8×10^4	CH_3CN/H_2O, 9:1	293
35c	407	2.9×10^4	CH_3CN/H_2O, 9:1	293

[a]LG = alkoxides, carboxylates, carbonates, carbamates, phosphates, thiols, sulfonates, azide, halides. [b]HEPES = 4-(2-hydroxyethyl)-1-piperazineethanesulfonic acid; MOPS = 3-(*N*-morpholino)propanesulfonic acid; PBS = phosphate buffer saline.

bathochromic shift in λ_{max}^{abs},[303,304] while derivatives with stronger EDGs such as hydroxy ((7-hydroxycoumarin-4-yl)methyl, **29a**) and methoxy ((7-methoxycoumarin-4-yl)-methyl, **29b**) exhibited more pronounced effects (Table 7). The(7-carboxymethoxycoumarin-4-yl)methyl derivative **29c** was designed to provide improved water solubility,[184,301,305−307] while esters **29d** ((7-acetoxycoumarin-4-yl)methyl) and **29e** ((7-propionyloxycoumarin-4-yl)methyl) were introduced to improve membrane permeability.[308−311] After penetration into live cells by diffusion, the esters of **29d** and **29e** are hydrolyzed by endogenous esterases to form the more polar phenolic derivative **29a**, which has negligible membrane permeability and thus accumulates inside cells.[309,310] A genetically encodable lysine caged by **29a** was developed to control protein functions in cell cultures and *in vivo*.[312−316] The photoexcitation of **29a−e** and their derivatives is usually restricted to the 300−350 nm wavelength range. Photouncaging of phosphates, sulfonates, and quaternary amines from **29a−e** and their derivatives typically occurs with Φ_r values of 0.05−0.39,[276,278,281,290,301,309,317,318] whereas poorer leaving groups, such as carboxylic,[184,276,278,319,320] carbonic,[319,321−323] and carbamic[305,313,319,324−326] acids are liberated less efficiently (Φ_r = 0.004−0.03). The photorelease efficiencies of amino acids connected to **29a** and **29b** through different linkers declined in the following order: anhydride > ester > carbamate > carbonate.[319] The carbonic or carbamic acids initially liberated by photorelease from these linkers are unstable and undergo decarboxylation to give the corresponding free alcohol or amine, respectively. These decarboxylation reactions usually have quite low rates, with k_{-CO_2} on the order of 10^{-3} s^{-1}, and they are subject to both acid and base catalysis.[327−330] A single example of a C−N bond cleavage from **29b** was reported.[331] This reaction proceeded efficiently only in the presence of an excess of a hydrogen-atom donor

https://dx.doi.org/10.1021/acs.chemrev.0c00663
Chem. Rev. 2020, 120, 13135−13272

such as *n*-decanethiol or 1,4-cyclohexadiene. A radical mechanism was proposed (Scheme 7), involving electron

Scheme 7. Photouncaging of Amines via Direct C−N Bond Cleavage[331]

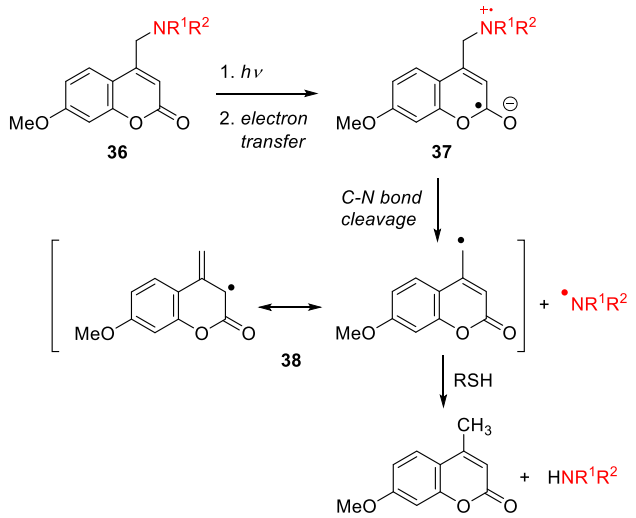

transfer between the amine and coumarinylmethyl moieties in **36** to form the intramolecular radical ion pair **37**. The subsequent cleavage of the C−N bond generates an aminyl radical and a resonance-stabilized coumarinylmethyl radical **38**, both of which can be trapped by hydrogen-atom donors.

The introduction of a 7-NH_2 substituent ((7-aminocoumarin-4-yl)methyl, **30a**)[324] caused a ∼40−45 nm bathochromic shift of λ_{max}^{abs} (Figure 3), and the liberation of carboxylic acids and amines from the corresponding esters and carbamates of **30a** proceeded with Φ_r values of 0.003−0.6 (λ_{irr} = 350 or 419 nm).[308,324,339,340] Alkylation of the 7-amino moiety, which increases its electron-donating ability, resulted in a more red-shifted and intense absorption band in [7-(dimethylamino)coumarin-4-yl]methyl derivative **30b**[290,334,341] and [7-(diethylamino)coumarin-4-yl]methyl analog **30c**[301,334] (Table 7).[278,290,301] The photorelease quantum yields for **30b** and **30c** exceeded those for all other compounds in this series. This was attributed to greater stabilization of the (coumarin-4-yl)methyl carbocation by the electron-donating dialkylamino substituents, leading to more efficient LG liberation from the TIP intermediate.[276,278,290] For example, the Φ_r values for cAMP release from **30b** and **30c** were 0.28 and 0.21, respectively, around twice that for **29b** (Φ_r = 0.13).[278,290] The release of carboxylic acids from **30b** and **30c** occurred with Φ_r values of 0.003−0.12,[291,321,332,333] whereas amines (as carbamic acids),[278,342−346] alcohols (as carbonic acids),[293,344,347] and thiols (as thiocarbonic acids)[348−350] were liberated with Φ_r = 0.01−0.09. The direct release of phenols occurred with Φ_r = 0.02−0.26, but competing recombination of the primary products proceeded with similar or even higher efficiency with these LGs.[345,351−353] The favorable spectroscopic and photochemical properties of **30c**, such as its absorption above 400 nm,[332,333] have made it one of the most popular PPGs. For more examples of its applications, the reader is referred to several review articles.[10,16,19,21,22,26,285]

Derivative **30d** was shown to have similar spectroscopic and photochemical properties to **30c** (Table 7)[354] while providing an additional derivatization point for further modulation of its properties and functions.[354−360] The alkyl substituents of the (7-dialkylaminocoumaryl)methyl group can easily be replaced with other functional moieties without significantly affecting the molecule's photophysical and photochemical properties,[361] allowing other properties to be tuned to expand the PPG's utility. For example, long alkyl chains have been appended to the 7-amino group to increase hydrophobicity,[362−366] and highly polar or charged moieties such as bis(carboxymethyl),[283,306,367−375] bis((dimethylamino)ethyl)carboxamide,[376] and bis(ethylsulfonate)[377,378] groups have been used to increase water solubility and control cellular permeability. Other functionalities have been appended to the 7-amino group to enable conjugation to (sub)cellular targeting motifs,[377,379−382] binding to surfaces and nanoparticles,[383−388] or incorporation into polymer backbones.[389,390] Analyte-dependent photoactivatable derivatives have also been reported.[383,391,392]

Derivatives bearing a conformationally locked electron-donating julolidine motif[393,394] exhibited a 10−15 nm bathochromic shift of λ_{max}^{abs} relative to their corresponding open-chain analogs (Table 7) and were photolyzed with higher quantum yields.[294,335−337] For example, the liberation of benzoic acid derivatives from coumarin **31** was 5−7-times more efficient than from **30c** under the same conditions (λ_{irr} = 405 nm).[337] The 7-azetidinyl and 7-aziridinyl substitutions significantly increased fluorescence quantum yields in coumarin fluorophores, which was related to a decrease in the population of twisted intramolecular charge transfer (TICT) states[395] upon excitation.[313,396] Rivera-Fuentes and co-workers synthesized 7-azetidinyl coumarin **32**, which released carboxylic acids with Φ_r = 1.4−1.6 × 10^{-2} upon irradiation at 405 nm.[337] The authors suggested that this increase in photouncaging efficiency is not due to the substituent's effect on the population of TICT states (as was suggested for the fluorescence enhancement[313,396]) but rather to suppression of an unproductive H-bond-induced non-radiative decay[397−399] (HBIND) channel.[337] Photouncaging (λ_{irr} = 405 nm) of a fluorescein derivative from **32** in live cells was demonstrated.[337] Singh and co-workers synthesized the squaric acid−coumarin conjugate **33** (LG = the anticancer drug chlorambucil, Table 7). An organic nanoparticle formulation of this compound exhibited a hypsochromically shifted and broadened absorption spectrum (λ_{max}^{abs} ≈ 410 nm) relative to that of the free molecular species.[338] Photoexcitation of **33**−nanoparticle conjugates (λ_{irr} = 410 nm) led to the simultaneous release of chlorambucil (Φ_r = 0.083) and generation of singlet oxygen (Φ_Δ = 0.51) from the excited squaraine moiety.[400−402] This simultaneous release of a strong oxidant and an anticancer drug had synergistic effects on cell viability in cultured HeLa cells.[338]

Gonçalves and co-workers expanded the coumarin π-system by substituting the 7-position with phenyl (**34a**) or *p*-methoxyphenyl (**34b**) groups, resulting in bathochromic shifts in the absorption of 19 and 31 nm, respectively, relative to the parent coumarin **28a** (Table 7). However, detectable carboxylic acid release from these derivatives occurred only upon irradiation below 350 nm.[339] The introduction of a 7-styryl group[293,339] in **35a** caused a more significant bathochromic shift of λ_{max}^{abs} that was further enhanced by substituting the *para*-position with EDGs (**35b** and **35c**, Table 7; Figure 3).[293] The liberation of alcohols (caged through a carbonate linker) from **35c** proceeded with Φ_r = 8.3 × 10^{-4} (λ_{irr} = 420 nm), which is ∼50-times lower than the

https://dx.doi.org/10.1021/acs.chemrev.0c00663
Chem. Rev. 2020, 120, 13135−13272

Table 8. Coumarin PPGs Substituted at the 6-Position

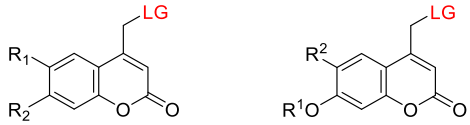

39a: R_1 = OCH_3, R_2 = H
b: R_1 = R_2 = OCH_3
c: R_1 = R_2 = CH_2CO_2H
d: R_1 = R_2 = CH_2CO_2Et

40a: R_1 = H, R_2 = Br
b: R_1 = H, R_2 = Cl
c: R_1 = $COCH_3$, R_2 = Br
d: R_1 = alkyl, R_2 = Br

PPG	λ_{max}^{abs} (nm)	ε_{max} (M^{-1} cm^{-1})	leaving groups[a]	Φ_r (λ_{irr}/nm)	solvent[b]	ref
39a	337−346	4.2−4.5 × 10^3	cAMP	0.02-0.055 (333)	CH_3OH/HEPES buffer pH 7.2, 1:1	278, 290
39b	341−349	1.1−1.2 × 10^4	cAMP	0.04 (333)	CH_3OH/HEPES buffer pH 7.2, 1:1	278, 290
39c	346−347	1.1−1.2 × 10^4	cAMP	0.08−0.10 (333)	CH_3CN/HEPES buffer pH 7.2, 1:20 or HEPES buffer pH 7.2	301
40a	370−375	1.5−1.7 × 10^4	acetic acid	0.37 (365)	MOPS buffer, pH	165
			cAMP	0.1 (350)	7.2	403
40b	370	1.6 × 10^4	acetic acid	0.01 (365)	MOPS buffer, pH 7.2	165
40c	320	0.6 × 10^4	cAMP	0.074 (350)	MOPS buffer, pH 7.2	403
40d	329−330	0.5−1.0 × 10^4	2′-deoxycytidines	0.24−0.30 (350)	MOPS buffer, pH 7.2	404

[a]Only selected LGs are shown. [b]HEPES = 4-(2-hydroxyethyl)-1-piperazineethanesulfonic acid; MOPS = 3-(*N*-morpholino)propanesulfonic acid; cAMP = cyclic adenosine monophosphate.

corresponding value for coumarin **30c** (Φ_r = 4.5 × 10^{-2}). Nevertheless, the uncaging cross section of **35c** upon irradiation at 430 nm was around 4-times that of **30c** ($\Phi_r\varepsilon_{430}$ = 8.28 and 2.29 M^{-1} cm^{-1} for **35c** and **30c**, respectively).[293] Because of its extended D−π−A backbone,[267] **35c** exhibited a much stronger 2P absorption than **30c** (309 vs 2.3 GM at 800 nm) and a ∼2-fold higher 2P uncaging cross section (δ_{unc} = 0.26 vs 0.12 GM at 800 nm).[293]

Coumarin derivatives bearing EDGs at the 6-position exhibited greater bathochromic shifts in absorption than their 7-EDG counterparts,[278,290,405,406] but usually also exhibited less efficient photorelease (Table 8).[278,290] For example, the (6-methoxycoumarin-4-yl)methyl compound **39a** had a 20 nm bathochromic shift of λ_{max}^{abs} relative to its 7-methoxy analog **29b** and was photolyzed to release cAMP as an LG ∼4-times less efficiently.[278,290] The spectroscopic and photochemical properties of the 6,7-dialkoxy derivatives **39b−d** resembled those of their 6- or 7-monosubstituted analogs. Sulfonates and phosphates such as cAMP and cGMP were released from **39b−d** with Φ_r = 0.08−0.14,[278,290,301,407−410] while poorer LGs such as carboxylic and carbamic acids were released with Φ_r = 0.6−2.0 × 10^{-2}.[305,321] The uncaging of cysteine residues protected with **39b** in proteins was used to study their folding kinetics on a sub-microsecond time-scale.[411,412] The (6,7-dicarboxymethoxycoumarin-4-yl)methyl derivative **39c** was designed to provide increased water solubility,[301,305,410] and the diethyl ester **39d** was synthesized to improve membrane permeability.[413]

The effect of electron-withdrawing groups (EWGs) at the 6-position has mainly been explored in combination with an EDG at the 7-position. Introducing an EWG in the 6-position had only a minor effect on the absorption spectrum relative to the parent PPG (causing bathochromic shifts of ∼5−15 nm) and often led to reduced photouncaging quantum yields,[165,285,303] presumably due to interference with through-bond electron transfer to the C2 carbonyl in the excited state.[285] Two exceptions to these effects were observed for the (6-bromo-7-hydroxycoumarin-4-yl)methyl compound **40a** by Tsien and co-workers.[165] First, the 6-bromo substituent increased the acidity of the 7-OH group relative to **29a** (pK_a = 6.2 vs 7.9), causing **40a** to be predominantly anionic at physiological pH. Consequently, **40a** has an absorption maximum at 375 nm, compared to 330 nm for its protonated form and 325 nm for **29a**, and is more water-soluble.[165,414] These effects were also observed for the 6-chloro derivative **14b**.[165,415] Second, acetate was liberated from **40a** ∼1.5-times more efficiently than from **29a** (Φ_r = 0.037 vs 0.025).[165] It was suggested that the heavy bromo substituent of **40a** promotes ISC to the triplet excited state and that this effect outweighs its interference with through-bond electron transfer to the C2 carbonyl, resulting in increased quantum efficiency.[165,285] The introduction of an electron-withdrawing chlorine atom at the 6-position led to a lower photorelease quantum efficiency in **40b**, but the heavy atom effect of two additional bromo substituents at the 3- and 8-positions increased efficiency in the case of **40a** (Φ_r = 0.065), suggesting that the triplet excited state is productive in these derivatives.[165] Phosphates (e.g., cAMP, cGMP, deoxycytidines; Φ_r = 0.09−0.1),[403,404] carboxylic acids (Φ_r = 0.02−0.13),[165,416,417] amines (as carbamic acids; Φ_r = 0.04−0.16),[418,419] alcohols (as carbonic acids; Φ_r = 0.01−0.4),[321,342,420,421] diols (Φ_r = 0.004−0.06),[422,423] and alkoxyamines[424] have all been successfully released from **40a**. The 2P uncaging cross section of **40a** at 740 nm ranged from 0.35 to 2.0 GM depending on the caged substrate.[165,404,417,419,423] Despite several reports of successful liberation of thiols from **40a**-thioethers,[425−428] photoisomerization of the by-product **42** occurred with higher efficiency (Scheme 8). Blocking the 3-position with a methyl group as in **41** prevented the formation of **42**, facilitating the clean formation of **43** and the liberation of free thiols, albeit with lower quantum efficiencies than were achieved with **40a** (Φ_r = 0.01 and 0.04, respectively).[429,430]

Similarly, phenols could be liberated directly from **40a**, but competing recombination of the primary products was observed.[345,352,431] For example, a photo-Claisen rearrangement was found to proceed ∼2.5-times more efficiently than LG photorelease from **44** (Scheme 9).[345]

The favorable spectroscopic and photochemical properties of **40a** were found to be useful not only for the photorelease of bioactive small molecules[421,427,432−438] but also in the development of photoresponsive polymers,[426,439−446] dendrimers,[447] and supramolecular materials.[448−451] A genetically

https://dx.doi.org/10.1021/acs.chemrev.0c00663
Chem. Rev. 2020, 120, 13135−13272

Scheme 8. Photochemistry of Thioethers 40a and 41[429,430]

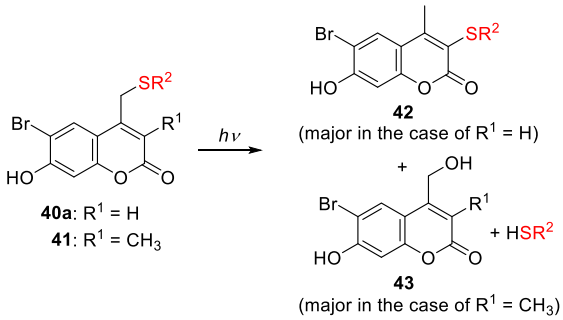

encodable lysine caged by **40a** was also reported.[325] Compound **40c** (LG = acetate) was introduced as a more cell-permeable version of **40a**, which can be trapped inside cells after hydrolysis of the ester bond.[403] The 6-bromo-7-alkoxy derivatives of **40d** had spectroscopic properties comparable to those of the protonated form of **40a**, and were shown to release various LGs with Φ_r = 0.01−0.3 at λ_{irr} = 350 nm.[342,347,404,421,452,453]

Singh and co-workers developed coumarin **45** as a photoresponsive, dual-channel sensor for hypoxia and nitric oxide (NO; see also section 4.2) with λ_{max}^{abs} = 410 nm and very weak fluorescence (Φ_F = 0.01; Scheme 10).[454] Reduction of the 6-NO_2 group to an NH_2 group (**46**) led to a hypsochromic-shift in the absorption maximum (λ_{max}^{abs} = 387 nm) and intense fluorescence emission centered at 535 nm (Φ_F = 0.55). Further reaction of the diamino moiety in **46** with NO[455−457] provided triazole **47** with λ_{max}^{abs} = 355 nm and fluorescence emission at 500 nm. The liberation of chlorambucil from **47** took place with Φ_r = 0.04 (λ_{irr} ≥410 nm) and a chemical yield of 90%. Hypoxia-dependent detection of NO based on changes in fluorescence and subsequent light-mediated release of chlorambucil was demonstrated in cultured HeLa cells.[454]

EWGs or EDGs at the 8-position do not significantly affect the absorption spectra of coumarins;[406,458] thus, substitution at this position was used to tune the non-photochemical properties of coumarin-based PPGs. For example, the 7,8-dihydroxy derivative **48a** and the bis(carboxymethoxy)-substituted coumarin **48b** exhibited similar spectroscopic properties (Table 9) to their analogs **29a** and **29c** (Table 7).[367,459] The catechol motif in **48a** enabled its attachment to

Scheme 10. Photochemistry of the Hypoxia and NO Dual-Channel Sensor 45[454]

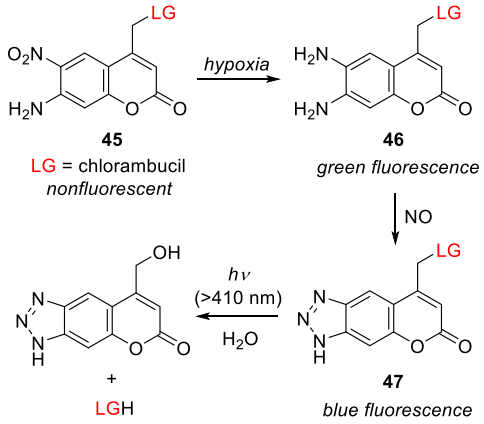

TiO_2 nanoparticles; photorelease of chlorambucil (Cbl) from **48a** (LG = Cbl) bound to such nanoparticles (λ_{irr} >410 nm) was accompanied by $^1O_2$ generation by excited TiO_2 (Φ_Δ = 0.29).[459] The bis(carboxymethoxy) moiety of **48b** conferred increased water solubility (up to 2.7 mM in acetonitrile/HEPES buffer 5:95, pH 7.2).[367] The dialkylaminomethyl C8 substituents of **49a−d** (Table 9) significantly reduced the acidity of the 7-OH group in **49c** (pK_a = 4.9)[460] and **49d** (pK_a = 3.8)[461] relative to the parent **40a** (pK_a = 6.2), presumably because the aminomethyl group forms an intramolecular hydrogen bond with the phenolic hydroxyl group,[462] leading to greater photouncaging efficiency at the lower end of the physiological pH range. The liberation of carboxylic acids, diols, amines (as carbamic acids), and phenols (as carbonic acids) from **49a−d** occurred with quantum efficiencies similar to or slightly exceeding that for **40a** upon both 1P (Φ_r = 0.06−0.014, λ_{irr} = 360 nm) and 2P excitation (δ_{unc} = 0.5−1.4 GM, 755 nm).[418,460,461,463] The 8-bis(carboxymethyl)aminomethyl moiety of **49c** increased water solubility[418,460] (to >2 mM in acetonitrile/HEPES buffer 5:95, pH 7.2), and the appended alkyne of **49d** enabled further conjugation of the PPG via copper-mediated click chemistry.[461,463] Singh and co-workers developed the π-extended coumarin derivatives **50** and **51** (Table 9),[464,465] which exhibited broad-range absorption extending to 400 or 550 nm, respectively. The 2-(2′-hydroxyphenyl)benzothiazole[466] (HBT) moiety in **50** facilitated pH-dependent excited-state intramolecular proton trans-

Scheme 9. Photochemistry of 44[345]

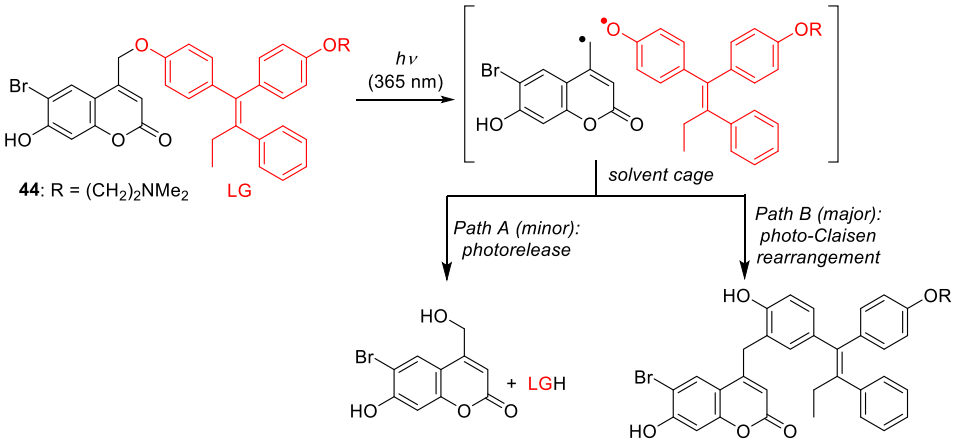

https://dx.doi.org/10.1021/acs.chemrev.0c00663
Chem. Rev. 2020, 120, 13135−13272

Table 9. Coumarin PPGs Substituted at the 8-Position

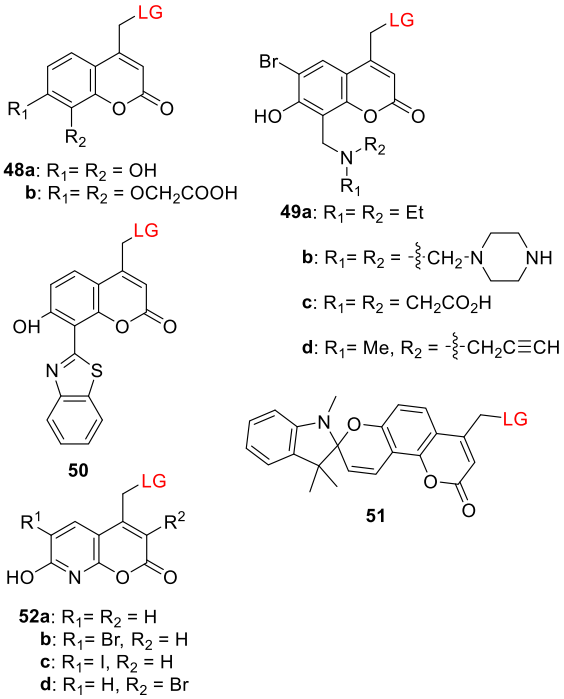

PPG	λ_{max}^{abs} (nm)	ε_{max} (M^{-1} cm^{-1})	leaving groups[a]	Φ_r (λ_{irr}/nm)	solvent[b]	ref
48a	~325	not reported	chlorambucil	0.034 (410)	ethanol	459
48b	324	1.1×10^4	Fmoc-cysteine	0.06 (350)	CH_3CN/HEPES buffer pH 7.2, 1:20	367
49a−c	371−376	$1.2-1.8 \times 10^4$	benzoic acid, dopamine and octopamine (as carbamic acids), capsaicin (as a carbonic acid), benzaldehyde (as a diol)	0.06−0.16 (360 or 365)	CH_3CN/PBS buffer pH 7.2, 1:20 or CH_3CN/HEPES buffer pH 7.2, 1:20	418, 460
49d	359	0.9×10^4	arachidonic acid, paclitaxels	0.06−0.14	MOPS buffer, pH 7.2	461
50	330	not reported	chlorambucil	0.006 (365)	ethanol	464
51	~330	not reported	chlorambucil	(410)	CH_3CN/H_2O, 7:3	465
52a	356	2.1×10^4	acetic acid	0.026 (350)	MOPS buffer, pH 7.2	416
52b	362	2.3×10^4	acetic acid	0.059 (350)	MOPS buffer, pH 7.2	282, 416, 469
				0.11 (365)	PBS buffer pH 7.4	131
52c	365	2.3×10^4	acetic acid	0.52 (365)	MOPS buffer, pH 7.2	282
52d	378	2.7×10^4	acetic acid, glutamate (as ester or as carbamic acid)	0.17−0.43	PBS buffer pH 7.4	282, 469

[a]Only selected LGs are shown. [b]HEPES = 4-(2-hydroxyethyl)-1-piperazineethanesulfonic acid; MOPS = 3-(*N*-morpholino)propanesulfonic acid; PBS = phosphate buffer saline.

fer[467] (ESIPT); at pH < 7.4, the 7-OH group enabled an ESIPT process resulting in emission at 528 nm, but at higher pH values, the hydroxy group was ionized and ESIPT was prevented, resulting in blue-shifted emission with λ_{max}^{em} = 480 nm.[464] The acidochromic spiropyran moiety[468] in **51** allows this PPG to undergo a reversible pH-dependent transformation between two species with distinguishable absorption spectra (Scheme 11; see also section 8).[465] The closed form of the spiropyran ($\mathbf{51}_{SP}$) has a C_{spiro}−O bond and has an absorption spectrum typical of 7-OR coumarin derivatives ($\lambda_{max}^{abs} \approx$ 325 nm). Under acidic conditions (pH < 5.4), the Cspiro−O bond was cleaved to form the zwitterionic merocyanine isomer ($\mathbf{51}_{MC}$), which has a more intense and red-shifted absorption spectrum extending up to 550 nm. The $\mathbf{51}_{MC}$ form can thus be selectively photolyzed at λ_{irr} >410 nm. Chlorambucil liberation was observed upon irradiation of **50** and **51** (LG = Cbl) at 365 and 410 nm, respectively.[464,465]

Scheme 11. Photochemistry of Spiropyran-Coumarin 25[465]

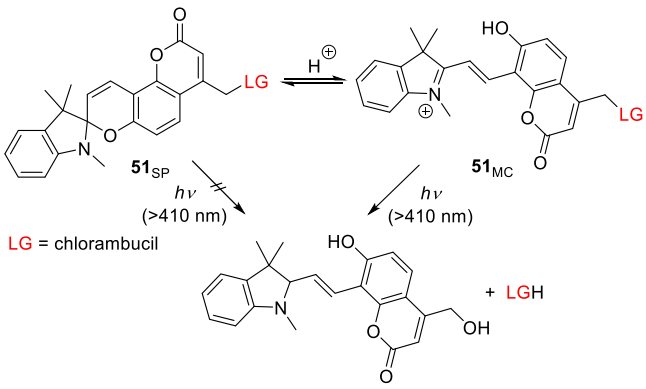

https://dx.doi.org/10.1021/acs.chemrev.0c00663
Chem. Rev. 2020, 120, 13135−13272

Table 10. Coumarin PPGs Substituted at the 3-Position

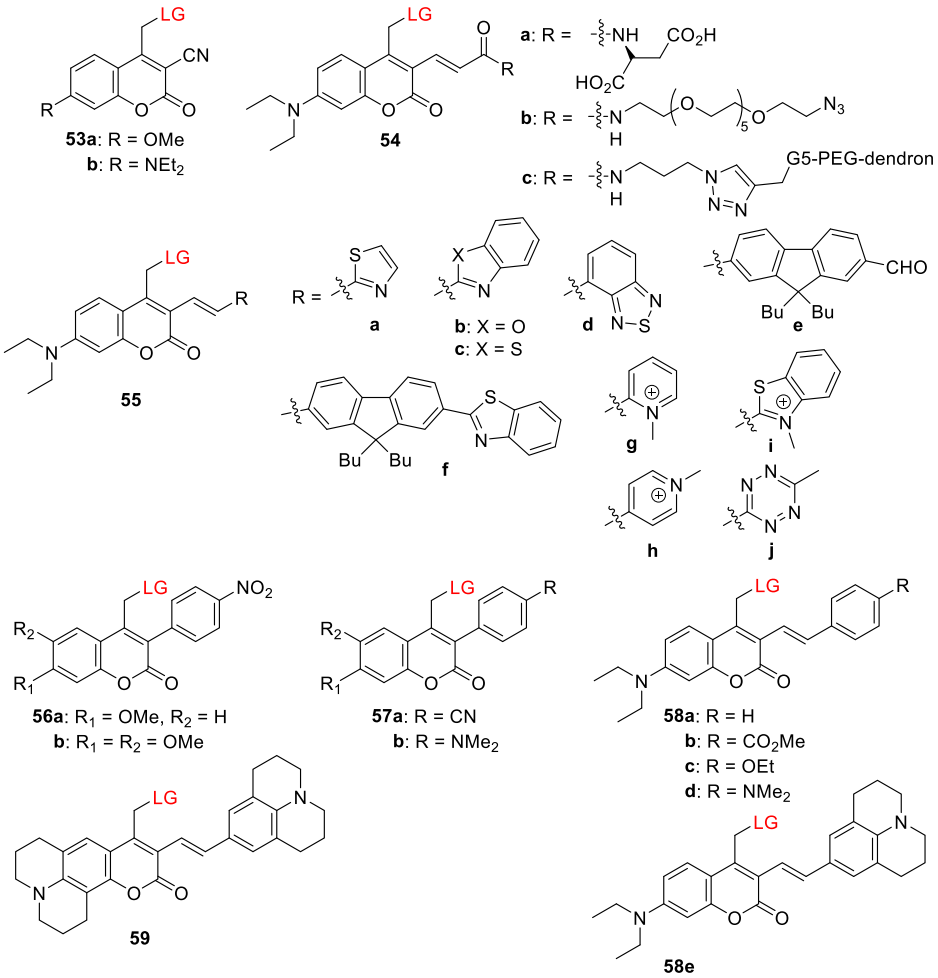

PPG	λ_{max}^{abs} (nm)	ε_{max} (M^{-1} cm^{-1})	leaving groups[a]	Φ_r (λ_{irr}/nm)	solvent[b]	ref
53a	360	2.5×10^4	benzoic acid	not reported	CH_3CN/Tris buffer (1:1), pH 7.2	291
53b	443	2.6×10^4	benzoic acid	0.04	CH_3CN/Tris buffer (1:1), pH 7.2	291
54a	450	4.3×10^4	glutamate	0.39 (473)	phosphate buffer, pH 7.4	292
55a−f	457−472	$3.3–4.7 \times 10^4$	Fmoc-Gly-OH	0.09-0.45 (455)	DMSO	470
55g−i	482−538	$3.0–4.0 \times 10^4$	3,5-dimethyl benzoic acid	0.001−0.01 (544)	H_2O	295
55j	470	3.5×10^4	Boc-Phe-OH	0.0044 (463)	CH_3CN/HEPES buffer (2:1), pH 7.0	471
56a	345	2.3×10^4	benzoic acid	0.09 (360)	DMSO	472
56b	369	1.7×10^4	benzoic acid	0.03 (360)	DMSO	472
57a	407	not reported	glutamate	0.05 (410)	HEPES buffer, pH 7.4	140
57b	407	2.4×10^4	benzoic acid	0.16 (400)	DMSO	473
58a−e	430−456	$3.0–4.4 \times 10^4$	4-methoxy benzoic acid	0.04−0.45 (430−456)	CH_3OH/H_2O (9:1)	294
59	467	3.5×10^4	4-methoxy benzoic acid	0.41 (467)	CH_3OH/H_2O (9:1)	294

[a]Only selected LGs are shown. [b]Tris = tris(hydroxymethyl)aminomethane; DMSO = dimethyl sulfoxide; HEPES = 4-(2-hydroxyethyl)-1-piperazineethanesulfonic acid.

Tamamura and co-workers developed 8-azacoumarin derivatives **52a−c**, whose absorption maxima are bathochromically shifted by ∼30 nm relative to **29a** (Table 9). These compounds have rather acidic phenolic OH groups (with pK_as of 4.22−5.67) and high water solubility (5−10 mM in PBS buffer).[282,416,469] The observed trend in the efficiency of acetic acid photorelease from **52a−c** (**c** > **b** > **a**) was attributed to the heavy atom effect of the 6-substituents on the ISC rate.[282,416,469] The bromine atom at the 3-position of **52d** induced an additional bathochromic shift, approximately doubled the photouncaging efficiency, and increased the pK_a of the phenolic OH group to 5.1.[282,416]

Extending the π-system at the 3-position is a well-establishedand useful way to bathochromically shift the absorption and emission maxima of coumarin fluorophores.[474−479] Jullien and co-workers synthesized 3-cyano coumarins **53a** and **53b**, which exhibited bathochromic shifts in λ_{max}^{abs} of 37 and 58 nm, respectively, relative to the parent coumarins **29b** and **30c** (Table 10).[291] The photorelease of benzoic acid from **53b** was ∼5-times less efficient than from **30c**. A 3-iodo derivative of **30c** had a similar λ_{max}^{abs} to **53b** (441 nm) but released pyridine derivatives more efficiently than **30c** ($\Phi_r\varepsilon_{405}$ = 202.0 vs 0.3 M^{-1} cm^{-1}, respectively), presumably due to less efficient PeT from the pyridine to the coumarin.[480]

https://dx.doi.org/10.1021/acs.chemrev.0c00663
Chem. Rev. 2020, 120, 13135−13272

Scheme 12. Photochemistry of DEAC450 PPG 54a[292]

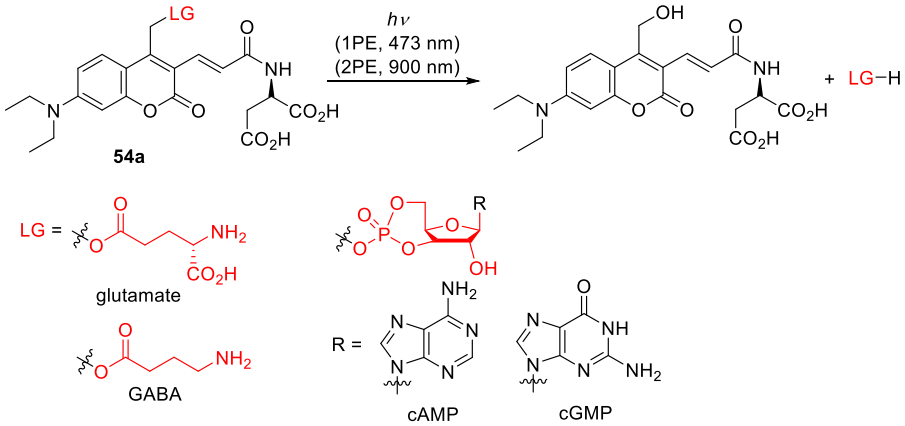

Scheme 13. BRET-Induced Photouncaging of Ibrutinib in Live Cells[487]

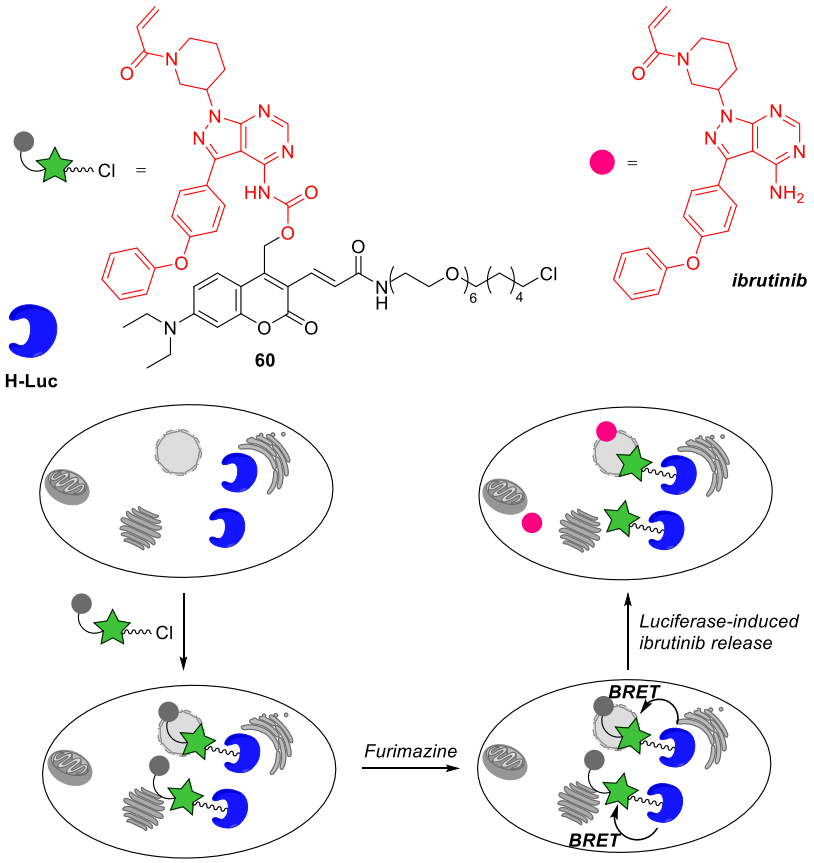

Ellis-Davies and co-workers introduced the water-soluble 3-[3-(methylamino)-3-oxoprop-1-en-1-yl] coumarin derivative **54a** (DEAC450; Figure 3), which strongly absorbs blue light.[292] The release of carboxylic acids (e.g., glutamate, GABA), cyclic adenosine monophosphate (cAMP), and cyclic guanosine monophosphate (cGMP) from **54a** proceeded quantitatively and efficiently upon either 1P (λ_{irr} = 473 nm, Φ_r = 0.18−0.78) or 2P (δ_{unc} = 0.5 GM, 900 nm) excitation, and a solvent-captured species was identified as the sole photoproduct (Scheme 12).[140,292,481,482]

Coumarin **54a** absorbs weakly in the UV region, especially in the range of 340−360 nm,[140,292] which enabled its selective and orthogonal 1P (473 and. 355 nm) and 2P (900 and 720 nm) excitation in the presence of shorter-wavelength activatable PPGs such as 4-carboxymethoxy-7-nitroindolinyl (CDNI) or dicarboxylate 2-(*p*-phenyl-*o*-nitrophenyl)propyl (dcPNPP).[140,481,483] Derivatives in which the 3-acrylamide moiety is conjugated with *O*-(aminoethyl)-2-azidoethyl-pentaethylene glycol (**54b**) or a PEG dendron (**54c**) were developed to increase the water solubility of caged GABA[481,483,484] and reduce antagonism towards GABA-A receptors.[481,485] Winssinger and co-workers reported that bioluminescence resonance energy transfer (BRET) from the Nanoluc-Halotag[486] fusion protein (H-Luc) to coumarin **60** was sufficient to induce uncaging of the kinase inhibitor ibrutinib (Scheme 13).[487] Accordingly, treatment with **60** caused furimazine-dependent covalent inhibition of the ErbB2

https://dx.doi.org/10.1021/acs.chemrev.0c00663
Chem. Rev. 2020, 120, 13135−13272

Scheme 14. Proposed Mechanism for the Uncaging Reaction of 57b[473]

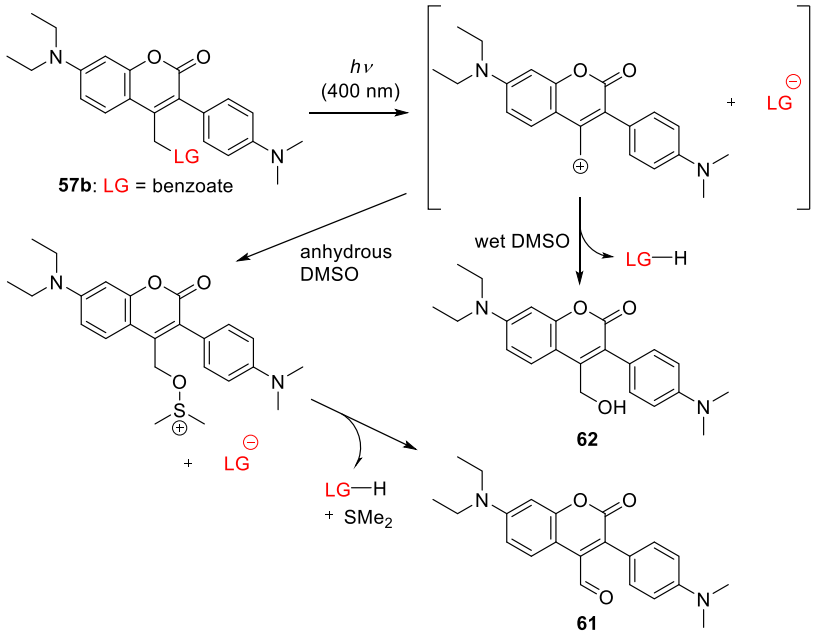

protein kinase in NanoLuc-HaloTag-expressing SKBR3 cells.[487]

Blanchard-Desce, Kele, and co-workers independently developed a series of 3-π-extended 7-(diethylamino)-coumarinylmethyl derivatives bearing electron-withdrawing end-groups (**55a−i**, Table 10).[295,470] Coumarins **55a−f** had absorption maxima at 457−472 nm, and the charged pyridinium and benzothiazolium derivatives **55g−i** exhibited even more pronounced bathochromic shifts in λ_{max}^{abs}.[295,470] The 66 nm difference in λ_{max}^{abs} between **55c** and **55i** (472 and 538 nm, respectively; Figure 3) can be attributed to the effect of the *N*-alkyl moiety on the benzothiazolyl end-group. The release of carboxylic acids from **55a−c** and **55e−f** proceeded with Φ_r = 0.09−0.45, but **55d** was photolyzed with Φ_r < 0.001. The authors explained this discrepancy by noting that the benzothiadiazolyl end-group of **55d** is the strongest EWG in this series and suggesting that its strong electron-withdrawing effect gives rise to a strongly polarized excited state with pronounced photoinduced ICT that hinders photorelease.[470,488] Accordingly, carboxylic acid liberation was less efficient from **55g−i**, which have strong cationic EWGs.[295] The 2PE cross section for these compounds was larger in the 700−750 nm region (δ = 175−1304 GM) than in the 940−970 nm region (δ = 59−371 GM).[295,470] Coumarin **55f** had the highest photoreaction efficiency for both 1PE (Φ_r = 0.45) and 2PE (δ_{unc} = 442 and 64 GM, at 730 and 940 nm, respectively) in this series.[470] Visible-light activated liberation of carboxylic acid LGs from coumarin **55j** was demonstrated to occur only after bioorthogonal transformation of the modulating tetrazine moiety.[471]

The introduction of 3-phenyl groups bearing either a strong EWG (**56a,b** and **57a**) or a strong EDG (**57b**) in the *para* position to create D−π−A or D−π−D systems, respectively, resulted in a ∼25−30 nm bathochromic shift of λ_{max}^{abs} relative to the parent coumarin (Table 10).[140,472,473] Photolysis of **56a,b** and **57a,b** led to quantitative carboxylic acid release; D−π−D derivative **57b** had the highest quantum yield in this series.[140,472,473] The 2PE uncaging cross section was determined to be 3.4 GM (710 nm) for **56a** and 2.1 GM (740 nm) for **56b**;[472] that for **57b** was estimated to be 16 GM (680 nm).[473] Aldehyde **61** was the major photoproduct (70%) formed upon irradiation of **57b** in anhydrous DMSO; the expected alcohol **62** was obtained only in the presence of water.[473] A proposed mechanism is shown in Scheme 14.

Zhu and co-workers observed similar photochemical behavior in the D−π−A and D−π−D systems **58a−e** and **59**, which were formed by extending the π-systems of 3-styryl coumarins at the 3-position (Table 10).[294] Coumarin **58a** exhibited a 48 nm bathochromic shift in λ_{max}^{abs} relative to **30c**, and it was photolyzed to release *p*-methoxybenzoic acid with a similar quantum yield (Φ_r = 0.05 and 0.04, respectively) upon irradiation at the corresponding absorption maxima.[294] The introduction of either an EDG or an EWG at the 3-styryl *para* position (**58b−e**) caused a further bathochromic shift. The uncaging quantum yields for D−π−D derivatives **58c−e** were 5−10-times higher than that for D−π−A derivative **58b** (Φ_r = 0.19−0.45 vs 0.04, respectively).[294] The ∼40 nm difference between the absorption maxima of **58d** and **58b** is probably related to the presence of the π-bridge. Bis(julolidine) derivative **59**, which bears the strongest electron donors in this series,[393] also had the most bathochromically shifted λ_{max}^{abs} (Figure 3) and was photolyzed with the highest efficiency ($\Phi_r\varepsilon_{467}$ = 14.3 M^{-1} cm^{-1}).[294] The 2PE uncaging cross sections determined for D−π−D systems **58c−e** and **59** were ∼5−10-times larger than that for D−π−A system **58b** (δ_{unc} = 17.7−39.6 vs 3.2 GM at 730 nm, respectively).

Benzocoumarin derivatives typically have similar or slightly hypsochromically shifted absorption maxima relative to 4-methylcoumarin[406,489,490] (λ_{max}^{abs} = 274−321 nm vs 310 nm), but their spectroscopic properties can be modified by introducing EDGs or EWGs to modulate their ICT states.[490] Gonçalves, Costa, and co-workers reported on several benzocoumarin PPGs (**63−68**); their structures and photophysical and photochemical properties relating to the photorelease of various carboxylic acids are shown in Table 11.[320,491−500]

The absorption maxima of coumarins can be significantly red-shifted by increasing the electron-withdrawing capacity at

https://dx.doi.org/10.1021/acs.chemrev.0c00663
Chem. Rev. 2020, 120, 13135−13272

Table 11. Spectroscopic and Photochemical Properties of Benzocoumarin-Derived PPGs

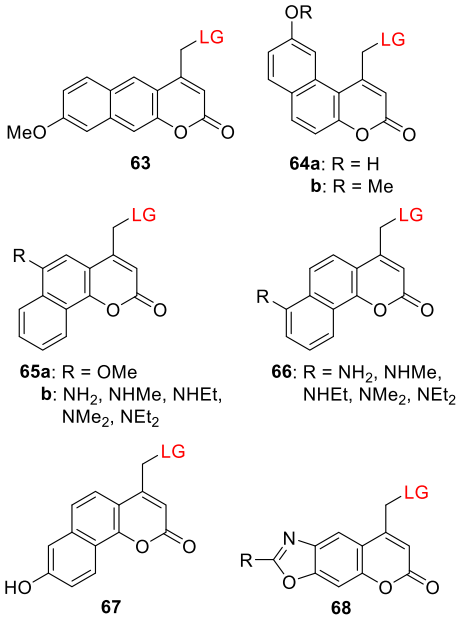

PPG	λ_{max}^{abs} (nm)	ε_{max} (M^{-1} cm^{-1})	leaving groups[a]	Φ_r (λ_{irr}/nm)	solvent[b]	ref
63	345	0.8×10^4	GABA−OH	0.7×10^{-5} (350)	ethanol	320
64a	360	1×10^4	Phe-OH		ethanol	491−493
64b	344−348	$0.6-1.8 \times 10^4$	various amino acids	$0.1-6.2 \times 10^{-5}$ (350)	ethanol or CH_3OH/HEPES pH 7.2, 4:1	320, 491−493
65a	371−376	4.1×10^3	GABA, various amino acids, 5-aminolevulinic acid	$2-24 \times 10^{-5}$ (350)	CH_3OH/HEPES pH 7.2, 4:1	494, 496, 497
				$0.4-16 \times 10^{-5}$ (419)		494, 496, 497
65b	377−418	$0.7-7.7 \times 10^3$	butyric acid, 5-aminolevulinic acid	$0.8-25.0 \times 10^{-5}$ (350)	CH_3OH/HEPES pH 7.2, 4:1	495, 497, 498
				$0.5-31.0 \times 10^{-5}$ (419)		495, 497, 498
66	377−398	$0.7-7.7 \times 10^3$	butyric acid	$0.7-13.0 \times 10^{-5}$ (350)	CH_3OH/HEPES pH 7.2, 4:1	497, 498
				$0.6-7.0 \times 10^{-5}$ (419)		497, 498
67	362	1.1×10^4	glutamate	0.006 (355)	$CHCl_3$	499
68	339−361	$0.3-1.1 \times 10^4$	butyric acid	$8.6-12.0 \times 10^{-5}$ (350)	CH_3OH/HEPES pH 7.2, 4:1	497, 500
				$0.04-1.0 \times 10^{-5}$ (419)		497, 500

[a]Only selected LGs are shown. [b]GABA−OH = 4-(benzyloxycarbonylamino)butanoic acid; Phe-OH = *N*-(carbobenzyloxy)-L-phenylalanine; HEPES = 4-(2-hydroxyethyl)-1-piperazineethanesulfonic acid.

the 2-position.[501−504] For example, the singlet excited states of thiocarbonyls are lower in energy than those of their carbonyl analogs, so their light absorption is bathochromically shifted.[505,506] This effect was also observed for coumarins.[507−510] Costa, Jullien, and co-workers studied thionated coumarin **69a**, which had a 73 nm bathochromic shift of λ_{max}^{abs} relative to its carbonyl analog, yet it released carboxylic acids with a low quantum efficiency (Table 12).[291,304,511] The absorption maximum of 7-NEt_2 thiocoumarin **69b** was bathochromically shifted by 87 nm relative to its carbonyl analog (Figure 3), and it photoreleased benzoic acid with Φ_r = 0.18, which was 2 orders of magnitude higher than the corresponding value for the carbonyl analog when both were irradiated at their absorption maxima.[291] The liberation of benzoic acid from **69b** was induced by irradiating Er^{3+}- or Tm^{3+}-based upconverting nanoparticles (see also section 6.4.2) at 974 nm.[512] However, the release quantum yield of **69b** was found to be concentration-dependent, decreasing ∼30-fold when its concentration in the irradiated solution was lowered from 25 to 4 μM.[291] The photouncaging of a carbamate-linked cyclofen analog[431,513] from **75** was demonstrated (Scheme 15).[514] The solvent-captured derivative **76** was identified as the sole photoproduct of this reaction, and the cyclofen derivative was liberated in high chemical yield (90%, $\Phi_r = 5 \times 10^{-3}$) at λ_{irr} = 470 nm. The chromatically orthogonal photoactivation of **75** and 13-*cis*-retinoic acid (using blue-cyan- and UV-light sources, respectively) was used to control the development of live zebrafish embryos.[514] Additionally, the photouncaging of a Cas9 activator, trimethoprim, from **69b** was used to control the activity of a CRISPR-Cas9 system in cell cultures.[515]

Gonçalves and co-workers studied several thionated benzo-[*f*]coumarins (**70a−c**) that exhibited bathochromic shifts of ∼65 nm relative to their carbonyl analogs and released carboxylic acids, with 3−20-times higher quantum yields upon

https://dx.doi.org/10.1021/acs.chemrev.0c00663
Chem. Rev. 2020, 120, 13135−13272

Table 12. Spectroscopic and Photochemical Properties of Thionated Coumarin PPGs

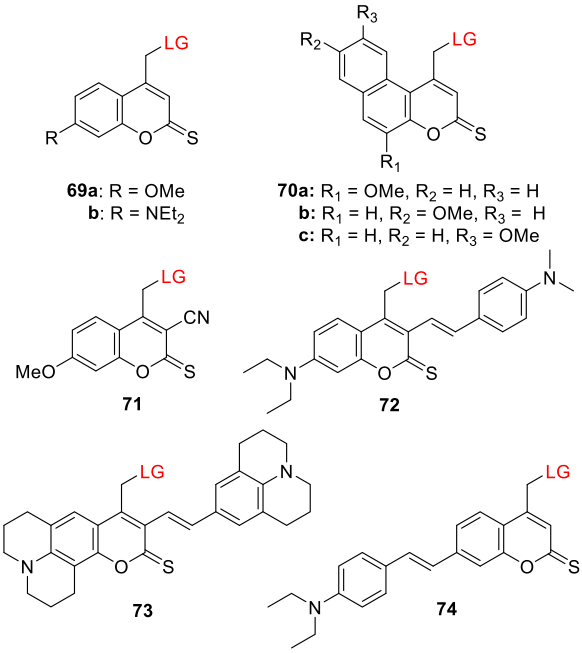

PPG	λ_{max}^{abs} (nm)	ε_{max} (M^{-1} cm^{-1})	leaving groups[a]	Φ_r (λ_{irr}/nm)	solvent[b]	ref
69a	395−398	1.4−1.7 × 10^4	benzoic acid, Z-Phe-OH	2−7 × 10^{-5} (365, 419)	ethanol or CH_3CN/Tris buffer pH 7.5, 1:1	291, 304, 511
69b	472	3.1 × 10^4	benzoic acid	0.12 (365), 0.18 (487)	CH_3CN/Tris buffer pH 7.5, 1:1	291
70a−c	400−431	0.7−2.7 × 10^4	butyric acid, various amino acids	1.0−13.0 × 10^{-5} (419)	CH_3OH/HEPES pH 7.2, 4:1	335, 516, 517
71	427	1.8 × 10^4	benzoic acid		CH_3CN/Tris buffer pH 7.5, 1:1	291
72	490	3.0 × 10^4	4-methoxybenzoic acid	0.4 (490)	CH_3OH/H_2O 9:1	294
73	515	2.5 × 10^4	4-methoxybenzoic acid	0.7 (515)	CH_3OH/H_2O 9:1	294
74	479	1.0 × 10^4	acetic acid	0.071 (475)	H_2O	284

[a]Only selected LGs are shown. [b]Tris = tris(hydroxymethyl)aminomethane; HEPES = 4-(2-hydroxyethyl)-1-piperazineethanesulfonic acid; Z-Phe-OH = *N*-(carbobenzyloxy)-L-phenylalanine.

Scheme 15. Photochemistry of Thiocoumarin 75[514]

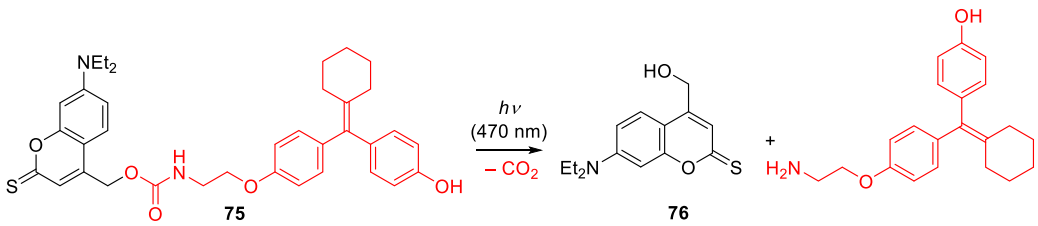

irradiation at 419 nm (Table 12).[335,516,517] The thiocarbonyl motif proved to be compatible with other structural modifications that caused further bathochromic shifts in absorption. For example, the 3-CN derivative **71** had a λ_{max}^{abs} of 427 nm, although it was thermally unstable in a Tris buffer/acetonitrile solution (pH = 7.5).[291] Conversely, coumarin derivatives **72** and **73** bearing electron-rich *p*-aminostyryl moieties in the 3-position had significantly bathochromically-shifted absorption spectra (λ_{max}^{abs} = 490 and 515 nm, respectively) but were thermally stable.[294] Irradiation of **72** and **73** at their λ_{max}^{abs} induced photorelease of *p*-methoxybenzoic acid with Φ_r = 0.4 and 0.7, respectively. The cyclized derivative **78**, rather than the expected 4-hydroxymethyl-coumarin, was identified as the main photoproduct of photolysis of **77**. The mechanism proposed to explain this observation is shown in Scheme 16. Similar photoproducts are formed from **72** and **73**; in all three cases, the loss of π-conjugation at the 3-position in the photoproducts causes a hypsochromic shift of λ_{max}^{abs} (to 470 nm).[294]

Howorka and co-workers reported that the absorption maximum of thiocoumarin **74**, which has an electron-rich *p*-diethylaminostyryl moiety at the 7-position, is at ∼480 nm (Table 12).[284] Irradiation of **74** in DMSO or water liberated acetic acid with Φ_r = 0.024 and 0.071, respectively. On the basis of transient-absorption spectroscopy and steady-state kinetic studies in the presence and absence of oxygen, the authors proposed that the photorelease of the LG in DMSO proceeds through the triplet excited state, while a charge-separated state is more populated in water.[284]

Imino and hydroxyimino derivatives **79a** and **79b** (Figure 4) exhibited only minimal shifts in λ_{max}^{abs} relative to the carbonyl analog **29b**.[291] Compound **79a** was thermally unstable in a tris

https://dx.doi.org/10.1021/acs.chemrev.0c00663
Chem. Rev. 2020, 120, 13135−13272

Scheme 16. Proposed Photolysis Mechanism for 3-Styryl-Conjugated Thiocoumarins[294]

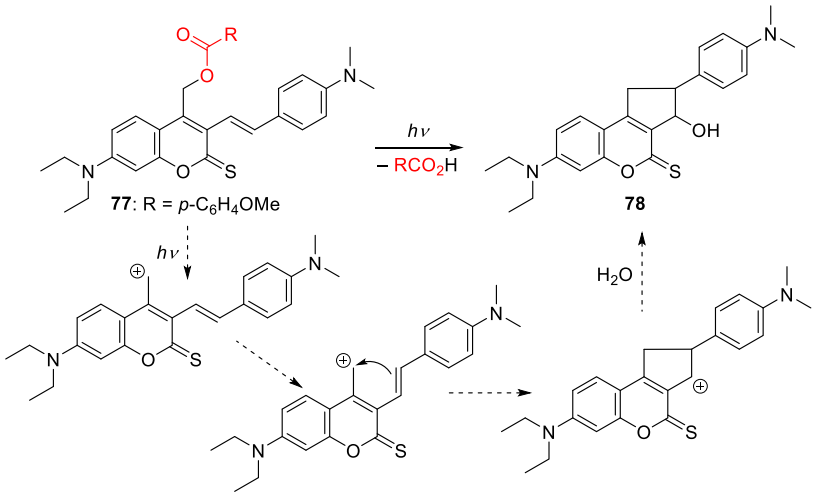

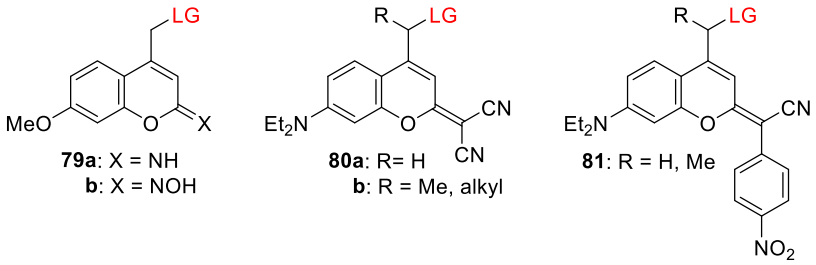

Figure 4. Structures of coumarin PPGs substituted at the 2-position. LG = alkoxide, carboxylate, or amine (as a carbamate).

buffer/acetonitrile solution (pH 7.5), while **79b** was photochemically inactive; it did not release acetic acid as a LG upon irradiation at 365 nm.[291] Conversely, 7-(*N*,*N*-diethylamino)-dicyano derivative **80a** (λ_{max}^{abs} = 487 nm, ε_{487} = 3.3 × 10^4 M^{-1} cm^{-1})[291] released carboxylic acids in high chemical yield (>90%) upon irradiation at 487 or 505 nm with Φ_r = 0.3−1.5 × 10^{-3}.[291,518,519] However, the liberation of an amine (as a carbamic acid) from **80a** proceeded ∼3-times less efficiently than that of a comparable carboxylic acid.[519] Marchán and coworkers reported that the release quantum yields of carboxylic acids and amines from dicyano derivative **80b** (R = Me) were up to 2.5-fold higher than those for release from **80a**.[518,519] Additionally, **80b** was more stable than its thiocarbonyl analog in the presence of acids and bases commonly used in Fmoc/*t*-Bu solid-phase peptide synthesis. It was therefore used to cage a cyclic RGD peptide-drug conjugate (**82**, Figure 5).[518] Photouncaging of the peptide-drug conjugate from **82** (λ_{irr} = 505 nm) proceeded with Φ_r = 7.2 × 10^{-3}.

An analog of **80b** (R = alkyl) was used to prepare caged morpholino oligonucleotides[212,520−523] (cMOs) capable of perturbing targeted RNAs *in vivo*.[356] Although the caged cMOs were successfully uncaged in live zebrafish embryos (λ_{irr} = 470 nm), their thermal stability *in vivo* was significantly lower than that of their carbonyl analogs.[356] Increasing the system's electron-withdrawing capacity at the 2-position by replacing one cyano group with a *p*-nitrophenyl moiety (**81**) caused an additional ∼15 nm bathochromic shift of the absorption maximum (λ_{max}^{abs} ≈ 502 nm) but also significantly reduced the photouncaging quantum yield (Φ_r = 0.5−2.3 × 10^{-6}).[519]

A different way of utilizing the coumarin scaffold for photorelease was demonstrated by introducing a photoreactive oxime ester[524] in the 3-position (**83**, Figure 6).[525] The

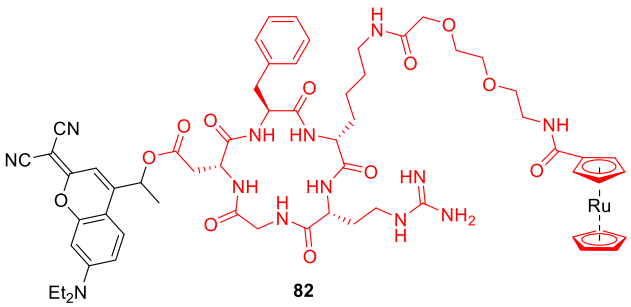

Figure 5. Structure of the **80b**-caged c(RGDfK)-ruthenocene conjugate **82**.

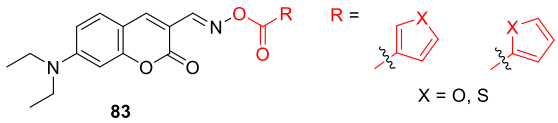

Figure 6. Structure of coumarin-oxime-ester PPG **83**.

excitation of oxime esters typically results in homolytic scission of the N−O bond and the formation of a caged radical pair.[526−528] Photoexcitation of **83** (λ_{max}^{abs} = 436 nm, ε_{436} = 3.9−4.2 × 10^4 M^{-1} cm^{-1}) at 450 nm led to the formation of heterocyclic radicals, and the system was used as a photoinitiator for radical polymerization of acrylate monomers.[525]

2.3. Arylmethyl and Arylcarbonylmethyl Groups

Polyaromatic cores provide convenient platforms for developing π-extended arylmethyl and arylcarbonylmethyl PPGs. For example, the (anthracen-9-yl)methyl group was introduced as a polyaromatic benzyl-type PPG for carboxylates, alcohols, and

https://dx.doi.org/10.1021/acs.chemrev.0c00663
Chem. Rev. 2020, 120, 13135−13272

hydroxylamines with a bathochromically shifted absorption band ($\lambda_{max}^{abs} \approx 385$ nm)[529] relative to those of benzyl[1] ($\lambda_{max}^{abs} \approx 254$ nm) and 2-naphthylmethyl[317] ($\lambda_{max}^{abs} \approx 280$ nm) chromophores.[323,529−531] Lam and co-workers prepared an (anthracen-9-yl)methyl that absorbs above 400 nm by extending its π-conjugation through the 10-position (**84a−f**, Figure 7).[532]

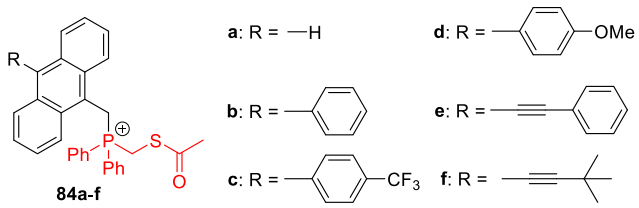

Figure 7. π-Extended (anthracen-9-yl)methyl PPGs.

The absorption spectra of compounds **84b−d** ($\lambda_{max}^{abs} \approx 405$ nm) are bathochromically shifted relative to that of **84a** ($\lambda_{max}^{abs} = 376$ nm). Although these compounds have different substituents at the *para* position of the phenyl moiety, their spectra are similar. This was attributed to steric hindrance, which may cause the phenyl ring to be oriented orthogonally to the anthracenyl core.[533] The presence of an acetylene bridge in **84e** and **84f** eliminates this steric hindrance;[534] accordingly, the absorption maxima of these compounds are bathochromically shifted by ∼30−40 nm (λ_{max}^{abs} = 425−440 nm). The photorelease of the diphenylphosphinothioester LG from **84b−f** in a THF/water mixture (3:1, λ_{irr} >420 nm) was demonstrated, and **84f** showed the highest release efficiency within this series. The photoinduced heterolytic cleavage of the (anthracen-9-yl)methyl−phosphorus bond in **84f** at λ_{irr} = 366 and 416 nm occurred with Φ_r = 0.08 and 0.025, respectively; these values are comparable to those for previously reported 4,5-dimethoxy-2-nitrobenzyl[535] (DMNB) and (anthracen-9-yl)methyl[536] caged phosphines (λ_{irr} = 360−400 nm). A phototriggered (λ_{irr} > 420 nm) traceless Staudinger ligation[537] of caged oligopeptides (**85**) with azide-containing amino acids was shown to form the expected oligopeptides in chemical yields of 31−43% (Scheme 17).

Scheme 17. Visible-Light Triggered Traceless Staudinger Ligation[532]

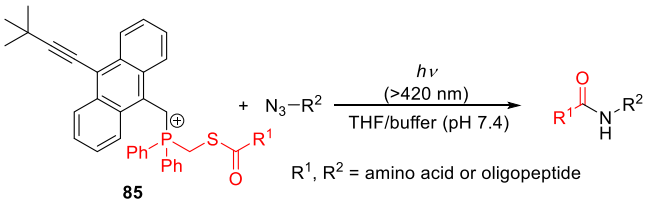

The (acridin-9-yl)methyl group (**86**) was introduced by Zhang and co-workers as a UV-activatable ($\lambda_{max}^{abs} \approx 355$ nm, $\varepsilon_{360} \approx 1 \times 10^4$ M^{-1} cm^{-1}) PPG for alcohols[538] and was later used with carboxylic acids.[335,517,539,540] Its tail absorption in the visible range enabled photolysis at λ_{irr} = 419 nm, albeit with low quantum efficiency (Φ_r = 0.5−1.6 × 10^{-4}).[335,540] The photoreaction was proposed to proceed through an ion-pair intermediate.[539] Singh and co-workers introduced the π-extended [benzo(*a*)acridin-12-yl]methyl derivative **87**, which exhibits a bathochromic shift of ∼20 nm ($\lambda_{max}^{abs} \approx 374$ nm, $\varepsilon_{max} \approx 5 \times 10^4$ M^{-1} cm^{-1}) and extended absorption up to ∼425 nm (Scheme 18).[541] Photorelease ($\lambda_{irr} \geq 410$ nm) of carboxylic acids from **87** proceeded in excellent chemical yields (80−92%) and with significantly higher quantum efficiencies (Φ_r = 0.08−0.13) than for **86**; solvent-captured (benzo(*a*)acridin-12-yl)methylalcohol was identified as the sole side-photoproduct (Scheme 18).[541] A (benzo(*a*)acridin-12-yl)methyl-caged chlorambucil derivative was also shown to accumulate in the nuclei of cultured HeLa cells, presumably due to the acridine scaffold's capacity to intercalate with DNA,[542−544] and exhibited light-dependent cytotoxicity.[541]

Singh and co-workers also introduced 1-(hydroxyacetyl)-pyrene[545] **88** as a variant of the well-established (pyren-1-yl)methyl PPG (Scheme 19).[322,546−549] In contrast to (pyren-1-yl)methyl, which absorbs only in the UV region (with a solvent-dependent λ_{max}^{abs} = 320−340 nm), the addition of a hydroxyacetyl group in **88** caused a bathochromic shift of λ_{max}^{abs} (∼355 nm), resulting in sufficient absorption above 400 nm (ε_{410} = 2.7−3.9 × 10^3 M^{-1} cm^{-1}) to enable visible light-induced photolysis.[545] The photorelease ($\lambda_{irr} \geq 410$ nm) of carboxylic acids[545,550] and alcohols[551] (as carbonates) in a 1:1 acetonitrile/H_2O solution proceeded with near-quantitative chemical yields (>94%) and high quantum efficiencies (Φ_r = 0.30−0.41 and 0.17−0.20, respectively; Scheme 19). These results can be compared to those achieved with a (pyren-1-yl)methyl group, which released carboxylic acids and alcohols with (solvent dependent) Φ_r = 0.0029−0.139 upon excitation at 350 nm.[322,546−548] The inherent fluorescence of 1-acetylpyrene[552] (λ_{max}^{abs} = 439 nm, Φ_F = 0.02) enabled imaging of **88** in fixed cells.[551] The efficiency of photorelease from **88** depended strongly on the water content of the reaction

Scheme 19. Photochemistry of 1-(Hydroxyacetyl)pyrene PPG[551]

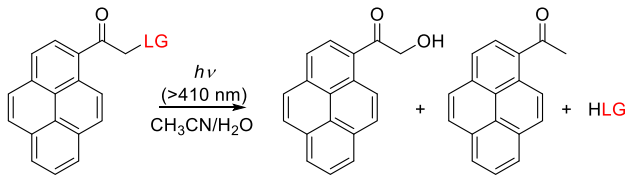

Scheme 18. (Acridin-9-yl)methyl PPGs 86 and 87[541]

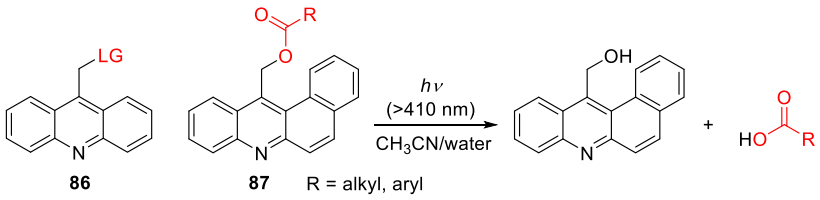

https://dx.doi.org/10.1021/acs.chemrev.0c00663
Chem. Rev. 2020, 120, 13135−13272

Scheme 20. Photorelease from 1-Acetylpyrene PPG (88)[551]

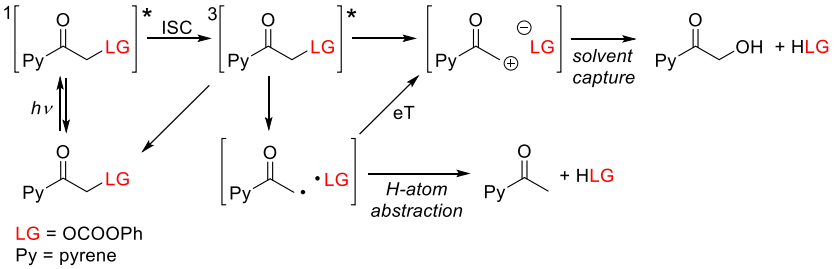

mixtures and decreased in the presence of a triplet quencher (potassium sorbate). Three photoproducts (the leaving group, 1-hydroxyacetylpyrene, and acetylpyrene) were formed upon irradiation; Scheme 20 shows a mechanism explaining these results.[545,551]

Another arylmethyl-type PPG studied by Singh and co-workers is the (perylen-3-yl)methyl group (**89**), which absorbs in the visible range (λ^{abs}_{max} = 438 nm, ε_{max} = 2.4−3.5 × 10^4) and displays characteristic fluorescence (λ^{F}_{max} = 445 nm, Φ_F = 0.9; Scheme 21).[553] Carboxylic acids and alcohols (attached as carbonates) were successfully photoreleased from **89** (λ_{irr} ≥ 410 nm) in an acetonitrile/H_2O (3:1) solution with high chemical yields (>89%) and moderate quantum efficiencies (Φ_r = 7.7−9.3 × 10^{-2}).

Scheme 21. Photochemistry of the (Perylen-3-yl)methyl PPG[553]

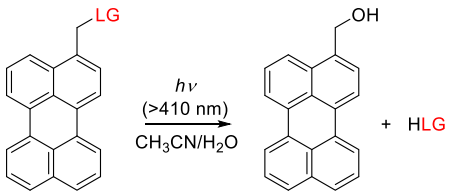

89: LG = carbonates, carboxylates

Similar to other polyaromatic arylmethyl-type PPGs,[529] the photoreaction mechanism of **89** was proposed to proceed through the singlet excited state, followed by heterolysis of the C−O bond and solvent capture to afford the photoproducts.[553] Heterolysis of the C−O bond was previously calculated to be energetically preferable to homolysis, especially when the carbocation is stabilized,[554−556] although homolysis dominates in simple benzyl derivatives.[557] Zhao and co-workers further demonstrated that carboxylic acid leaving groups (e.g., chlorambucil) can be released from perylene **90** (Scheme 22), although quantitative chemical yields were not reported.[558]

Scheme 22. Photorelease of Chlorambucil from a Single (Perylen-3,4,9,10-yl)tetramethyl PPG (90)[558]

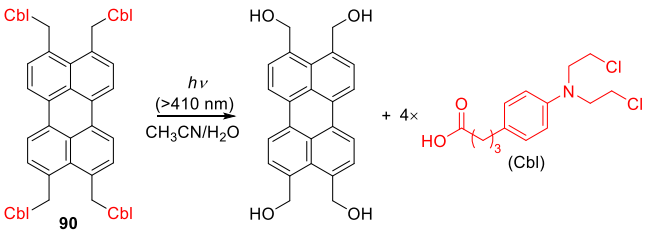

The inherent hydrophobicity of polyaromatic PPGs limits their applicability in aqueous media. However, their incorporation into larger molecular structures has been demonstrated. For example, **89** was used to prepare photodegradable hydrogels[559,560] and polymer nanoparticles.[561−563] Additionally, Singh and co-workers used a reprecipitation technique[564] to formulate (perylen-3-yl)methyl-caged chloambucil[565] and pesticide 2,4-D[566] (**91** and **92**, Figure 8) as globular organic nanoparticles with an average particle size of 25−30 nm, broad absorption spectra extending into the visible range (350−550 nm), and fluorescence emission at 625 nm. These nanoparticles were photolyzed (λ_{irr} ≥ 410 nm) to release the parent compound (perylen-3-yl)methanol and the corresponding leaving group. In the absence of light, 2−5% of the starting material hydrolyzed upon incubation in water or 10% fetal bovine serum (FBS) at 35−37 °C over 2−7 days. Photorelease (λ_{irr} ≥410 nm) from nanoparticles of **91** and **92** was also demonstrated in cultured HeLa cells[565] and plants[566] (*Cicer arietinum*), respectively, and light-dependent biological effects of the corresponding bioactive leaving groups were observed. Leaving group release could be monitored in real time because it caused the fluorescence emission band to shift from 625 nm (nanoparticle) to 450 nm ((perylen-3-yl)methanol). Similarly, the antimicrobial compound salicylic acid was caged with 1-(hydroxyacetyl)pyrene via an ester linkage (**93**, Figure 8), and the resulting conjugate was formulated into light-responsive (λ_{irr} ≥ 410 nm) organic nanoparticles whose photoactivation was demonstrated.[567]

2.4. The (Benzothiadiazol-6/7-yl)methyl Group

VanVeller and co-workers studied compounds **94** and **95** as benzyl-type PPGs with a π-expanded heteroaromatic benzothiadiazole core (Figure 9).[568] Their photoreactivity was explained based on the redistribution of electron density from the EDGs in the *o*- and *m*-positions upon excitation.[554,555,557] Although the *meta* effect was established for methoxy-substituted benzyl derivatives over 50 years ago,[556] the corresponding NR_2 analogs were only studied recently[569−576] and achieved high photoreaction quantum yields (up to 0.45[570]). Derivatives **94** and **95** had broad absorption bands extending up to 500 nm with maxima at 420 nm. Acetate was photoreleased from **94a** and **95** with comparable quantum yields (Φ_r = 0.067 and 0.061, respectively; λ_{irr} = 455 nm), and ethanol was liberated from **95** with Φ_r = 0.04.[568] The presence of a bromo substituent in the 7-position (**94b**) roughly halved the quantum yield,[568] presumably because of competing photochemical processes such as C−Br scission.[577]

2.5. The (*N*-Methyl-7-hydroxyquinolinium-2-yl)methyl Group

The photochemistry of the (7-hydroxyquinoline-2-yl)methyl group was initially explored and exploited by Dore and co-

https://dx.doi.org/10.1021/acs.chemrev.0c00663
Chem. Rev. 2020, 120, 13135−13272

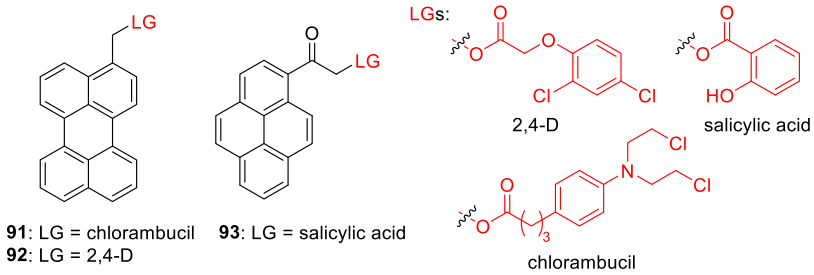

Figure 8. Structures of (perylen-3-yl)methyl and 1-(hydroxyacetyl)pyrene derivatives.

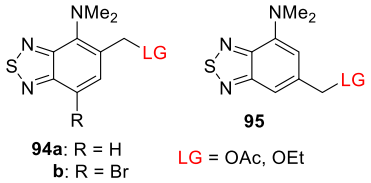

Figure 9. (Benzothiadiazol-6/7-yl)methyl PPGs.

workers, who identified the (8-bromo-7-hydroxyquinoline-2-yl)methyl (BHQ)[578] and (8-cyano-7-hydroxyquinoline-2-yl)-methyl (CyHQ)[579] groups (among others) as efficient PPGs for carboxylates, phosphates, diols, phenols, and amines.[578,580−584] Derivatives of the (7-hydroxyquinoline-2-yl)methyl group can also be removed by 2P excitation, which reportedly proceeds with δ_{unc} values of up to 2.6 GM (740 nm) for carboxylate LGs.[579,585] The photochemical properties of (7-hydroxyquinoline-2-yl)methyl could be adjusted by varying the substituents on the quinoline core, although the λ_{max}^{abs} remained in the range of 320−385 nm.[579,585,586] Singh and co-workers showed that attaching an (8-alkoxyquinoline-2-yl)methyl derivative to carbon dots enabled their photolysis with $\lambda_{irr} \geq 410$ nm to release H_2S (see also section 4.3).[587] Additionally, Narumi and co-workers[588,589] extended the absorption wavelengths of quinoline-derived PPGs above 400 nm by *N*-alkylation of the quinoline nitrogen, a modification known to shift the absorption spectrum bathochromically.[590,591]

The *N*-methyl-7-hydroxyquinolinium group **96** (*N*-Me-7HQm, λ_{max}^{abs} = 418 nm) photoreleased acetic acid as an LG upon irradiation with blue light (λ_{irr} = 458 nm, Φ_r = 0.045), with concomitant formation of (*N*-methyl-7-hydroxyquinolinium-2-yl)methanol as the sole additional photoproduct (Scheme 23). It is not yet known whether the

Scheme 23. Photochemistry of *N*-Methyl-7-hydroxyquinolinium PPG[588]

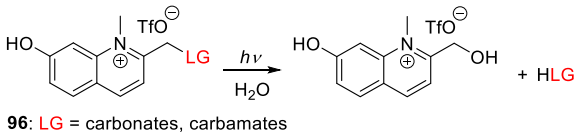

mechanism of this photoreaction is similar to that of other (7-hydroxyquinoline-2-yl)methyl derivatives, in which heterolysis of the C−O bond proceeds from the triplet-excited state to generate an ion pair that subsequently collapses into the free leaving group and a solvent-captured side product.[578,582,592,593] Methylation of the 7-hydroxy group caused a 60 nm hypsochromic shift of λ_{max}^{abs} but terminated the photoreaction. 7-NMe_2 derivatives exhibited a λ_{max}^{abs} at ∼445 nm and were photolyzed with lower quantum yields (Φ_r = 1.2−2.8 × 10^{-3}) than the 7-hydroxy derivative, presumably due to the contribution of the NMe_2 group in the twisted intramolecular charge-transfer (TICT) excited state.[395,594] Increasing the system's electron density by introducing an ethyl group in the 4-position more than doubled the quantum yield. As a salt, **96** was highly soluble in water (up to 20 mM, depending on the leaving group) and was successfully used for the photorelease of several amino acids and neurotransmitters (caged via their amino groups as carbamates), achieving Φ_r values of 0.025−0.068 and $\Phi_r\varepsilon(\lambda_{irr})$ values at 458 nm in the range of 96−272 M^{-1} cm^{-1}.[588,589]

2.6. The Bimane Group

Singh and co-workers repurposed the fluorescent molecule bimane, often used in biochemistry for fluorescence labeling of proteins,[595−597] as a photoremovable protecting group by introducing carboxylate leaving groups on the 3-methyl or 3,5-dimethyl substituents (**97** and **98**, respectively, Figure 10).[598]

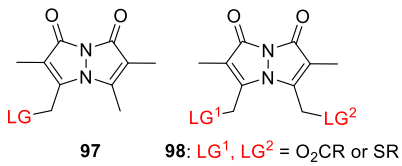

Figure 10. Bimane PPGs.

These compounds had a λ_{max}^{abs} at ∼380 nm with tail absorption above 400 nm and a fluorescence λ_{max}^{em} between 460 and 480 nm (Φ_F = 0.6−0.8). These values are similar to those for unsubstituted bimane.

Photorelease ($\lambda_{irr} \geq 410$ nm) of various aliphatic and aromatic carboxylic acids from bimane **97** proceeded with good chemical (75−85%) and moderate quantum yields (Φ_r = 0.06−0.07)[598] that increased with the solvent's water content.[598] The authors proposed that the photoreaction proceeds through the singlet excited state and involves heterolytic C−O bond cleavage to generate an ion-pair that then undergoes solvent-mediated separation, leading to solvent capture of the bimane methyl cation (Scheme 24). In the case of **98**, the captured product underwent a second photoreaction to release another equivalent of the LG with a quantum efficiency similar to that for the first LG liberation (Φ_r = 0.04).[598]

The photorelease of thiols from bimane **97** upon irradiation at 420 nm proceeded with a high chemical yield (70%) and Φ_r = 0.02.[599] Because of the high nucleophilicity of thiols, the presence of strong electrophiles was required to prevent recombination of the resulting ion pair; in their absence, no photoproducts were detected. Similar behavior was observed

https://dx.doi.org/10.1021/acs.chemrev.0c00663
Chem. Rev. 2020, 120, 13135−13272

Scheme 24. Proposed Mechanism of Photorelease from Bimane-Derived PPGs[598]

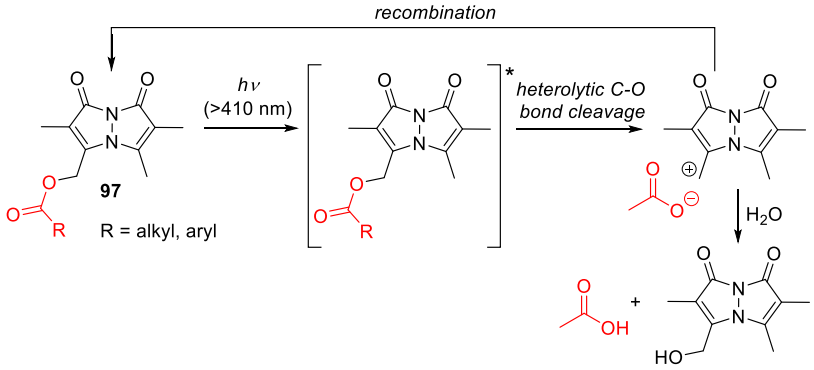

for the release of thiols from 3-(hydroxymethyl)-2-naphthol derivatives.[600] Photouncaging (λ_{irr} = 420 nm) of thiols from the corresponding tetra-bimane-protected dendrimeric monomer **99** in the presence of a dendritic monomer functionalized with strong electrophiles led to the formation of a photo-induced crosslinked polymeric network (Scheme 25) capable of entrapping live cells while preserving their viability.[599]

Scheme 25. Polymer Cross-Linking via a Light-Induced Thiol-Electrophile Reaction[599]

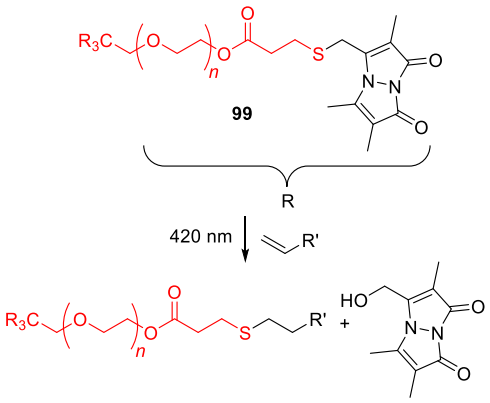

2.7. Arylcarbonylmethyl Groups

Aromatic ketones are synthetically accessible, thermally stable, and photochemically reactive moieties that have been used extensively as PPGs.[10] Both their lowest energy transition (n,π*) and the higher energy π,π* absorption bands are typically in the UV range. The liberation of leaving groups from arylcarbonylmethyl groups (Figure 11) can proceed via different reaction mechanisms depending on the substitution of the arene; for details, see an earlier review.[10] Simple phenacyl PPGs (**100**) liberate LGs via H atom abstraction[601−603] or electron transfer (see section 6.2), *o*-methylacetophenones (**101**) react through an intramolecular H-transfer process,[235,604−610] *p*-hydroxyphenacyl moieties (**102**) release LGs via a photo-Favorskii rearrangement,[611−613] and benzoin derivatives (**103**) release LGs via photocyclization to form 2-phenylbenzofuran as a side-product.[275,614−616] Here, we discuss only arylcarbonylmethyl PPGs that absorb above 400 nm.

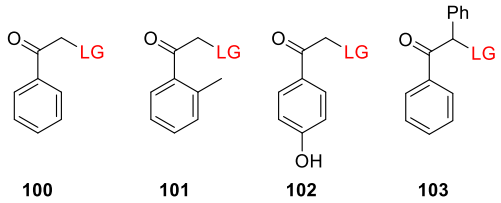

Figure 11. Arylcarbonylmethyl PPGs.

A phenacyl-based polyaromatic scaffold containing tetraphenylethylene[617] was used by Singh and co-workers to create a PPG with an aggregation-induced emission chromophore[618,619] by installing a pendant acetyl group on each aryl ring (**104**).[620] Sequential photorelease ($\lambda_{irr} \geq$ 410 nm) of four carboxylic acid moieties (chlorambucil, Cbl) from an organic nanoparticle formulation of **104** was demonstrated (Scheme 26).[620] The chemical yield and quantum efficiency of release depended strongly on the water fraction of the solution (f_w): there was no appreciable release below f_w = 85% but photorelease proceeded in chemical yields of up to 96% for f_w = 99% (Φ_r = 0.52). It was suggested that the photoreaction requires a restriction of intramolecular rotation (RIR)[621] that is imposed in the aggregated state. Singlet oxygen generation by both **104** as a nanoparticle and the photoproduct **105** (Φ_Δ

Scheme 26. Photorelease of Chlorambucil from a Phenacyl-type Tetraphenylethylene PPG (104) via a Photoreaction That Occurs Only in an Aggregated State[620]

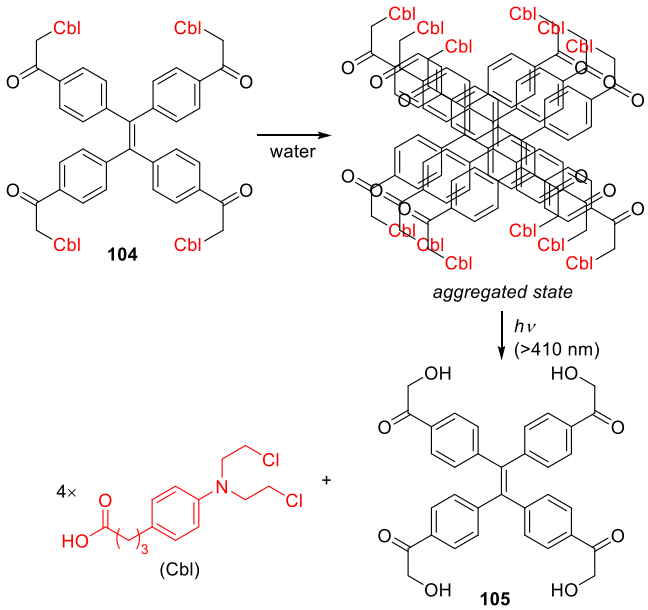

https://dx.doi.org/10.1021/acs.chemrev.0c00663
Chem. Rev. 2020, 120, 13135−13272

= 0.31 and 0.27, respectively) provided a complementary cell-killing mechanism whose effects were additive with those of the photoreleased drug in HeLa cells.[620]

The *p*-hydroxyphenacyl (pHP) group (**102**) is an established[612] UV-excitable (λ_{max}^{abs} ~ 275 nm), arylcarbonylmethyl-type[622] PPG with several favorable properties including high rate constants (10^7–10^8 s^{-1}), quantum yields (0.2–1.0), and chemical yields (typically 60–90%) for LG release, and the formation of a major biocompatible photoproduct (*p*-hydroxyphenylacetic acid) with a hypsochromically-shifted absorption spectrum. It has therefore found many applications in chemistry and biology.[22,622] The mechanism of the photoreaction has been studied extensively and previously reviewed.[22,622] Briefly, photoexcitation and subsequent ISC are thought to generate an intermediate[622−628] reminiscent of a Favorskii rearrangement[624−626] cyclopropanone intermediate (**106**) that either hydrolyzes to form *p*-hydroxyphenylacetic acid or undergoes decarbonylation to form *p*-hydroxybenzylalcohol (Scheme 27).[629,630]

Scheme 27. Photochemistry of 102 (pHP) as a PPG[613]

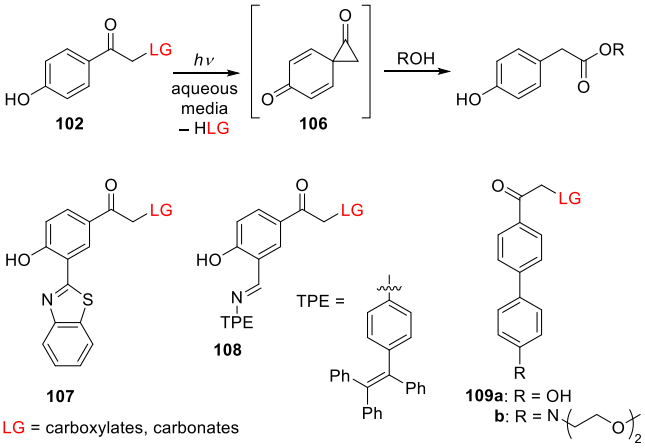

A bathochromic shift in the absorption spectrum of pHP was induced by extending its π-system at the 3-position (**107** and **108**, Scheme 12; λ_{max}^{abs} ≈ 380 nm in polar protic solvents). The nitrogen-containing substituents in **107** and **108** are positioned in a way that was expected to facilitate an excited-state intramolecular proton transfer (ESIPT) that would assist in the deprotonation of the *p*-hydroxyl group. Specifically, it was proposed that upon excitation to the singlet excited state, an ESIPT would occur,[631] followed by a transition to a triplet excited state, allowing the reaction to proceed as shown in Scheme 27.[631−633] The hydrophobicity of the tetraphenylethylene[617] moiety in **108** enabled the formation of organic nanoparticles[633] using a reprecipitation technique.[564] Visible light-mediated photorelease (λ_{irr} ≥ 410 nm) of a carboxylic acid[631,633] (chlorambucil) and a hydroxylamine[632] (an NO-donating NONOate;[634] see section 4.2) from **107** and **108** proceeded in high chemical yields, with the corresponding *p*-hydroxyphenylacetic acid derivative being the sole additional photoproduct[631,633] (Scheme 28). Uncaging was accompanied by a 70–100 nm blue-shift of the fluorescence emission spectrum, enabling real-time quantitative monitoring of the reaction's progress in live cultured cells.[631−633]

A two-step activation system was developed by capping the *p*-hydroxyl group in **110** with a 4-benzylboronic acid pinacol ester.[636] Phenylboronic acid and its esters react with hydrogen peroxide (H_2O_2) to form the corresponding phenol,[637−639] which in turn can lead to the release of a leaving group from the *p*-benzyl position via 1,6-elimination.[640−642] The photorelease of chlorambucil from **110** thus occurred only in the presence of H_2O_2 (Scheme 29).[636]

Goeldner and co-workers introduced donor–acceptor biphenyl pHP derivatives **109a** and **109b** (λ_{max}^{abs} = 313 and 369 nm, respectively; Scheme 27).[255] The photorelease of glutamate was more efficient from **109a** than from **109b** (Φ_r = 0.21 and 0.015, respectively). The 2P-uncaging cross section of glutamate liberation from **109a** was 0.21 GM at 740 nm,[255] which is comparable to the values previously observed for 2P release of diethyl phosphate and ATP from the parent pHP (0.5–1.1 GM at 550 nm).[643]

2.8. The 4-(*p*-Hydroxybenzylidene)-5-imidazolinone Group

Campbell and co-workers developed a photocleavable variant (PhoCl) of the photoconvertible fluorescent protein mMaple[644] that exploits the phototransformation of the protein's chromophore, a 4-(*p*-hydroxybenzylidene)-5-imidazolinone group formed autocatalytically from the tripeptide serine-tyrosine-glycine in the presence of oxygen.[645] This moiety is non-fluorescent in its neutral form (**111**; Scheme 30). Upon excitation with UV or violet (~400 nm) light, it is deprotonated to form an excited intermediate, **112***,[646,647] which undergoes irreversible β-elimination to liberate a carboxamide-containing peptide.[648] The photocleavage of

Scheme 28. Photouncaging of Chlorambucil and DEA NONOate from 107[631,632,635]

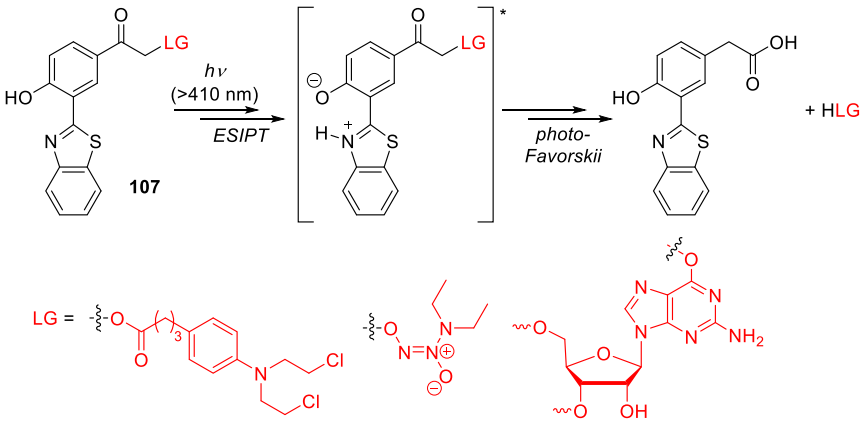

https://dx.doi.org/10.1021/acs.chemrev.0c00663
Chem. Rev. 2020, 120, 13135−13272

Scheme 29. Two-Step Sequential Uncaging of Chlorambucil (Cbl) from 110[636]

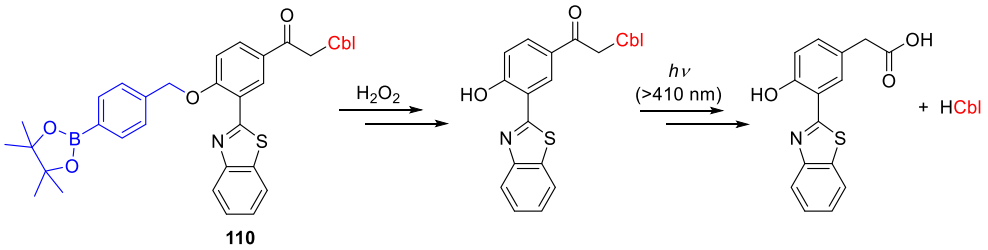

Scheme 30. Photocleavage of a Peptide in PhoCl[648]

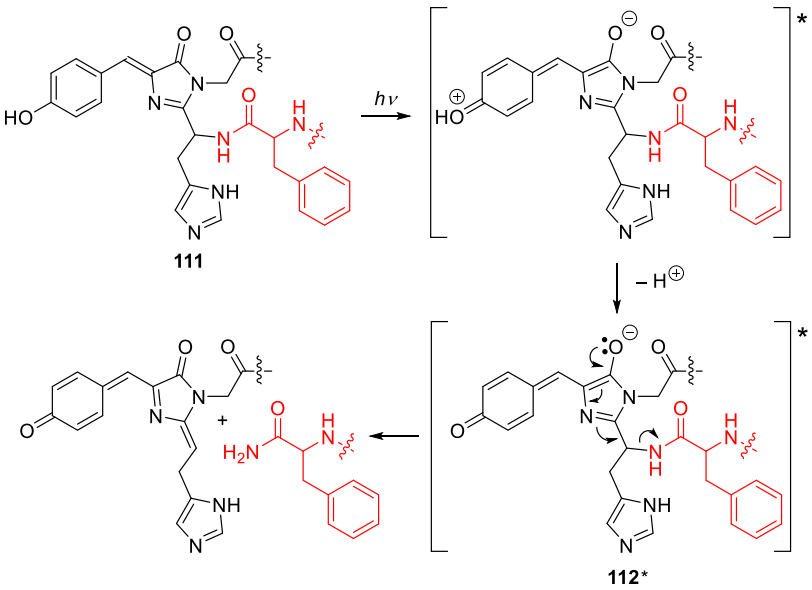

PhoCl has been used in several applications, for example, to control protein function[645,649−652] or modulate the mechanical properties of hydrogels.[653]

2.9. The Stilbene Group

Singh and co-workers harnessed the photocyclization of stilbenes to induce elimination of alcohol and carboxylic acid leaving groups from the 2-position of *E*-4-(*N*,*N*-dimethylamino)-4′-nitrostilbene[654] (DANS, **113**, Scheme 31). The light-mediated *E*−*Z* isomerization of stilbenes followed by a photochemically allowed conrotatory 6π-electrocyclization to form an *E*-dihydrophenanthrene is a well-studied process.[655−657] This intermediate tends to spontaneously undergo a subsequent oxidative dehydrogenation to yield a phenanthrene derivative.[656−658] However, in the absence of an oxidant, the dihydrophenanthrene intermediate may reversibly open to give the corresponding *Z*-stilbene; alternatively, if suitable substituents are present, hydrogen-shift processes may occur.[659,660] However, the presence of substituents such as methoxy[661−663] or halide[663,664] groups in the 2-position resulted in thermal non-oxidative elimination to form a phenanthrene derivative **114** (Scheme 31).

Scheme 31. Photorelease from *E*-4-(*N*,*N*-Diethylamino)-4′-nitrostilbene (DANS) PPG[654]

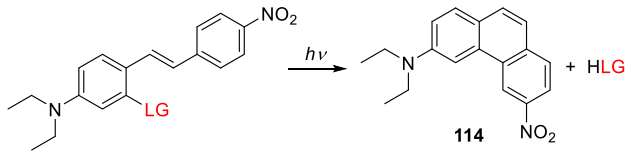

113: LG = carboxylates, alkoxides

The spectroscopic properties of **113** were solvent-dependent: on going from non-polar to polar solvents, λ^{abs} shifted from 410 to 430 nm, λ^{em}_{max} shifted from 502 to 720 nm, and there was a marked decrease in the fluorescence quantum yield (from 0.55 to <0.002), presumably because of the formation of a TICT state.[665] The molar absorption coefficient remained relatively constant (ε_{max} = 2.5−2.8 × 10^4 M^{-1} cm^{-1}). Photorelease of alcohols and carboxylic acids from **113** was demonstrated in hexane, acetonitrile, and water. In acetonitrile, the Φ_r was in the range of 0.10−0.14 for all tested leaving groups, and the chemical yields of photorelease were between 88 and 93%. On the basis of previous studies,[661,666−668] a photoreaction mechanism was proposed (Scheme 32) in which photoexcitation of **113** leads to a singlet excited state, allowing the *E*-stilbene to isomerize into its *Z*-isomer. The subsequent photoexcitation of the *Z*-isomer to its singlet state leads to a conrotatory 6π-electrocyclization to form *E*-dihydrophenanthrene. Orbital symmetry and energy considerations[669] suggest that the relative configuration of the dihydrophenanthrene product is *E*. Spontaneous re-aromatization of the *E*-dihydrophenanthrene by elimination then yields phenanthrene **114** and releases the leaving group. The fluorescence of the phenanthrene photoproduct (λ^{em} = 450 nm) was monitored to follow the reaction in real time. The photorelease of chlorambucil from **113** (λ_{irr} ≥ 410 nm), giving

https://dx.doi.org/10.1021/acs.chemrev.0c00663
Chem. Rev. 2020, 120, 13135−13272

Scheme 32. Proposed Release Mechanism from Stilbene Derivatives 113[654]

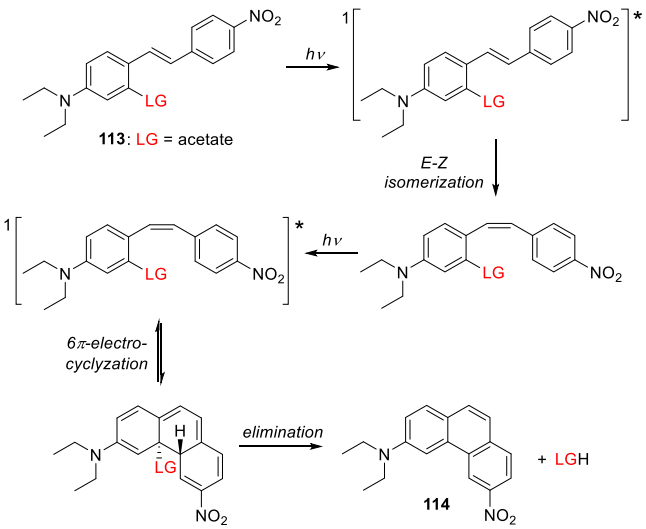

rise to light-dependent cytotoxicity, was observed in MCF-7 breast cancer cell lines.[654]

2.10. Quinones

The photoreduction of quinones has been studied extensively.[670−675] The reaction can proceed intermolecularly in the presence of a hydrogen donor[676−681] (e.g. an alcohol or amine) or intramolecularly via H atom transfer[682−689] from a favorably positioned C−H bond on a side-chain. Examples of hydrogen abstraction from the C−H bonds of amino[690−693] and sulfido[694,695] substituents are also known.

Iwamura and co-workers were the first to exploit the solvent-assisted intermolecular photoreduction of quinones to release leaving groups.[317] The (anthraquinon-2-yl)methyl derivative **115** (λ_{max}^{abs} = 325 nm), originally developed as a protecting group for carboxylic acids that could be removed with reducing agents,[696] efficiently released cyclic adenosine monophosphate (cAMP, Φ_r = 0.2) upon irradiation at 350 nm (Scheme 33).

Scheme 33. Photorelease of cAMP from an (Anthraquinon-2-yl)methyl PPG[317]

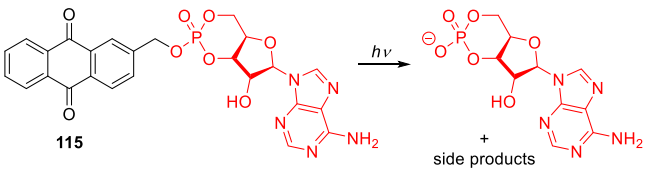

This photoreaction was proposed to involve two photochemical steps.[697−699] The first is quinone photoreduction via H atom transfer from the solvent in the triplet excited state to form a ketyl radical that gives rise to the final 1,4-dihydroxyanthraquinone derivative. The second is the photorelease of the leaving group from the resulting dihydroxyanthraquinone via a mechanism similar to that of photorelease from *o*-hydroxybenzyl PPGs.[570,700−702] Photochemical liberation (λ_{irr} = 350 nm) of alcohols,[322,697] carboxylates,[698,699] and ketones/aldehydes[703] from **115** (and derivatives thereof) proceeded with Φ_r = 0.03−0.12. However, the solvent-dependence of the intermolecular photoreduction of **115** may limit its usefulness.[322,697,698]

The presence of electron donors on the quinone core can give rise to broad charge-transfer absorption bands in the visible range.[704] Although 1,4-naphthoquinone and 1,4-anthraquinone appear to have more extended π-systems than 1,4-benzoquinone, a hypsochromic shift in λ_{max}^{abs} of ∼50 nm was observed for each fused benzene ring.[705] The photochemistry of naphthoquinone and anthraquinone derivatives resembles that of benzoquinones bearing aryl substituents. However, the presence of electron donors and acceptors on the distal rings causes substantial absorption spectrum shifts.[706] For example, the absorption of 1,4-benzoquinone (λ_{max}^{abs} = 281 nm) was significantly extended into the visible range (400−600 nm) upon introducing electron-donating substituents.[707−710] The magnitude of this shift correlated qualitatively with the magnitude of the HOMO and LUMO coefficients in the substituted quinone.[711]

Chen and Steinmetz used the photocyclization of 2-dialkylamino-1,4-benzoquinones[690,691,712,713] into benzoxazoline photoproducts to drive 1,4-elimination of carboxylates and phenolates bound through the 5-methylene group (**116**, Scheme 34).[714,715]

2-Pyrrolidino-1,4-benzoquinone **116a** exhibited a strong absorption band in the UV region and a weaker charge-transfer absorption band extending into the visible range (450−650 nm, ε = 1.9−2.6 × 10^3 M^{-1} cm^{-1}),[697,714−716] which is typical for amino-substituted quinones.[717,718] Carboxylates were released from **116a** (λ_{irr} = 458 or 532 nm) in chemical yields of 50−60% at full conversion. An additional photoproduct resulting from cycloaddition of an *o*-quinone methide photoproduct with **116a** was formed with a chemical yield of 36%. The photorelease yield increased to 89−92% upon irradiation in the presence of 3-(dimethylamino)cyclohexen-1-one (0.1 M) as an *o*-quinone methide trapping agent.[715] The quantum yield for the disappearance of **116a** was similar to that for carboxylate formation and was sensitive to solvent polarity (dropping from 0.10 in dichloromethane to ∼0.005 in water) but not to the presence of oxygen. Kalow and co-workers improved the quantum efficiency of release in water by changing the substituents around the side-chain γ-hydrogen:[697,716] replacing the pyrrolidine in **116a** with an isoindoline (**116c**) or tetrahydroisoquinoline (**116d**), in which the C−H bond is weaker, led to an 8- to 10-fold increase in Φ_r in water (5.8 × 10^{-3} vs 4.7 × 10^{-2} and 5.7 × 10^{-2}, respectively). The release efficiency correlated strongly with the leaving group pK_a,[714,715] suggesting that the thermal 1,4-elimination step is rate determining. Rate constants for the release of phenols in this step were in the range of k = 5.1−20.1 × 10^{-4} s^{-1},[715] in keeping with previous measurements.[719,720] The proposed photoreaction mechanism is shown in Scheme 35.

The sensitivity of the reaction's quantum yields to solvent polarity suggested the involvement of an intramolecular charge-transfer (ICT) excited state[679,721,722] (**117**) formed prior to excited-state hydrogen transfer from the pyrrolidino group to benzoquinone (**118**). The initial ICT excited state undergoes rapid back electron transfer (eT) to regenerate the ground state **116a**, competing with the hydrogen-transfer step. A possible immediate precursor to benzoxazoline **121** in the photocyclization is the ground-state zwitterionic species **119**.[684,685,723] In keeping with this hypothesis, photolysis of α-keto amides bearing leaving groups at the α-position yielded intermediates analogous to **119** that could cyclize with concomitant expulsion of a phenolate or carboxylate leaving group.[724] Alternatively, leaving groups can be liberated from

https://dx.doi.org/10.1021/acs.chemrev.0c00663
Chem. Rev. 2020, 120, 13135−13272

Scheme 34. (1,4-Benzoquinon-5-yl)methyl Derivatives 116 as PPGs[715]

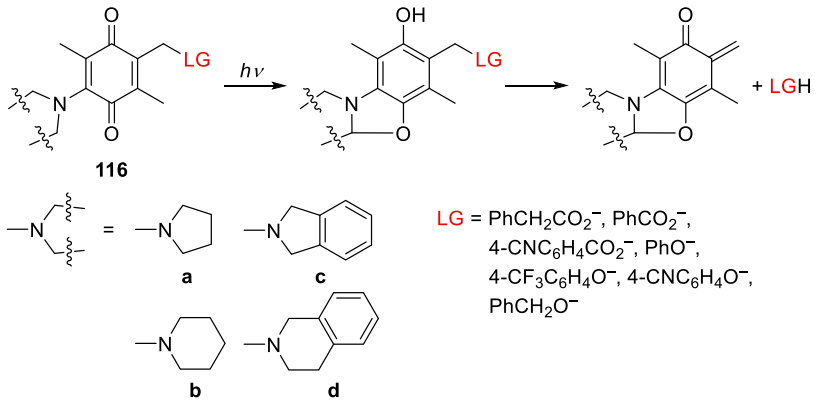

Scheme 35. Proposed Release Mechanism from a 2-Pyrrolidino-1,4-Benzoquinone PPG[715]

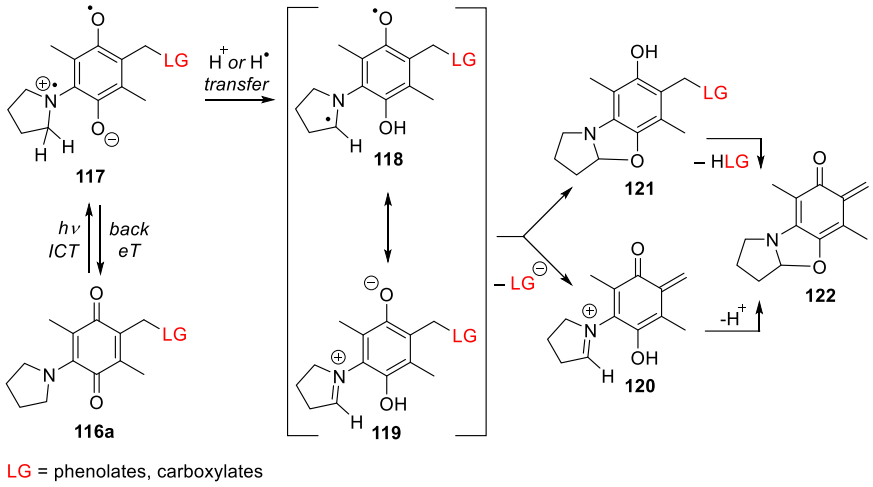

Scheme 36. Photochemistry of 1,4-Benzoquinone Trimethyl Lock PPGs[723]

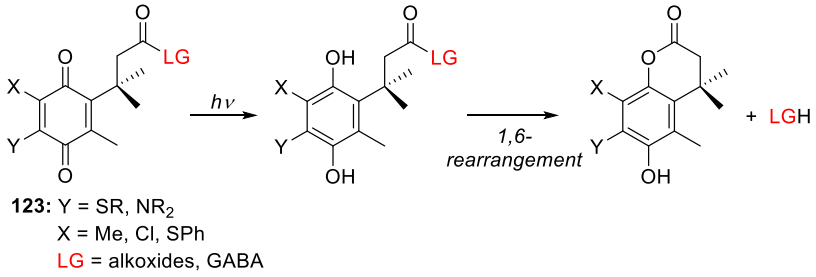

121 via deprotonation and subsequent 1,4-elimination.[725] Evidence for this pathway was obtained by isolating intermediate **121** (with LG = OPh) and showing that it could undergo elimination under sufficiently basic conditions.[715] Additionally, nanosecond laser flash photolysis experiments provided no evidence supporting direct elimination of carboxylates from **119**.[715] Chromatically orthogonal photorelease from **116d** (λ_{irr} = 626 nm) and a 2-nitrobenzyl derivative (λ_{irr} = 365 nm) has been demonstrated.[716]

Almutairi and co-workers overcame the inefficiency of photorelease from **116a** in water by formulating **116a**-caged drug systems (with drugs including paclitaxel, dexamethasone, and chlorambucil) by applying a microemulsion probe-sonication method to a mixture of poloxamer 407 (1% w/v) in water to form monodisperse water-dispersible nanoparticles with hydrophobic interiors. The particles had diameters of 108 ± 20 to 305 ± 101 nm, and their caged drug content ranged from 69 to 94 mol %.[726] Photolysis of these nanoparticles (λ_{irr} > 590 nm) using various mouse tissue filters released the caged drugs, and the progress of the photorelease process was monitored by co-loading fluorescent dyes (DiD and IR780) into the nanoparticles.[726]

Dougherty and co-workers[723,727] studied analogs of **123**, an *o*-hydroxydihydrocinnamic acid derivative with a conformationally restrictive "trimethyl lock" that enables thermal uncaging and photoreduction to release alcohols and amines via a 1,6-rearrangement mechanism[728−730] (Scheme 36). The UV-light-induced release of 2-nitrobenzyl-protected phenols to activate the trimethyl lock mechanism has been demonstrated previously.[223,731−733]

The broad visible absorption bands of **124**, **125** (400−600 nm), and **126** (350−500 nm; Figure 12) are indicative of

https://dx.doi.org/10.1021/acs.chemrev.0c00663
Chem. Rev. 2020, 120, 13135−13272

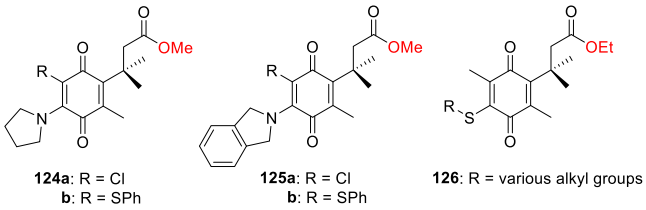

Figure 12. Structures of 2-amino- and 2-sulfido-substituted 1,4-benzoquinone trimethyl lock PPGs.

transitions to charge-transfer states.[707] The absorption maxima of **124** and **125** are bathochromically shifted relative to that of **116**,[715,716] which was attributed to the steric effect of the trimethyl lock moiety. Photolysis of **126** (λ_{irr} = 455 nm), **124** (455 nm), and **125** (565 nm) in polar protic solvents liberated caged alcohols in quantitative chemical yield.[723] Additionally, the orthogonal release of two different alcohols from **126** (R = Me) and **124a** was demonstrated (λ_{irr} = 455 and 565 nm, respectively),[727] and a mechanism for their photoreaction was proposed on the basis of studies on **126**[723] (Scheme 37).

Zwitterion **127** was proposed to be the penultimate intermediate in this photoreaction; it can undergo nucleophilic capture at the carbocationic center by the solvent or an intramolecular nucleophile to give **128** or **129**, respectively. Either of these species can then undergo trimethyl lock-facilitated ring closure to provide the final products in high chemical yield (>95%).[723] The singlet excited state, ^{1}**126***, has a charge-transfer character. In contrast to the photoreactions of typical benzoquinones, which undergo ISC to their triplet excited state with a near-unity quantum yield,[734] ^{1}**126*** predominantly undergoes nonemissive return to the ground state (with >90% efficiency). The triplet excited state ^{3}**126*** is formed with low efficiency (Φ_{ISC} = 1−5%) and was suggested to have a charge-transfer character based on a spin density calculation (DFT M06/6-311++G**),[723] in contrast to the n,π* triplet-excited state of simple benzoquinones.[735] It is still unclear whether the nonproductive triplet decay of ^{3}**126*** to **127** occurs directly or via ^{3}**127***. Formation of **127** can thus occur through both the singlet and triplet manifolds. For simple *S*-alkyl derivatives, product formation via the singlet pathway dominated, but the triplet pathway contributed more substantially in the case of *S*-benzyl analogs.[723] Although the triplet excited state is formed with low efficiency, it forms the product more efficiently than the singlet excited state.

The fluorophore 4-methylumbelliferone and the neurotransmitter GABA were both successfully photoreleased from derivatives of **126** under physiological conditions.[723] Additionally, Forsythe and co-workers[736] showed that *S*-substituted analogs of **126** can be formed in water under slightly basic conditions via a thio-bromo coupling.[737,738] Dendrimeric monomers with bromo-substituted 1,4-benzoquinone trimethyl lock moieties (**132**) were reported to react with dendrimeric monomers bearing sulfhydryl end groups (**133**) to form a polymeric network with sulfido-substituted 1,4-benzoquinone trimethyl lock PPGs incorporated into its backbone (Scheme 38).[736] Encapsulation of cells (mouse fibroblast L929, human foreskin fibroblast, and human mesenchymal stem cells) in this polymeric network and their subsequent release by photodegradation of the polymer (λ_{irr} > 420 nm) were demonstrated, with the cells retaining high viability throughout the process.[736]

Scheme 37. Proposed Uncaging Mechanism of Photoinduced Quinone Trimethyl Lock PPGs[723a]

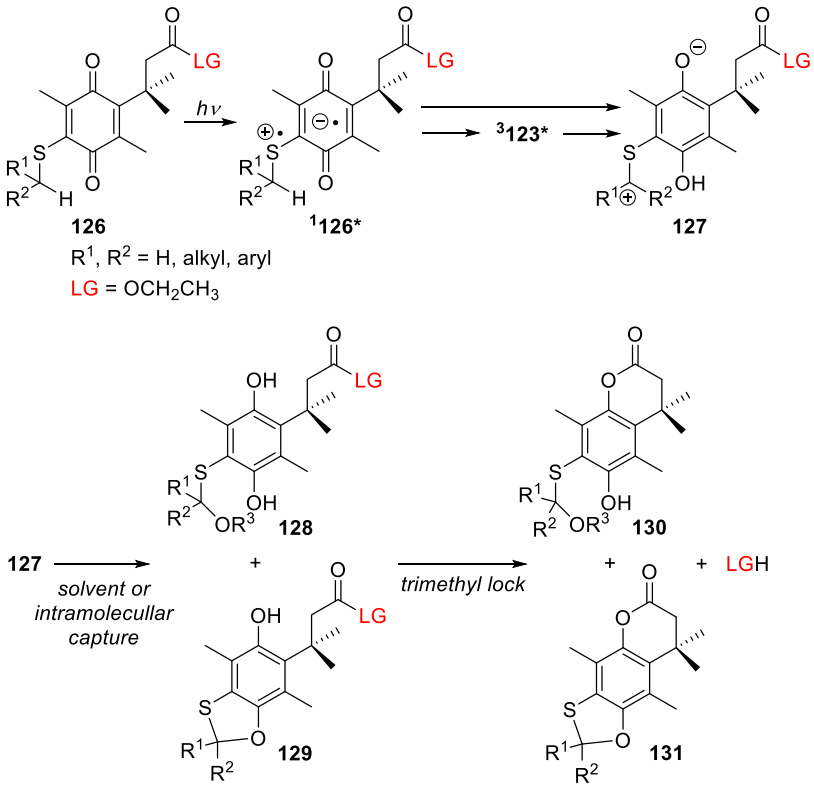

[a]Photochemical transformations are shown for R^1 = R^2 = H or Ph.

https://dx.doi.org/10.1021/acs.chemrev.0c00663
Chem. Rev. 2020, 120, 13135−13272

Scheme 38. Photocleavable Polymer Based on a Sulfido-Group-Substituted 1,4-Benzoquinone Trimethyl Lock PPG[736]

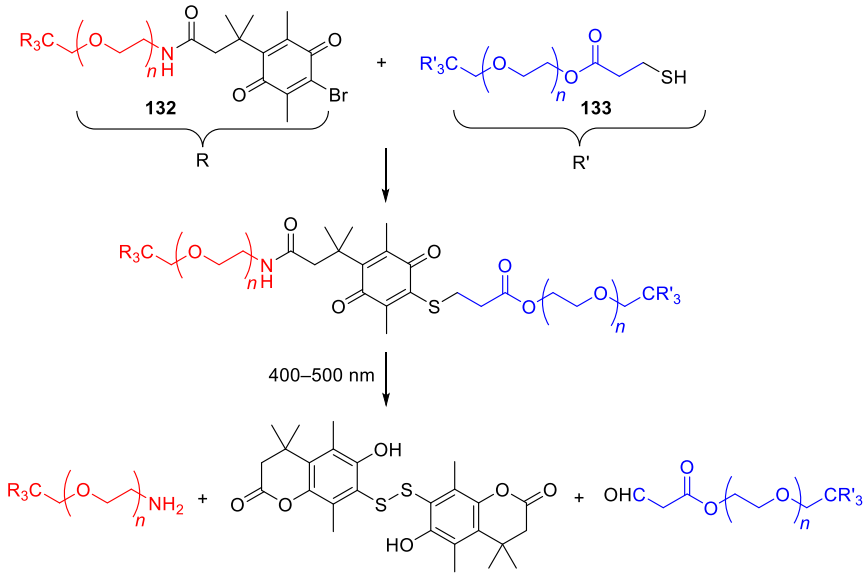

The 2-hydroxycinnamyl moiety (**134**, Scheme 39) was first utilized as a PPG by Porter and co-workers to achieve photochemical activation of thrombin.[739,740] This system undergoes an initial photoinduced isomerization followed by cyclization to form a coumarin derivative, causing the release of caged substrates such as alcohols.[741−750] The cyclization rates of 2-hydroxycinnamyl esters or amides approached those of the trimethyl lock system (k = 0.03−50 × 10^5 s^{-1}).[723,728,729,751−754] The absorption maxima of **134** could be further bathochromically shifted (up to λ_{max}^{abs} = 394 nm) by introducing electron-donating substituents on the phenyl ring[743,755,756] or extending the system's π-conjugation.[750,757] A small set of 2-hydroxycinnamic derivatives was synthesized to study and improve the 2P-absorption-mediated release process.[755,756,758]

Scheme 39. Photochemistry of *o*-Hydroxycinnamic Derivatives[740]

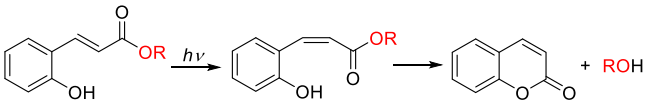

Dougherty and co-workers incorporated conformationally locked *Z*-cinnamyl esters (with a *cis*-alkenyl lock[759]) into amino-substituted 1,4-benzoquinones **135** and **136**, and 1,4-naphthoquinone **137** (Figure 13), enabling visible-light mediated quinone photoreduction to serve as an intramolecular cyclization initiator and leaving-group release trigger (Scheme 40).[760]

Amino-substituted quinones **135**−**137** have broad charge-transfer absorption bands in the range of 495−535 nm (ε_{max} = 2.9−3.6 × 10^3 M^{-1} cm^{-1}). Upon irradiation at 565 nm, methanol or ethanol was liberated with Φ_r = 0.03−0.04 in quantitative chemical yield.[760] Solvent effects on the photoreduction[715] and cyclization[759] processes were observed as expected; in polar protic solvents, photoreduction was less efficient and cyclization was more efficient, whereas the opposite was true in non-polar aprotic solvents.[760]

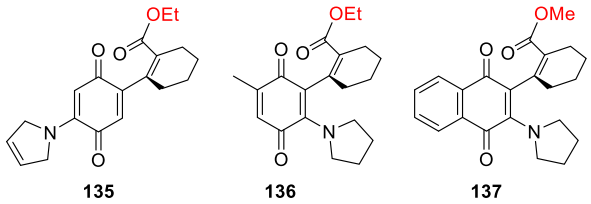

Figure 13. Structures of amino-substituted 1,4-benzo- and naphthoquinone *cis*-alkenyl lock PPGs.

A different mechanism involving photoenolization[609,761] followed by heterolytic elimination[230,231,233,762] was demonstrated by Kamdzhilov and Wirz[232] for substituted 5-(ethylene-2-yl)-1,4-naphthoquinone **138** (Scheme 41), which absorbs below 405 nm. This compound released HBr and diethyl phosphate upon irradiation at 365 nm (Φ_r = 0.35 and 0.70, respectively) in a neutral aqueous solution, but a poorer leaving group (acetic acid) was released less efficiently (Φ_r < 0.01). Unfortunately, the sensitivity of this photoreaction to acids and the instability of naphthoquinones toward bases limit the use of this photochemical protecting group.

2.11. Xanthene and Pyronin Groups

Wirz, Klán, and co-workers showed that acetate and diethyl phosphate can be released from a 1:1 complex of **139** with 2,3-dichloro-5,6-dicyano-1,4-benzoquinone (DDQ) upon irradiation at >500 nm with Φ_r = 0.3−2.4 × 10^{-2} (Scheme 42).[763] This relatively low photorelease quantum yield was compensated for by a large molar absorption coefficient at the irradiation wavelength ($\varepsilon \approx 4 \times 10^4$ M^{-1} cm^{-1}), resulting in an uncaging cross section $\Phi_r\varepsilon(\lambda_{irr})$ of ∼100 M^{-1} cm^{-1}.[763] Efforts to synthesize **139** by alternative methods or to separate this DDQ complex were unsuccessful.[11,763] It was assumed that the primary photoproduct in aqueous solutions, a *meso*-methylhydroxy derivative formed from the corresponding cationic intermediate, is further oxidized by DDQ to give 6-hydroxy-3-oxo-3*H*-xanthene-9-carboxylic acid (**140**) as the major photoproduct. HMO calculations of the xanthene frontier molecular orbitals revealed that the HOMO and LUMO are disjoint at the *meso*-position, resulting in an increase in its negative charge upon HOMO−LUMO excitation. This behavior was linked to

https://dx.doi.org/10.1021/acs.chemrev.0c00663
Chem. Rev. 2020, 120, 13135−13272

Scheme 40. Photochemistry of 1,4-Benzoquinone *cis*-Alkenyl Lock PPG 18[760]

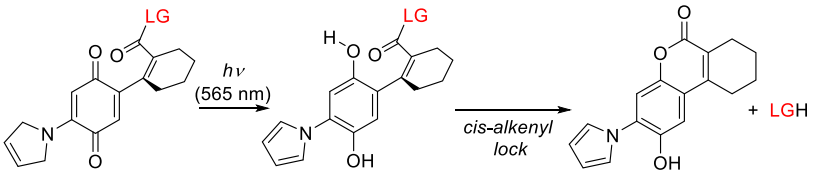

Scheme 41. Photochemistry of 5-(Ethylene-2-yl)-1,4-naphthoquinone PPG[232]

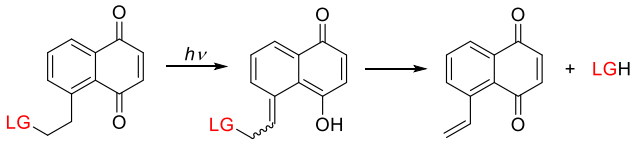

LG = Br, dialkylphosphate, carboxylate

Scheme 42. Photochemistry of Xanthene PPG 139[763] **and Schematic Representation of the HOMO and LUMO of Its π-System**[11]

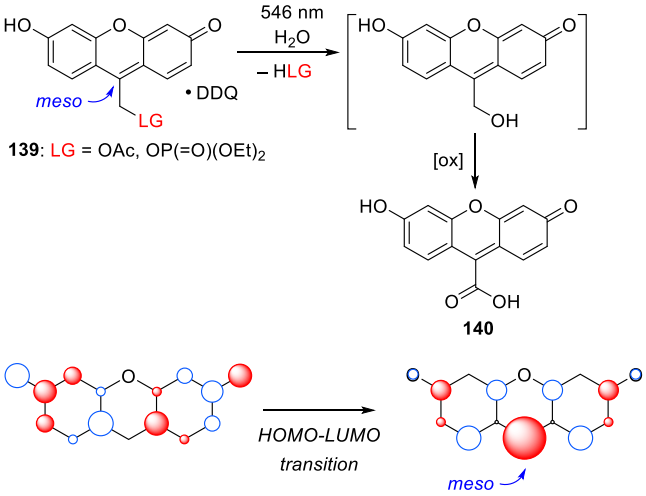

specific photoreactivity such as the extrusion of leaving groups (Scheme 42)[11] (see also section 2.12).

A different approach involved placing a 1,3-dithian-2-yl substituent at the *meso*-position of pyronin **141** (Scheme 43).[764] The resulting compound exhibited strong absorption (λ_{max}^{abs} = 584 nm) and emission (λ_{max}^{F} = 607 nm) bands in aqueous solution, and irradiation in its major absorption band ($\Phi_r = 3 \times 10^{-4}$) gave a stable photoproduct that absorbed at 382 nm and emitted at 448 nm. It was proposed that direct thiolate release could explain the observed *meso* C−C bond cleavage in the pyronin chromophore.[764] Recently, Klán, Roithová, and co-workers subsequently showed that transformation of **141** is a multi-photon multi-step process. Many intermediates in this process were identified and their interrelationships were clarified using steady-state and time-resolved optical spectroscopy, mass spectrometry, and NMR spectroscopy.[765] Scheme 43 presents a simplified mechanism for this complex reaction, which involves at least three light-initiated steps. A different mechanism involving photooxidative cleavage by singlet oxygen was observed for the photolysis of *exo*-alkylidene xanthenes.[766]

Scheme 43. Photochemistry of Pyronin 141[764,765]

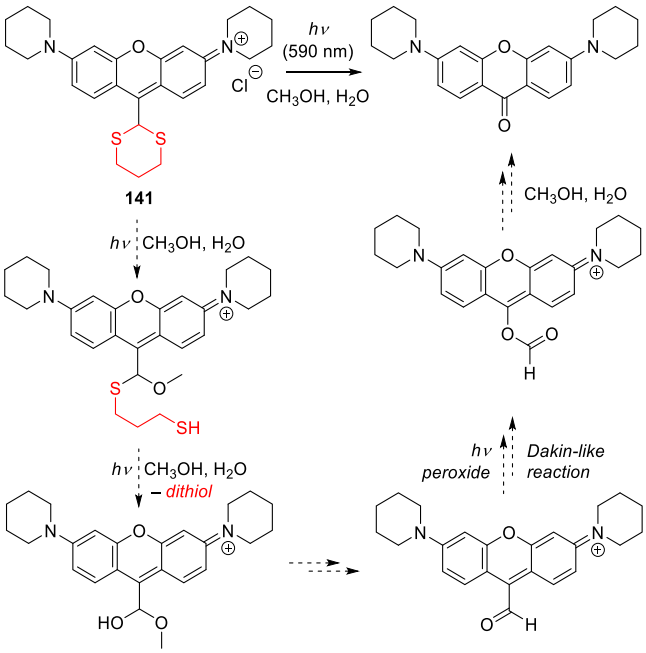

Jo and co-workers recently demonstrated the release of 10-*N*-carbamoyl substituents from a 3,7-bis(dimethylamino)-10*H*-phenothiazine chromophore upon excitation with red light in aqueous solution (**142**, Scheme 44).[767] The side product of this transformation is the fluorescent indicator methylene blue. Because 3,7-bis(dimethylamino)-10*H*-phenothiazine is a UV-light absorbing chromophore,[768] its excitation at 660 nm was unexpected. Although no mechanistic details were provided in the report, the authors suggested that the reaction starts with the heterolytic cleavage of the N−C(O) bond upon irradiation.

2.12. BODIPY Groups

4,4-Difluoro-4-bora-3a,4a-diaza-*s*-indacene (BODIPY) and its derivatives are highly fluorescent dyes that are widely used in chemistry[769−773] and biology.[774−778] Their favorable spectroscopic properties are mainly due to their relatively compact, rigid, and planar structures, which make the potential energy surfaces of their S_0 and S_1 states very similar. Consequently, narrow Gaussian-shaped absorption and emission bands are typically observed for their lowest energy transition.[779,780] These compounds have high Φ_{HF} values (typically >0.5) because of inefficient nonradiative decay and ISC.[781,782] Simple BODIPY chromophores typically have two narrow absorption bands in the visible range ($\lambda_{max} \approx 490-540$ nm, $\varepsilon \approx 3-9 \times 10^4$ M^{-1} cm^{-1}): an intense 0−0 band due to the S_0-S_1 transition, and a shoulder attributed to the 0−1 vibrational transition.[783−787] The BODIPY scaffold tends to resist photobleaching[781,788,789] and degradation by acids/bases,[790,791] but it is highly amenable to synthetic trans-

https://dx.doi.org/10.1021/acs.chemrev.0c00663
Chem. Rev. 2020, 120, 13135−13272

Scheme 44. Photorelease from 10*H*-Phenothiazine Derivatives[767]

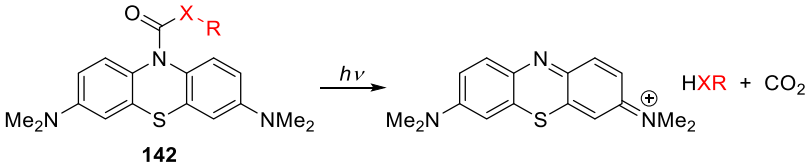

formations that modulate its spectral properties.[779,780,792,793] This section focuses on the different strategies reported to date utilizing the BODIPY chromophore as a photoreleasing system (Figure 14).

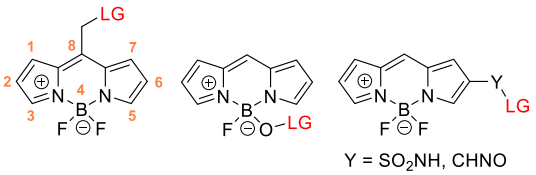

Figure 14. Structures of BODIPY PPGs with LGs at different positions.

The groups of Winter[795] and Weinstain[794] independently studied the release of leaving groups from *meso*-methyl BODIPY derivatives upon photoexcitation with green light (a general structure **143** is shown in Scheme 45). The basis for

Scheme 45. Photorelease of LG from *meso*-Methyl BODIPY Derivatives,[794] and Schematic Representation of the HOMO and LUMO of the BODIPY π-System (BF_2 Is Omitted)[11]

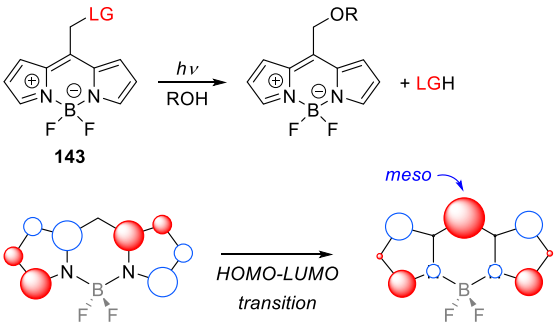

this photoreactivity can be traced to the properties of the chromophore's *meso* position. Heterolytic photodissociation to give a *meso*-methyl carbocation is favored when electronic excitation to the lowest singlet-excited state involves a substantial transfer of electron density to the sp^2 carbon atom of a chromophore bearing a LG in the α-position such that the antibonding σ* orbital is mixed with the chromophore's LUMO.[11] In such cases, the promotion of an electron from the HOMO to the LUMO weakens the C−LG bond, facilitating heterolytic dissociation of the leaving group. This mechanism is responsible for, among other things, Zimmerman's *meta*-effect in the photosolvolysis of methoxybenzyl acetates[556] and the photochemical reactivity of coumarinyl-4-methyl PPGs (section 2.2).[22,278] HMO calculations suggested that BODIPY also reacts in this way because its HOMO and LUMO are disjoint at the *meso* position (Scheme 45), and the negative charge at this position increases upon excitation,[11,780] as also predicted for xanthene chromophores (Scheme 42). *meso*-Methyl carbocations were reported to have a low-lying excited state with a vertical S_0−S_1 energy gap of 8−13 kcal mol^{-1} (TD-DFT), suggesting a near-degenerate diradical configuration.[795] Such low-energy diradicals can have a close-lying conical intersection between the closed-shell singlet and singlet diradical forms.[796] The photoheterolysis of C−LG bonds to generate ion pairs was shown to be favored when the ion pair has access to a nearby productive conical intersection that provides an efficient channel for the excited state of the precursor to decay to the ground-state ion pair.[796,797]

The synthesis of *meso*-methyl functionalized BODIPYs generally follows known routes,[481,779,780,792,793] and the attachment of a leaving group is achieved by one of (a) incorporation during BODIPY core synthesis,[795,798−801] (b) displacement of a formerly installed good leaving group,[295,798,801−803] (c) utilizing a *meso*-methylhydroxy derivative as a nucleophile to attack a pre-activated form of the leaving group,[795,804−808] or (d) modifying a previously installed carbonic acid derivative[794,805,809−811] (Scheme 46). The latter process was shown to compete with an undesired direct attack at the *meso*-methyl position.[809]

Scheme 46. Synthetic Pathways to *meso*-Methyl BODIPY PPGs

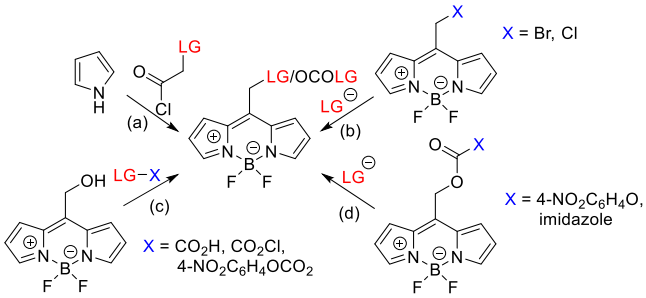

meso-Methyl BODIPY PPGs such as **144**, **145**, and **146** (Figure 15) typically have absorption bands with λ_{max}^{abs} at 490−545 nm (Figure 16), although a family of π-extended *meso*-methyl BODIPYs with λ_{max}^{abs} at 586−693 nm was also reported (**147**; Figure 16).[807,812] The absorption spectra of representative *meso*-methyl BODIPY PPGs discussed in this section are shown in Figure 16.

The photorelease of diverse functional groups, including primary and secondary amines[794,805,809,810,812] (as carbamates), carboxylic acids,[295,794,795,798,802,804,806−808] alcohols[794,798,805] (as carbonic acid esters[794] or ethers[798,801,805]), halogens,[798] hydroxylamines,[803] thiocarbamic acid,[799] thioacetic acid,[798] and thiols[800] (Figure 15) from BODIPY-based PPGs, has been reported. The liberation efficiency of LGs correlated well with the pK_a of their conjugate acids,[794,798,809] and the photoreaction quantum efficiency of unsubstituted BODIPYs (other

https://dx.doi.org/10.1021/acs.chemrev.0c00663
Chem. Rev. 2020, 120, 13135−13272

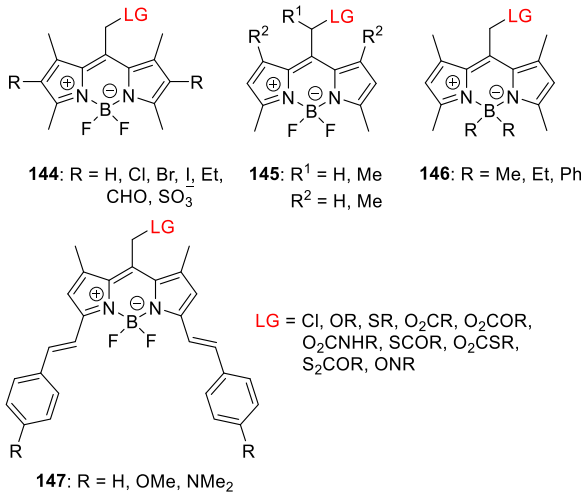

Figure 15. Structures of *meso*-methyl BODIPY PPGs.

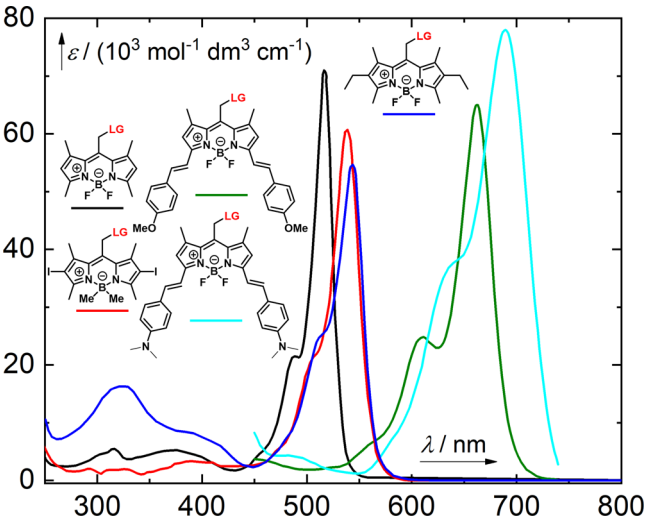

Figure 16. Absorption spectra of selected *meso*-methyl BODIPY PPGs. Black line, 1,3,5,7-tetramethyl derivative (LG = acetate);[795] blue line, a 2,6-diethyl-1,3,5,7-tetramethyl derivative (LG = (4-nitrophenyl)carbamate);[794] red line, a 2,6-diiodo-*B*-dimethyl derivative (LG = acetate);[798] green line, a bis(*p*-methoxystyryl) derivative (LG = benzoate);[807] cyan line, a bis(*p*-dimethylaminostyryl) derivative (LG = benzoate).[807]

than 1,3,5,7-tetramethyl derivatives) was moderate to low. The photoreaction quantum yields determined in aerated protic solvents were around half those measured in degassed solutions.[798] The typically small values of Φ_r for these systems (Φ_r^{aer} = 1−800 × 10^{-4}) are compensated by high molar absorption coefficients (typically, ε_{max} = 3−7 × 10^4 M^{-1} cm^{-1}), giving rise to uncaging cross sections, $\Phi_r\varepsilon(\lambda_{irr})$, of 1−100 M^{-1} cm^{-1}, that are similar in magnitude to those of traditional UV-absorbing PPGs.[10] The major side-photoproducts were identified as solvent-captured *meso*-methyl BODIPY derivatives (Scheme 45).[719,794,795,798,803,808] These compounds (e.g., *meso*-methyl ethers formed when using methanol as the solvent) absorb at very similar wavelengths to the original PPG and may thus act as internal optical filters, but they are eventually degraded upon extensive irradiation.[798]

Klán, Weinstain, Winter, and co-workers showed that in addition to the nature of the LG, the efficiency of photorelease from BODIPY chromophores depended on their substitution: halogen substituents at the 2,6-positions increased both the reaction efficiency and Φ_{ISC},[795,798] with a substituent heavy-atom effect that decreased in the order I > Br > Cl > H.[813,814] However, electronegative halogen substituents increased the electrophilicity of the *meso*-methyl position, making it prone to nucleophilic attacks that caused LG liberation even in the dark.[809] Stronger EWGs such as aldehydes or sulfonates in the 2,6-positions substantially raised the barrier to C−O bond heterolysis on the triplet surface of **144** and thus impeded photorelease.[811] For example, the calculated C−O bond (heterolytic) dissociation energies for derivatives of **144** bearing 2,6-disulfonate, -dihydrogen, and -diethyl substituents were 18.9, 15.7, and 13.5 kcal mol^{-1}, respectively, with photouncaging quantum yields of 0, 0.6 × 10^{-4} and 3.9 × 10^{-4}, respectively.[811] The absence of the 1,7-methyl groups reduced Φ_r by a factor of ∼1.5, probably due to a reduced electron density in the BODIPY core and thus a reduced capacity to stabilize the putative cationic diradical intermediate.[795,798] In addition, dialkylborano analogs had significantly higher Φ_r values than their BF_2 counterparts (up to 30-fold).[798,801,807,812] These substituent effects were additive: the Φ_r of **149** (Figure 16) was 100-times that of **148** (Figure 17).[798]

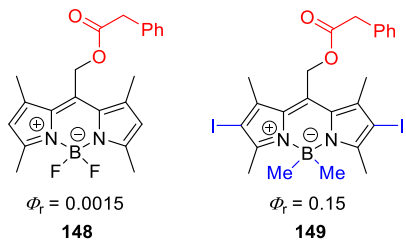

Figure 17. Structures and quantum efficiencies of BODIPY PPGs **148** and **149**, the latter of which combines the 2,6-diiodo and BMe_2 modifications.

Winter and co-workers recently studied conformationally-restrained π-extended boron-methylated *meso*-methyl BODIPYs that absorb light at around 700 nm to liberate acetic acid with Φ_r = 0.018−0.037. These efficiencies are ∼50-times those reported for the comparable non-restrained **147** derivatives.[815] It was suggested that conformational restriction inhibited competing excited state decay pathways such as internal conversion, leading to higher photorelease quantum yields. The Jabłoński diagram describing the photochemistry of **150** shown in Figure 18 indicates that photorelease proceeds from both the singlet and triplet excited states.[798] The increase in quantum efficiency correlated with enhanced ISC,[795,798] which can reduce competition from radiative (Φ_F) and nonradiative (Φ_{NR}) processes.[798] It should be noted that the reaction efficiencies are relatively low for mediocre LGs such as carboxylates, presumably because of ion-pair recombination and nonradiative decay from the triplet excited state, which do not occur during photolysis of good LGs such as Cl^-.[798]

Photorelease from *meso*-methyl BODIPYs has been used in various biological and synthetic applications. For example, the uncaging of signaling molecules including the gasotransmitter H_2S (see also section 4.3),[799] histamine, and the neurotransmitter dopamine,[794,811,812] has been demonstrated in cellular environments. Sortino and co-workers reported that light-dependent NO-induced vasodilatation of rat aorta can be achieved by uncaging the NO donor (see also section 4.2) *N*-nitroso-*N*-phenylhydroxylamine.[803] Weinstain and co-workers

https://dx.doi.org/10.1021/acs.chemrev.0c00663
Chem. Rev. 2020, 120, 13135−13272

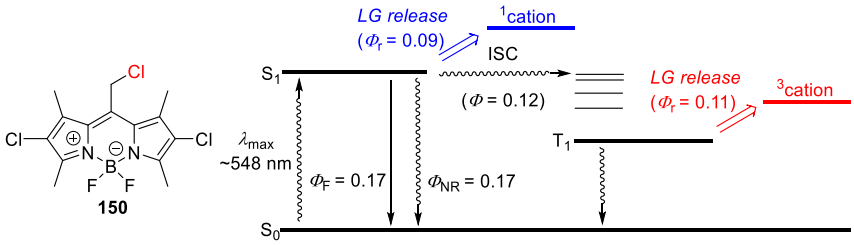

Figure 18. Jabłoński diagram of the photochemistry of **150**.[798]

introduced a protecting-group-free, late-stage functionalization of *meso*-methyl BODIPYs that enabled their targeting to specific cellular organelles[805] and the development of water-soluble derivatives.[811] Other notable applications include the selective photorelease of the protonophore 2,4-dinitrophenol in mitochondria and the protein synthesis inhibitor puromycin in the endoplasmic reticulum,[805] as well as the light-dependent delivery of cytotoxic molecules including chlorambucil and a cathepsin B inhibitor (CA-074[816]) to cells.[804,806] In both of the latter cases, the observed cytotoxicity was partly due to photosensitized $^1O_2$ generation by the BODIPY PPG.[804,806] Sebastián and co-workers used a *meso*-methyl BODIPY-caged diethylamine as an organic light-responsive nucleophilic cyanoacrylate initiator capable of fast on-demand photocuring of commercial formulations of various cyanoacrylates including biologically-relevant long alkyl chain monomers.[810] Klán and co-workers reported that controlled photorelease of alkynoic acids was followed by efficient decarboxylation, giving terminal alkynes that could subsequently undergo Cu^I-catalyzed azide/alkyne cycloaddition reactions.[802] Similarly, Truong and co-workers developed a phototriggered thiol-propiolate addition that is initiated by uncaging methyl-3-mercaptopropionate.[719] The utility of this photochemical ligation strategy was demonstrated by fabricating hydrogels with specific architectures, photo-immobilization of biomacromolecules, and live-cell encapsulation within a hydrogel scaffold.[800]

The BODIPY boron center has also been identified as a photoreactive center. Urano, Nagano, and co-workers showed that the B−O bond in 4-aryloxy BODIPYs can be photolyzed (λ_{irr} = 475−490 nm) to release phenols (Scheme 47).[817,818] The absorption/emission wavelengths (λ^{abs} = 495−525; λ^{em} = 506−541 nm) and molar absorption coefficients (ε_{max} = 6.2−9.8 × 10^4 M^{-1} cm^{-1}) of derivatives **151** were only slightly affected by modulation of the HOMO/LUMO energy gap. However, their fluorescence quantum yields, Φ_F, decreased dramatically upon raising the HOMO energy of the aryl group

Scheme 47. Photorelease of Phenols by B−O Photolysis[818]

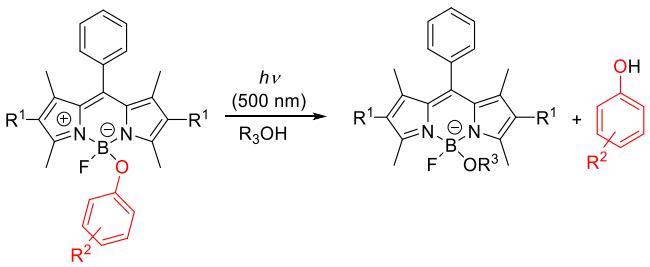

151: R^1 = Et, H, Cl, CO_2R, CO_2−
R^2 = 4-CO_2Me, 4-CH_2CO_2Me, 4-Me, 4-OMe, 4-NO_2, 4-CN, 3-NMe_2, 3,4-di-OMe
R^3 = H, Me

or reducing the LUMO energy of the BODIPY core.[817,818] This effect on Φ_F was attributed to electron transfer (eT) from the adjacent aryl group to the BODIPY core.[819] The release quantum efficiencies were generally inversely correlated with Φ_F, suggesting that the photoreaction proceeds via a competing PeT process in which B−O bond solvolysis is preceded by the formation of a charge-separated intermediate with a cationic aryl group radical and an anionic radical BODIPY core. Derivatives with a high calculated PeT driving force[820] had low uncaging efficiencies (Φ_r = 0.3−2 × 10^{-3}). The same was true when the calculated PeT driving force was low (Φ_r = 0.7−2.6 × 10^{-3}), presumably because fast reverse-electron transfer from a charge-separated intermediate[821] competes with uncaging. Derivatives with moderate predicted PeT driving forces thus had the highest uncaging efficiencies (Φ_r = 1.4−5.4 × 10^{-3}).[817,818] Photouncaging of phenols from π-extended BODIPY analogs at λ_{irr} = ∼620 nm was demonstrated, albeit with very low quantum efficiencies (Φ_r = 1.5 × 10^{-7}−7.4 × 10^{-5}).[818] This capability was used to achieve intracellular photorelease of the transient receptor potential cation channel V1 (TRPV1) agonist capsaicin in cultured HEK293 cells transiently transfected with TRPV1, leading to the induction of light- and ligand-dependent Ca^{2+} uptake.[817]

The range of functionalities releasable via B−O bond photocleavage was expanded[818,822−824] by introducing a benzyloxycarbonyl linker that undergoes a spontaneous 1,6-elimination to release a leaving group from its benzyl position after the phenol moiety is liberated (Scheme 48).[825] For example, a carboxylic acid derivative of the fluoroquinolone antibiotic levofloxacin was directly photoreleased (λ_{irr} = 470 nm) from ester **152** in 31% chemical yield.[822] As a result, this ester exhibited light-dependent bactericidal effects in *E. coli* and the Gram-positive *S. aureus*. The terminal primary amine of biogenic histamine was similarly caged through a carbamate bond (**153a** and **153b**), and its subsequent photorelease (λ_{irr} = ∼480 nm) was achieved in 40% chemical yield with Φ_r = 3−3.9 × 10^{-4}.[818] Photoexcitation (λ_{irr} = 488 nm using an argon laser) of the cell-impermeable **153b** in HeLa cells induced light- and H_1-receptor-dependent Ca^{2+} oscillations. The photolysis of carbamothioate **154** (λ_{irr} = 470 nm) also resulted in the release of a free amine;[823] the carbamothioic acid subsequently underwent thermal B−O bond cleavage (k = 0.02 min^{-1}, pH 7.4) to release carbonyl sulfide (COS) and a free amine.[823,826] COS is hydrolyzed into CO_2 and H_2S (spontaneously or under carbonic anhydrase catalysis[827]), making it a useful H_2S generator for research with potential therapeutic applications (see also section 4.3).[799,828−830]

Smith, Winter, and co-workers developed **155** as a photoswitchable probe[831] for single-molecule localization spectroscopy,[832] demonstrating that the B−C bond is also amenable to photocleavage. Photoexcitation of **155** (λ_{irr} = 488

https://dx.doi.org/10.1021/acs.chemrev.0c00663
Chem. Rev. 2020, 120, 13135−13272

Scheme 48. Expansion of Chemical Functionalities Amenable to Uncaging from BODIPYs via B−O Photolysis Using a Self-Immolative Linker[818,822−824]

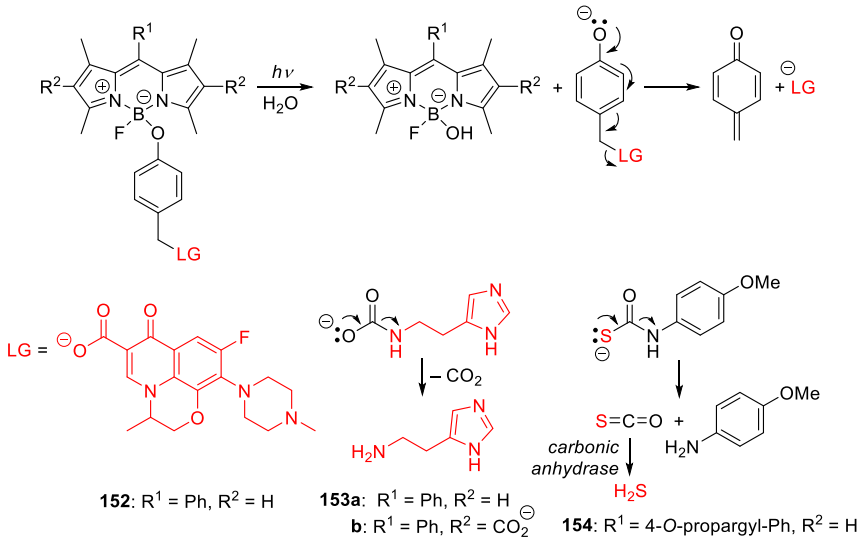

or 532 nm) caused the cleavage of its two *B*−alkyl groups and their subsequent replacement by solvent adducts (**156**), which was accompanied by a ∼6-fold increase in Φ_F (from 0.15 to 0.96; Scheme 49). Conjugation of **155** with paclitaxel via its

Scheme 49. Photoswitchable BODIPY Probe Based on B−C Bond Photocleavage[831]

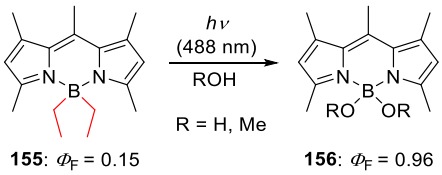

styryl group enabled super-resolution imaging of microtubules in live HeLa cells with an average full-width-at-half maximum (FWHM) diameter of 94 ± 10 nm.[831] The photoactivation of **155** required only a single laser wavelength and relatively low laser power.[833−835]

A different approach to using BODIPY scaffolds for photorelease is to introduce photoreactive functional groups in the 2,6-positions (**157**).[836,837] This approach is exemplified by the photorelease of amines from sulfonamide groups in the BODIPY 2,6-positions (λ_{irr} = 470 ± 20 nm, chemical yields = 45−50%, Φ_r = 0.022−0.11).[836] These photoreactions were insensitive to the presence of oxygen, required a carboxylic functional group in the α-position of the amide chain, and exhibited pH-dependent rates, proceeding less efficiently under acidic conditions. These observations are consistent with the known photochemistry of arylsulfonamides,[838] which have been studied extensively in the context of their use as potential PPGs[839−842] and due to their prevalence in pharmaceuticals.[843−845] The proposed photoreaction mechanism involves a sequence of electron-transfer, decarboxylation, hydrogen-transfer, and fragmentation steps that are shown in Scheme 50.

The key steps in this reaction are electron transfer from the donor (carboxylate) to the acceptor (sulfonamide)[839,840,846] and the subsequent formation of a charge-separated state.[845,846] In the case of **157**, the ability of carboxylates to transfer a single electron to the excited BODIPY is yet to be established, but a similar process was proposed for the closely related compounds **225a,b** (section 4.1.1).[847] The formation of a charge-separated state was supported by the need for the carboxylate and sulfonamide groups to be in close proximity.[836,848] Decarboxylation occurs from this state[842,849] and is followed by a radical reaction that can proceed through competing pathways, resulting in either the cleavage of the S−N bond with the formation of a reduced BODIPY derivative (pathway a) or deboronation (pathway b).[850] In both cases, back electron transfer terminates the reaction. The formation of equal amounts of amine and aldehyde in the pathway suggests the formation of an imine intermediate that is subsequently hydrolyzed.[836] The observed chemical yields of pathways a and b were consistent with previous observations of competition between different reaction pathways in arylsulfonamides.[849,850] When the carboxylate group is not ionized, the yields of the amine are reduced; this was attributed to a need for H atom transfer[847,851] and makes other reaction pathways more competitive.[850] Photolytic cleavage of GABA from **158** (λ_{irr} = 488 nm; Scheme 51) enabled the controlled induction of light-triggered membrane-potential responses in patch-clamped mouse basolateral amygdala brain slices.[836]

Zhang and co-workers introduced a PPG based on a BODIPY derivative bearing photoreactive oxime esters[524] at the 2-position (Scheme 52).[837] Compounds **159a** and **159b** have strong absorption bands centered at 507 and 516 nm (ε_{max} = 5.2−5.7 × 10^4 M^{-1} cm^{-1}) with low Φ_F values (0.09−0.12). This was attributed to the proximity of the $^3n,\pi^*$ state to the lowest $^1\pi,\pi^*$ excited state, suggesting that ISC competes with fluorescence. The quantum yields of photorelease for carboxylic acid LGs at λ_{irr} = 503 nm were comparable to those for other BODIPY PPGs (Φ_r = 5.2−7.2 × 10^{-4}). The proposed photoreaction mechanism for this process is shown in Scheme 53. The excitation of oxime esters was shown to result in homolytic scission of the N−O bond and formation of a caged radical-pair.[526−528] This process is considered to occur mainly from the triplet-excited state,[852−856] although dissociation proceeded efficiently from the singlet-excited state in some oxime esters.[854] The caged radical pair can undergo recombination or in-cage reactions,[854] but escape of the carboxyl radical from the cage and subsequent hydrogen atom

https://dx.doi.org/10.1021/acs.chemrev.0c00663
Chem. Rev. 2020, 120, 13135−13272

Scheme 50. Proposed Mechanism for Photolysis of 157[836]

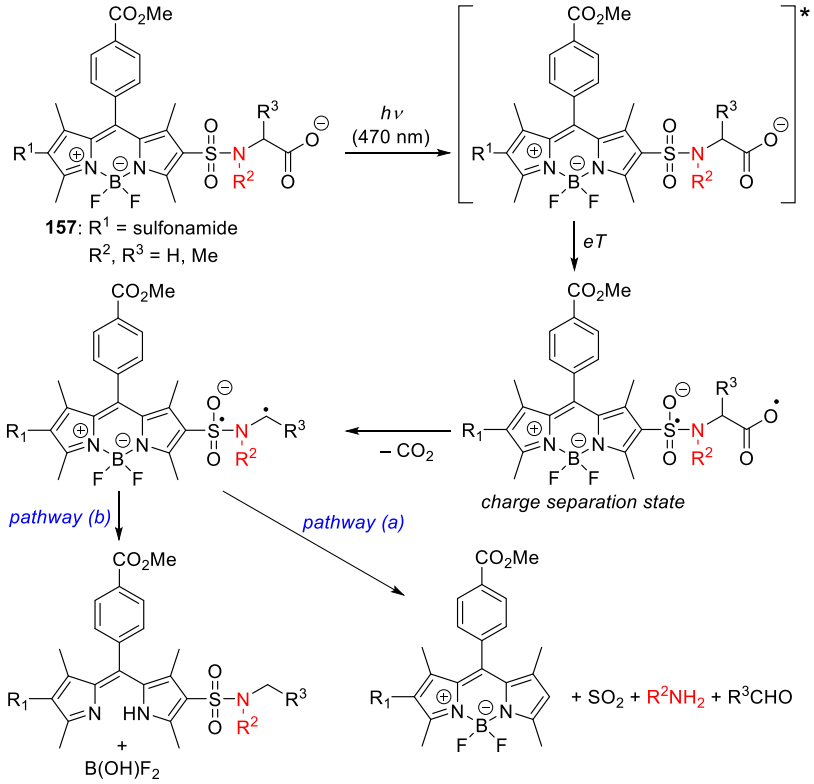

Scheme 51. Release of GABA upon Photolysis of 158[836]

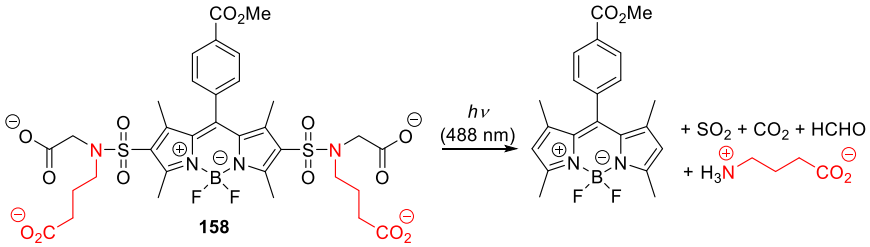

Scheme 52. Photorelease of Carboxylic Acids from BODIPY Oxime Esters[837]

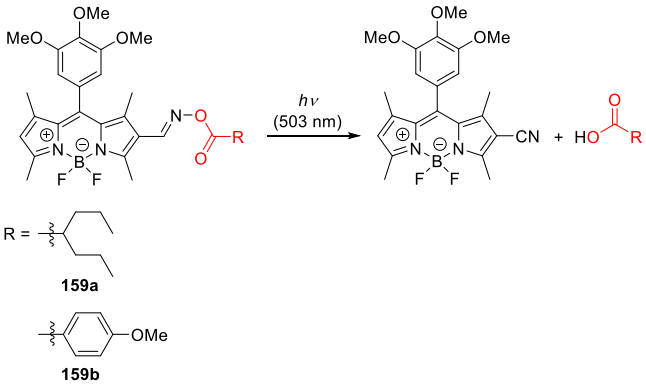

abstraction from a polar protic solvent creates a carboxylic acid leaving group.[412,528,837,856] The corresponding iminyl radical can undergo several transformations[796,857,858] or fast back-electron transfer to form an iminyl cation that is subsequently converted into a nitrile by deprotonation.[859] In the case of **159**, back electron transfer was found to be favorable; the 2-cyano BODIPY photoproduct was obtained in 60% chemical yield.[837] The histone deacetylase inhibitor valproic acid (VPA) was caged as a BODIPY oxime ester in this way; in HeLa cells, this compound caused light- and dose-dependent toxicity with an IC_{50} 100-times lower than that of free VPA.[837]

3. PHOTORELEASE FROM COORDINATION COMPOUNDS

Coordination compounds, which consist of a central (usually metal) atom or ion surrounded by ligands, have rich and varied photochemistry.[860,861] They often have unique ground- and excited-state properties that can be tuned by varying the central atom or the coordinating ligands to allow light-triggered release of chemically or biologically active species. Many organometallic complexes also exhibit photonuclease, photo-crosslinking, or photocytotoxic activities, accompanied by diverse types of photofragmentation reactions or photodynamic effects.[862−869] This section surveys coordination compounds that have been used as photoreleasable systems activated by visible/NIR light in the past decade. However, comprehensive coverage of all their applications would be beyond the scope of this review. A more extensive discussion

https://dx.doi.org/10.1021/acs.chemrev.0c00663
Chem. Rev. 2020, 120, 13135−13272

Scheme 53. Proposed Mechanism for Photolysis of 159[837]

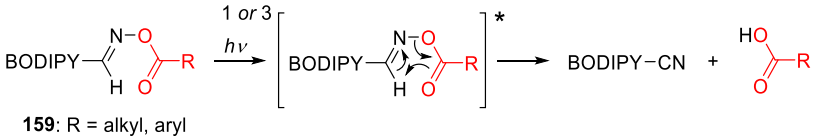

of these applications can be found in several review articles and perspectives that have been published in recent years.[8,40,58,65,66,68,69,76,98,107,113,869−876] Representative spectra of selected PPGs discussed in this section are shown in Figure 19.

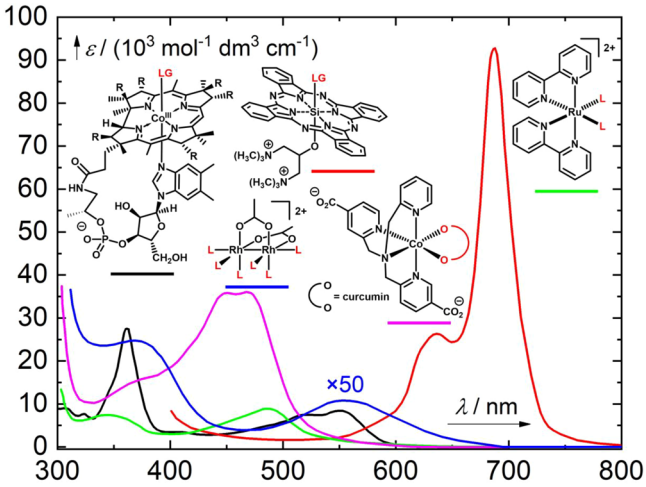

Figure 19. Representative spectra of transition metal-containing PPGs: black line, a vitamin B_{12} derivative[877] (LG = alkyl; section 3.1); red line, a phthalocyanine derivative (LG = aryloxy; section 3.2);[878] green line, a ruthenium(II) bipyridyl derivative (L = tyramine; section 3.3);[879] blue line, a dirhodium(II,II) derivative (L = acetonitrile; section 3.4; the ε values are 50-fold smaller than shown);[880] and magenta line, a cobalt(III) derivative (section 3.5).[881]

Transition-metal complexes are usually colored compounds and are therefore readily excited using visible light. The accessibility of multiple excited states with different spin multiplicities[882] and competing photophysical and chemical processes can result in complex and sometimes unpredictable photochemistry. Many different primary photophysical processes, including metal-to-ligand charge transfer (MLCT), ligand-to-metal charge transfer (LMCT), and ligand-to-ligand charge transfer (LLCT), may precede the release of species.[883,884] However, ligand exchange is usually the key process in ligand (species) liberation.

3.1. Photochemistry of Vitamin B_{12} Derivatives

Vitamin B_{12} is a water-soluble metal complex bearing a cobalt ion in the center of a conjugated corrin ring; its photophysical and photochemical properties are relatively well understood.[60−62,64,67,885,886] The corrin Co^{III} complex absorbs light below 580 nm,[877] and its derivatives such as **160** (Scheme 54, Figure 19; LG = alkyl, CN, OH, oradenosyl) can undergo homolysis[887] of the Co−C bond (BDE = 30−44 kcal mol^{-1})[886] in the singlet excited state[888] to give a charge-transfer Co^{III} intermediate within tens of picoseconds.[877,889−896] The intermediate then dissociates into a close radical pair of $LG^{\bullet}$ and Co^{II} side-product radicals that either recombine within nanoseconds or escape the solvent cage (Scheme 54).[61,67,885,886,892,897−900] The solvent's properties affect the efficiency of recombination.[901] Depending on the ligands, the relaxed singlet excited states have been characterized as either MLCT or LMCT states using DFT and TD-DFT methods.[62,886,902−912] In addition, magnetic field effects on the photolysis of 5′-deoxyadenosylcobalamin have been reported.[913,914] The rate of radical pair recombination was found to be sensitive to external magnetic fields on the order of tens to hundreds of mT in viscous solutions. Although the involvement of a triplet state in the dissociation of ligands from cobalamin complexes has not been precluded by calculations,[886,909] the formation of a triplet radical pair seems inconsistent with the observed magnetic field effects.[895,913] The photobiological role of vitamin B_{12} in the photoreception of photosynthetic and non-photosynthetic bacteria was studied by Kutta, Jones, and co-workers.[915] In contrast to the mechanism described above, the photochemistry of the coenzyme B_{12}-dependent photoreceptor protein, a bacterial transcriptional regulator that controls carotenoid biosynthesis, does not proceed via radical pair intermediates but through Co−C bond heterolysis.

It was demonstrated that visible-light-induced hydrogel formation can be facilitated using alkyl-cobalamin-based

Scheme 54. Vitamin B_{12} PPGs[877]

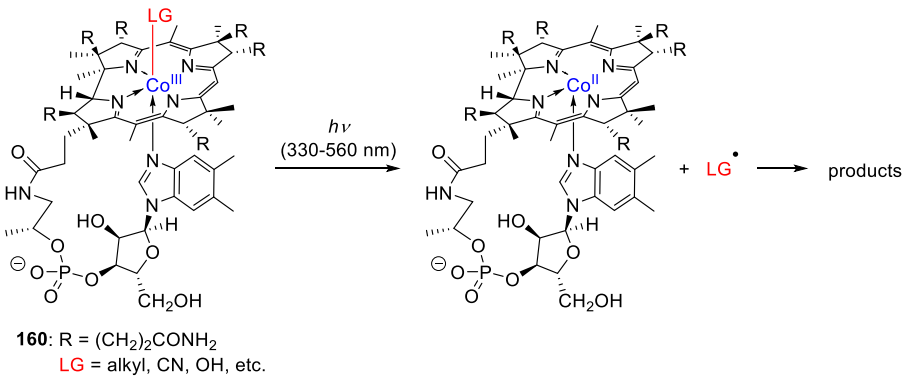

https://dx.doi.org/10.1021/acs.chemrev.0c00663
Chem. Rev. 2020, 120, 13135−13272

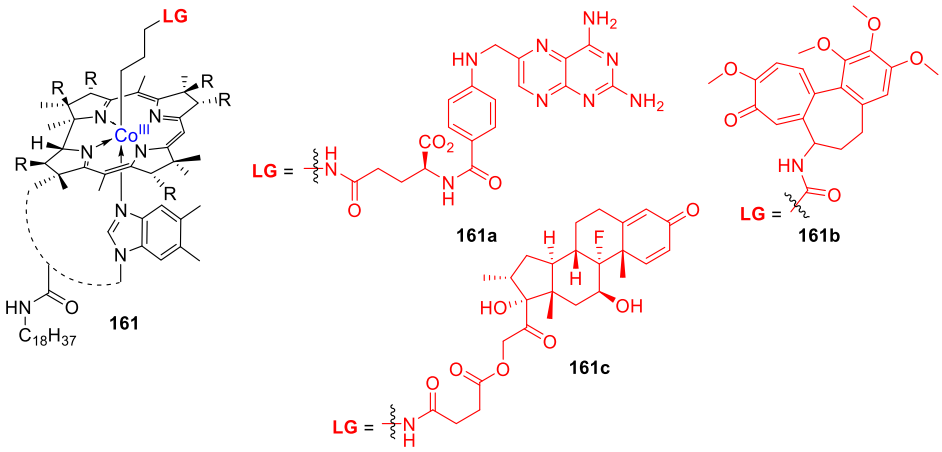

Figure 20. Cobalamin PPGs designed to release methotrexate (**161a**), colchicine (**161b**), and dexamethasone (**161c**).[932]

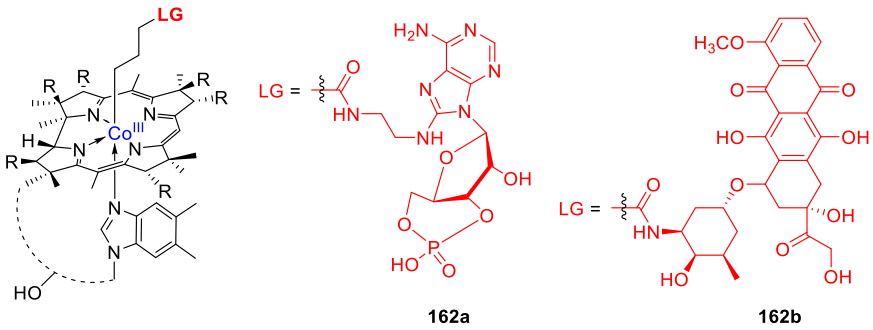

Figure 21. Cobalamin PPGs designed to release cyclic adenosine monophosphate (**162a**) and doxorubicin (**162b**).[930]

photoinitiators whose photochemistry induces radical photopolymerization.[916] The production of free radicals from thiolato-Cob(III)alamins was also supported by electron paramagnetic resonance.[917] Irradiation of alkylcobalamins using >500 nm light was shown to form carbon-centered radicals that cause DNA damage via strand scission of polynucleotides.[918] Additionally, in the presence of reductants such as TiO_2 or Zn/NH_4Cl, cobalamin derivatives undergo photochemical reduction to strongly nucleophilic Co^I complexes that can react with electrophiles via an S_N2 mechanism.[919]

The quantum yields of LG release from cobalamin derivatives are often irradiation-wavelength dependent.[892,894,920] For example, the Φ_r for $^{\bullet}CH_3$ liberation from methylcobalamin in aerated aqueous solutions varies from 0.35 at λ_{irr} = 490 nm to 0.24 at Φ_r = 550 nm.[921,922] Similarly, 5′-deoxyadenosylcobalamin undergoes Co−C bond cleavage with Φ_r = 0.20 under anaerobic conditions,[923] although a near-unity quantum yield for bond homolysis in aqueous solution has also been reported for this compound.[924] The Co^{II} side-product can be trapped by oxygen.[923,925,926] The photolysis mechanism and release quantum yields depend not only on the type of LG but also on experimental parameters including the solvent, the pH, the presence of specific enzymes,[888,894,901,927−929] and the nature of the lower axial base.[895,923] Cobalamin release mechanisms are discussed in more detail in a recent review by Jones.[61]

Photoactivatable vitamin B_{12} systems have been used for visible-light-initiated drug release. The absorption limit of the corrin ring (>580 nm) can be extended by appending a sensitizer absorbing in the NIR region, by exploiting 2P excitation, or via upconversion (see section 6.4.2).[885,930] Building on the earlier studies on the photochemical decomposition of adenosylcobalamin and other vitamin B_{12} analogs discussed above, Lawrence and co-workers showed that the photochemical cleavage of the Co−C bond in cobalamins can be used in the design of caged compounds.[885] Cobalamin **160**, which bears a rhodamine fluorophore as an LG connected through an alkyl linker, was shown to undergo selective photochemical homolysis upon irradiation at 560 nm in high chemical yield (97%), even when mixed with two different caged compounds absorbing only UV light.[931] The fluorescence of the appended rhodamine in **160** is quenched by the cobalamin, allowing its release to be monitored by observing its fluorescence under a confocal microscope in microwells and living cells.

The portfolio of leaving groups used with these PPGs was subsequently extended beyond fluorophore indicators by caging biologically active species including the anti-inflammatory agents methotrexate (**161a**), colchicine (**161b**), and dexamethasone (**161c**) with the cobalamin lipid conjugate **161** (Figure 20).[932] These caged derivatives were loaded onto human erythrocytes and the agents (which were connected via an auxiliary linker that was subsequently removed by esterase hydrolysis) were released in quantitative yield upon irradiation at 525 nm. To shift the absorption into the phototherapeutic window, the C_{18} derivatives of pentamethine cyanine (Cy5; λ_{irr} = 646 nm), AlexaFluor700 (λ_{irr} = 700 nm), heptamethine cyanine (Cy7; λ_{irr} = 747 nm), and DyLight 800 (λ_{irr} = 784 nm) were used as sensitizers. Irradiation at the dyes' maxima led to drug release and the induction of the expected biological responses.[932] A similar strategy was used to release cAMP from

https://dx.doi.org/10.1021/acs.chemrev.0c00663
Chem. Rev. 2020, 120, 13135−13272

conjugate **162a** to control the activity of a cAMP-dependent protein kinase and to release the anticancer agent doxorubicin from **162b** (Figure 21).[930] In these studies, several commercially available sensitizers including 5-carboxytetramethylrhodamine, SulfoCy5, Atto725, DyLight800, Alexa700, and BODIPY650 were used to facilitate excitation of cobalamin conjugates with visible-to-NIR light.

A photorelease strategy for liberating membrane-permeable bioagents such as colchicine, paclitaxel, and methotrexate from cobalamin−bioagent conjugates confined within lipid-enclosed compartments in the interior of erythrocytes was reported by Lawrence and co-workers.[933] Upon photolysis of the conjugates by visible-to-NIR light, enabled by a Cy5 sensitizer attached via a dimethylbenzimidazole ligand, the drugs were liberated inside red blood cells. Janovjak and co-workers recently used the 5′-deoxyadenosylcobalamin binding domains of bacterial CarH transcription factors to induce growth factor receptor 1 dissociation.[934] Several other relevant biological applications of cobalamin photochemistry have also been reported.[935−937]

3.2. Photochemistry of Phthalocyanine and Porphyrin Derivatives

Si-phthalocyanine macrocycles (Figure 22) are photostable, hydrophobic, and non-toxic.[938−940] Their usefulness in aqueous media is limited by their low aqueous solubility, although this can be overcome through structural modification.[941−943] Their absorption spectra feature an intense Q-band at approximately 670 nm and a Soret band in the region of 300−400 nm,[939,944] and the quantum yield of ISC is reduced by dye aggregation.[944] Interestingly, however, the efficiency of singlet oxygen production by the triplet state is very similar to that for the singlet states.[945] These complexes can thus serve as efficient oxygen photosensitizers in photodynamic therapy (see also section 6.3),[938,940,946−948] although photobleaching by self-sensitized photooxidation can limit their usefulness.[945] Interestingly, the properties of the axial ligands (Figure 22, R and R′) and the pH of the solution were found to profoundly affect their photophysics.[939]

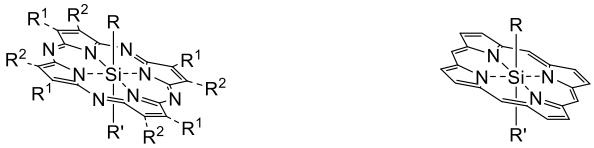

Figure 22. Si-phthalocyanine macrocycles as PPGs.

Axial alkyl ligands in various Si-porphyrin derivatives (Figure 22) undergo homolytic cleavage upon irradiation with visible light;[949−951] the dissociation energy of the axial Si−C bond is relatively low[950] (around 40 kcal mol^{-1}).[952] Accordingly, Ziady, Burda, and co-workers found that an axial alkyl tether used to link Si-phthalocyanines to Au nanoparticles (**163**) underwent efficient photochemical homolytic cleavage upon irradiation with 660 nm light (Scheme 55).[953] This Au-drug delivery system is initially PDT-inactive because the excited state of the Si-phthalocyanine is quenched by the Au nanoparticle (see also section 6.4). Upon irradiation, the chromophore is liberated and undergoes ligand exchange[950] with water to give a PDT-active species that produces singlet oxygen with a quantum yield of 49%. The homolytic photocleavage of axial alkyl groups was also investigated in methanol,[954] and a mechanism was proposed involving the initial formation of a radical centered on the Si atom of the Si-phthalocyanine and an alkyl radical that subsequently abstracts hydrogen from methanol. Several Si-phthalocyanine derivatives bearing amino acrylate axial linkers cleavable by singlet oxygen produced by *in situ* phthalocyanine sensitization have been reported.[955−957]

The dissociation energy of axial Si−O bonds in Si-phthalocyanines is much higher (≥80 kcal mol^{-1}) than that of comparable Si−C bonds.[952] Irradiation of Si-phthalocyanines bearing both axial alkyl and alkylsiloxy ligands (Figure 22, R = alkyl, R′ = alkylsiloxy groups) leads to the exclusive homolytic liberation of the alkyl group.[952]

The photochemistry of a series of Si-octaphenoxyphthalocyanines bearing aryloxy, siloxy, aminoalkoxy, carboxyl, and sulfonyloxy groups as axial ligands was studied by Nyokong and co-workers.[945] Axial ligand exchange to give the corresponding hydroxy derivatives in DMSO solutions was suggested to proceed via intermolecular electron transfer between the phthalocyanine π,π^* excited state and an electron acceptor. Schnermann and co-workers showed that the Si−OAr bond in Si-phthalocyanines with axial aryloxy ligands can be cleaved in aqueous solutions using NIR light.[878] Scheme 56 shows the synthesized aryloxy derivatives **164** (Figure 19), which liberated substituted coumarin and stilbene moieties in degassed (hypoxic) aqueous solutions upon irradiation at 690 nm. Complex **164a** released the fluorescent reporter 4-methylumbelliferone, and the photorelease of combretastatin-A4 and its *E*-isomer from **164b** and **164c**, respectively, was

Scheme 55. Si-Phthalocyanine Attached to Au Nanoparticle as a PPG[953]

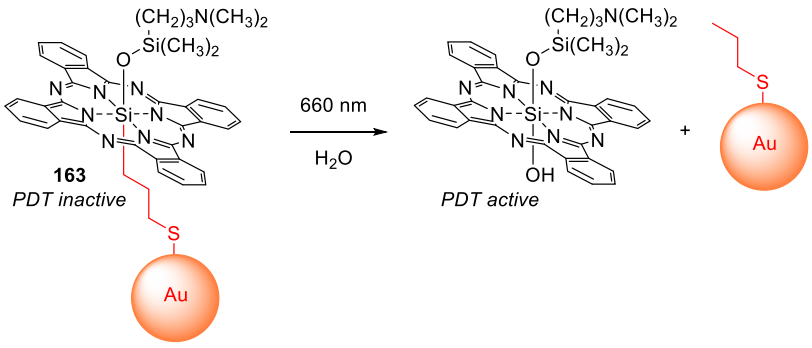

https://dx.doi.org/10.1021/acs.chemrev.0c00663
Chem. Rev. 2020, 120, 13135−13272

Scheme 56. Si-Phthalocyanine PPGs to Release Aryloxy Groups[878]

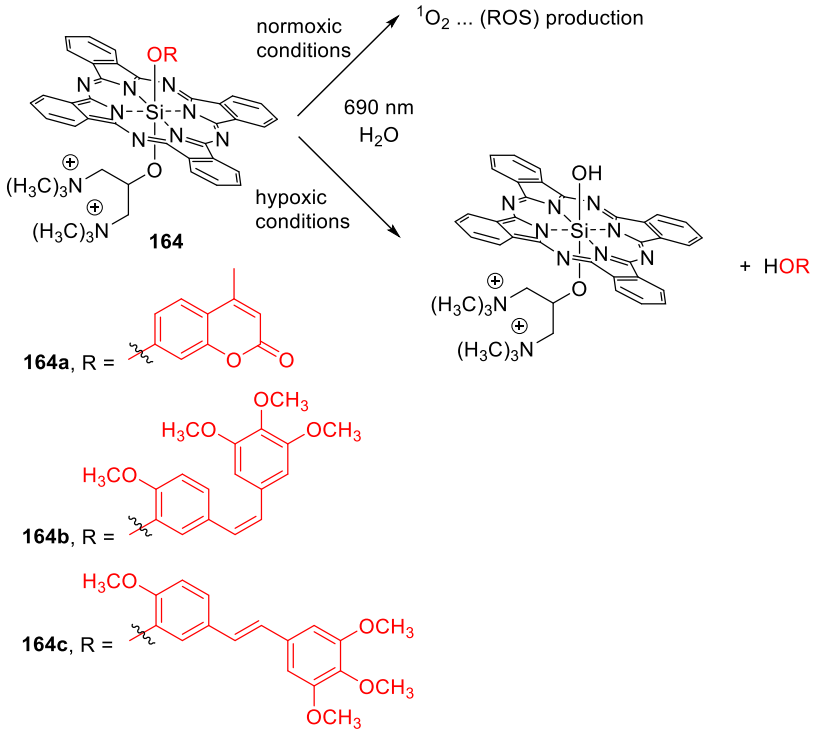

Scheme 57. Ligand Exchange in a Si-Phthalocyanine PPG[958]

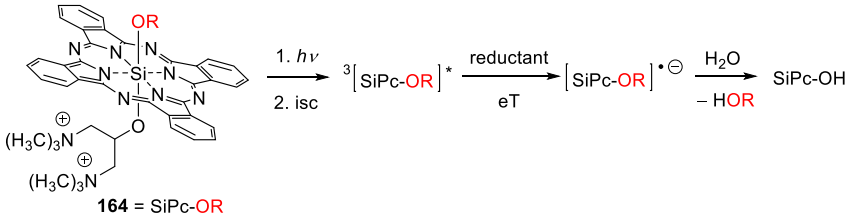

Scheme 58. Ligand Exchange in the Phthalocyanine IR700[959]

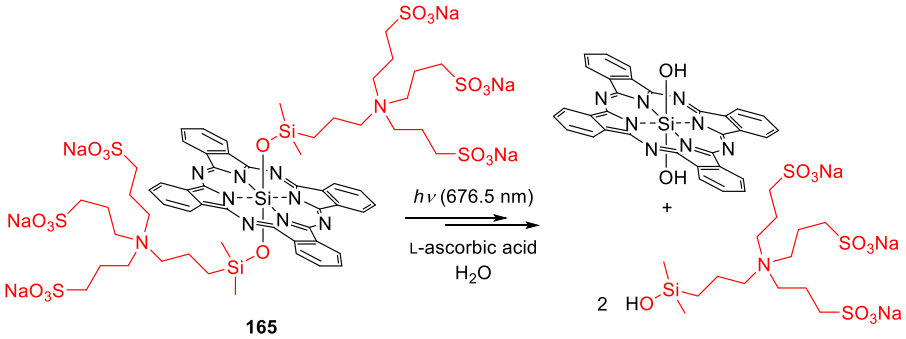

used to study the effects of tubulin polymerization inhibition under low-O_2 conditions typical of tumor microenvironments. Under normoxic (normal oxygen concentration) conditions, complexes **164** exhibited reactive oxygen species-mediated phototoxicity. Both spectroscopic and computational studies provided evidence of photoinduced electron transfer to the Si-phthalocyanine triplet to form a radical anion intermediate that undergoes ligand exchange with water[958] (Scheme 57). DFT calculations indicated that the attack of water as a nucleophile on the radical-anion center is more feasible than an attack on the neutral complex.[958]

A different way of exploiting photoinduced ligand release from Si phthalocyanines is embodied by the phthalocyanine derivative IR700 (**165**, Scheme 58), which releases a ligand upon irradiation at 676.5 nm in the presence of L-ascorbate as an electron donor.[959,960] It was proposed that this reaction changes the dye's hydrophilicity and propensity to aggregate in aqueous solutions, which contributes significantly to the induction of cell death.

Herges and co-workers designed Ni^{II}-porphyrin systems **166**, which undergo photochemical axial coordination/de-coordination (Scheme 59)[961,962] in a manner that enables

https://dx.doi.org/10.1021/acs.chemrev.0c00663
Chem. Rev. 2020, 120, 13135−13272

Scheme 59. Ni^{II}−Porphyrin PPGs

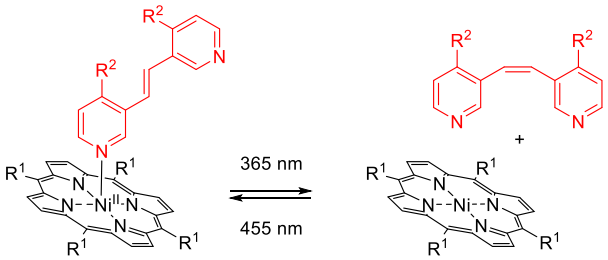

controlled coordination-induced spin-state switching.[963] Photochemical isomerization of the *E*-azopyridine ligand to the *Z* form weakens its binding due to steric clashing between the substituents at the 2-positions of the pyridyl rings, resulting in ligand release. When the axial ligand is bound, the Ni complex is pentacoordinate, high spin, and paramagnetic; dissociation of the axial ligand causes switching to the diamagnetic tetracoordinate low spin state. Similarly, the spin state of Fe^{III} porphyrins bridged with 1,2,3-triazole ligands can be changed by adding phenylazopyridine as a photodissociable ligand,[964] or the pyridine-bearing dithienylethene (DTE) photoswitch can be used to induce metal−ligand interaction between two Zn^{II}-porphyrin moieties connected through a diethyne linker.[965]

3.3. Photochemistry of Ruthenium(II) Polypyridyl Complexes

The photochemical activity of metal polypyridyl complexes has been known for decades, and the archetypical chromophore of this type, the $[Ru(bpy)_3]^{2+}$ cation (bpy = 2,2′-bipyridyl; Figure 23), has received considerable attention because of its unique

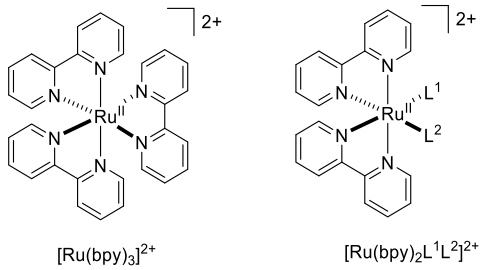

Figure 23. Ru^{II} polypyridyl complexes.

optical and physicochemical properties.[56,70,860,966,967] It absorbs in the visible region ($\lambda_{max}^{abs} \approx 450$ nm) and the metal-to-ligand charge-transfer (MLCT) d → π^* transition populates the singlet state, formally represented as a Ru^{III}−bpy^- state, which is converted into the triplet ^{3}MLCT state in about 10 fs[968] with an ISC quantum yield of almost unity.[966] The long-lived triplet state ^{3}MLCT can be deactivated by radiative, non-radiative, and electron transfer pathways or be thermally activated to give a low-lying triplet ligand-field state (^{3}LF) with an Ru−ligand antibonding character that can lead to ligand release.[70,72,969−971] A relationship between the π-accepting ability of the ligands and the photosubstitution efficiency has been demonstrated.[972−975] In the triplet state, this complex is an efficient oxygen sensitizer.[976] The photochemical applications of $[Ru(bpy)_3]^{2+}$ range from solar energy conversion, photocatalysis, and sensing to photochemotherapy and bioimaging.[57,70,71,966]

The photoreactions of analogous $[Ru(bpy)_2L^1L^2]^{2+}$ complexes (where L^1 and L^2 may belong to the single or separate ligands; see Figure 23) have attracted great interest in the context of photocaging and are discussed at length in recent reviews and perspectives.[70,72,977−979] The major advantage of these and many other transition metal-containing photoactivatable systems is that they can release neutral bioactive small molecules (ligands) including nitriles, amines, and aromatic heterocycles.[980,981] The absorption spectra of $[Ru(bpy)_2L^1L^2]^{2+}$ feature strong bands in the visible region ($\lambda_{max}^{abs} \approx 420$ nm), but larger conjugated terpyridine or bisquinoline ligands shift the absorption maximum up to as much as 600 nm, with tail absorption extending into the phototherapeutic window in the NIR and IR regions.[982] In an early study, Pinnick and Durham found that the quantum yields of photosubstitution (ligand exchange) in $[Ru(bpy)_2L^1L^2]^{2+}$ derivatives correlated with the energy of the lowest energy charge-transfer transition.[983] It has been suggested that the direct population of the reactive ^{3}LF state from ^{1}MLCT along with the population of the emissive ^{3}MLCT state are the first photophysical events to occur in these complexes.[969,977,984] However, Dunbar and Turro showed that the population of ^{3}MLCT competes with ligand liberation on time scales of fs to ps.[985,986] In their work, irradiation of $[Ru(bpy)_2(CH_3CN)_2]^{2+}$ in water resulted in stepwise CH_3CN release to give $[Ru(bpy)_2(CH_3CN)(H_2O)]^{2+}$ and $[Ru(bpy)_2(H_2O)_2]^{2+}$ as the first and second intermediates, with the former complex being detected after only 77 ps.

Etchenique and co-workers created a $[Ru(bpy)_2L^1L^2]^{2+}$ PPG by coordinating two K^+ channel-blocking 4-aminopyridine (4AP) ligands to obtain complex **167** (Scheme 60). These ligands were released sequentially upon irradiation at 480[987] or 800 nm (2P absorption).[988] A similar strategy was used to cage nicotine,[989] γ-aminobutyric acid (GABA, for which the release quantum yield was 0.036[990]) and other amines.[879,991−993] When one of the monodentate ligands is triphenylphosphine, which is a weaker σ-donor than an amine but a stronger π-acceptor (**168**, Scheme 60, Figure 19), the Ru^{II} center becomes

Scheme 60. $[Ru(bpy)_2L^1L^2]^{2+}$ Complexes 167[988] (4AP = 4-Aminopyridine) and 168[990] as PPGs

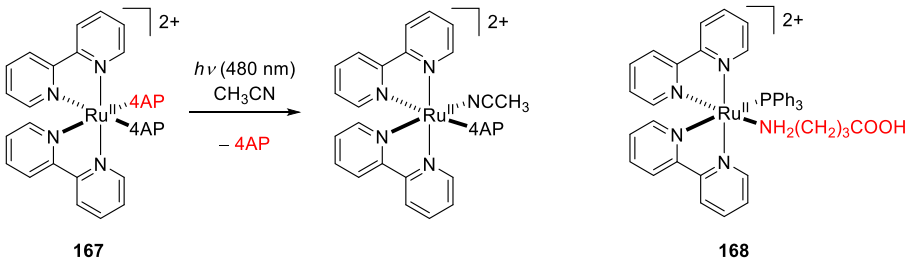

https://dx.doi.org/10.1021/acs.chemrev.0c00663
Chem. Rev. 2020, 120, 13135−13272

Scheme 61. Ru^{II} Complexes 169[999] and 170[1005] as PPGs

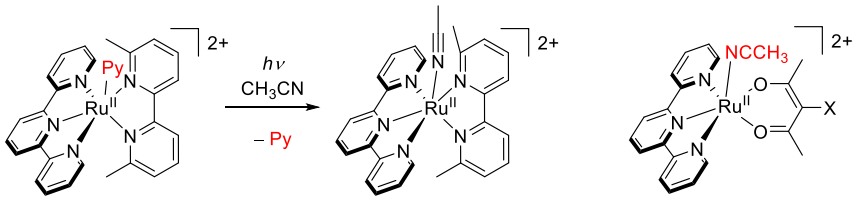

electronically depleted, resulting in more efficient GABA liberation (Φ_r > 0.21).[990] A kinetic flash photolysis study showed that [Ru(bpy)$_2$(PMe$_3$)(glutamine)] photoreleases glutamine within 50 ns.[994] The analogous [Ru(bpy)(dcbpy)-py$_2$]$^{2+}$ and [Ru(dcbpy)$_2$ py$_2$]$^{2+}$ complexes (bpy = 2,2′-bipyridine, dcbpy = 4,4′-dicarboxy-2,2′-bipyridine, and py = pyridine) released their pyridine ligands upon irradiation at 450 nm at physiological pH.[995] Similarly, [Ru(ane)(chel)-(py)]$^{2+}$ (ane = 1,4,7-trithiacyclononane, chel = chelating diimine) photoreleased pyridine at 470 nm.[996] In another application, a weakly fluorescent rhodamine-substituted Ru^{II} complex was shown to photorelease a rhodamine dye, increasing its fluorescence intensity almost six-fold.[997]

Sterically bulky ligands were introduced to distort the pseudo-octahedral geometry of the Ru^{II} complexes, which reduces the energy of the locally-excited ^{3}LE state, and increases the efficiency of ligand exchange.[70] For example, 2,2′-biquinoline (biq) is photoreleased from [Ru(biq)(phen)$_2$]$^{2+}$ (phen = 1,10-phenathroline), whereas [Ru(phen)$_3$]$^{2+}$ is photochemically inactive.[998] This phenomenon was demonstrated by Turro and co-workers in a series of Ru complexes bearing tridentate ligands, such as [Ru(tpy)(Me$_2$ bpy)(py)]$^{2+}$ (Me$_2$ bpy = 6,6′-dimethyl-2,2′-bipyridine, tpy = terpyridine, py = pyridine).[999] As shown in Scheme 61, this complex (**169**) undergoes ligand exchange with a quantum yield of 0.16 upon irradiation at 500 nm. This value is approximately 3 orders of magnitude higher than that for [Ru(tpy)(bpy)(py)]$^{2+}$, which features the sterically undemanding bpy ligand rather than the sterically bulky Me$_2$ bpy. The ^{3}LE state was found to form within 3−7 ps, and it can be deactivated by ligand dissociation or non-radiative decay. Building on preceding theoretical studies,[1000,1001] Alary and co-workers performed DFT calculations indicating that these results can be attributed to the formation of a quasi-degenerate triplet metal-centered state and triplet excited-state potential energy surfaces with differing topologies.[1002,1003] An analogous photoactivatable ruthenium complex [Ru(tpy)(bpy)(L)]$^{2+}$, where L is a rigidin derivative caged through its thioether group, released the caged ligand upon irradiation at 530 nm.[1004] The rigidins are cytotoxic marine alkaloids known to kill cancer cells. A series of related Ru terpyridine complexes bearing acetylacetonate-based ligands (Scheme 61, **170**, X = H or halogen) was synthesized to bathochromically shift the absorption of these systems (λ_{max}^{abs} < 517 nm).[1005] These complexes exhibited quantum yields of ligand release five- to seven-times higher than that of [Ru(tpy)(bpy)(CH$_3$CN)]$^{2+}$.

Another class of Ru^{II} complexes features tetradentate ligands such as tris(2-pyridylmethyl)amine **171** (Figure 24).[72,977,1006−1008] These stable complexes can cage a wide range of different ligands L, including the cathepsin K inhibitor Cbz-Leu-NHCH$_2$CN and nicotinamide, which are released upon irradiation at >400 nm. The selective release quantum

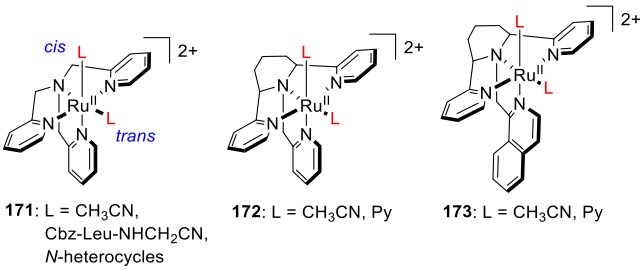

Figure 24. Ru^{II} complexes with the tetradentatetris(2-pyridylmethyl)-amine ligand and its analogs as PPGs.

yields of *cis*-nitrile ligands (∼0.01) were higher than those for *cis*-heterocyclic ligands in water, which was attributed to aromatic heterocycles being stronger σ-donors than nitriles.[977] Rigid complexes **172** and **173** bearing tetradentate piperidine ligands (Figure 24) also underwent photochemical ligand exchange with quantum yields of 0.001−0.03.[1009] DFT studies on the two isomers of the tris(2-quinolinylmethyl)amine (TQA) complexes [Ru(TQA)(MeCN)$_2$]$^{2+}$ **172**[970] and **173**[1009] showed that orbital mixing is crucial for effective ligand photodissociation.

Bonnet and co-workers demonstrated the photorelease of 2-(methylthio)ethanol from Ru^{II} complexes such as **174** (Scheme 62).[1010] This ligand was released in water upon

Scheme 62. Ru^{II} Photoreleasable Complex 174[1010]

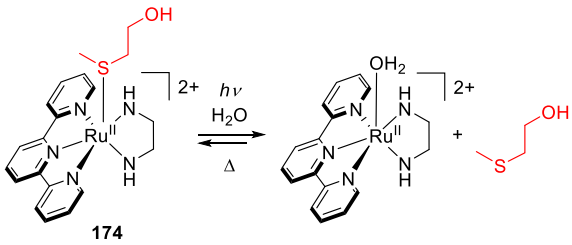

irradiation at 465 nm with a quantum yield of 0.13. An analogous complex bearing 6,6′-dichloro-2,2′-bipyridine as a ligand was used to control light-responsive supramolecular interactions.[1011] The photorelease of a microtubule-targeted rigidin analog from [Ru(tpy)(bpy)L]$^{2+}$ derivative **175** (Figure 25) in hypoxic cancer cells is another notable practical application of Ru^{II}-based PPGs.[1004] A series of Ru^{II} polypyridyl complexes bearing 6-mercaptopurine as a photocleavable ligand was prepared by Renfrew and co-workers.[1012] The highest release quantum yield (0.6) in this series was achieved with complex **176** (Scheme 62), which liberates 6-mercaptopurine upon irradiation at 465 nm in acetonitrile. The 1,4,7-trithiacyclononane Ru^{II} complexes **177**−**179** (Figure 25), bearing photocleavable pyridine, DMSO, 3-acetylpyridine, and imidazole ligands, were designed and studied by Alessio,

https://dx.doi.org/10.1021/acs.chemrev.0c00663
Chem. Rev. 2020, 120, 13135−13272

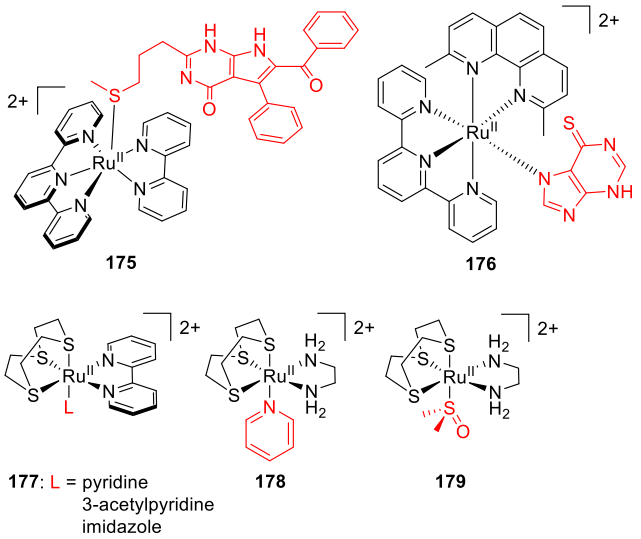

Figure 25. Ru^{II} complexes as PPGs.

Sadler, and co-workers.[1013−1015] These complexes release their ligands upon irradiation with blue light (400−490 nm).

Many other applications of Ru^{II} complexes as photoactivatable groups have been reported. The liberation of neurotransmitters to enable control over receptor activity in neuronal cells was mentioned above.[56,879] These complexes have also been used for controlled release of small molecule drugs and enzyme inhibitors. Enzymes successfully targeted in this way include proteases,[1016] cathepsin B (inhibited with a novel dipeptidyl nitrile[1017]),[980,1018] nicotinamide phosphoribosyl transferase,[1019] cytochromes P450,[1020] and CYP17A1.[1021] Drugs successfully photoreleased from Ru^{II} complexes include the anticancer agent CHS-828,[1022] the imidazole-based cytotoxic drug econazole,[1023] the anti-tuberculosis drug isoniazid,[1024] and 5-cyanouracil.[1025,1026] Additionally, a photoactivatable histidine building block for Fmoc/*t*-Bu solid-phase peptide synthesis based on a Ru^{II} complex with an imidazole ligand was used to prepare caged histidine peptides.[1027] A library of tetra- and pentadentate ligands was attached to a polystyrene resin to prepare the corresponding photolabile Ru^{II} complexes for a solid-phase synthesis application.[1028] $[Ru(bpy)_2(4AMP)_2]$ (4AMP = 4-(aminomethyl)pyridine) was incorporated into polyurea organo- and hydrogels and used as a photoremovable moiety to induce de-gelation upon 1P or 2P excitation.[1029] Similarly, supramolecular crosslinked gels with a photosensitive ruthenium bipyridine complex functioning as a crosslinker and poly(4-vinylpyridine) as a macromolecular ligand were developed by Teasdale and Monkowius.[1030] Photolysis of these organogels with visible (>395 nm) and NIR light (1028 nm; a multiphoton process) resulted in the liberation of the pyridine moieties and degelation.

Photoinduced ligand dissociation from ruthenium complexes can also be accompanied by singlet oxygen production.[70] Turro and co-workers showed that the triplet excited state of the $[Ru(bpy)(dppn)(CH_3CN)_2]^{2+}$ (dppn = benzo[*i*]-dipyridophenazine) complex efficiently sensitizes oxygen to give $^1O_2$ in aqueous solution (Φ_Δ = 0.72) and also releases acetonitrile in a less efficient competing process (Φ_r <0.01).[1031] Similar dual reactivity was demonstrated for $[Ru(tpy)(Me_2\ dppn)(py)]^{2+}$ (dppn = dimethylbenzo-[*i*]-dipyridophenazine)[1032] and $[Ru(pydppn)(biq)(py)]^{2+}$ (pydppn = (pyrid-2-yl)benzo[*i*]dipyridophenazine)[1033] complexes. Additionally, a structurally distinct nitrosyl phthalocyanine ruthenium complex was shown to produce singlet oxygen and release nitric oxide (see section 4.2).[1034]

Rh^{III} complexes with polypyridyl and phenanthrene quinone diamine ligands are also photoactive and have been used to achieve photoinduced DNA cleavage. However, ligand exchange reactions are not the primary processes responsible for their photochemical activity.[113]

3.4. Photochemistry of Dirhodium(II,II) Complexes

Dirhodium (Rh^{II}−Rh^{II}) complexes have also attracted attention as photoactivatable species,[71,113] although there have been few studies on this aspect of their behavior. The complex **180**, reported by Turro and co-workers, has an absorption maximum at 525 nm (ε_{max} = 218 M^{-1} cm^{-1}; Scheme 63; Figure 19) in acetonitrile, which was attributed to a $Rh_2(\pi^*) \rightarrow Rh_2(\sigma^*)$ transition on the basis of TD-DFT calculations.[880] This compound selectively exchanges its axial CH_3CN ligands with H_2O in aqueous solutions in the dark. Upon irradiation of the product with visible light, two equatorial CH_3CN ligands dissociate and are replaced with water to give three different isomers of *cis*-$[Rh_2(\mu\text{-}O_2CCH_3)_2(CH_3CN)_2(H_2O)_4]^{2+}$, causing a slight bathochromic shift of the absorption maximum. The liberation quantum yields depended on the irradiation wavelength: $\Phi_{355\ nm}$ = 0.37 and $\Phi_{509\ nm}$ = 0.09. Irradiation of **180** in water in the presence of 2,2′-bipyridine or 9-ethylguanine led to the coordination of these ligands to the dirhodium core. Similar results were obtained with *cis*-$[Rh_2(HN(O)CCH_3)_2(CH_3CN)_6]^{2+}$, which releases two molecules of acetonitrile upon irradiation at >495 nm to form bis-aqua products,[1035] and with $[Rh_2(O_2CCH_3)_2(CH_3CN)_6]^{2+}$, which releases its axial CH_3CN ligands upon irradiation at >455 nm.[1036]

The 1,10-phenanthroline complex **181** was shown by Turro and Dunbar to release two equatorial CH_3CN ligands in water upon irradiation with visible light (λ_{irr} >590 nm), whereas mononuclear radical Rh^{II} fragments were formed upon homolytic photocleavage of the metal−metal bond (Figure 26).[1037] Remarkably, the release quantum yield measured upon irradiation at 550 nm exceeded unity (Φ_r = 1.38), suggesting that a dark release follows the initial photoreaction. Another photoactivatable dirhodium complex, **182**, bearing a benzo[*i*]-dipyridoquinoxaline ligand (Figure 26) was designed to serve

Scheme 63. Dirhodium (Rh^{II}−Rh^{II}) Complex as a PPG[880]

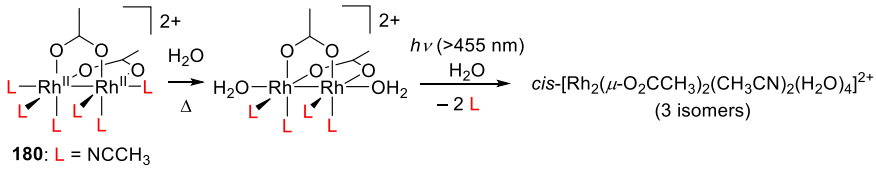

https://dx.doi.org/10.1021/acs.chemrev.0c00663
Chem. Rev. 2020, 120, 13135−13272

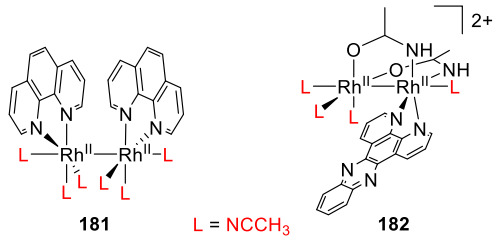

Figure 26. Dirhodium (Rh^{II}–Rh^{II}) complexes **181**[1037] and **182**.[1038]

as a DNA-intercalating singlet oxygen generator (Φ_Δ = 0.22 at 477 nm) thanks to its low-lying dppn-centered $^3\pi,\pi^*$ state.[1038] Upon irradiation in water, acetonitrile is released from this compound and replaced by H_2O as a ligand (Φ_r = 0.0033 at 450 nm).

3.5. Photochemistry of Pt-, Co-, and Fe-Containing Organometallic Complexes

Usually unreactive Pt^{IV} prodrugs are important anticancer compounds[1039] that are designed to be converted into toxic Pt^{II} species *in vivo* by reducing agents such as ascorbic acid.[1040] Well-known Pt^{II} drugs such as cisplatin and carboplatin have very narrow therapeutic indexes, so there is great interest in their controlled photochemical production in target tissues. Several visible-light absorbing photoactivatable Pt^{IV} complexes with the general structure *trans,trans,trans*-[$Pt(N_3)_2(OH)_2(N^1)(N^2)$] (**183**, N^1, N^2 = pyridine or amines; Figure 27) were studied by Sadler and co-workers and shown

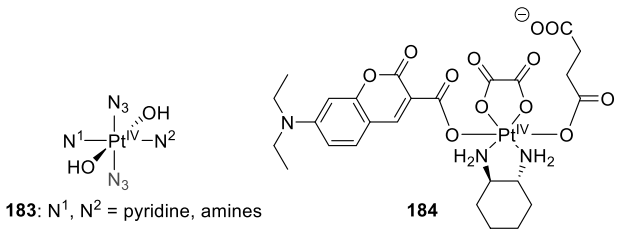

Figure 27. Pt^{IV} complexes as PPGs.

to be cytotoxic to cancer cells upon irradiation with blue light.[1041−1044] Compounds **183** do not liberate pyridine or amines upon excitation but do exhibit Pt–N_3 bond elongation, eventually leading to the release of azidyl radicals.[1041] This concept was also used in the design of a photoactivatable dopamine-conjugated Pt^{IV} anticancer complex that was incorporated into borate hydrogels,[1045] as well as Pt^{IV} triazolato azido complexes that photorelease Pt^{IV} and Pt^{II} 5′-guanosine monophosphate species.[1046] Additionally, the oxaliplatin-based photocaged Pt^{IV} prodrug coumaplatin (**184**), was shown to release an axial ligand upon irradiation at 450 nm, forming a cationic Pt^{IV} intermediate that oxidizes water and generates oxygen under biological conditions.[1047]

Chakravarty and co-workers showed that curcumin (**185**, Figure 28), a compound with significant antioxidant, anti-inflammatory, antiseptic, and anticancer activities,[59] can form photoactivatable Pt^{II} complexes.[1048−1050] For example, [$Pt(NH_3)_2$(cur)](NO_3) (**186**, cur = curcumin) exhibits a strong absorption band with a λ_{max}^{abs} of ∼430 nm and releases two anticancer agents, curcumin and a cisplatin analog (which crosslinks DNA), upon irradiation with visible light.[1048] The analogous [Pt(en)(cur)](NO_3) and [Pt(dach)(cur)](NO_3) (**187**, en = ethylenediamine, dach = 1*R*,2*R*-(−)-1,2-diaminocyclohexane) complexes also liberated curcumin under similar conditions.[1049] The use of a photosensitizer as a ligand (see also section 6) can lead to dual photochemotherapeutic effects. This was demonstrated using [Pt(L)(R-BODIPY)]Cl complexes, where R-BODIPY is a distyryl-BODIPY derivative (sensitizer) and L are different terpyridine ligands. Irradiation of these species with red light (600−720 nm) caused both singlet oxygen production and the release of photoactive BODIPY ligands, resulting in appreciable photocytotoxicity.[1051] Similarly, platinum(II) ferrocenylterpyridine (Fc-tpy) complexes [Pt(Fc-tpy)(L)]Cl (L = a biotin-containing ligand) released their biotinylated ligands upon irradiation with red light (647 nm) because of the photosensitizing behavior of the Fc-tpy ligand.[1052] Finally, the very interesting heptamethine cyanine-based Pt^{II} complex **188** (Figure 28) was reported to undergo Pt–O bond scission and to generate singlet oxygen upon irradiation with near-IR light.[1053]

Unlike Ru^{II} and Pt^{IV} complexes, Co^{III} complexes (see also section 3.1) usually have very weak absorption bands in the visible region.[875] Therefore, strongly absorbing ligands that can photoreduce the Co^{III} ion to induce ligand release have been developed. The first reported complex of this type was the Ru^{II}–Co^{III} heterodinuclear species **189** (Figure 29), which has an absorption maximum close to 400 nm.[1054] Upon irradiation with visible light, the Ru^{II} moiety probably transfers an electron

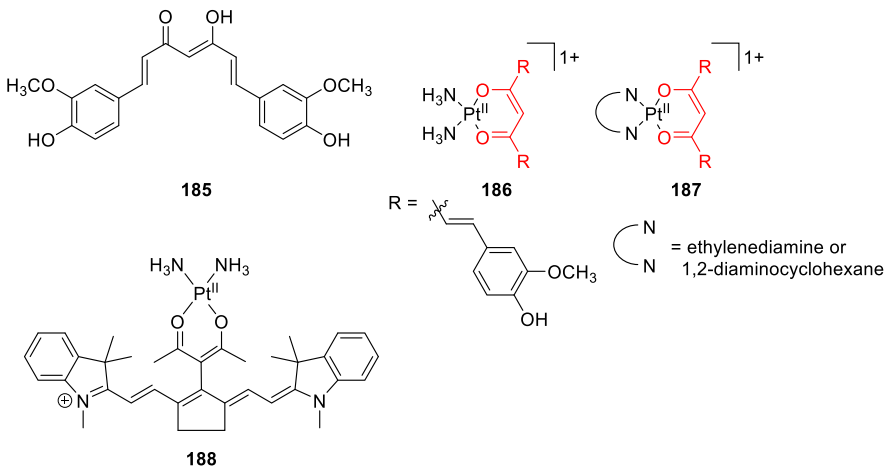

Figure 28. Photoactivatable Pt^{II} complexes.

https://dx.doi.org/10.1021/acs.chemrev.0c00663
Chem. Rev. 2020, 120, 13135−13272

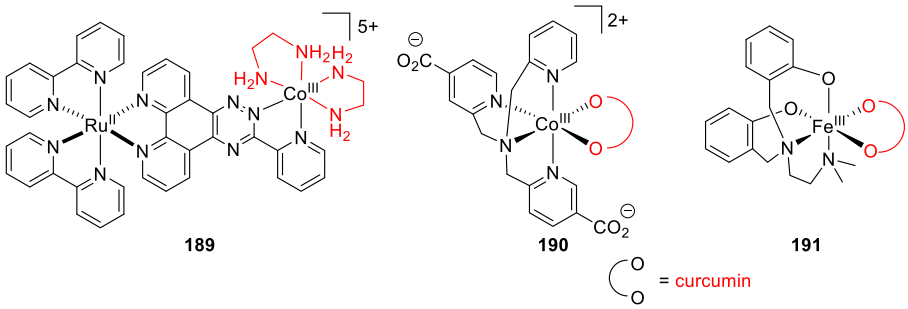

Figure 29. Ru^{II}–Co^{III}, Co^{III}, and Fe^{III} complexes.

to the Co^{III} complex to produce a Co^{II} species with concomitant release of the ethylenediamine ligands. Renfrew and co-workers reported the release of curcumin from Co^{III} curcumin complexes such as **190** (Figure 29, Figure 19).[881] This complex absorbs at λ_{max}^{abs} = 451 nm, and the authors hypothesized that irradiation at 520 nm causes electron transfer from curcumin to the cobalt ion. The photodegradation quantum yield for this compound was found to be 0.01. A similar strategy was demonstrated using ternary Co^{III} complexes of mitocurcumin (a water-soluble curcumin derivative) bearing a tetradentate phenolate-based ligand.[1055] Mitocurcumin was released upon irradiation with visible light and was shown to act as a phototoxin that generated reactive oxygen species in cells.

The analogous charge-neutral Fe^{III} complex **191** (Figure 29) and two other high-spin iron complexes reportedly released curcumin upon irradiation with visible light, and thus exhibited cytotoxicity in multiple cell lines.[1056] In addition, Fe^{III}–polysaccharide hydrogels were found to be visible-light (405 nm) responsive because of the photoreduction of the Fe^{III} ions to Fe^{II}, which rendered the Fe complexes incapable of functioning as cross-linkers for the polymer.[1057]

4. PHOTORELEASE OF GASOTRANSMITTERS

Gasotransmitters are small gaseous endogenously-produced signaling molecules that are involved in the control of a vast array of physiological processes in the cardiovascular, nervous, gastrointestinal, excretory, and immune systems as well as cellular functions including apoptosis, proliferation, inflammation, metabolism, oxygen sensing, and gene transcription.[1058] The most important gasotransmitters identified to date are nitric oxide (NO), carbon monoxide (CO), and hydrogen sulfide (H_2S). These small molecules are freely permeable through membranes and are perceived without cognate receptors.[1059] Their molecular targets can be divided into two groups. The first are metal-containing prosthetic groups of proteins that form coordination complexes with CO and NO; examples include heme-imidazoles (as in hemoglobin and cytochrome c oxidase), thiolated hemes (as in cytochromes P450), and non-heme iron complexes (as in prolyl hydroxylase and superoxide dismutase). The second group consists of organic thiols, which can be nitrosylated by NO and sulfhydrated by H_2S.[1058] Gasotransmitter perception can induce diverse macroscopic biological responses, many of which are therapeutically relevant such as vasodilatation,[1060,1061] protection of tissues against hypoxia,[1062] anti-inflammatory processes,[1063] wound healing,[1064,1065] platelet aggregation inhibition,[1066] postsynaptic plasticity augmentation, and hormone secretion.[1067] The simplest method of administering gasotransmitters is by direct inhalation of small quantities of the gaseous species. While this approach induces therapeutic effects in some contexts,[1068,1069] its usefulness is limited by narrow pharmaceutical windows and it requires precise control of the gasotransmitter's concentration, which is very difficult to achieve.[1070] Consequently, there is considerable interest in the development of gasotransmitter-releasing molecules.[80,82,94]

Most known gasotransmitter-releasing molecules are based on metal complexes that release a weakly bound gasotransmitter ligand via simple hydrolytic ligand exchange upon dissolution in aqueous media. Such complexes are prone to rapid initial releases of the bound gasotransmitter prior to administration to the target organism but do not allow for precise control over the release. Enzymatically triggered reactions that offer more controlled release profiles have also been demonstrated.[1071] An alternative activation strategy that enables precise spatial and temporal control over gasotransmitter release is to use photochemically activatable gasotransmitter-releasing molecules such as photoactivatable CO-releasing moieties (photoCORMs) or photoactivatable nitric oxide-releasing moieties (photoNORMs).[77−114] In therapeutic applications, organic (transition-metal-free) photoCORMs can have important advantages over metal carbonyl complexes such as more favorable biodistribution and lower toxicity.[80−82] Because of their distinct physicochemical properties (which typically include small size or neutral charge), the photorelease of gasotransmitters requires unique and highly specific strategies that may differ appreciably from those used for photorelease of larger ligands. Therefore, we present this research area in its own section. Research on photochemically activatable gasotransmitter-releasing molecules has advanced rapidly in the past decade, and many reviews are available.[49,80−102,1072−1074] This section focuses solely on visible-light-absorbing photorelease systems. Figure 30 shows the absorption spectra of selected transition-metal-free molecules that release gasotransmitters upon excitation with visible or NIR light, and Figure 31 shows the absorption spectra of some transition metal complexes with such activity.

4.1. Release of Carbon Monoxide

4.1.1. Transition-Metal-Free PhotoCORMs. The lowest excited state of simple ketones and aldehydes corresponds to the excitation of an electron from the n lone pair to the π^* molecular orbital.[136] n,π^*-Transitions are generally weak and often hidden by the red tail of a stronger π,π^*-absorption. Homolytic cleavage of the α-bond in ketones (α-cleavage; Norrish type I reaction) often results in decarbonylation, that is, carbon monoxide (CO) release. Therefore, carbonyl compounds have been widely used as photoCORMs.[80,82]

https://dx.doi.org/10.1021/acs.chemrev.0c00663
Chem. Rev. 2020, 120, 13135−13272

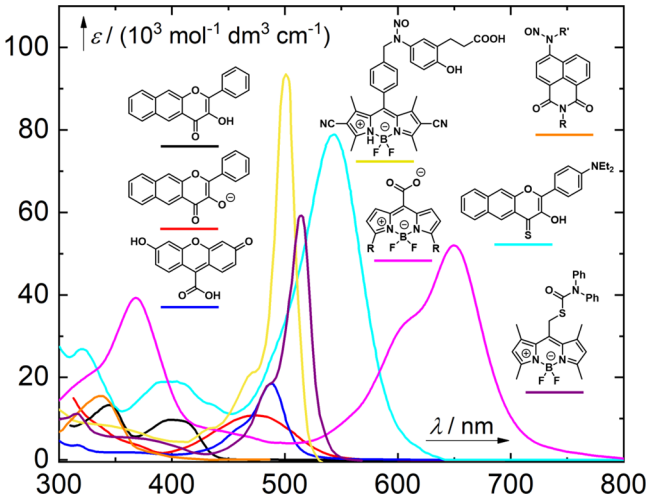

Figure 30. Representative absorption spectra of transition-metal-free molecules that photorelease CO, NO, and H_2S. Black,[1075] red,[1075] cyan[1076] lines, flavonol-based photoCORMs (section 4.1.1); blue line, a xanthene-based photoCORM (section 4.1.1);[763] magenta line, a BODIPY-based photoCORM (R = a styryl group; section 4.1.1);[847] yellow line, a BODIPY-based photoNORM (section 4.2.1);[1077] orange line, a naphthalimide-based photoNORM (section 4.2.1);[1078] violet line, a BODIPY-based H_2S releasing molecule (section 4.3).[799]

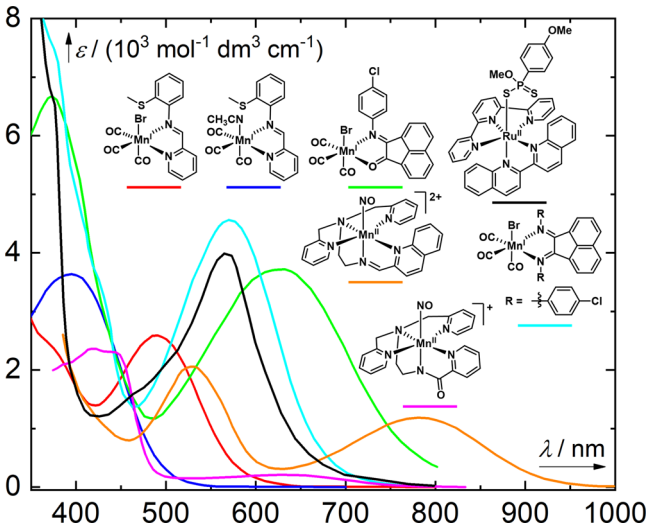

Figure 31. Representative spectra of transition-metal complexes photoreleasing CO, NO, and H_2S. Red,[1079] blue,[1079] green,[1080] cyan[1080] lines, Mn^{II} tricarbonyl photoCORMs (section 4.1.2); magenta[1081] and orange[1082] lines, Mn^{II} photoNORMs (section 4.2.2); black line, a Ru^{II}-based H_2S releasing complex (section 4.3).[1083]

The release of CO from prototypical aliphatic acyclic and especially small cyclic ketones by radical decarbonylation occurs only at the edge of the vacuum UV range (e.g., λ_{irr} = 193 nm for 3-cyclopentenone).[1084] However, an extension of the ketone π-system results in bathochromic shifts of their absorption maxima.[136] 1,2-Dicarbonyl compounds (which typically absorb above 300 nm) can also be photolyzed to produce CO.[1085] Irradiation of bicyclo[2.2.2]octane-2,3-dione **192a** in toluene at the edge of the visible region (395 ± 25 nm) resulted in the formation of aromatic side-products **193a−f** and the release of two equivalents of CO (Φ_r = 0.02, $\varepsilon\Phi_{CO}$ = 6 at 395 nm) (Scheme 64).[1085] 1,2-Diketone **192a** was used as an additive in poly(ε-caprolactone) electrospun

Scheme 64. 1,2-Diketones as PhotoCORMs[1085−1087]

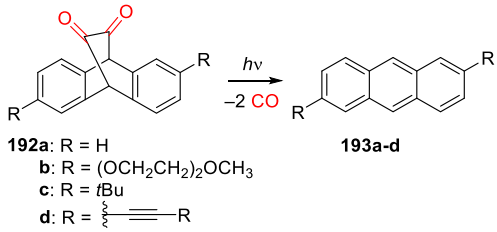

scaffolds designed for vascular tissue engineering[1086] and was shown to release CO upon irradiation at λ_{irr} = 470 nm in this environment.[1086,1087] To increase the hydrophilicity of the bicyclo[2.2.2]octane-2,3-dione scaffold, a derivative substituted with oligo-(ethylene)glycol side chains (**192b**) was prepared.[1087] However, **192b** did not release CO when dissolved in a water/DMSO (99:1) mixture due to hydration of the carbonyl groups. This was circumvented by encapsulating **192b** in micelles of Pluronic F127, a biocompatible block copolymer of poly(ethylene oxide) and polypropylene oxide. The encapsulated compound efficiently released CO upon irradiation at 470 nm, and the system was successfully used *in vitro*.[1087]

Liao and co-workers recently overcame the hydration-induced deactivation of photoactivity in bicyclo[2.2.2]octane-2,3-dione by preparing derivative **192c**, which carries *t*-butyl substituents (Scheme 64) that sterically hinder hydrate formation.[1088] This compound was incorporated into poly(butyl cyanoacrylate) nanoparticles and used as a tissue adhesive with possible applications in CO delivery to the brain. Additionally, Raymo and co-workers have designed an autocatalytic reaction based on the photoinduced decarbonylation (λ_{irr} = 420 nm) of **192a** and **192d**, which is sensitized by its own photoproducts, the anthracene derivatives **193**. The quantum yields of decarbonylation for **192a** and **192d** were 0.20 and 0.50, respectively.[1089]

The group of Yamada substituted the bicyclo[2.2.2]octane-2,3-dione scaffold with BODIPY antennas to obtain **192e** and **192f** (Figure 32).[1090] These compounds have a major absorption maximum in the green-to-yellow region (λ_{max}^{abs} = 534 nm for **192e** and λ_{max}^{abs} = 605 nm for **192f**) and release CO

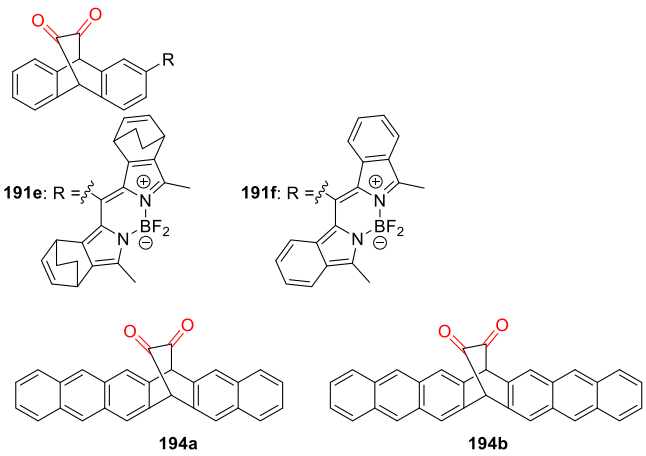

Figure 32. 1,2-Dicarbonyl PhotoCORMs.

https://dx.doi.org/10.1021/acs.chemrev.0c00663
Chem. Rev. 2020, 120, 13135−13272

Scheme 65. Photolysis of 2-Ketocarboxylic Acids (R = *i*Pr, Ph)[1093]

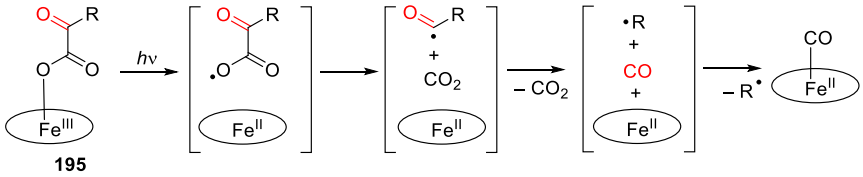

upon irradiation at 450 nm via initial photoinduced electron transfer from the BODIPY moiety to the 1,2-diketone functionality. Moreover, **192e** releases 2 equiv of ethylene via a thermal process that occurs upon heating to 220 °C. The release of CO and ethylene are thus orthogonal and can be performed sequentially. Unfortunately, **192e** and **192f** are insoluble in polar media, which limits their biological applications. Diketones **194a** and **194b** (Figure 32) decarbonylate upon irradiation at λ_{irr} = 395 ± 25 nm, but their aromatic photoproducts (hexacene and heptacene, respectively) do not accumulate in the reaction system due to their fast oxidation and dimerization.[1085,1091,1092]

2-Ketocarboxylic acids can also be used as photoCORMs. Visible light irradiation (>390 nm) of the tetra-(2-*N*-methylpyridyl)porphyrin-Fe^{III} complex with 2-ketocarboxylic acid **195** led to photoinduced electron transfer from the carboxylate anion to the central metal ion, yielding an Fe^{II} complex and a carboxyl radical (Scheme 65)[1093] that underwent simultaneous decarboxylation and decarbonylation. The released CO was then efficiently trapped by the Fe^{II}-porphyrin complex in the solvent cage.

Flavonol or 3-hydroxyflavone (3-hydroxy-2-phenylchromen-4-one; **196**, Scheme 66) belongs to the family of flavonoids,

Scheme 66. Photodecarbonylation of 3-Hydroxyflavone[1096]

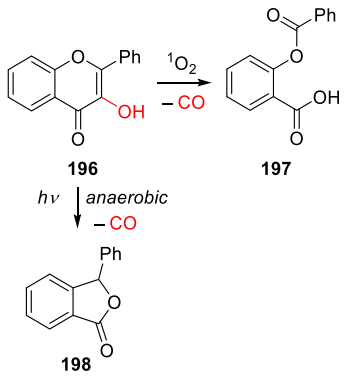

well-known natural antioxidants[1094,1095] that have been recognized as CO-releasing molecules. Unsubstituted flavonols absorb only in the UV region and, thanks to their biological relevance, the photodecomposition mechanism responsible for the resulting CO release has been studied since the 1960s. The photosensitized oxygenation of **196** by singlet oxygen generated photochemically *in situ* was reported in the seminal work of Matsuura and co-workers,[1096] who showed that it results in the formation of CO together with *o*-benzoyl salicylic acid **197** as a side-photoproduct. The reaction was suggested to proceed via an endoperoxide intermediate. In the absence of oxygen, 3-hydroxyflavone rearranges into the 3-arylphthalide derivative **198** with concomitant CO liberation. The 3-hydroxy group was found to be essential for this reaction because the analogous 3-methoxyflavone derivative is photostable. These mechanistic pathways were later studied in detail.[1097−1100] Kubinyi and co-workers introduced the push-pull substituted 4′-diethylamino-3-hydroxyflavone and its Mg^{II} complex.[1101] However, despite the ESIPT character of this compound and its absorption in the visible part of the spectrum, only UV-light-initiated CO release was studied. The photochemistry of flavonol-based CORMs was recently reviewed.[92]

Flavonols are excellent ligands for d-block elements; complexation of metal cations with flavonolate anions causes bathochromic shifts of their lowest energy absorption bands into the visible part of the spectrum and also increases their molar absorption coefficients in some cases.[1099] Because of their biological relevance in plant metabolism and occurrence in soil,[1102] the photochemistry of these metal complexes has been studied in detail. The photoreactivity of Pb^{II} and Al^{III} flavonolato complexes is suppressed, whereas Zn^{II} complexes exhibit similar reactivity to free 3-hydroxyflavone.[1099] The flavonolate complex $[(6\text{-}R_2TPA)Zn(3\text{-}Hfl)]ClO_4$ (TPA = tris(2-pyridylmethyl)amine) **199** (Figure 33),[1103] Zn^{II} complexes bearing tetradentate tripodal nitrogen donor ligands and flavonol derivatives **200** or **201**,[1104] and the bipyridine-ligated Zn^{II} complex **202** with a bridging flavonolate ligand[1105] all

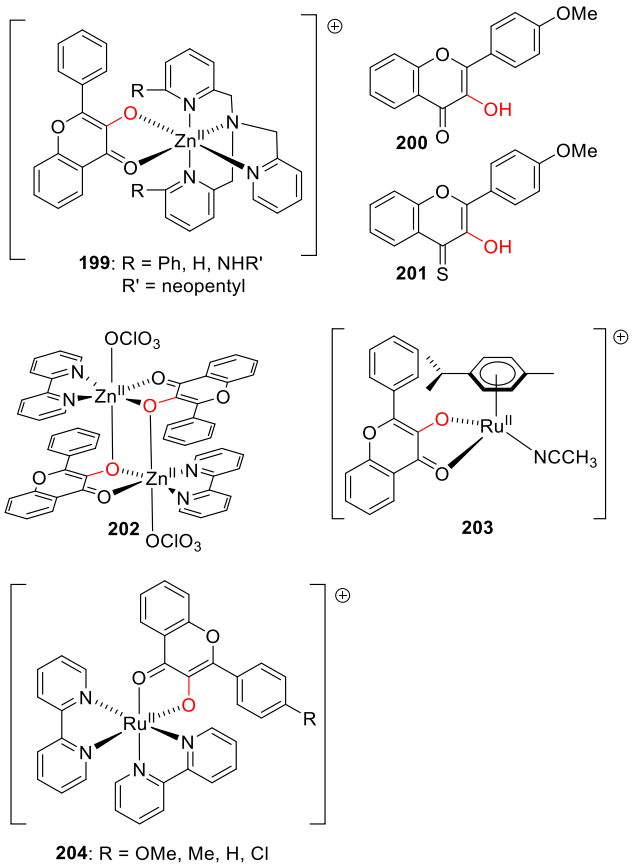

Figure 33. Metal flavonolato complexes and their ligands.

https://dx.doi.org/10.1021/acs.chemrev.0c00663
Chem. Rev. 2020, 120, 13135−13272

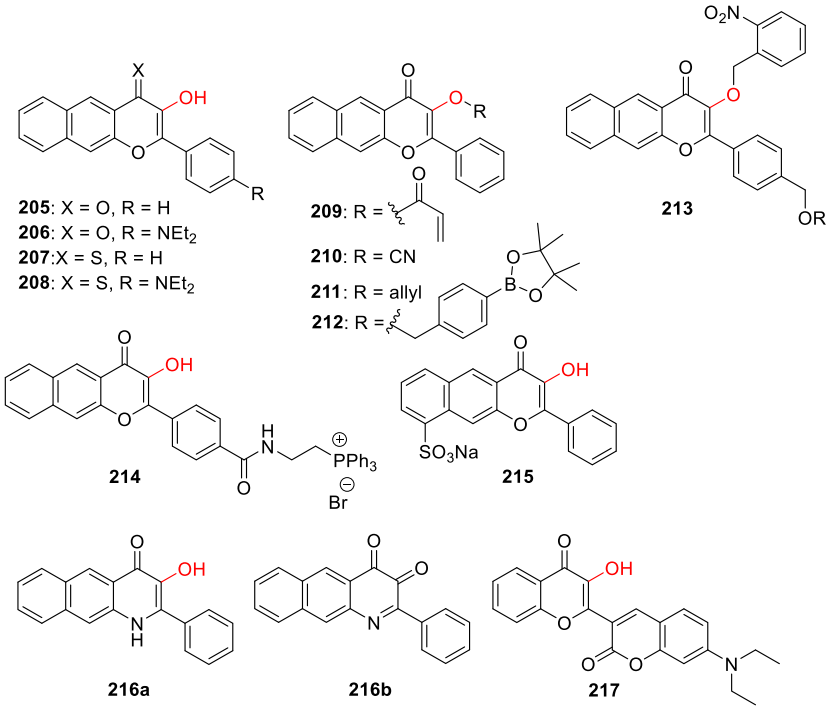

Figure 34. π-Extended flavonol derivatives.

Scheme 67. Photochemistry of Conjugate Acid 205a[1075]

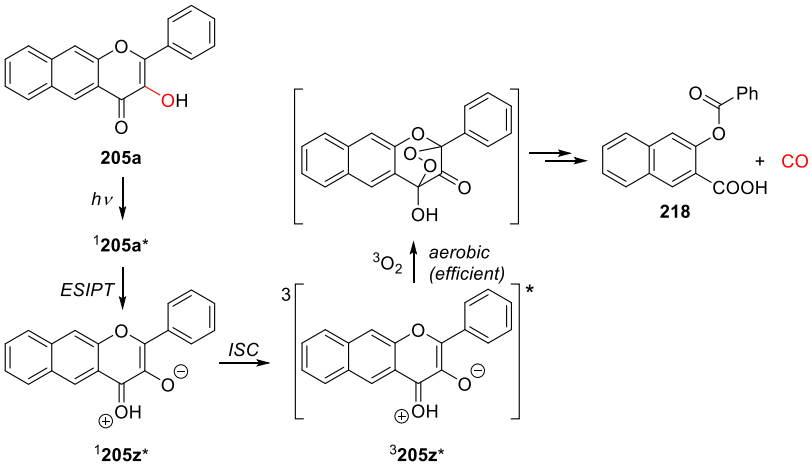

released CO upon irradiation at λ_{irr} > 400 nm. In addition, the Ru^{II} cymene complex **203** released CO upon irradiation at either 300 or 419 nm.[1106] Additionally, Farmer and co-workers synthesized and characterized a series of Ru^{II} bipyridine-substituted flavonolato complexes **204**,[1107,1108] and studied the mechanism of their photooxygenation by $^1O_2$ at low temperatures. Their results suggest that this process occurs via 1,2- or 1,3-addition to the flavonol core.

The π-extended 3-hydroxyflavone **205** (Figure 34) and its derivatives absorb in the visible region.[1076,1109] Displaying photochemistry similar to that of **196**, Berreau and co-workers have demonstrated that 1 equiv of CO is photoreleased from **205**. The reported quantum yield of CO release for **205** (Φ_r = 0.007, λ_{irr} = 419 nm) in DMSO/aqueous buffer (1:1, v/v, pH = 7.4) increased by a factor of 2 upon complexation with Zn^{II} but was reduced by an order of magnitude upon binding to bovine serum albumin.[1110] The 4′-diethylamino-substituted **206** exhibits bathochromically shifted absorption (λ_{max}^{abs} = 442 nm) but with an unchanged photochemical efficiency of CO release.[1076] The structure of **205** was further modified to obtain 4-flavonothione analog **207** and the 4′-diethylamino derivative **208**, which have bathochromically shifted absorption bands (Figure 30).[1076] Compound **207** also had a higher quantum yield of CO release than **205** (Φ_r = 0.4 at 419 nm). Because a free 3-hydroxy group was found to be essential for the photoreactivity of **205**, its substitution with a protecting group sensitive to an external trigger allowed Berreau and co-workers to construct a series of RS^- co-triggered "AND logic gates" that release CO only in the simultaneous presence of oxygen, light, and a thiol. An acryloyl-protected derivative **209**[1111,1112] was activated by thiols including cysteine, while the cyanate-substituted compound **210** proved suitable for intracellular H_2S sensing.[1111] When combined with $PdCl_2$, the allyl-protected flavonol derivative **211** was shown to act as an OFF-ON fluorescent CO sensor that replenishes the CO consumed during detection.[1113] A similar approach was used

https://dx.doi.org/10.1021/acs.chemrev.0c00663
Chem. Rev. 2020, 120, 13135−13272

by Tang and co-workers, who designed the hydrogen peroxide-sensitive compound **212**.[1114] Oxidation of this compound's pinacol boronate ester by hydrogen peroxide liberates free **205**, which can subsequently photorelease CO. The 2-nitrobenzyl-protected flavonol **213** was used by Hu and co-workers to prepare CO-releasing micelles that undergo a tandem photochemical reaction in which 2-nitrobenzyl deprotection is followed by CO release, accompanied by a dual fluorescence response.[1115,1116] Flavonol derivatives substituted with polar groups such as triphenylphosphonium (**214**) were found to target mitochondria and affect cellular bioenergetics.[1117] However, the sulfonated analog **215** did not penetrate through the cell membrane and thus enabled extracellular CO release.[1118] Both derivatives had photochemical properties similar to **205**, allowing Berreau and co-workers to compare the effects of extracellular (**215**), cytosolic (**205**), and mitochondrial-localized (**214**) photoinduced CO release.[1117,1118] The 3-hydroxybenzo[*g*]quinolone derivative **216a** releases one equivalent of CO upon illumination at 465 nm under physiological conditions.[1119] **216b**, an oxidized form of **216a**, is photochemically stable and can act as a prodrug that is activated by thiol-mediated reduction *in vivo*.[1119] The group of Feng recently introduced a coumarin-flavone hybrid **217** that combines the excellent absorption properties of the 7-(diethylamino)coumarinyl moiety with the CO-releasing ability of 3-hydroxyflavone.[1120] Upon irradiation at 460 nm, the excited coumarinyl moiety transfers energy to the fluorescent flavone CO-releasing group. Following CO release, the molecule is transformed into a coumarinyl-substituted salicylic acid derivative with fluorescence similar to that of free 7-diethylaminocoumarin.

The mechanism of the aerobic photodecarbonylation of **205** was the subject of several investigations.[1109,1110] Like its parent flavonol **196**,[1110,1121,1122] the visible-light absorbing **205** exists in both acid (**205a**) and base (**205b**) forms (Schemes 67 and 68; Figure 30).[1123] Klán and co-workers showed that the

Scheme 68. Photochemistry of the Conjugate Base 205b[1075]

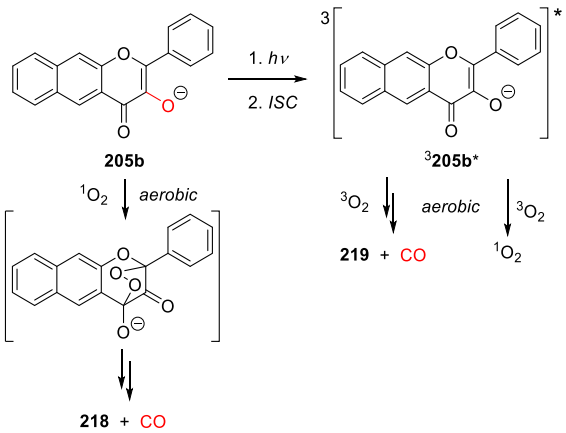

singlet excited state of **205a** undergoes rapid excited-state intramolecular proton transfer (ESIPT) in methanol to give ^{1}**205z*** (z = zwitterion), which intersystem crosses to the triplet ^{3}**205z***. The triplet then reacts with ground-state oxygen, possibly via an endoperoxide intermediate, to release CO (Φ_r = 0.031; Scheme 67).[1075] The conjugate base **205b** releases CO via an oxygenation reaction with singlet oxygen formed by the sensitizing action of the triplet ^{3}**205b*** (Φ_Δ = 0.07; Φ_r = 0.018), and partially via oxidation with $^3O_2$ (Φ_r = 0.003; Scheme 68). There are thus three major orthogonal pathways of CO release. In addition, both forms undergo a very inefficient photorearrangement to release CO in the absence of oxygen. An isotopic labeling study with $^{18}O_2$ revealed that the photoproduct **218** exclusively incorporates ^{18}O atoms.[1076]

Štacko, Klán, and co-workers developed a new class of transition-metal-free photoCORMs by fusing two CO-releasing flavonol moieties with a heptamethine cyanine chromophore (**219a**,**b**, Figure 35).[1124] The resulting hybrids

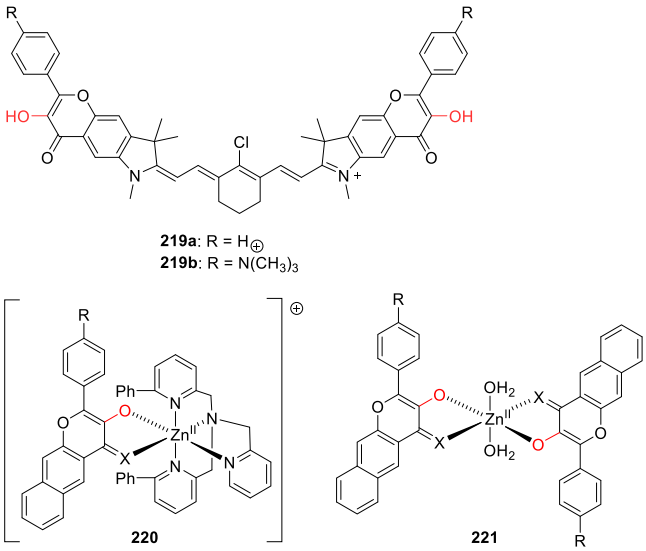

Figure 35. Cyanine-flavonol hybrid **219**[1124] and Zn^{II} complexes **220** and **221**.

released CO in high chemical yields of ∼130% (in principle, 2 equiv of CO can be liberated) upon activation with NIR light of up to 820 nm, with excellent uncaging cross sections ($\Phi_r\varepsilon(\lambda_{793\ nm})$ = 75 for **219b**). The biocompatibility and applicability of these systems *in vitro* and *in vivo* were also demonstrated.

Complexation of **205**, **207**, and **208** with $[Zn^{II}(Ph_2TPA)]^{2+}$ (TPA = tris(2-pyridylmethyl)amine) in **220** (Figure 35) bathochromically shifts their absorption bands by 60−80 nm (e. g., λ^{abs}_{max} = 600 nm for **220**, X = S, R = NEt_2) and increases the CO release quantum yield to almost unity (Φ_r = 0.95 for both **220**, X = S, R = H, and **220**, X = S, R = NEt_2).[1125,1126] One equivalent of CO is always released upon irradiation, and the complexes are active in both the solution and solid phases. In the absence of the TPA ligand, bis-flavonolato-Zn^{II} complexes **221** are formed. These compounds have even more bathochromically shifted absorption spectra (by ∼10 nm) and can release, in principle, 2 equiv of CO originating from the two flavonolato ligands upon irradiation at >545 nm.[1125]

Cyclopropenones are strained systems that liberate CO upon irradiation by UV light.[1127] Most 2,3-alkylcyclopropenones absorb only in the deep UV-region, but their absorption band can be bathochromically shifted by substitution, for example, 2,3-bis(4-methoxyphenyl)-cyclopropenone **222** has a λ^{abs}_{max} of 340 nm (Figure 36).[1127] 2,3-Bis-naphthyl-cyclopropenone derivatives **223** have an absorption tail in the range of 400−440 nm, but 1P absorption leading to decarbonylation occurs only under illumination with UV light

https://dx.doi.org/10.1021/acs.chemrev.0c00663
Chem. Rev. 2020, 120, 13135−13272

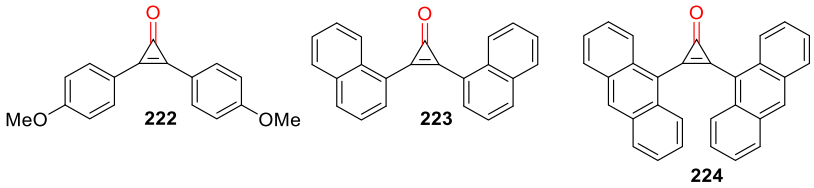

Figure 36. Cyclopropenone photoCORMs.

(λ_{irr} = 350−380 nm).[1128] However, they also efficiently decarbonylate upon non-resonant two-photon absorption at 800 nm. Unfortunately, their strong π-stacking makes them poorly soluble in polar protic solvents, which often limits their usefulness as photoCORMs.

The doubly 9-anthryl substituted cyclopropenone **224** absorbs in the visible region (λ_{max}^{abs} = 465 nm), although excitation at these wavelengths does not induce decarbonylation.[1129,1130] The lowest absorption band of this compound corresponds to an intramolecular excimer of the 9-anthryl substituents and does not weaken the C−C bonds in the cyclopropenone moiety. Derivative **224** thus releases CO only upon excitation with shorter wavelength light (λ_{irr} = 366 nm) due to a very fast adiabatic reaction from an upper excited state that is largely localized in the cyclopropenone chromophore.[1131]

Klán and co-workers discovered that xanthene-based carboxylic acid **140**, isolated as a product from the photoreaction of **139** (Scheme 42, section 2.11), can release carbon monoxide via the triplet-excited state with $\Phi_r = 6.8 \times 10^{-4}$ in aqueous solutions of pH 7.4 upon irradiation at 500 nm (Scheme 69).[763] A 6-fold increase in the quantum yield was obtained at pH 5.7; under these conditions, **140** and its conjugate base exhibit equal absorbance at the irradiation wavelength (Figure 30). The photoreaction cross section $\Phi_r\varepsilon(\lambda_{irr})$ for **140** was on the order of 10 M^{-1} cm^{-1} at λ_{irr} ~500 nm and pH 7.0 (Table 13). Irradiation of **140** at 503 nm in the presence of non-complexed methemoglobin (MetHb, Fe^{II}) in aqueous solution led to the formation of carbonylhemoglobin (COHb). Studies on isotopically labeled **140** ($C^{18}O_2H$) and DFT calculations suggested that an α-lactone intermediate is formed upon irradiation (via a mechanism analogous to that shown for BODIPY-based photoCORMs, *vide infra*), which subsequently thermally decarbonylates to release CO[847,1132,1133] and form 3,6-dihydroxy-9*H*-xanthen-9-one as a photoproduct.[763]

Scheme 69. Photochemistry of photoCORM 140[763]

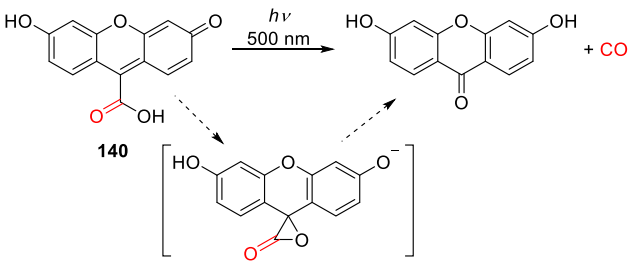

Klán and co-workers also introduced two organic photoCORMs[10,80] based on the BODIPY chromophore, **225a** and **225b**[847] (Scheme 70). The release of CO from **225a** was achieved in 45% chemical yield with $\Phi_r = 1.1 \times 10^{-4}$ in an aerated PBS solution (pH = 7.4) to give 2-methylpyrrole and 2*H*-pyrrole-4-carbaldehyde as the major additional photoproducts.[847] These compounds are typical products of photochemical degradation of BODIPYs.[1134] The release of CO from the π-extended BODIPY **225b**[847] (λ_{irr} = 652 and 732 nm; Figure 30) occurred with a lower quantum efficiency ($\Phi_r = 1.4 \times 10^{-5}$), presumably due to an enhancement of radiationless decay related to the presence of the two flexible styryl groups.[1135,1136] Nevertheless, the release was efficient enough for use *in vivo*: white light-induced photoactivation of **225b** in mice noticeably increased CO levels in the blood and

Scheme 70. Photorelease of CO from BODIPY PhotoCORMs[847]

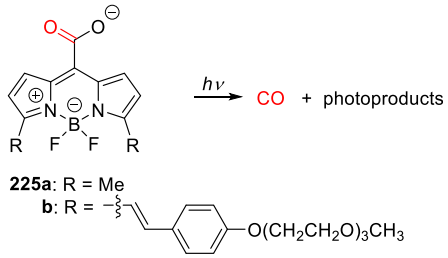

Table 13. Photophysical Properties of Some Organic PhotoCORMs

CORM	λ_{max}^{abs} (nm)	ε_{max} (M^{-1} cm^{-1})	n_{CO}	Φ_r (λ_{irr}/nm)	solvent	ref
140	488	18.6×10^3	(1)[a]	6.8×10^{-4} (500)	PBS	763
191a	461	0.3×10^3	(2)[a]	0.02 (395)	toluene	1085
191e	534	53.8×10^3	(2)[a]	n.d. (450)	DCM	1090
191f	605	135×10^3	(2)[a]	n.d. (450)	DCM	1090
205	409	16.2×10^3	0.96	0.0073 (419)	CH_3CN	1075, 1076, 1109
208	543	79.4×10^3	1.00	n.d.	CH_3CN	1076
224	465 (inactive)	17.8×10^3				
	374 (active)	8.9×10^3	(1)[a]	0.14 (366)	cyclohexane	1131
225a	502	49.0×10^3	0.87	2.7×10^{-4} (500)	PBS	847
225b	652	52.5×10^3	0.91	1.2×10^{-5} (365)	PBS	847

[a]Theoretical yield of CO equivalents. PBS = phosphate-buffered saline; DCM = dichloromethane.

https://dx.doi.org/10.1021/acs.chemrev.0c00663
Chem. Rev. 2020, 120, 13135−13272

some tissues.[847] The involvement of a triplet excited state was established by transient spectroscopy, oxygen quenching experiments, and experiments using CsCl as a heavy-atom-effect mediator.[1137] The benzyl ester derivative of **225a** was photostable, and the photolysis of **225a** at pH 2.5 proceeded with a ∼4-fold lower quantum efficiency than at pH = 7.0. This was in agreement with the calculated ΔG_{eT}, which predicted a more efficient intramolecular electron transfer from the carboxylate to the triplet-excited BODIPY core than for the protonated form.[847] The proposed mechanism of the photoreaction is shown in Scheme 71. Upon excitation, a strongly

Scheme 71. Proposed Mechanism of CO Photorelease from BODIPY PhotoCORMs 225a,b[847]

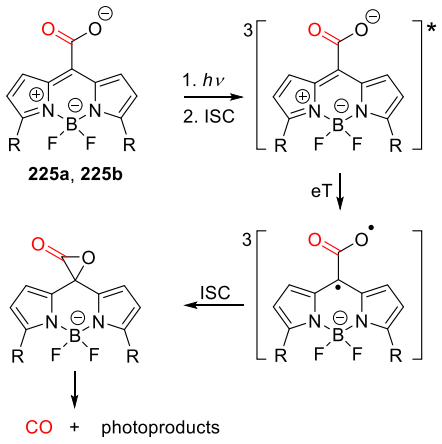

fluorescent singlet excited state of **225** undergoes relatively inefficient ISC to the triplet state followed by an exergonic electron transfer (eT) from the carboxylate to the BODIPY core to form an oxyallyl-type triplet diradical.[1138] The diradical then intersystem crosses to an open-shell singlet state, followed by the formation of α-lactone on the singlet ground-state potential energy surface.[847] Finally, thermal fragmentation of the lactone releases CO.[1132,1133]

4.1.2. Release of Carbon Monoxide from Transition-Metal-Containing PhotoCORMs. Most of the known photochemically activatable CO-releasing molecules (photoCORMs) are based on metal carbonyl complexes that undergo photoinduced cleavage of the carbonyl moiety followed by the addition of a solvent molecule to the vacant position in the metal's coordination sphere.[83] The mechanisms of photochemical CO release from the coordination sphere of a transition metal have been studied in detail.[1139−1141] The carbonyl−metal bond is relatively strong (∼20−40 kcal mol^{-1})[1142] because of its π-backbonding character. Delocalization of the LUMO on the carbonyl moiety is a general requirement for the photochemical liberation of CO.[1140] The photocleavage is a reversible process; the recombination of the liberated CO molecule with the vacancy on the metal's coordination sphere regenerates the photoCORM and thus reduces the quantum yield of CO release. This can be avoided by using ancillary ligands that shift electron density away from the metal center and reduce the amount of metal−CO backbonding.[1139] It has been shown that not all carbonyl ligands are cleavable from complexes containing multiple carbonyl moieties and not all CO molecules are released in the primary photochemical step. CO can also be liberated by subsequent solvolysis or oxidative steps.[82,1140,1143]

The first report on a photoCORM was published by Motterlini and co-workers, who described the photodissociation of $Fe(CO)_5$ and complex **226** (Figure 37).[1144] The term

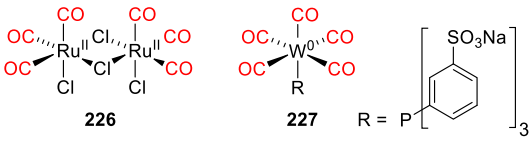

Figure 37. Structures of some UV-absorbing photoCORMs.

photoCORM was introduced by Rimmer and co-workers in reference to W^0 complex **227** (Figure 37), which releases one equivalent of CO upon irradiation.[1143] The first transition-metal-containing photoCORMs required excitation at wavelengths in the range of 310−360 nm,[1139,1145] but strategies for bathochromically shifting their spectra were introduced by Mascharak and co-workers.[1146] The use of nitrogen-based ligands with extended π-conjugation can lower the energy of the LUMO, while strongly donating ancillary σ-and π-donors raise the HOMO energy. The combination of such ligands with highly thermostable carbonyl complexes of electron-rich d^6 metal ions such as Mn^I, Re^I, Fe^{II}, or Ru^{II} gives rise to bathochromically shifted MLCT absorption bands.

Many visible-light-absorbing photoCORMs are based on Mn^I complexes. For example, Mn^I complexes with bidentate heteroaryl-imine ligands (Table 14) exhibit absorption maxima in the range of 390−700 nm. The absence of the σ-donating ligand Br^-(as in **228b**, **229b**, and **231b**) caused a hypsochromic shift of 60−110 nm (Figure 31) and reduced the CO release efficiency by a factor of ∼1.1−3.5 relative to the reference analogs (**228a**, **229a**, and **231a**).[1079,1146,1147] Extending the conjugation of the aromatic ligand, for example, by replacing pyridine with quinoline (as in complexes **229a**, **229b**, and **234**), bathochromically shifted the MLCT band absorption maximum by ∼35−45 nm and also increased the quantum yield of CO release. Complexes **232**, **233**, and **234** (Table 14) containing α-diimine ligands were designed to be more soluble in water.[1148] Irradiation of **233** released 3 equiv of CO, but the quantum yield of this process declined by factors of ∼2 and 3 in dichloromethane and aqueous solutions, respectively. The CO release efficiency of these complexes increased in the order **232** < **233** < **234**, paralleling the increase in the electron-donating abilities of their ligands. Studies on analogous Mn^I and Re^I complexes containing 4-aminophenyl instead of adamantyl ligands revealed that only manganese complex **235** photoreleased CO upon visible light irradiation.[1149] Zobi and co-workers studied a series of Mn^I-tricarbonyl complexes bearing azobipyridine ligands (**236a−e**, Table 14).[1150] CO was liberated upon their illumination with red light (≥625 nm), and DFT calculations indicated that electron-withdrawing substituents lowered the LUMO energy more than that of the HOMO, resulting in a bathochromic shift of the MLCT band maximum. Complex **236e**, which bore the strongest electron-withdrawing groups (CF_3 and Cl) was even activatable at the tail of the absorption range (810 nm). In the dark, complexes **236a** and **236b** were stable but the electron-poor complexes **236c−e** slowly released CO. A series of 8 benzimidazole-based photoCORMs **230** was recently studied by Schatzschneider.[1151] These compounds rapidly released CO upon illumination, and their photochemistry was sensitive to their substitution. The 4-NO_2 substituted derivative **230** exhibited the most bathochromically shifted

https://dx.doi.org/10.1021/acs.chemrev.0c00663
Chem. Rev. 2020, 120, 13135−13272

Table 14. Mn^{I}-Based photoCORMs Containing Bidentate Heteroaryl-Imine Ligands[a]

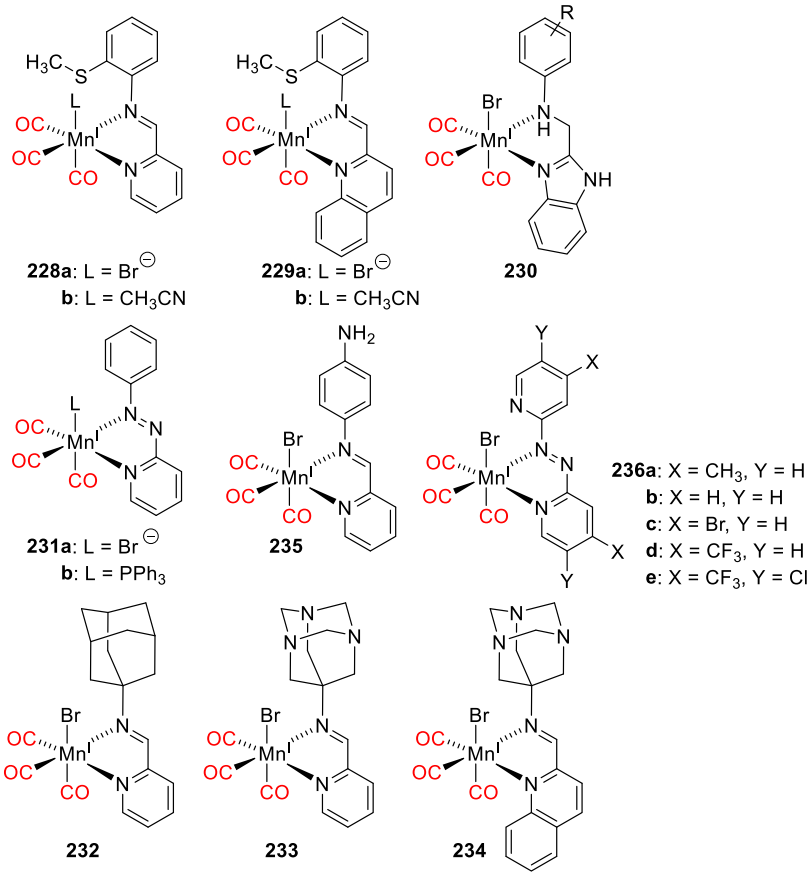

CORM	λ_{max}^{abs} (nm)	ε_{max} (M^{-1} cm^{-1})	n_{CO}	Φ_r (λ_{irr}/nm)	solvent	ref
228a	500	2.5×10^3	<3	0.34 (509)	THF	1079
228b	390	3.6×10^3	<3	0.12 (509)	CH_3CN	1079
229a	535	2.2×10^3	<3	0.37 (509)	THF	1079
229b	435	3.7×10^3	<3	0.34 (509)	CH_3CN	1079
230	386−495	$1.3–2.2 \times 10^3$	0.8−1.8	n.d. (412 or 468)	DMSO	1151
231a	586	3.9×10^3	n.d.	0.48 (550)	CH_3CN, DCM	1146, 1147
231b	520	4.1×10^3	n.d.	~0.33[b] (420)	DCM	1146, 1147
232	445	1.8×10^3	n.d.	~0.18[b](≥450)[e]	DCM	1148
233	455	2.1×10^3	3	0.35 (≥450)[e]	DCM	1148
				~0.16[b]	PBS	
				~0.10[b]	H_2O	
234	490	1.9×10^3	n.d.	~0.78[b](≥450)[e]	DCM	1148
235	437	n.d.	3	n.d. (525 or 468)	DMSO	1149
236a	625	4.35×10^3	n.d.	n.d.	DCM	1150
				($\tau_{1/2}$ = 3.52 h)[c]	(H_2O)[d]	
236b	630	4.43×10^3	n.d.	n.d.	DCM	1150
				($\tau_{1/2}$ = 3.60 h)[c]	(H_2O)[d]	
236c	661	3.46×10^3	n.d.	n.d.	DCM	1150
				($\tau_{1/2}$ = 1.21 h)[c]	(H_2O)[d]	
236d	678	3.76×10^3	n.d.	n.d.	DCM	1150
				($\tau_{1/2}$ = 0.48 h)[c]	(H_2O)[d]	
236e	693	4.85×10^3	n.d.	n.d.	DCM	1150
				($\tau_{1/2}$ = 0.41 h)[c]	(H_2O)[d]	

[a]n.d.: not determined, PBS = phosphate-buffered saline, THF = tetrahydrofuran, DMSO = dimethyl sulfoxide, DCM = dichloromethane. [b]Values estimated from the relative apparent CO release rates (k_{CO}). [c]Relative half-lives in the series **236a−e**; samples were irradiated at λ_{max}^{abs}. [d]Aqueous solutions were used in the Mb assay[1152] to determine CO release. [e]Broadband visible light with a cut-off filter was used.

absorption but released CO with the lowest observed chemical yield because of a competing photodecomposition process.

α,α′-Diimines and related ligands can also be used to tune the properties of Mn^{I}-based photoCORMs. For example, the Mn^{I} *fac*-complex **237** (Table 15, L = Br^-, Ar = 2,6-*i*Pr_2Ph)

https://dx.doi.org/10.1021/acs.chemrev.0c00663
Chem. Rev. 2020, 120, 13135−13272

Table 15. Mn^I-Based PhotoCORMs Containing α,α'-Diimino, Iminoketone, or Carbothioamide Ligands[a]

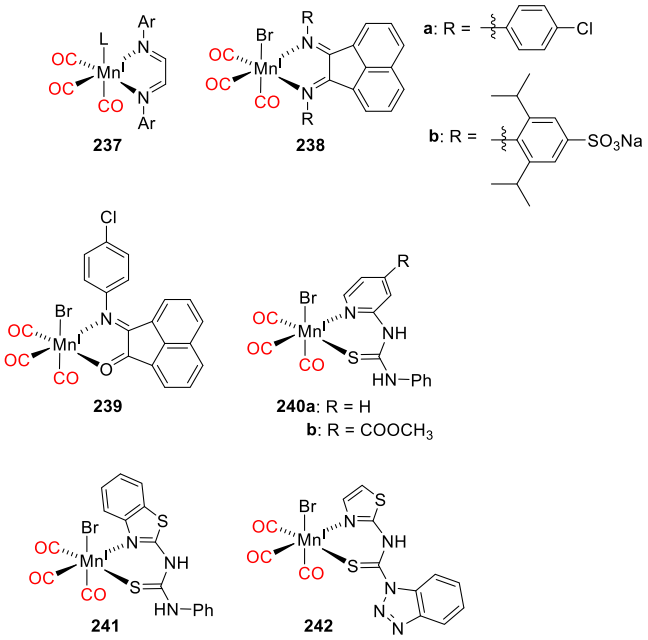

CORM	λ_{max}^{abs} (nm)	ε_{max} (M^{-1} cm^{-1})	n_{CO}	Φ_r (λ_{irr}/nm)	solvent	ref
237 (L = Br^-)	582	n.d.	<1	n.d. (560)	THF	1153
238a	570	4.6×10^3	3	0.70 (545)	CH_3CN	1080
238b	513 (H_2O)	2.1×10^3	1	0.54 (545)	H_2O	1154
	568 (MeOH)			0.30 (623)		
				0.38 (623, deg.)[c]		
239	630	3.7×10^3	n.d.	~0.46[b] (>520)	CH_3CN	1080
240a	398	n.d.	2	n.d. (468)	DMSO	1156
240b	407	n.d.	2	n.d. (468)	DMSO	1156
241	387	n.d.	1	n.d. (468)	DMSO	1156
242	437	6.1×10^3	1.5	n.d. (468 or 525)	DMSO	1157

[a]THF = tetrahydrofuran, DMSO = dimethyl sulfoxide. [b]Values estimated from relative apparent CO release rates (k_{CO}). [c]deg.: degassed.

releases CO upon irradiation with green light.[1153] Its photoactivity can be attributed to an MLCT transition from the Mn^I−CO π and Br-centered orbitals to the π^* orbitals of the diamine ligand, which weakens Mn−CO π-backbonding and thus facilitates CO release. The substitution of the bromide ligand with a neutral molecule (**237**, L = CO, THF, CH_3CN, *t*BuCN) afforded complexes absorbing at 420 nm. A tetracarbonyl complex (**237**, L = CO) was reactive in the dark and rapidly released CO upon dissolution in acetonitrile or THF. UV-photolysis of **237** (L = Br^-) in THF released one equivalent of CO along with the Br^- ligand isomerization, and the resulting dicarbonyl complex coordinated CO to form meridional isomer of **237**. The complexation of highly conjugated ligands derived from α,α'-diimines with the [$Mn(CO)_3Br$] moiety, as in **238a** (Figure 31) and **238b** (Table 15), led to exceptionally efficient CO release.[1080,1154] Complex **238b** reportedly released CO in the IR region upon irradiation above 780 nm, where the compound does not absorb noticeably.[1154] The authors attributed this to a weak but not completely forbidden optical population of the lowest triplet excited state of the complex. Similar S_0−T_1 absorption was later observed for carbazole derivatives.[1155] The complex **238b** exhibited strong solvatochromism, which was rationalized by suggesting that its lowest-lying singlet excited state has a charge-transfer character. Complex **239** (Table 15), bearing an iminoketone ligand, has a significantly bathochromically-shifted absorption maximum at 630 nm (Figure 31) and retains CO releasing ability.[1080] A series of thiourea- and thiazolyl-benzotriazolyl-carbothioamide-based Mn^I photoCORMs **240a**, **240b**, **241**, and **242** (Table 15) were also reported to release 1-2 equiv of CO.[1156,1157]

A Mn^I tricarbonyl structural motif was used to develop several bipyridine-based visible-light absorbing photoCORMs. Polypyridyl-containing metallodendrimers **243** (Table 16, n = 4, 8; R = 1,4-diaminobutane-poly(propyleneimine); DAB-PPI) released ~65% of their total content of CO ligands upon irradiation with 410 nm light.[1158] Complex **244** (Table 16) releases CO upon irradiation with blue light, while photoCORMs combining **244** and lanthanide ion-doped upconversion nanoparticles (see section 6.4.2) based on Yb^{III}- and Tm^{III}-doped Gd^{III} salts coated with a polymer matrix consisting of phospholipid-functionalized poly(ethylene glycol) released CO upon irradiation at 980 nm.[1159] Blakemore, Elles, and coworkers recently studied 4,4′-disubstituted 2,2′-bipyridyl complexes **245** (R_1 = R_2 = NO_2, CF_3, H, *t*Bu; Table 16) and the influence of the ligand's electronic properties on the CO release rate,[1160] showing that irradiation into the MLCT band caused rapid CO release (τ_{CO} = 0.46−0.68 ps) followed by solvent coordination (τ_{solv} = 18−39 ps). A recent mechanistic study by Pordel and White examined a series of tricarbonylmanganese(I) complexes with 4,4′-substituted 2,2′-bipyridine ligands (bpy′) *fac*-[Mn(bpy′)$(CO)_3$L; L = Br^- or

https://dx.doi.org/10.1021/acs.chemrev.0c00663
Chem. Rev. 2020, 120, 13135−13272

Table 16. Mn^{I}-Based PhotoCORMs with Heteroaryl Bidentate Ligands and Their Analogs[a]

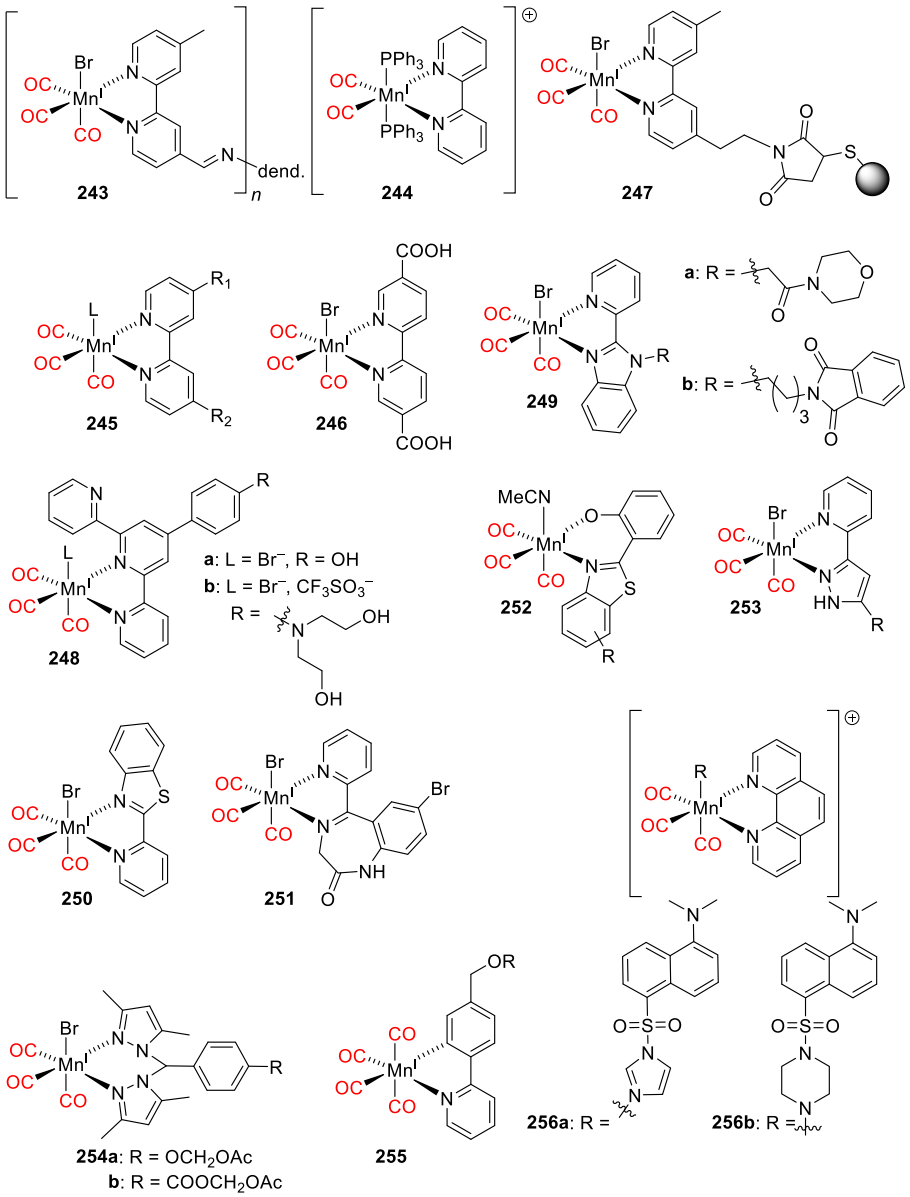

CORM	λ_{max}^{abs} (nm)	ε_{max} (M^{-1} cm^{-1})	n_{CO}	Φ_r (λ_{irr}/nm)	solvent	ref
243, n = 4	410	10.3×10^3	7.56	2.66×10^{-3} (410)	DMSO:H_2O	1158
n = 8	420	18.8×10^3	15.24	2.71×10^{-3} (410)	1:9, v/v	
244	400	5.4×10^3	1.85	0.26 (470)	DCM	1159
245						
L = Br^-, R_1 = R_2 = CO_2Me	460	3.2×10^3	~3	0.32 (405)	CH_3CN	1161
L = Br^-, R_1 = R_2 = H	416	2.9×10^3	~3	0.22 (405)	CH_3CN	
L = Br^-, R_1 = R_2 = Me	411	2.9×10^3	~3	0.20 (405)	CH_3CN	
L = py, R_1 = R_2 = CO_2Me	420	4.0×10^3	~3	0.19 (405)	CH_3CN	
L = py, R_1 = R_2 = H	383	3.4×10^3	~3	0.17 (405)	CH_3CN	
L = py, R_1 = R_2 = Me	378	3.4×10^3	~3	0.15 (405)	CH_3CN	
L = Br^-, R_1 = R_2 = *t*Bu	412	2.4×10^3	n.d.	n.d. (415)	CH_3CN	1160
L = Br^-, R_1 = R_2 = H	415	2.3×10^3	n.d.	n.d. (415)	CH_3CN	
L = Br^-, R_1 = R_2 = CF_3	457	1.5×10^3	n.d.	n.d. (415)	CH_3CN	
L = Br^-, R_1 = R_2 = NO_2	510	0.2×10^3	n.d.	n.d. (415)	CH_3CN	
246	410	n.d.	3	n.d. (460)	DMSO	1164
247	385	n.d.	2.84	n.d. (456)	PBS, pH = 7	1165
248a, R = OH	422	n.d.	n.d.	(k_{CO} = 0.07 min^{-1})[b] (410)	CH_3CN	1166
R = O^-	490	n.d.		(k_{CO} = 0.81 min^{-1})[b] (410)	CH_3CN	
248b, L = Br^-	428	35.3×10^3	3	0.19 (451)[c]	ethanol:PBS	1167

https://dx.doi.org/10.1021/acs.chemrev.0c00663
Chem. Rev. 2020, 120, 13135−13272

Table 16. continued

CORM	λ_{max}^{abs} (nm)	ε_{max} (M^{-1} cm^{-1})	n_{CO}	Φ_r (λ_{irr}/nm)	solvent	ref
L = $CF_3SO_3^-$	428	28.6×10^3	3	0.04 (451)[e]	2:1, v/v	
				0.22 (451)[c]		
				0.06 (451)[e]		
249a	396	n.d.	~2.5	($k_{CO} = 16 \times 10^{-4} s^{-1}$)[d](468)	DMSO	1168
249b	401	n.d.	~2.5	($k_{CO} = 37 \times 10^{-4} s^{-1}$)[d] (468)	DMSO	1168
250	450	3.2×10^3	n.d.	n.d. (>440)	DCM	1169
251	465	3.2×10^3	2.85	n.d. (470)	DMSO	1170
252	440−640	$0.15-3.0 \times 10^3$	n.d.	n.d. (400−700)	CH_3CN	1171
253	393	n.d.	0.09[f]	n.d. (480)	CH_3OH	1172
254a	375	1.5×10^3	3	0.18 (405)	PBS	1173
				0.31 (470)		
254b	379	1.4×10^3	3	0.17 (405)	PBS	1173
				0.43 (470)		
255	340	3.6×10^3	2.5	n.d. (400)	DMSO	1174
256a	370	5×10^3	3	0.35 (380)	CH_3CN	1175
256b	350	6.2×10^3	3	0.39 (>410)	CH_3CN	1176

[a]DMSO = dimethyl sulfoxide, DCM = dichloromethane, PBS = phosphate buffer saline. [b]Relative rate of the CO release of **248a**. [c]Quantum yield for the release of the first equivalent of CO. [d]Quantum yield for the release of the second equivalent of CO. [e]Relative rates of CO release from **249a** and **249b**. [f]Measured by irradiation of solid crystalline phase. dend. = 1,4-diaminobutane dendrimer. **247**: the sphere represents the membrane-puncturing needle domain of bacteriophage T4.

py] **245** (Table 16).[1161] In accordance with the findings of Mascharak and co-workers,[86] substituting the electron-donating Br^- ligand with a π-accepting pyridine stabilized the Mn^I-based HOMO, causing a hypsochromic shift of the absorption maxima (by 100−150 nm), and reduced the quantum yield of CO release. The regioselectivity of CO release could also be tuned: the CO ligand *cis* to L was liberated first when L = Br^-, but the *trans*-CO was liberated first when L = py. Increasing the π-acidity of the bipyridine ligands also increased the efficiency of the CO release, although this effect was comparatively weak. The absorption spectra and energies of the MLCT states of 50 different *fac*-$[M(CO)_3]^+$ complexes (M = Mn^I, Re^I) evaluated as potential photoCORMs were recently analyzed and mathematically correlated by the group of Zobi.[1162]

Zobi and co-workers also developed hybrid systems referred to as quantum-CORMs that combine Mn^I-tricarbonyl complexes **245** (Table 16) with bipyridyl ligands containing anchoring groups (R_1 = H, COOH; R_2 = COOH, NH_2, (4-carboxyphenyl)ethynyl, and (4-aminophenyl)ethynyl) that were used to bind the Mn complexes to the surfaces of CdSe/ZnS core/shell semiconductor quantum dots (see also section 6.4.1).[1163] These quantum dots have a band-gap wavelength of 504 nm and bright emission at 512 nm. Upon irradiation at 510 nm, they sensitize the release of CO from the photoCORM, increasing its efficiency 2- to 6-fold compared to non-sensitized excitation.

Furukawa and co-workers developed light-responsive metal-organic frameworks as controllable CO-releasing cell-culture substrates.[1164] These materials combine a Mn^I tricarbonyl bipyridyl complex **246** (Table 16) with a highly robust Zr^{IV}-based MOF. The group of Ueno developed a construct containing an artificial protein needle by conjugating the membrane puncturing needle domain of bacteriophage T4 to the Mn^I carbonyl photoCORM complex **247** (Table 16) via a maleimide thiol linkage.[1165] This system was used as an *in vivo* magnetic-resonance-imaging contrast reagent. Allosteric regulation of CO release was demonstrated in complex **248a** (Table 16),[1166] in which the phenolic substituent of the terpyridyl ligand responds to fluoride ions by undergoing deprotonation, leading to allosteric activation of CO release; the deprotonated complex released CO approximately 1 order of magnitude more efficiently than its neutral form. Ford and co-workers synthesized another terpyridine-based manganese tricarbonyl complex **248b** (Table 16), which can release CO both by 1-photon excitation in the visible region and also by 2-photon excitation at 750 and 800 nm because the terpyridine ligand acts as an efficient 2-photon antenna.[1167]

Potentially bioactive Mn^I tricarbonyl complexes with 2-(2′-pyridyl)benzimidazole ligands bearing morpholino (**249a**) or phthalimido (**249b**, Table 16) substituents were studied spectroscopically and computationally by Mansour and Ragab.[1168]

Another Mn^I tricarbonyl photoCORM, **250** (Table 16), contains a benzothiazole ligand that functions as a turn-on fluorescent signal.[1169] Upon photoexcitation, this complex releases both CO and the 2-(2-pyridyl)-benzothiazole ligand, whose fluorescence was successfully used to monitor the CO-induced death of human breast cancer cells treated with **250**. The similar Mn^I complex **251** (Table 16), which has a ligand derived from the anti-anxiety drug bromazepam, was reported by Mansour.[1170]

A series of four photoCORMs **252** (Table 16) bearing 2-(benzo[*d*]thiazol-2-yl)phenol ligands, was developed by Roy and co-workers,[1171] and tricarbonyl Mn^I complexes with 3-(2-pyridyl)pyrazole ligands **253** (Table 16) were shown to release CO independently of the choice of R substituents.[1172]

Mn^I tricarbonyl photoCORMs **254a** and **254b** (Table 16), containing substituted bispyrazolylmethane ligands, were prepared by the group of Westerhausen.[1173] These complexes are initially neutral but their ligands have terminal acetyl groups that are hydrolyzed into carboxylates upon cellular uptake. As a result, the photoCORMs become anionic and are trapped inside the cells. Fairlamb, Lynam, and co-workers synthesized a series of biotin-conjugated Mn^I-based photoCORMs **255** (R = biotin; Table 16) that release CO upon irradiation at 400 nm and bind efficiently to avidin.[1174]

Fluorescent dansylimidazole-substituted complex **256a** (Table 16) released CO upon irradiation with visible light.[1175] Its analog **256b** exhibited strong green luminescence

https://dx.doi.org/10.1021/acs.chemrev.0c00663
Chem. Rev. 2020, 120, 13135−13272

that could be visualized *in vitro*.[1176] This class of luminescent Mn^I-based photoCORMs was extended by preparing dansyl-imidazole complexes with diazabutadiene ligands bearing sterically similar adamantyl (lipophilic) or 1,3,5-triaza-adamantyl (hydrophilic) substituents.[1177] Changing the ligand's lipophilicity altered the localization of the photoCORMs in cellular organelles.

Tridentate heteroaryl ligands form stable complexes with Mn^I and were used for the successful design of photoCORMs. Very recently, the group of Schiller introduced a novel class of 2-photon absorbing naphthalimide-containing photoCORMs **257** (Figure 38).[1178] These compounds release CO by both 1-(405 nm) and 2-photon (800 nm) excitation. CO liberation is accompanied by the release of the naphthalimide ligands, which are fluorescent in solution, in non-woven fabrics, and in HeLa cells. Similar naphthalimide-substituted photoCORMs **257** (X = NR) were used to synthesize green light-responsive (550 nm) CO-releasing polymeric materials by ring-opening metathesis polymerization.[1179]

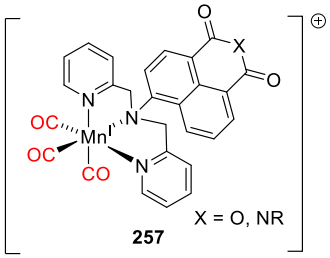

Figure 38. Naphthalimide substituted photoCORM.

Schiller and co-workers developed the dabsyl-substituted Mn^I tricarbonyl complex **258** (Figure 39), which releases CO upon irradiation at 405 nm.[1180] The complex was loaded onto paper strips to form a material whose light-triggered CO release could be monitored with the naked eye by observing the change in its color. An analogous approach was used in the design of the colorimetric and fluorometric dual response photoCORM **259** (Figure 39), which is based on the nitrobenzoxadiazole fluorophore and releases CO upon irradiation at 490 nm.[1181]

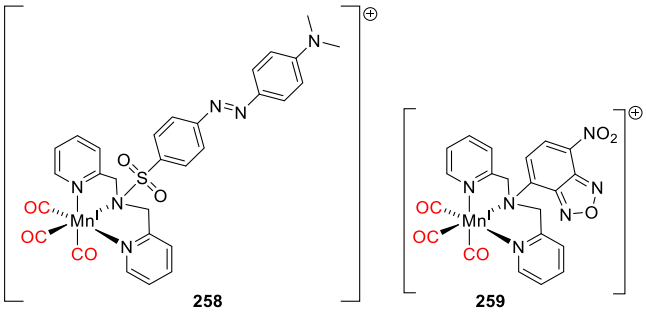

Figure 39. Dabsyl- and nitrobenzoxadiazole-substituted photoCORMs.

Mn^I-based photoCORMs with other structures have also been reported (Table 17). For example, Ueno and co-workers developed a series of engineered protein crystals using the photoCORM $Mn(CO)_5Br$.[1182] Polyhedral crystals containing histidine as a ligand were used to immobilize the Mn^I carbonyl complex **260** (Table 17). Two proteins were prepared, a wild-type (WT) with 3 histidine units and mutants with hexahistidine tags containing 3 or 6 equiv of the photoCORM. The CORM loading and the corresponding quantum yields of CO release correlated with the number of histidine residues in the protein.

Mn^I tricarbonyl complexes with tazarotene (**261**) and metamizole (**262**) as bidentate and tridentate ligands, respectively, were developed by Mansour and Shebab (Table 17).[1183] Both ligands dissociate from the metal center upon the CO photorelease. In addition, Manimaran and co-workers developed a series of 10 Mn^I-based aminoquinonato-bridged dinuclear complexes **263** (Table 17) that release CO upon irradiation with green light.[1184] The mechanism of CO release from the Mn^I tryptophanate complex **264** (Table 17)[1185] was studied by time-resolved ultrafast infrared spectroscopy (TRIR) and TD-DFT,[1186] which revealed that excitation leads to an LMCT from the indole moiety of the tryptophan ligand to the metal d-orbitals. The loss of CO then occurs within 3 ps, resulting in the formation of the triplet state of the dicarbonyl product $^3[Mn^I(tryp)(CO)_2(MeCN)]$, which is solvated within 20 ps. The mechanism of CO release from **264** was further studied by laser-interfaced mass spectrometry (LIMS) across a wide wavelength range (λ_{irr} = 234−580 nm).[1187]

Zobi and co-workers studied a *fac*-Mn^I tricarbonyl complex with a tetraazacyclotetradecane ligand attached to the 5′−OH ribose group of vitamin B_{12} (**265**, Table 17).[1188] Vitamin B_{12} acts as a biocompatible water-soluble scaffold that allows the photoCORM to be actively transported into cells. Because of its remote attachment, it does not affect the photochemistry of the Mn^I complex. The compound was successfully delivered into fibroblasts, where the photoinduced release of CO protected them against death under conditions of hypoxia and metabolic depletion.

The group of Westerhausen developed a series of water-soluble manganese tricarbonyl complexes **266** and **267** (Table 17) based on tridentate aminoalkylsulfide ligands.[1189] Accumulation of these complexes inside cells was observed by FT-IR imaging. Peralta and co-workers recently synthesized three analogous water-soluble complexes **268** and **269** (R = H, CH_3) that sequentially release three equivalents of CO upon irradiation with blue light.[1190] The thiolato-bridged Mn^I-dimer **270** (Table 17) prepared from cysteamine by Westerhausen and co-workers was shown to photochemically release all 6 of its bound CO ligands.[1191]

Schiller and co-workers demonstrated the photochemically controlled release of CO from non-woven polylactide fibers containing the Mn^0 decacarbonyl complex ($Mn_2(CO)_{10}$, CORM-1).[1192] They later constructed a device for remote-controlled delivery of CO using tetranuclear Mn^I-based complexes **271** (Table 17, R = *n*Pr, *n*Bu) embedded in non-woven polylactide or polymethacrylate fabrics[1193] that were shown to be nontoxic towards 3T3 mouse fibroblast cells.

A new strategy for triggering the photochemical release of caged CO using long-wavelength and NIR light was described by Ford and co-workers using dinuclear Rh^0−Mn^0 carbonyl complexes **272** (Table 17).[1194] These complexes have strong metal−metal-bond-to-ligand charge-transfer (MMLCT) absorption bands from ∼550 to ∼720 nm. Their photoexcitation leads to homolytic cleavage of the Re−Mn bond, yielding mononuclear metal radicals that tend to recombine in the absence of trapping agents but react with dioxygen to form active species that efficiently release CO via secondary thermal

https://dx.doi.org/10.1021/acs.chemrev.0c00663
Chem. Rev. 2020, 120, 13135−13272

Table 17. Other Mn-Based PhotoCORMs[a]

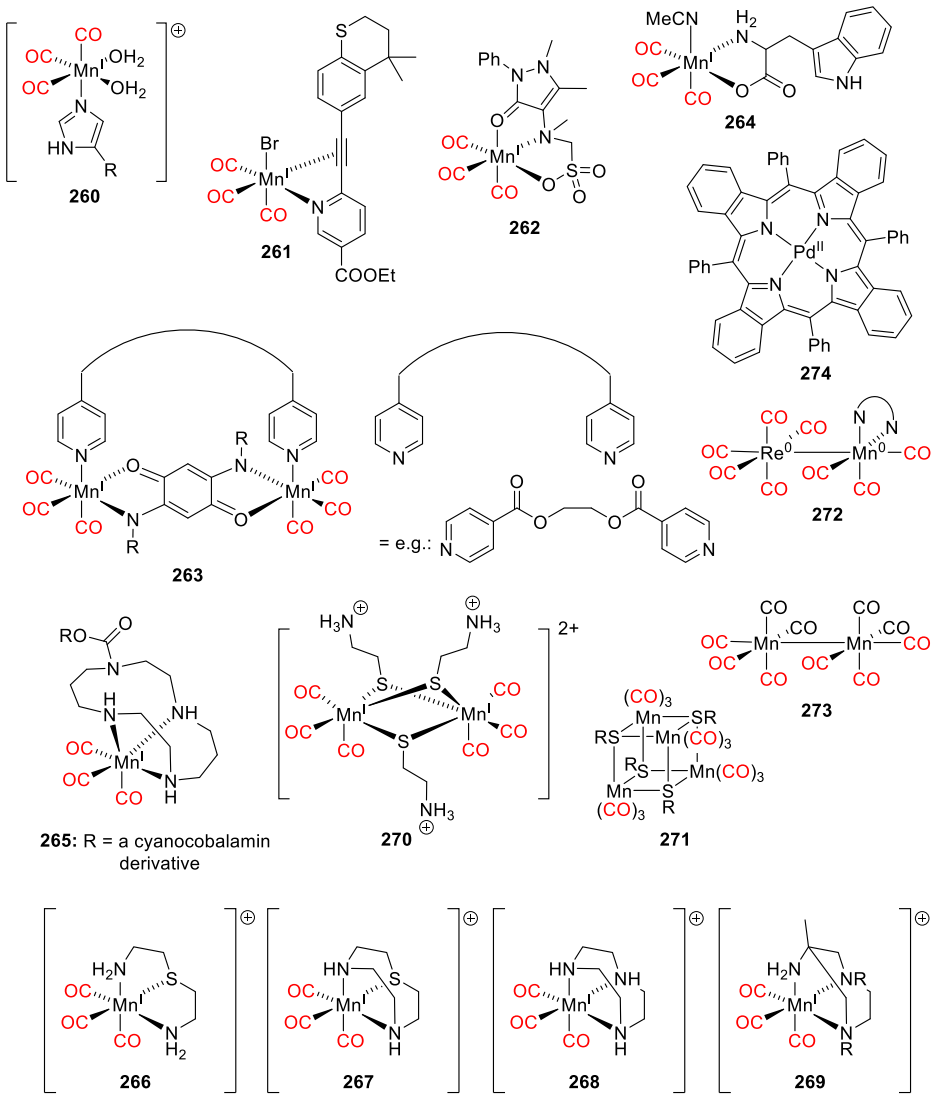

CORM	λ_{max}^{abs} (nm)	ε_{max} (M^{-1} cm^{-1})	n_{CO}	Φ_r (λ_{irr}/nm)	solvent	ref
260	n.d.	n.d.	1.9[b]	0.013[b] (456)	PBS	1182
			2.9[c]	0.047[c] (456)		
261	435	n.d.	~1	n.d. (468)	DMSO	1183
262	395	n.d.	~0.5	n.d. (410)	DMSO	1183
263	465−486	n.d.	1.7−1.9	n.d. (520−560)	DCM	1184
264	360	1.4×10^3	2	n.d. (400)	CH_3CN	1185
			1.4	n.d. (465)		
265	388	n.d.	3	n.d. (470)	H_2O	1188
266	354	n.d.	2.86 (405)	0.1 (365)	PBS	1189
267	350	n.d.	2.61 (405)	0.06 (365)	PBS	1189
268	344	1.1×10^3	3	0.054 (385)	H_2O	1190
				0.030 (410)		
269					H_2O	1190
R = H	349	1.3×10^3	3	0.058 (385)		
				0.044 (410)		
R = CH_3	354	1.4×10^3	3	0.081 (385)		
				0.033 (410)		
270	384	n.d.	6	0.11 (365)	PBS	1191
				0.06 (470)		
271						1193
R = *n*Pr	385	1.8×10^3	n.d.	n.d. (405)	$CHCl_3$	
R = *n*Bu	n.d.	n.d.	n.d.	n.d. (405)	$CHCl_3$	
272						1194

https://dx.doi.org/10.1021/acs.chemrev.0c00663
Chem. Rev. 2020, 120, 13135−13272

Table 17. continued

CORM	λ_{max}^{abs} (nm)	ε_{max} (M^{-1} cm^{-1})	n_{CO}	Φ_r (λ_{irr}/nm)	solvent	ref
N∩*N* = phe	550	5.8×10^3	2	0.41 (659)	CH_3CN	
N∩*N* = bpy	550	4.9×10^3	n.d.	0.39 (659)	CH_3CN	
N∩*N* = biq	719	1.3×10^3	n.d.	0.24 (659)	CH_3CN	
N∩*N* = phen−CHO	652	7.6×10^3	n.d.	0.02 (659)	CH_3CN	
273	340	n.d.	5.3	0.24 (405)[d]	DMA	1195
				0.006 (635)[e]		

[a]PBS = phosphate buffer saline, DMSO = dimethyl sulfoxide, DCM = dichloromethane, Phe = 1,10-phenanthroline, Bpy = 2,2′-bipyridyl, Biq = 2,2′-biquinoline, Phen-CHO = phenanthrolinecarboxaldehyde, DMA = dimethylacetamide. [b]Wild-type protein (3 histidine units). [c]Mutant protein with hexahistidine tag. [d]Direct irradiation. [e]Sensitized release.

or photochemical processes in aerated solutions. Schiller and co-workers combined the classical UV-absorbing photoCORM $Mn_2(CO)_{10}$ **273** (Table 17) with the Pd^{II} tetraphenyltetrabenzoporphyrin complex **274**, which is a triplet photosensitizer (see also section 6.1) excitable by red or NIR light.[1195] The triplet-excited photosensitizer transfers its energy to the photoCORM, which then liberates CO. The authors combined these components in the solid state to prepare a CO-releasing material supported on electrospun non-woven fabrics.

Ru^{II} complexes have d^6 configurations similar to those of Mn^I complexes and have also been successfully used as visible-light activatable photoCORMs. Ru^{II} analogs of **229a** (Table 14), **275**, and **276** (Figure 40) are carbonyl complexes where

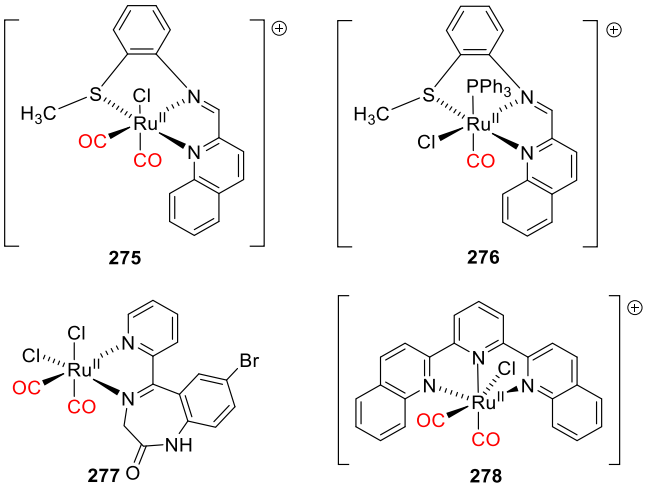

Figure 40. Ru^{II}-based photoCORMs.

the 2-quinoline-*N*-(2′-methylthiophenyl)-methylenimine (qmtpm) moiety acts as a tridentate ligand due to the high affinity of Ru^{II} for sulfur. Complex **275** has a MLCT band at λ_{max}^{abs} = 405 nm.[1196] The replacement of a strongly π-accepting CO ligand with PPh_3 resulted in a bathochromic shift of the MLCT band to 465 nm. Complex **275** releases CO only in acetonitrile upon UV-light (310 nm) irradiation, whereas phosphine-substituted complex **276** is active in the visible region and releases CO under visible light (≥440 nm). Mansour studied the Ru^{II} dicarbonyl complex **277** (Figure 40), which incorporates a ligand derived from the anti-anxiety drug bromazepam and liberated 2 equiv of CO upon excitation with 470 nm light.[1170] The complexation of this photoCORM to bromozepam increased its antibacterial toxicity relative to the non-complexed drug. Complex **278**, which has a bisquinoline ligand, sequentially releases two equivalents of CO upon irradiation at 350 or 420 nm, with the first equivalent being liberated more efficiently.[1197] Finally, Oyama and co-workers recently introduced a series of Ru^{II} dicarbonyl photoCORM complexes with asymmetric bipyridine ligands.[1198]

Some Fe^{II} carbonyl complexes were reported as visible-light excitable photoCORMs. For example, irradiation of complex **279** (Figure 41) at 470 nm resulted in decarbonylation, which was monitored using a myoglobin assay and ion channels sensitive to CO.[1199,1200] The diiron hexacarbonyl complex **280** (Figure 41)[1201] is a water-soluble analog of an iron−iron hydrogenase model complex[1202] and can liberate 6 equiv of CO upon irradiation at 390 nm. It is not clear whether all 6 CO ligands are liberated from the excited state. Nakajima and co-workers reported a series of *N*,*C*,*S*-pincer iron(III) carbonyl complexes **281** (Figure 41) with two phosphorous ligands (**281a**: R_1 = Me, R_2 = Ph; **281b**: R_1 = R_2 = Me; **281c**: R_1 = R_2 = OEt) in the *trans*-positions.[1203] A detailed study of their wavelength dependence showed that all of these complexes released CO upon irradiation at <500 nm and that complex **281c** was photoactive even at 800 nm. The release quantum yields were in the range of 0.03−0.01 for all complexes. A core-shell-based material that releases CO via an upconversion process (see section 6.4.2) was developed by Liu and co-workers.[1204] The core, in this case, consists of upconverting nanoparticles of β-$NaYF_4$:Yb^{III}/Er^{III}, while the shell consists of $[Fe^{II}(\eta^5\text{-Cp})(CO)_2]$ complexes with the structure **282** (Figure 41) that are anchored to the surfaces of the nanoparticles via thiol groups. Irradiation of this material with a 980 nm laser led to the sensitization and subsequent decarbonylation of the CORM shell. Wright and co-workers introduced 2-aminopyridine and 1-aminoisoquinoline-based iron(II) complexes **283** bearing two CO molecules[1205] that can be substituted by thioglucose to obtain the ferracyclic dimeric complexes **284**, which exhibit enhanced water solubility and Φ_r values of 0.9−1.7×10^{-4}.

Re^I complexes **285** (L = Br^-, PPh_3, Figure 42), which are analogous to Mn^I-based complexes **231** (Table 14), were found to release CO only under UV illumination.[1146] This was rationalized by TD-DFT calculations indicating that ISC to the triplet state promoted by strong spin-orbit coupling competed with CO release. Conversely, the water-soluble Re^I-based photoCORM **286** (Figure 42) released 1 equiv of CO upon irradiation at 405 nm with Φ_r = 0.11[1206] (Φ_r (365 nm) = 0.024).[1207] This complex and its photoproduct are both fluorescent, with distinguishable maxima at 515 (Φ_F (365 nm) = 0.08) and 585 nm, respectively, enabling qualitative monitoring of CO release in cells using confocal fluorescence microscopy.

https://dx.doi.org/10.1021/acs.chemrev.0c00663
Chem. Rev. 2020, 120, 13135−13272

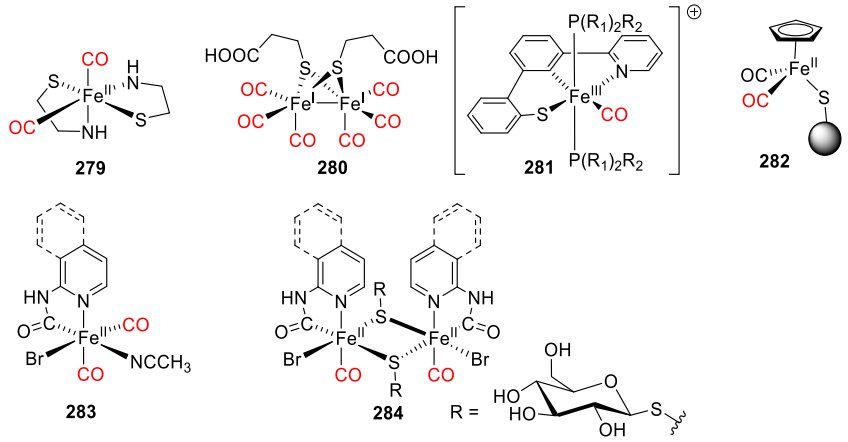

Figure 41. Iron-based photoCORMs.

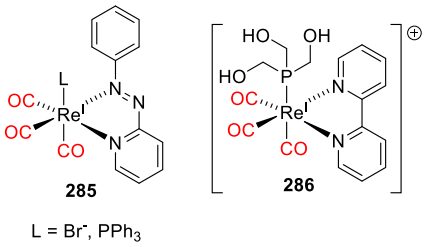

Figure 42. Re^{I}-based photoCORMs.

4.2. Release of Nitric Oxide

Nitric oxide (NO) is a gasotransmitter with many important biological roles[1208] in processes including vasodilatation,[1061,1209−1212] platelet aggregation inhibition,[1066] wound healing,[1065] postsynaptic plasticity augmentation, and hormone secretion.[1067] The development of NO-releasing molecules (NORMs) is therefore of interest for both therapeutic applications[1213] and mechanistic chemico-biological studies. Advances in the photochemical release of NO from photoNORMs have been reviewed previously.[103−109]

4.2.1. Transition-Metal-Free PhotoNORMs. There are three types of transition-metal-free photoactivatable nitric oxide (NO) donors (often termed photoactivatable nitric-oxide-releasing moieties, or photoNORMs): (i) *N*-nitroso amines, (ii) diazeniumdiolates (NONOates, $R_2N-(NO^-)-N{=}O$) and related structures, and (iii) *o*-substituted nitroarenes and their derivatives. NO release from these species can be induced by direct excitation or energy/electron transfer from an excited sensitizer.

N-Nitroso amines (Scheme 72) are popular NO donors because they are easily prepared by nitrosylation of amines.[1214] The N−NO bond is typically very weak (~39 kcal mol^{-1}); its energy is comparable to that of a photon with a wavelength of ~730 nm.[103] However, the N−NO group exhibits very limited absorption in the visible/NIR part of the spectrum and is therefore always combined with a suitable sensitizer. Upon NO photorelease, *N*-nitroso amines form aminyl radicals that may abstract hydrogen atoms from other molecules or undergo reduction or oxidation.[1215,1216] They can also transnitrosate with nucleophiles such as thiols.[1217]

The thermally stable and non-cytotoxic aza-BODIPY-based *N*-nitrosamine **287** (Figure 43) was shown to release NO upon irradiation at λ_{irr} = 700 nm *in vitro* and *in vivo*.[1218] This molecule also acts as an excellent photoacoustic sensor,

Scheme 72. Photoreactions of *N*-Nitroso Amines[1214,1215,1217]

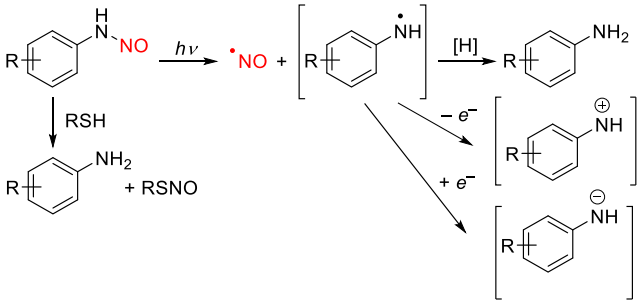

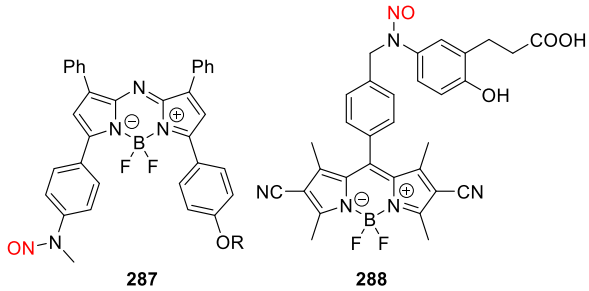

Figure 43. Structures of BODIPY *N*-nitroso amine-based photoNORMs.

allowing the local, irradiation-dependent release of NO to be monitored *in vivo* by photoacoustic tomography. The BODIPY scaffold was also used to prepare **288**,[1077] which releases NO upon irradiation at wavelengths in the range λ_{irr} = 470−500 nm with a Φ_r of 0.0019 at 488 nm (Figure 30).

Like **288**, the rosamine photoNORM **289** releases NO upon irradiation at λ_{irr} = 530−590 nm (Scheme 73).[1219] The suggested mechanism involves photoinduced electron transfer from the *N*-nitrosoaminophenol group to the excited rosamine moiety to form unstable phenoxyl radical **290**, which decomposes to release NO and form the stable quinoneimine **291**.

This approach was further developed by the synthesis of photoNORMs **292** and **293** (Figure 44), and it was found that the distance between the NO-releasing *N*-nitrosoaminophenol group and the rosamine sensitizer profoundly affects the efficiency of **NO** release.[1220] Compound **293** exhibited the most efficient NO release (Φ_r = 1.01 × 10^{-3}); the other

https://dx.doi.org/10.1021/acs.chemrev.0c00663
Chem. Rev. 2020, 120, 13135−13272

Scheme 73. Mechanism of Photochemical Release of NO from 289[1219]

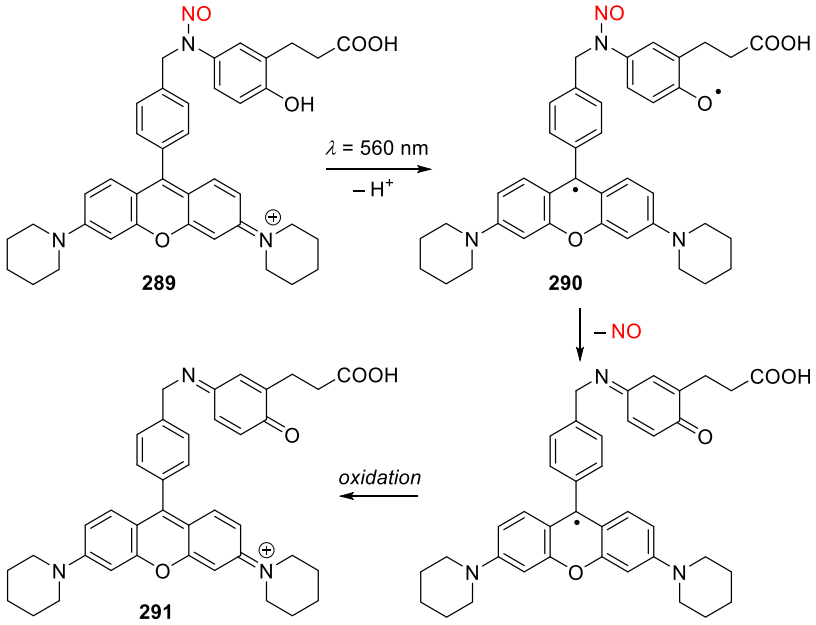

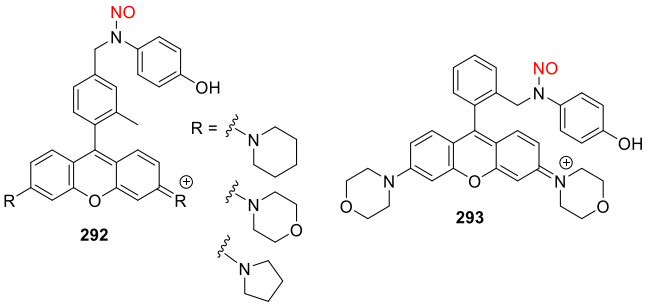

Figure 44. Structures of rosamine-based photoNORMs.

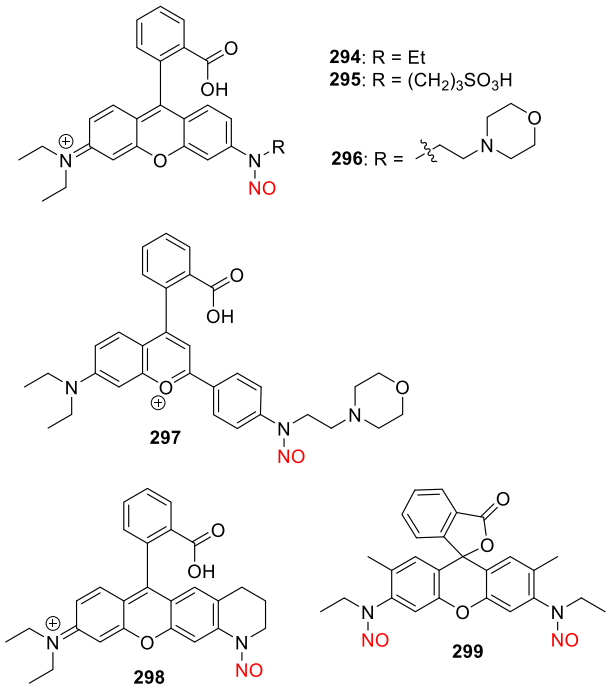

Figure 45. *N*-Nitroso amine-based photoNORMs.

derivatives were strongly fluorescent. This proximity effect was attributed to $\pi-\pi$ stacking and the formation of conformational isomers that enable efficient electron transfer. Conjugation of D-galactose with the phenolic hydroxy group completely blocked NO release, which was restored by selective enzymatic hydrolysis with β-galactosidase, enabling NO release using two independent triggers that can be activated simultaneously. The formation of phenoxyl radical **290** (Scheme 73) was shown to be the key step in NO release. The release of NO from compound **293** upon irradiation at 530−590 nm was tested in HET293T cells and used to control the response of rat aortas to NO in an *ex vivo* system.[1221] Compounds **288**, **289**, and **293** were subsequently evaluated as potential NO donors for treatment of erectile dysfunction.[105]

Yang and co-workers recently developed a visible-light absorbing photoNORM based on *N*-nitroso rhodamine derivative **294** (Figure 45).[1222] Upon irradiation with λ_{irr} = 532 nm, the weakly fluorescent molecule **294** was converted into NO and a fluorescent rhodamine-based photoproduct (Φ_F = 0.43 at 560 nm in phosphate buffer, pH = 7.4), which was used to monitor the localization, flux, and dose of the released NO. NO release was found to occur within 7 ps after excitation. A sulfonate group was attached to the *N*-nitrosamino group in photoNORM **295** to increase its water solubility,[1223] while the morpholine-substituted derivative **296** was designed to target the lysosomes and release NO in living cells and zebrafish.[1224] Interestingly, a chromenylium analog of **296**, **297**, released NO in 91% yield only upon excitation with 365 nm light despite absorbing in the visible region (λ_{max}^{abs} = 537 nm).[1225] Additionally, the dihedral angle between the nitroso moiety and the rhodamine core was found to influence the efficiency of NO photorelease. The nitrosamine group is almost orthogonal to the plane of the chromophore in **294**−**296**, whereas in the ring-restricted compound **298**, the nitrosamine moiety is locked in a coplanar geometry.[1216] The direct conjugation of the chromophore and nitrosamine systems enables more efficient photoinduced intramolecular charge transfer, leading to NO release at λ_{irr} = 532 nm, ∼20-times more efficiently than from **294**. A doubly *N*-nitrosylated

https://dx.doi.org/10.1021/acs.chemrev.0c00663
Chem. Rev. 2020, 120, 13135−13272

analog of **294**, **299**, released NO only upon UV light irradiation (λ_{irr} = 365 nm; Figure 45).[1226] Unlike **294**, which exists as an equilibrating mixture of a fluorescent visible-light-absorbing open form and a non-fluorescent UV-light-absorbing lactone form, photoNORM **299** exists exclusively as a lactone. This molecule was used to study changes in mitochondrial dynamics following NO release induced by irradiation at 375 nm.[1227]

The naphthalimide derivative **300** is another notable *N*-nitrosoamino photoNORM (Figures 46 and 30).[1078] It releases

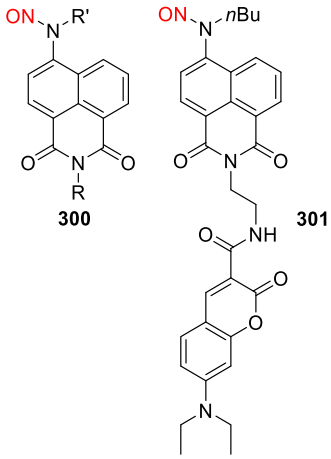

Figure 46. Napththalimide-based photoNORMs.

NO only upon irradiation with UV light (λ_{irr} = 365 nm) or 2P excitation at λ_{irr} = 740 nm. Its coumarinyl-substituted analog **301** also releases NO upon UV irradiation or 2P excitation at λ_{irr} = 800 nm, with a chemical yield of 79%.[1228]

Diazeniumdiolates (NONOates) release two equivalents of NO via thermal processes and have been investigated by Keefer and co-workers as potential liver-selective NO donating prodrugs.[1229] NONOates release NO in neutral aqueous solutions at a rate that depends on their structure. Because of their simple preparation[1230] and generation of predictable amounts of NO, they have attracted considerable attention as NORMs.[1231,1232] NO release from NONOates is insensitive to biological factors, so they do not induce resistance.[1233] The first attempt to control NO release from NONOates with light was reported by Tsien and co-workers, who used the *o*-nitrobenzyl protecting group (section 2.1.1) as a PPG in **302** (Scheme 74).[1234] This group is activated only by UV-irradiation (λ_{irr} = 365 nm); upon deprotection of the NO group, it thermally releases two equivalents of NO and a secondary amine. Another approach was used by Sortino and

Scheme 74. Photochemical Deprotection of NONOates[1234]

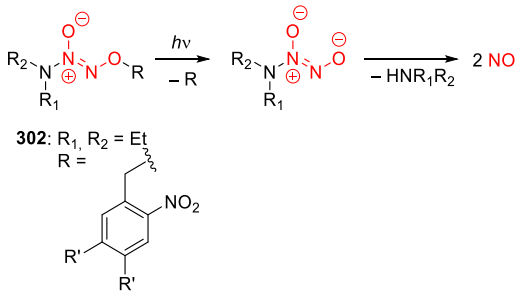

co-workers, who used the thermal NO releaser cupferron (which exists in two resonance forms: phenyldiazenium diolate **303** and *N*-nitroso-*N*-phenylhydroxylaminate **304**)[634] in the BODIPY-based (see section 2.11) photoNORM **305** (Figure 47).[803] Its irradiation at 530−550 nm resulted in the heterolytic cleavage of the BODIPY protecting group, unmasking cupferron, which thermally releases 1 equiv of NO (Φ_r = 0.008 ± 0.001 at 532 nm; $\Phi_r\varepsilon(\lambda_{irr})$ = 550 M^{-1} cm^{-1}). Iodo analog **306** was introduced as a photosensitizer for photodynamic therapy that simultaneously photoreleases NO (Figure 47).[798] The iodine atoms enhance the quantum yield of ISC, which increases singlet oxygen production in aerated solutions because of the sensitizing effect of the triplet-excited BODIPY group.

o-Substituted nitroarenes have also been identified as potential photoNORMs. The *o*-trifluoromethyl nitrobenzene derivatives **307** (R = H, Scheme 75) isomerize upon irradiation with UV light (λ_{max}^{abs} ≈ 300 nm) to give arylnitrite derivatives **308**,[1235] which thermally release NO to form phenoxy radicals **309**. These radicals subsequently abstract hydrogen atoms to give phenol derivatives **310**. The substituent in the *ortho*-position plays a key role in this process because it forces the nitro group to adopt a twisted geometry. Introducing an amino substituent *para* to the nitro group yields a chromophore with push-pull character, bathochromically shifting the absorption bands by ∼80 nm (**307**, R = NHR′, R′ = alkyl, acyl).[1235]

Hexadecylamine-substituted 4-nitro-3-(trifluoromethyl)-aniline **311** (Figure 48) was used by Jose and co-workers to prepare nanoscale lipid vesicles for photoinduced NO delivery (λ_{irr} = 410 nm).[1236] However, even push-pull-substituted nitroarenes are poor chromophores (ε_{max} ≈ 1000 M^{-1} cm^{-1}) and must be sensitized to enable visible-light activation. Sortino and co-workers introduced the anthracene-based photoNORM **312**, which releases NO upon irradiation with 420 nm light.[1237] **312** was used as a photoNORM in the construction of a fluorescein-labeled *β*-cyclodextrin-based supramolecular nanoassembly with a red-emitting singlet oxygen photosensitizer (zinc phthalocyanine).[1238] This system exhibits "five-in-one" photochemical features: visible-light or 2P (740 nm) excitation, facile visualization due to distinct fluorescence, production of cytotoxic singlet oxygen, and NO release. The coumarin-based compound **313** was incorporated into photo-antimicrobial polymeric films to release NO upon irradiation at λ_{irr} > 400 nm.[1239] *o*-Trifluoromethyl-substituted nitroarenes were similarly used to prepare diketopyrrolo-pyrrole-based nanoplatforms for pH-responsive photodynamic/photothermal synergistic cancer therapy.[1240]

Miyata and co-workers developed a series of 2,6-dimethyl-nitrobenzene-based photoNORMs with properties similar to their trifluoromethyl analogs.[110,1241] However, *π*-extension of the aromatic system did not lead to visible-light activated NO release. The most active derivative **314** (Table 18) generated 0.55 equiv of NO upon irradiation with UV light. The attachment of fluorescein as a sensitizer generated the visible-light-absorbing molecule **315**, which releases NO only upon UV-irradiation or 2P excitation (σ_{TPA} = 0.12 GM).[1242,1243] The conjugated analog **316** releases NO both by 1P and 2P excitation with a 2P absorption cross section 8-times higher than that of **315** (σ_{TPA} = 0.98 GM).[1244] A similar approach is embodied in rhodamine-based derivatives **317**, which liberate NO upon irradiation with yellow light,[1245] and in compound

https://dx.doi.org/10.1021/acs.chemrev.0c00663
Chem. Rev. 2020, 120, 13135−13272

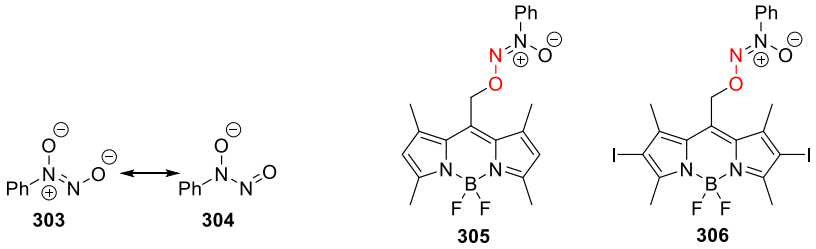

Figure 47. Structures of cupferron and cupferron-based photoNORMs.

Scheme 75. Photochemical Release of NO from *o*-Substituted Nitroarenes[1235]

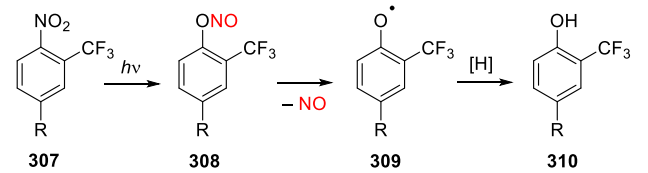

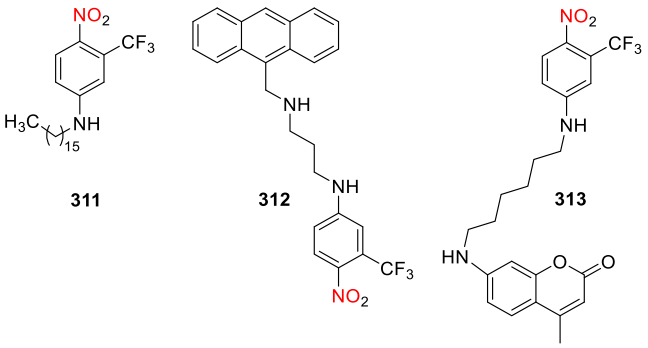

Figure 48. Structures of *o*-trifluoromethyl substituted nitroarene-based photoNORMs.

318, which incorporates 6-bromo-7-hydroxycoumarin as a sensitizer.[1246]

Sortino and co-workers recently synthesized two hybrid fluorescent photoNORMs **319a** and **320** (Figure 49) that combine an *N*-nitrosamine moiety with an *o*-trifluoromethyl nitroarene and a BODIPY or rhodamine sensitizer.[1247] Both compounds released NO upon irradiation with green light (λ_{irr} = 510 nm for **319a** and 532 nm for **320**), but release was more efficient from the BODIPY-substituted derivative **319a** (Φ_r = 0.031) than from the rhodamine-substituted compound **320** (Φ_r = 0.001). The reaction was suggested to be initiated by electron transfer from the N−NO group to the excited dye moiety. While these compounds should release 2 equiv of NO (one from the *N*-nitrosamine and one from the aryl nitro group), only the cleavage of the *N*-nitrosamine N−NO bond was observed. The iodo analog of **319a**, **319b**, releases NO upon irradiation with 532 nm light, which is accompanied by singlet oxygen production.[1248]

4.2.2. Transition-Metal-Containing PhotoNORMs. The most accessible sources of NO are nitrosyl and nitrito transition metal complexes with weakly bound NO ligands that can be released by external triggers. The oldest and best known NO donors are pentacyanonitrosylmetallates such as disodium pentacyanonitrosylferrate (sodium nitroprusside), which has been known since the mid-19th century.[1249−1251] The M−NO bond is readily cleaved by excitation into the MLCT ($d_M \rightarrow \pi^*_{NO}$) band of an organometallic complex. These bands exist in the visible region (above 400 nm); excitation weakens π-back-bonding to the NO ligand and facilitates electron transfer from the metal center to NO^+, which is then liberated as a neutral NO molecule.[1252] Transition metal complexes releasing NO have been reviewed by Ford[77−79,98,107] Mascharak,[63] and Liu[1253] and their co-workers.

The nitrito complex *trans*-$[Cr^{III}(cyclam)(ONO)_2]^+$ **321** (Scheme 76) was shown to release one equivalent of NO upon irradiation at 436 nm with Φ_r = 0.0092 in a degassed aqueous solution.[1254] Upon irradiation in aerated aqueous solutions, the complex releases NO with Φ_r = 0.25. This dichotomy was attributed to oxidation of the Cr^{IV} complex formed upon NO release by O_2 to give Cr^V species **322**. The presence of glutathione increased the quantum yield of NO release to Φ_{NO} = 0.25 by reducing an intermediate Cr^{IV} complex to a Cr^{III}−OH complex.[1255,1256] Complex **321** was combined with anthracene or pyrene "antenna" ligands (**323a** and **323b**, Figure 50) that harvest light and act as fluorescent reporters.[1255,1256]

Ford and co-workers recently developed a Cr^{III} nitrito complex **324** (Figure 51), which photoreleased NO upon irradiation at 451 nm[1257] and also upon irradiation at 800 nm when loaded onto polymer disks containing Nd-sensitized upconverting nanoparticles (see also section 6.4.2).

Fe^{III} and Fe^{II} nitrosyl complexes have long been known as photoNORMs. The most established Fe^{II} nitrosyl complex, sodium nitroprusside **325** (Scheme 77), was shown to photochemically release both CN^- and NO upon irradiation with 314−456 nm light.[1250] When irradiated in aqueous solution at >480 nm, NO was the sole photoproduct together with the oxidized Fe^{III} aqua complex as a side-product. NO release from nitrosyl complexes of electron-rich d-elements generally proceeds via electron transfer from the metal center to the NO^+ ligand and subsequent release of the NO radical.

Roussin's black salt **326** (Figure 52) and Roussin's red salt **327** were also found to release NO (5.9 equiv for **326** and 4 equiv for **327**) upon photolysis at wavelengths of 313−546 nm.[1141] The NO release quantum yield of **326** was Φ_r = 0.007, while that of **327** was one order of magnitude higher. Like Cr^{III} complexes **321**, the NO release efficiency was increased in the presence of oxygen. Encapsulation of **326** in NIR-absorbing nanocarriers resulted in efficient NO photorelease upon 980 nm excitation.[1258,1259] Derivatives of **327** and **328** were used as photoNORMs to efficiently release NO in aerated solutions.[1260−1263] Protoporphyrin IX was used to sensitize NO release from compound **328** (R = CH_2CH_2OH) at 436 and 546 nm with quantum yields of $\Phi_r = 5.2 \times 10^{-4}$ and 2.5×10^{-4}, respectively.[1262] Ford and co-workers showed that **328** (R = CH_2CH_2OH) could also be activated by attaching either sensitizing fluorescein derivatives absorbing at λ_{irr} = 400 (1PE) and 800 nm (2PE)[1260] or a benzothiazolyl-substituted

https://dx.doi.org/10.1021/acs.chemrev.0c00663
Chem. Rev. 2020, 120, 13135−13272

Table 18. 2,6-Dimethylnitrobenzene-Based PhotoNORMs

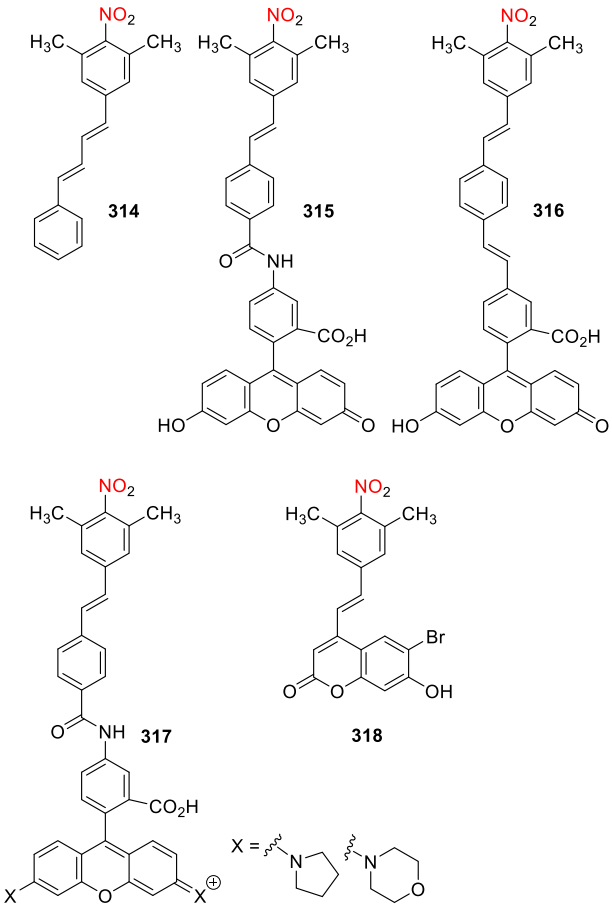

NORM	λ_{max}^{abs} (nm)	ε_{max} (M^{-1} cm^{-1})	λ_{irr} (nm)	Φ_r (λ_{irr}/nm)	solvent	ref
314	335	n.d.	UV[a]	n.d.	H_2O:DMSO 3:1 (v/v)	110, 1241
315	452	n.d.	330−380 450−480 720−735[c]	n.d.	H_2O:DMSO 3:1 (v/v)	1242
316	450	n.d.	450−480 720[c]	n.d.	H_2O:DMSO 3:1 (v/v)	1244
317, X = pyrrolidine	563	26 300	530−590	0.0023 (550)	phosphate buffer[b]	1245
317, X = morpholine	553	15 500	530−590	n.d.	phosphate buffer[b]	1245
318	360	11 200	400−430	0.053 (358)	H_2O:DMSO 1:1 (v/v)	1246

[a]UV irradiation with a Pyrex filter. [b]Sodium phosphate buffer, c = 100 mM, 1% DMSO (v/v). [c]2-photon excitation.

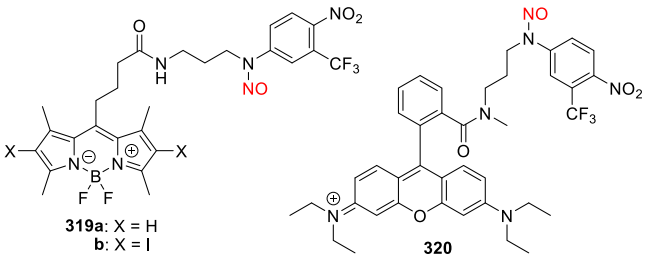

Figure 49. Hybrid photoNORMs combining *N*-nitrosamines and *o*-trifluoromethyl nitroarenes.

fluorenyl two-photon antenna with a large 2P absorption cross section (σ_{TPA} = 246 GM).[1264] Patra, Mascharak, and co-workers prepared Fe^{III} complex **329** (Figure 52), which incorporates pentadentate carboxamide-containing ligands.[63,1265,1266] This complex releases NO upon irradiation with visible light at 500 nm with Φ_r = 0.19. Lee, Chiang, Tsai, and co-workers recently introduced novel Fe^{II}-based photoCORMs with pendant thiols or thioethers (**330**, R = H, CH_3).[1267] The *S*-methylated complex releases NO upon irradiation with visible light (λ_{irr} > 400 nm), but the free thiol in **330** (R = H) interacts with the departing NO, generating HNO as the main photoproduct.

Complex **331**, a Mn^{II} analog of complex **329** (Table 19; Figure 31), irreversibly released NO upon visible-light activation[1081,1268] and was used to construct NO-releasing polyurethane-coated sol-gel hybrid materials.[1269] Replacing one pyridyl ligand of **331** with a quinoline unit yielded complex **332**, in which the absorption band is bathochromically shifted but photoactivity upon irradiation is retained at up to 810 nm.[1081] Additionally, the absorption maxima of the

https://dx.doi.org/10.1021/acs.chemrev.0c00663
Chem. Rev. 2020, 120, 13135−13272

Scheme 76. Cr^{III}-Nitrito Complexes and Their Photochemistry[1254]

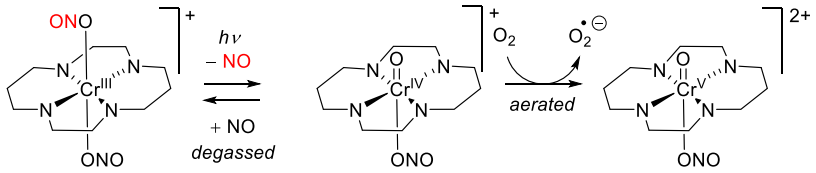

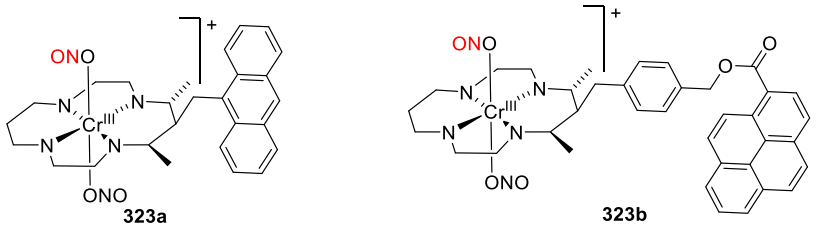

Figure 50. Cr^{III}-Nitrito complexes substituted with antenna ligands.

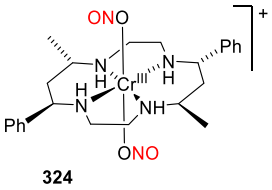

Figure 51. Cr^{III} nitrito complex **324**.

Scheme 77. Photochemistry of Sodium Nitroprusside[1250]

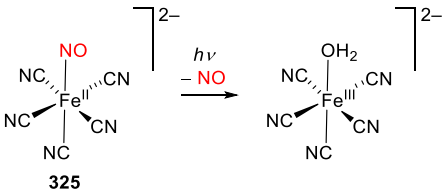

related complexes **333** and **334** (Figure 31), which contain imine nitrogens *trans* to the NO ligand, are bathochromically shifted by ∼100 nm relative to their carboxamide counterparts **331** and **332**.[1082]

Hitomi and co-workers studied the effects of varying the electronic properties of the ligands and the irradiation wavelength on the NO photorelease quantum yields of substituted complexes **335**.[1270] Electron-neutral and electron-donating groups gave the highest NO liberation efficiency at 460 nm, whereas electron-withdrawing groups provided the most efficient release at 650 nm.

Thanks to their robustness, thermal stability, and photoreactivity, Ru^{II} nitrosyl complexes have become established as useful photoNORMs.[113,1271−1286] The applications of these complexes are quite broad and beyond the scope of this review. Several representative complexes of this type, namely the nitrosyl-substituted Ru^{II} trichloride complex **336**,[1277] *trans*-tetraamine Ru^{II} nitrosyl complex **337** substituted with *N*- or *P*-based ligands,[1276] and theporphyrin-based Ru^{II} nitrosyl complexes **338**,[1278] are shown in Figure 53.

Cyclam Ru^{II} complex **339**, prepared by Tfouni and co-workers, releases NO only upon irradiation with near-UV light (Φ_r = 0.14 at 355 nm).[1287] Salen complexes **340** bearing π-extended ligands were extensively studied as potential photoNORMs because of their visible-light absorption.[1275,1283,1288] Upon irradiation at λ_{irr} = 546 nm, **340** (in

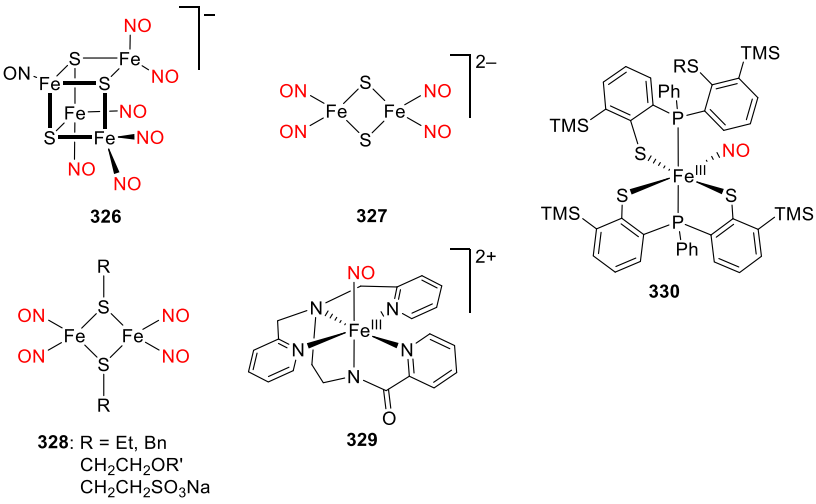

Figure 52. PhotoNORMs based on iron−sulfur clusters.

https://dx.doi.org/10.1021/acs.chemrev.0c00663
Chem. Rev. 2020, 120, 13135−13272

Table 19. Manganese(II) Multidentate Complexes Activatable in the Visible and NIR Region

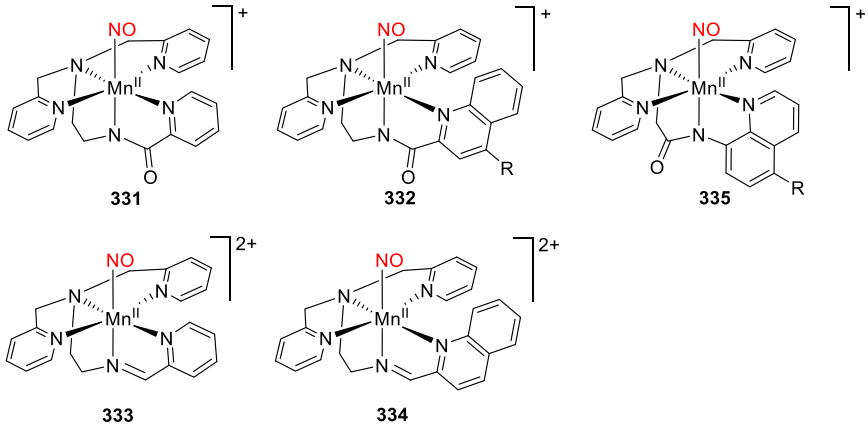

NORM	λ_{max}^{abs} (nm)	ε_{max} (M^{-1} cm^{-1})	λ_{irr} (nm)	Φ_r (λ_{irr}/nm)	solvent	ref
331	635	220	500, 550	0.326 (500)	CH_3CN	1081, 1268
				0.309 (550)	CH_3CN	
				0.400 (500)	H_2O	
				0.385 (550)	H_2O	
332	650	450	500, 550	0.623 (500)	CH_3CN	1081
				0.579 (550)	CH_3CN	
	670			0.742 (500)	H_2O	
				0.694 (550)	H_2O	
333	720	750	500, 550	0.41 (500)	CH_3CN	1082
				0.58 (550)		
334	785	1200	500, 550	0.39 (500)	CH_3CN	1082
				0.43 (550)		
335			460, 530, 650		MES[a]	1270
R = OCH_3	457	4740		0.58 (460)		
				0.47 (530)		
				0.49 (650)		
R = H	461	3120		0.61 (460)		
				0.51 (530)		
				0.47 (650)		
R = Cl	475	6940		0.66 (460)		
				0.66 (530)		
				0.73 (650)		
R = NO_2	523	13.6×10^3		0.61 (460)		
				0.63 (530)		
				0.78 (650)		

[a]MES = a 2-(*N*-morpholino)ethanesulfonic acid-based buffer.

which X = Cl^-) released NO more efficiently (Φ_r = 0.07) than complexes with other X ligands (ONO^- or H_2O).[1275,1283]

Mascharak and co-workers developed a series of Ru^{II} complexes **341** bearing tetradentate ligands.[1272,1289,1290] A systematic study of complexes in this series with π-extended ligands revealed factors important for release in the visible region.[1272] For example, **341** (R = OMe, X = Cl^-) releases NO with Φ_r = 0.01 at 500 nm (λ_{max}^{abs} = 420 nm), while its π-extended quinoline analogue (**341**, R = OMe, X = Cl^-, quinoline ligand) is photolyzed more efficiently (Φ_r = 0.025 at 500 nm, λ_{max}^{abs} = 490 nm).[1289] Ru^{II} nitrosyl complex **342** containing a tridentate *N*-(pyridin-2-ylmethylene)quinolin-8-amine ligand released NO upon irradiation with both 365 nm UV light and visible light with Φ_r = 0.004 (at 365 nm) in acetonitrile.[1291] Similarly, Ru^{II} complexes **343** and **344** (Figure 54) released NO upon irradiation at 355 nm in water (Φ_r = 0.12 and 0.20, respectively) and at 410 nm in acetonitrile (Φ_r = 0.05 and 0.17, respectively).[1292]

Malfant and co-workers investigated the mechanism of NO photorelease in Ru^{II} nitrosyl complexes with terpyridyl ligands bearing substituents having different electron-donating abilities (**345a−345c**; Table 20),[1293,1294] showing that low-lying electronic transitions that drive NO release exhibit strong charge-transfer interactions with the nitrosyl moiety. Upon excitation, the nitrosyl MLCT state is reduced to form a free NO radical and an oxidized Ru^{III} metal complex. Additionally, the 9-dibutyl-9*H*-fluoren-2-yl substituted Ru^{II} terpyridine complexes **346** (Table 20) released NO upon irradiation with blue light.[1295] The fluorenyl substituents of these complexes make them excellent chromophores, with a 2-photon absorption cross section of σ_{TPA} = (156 ± 23) GM. Substitution of the 9-dihexyl-9*H*-fluoren-2-yl groups in **347a** with *N*-ethylcarbazol-3-yl ligands (as in **347b**) strengthened the bathochromic shift of the charge-transfer transitions toward the electron-withdrawing Ru-NO fragment, resulting in excellent 2-photon absorption (σ_{TPA} = (159 ± 22) GM) but

https://dx.doi.org/10.1021/acs.chemrev.0c00663
Chem. Rev. 2020, 120, 13135−13272

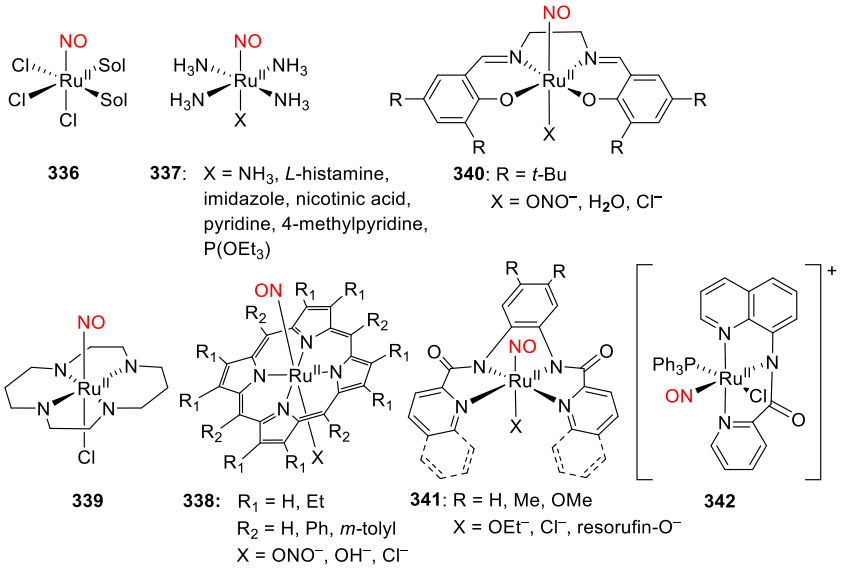

Figure 53. Structures of some Ru^{II}-based photoNORMs, Sol = DMSO, CH_3CN.

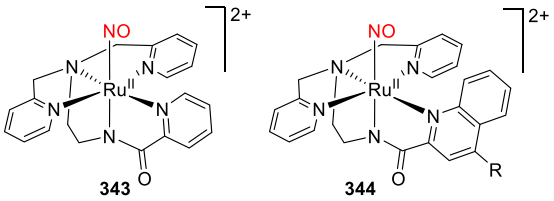

Figure 54. Structures of Ru^{II} NO complexes with pentadentate ligands.

reducing the rate of NO release.[1296] A similar group of complexes **348** (Table 20) bearing zero, one, two, or three 4′-(4-methoxyphenyl) electron-donating substituents was also investigated.[1297] The degree of intramolecular charge-transfer toward the strongly electron-withdrawing nitrosyl ligand increased with the number of methoxyphenyl substituents. However, irradiation of these complexes in the charge-transfer absorption band revealed only minor differences in the quantum yield of NO release, indicating that the CT band is not the sole determinant of NO release efficiency and that other factors must be involved. Malfant and co-workers further extended the study of terpyridine Ru^{II} complexes by examining derivatives **349** (Table 20),[1298] which released NO upon green-light irradiation. Similar complexes were used by Liu and co-workers to create NO-releasing Ru^{II} nitrosyl-containing nanoplatforms bearing BODIPY (**350**)[1299] or naphthalimide (**351**) ligands.[1300] Maji and co-workers recently synthesized two nitrosyl complexes **352**, which can be classified as $\{RuNO\}^6$ and $\{RuNO\}^7$ complexes using Enemark-Feltham notation.[1301] Irradiation with visible light caused NO release from both complexes, but the $\{RuNO\}^7$ complex (**352**$^{2+}$) was more active. This was attributed to the more efficient formation of the MLCT state in the $\{RuNO\}^7$ complex, which contains a Ru^{II}−NO• fragment, than in the $\{RuNO\}^6$ complex containing a Ru^{II}−NO^+ fragment.

Slep and co-workers studied complexes **353**−**355** (Figure 55), which release NO upon visible-light irradiation (λ_{irr} = 455 nm).[1302] Their quantum yields of NO release span 3 orders of magnitude, ranging from $\Phi_r = 0.06 \times 10^{-3}$ for 353, to $\Phi_r = 1.63 \times 10^{-3}$ for **355**, and $\Phi_r = 0.04$ for **354**. DFT analysis revealed that the presence of a second Ru^{II} center increases the molar absorption coefficient but does not necessarily influence the electronic distribution of the excited state responsible for NO release. Nikolaou and co-workers developed a ruthenium-based trinuclear complex $[Ru_3O(CH_3COO)_6(4\text{-pic})_2(NO)]PF_6$ ((4-pic) = 4-methylpyridine) that releases NO upon irradiation at λ_{irr} = 532 nm.[1303]

Cho and co-workers recently synthesized a Co^{III}-nitrosyl complex **356** (Figure 56) that efficiently released NO upon white-light irradiation (λ_{irr} = 385−740 nm; $\Phi_r = 0.78$)[1304] and was used in a real-time simulation of cell signaling to study extracellular signal-regulated kinases.

4.2.3. Sensitized Release of NO from Metal Nitrosyl Complexes. Transition metal nitrosyl complexes are often efficient photoNORMs that can be activated by visible light. However, their absorption bands have often lower molar absorption coefficients than common organic dyes ($\varepsilon \approx 10^3$ M^{-1} cm^{-1})[1082] and absorption maxima in the 400−500 nm region, which is unsuitable for deep tissue irradiation. Unfortunately, modifications that bathochromically shift their absorption into the 600−800 nm region often render these complexes unstable to hydrolysis (i.e., NO and ligand solvolysis).[98] Many alternative strategies have therefore been developed to shift their absorption maxima into the red and infrared regions while maintaining good dark stability and enhancing their molar absorption coefficients. These include (i) conjugation of photoNORMs with antenna moieties,[1081,1255,1261,1270,1272,1305,1306] (ii) multiphoton excitation of photoNORMs,[78,79,1243,1260,1305] (iii) the use of semiconductor quantum dots (see also section 6.4.1),[79,1305,1307] and (iv) combining photoNORMs with upconverting nanoparticles (see also section 6.4.2).[1258,1259,1305]

Chromium(III) nitrito complexes **323a** and **323b** (Figure 50) that release NO upon intramolecular sensitization by pyrene or anthracene antennae are representative implementations of the first strategy.[1255] These complexes typically become fluorescent after releasing NO, enabling the reaction to be monitored. Roussin's red salt derivatives **328** (R = CH_2CH_2OH, Figure 52) bearing protoporphyrin IX as a sensitizer are another notable implementation.[1262] Ru^{II} complexes **357** (Figure 57), which have tetradentate quinoline-based ligands containing various antennae (X = O,

https://dx.doi.org/10.1021/acs.chemrev.0c00663
Chem. Rev. 2020, 120, 13135−13272

Table 20. Structures and Properties of Ru^{II} PhotoNORMs with Terpyridine Ligands[a]

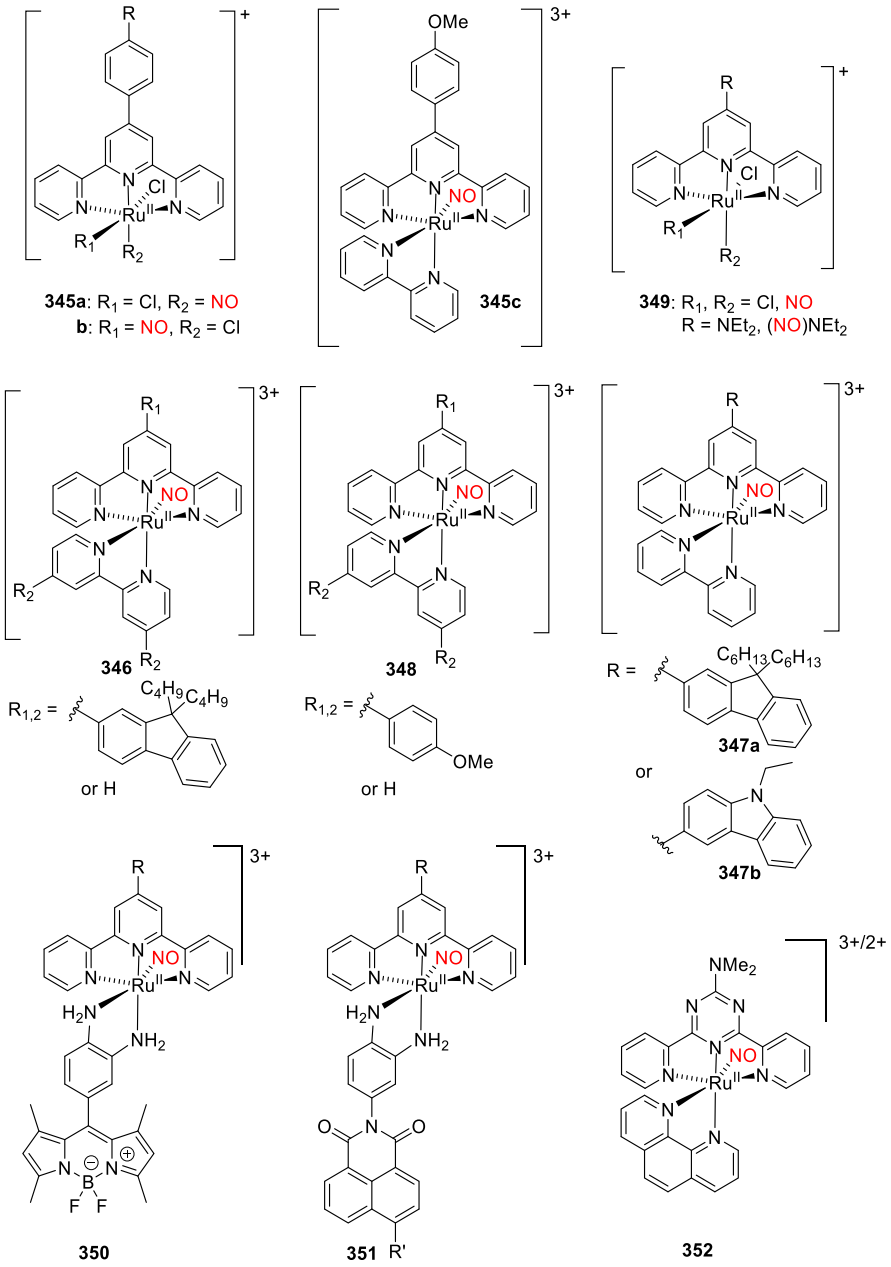

NORM	λ_{max}^{abs} (nm)	ε_{max} (M^{-1} cm^{-1})	λ_{irr} (nm)	Φ_r (λ_{irr}/nm)	solvent	ref
345a − *trans*			365		CH_3CN	1294
R = NO_2	357	9900		0.05		
R = H	350	18 000		0.12		
R = Br	354	22 900		0.11		
R = OCH_3	387	18 500		0.07		
345b − *cis*			365		CH_3CN	1294
R = NO_2	352	6700		0.24		
R = H	330	17 400		0.39		
R = Br	340	23 600		0.32		
R = OCH_3	366	15 600		0.28		
345c	420	12.4 × 10^3	365, 436	0.08 (365) 0.03 (436)	CH_3CN	1293
346			400, 405		CH_3CN	1295
R_1 = Fl, R_2 = H	455	16 700		0.06 (400)		
R_1 = H, R_2 = Fl	362	39 400		0.033 (400)		
347a	453	16 700	405, 436	0.06 (405) 0.03 (436)	CH_3CN	1296

https://dx.doi.org/10.1021/acs.chemrev.0c00663
Chem. Rev. 2020, 120, 13135−13272

Table 20. continued

NORM	λ_{max}^{abs} (nm)	ε_{max} (M^{-1} cm^{-1})	λ_{irr} (nm)	Φ_r (λ_{irr}/nm)	solvent	ref
347b	517	14 600	436	0.01	CH_3CN	1296
348			365, 436		CH_3CN	1297
R_1 = H, R_2 = H	352	n.d.		0.086 (365)		
R_1 = Ar, R_2 = H	425	n.d.		0.011 (436)		
R_1 = H, R_2 = Ar	360	33 000		0.024 (365)		
R_1 = Ar, R_2 = Ar	365	39 000		0.002 (436)		
	421	n.d.[b]				
349 − *trans*			365, 546		CH_3CN	1298
R = NEt_2	550	20 200		0.09 (365)		
				0.01 (546)		
R = (NO)NEt_2	497	3200		0.13 (365)		
349 − *cis*			365, 546		CH_3CN	1298
R = NEt_2	516	17 200		0.12 (365)		
				0.045 (546)		
350	548	n.d.	>400, 470, 530, 672	0.034 (470)	H_2O	1299
				0.083 (530)		
				0.017 (627)		
351	519	n.d.	808	0.017	saline[c]	1300
352			–[d]	n.d.	CH_3CN	1301
{RuNO}^{6}	298	34 500		(74 min)[e]		
{RuNO}^{7}	479	15 400		(17 min)[e]		

[a]Fl = 9,9′-dibutyl-9*H*-fluoren-2-yl, Ar = 4′-(4-methoxyphenyl). [b]A shoulder in the absorption spectrum. [c]NaCl aqueous solution (c = 150 mM). [d]Unspecified wavelength, Xe light source. [e]Half-life of the NO release for **352**.

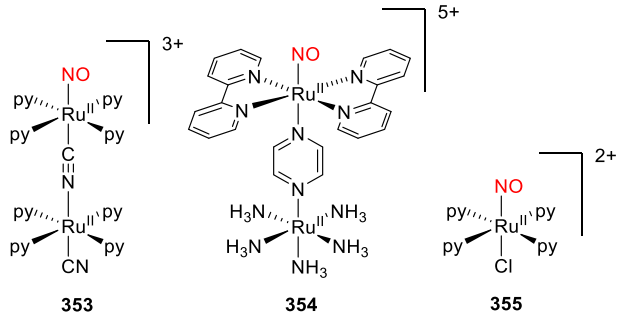

Figure 55. Ru^{II}-based dinuclear photoNORMs.

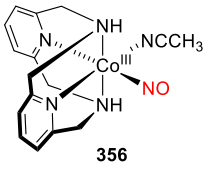

Figure 56. Co^{III}-nitrosyl photoNORM.

resorufin; X = S, thionol; X = Se, selenophore) were developed by Mascharak and co-workers.[1289,1308,1309] The attachment of the dye antenna introduces an absorption band ($\varepsilon \approx 28\ 000$ M^{-1} cm^{-1}) in the visible region (500−550 nm), and sensitized NO release occurs with Φ_r = 0.1−0.2. The derivative **357** (X = Se) was shown to be photoactive even at λ_{irr} = 600 nm with Φ_r = 0.04.[1309] Fluorescein- and dansyl-substituted analogs **358**[1310] and **359**[1311] also efficiently released NO (**358**: Φ_r = 0.306 ± 0.01 at 500 nm; **359**: Φ_r = 0.08 at 400 nm) upon irradiation with visible light. Complex **358** has an internal fluorescence turn-on indicator of NO release because release is accompanied by the photochemical formation of a highly emissive fluorescein methyl ester, while complex **359** acts as a fluorescence turn-off indicator of NO release because it is converted into a non-emissive paramagnetic Ru^{III}-dansyl aqua

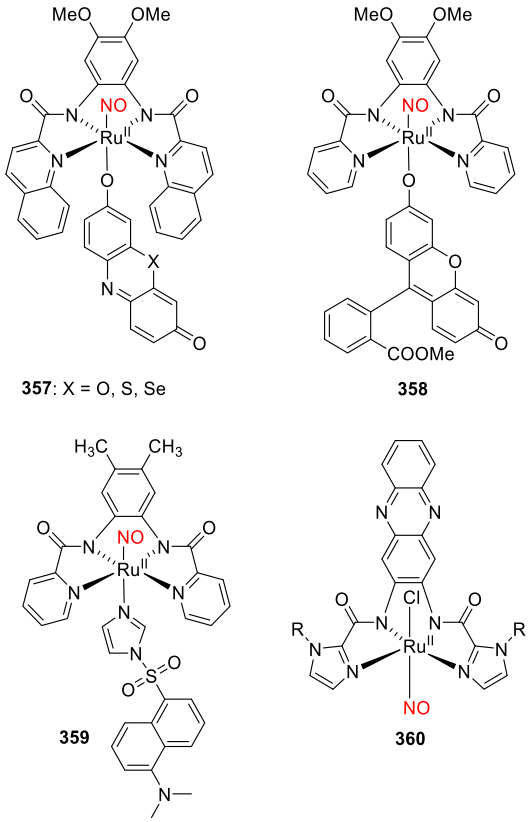

Figure 57. Ru^{II} photoNORMs with antennae.

complex upon irradiation.[1310,1311] Schiller and co-workers reported a combined spectroscopic-theoretical investigation of Ru^{II} complex **360**,[1312] which has a tetradentate ligand and releases NO upon irradiation at 475 nm.

Multiphoton excitation is another approach for NIR activation of NO release.[1258,1260,1263,1264] The fluorescein-

https://dx.doi.org/10.1021/acs.chemrev.0c00663
Chem. Rev. 2020, 120, 13135−13272

conjugated iron−sulfur cluster **361** (Figure 58) releases 4 equiv of NO upon both 2P- (λ_{irr} = 800 nm) and 1P- (λ_{irr} = 436 nm; Φ_{NO} = 0.014, calculated per NO molecule) excitation.[1313] Similar complexes were used to deliver NO to cells and tissues.[1258,1263]

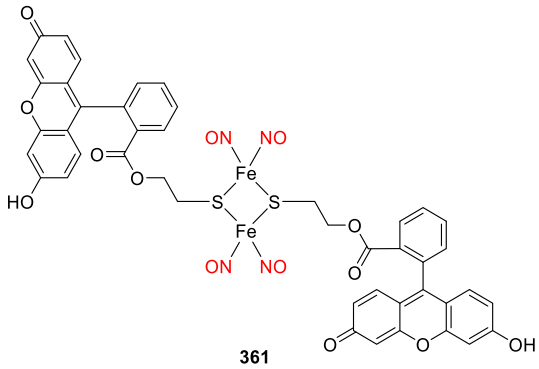

Figure 58. PhotoNORM based on an iron−sulfur cluster sensitized with fluorescein.

Semiconductor quantum dots (see also section 6.4.1) and related nanoparticles can also be used to induce NO release upon irradiation with red or NIR light.[1258,1259,1314−1319] This approach is exemplified by the photosensitized release of NO from Cr^{III} nitrito complex **321** (Scheme 76) with CdSe(ZnS) core/shell quantum dots upon irradiation with 450 nm light.[1307,1320] Tan and co-workers used a similar approach to design Mn^{II}-doped ZnS quantum dots that were encapsulated in the polysaccharide chitosan and conjugated to Roussin's black salt **326** (Figure 52).[1321,1322] NIR excitation (λ_{irr} = 1160 nm) of this system caused 2P-induced photoluminescence at λ^{em}_{max} = 589 nm. The emitted photons were then absorbed by **326**, inducing NO release.

A fourth way of inducing NO release with long-wavelength light is to use upconverting nanoparticles (see also section 6.4.2)[1258,1323−1325] that are excited via sequential absorption of 2 or more NIR photons and then emit upconverted blue-shifted light that is absorbed by attached photoNORMs. Nanoparticles of this type have been used in combination with Roussin's black salt **326**[1258,1259] and chromium(III) nitrito complex **321**.[1326]

4.2.4. NO-Photoreleasing Materials. NO-releasing materials (see also section 6.4) have attracted considerable research interest because of their potential to offer lower toxicity and better solubility and photoreactivity than molecular photoNORMs. This field has recently been thoroughly reviewed,[98,104,106,107,803] and a comprehensive discussion would be beyond the scope of this review. In general, NO-releasing materials contain NO donors attached to an inert carrier, which increases water solubility and may influence many (bio)physical properties including *in vivo* stability, biodistribution, and pharmacokinetics. NO donors are often coupled with a visible-light absorbing sensitizer or a NIR-absorbing upconverting species to improve photorelease.[104] The carriers are often biocompatible polymers,[1257] and the NO donors may either be present in a mixture or covalently attached.[1327] Polymeric gels are another common tool for delivering NO into organisms.[1081,1288,1309,1328−1330] For example, a Mn^{II} nitrosyl complex-based sol-gel was demonstrated to release NO upon irradiation at 780 nm.[1081] Additionally, self-assembled NO-releasing amphiphiles based on *N*-nitrosamine moieties have been used to achieve NO delivery with polymersomes.[1331] Another common strategy is to combine polymers with NIR-active nanoparticles[1322,1332] and upconverting nanoparticles.[1258,1323,1325,1333] Finally, Furukawa and co-workers introduced an alternative approach for NO release using a zeolitic imidazole framework with nitroimidazole ligands.[1334]

4.3. Release of Hydrogen Sulfide and Sulfur-Based Small Molecules

Hydrogen sulfide is a gasotransmitter produced endogenously from cysteine and homocysteine.[1335] It acts as a signaling agent involved in antioxidative, antiinflammatory, vasorelaxant, and cytoprotective processes,[1336−1338] and there have been several efforts to develop methods for its controlled release. Various H_2S-liberating systems activatable by pH, the presence of thiols, redox processes, and light, have been designed.[826,828,1339,1340] A complementary approach for H_2S release is to exploit photothermal effect using NIR light.[1341,1342] Developments in this field have been summarized in several reviews.[110−112]

The first H_2S-releasing systems activatable by UV light were reported only recently.[1343] The *o*-nitrobenzyl caged geminal dithiol **362** (Figure 59) was prepared by the $TiCl_4$-catalyzed condensation of the corresponding thiol with acetone. Upon irradiation of this compound at 365 nm in the presence of water, the free *gem*-dithiol is released and then hydrolyzed to

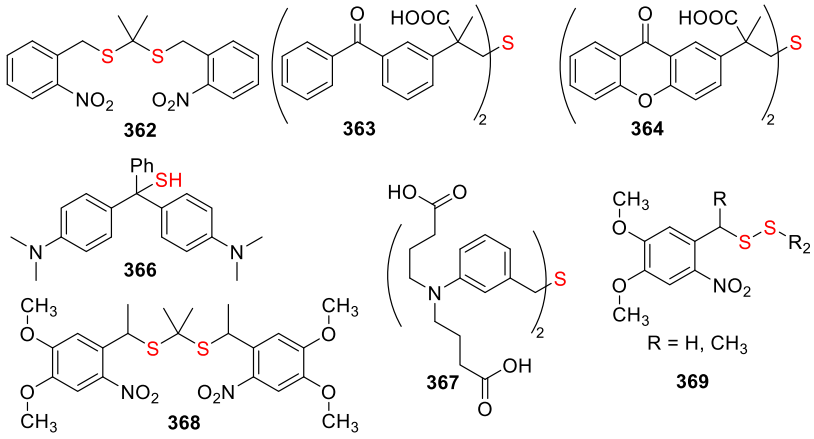

Figure 59. H_2S-releasing systems.

https://dx.doi.org/10.1021/acs.chemrev.0c00663
Chem. Rev. 2020, 120, 13135−13272

Scheme 78. UV-Absorbing H_2S Photodonors

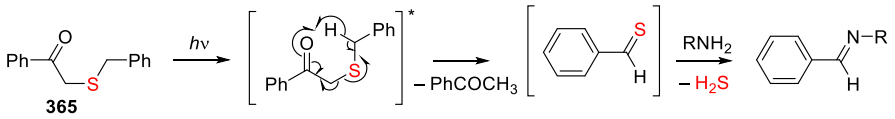

liberate H_2S.[1344] The ketoprofenate-based donor **363** also releases H_2S with simultaneous decarboxylation upon irradiation at 300−350 nm,[1345] while its xanthone analog **364** liberates H_2S under UVA irradiation (325−385 nm).[1346] Other H_2S-releasing systems are based on the Norrish type II hydrogen abstraction-induced photoproduction (λ_{irr} = 365 nm) of thiobenzaldehydes[1347] from compounds such as **365**. The thiobenzaldehydes formed in this way release H_2S in the presence of amines (Scheme 78).[1348] Another successful system was prepared by encapsulating the hydrosulfide-containing leuco-form of malachite green **366** into vesicles that released H_2S upon irradiation with UV light (Φ_r = 0.01 at 365 nm; Φ_r = 0.22 at 254 nm).[1349] Interesting results were also achieved with the *meta*-effect-based H_2S photodonor **367**, which bears water-solubilizing substituents (Φ_r = 0.14 at 365 nm).[573] Compound **368** is an analog of **362** that also releases H_2S upon irradiation with UV light. It was also used in combination with upconverting nanoparticles based on $LiYF_4$:Yb/Tm coated with polyethylene glycol-octadecylamine, which convert NIR excitation (λ_{irr} = 980 nm) into UV photoemission (λ^{em} = 365 nm) to trigger H_2S liberation.[1350] Finally, compounds **369** release biologically active persulfides upon irradiation at 365 nm with Φ_r = 0.07 for **369** (R = H) and Φ_r = 0.36 for **369** (R = CH_3).[1351]

Chakrapani and co-workers were the first to develop an H_2S photodonor activatable by direct excitation with visible light.[823] Their BODIPY-based molecule **370** undergoes photoinduced B−O bond cleavage (section 2.12) to release a thiocarbamate-substituted phenolate upon irradiation with 470 nm light. Subsequent thermal self-immolation of this phenolate (k_{immol} = 0.02 min^{-1}) then liberates carbonyl sulfide (COS), which is transformed to H_2S (k_{hydrol} = 1.82 s^{-1}) in the presence of carbonic anhydrase, an omnipresent enzyme that catalyzes the hydration of carbon dioxide and the dehydration of bicarbonate.[1352] The H_2S yield was 30−40% and its formation was tracked *in vitro* by monitoring the fluorescence enhancement due to the highly emissive photoproduct.

Štacko, Klán, and co-workers developed H_2S-releasing molecules **371**−**373** (Figure 60; **371**: Figure 30) based on a BODIPY PPG (section 2.12).[799] Upon photochemical excitation of the BODIPY core, the thiocarbamate leaving group installed at its *meso*-methylene position dissociates, leading to the release of COS, which is then converted into H_2S using carbonic anhydrase. Unlike **371**, the polyethylene glycol-substituted analog **372** is water-soluble and efficiently releases COS together with Ph_2NH (λ^{abs}_{max} = 513 nm in degassed aq. PBS, Φ_r = 15.1 × 10^{-2} at 365 nm; yield ≈ 86%). The π-extended derivative **373** has a bathochromically shifted absorption band and photoreleases H_2S upon irradiation at 700 nm (λ^{abs}_{max} = 688 nm in degassed aq. PBS, Φ_r = 9.7 × 10^{-2} at 365 nm, yield 69%). Oxygen quenches the productive triplet state, but H_2S release can proceed through both the singlet and triplet states.[798] The thiocarbamates are synthesized by the reaction of thiols with a suitable carbamoyl donor (4-nitrophenyl carbamate[823] or carbamoyl chloride,[799] Figure 60). The strategy of thiocarbamate caging and COS release

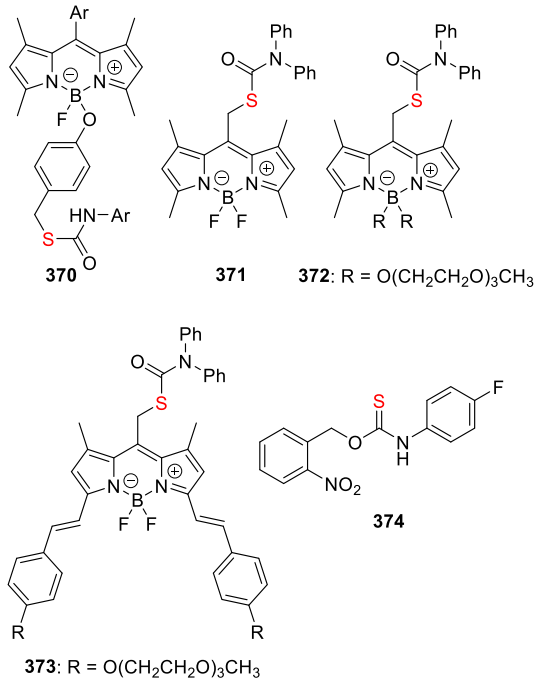

Figure 60. H_2S photoreleasing molecules.

was originally conceived by Pluth and co-workers and implemented in the form of compound **374**, which bears an *o*-nitrobenzyl PPG (section 2.1.1) and absorbs below 400 nm.[1353]

Singh and co-workers developed tetraphenylethylene-conjugated *p*-hydroxyphenacyl H_2S donors **375** (Scheme 79), which aggregate in aqueous media to form visible-light activatable (λ_{irr} >410 nm) nanoparticles that exhibit both aggregation-induced emission (AIE) and excited-state intramolecular proton transfer (ESIPT).[1354] These nanoparticles material offer efficient H_2S release (Φ_r = 0.18) that can be monitored in real time due to a fluorescence color change (λ_{em} = 549 nm for the starting material and 486 nm for the photoproduct).

Scheme 79. Tetraphenylethylene-Conjugated *p*-Hydroxyphenacyl-Based H_2S Donor

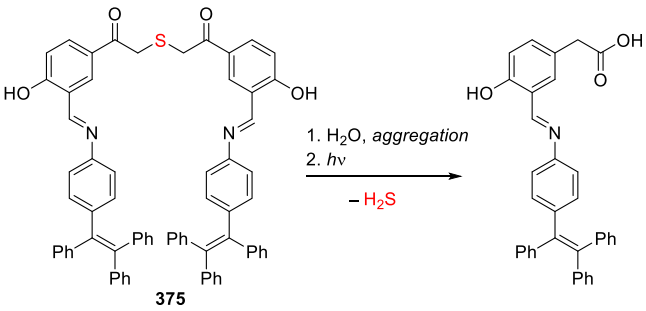

https://dx.doi.org/10.1021/acs.chemrev.0c00663
Chem. Rev. 2020, 120, 13135−13272

Singh and co-workers also reported H_2S photorelease from the benzo[*d*]thiazol-2-yl-substituted *p*-hydroxyphenacyl compound **376** (Figure 61) upon irradiation with visible light (λ_{irr} > 410 nm).[1355] The closely related derivative **377** liberated hydrogen persulfide (H_2S_2) under similar conditions,[1356] while sulfide dimers analogous to **376** photoreleased H_2S when formulated as organic nanoparticles.[633]

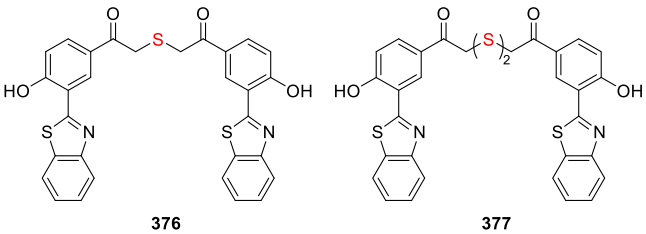

Figure 61. *p*-Hydroxyphenacyl-based H_2S photodonors.

Another H_2S releasing system developed by Singh and co-workers is the visible light-responsive (λ_{irr} > 410 nm) nanocarrier system **378**, which is based on a quinoline derivative (Figure 62) attached to a fluorescent carbon dot (see also section 6.4).[587] The system fluoresces in the visible region (λ^{em} = 425 nm, Φ_F = 0.078) and releases H_2S with a quantum yield of Φ_r = 0.09.

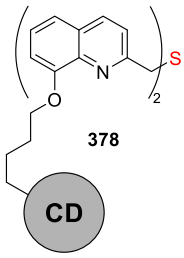

Figure 62. Fluorescent carbon dot-based H_2S photodonor (CD = carbon dot).

The group of You used a hybrid approach to develop Pluronic F-127-based vesicles containing a photosensitizer that generates singlet oxygen upon irradiation with visible light.[1357] Two such photosensitizers were tested, as shown in Scheme 80: Pt^{II} octaethylporphine **379** (Φ_r = 0.30) and [Ir^{III} bis(2-(3-methoxyphenyl)pyridinate)(1,10-phenanthroline)]PF_6**380** (Φ_Δ = 0.41). The singlet oxygen generated by these complexes upon irradiation (λ_{irr} = 500−550 nm for **379** and 380−500 nm for **380**) reacts with 1,3-diphenylisobenzothiophene **381** to form an endoperoxide, which then undergoes thermal decomposition to release H_2S (Φ_r = ∼2× 10^{-3}).

Scheme 80. Sensitizer-Based System for Photorelease of H_2S by Visible Light

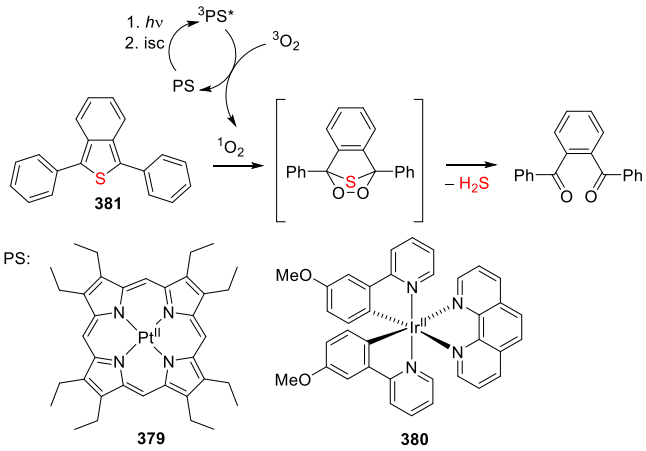

Visible light-induced H_2S release can also be achieved using organometallic complexes such as **382** and **383** (Figures 63 and 31), as demonstrated by Wilson and co-workers. These Ru^{II} terpyridyl complexes have low energy metal-to-ligand charge transfer (MLCT) absorption bands in the red region (λ^{abs}_{max} = 581 nm for **382** and 570 nm for **383**).[1083] Efficient ISC from ^{1}MLCT* leads to a dissociative triplet ligand-field excited state (^{3}LF) that liberates the monodentate ligand phosphinodithioate with near-quantitative quantum yields (Φ_r = 0.85 for **382**, Φ_r = 1.02 for **383** at 626 nm). The released phosphinodithioate acts as a thermal H_2S donor, undergoing hydrolytic decomposition to give two equivalents of H_2S.[1358,1359] Complexes **382** and **383** were used successfully in living cells both to protect H9c2 cardiomyoblasts and in an *in vitro* model of ischemia-reperfusion injury.

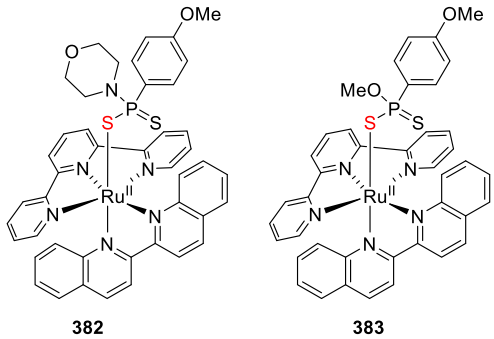

Figure 63. Ru^{II}-based H_2S donors.

Carbon disulfide is another small gaseous molecule that was recently identified as an important bioregulatory and therapeutic agent[1360] and has thus become an interesting target for uncaging and triggered delivery. Ford and co-workers developed a photocatalytic method for CS_2 production from potassium 1,1-dithiooxalate **384** (Figure 64) by oxidative cleavage photosensitized by CdSe quantum dots (see also section 6.4.1).[1361] This system releases CS_2 upon irradiation between 365 and 530 nm with Φ_r = 0.029−0.045. The mechanism of CS_2 release involves photoinduced two-electron oxidation of **384** to give CS_2 and CO_2.

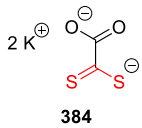

Figure 64. Carbon disulfide donor.

5. PHOTOACID AND PHOTOBASE GENERATORS

Photopolymerization processes use light to initiate polymerization, usually via radical reactions. Alternatively, polymerization may be triggered by an acid or a base formed by irradiation of a photoacid or photobase generator. This field has been covered by several recent reviews,[51,1362] so we discuss only a few particularly notable visible-light absorbing

https://dx.doi.org/10.1021/acs.chemrev.0c00663
Chem. Rev. 2020, 120, 13135−13272

generators. Thiophene-containing oxime sulfonates **385** release sulfonic acids upon irradiation at 365−475 nm (Figure 65).[1363]

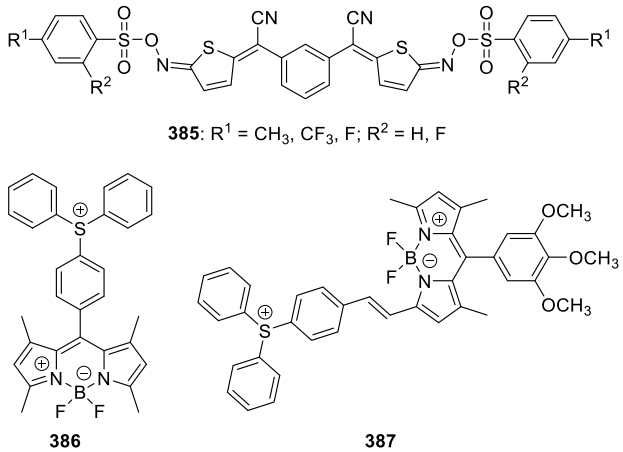

Figure 65. Photoacids **385**−**387**.

The first step in the release mechanism was proposed to be the liberation of the corresponding sulfonyl radical via homolytic cleavage of the N−O bond. Also notable are the BODIPY-based donor−acceptor triarylsulfonium salt-based photoacid generator systems **386** and **387**, which are photoactivated by green and red LED light, respectively, and were used to trigger cationic polymerization (Figure 65).[1364]

Visible-light initiated polymerization in the presence of merocyanine-based photoacid **388** was demonstrated by Boyer and co-workers (Scheme 81).[1365] The proton dissociation was reversible, enabling temporal control of the process.

Scheme 81. Photoconversion of Merocyanine-Based Photoacid 388[1365]

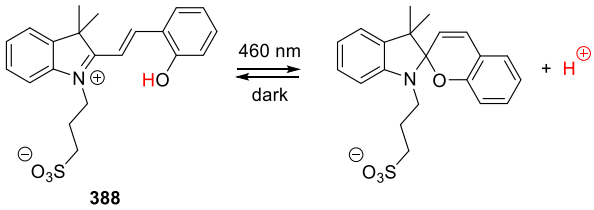

Scheme 82 shows a rare example of a visible-light absorbing photobase generator. In the first case, benzothiophene imino derivative **389** releases an amine base in a two-stage photoprocess.[1366] The oxamic acid ester **390** then undergoes homolytic N−O bond cleavage, followed by decarboxylation and radical addition into the adjacent aryl ring. In another example, tetramethyl guanidine (a basic polymerization initiator) was liberated from a coumarinyl-4-methyl PPG (see also section 2.2) upon irradiation at 400−500 nm.[346]

6. PHOTOSENSITIZED RELEASE: FROM SMALL MOLECULES TO NANOPARTICLES AND NANOMATERIALS

Photochemically induced uncaging using visible/NIR light can be achieved by various approaches. Direct release following one-photon (1P) absorption is the most desirable but is also rather challenging to achieve. The low energy of red and near-infrared photons is usually insufficient to initiate chemical processes; thus, a major goal when developing photoactivatable moieties is to identify feasible photochemical transformations. Many additional criteria may also need to be addressed; in particular, useful compounds must have suitable photochemical (good quantum yields and release rate constants, non-absorbing side-products), chemical (non-reactive side-products), and biological (non-toxicity of all species in the photoreaction pathway, and potentially water solubility) properties.[10] The release of a leaving group, usually an anion or neutral species, can generally proceed directly from an excited state of different multiplicity (Scheme 83a) or a reactive ground-state intermediate formed from the excited chromophore (Scheme 83b). Near-infrared absorption is often related to molecular overtone and combination vibrations that are forbidden by the quantum-physical selection rules, so the corresponding molar absorptivities are usually small.[1367] Only dyes with extensive conjugated systems such as cyanines or squaraines[1368] exhibit intense electronic transitions in the NIR region. A potentially expensive solution is to induce absorption of two (2P) or more photons (multi-photon absorption) by a single molecule using a high-power femtosecond laser, which enables access to excited states with energies equal to the sum of the absorbed photon energies.[1369,1370] This method can thus be used to excite chromophores absorbing in the UV region with NIR or visible light, as discussed extensively in our previous review.[10]

Another strategy for activating release with visible/NIR-light is to use two separate molecular components or bi-/multi-chromophoric systems, with one being a light-harvesting molecular or nanoscale sensitizer (see also section 6.1) that can transfer energy to[10,1371−1373] (Scheme 83c) or exchange an electron with[10,1374,1375] (Scheme 83d; the excited sensitizer is either an electron donor or acceptor) a separate molecule or complex bearing the leaving group. The excited chromophore can also be the photoremovable moiety, as in the case of Schemes **83a** and **83b**; in such cases, electron transfer to or from an auxiliary ground-state electron acceptor or donor, respectively, is responsible for leaving group release and the advantage of the auxiliary light-harvesting system is lost (Scheme 83e).

Scheme 83f depicts an alternative strategy that relies on a photosensitizer acting via the photodynamic effect: it generates singlet oxygen or another reactive oxygen species (ROS) upon irradiation,[1376−1379] which then reacts with an oxidizable moiety bearing the leaving group.

Scheme 82. Visible-Light Absorbing Photobase Generator[1366]

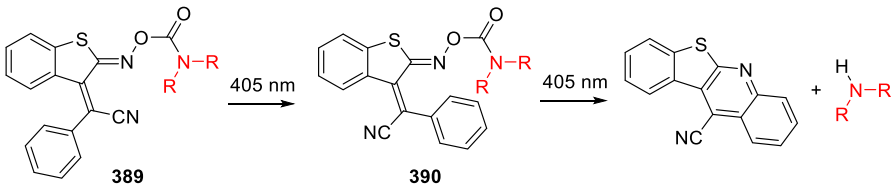

https://dx.doi.org/10.1021/acs.chemrev.0c00663
Chem. Rev. 2020, 120, 13135−13272

Scheme 83. Direct Photorelease versus Photosensitized Release

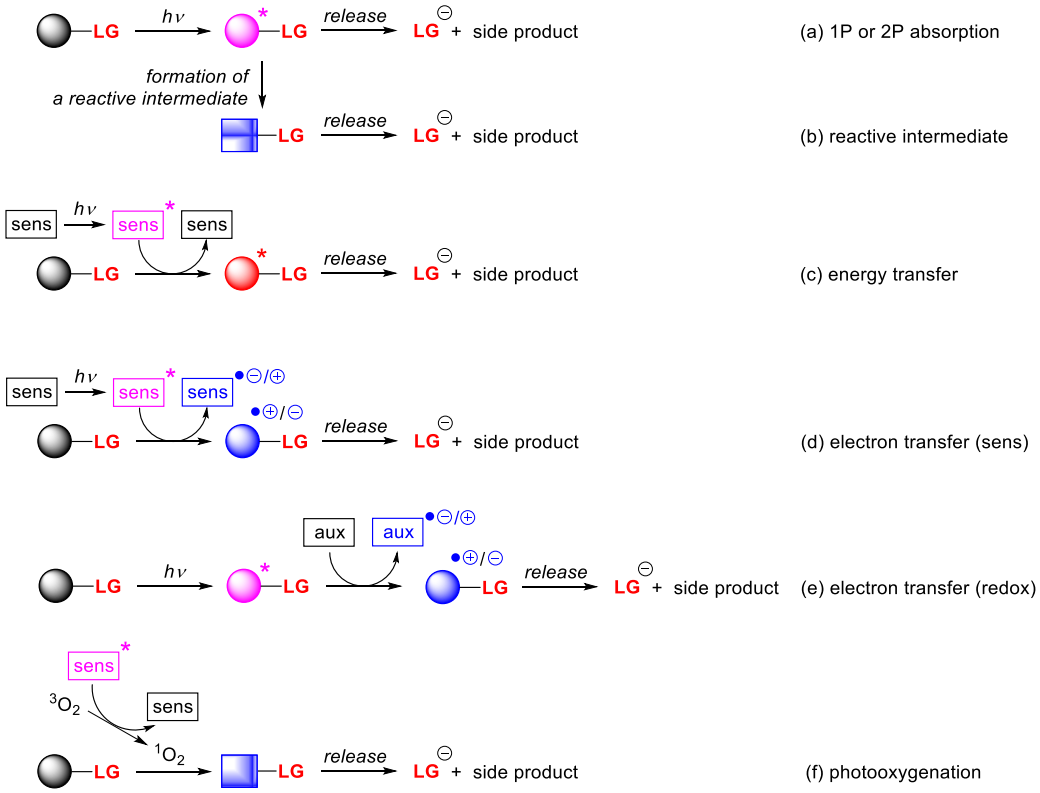

6.1. Molecular Photosensitizers: Energy Transfer

Photoinduced energy transfer is a practical way to generate (usually) a triplet excited state, particularly when the desired state is not accessible by direct excitation or the molecule does not absorb sufficiently at the desired wavelength.[136,1371] An efficient triplet−triplet energy transfer should be exergonic to avoid reverse transfer, and the sensitizer should have a high molar absorption coefficient, undergo efficient ISC, and have a sufficiently long triplet lifetime. Intramolecular energy transfer via either through-space or through-bond mechanisms might be preferred because it avoids the bimolecular entropic restrictions associated with diffusion and its efficiency can be finely tuned by adjusting the inter-chromophore distance.[10,1372,1373,1380,1381] Intramolecular energy transfer necessarily involves the use of an "equimolar" quantity of the sensitizer.

Several bichromophoric photoremovable protecting groups containing various UV-absorbing light-harvesting chromophores have been designed and studied by Corrie and co-workers over the past decade.[842,1382−1385] Benzophenone, which has substantially higher molar absorption coefficients above 300 nm than the photoactivatable nitroindoline group, was found to act as a triplet sensitizer to promote the nitroindoline moiety in compound **391** into its triplet state and trigger the subsequent release of a carboxylic acid (Scheme 84).[1385]

Steiner and co-workers used 9*H*-thioxanthen-9-one, which absorbs at slightly above 400 nm, to improve the light sensitivity of the weakly absorbing *o*-nitro-2-phenethyl PPG (see also section 2.1.2).[171,252,253,1386] For example, compounds **392** consisting of two chromophores connected via flexible tethers of different lengths were tested in the photolithographic synthesis of high-density DNA chips (Scheme 85).[253] It was

Scheme 84. Energy-Transfer-Mediated Release Involving the Nitroindoline Group[1385]

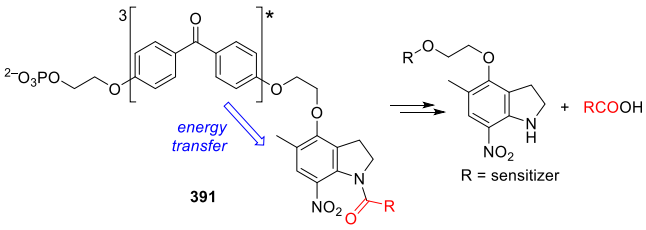

found that in addition to triplet−triplet energy transfer, the singlet excited state of the sensitizer was important, especially in systems with short tethers. Similarly, the photocleavage of the 2-(2-nitrophenyl)propyl group was sensitized intramolecularly by 9*H*-thioxanthen-9-one in the triplet excited state to release a fluorescent rhodamine dye.[1387]

The triplet excited state of 9*H*-thioxanthen-9-one was also shown to sensitize a linked benzothiophene-2-carboxanilide ring system (**393**, Scheme 86) via electrocyclic ring closure of the anilide moiety to liberate leaving groups including halides, thiolates, carboxylates, and phosphates (Φ_r = 0.14−0.41 at 395 nm).[1388]

Wang and co-workers recently demonstrated that intermolecular triplet−triplet energy transfer between a Pt^{II} tetraphenyltetrabenzoporphyrin sensitizer excited at 625 nm and a photoactivatable *meso*-methyl-substituted BODIPY derivative (**394**) (see also section 2.12) leads to the release of a carboxylate moiety (Scheme 87).[808,1389] The use of photosensitizers with a higher T_1 energy and a lower S_1 energy than that of the photocleavable group was recommended to enable exergonic energy transfer from a sensitizer excited at longer wavelengths.

https://dx.doi.org/10.1021/acs.chemrev.0c00663
Chem. Rev. 2020, 120, 13135−13272

Scheme 85. Energy-Transfer-Mediated Release Involving the *o*-Nitrobenzyl Group[253]

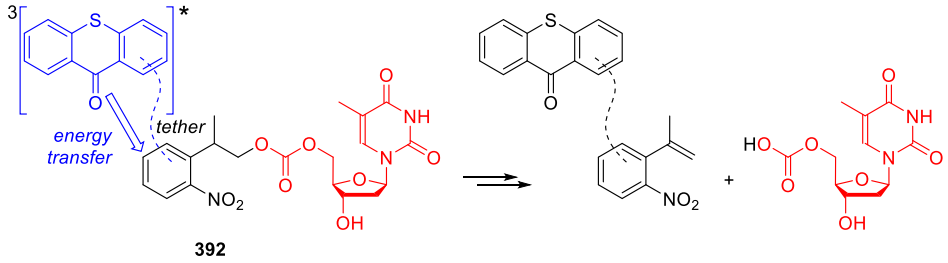

Scheme 86. Energy-Transfer-Mediated Release Involving the Benzothiophene-2-carboxanilide Group[1388]

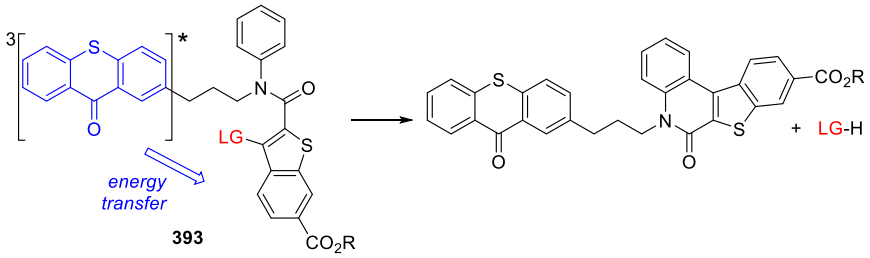

Scheme 87. Energy-Transfer-Mediated Release Involving the BODIPY PPG[808]

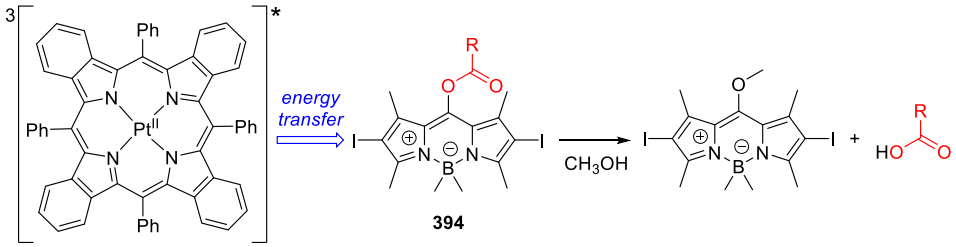

Scheme 88. Sensitized Release of Carboxylic Acids from Phenacyl Esters[1399]

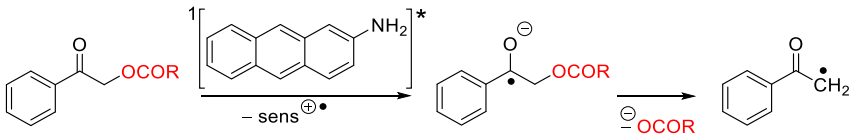

6.2. Molecular Sensitizers and Photocatalysts: Electron Transfer

The liberation of a leaving group can also be facilitated by (inter-/intramolecular) photoinduced electron transfer (PET), where the excited species is either the sensitizer or the substrate itself (Scheme 83d,e).[10,1374] For uncaging purposes, the sensitizer should have a high molar absorption coefficient and satisfy the other criteria mentioned in the previous section. If both reactants are neutral prior to the reaction, the resulting radical ion pair will undergo chemical transformations that eventually lead to leaving group release or recombination to restore the starting material. The Gibbs free energy of PET can be calculated from the corresponding redox potentials of both reactants and the excitation energy of the excited molecule.[10,136,1390−1392]

UV-light-initiated PET-assisted uncaging was reviewed several years ago.[10,1374] Hamada's pioneering photofragmentation of tosylamides in the presence of a reducing agent to give amines,[840] and especially the work of Falvey and co-workers on photosensitized uncaging of phenacyl esters,[1393,1394] picolinium esters,[1393,1395−1397] or 9-phenyl-9-tritylone[1398] were key studies in this area.

Falvey and co-workers also demonstrated that the sensitized release of carboxylic acids from phenacyl esters using a visible-light-absorbing electron donor (anthracen-2-amine; λ_{irr} > 400 nm) proceeds in near-quantitative chemical yield (Scheme 88).[1399] The sacrificial sensitizer can be regenerated in the presence of ascorbic acid by donating a hydrogen atom (or electron) to the aryloxy radical. Their experiments indicated that the phenacyl moiety interacts with the singlet excited state of the sensitizer.[1393] More recently, Speckmeier and Zeitler reported the catalytic deprotection of analogous phenacyl anddesyl (**395**) protecting groups using substoichiometric quantities of $[Ru(bpy)_3](PF_6)_2$ (1 mol %) as a photocatalyst excited at 455 nm and ascorbic acid (Asc−H) as a sacrificial electron donor (Scheme 89).[1400]

A similar strategy was used by Falvey's group to release carboxylic acids, amino acids, and phosphates from *N*-alkylpicolinium, which has a favorable reduction potential of E_{red} = −1.1 V. Scheme 90 shows a bimolecular photodeprotection of a carboxylic acid using BODIPY and coumarin derivatives as photosensitizers absorbing at $\lambda_{max}^{abs} \approx$ 500 and 467 nm, respectively.[1401] The PET-induced uncaging of carboxylic acids from an *N*-alkylpicolinium derivative by visible light was

https://dx.doi.org/10.1021/acs.chemrev.0c00663
Chem. Rev. 2020, 120, 13135−13272

Scheme 89. Photocatalyzed Release of Carboxylic Acids[1400]

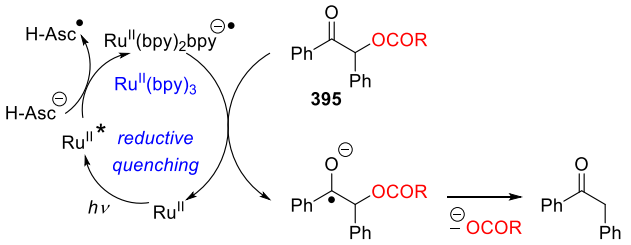

Scheme 90. Photosensitized Release from *N*-Alkylpicolinium Ions[1401]

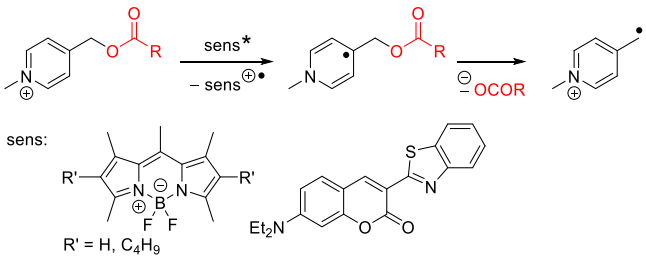

also demonstrated in the presence of substoichiometric amounts of tris(bipyridyl)ruthenium(II) ($\lambda_{max}^{abs} \approx 450$ nm) acting as both a sensitizer and a mediator of electron transfer between a good donor and the protecting group.[1402] Ascorbic acid, *N*,*N*-dimethylaniline, or 1,4-diazabicyclo[2.2.2]octane served as sacrificial electron donors in this case. Fluorescence quenching and transient spectroscopy experiments showed that the reaction rate constants were near the diffusion limit. Analogous visible-light promoted reactions were performed with ketocoumarin derivatives ($\lambda_{max}^{abs} \approx 450$ nm) as sensitizers/mediators,[1403] *N*-methylpyridinium iodide esters that undergo charge-transfer excitation,[1404] and an anthraquinone-based chromophore covalently attached to an *N*-alkylpicolinium ester.[1405] Similarly, Boncella and co-workers used tris(bipyridyl)ruthenium(II) to mediate PET to *N*-methylpicolinium carbamates to release amines in very high chemical yields,[1406] Cui reported the release of *N*-alkyl substituted 4-picolinium ions conjugated with self-assembled monolayers via an ester group using $[Ru(bpy)_3]^{2+}$ as a photocatalyst under irradiation at 452 nm,[1407] and Anderson, Flamigni, and co-workers showed that electron-accepting *N*-methylpyridinium, phenacyl, or *p*-nitrobenzoate moieties can be activated via intramolecular PET via two-photon absorption if covalently attached to electron-donating fluorene derivatives ($\lambda_{abs} < 450$ nm).[1408]

A photoactivatable system based on a 9-phenyltritylone protecting group that releases alcohols upon irradiation at 447 nm in the presence of *fac*-(tris(2,2′-phenylpyridine))iridium(III) (*fac*-$Ir(ppy)_3$) or tris(bipyridine)ruthenium(II) chloride ($[Ru(bpy)_3]^{2+}$) as photosensitizers and triethylamine as a sacrificial electron donor was reported by Falvey and co-workers.[1409] The authors proposed photodeprotection mechanisms involving both oxidative and reductive quenching scenarios (Scheme 91) corresponding to the general mechanism shown in Scheme 83d. In another case, these authors demonstrated the efficient release of calcium ions (Ca^{2+}) from an EDTA complex facilitated by photolysis of riboflavin photocatalysts at $\lambda_{irr} > 440$ nm.[1410]

An interesting visible-light uncaging reaction using photocatalytic deboronative hydroxylation was recently reported by

Scheme 91. Photocatalyzed Release of Alcohols[1409]

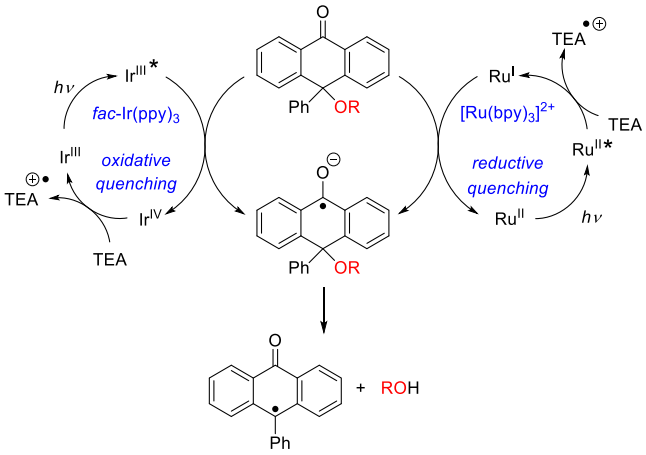

Chen and co-workers (one example is presented in Scheme 92.[1411] Phenol, alcohol, and amine derivatives were liberated

Scheme 92. Photocatalytic Deboronative Hydroxylation[1411]

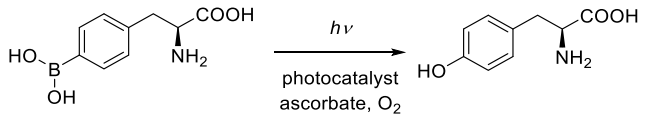

from the corresponding boronates in high chemical yields in bacteria and mammalian cells by reaction with transient hydrogen peroxides generated in the presence of molecular oxygen using fluorescein or rhodamine derivatives as photocatalysts and ascorbate as a reductant. In a different approach, Winssinger and co-workers used an azide-reduction-triggered immolative linker[1412] to release rhodamine using a $[Ru(bpy)_2phen]^{2+}$ conjugate as a photocatalyst in the presence of ascorbate.[1413]

6.3. Release via the Photodynamic Effect

A different way to release molecules of interest is to exploit the photodynamic effect, in which an excited photosensitizer and ground-state (triplet) oxygen ($^3O_2$) react to produce reactive oxygen species (ROS) or radicals that then react with molecules in the vicinity. The most common ROS is singlet oxygen ($^1O_2$) produced from $^3O_2$ by the triplet−triplet annihilation mechanism using triplet-excited organic dyes such as porphyrins, phthalocyanines, cyanines, pyropheophorbide, rhodamine, methylene blue, or eosin, which typically absorb in the red or NIR regions.[136] The use of this phenomenon to induce cell death in medical applications is known as photodynamic therapy. Diverse chemical functionalities and entities can be cleaved by reaction with singlet oxygen (Type II photooxygenation[136]) including olefins, vinyl ethers, vinyl disulfides, thioketals, and lipids.[1414,1415] Such singlet oxygen-sensitive groups can be inserted into tethers connecting drug molecules to structures such as membranes, nanomaterials, surfaces, or supramolecular carriers. The drug can then be liberated in the presence of a sensitizer, oxygen, and light.[1414−1417] The triplet-excited photosensitizer may also participate in electron exchange, that is, in Type I photooxygenation, as discussed in section 6.2.

In an early work, Anderson and Thompson demonstrated that singlet oxygen oxidation of liposome membranes by irradiating a membrane-incorporated sensitizing zinc phthalo-

https://dx.doi.org/10.1021/acs.chemrev.0c00663
Chem. Rev. 2020, 120, 13135−13272

cyanine at 640 nm resulted in the release of encapsulated glucose.[1418] The destruction of the membranes was attributed to a [2+2] cycloaddition reaction between $^1O_2$ and membrane alkenyl groups to form dioxetanes that subsequently decompose into two aldehydes.[1419] This mechanism was demonstrated to be responsible for the release of chlorin, which was used as a sensitizer (sens) that was covalently attached to silica via a tether containing a 1,2-diphenoxyethene unit (Scheme 93).[1417] Many other studies have exploited the reaction between $^1O_2$ and ethene derivatives such as vinyl ethers, bis(alkylthio)alkenes, or aminoacrylates for substrate liberation.[955,956,1420−1437] The uncaging photooxidation of lipids or liposomes[1438] in the presence of organic sensitizers may also proceed via mechanisms involving singlet oxygen.[1439−1446]

Scheme 93. Cleavage via the Photodynamic Effect (sens = Chlorin)[1417]

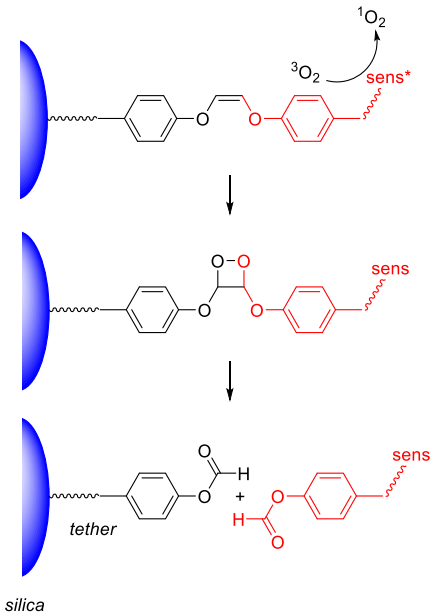

The second example of uncaging via the photodynamic effect is the release of siRNA bearing a 9-anthracenyl group and a photosensitizer (pyropheophorbide or eosin Y derivatives) attached to the 3′-terminus of the lagging strand (Scheme 94).[1447] Upon irradiation at 650 nm, singlet oxygen is formed by sensitization and attacks the 9-anthracene moiety to form an endoperoxide intermediate, which is then detached as anthracene-9,10-dione to liberate the siRNA strand. Similarly, methylene blue and alkoxyanthracene were used as a photosensitizer and a cleavable group, respectively, to disrupt micelles loaded with a chemotherapeutic agent.[1448] Other singlet-oxygen sensitive groups including thioketals,[1449−1462] thioethers,[1463] imidazoles,[1464] indolizines,[1465] and hydrazones,[1466] as well as selenium-[1467−1477] and tellurium-containing[1478−1480] moieties have also been used for uncaging. A qualitatively different photosensitizer, TiO_2 nanotube-doped PbS quantum dots combined with *S*-nitrosocysteine, was found to generate singlet oxygen upon irradiation at <600 nm, leading to the release of nitric oxide (Scheme 94).[1481]

An interesting approach to fluorophore photoactivation was recently reported by Wensel, Xiao, and co-workers,[1482] who replaced the carbonyl groups in common fluorophores with thiocarbonyl groups. This significantly reduced their fluorescence because of a photoinduced electron transfer-quenching mechanism. Upon irradiation, these compounds generate singlet oxygen, with which they then react to form their oxo derivatives, thereby restoring their original strong fluorescence (only one example is shown in Scheme 95).

Scheme 95. Fluorescence Switch via Self-Oxygenation[1482]

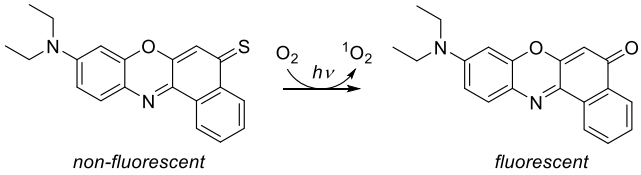

Two additional very interesting uncaging strategies involving photosensitized singlet-oxygen-mediated self-destruction of the photosensitizer leading to the release of a desired species are the liberation of carbon monoxide from flavonols (see section 4.1.1) and the use of cyanine dyes to release various leaving groups upon irradiation with red and NIR light (see below).

Cyanine dyes are invaluable fluorophores in chemistry and biology.[1483] They feature odd-numbered methine bridges connecting two nitrogen-containing heterocycles,[1484] which are responsible for their unique photophysical properties.[1485] In particular, heptamethine dyes with seven-carbon bridges are widely used as fluorescent tags in biological studies[1486−1488] and as markers in medical diagnostic tests.[1489,1490] Heptame-

Scheme 94. Photodynamic Cleavage of a 9-Anthracenyl Group from siRNA[1447]

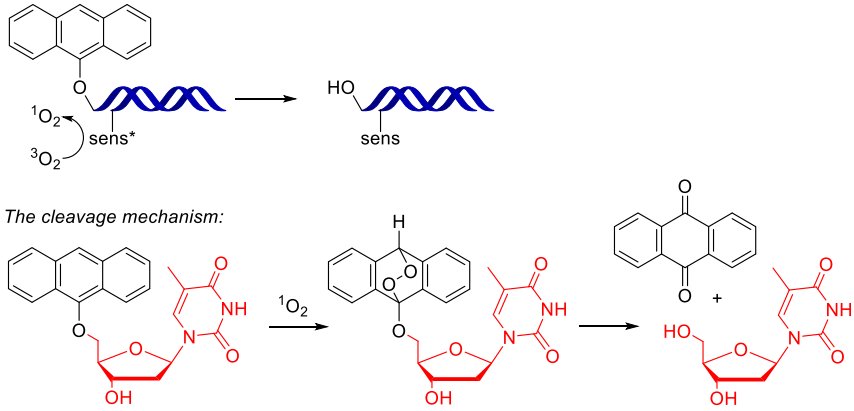

https://dx.doi.org/10.1021/acs.chemrev.0c00663
Chem. Rev. 2020, 120, 13135−13272

Scheme 96. Proposed Mechanism of Cy7 Photodegradation[1513]

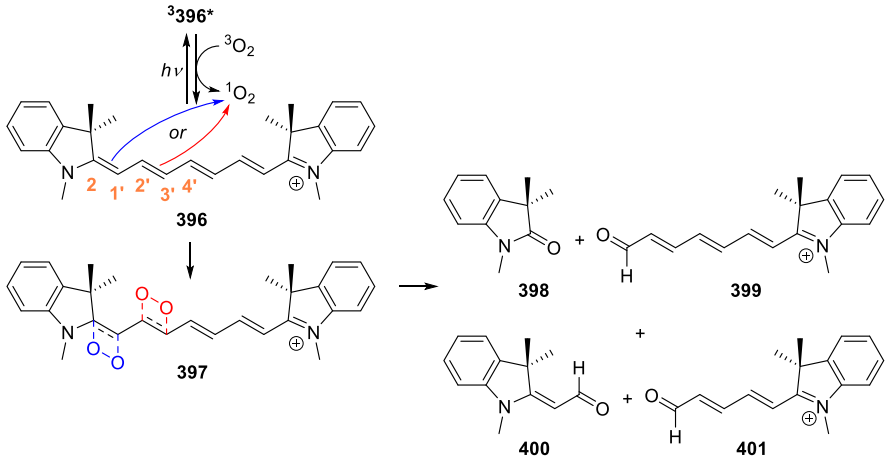

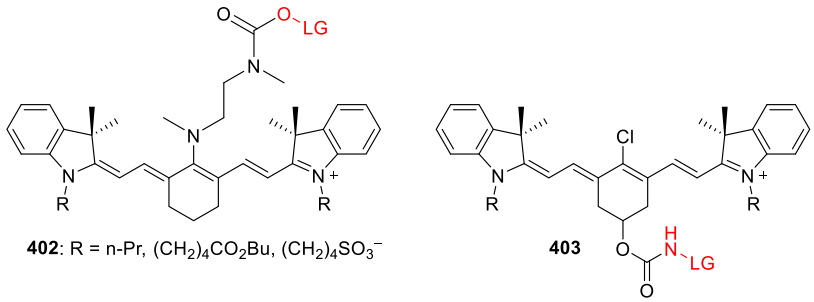

Figure 66. General structures of Cy7 photocages undergoing photooxidative-cleavage and C4′−N bond hydrolysis (**402**) or β-elimination (**403**).

thine cyanines (Cy7) have narrow absorption bands with high molar absorption coefficients (ε_{max} = 0.5−2.5 × 10^5 M^{-1} cm^{-1}) in the red to near-infrared (NIR) parts of the spectrum (650−800 nm). The peak absorption of heptamethine cyanines lies within the "first optical window" of mammalian tissue,[125,1486] where light attenuation due to absorption and scattering is minimal, making them particularly suitable for *in vivo* applications. This section focuses on the use of cyanine chromophores, particularly Cy7, as photoreleasing systems. Several aspects of this topic have been addressed by various recent review articles and perspectives.[20,21,50,878,890,1491−1494]

The photodegradation of heptamethine and other cyanines is a known phenomenon[1495] and has been shown to proceed via photooxidative cleavage of one or more heptamethine C=C bonds to form the corresponding carbonyl photoproducts.[1496−1506] The most common mechanism of Cy7 photooxygenation involves photosensitization of ambient (ground-state) molecular oxygen by the triplet excited state of Cy7 (^{3}**396***) to form singlet oxygen ($^1O_2$), followed by a [2+2] cycloaddition to form dioxetanes **397** that undergo thermal decomposition to form the carbonyl photoproducts (Scheme 96). Supportive evidence for this pathway include the findings that (1) triplet−triplet annihilation is exergonic[1507,1508] even though the quantum yields of $^1O_2$ production (Φ_Δ) tend to be low (∼0.01−0.001);[1509,1510] (2) the extent of photooxygenation depends on the oxygen concentration;[1501] (3) the reaction is suppressed in the presence of $^1O_2$ quenchers[1499,1501] or traps;[1497,1504,1511] (4) reaction rates are higher in deuterated solvents, which extend the lifetime of $^1O_2$;[1504] and (5) dioxetane intermediates can be detected by mass spectrometry.[1499,1512,1513] The generated singlet oxygen attacks the C2=C1′ or C2′=C3′ bonds to form the corresponding dioxetanes, which undergo thermal decomposition to give two carbonyl compounds.[1499,1512−1514] For example, the paired carbonyl products **398** + **399** and **400** + **401** were formed in a ∼4:1 concentration ratio during the photooxidative cleavage of **396**, accounting for 70% of the photodegradation chemical yield (Scheme 96).[1513] Computational analysis (B3LYP/cc-pVTZ) of **396** suggested that the observed regioselectivity is determined by the energies of the dioxetane intermediates; it was found that only dioxetanes at the C2/C1′ and C2′/C3′ positions, which give rise to carbonyl compounds **398**−**401**, are formed exergonically (ΔG = −2.8 and −0.7 kcal mol^{-1}, relative to **396**),[1513] in agreement with the experimental findings.[1494,1499,1512,1513] Cyanine photobleaching may also involve other pathways,[1501] such as photoinduced electron transfer from the Cy7 triplet state to oxygen to form O_2^-, which may subsequently generate hydroxyl radicals or other reactive oxygen species (ROS), together with a potentially reactive cyanine-radical cation.[1497,1498,1505,1515] The photodegradation of cyanines has mainly been studied to identify factors affecting their stability[1495,1502,1505,1516−1520] to improve their performance as fluorescent imaging agents,[1495,1521] although uses of their photodegradation, for example in sensing,[1522,1523] have also been reported.

Schnermann and co-workers pioneered the repurposing of heptamethine cyanines as photocages by developing two Cy7 scaffolds (**402** and **403**, Figure 66) that harness the regioselectivity of the photooxidative degradation process to drive either C−N bond cleavage[1491,1512,1524,1525] (**402**) or a β-elimination reaction[1514] (**403**), both ultimately leading to leaving group release. Both scaffolds contain a cyclohexenyl moiety attached at the C3′/C5′ positions of the heptamethine

https://dx.doi.org/10.1021/acs.chemrev.0c00663
Chem. Rev. 2020, 120, 13135−13272

bridge, which was originally used to increase the rigidity (and hence the fluorescence quantum efficiency) of Cy7.[1526,1527]

Cy7 derivatives **402** were synthesized from the corresponding cyanine dye featuring a chlorocyclohexenyl group.[1491,1512,1524,1525] The chlorine atom of this group is conveniently displaced via an $S_{NR}1$ reaction under mild conditions,[1528] in this case using ethylenediamine as the nucleophile. The leaving groups, such as chloroformate or *p*-nitrophenylcarbonate, were introduced in the last step. Photoexcitation (λ_{irr} = 690 nm) of **404** (λ_{max}^{abs} = 676 nm, ε = 5.15 × 10^4 M^{-1} cm^{-1}) resulted in the formation of products **405** and **406** in a ∼4:1 ratio (Scheme 97), as also observed for

Scheme 97. Mechanism of Uncaging from Cy7 Photocages 404[1512]

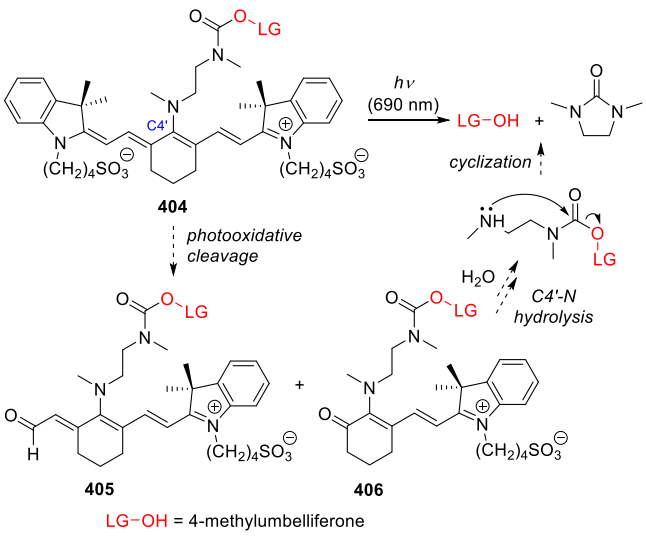

Cy7 **396**. The Cy7 derivative **404** is less prone to the hydrolytic release of the tertiary amine than the photooxidative cleavage products **405** and **406**, which was attributed to its more extensive π-conjugation, which reduces the electrophilicity of the key C4′−N bond (i.e., weakens its iminium character). Electrophilic reactivity at the C4′ position of heptamethine cyanines has previously been documented.[1529−1531] The inertness of the resulting aldehydes to both light and reactive oxygen species further supports the assumption that hydrolysis is the main pathway of amine release.[1512] The direct hydrolytic release of an aniline derivative (7-aminocoumarin) bound to the C4′ position was inefficient (with a chemical yield of <8%) despite rapid photooxidation of the corresponding heptamethine cyanine.[1514] It was therefore proposed that hydrolysis requires the prior protonation of the amine, and that the difference in the efficiency of hydrolysis between the tertiary amine and the aniline is due to their different basicities.[1514] Hydrolysis of the C4′−N bond is followed by intramolecular cyclization of the ethylenediamine linker,[1532,1533] resulting in the release of an alcohol as a leaving group.[1512,1524,1525,1534] Although the cyclization step is pH-dependent[1533] (proceeding more slowly at low pH), leaving group release efficiency was only reduced by a factor of 1.5 upon lowering the pH from 7.4 to 5.0.[1525] The overall chemical yield of uncaging (66−70%) correlated with the quantities of **405** and **406** formed during the reaction, suggesting that the light-independent steps are efficient.[1512] The kinetics of leaving group release appear to depend mainly on the rate of C4′−N bond hydrolysis.[1512]

The effects of structural variation of **404** on its spectroscopic and photochemical properties were also explored (Figure 67).[1524] Replacing the butyl sulfonic acid substituents on the indolenine nitrogens with *n*-propyl (**407**) or *n*-butyl pentanoates (**408**) did not affect the compound's spectroscopic and photochemical properties but significantly improved cellular penetration.[1491,1524] Replacing the *N,N′*-dimethylethylenediamine linker with *N,N′*-diethylethylenediamine (**409**) caused a 40 nm bathochromic shift of the absorption band, reduced the background (dark) hydrolysis rate (k_{rel} = 0.73), and increased the photooxidation rate (k_{rel} = 2.8) under the experimental conditions, although overall uncaging efficiency was reduced (k_{rel} = 0.81).[1524] Efforts to introduce more sterically demanding amines were hampered by the substantially lower reactivity of such amines in the chlorine substitution reaction.[1524] The lower background hydrolysis rate of **409** was attributed to increased steric hindrance either around the amine-heptamethine bond or the carbamate group.[1532] The introduction of sulfonates on the indolenine rings (**410**), which is often done to prevent aggregation,[1535] reduced photooxidation efficiency (k_{rel} = 0.43) and increased the rate of background hydrolysis (k_{rel} = 1.3) but also improved the kinetics of release (k_{rel} = 4.2).[1524] An alkyne group allowing the photocage to be connected to targeting molecules using click chemistry was introduced by using a branched carbamate linker (**411**).[1525] Replacing one (**412a**) or both (**412b**) flanking heterocycles with benzothiazole rings significantly improved oxidation efficiencies (k_{rel} = 3.7 and 6.7, respectively), in accordance with earlier studies on Cy7 fluorophores.[1504] However, this also dramatically increased the background hydrolysis rate (k_{rel} = 4.7 and 8.5, respectively).[1524] Replacing the central cyclohexenyl ring with a cyclopentenyl moiety (**413**) also increased the photooxidation rate (k_{rel} = 3.5) but significantly reduced the uncaging rate (k_{rel} = 0.013) and the overall uncaging chemical yield (<20%). The reason for the decreased uncaging efficiency was determined to be inefficient hydrolysis of the carbonyl intermediates.[1524] On the other hand, replacing the sulfonated indolenine rings with sulfonated benzindolenines and installing an alkoxy substituent on the cyclohexyl group (**414a** and **414b**) yielded PPGs with properties comparable to those of the original **404** but with a significantly red-shifted absorption spectrum (λ_{max}^{abs} = 690 and 732 nm, respectively).[1524] The individual contributions of each of these modifications have not yet been determined. In principle, the flexibility of the synthesis[1536−1538] and post-synthetic functionalization[1494,1531,1539,1540,1510] of cyanines enables useful structural modifications of the bridge or terminal heterocycles, providing considerable scope for modulation of their spectroscopic and photoreaction properties.

An analogous photooxidative cleavage mechanism was used by Schnermann and co-workers in the case of **403** (Figure 66) to drive the release of a leaving group through a β-elimination reaction.[1514] Several examples utilizing similar photooxygenation/β-elimination sequences to drive leaving group release have been reported.[187,1541−1545] Cy 7 photocages similar to **402** have mainly been used to release of phenols, while β-elimination of a carbamic acid functionality in **403** followed by spontaneous decarboxylation[1546] was used to release a free amine. Photoexcitation (λ_{irr} = 780 nm) of **415** (λ_{max}^{abs} = 781 nm, ε_{max} = 3 × 10^5 M^{-1} cm^{-1}, LG = coumarin 151) proceeded

https://dx.doi.org/10.1021/acs.chemrev.0c00663
Chem. Rev. 2020, 120, 13135−13272

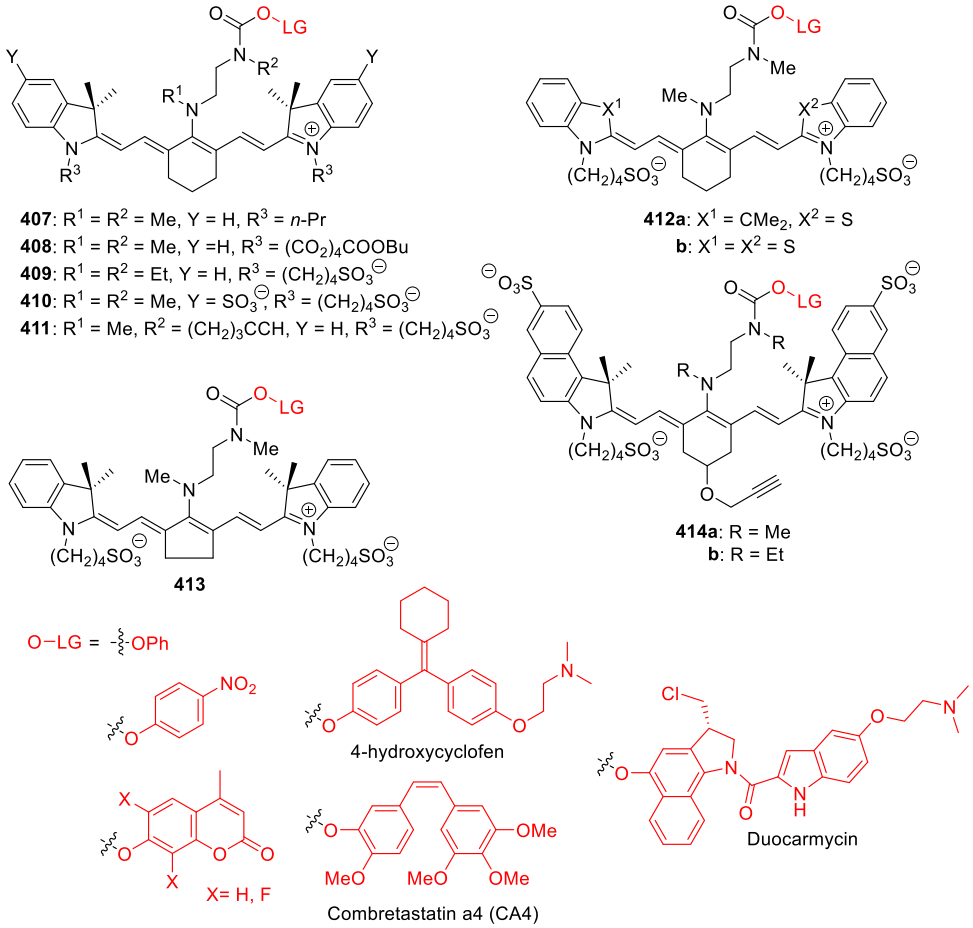

Figure 67. Structures of Cy7 photocage derivatives.

rapidly in PBS buffer to form two carbonyl intermediates, **416** and **417** (Scheme 98).[1514] Only **417** underwent efficient β-elimination, however. The formation ratio of **416** and **417** (~4:1; 70% chemical yield) explains the relatively low overall uncaging yield of this process (~14%).[1514]

Scheme 98. Mechanism of Uncaging from Cy7 PPGs via a Photooxidative Cleavage/β-Elimination Sequence[1514]

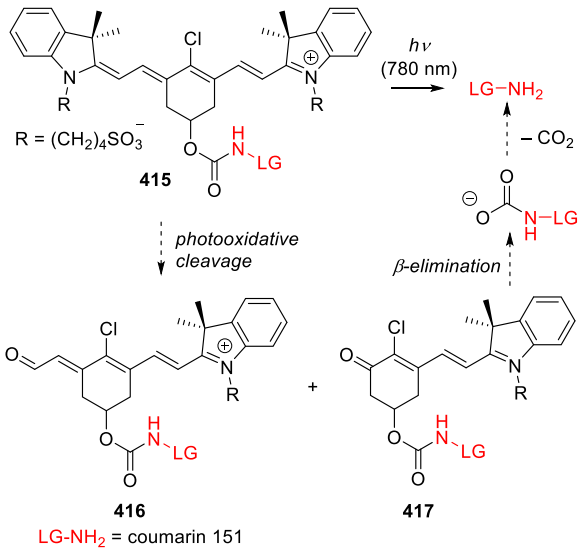

The photooxidative cleavage/β-elimination sequence was also applied to merocyanines such as **418** and **419** (λ_{max} = 664 and 713 nm, respectively).[1514] It was previously shown that oxidative cleavage takes place preferentially in the position adjacent to the more electron-rich heterocycle in unsymmetrical merocyanines.[1505,1511] Accordingly, irradiation of **418** and **419** (λ_{irr} ≈ 660 and 690 nm, respectively, in PBS buffer, pH 7.4) resulted in the release of coumarin **151** with chemical yields of 33% and 22%, respectively[1514] (Scheme 99). The

Scheme 99. Photochemistry of Merocyanine Photocages 418 and 419 Involving a Photooxidative Cleavage/β-Elimination Sequence[1514]

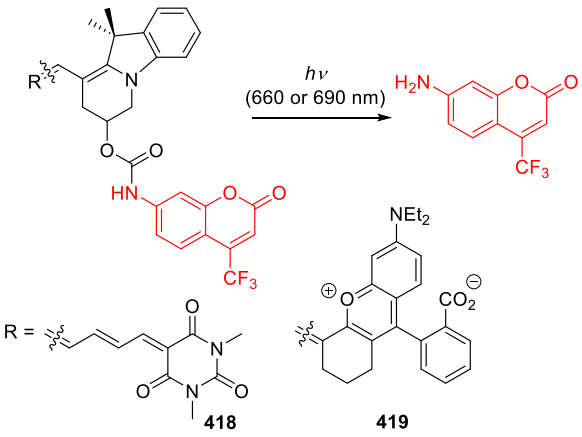

https://dx.doi.org/10.1021/acs.chemrev.0c00663
Chem. Rev. 2020, 120, 13135−13272

Scheme 100. Photouncaging of Cyclofen Derivatives from Cyanine Photocages[1512]

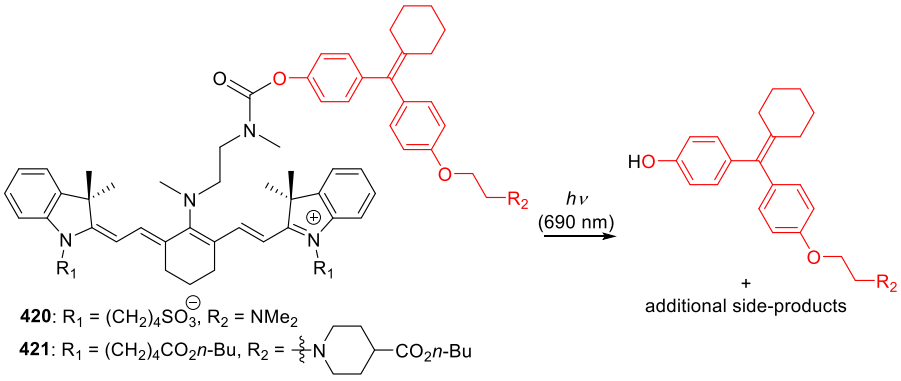

difference in yield was attributed to differences in the extent of dye aggregation in solution.[1514] For both compounds, additional release (4−5%) was observed after irradiation was stopped, suggesting that β-elimination is the rate-limiting step.[1514]

The estrogen receptor antagonist/agonist 4-hydroxycyclofen was caged with a Cy7 derivative (**420**) and its light-induced release was used to regulate gene expression in cell cultures (λ_{irr} = 690 nm; Scheme 100).[1491,1512] The reactive oxygen species generated during the photodecomposition process and the potentially reactive carbonyl photooxidation products were both well-tolerated in the studied cell cultures. Compound **420** also enabled light-mediated regulation of gene expression under similar irradiation conditions (λ_{irr} = 690 nm) in a CreER/LoxP system in transgenic mouse embryonic fibroblasts (MEFs).[1512] Exchanging the butyl sulfonic acids on the indolenine nitrogens with *n*-butyl pentanoates (**421**) significantly improved cellular penetration and increased spatial control over photoactivation by causing intracellular entrapment of the photocage.[1491] A prolonged irradiation time was required in experiments using this compound,[1491,1512] which was a limitation in applications requiring efficient substrate release. Fluorescence imaging of **420** in MEF and HeLa cells revealed that its intracellular distribution displayed a distinct punctate pattern and that it co-localized with LysoTracker staining,[1512] whereas **421** co-localized with MitoTracker.[1491] This difference in subcellular localization was attributed to the different charges of the two compounds. The cellular uptake mechanism was not determined, but other non-sulfonated heptamethine cyanines were shown to be captured by cells via endosomal uptake.[1547−1549]

Cy7 PPGs have also been used for antibody-targeted drug-release.[1534,1550,1551] The two strategies discussed above were used to non-specifically conjugate an NHS ester, the caged combretastatin A4[1525] (CA4, a microtubule polymerization inhibitor) derivative **422**, and the caged duocarmycin[1524,1552] (a DNA alkylating agent) derivative **423** to panitumumab (Pan), a clinically used anti-human epidermal growth factor receptor (EGFR) monoclonal antibody (Figure 68). The latter conjugate was injected *in vivo* into mice bearing MDA-MB-468 EGFR+ tumor xenografts, and the tumor area was irradiated at 690 nm 4 days after its administration. This single-dose treatment was sufficient to significantly reduce tumor size and improve overall survival compared to control groups.[1524] A combination therapy using **423** and Pan-IR700[947] (a near-IR photodynamic therapy agent) exhibited greater treatment efficacy than either therapeutic agent alone.[1552] The location

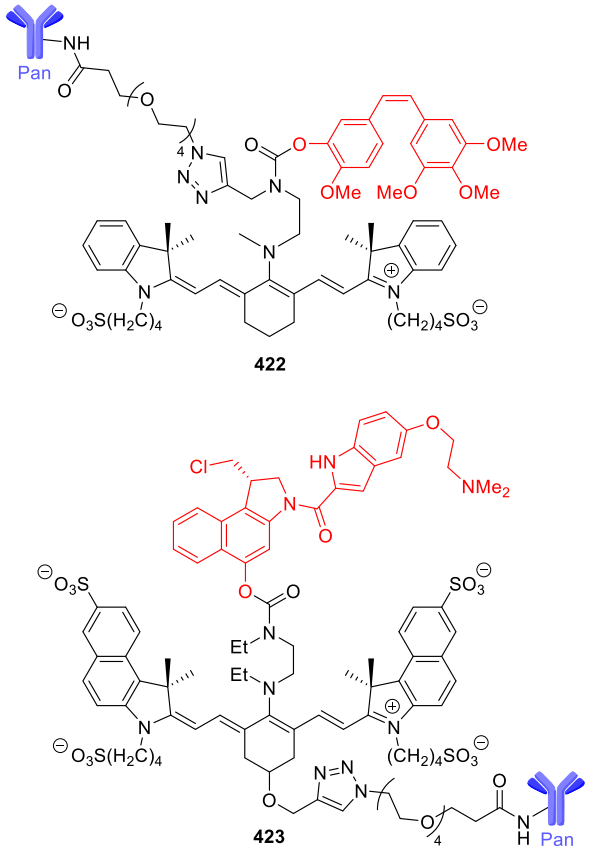

Figure 68. Structures of CA4 and duocarmycin caged with Pan-targeted heptamethine cyanine photocages.

of this antibody-drug conjugate was verified prior to its photoactivation by exploiting the fluorescence of the heptamethine cyanine photocage.[1524,1525,1552]

6.4. Photosensitization by Nanoparticles and Nanomaterials

Nanotechnology has found a remarkable array of applications in science and technology including biotechnology and biomedicine.[1553] Nanoparticles (NPs) and nanocarriers are frequently used for diagnostics, biosensing, photodynamic therapy, photothermal therapy, and targeted and controlled drug delivery/release. Developments in this field have been reviewed extensively in the past decade.[8,14,15,114,129,130,1415,1438,1554−1585] Various materials can be used in the design of nanocarriers including metal NPs, semiconductor NPs, nanocarbons, virus- and bacteriophage-

https://dx.doi.org/10.1021/acs.chemrev.0c00663
Chem. Rev. 2020, 120, 13135−13272

based NPs, microcapsules, and hydrogel-based systems.[1554,1556,1586] NPs can be both carriers (transporters) or active participants in drug (species) delivery. Photoactivatable NP systems may feature direct covalent bonds to drug molecules, or drugs may be encapsulated via non-covalent interactions. These systems must be stable in the relevant environment until an external trigger is applied to induce release. Light-activated release mechanisms include photochemical bond cleavage, photoreduction, photooxidation, photochemically-induced hydrophobicity switching, photocross-linking, photoisomerization, and photothermal processes.[1554] The following paragraphs briefly review the fundamental principles of species release from NPs upon irradiation with visible/NIR light and present some notable examples of related NP systems. This review is not fully comprehensive because many more specific reviews already exist, as noted above.

6.4.1. Photosensitization by Quantum Dots. Quantum dots (QDs), nanoscale semiconductor particles with interesting optical and electronic properties, typically consist of binary compounds such as PbS, PbSe, or CdS,[1587] although carbon[1588] and silicon quantum dots[1589] have also been used for uncaging purposes. They usually exhibit broad absorption spectra and narrow emission peaks and have large two-photon absorption cross sections. Their irradiation generally causes electron excitation from the valence band to the conduction band, and the resulting electron and hole can interact to produce an exciton. Their photophysics can be controlled using appropriate ligands.[1590,1591] Photoinduced energy transfer (Förster resonance energy transfer, FRET) or electron exchange between an excited QD and a ligand that undergoes subsequent chemical change is another way of using QDs for photosensitization.[1590,1592] QDs can interact with both electron acceptors and donors upon excitation. It should be noted that QDs are considerably larger than molecular species.

The QDs can serve as antennas that sensitize the photoreaction. Ford and co-workers reported that NO (section 4.2) is generated from electrostatic assemblies of water-soluble CdSe/ZnS and CdSeS/ZnS QDs loaded with negatively charged dihydrolipoic acid surface ligands and the cationic complex *trans*-Cr^{III}(cyclam)$(ONO)^{2+}$ (cyclam = 1,4,8,11-tetraazacyclotetradecane) upon irradiation with visible light (Scheme 101).[1593]

Scheme 101. QD-Mediated Photorelease[1593]

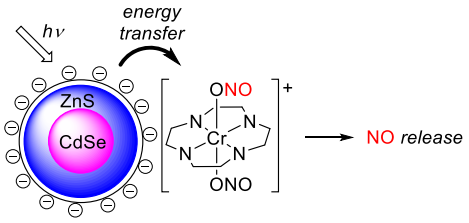

Carbon quantum dots (CQDs) have high photostability and large two-photon cross sections.[1588] CQDs covalently linked to a nitroaniline derivative as a NO photodonor were shown to release NO (section 4.2) upon one-photon (<450 nm) or two-photon (800 nm) absorption via anenergy-transfer mechanism.[1594] Another example of drug delivery from a CQD using a quinoline-based phototrigger was reported by Ghosh, Singh, and co-workers.[1595]

Photoinduced release via electron transfer from QDs to a ligand requires rather small nanoparticles to enable close contact between the two species.[1592] Bao, Zhu, and co-workers prepared water-soluble nanocrystalline CdSe/ZnS particles functionalized with an *N*-alkyl-4-picolinium ester linked to the anticancer drug 5-fluorouracil and L-cysteine (Scheme 102).[1596] Upon irradiation at λ_{irr} > 400 nm, 5-fluorouracil was liberated via electron transfer from the QD to the picolinium moiety, with L-cysteine acting as an electron donor.

Scheme 102. QD-Mediated Photorelease[1592]

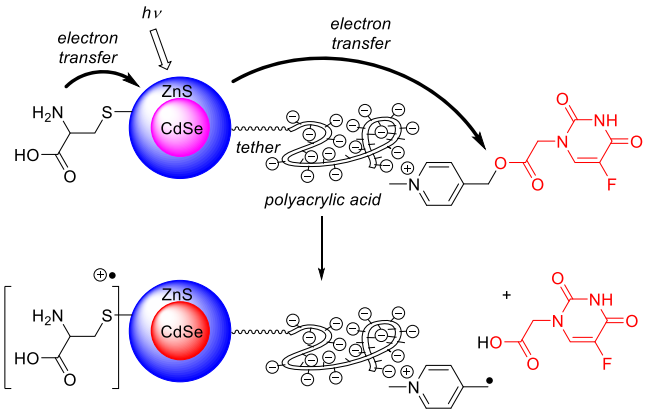

Water-soluble CdTe QDs capped with mercaptopropionic acid and a ruthenium nitrosyl complex *cis*-$[Ru^{II}(NO)(4AP)(bpy)_2]^{3+}$ (bpy = 2,2′-bipyridine, and 4AP = 4-aminopyridine) were shown by Ford, da Silva, and co-workers to release NO (section 4.2) upon irradiation at 530 nm via a charge-transfer mechanism.[1597] Visible light excitation of CdSe QDs was also demonstrated to trigger the release of coumarin from cinnamate surface ligands.[1598] In this system, electron transfer from the excited nanocrystal to the surface-bound cinnamate triggers *E*−*Z* isomerization and subsequent lactonization. *o*-Nitrobenzyl (oNB) groups can also be liberated from CdTe/CdS core/shell QDs under UV illumination to control QD emission.[1599] The possibility of exciton energy transfer was ruled out in this case, and because there was no overlap between QD emission and oNB absorption, it was suggested that an electron or hole transfer from the QD to the oNB occurred. Other examples of UV- or near-visible light-activated release via oNB group cleavage have also been reported.[197,1600,1601]

6.4.2. Photorelease Mediated by Upconversion and Second-Harmonic Nanoparticles. Several photophysical phenomena combine the energies of two or more photons to produce that of one higher-energy photon. Photon upconversion in organic molecules converts two or more low-energy photons into one higher-energy photon via two fundamental mechanisms: two (multi)-photon absorption (Figure 69b) or sensitized triplet−triplet annihilation (TTA).[136,1602] The former mechanism leads to an excited state of higher energy (which would also be accessible by one-photon absorption; see Figure 69a) via a virtual state, whereas the latter intermolecular process typically involves two molecules in their triplet states that interact to leave one molecule in the ground state with the second molecule being excited to a higher electronic state. Some nonlinear crystal materials and non-centrosymmetric compounds and structures can exhibit second-harmonic generation (SHG), in which two photons with the same

https://dx.doi.org/10.1021/acs.chemrev.0c00663
Chem. Rev. 2020, 120, 13135−13272

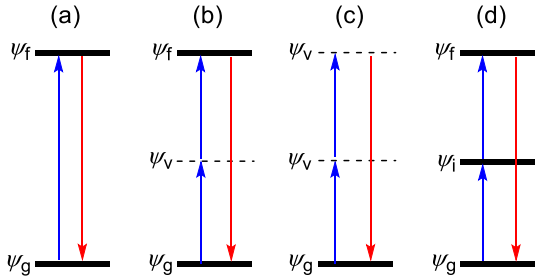

Figure 69. (a) Single-photon absorption; (b) two-photon absorption; (c) second-harmonic generation; (d) upconversion. ψ_g = ground state; ψ_f = final excited state; ψ_v = virtual state; ψ_i = intermediate state.

frequency interact with matter and coalesce to a virtual state (Figure 69c).[1603] The resulting second-harmonic photon is generated practically instantaneously (within a few fs), so the signal is coherent (frequency doubling). Another interesting phenomenon is observed in so-called upconversion nanoparticles (UCNPs), in which two or more sequentially absorbed photons are converted into one emitted photon with higher energy via real metastable excited states (Figure 69d).[1324,1604−1609] UCNPs typically absorb in the IR region and emit in the visible or ultraviolet regions. Most UCNPs consist of rare-earth-based lanthanide- or actinide-doped transition metals. The theoretical quantum yield of upconversion cannot exceed 0.5 because at least two photons are required to produce one upconverted photon.

Because of their unique optical and chemical properties, UCNPs can be used for drug release/delivery.[1610−1620] They are convenient and biologically favored "UV-vis light-bulbs"[49,1621] because of their ability to convert NIR light into UV and visible photons. Many conventional UV-absorbing photoactivatable groups that undergo photocleavage or photoswitching processes can thus be activated through the tissue-transparent window. Because of the many recent excellent reviews cited above, we discuss only a few illustrative examples.

An application using *o*-nitrobenzyl derivatives was presented by Liu, Xing, and co-workers (Scheme 103).[202] Monodispersed core-shell UCNPs consisting of $NaYF_4$ nanocrystals doped with Yb^{3+} and Tm^{3+} were functionalized with cationic photoreleasable linkers via covalent bonding, enabling the adsorption of anionic siRNA molecules via electrostatic interactions. Upon NIR light irradiation (980 nm), the photolabile linker was cleaved by upconverted UV light, initiating the intracellular release of the siRNA.

The literature provides many examples of applications in which different types of UCNPs serve as mediators in species release. Most works of this type published in recent years have used *o*-nitrobenzyl derivatives as photocleavable moieties.[203,1622−1641] However, other systems have also been studied, including coumarin-4-ylmethyl,[365] pyrenemethyl,[1642] or *o*-hydroxycinnamic[1643] PPGs as well as photoactivatable ruthenium,[1333,1644] platinum,[1645,1646] and manganese[1159] complexes, and Roussin's black salt.[1647] Photochromic moieties have also been used for species liberation involving UCNPs, for example, by incorporating azobenzene[1648−1650] or spiropyran/merocyanine[1651] photoswitches.

Second-harmonic emission has recently been used for uncaging. Bismuth ferrite harmonic nanoparticles (HNPs) were used to release L-tryptophan linked to a coumarin-4-ylmethyl photoactivatable group via a carbamate functionality (Scheme 104).[387] Light (790 nm) from a femtosecond pulsed laser was converted into emission at 395 nm, which was responsible for the excitation of the PPG.

6.4.3. Photothermally Controlled Release. Visible or NIR irradiation of some nanoparticles consisting of noble metals (gold or silver), carbon (graphene derivatives or carbon nanotubes), metallic composites (CuS, MoS_2), or polymers (polyanilines and liposomes) can result in the production of thermal energy (heat), which is dissipated into the surroundings of the nanostructure. This process is referred to as the photothermal effect,[1652,1653] and it can be regarded as a distinct type of photosensitization. Photothermal effects have

Scheme 103. Release of siRNA from UCNPs[202]

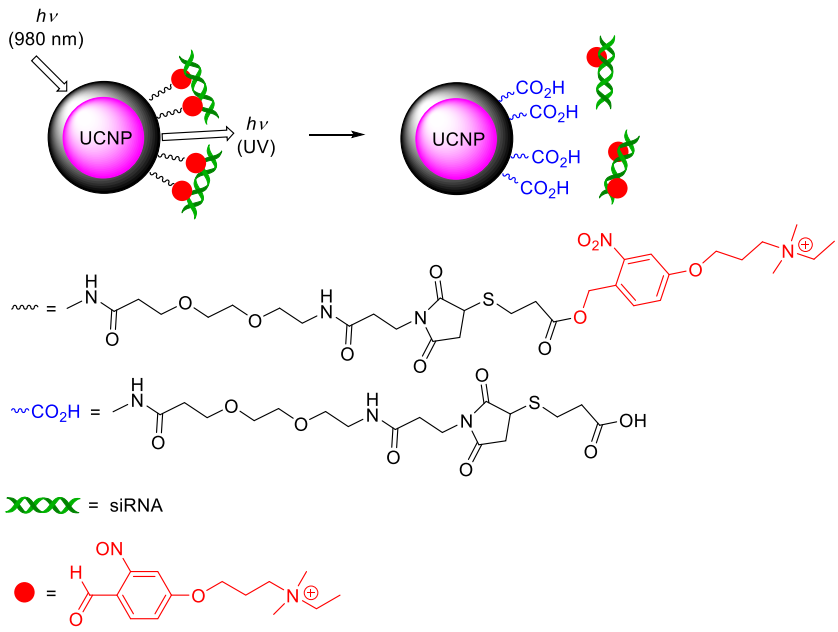

https://dx.doi.org/10.1021/acs.chemrev.0c00663
Chem. Rev. 2020, 120, 13135−13272

Scheme 104. Release of L-Tryptophan from UCNPs[387]

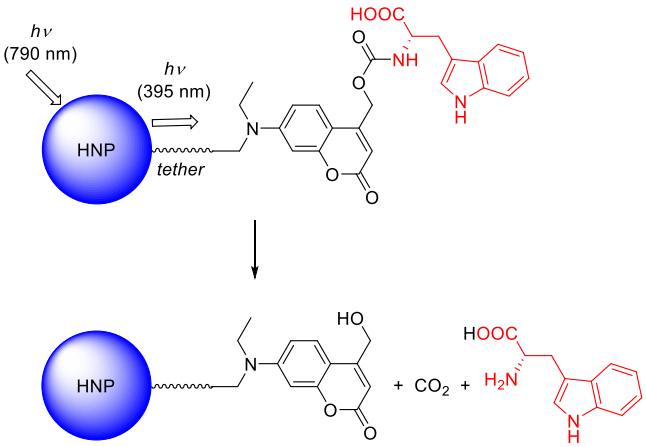

been used to achieve spatially and temporally controlled release of species such as drugs and metal ions.[1653−1656]

Upon excitation, noble metal nanoparticles (particularly those made of gold, AuNPs) exhibit localized surface plasmon resonance, that is, resonant oscillations of the conduction electrons, which are transformed into phonons, followed by rapid relaxation and heating.[1654] The wavelengths of the absorption maxima of AuNPs are related to the size of the particles: 10−40 nm AuNPs absorb in the green region, while larger particles have bathochromically shifted maxima. AuNPs have been used to uncage, among other things, (a) drugs embedded in a polymeric matrix surrounding AuNPs, (b) drugs embedded in liposomes together with AuNPs, and (c) drugs covalently or non-covalently attached to AuNPs via a tether.[1654] In all cases, photothermal heating disrupts the interactions confining the drug, leading to its release.

Scheme 105 shows a photothermally releasable system based on Au nanocages covered with poly(*N*-isopropylacrylamide)

Scheme 105. Au Nanocage Opening via the Photothermal Effect[1657]

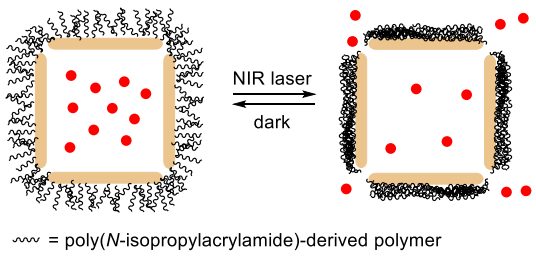

chains that undergo conformational changes when heated.[1657] Upon irradiation with a NIR laser, the light is absorbed by the AuNPs and is converted into heat via the photothermal effect. When the polymer chains collapse, a pre-loaded drug such as doxorubicin is released through the resulting pores. The polymer chains return to their original conformation in the dark and the pores close. Many other photothermal release systems using AuNPs have been reported.[1658−1672] Releasable systems consisting of cobalt nanowire-based particles,[1673] $NaYbF_4$:Er^{3+} UCNP nanocomposites,[1674] carbon nanotube thermosensitive hydrogel,[1675] biochar,[1676] and photothermal heating of water droplets confined in polymeric particles[1677] have also been reported.

7. PHOTOACTIVATABLE POLYMERS, MICELLES, AND VESICLES

Many photoactivatable polymeric materials, micelles, and vesicles have been developed for drug/species delivery in recent decades.[109,1573,1678−1689] Photocleavable polymer nanostructures are particularly interesting platforms for targeted drug delivery.[14] Several release mechanisms are available: these systems can serve as photoresponsive/degradable nanocarriers for drug delivery, polymeric films can facilitate photochemical species detachment or patterning,[1683] and hydrogels can alter the properties of biomaterials and affect the microenvironment.[1575,1690]

Photocleavage of covalent bonds in UV-absorbing chromophores such as *o*-nitrobenzyl or coumarin-4-ylmethyl groups[10,1683] connected to polymers and vesicles is an appealing strategy because the photochemistry and applications of these chromophores are well known.[1691] Their activation with red or NIR light is usually enabled by two-photon absorption or the use of upconverting nanoparticles (section 6.4.2). For example, two-photon or blue-light activation was used to remove *o*-nitrobenzyl-derived PPGs to release payloads from micelles[1692−1694] or polymers.[271,1695−1697] Similarly, coumarin-4-ylmethyl groups have been used to release drugs from micelles,[445] polymers,[1696,1698] hyaluronic acid nanogels,[1699] nanoparticles,[383,415] and nanocomposites.[364] Applications of photodegradable micelles consisting of amphiphiles containing a diazonaphthoquinone group have also been reported.[1700−1705]

One-photon visible-light photoactivation (at 420 nm) of cascade depolymerization of self-immolative polymersomes with photoremovable perylen-3-yl protecting groups[553] was shown to release encapsulated bioactive agents (section 2.3) via photosolvolysis (Scheme 106).[563]

Scheme 106. Photochemical Depolymerization of Self-Immolative Polymersomes[563]

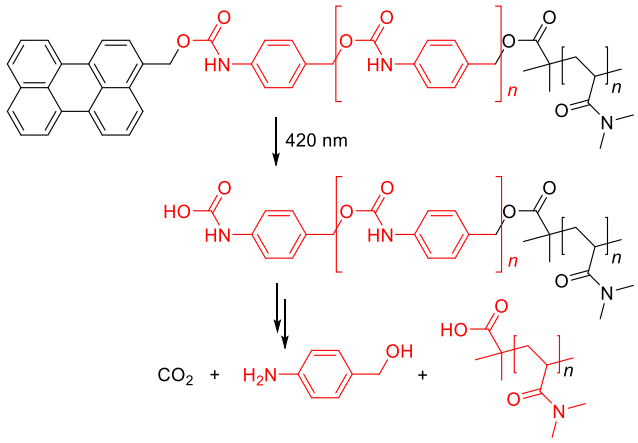

Wu and co-workers designed red-light-responsive Ru^{II}-containing block copolymers for anticancer phototherapy. These copolymers can be assembled into micelles, vesicles, or large compound micelles depending on their molecular weights (Scheme 107).[1483] Upon excitation at 656 nm, they release the $^1O_2$ generating anticancer agent $[Ru(tpy)(biq)(H_2O)]^{2+}$ via ligand exchange (see section 3). Similar strategies were used with block copolymers bearing $[Ru(Biq)_2(Hob)_2](PF_6)_2$ (Biq = 2,2′-biquinoline, Hob = 4-((6-hydroxyhexyl)oxy)-benzonitrile)[1706] or surface-grafted ruthenium complexes to

https://dx.doi.org/10.1021/acs.chemrev.0c00663
Chem. Rev. 2020, 120, 13135−13272

Scheme 107. Release from Ru^{II}-Containing Block Copolymers[1483]

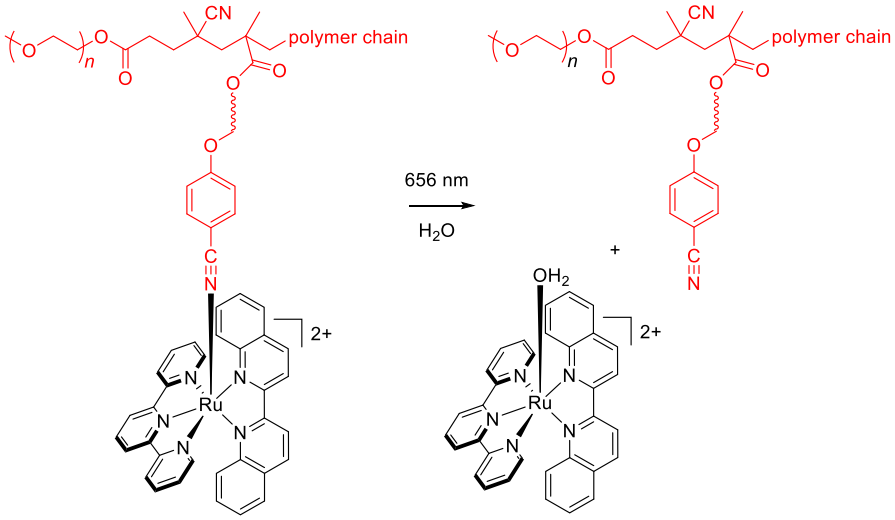

release cytotoxic molecules into cancer cells from mesoporous silica nanoparticles.[1274]

The amino-1,4-benzoquinone (**424**; see also section 2.10) photoactivatable moiety was used to prepare a nanoparticle-bound photocage−drug conjugate. Upon irradiation with red light, the nanoparticles dissolved in aqueous media, releasing the drug (Scheme 108; drug = paclitaxel, dexamethasone, or chlorambucil).[726] It was also shown that an encapsulated cyanine NIR-fluorescent dye such as DiD or IR780 could facilitate the location of the nanoparticles and monitoring of the photorelease process.

Scheme 108. Amino-1,4-benzoquinone Derivatives as PPGs for Drug Uncaging from Nanoparticles[726]

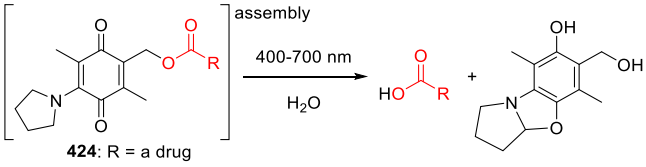

Photorelease from light-responsive polymeric micelles made from an amphiphilic block polymer incorporating a BODIPY derivative (see section 2.12) is shown in Scheme 109.[824] Upon irradiation, the micellar assembly of this polymer is disrupted due to the release of phenolate from the polymers to release a payload (Nile red). Another example of photoactivatable drug delivery is the photochemical release of dexamethasone from subcutaneously implanted polymeric particles, in which a π-extended *o*-nitrobenzyl derivative (section 2.1.1) absorbing below 500 nm serves as the photocleavable moiety.[261]

Mesoporous silica nanoparticles (MSNs) are important drug delivery nanocarriers with high surface areas and large pore volumes for drug loading, and they are readily functionalized with light-responsive groups or photoswitches.[1707−1710] Most known systems of this type rely on doped upconversion nanoparticles that convert NIR radiation into UV/vis radiation (section 6.4.2) or Au-based, CuS, or graphene oxide nanoparticles that absorb and convert NIR light into thermal energy via the photothermal effect (see section 6.4.3).

For example, 1P (420 nm) or 2P (800 nm) irradiation was used to release the anticancer drug chlorambucil, which was connected to a 7-amino-coumarin derivative and grafted onto the surface of aminopropyl-functionalized MSNs (Scheme 110).[384] The drug is liberated by a photosolvolysis reaction. Multi-photon-absorption (808 nm) leading to dissociation of *o*-nitrobenzyl-containing poly(ethylene glycol) on the surface of gold nanostars coated with a mesoporous silica shell was also shown to release doxorubicin.[1711]

Scheme 109. Release from BODIPY-Containing Amphiphilic Block Polymer[824]

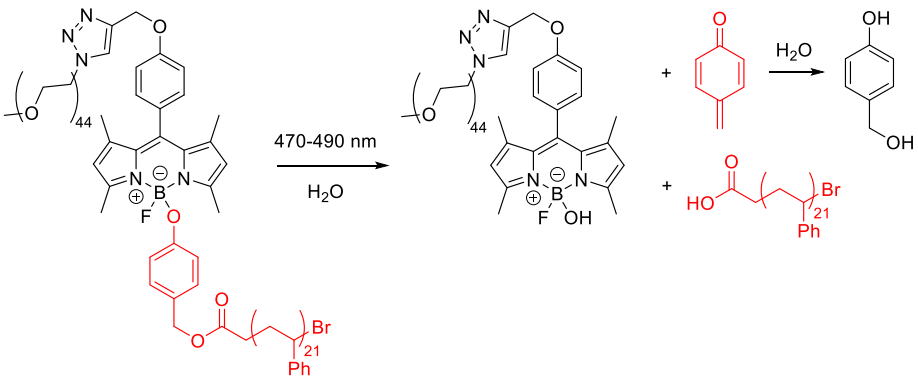

https://dx.doi.org/10.1021/acs.chemrev.0c00663
Chem. Rev. 2020, 120, 13135−13272

Scheme 110. Release from Aminopropyl-Functionalized MSNs[384]

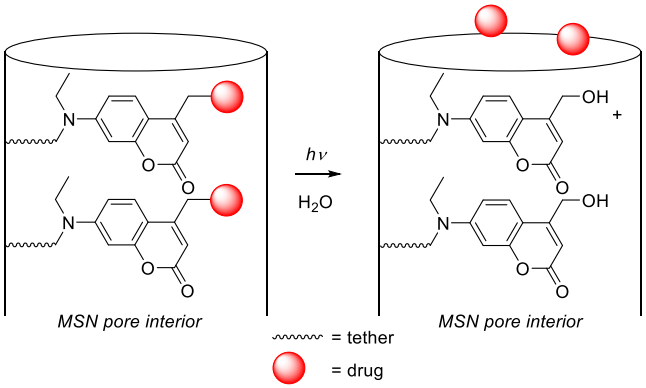

8. RELEASE MEDIATED BY PHOTOSWITCHING

Host−guest interactions are affected by several factors, such as the nature of the host and guest molecules and the properties of the solvent.[1712] The host entity can consist of a single molecule, usually a photoswitchable (photochromic) system whose photoreaction leads to the release of a guest molecule due to a change in binding affinity. The two isomers of a photoswitchable molecule have distinct chemical, physical and optical properties, which can be used to tune the properties of the host material. The most commonly used photoswitches[1713] for this purpose are azobenzene,[1714] spiropyran, and diarylethene derivatives (whose photoswitching involves ring-opening/closing) (Scheme 111), but stilbene and fumaric acid derivatives (which undergo light-induced $E-Z$ isomerization) or anthracene and coumarin chromophores (which undergo reversible photodimerization) have also been used.[1712] An alternative approach uses multi-component supramolecular cages or capsules that incorporate a photoactivatable moiety to control guest release. To achieve visible or NIR light absorption, UV-absorbing chromophores can be modified by π-extension to bathochromically shift their absorption bands. Alternatively, they can be excited via a 2-photon absorption, upconversion emission, or sensitization.[1411,1715] Research in this area has been reviewed on several occasions in the past decade,[1712,1714−1722] so here we present only some particularly notable systems bearing chromophores absorbing over 400 nm.

Since Ueno and co-workers showed in 1978 that azobenzene-capped β-cyclodextrin can regulate the binding of various substrates (including toluene, cyclohexanol, and geraniol) upon irradiation at wavelengths of 320−390 nm,[1723] the azobenzene unit has become one of the most widely used photoswitches. Azobenzene-bridged cryptand **425** is a typical example; its irradiation with visible light selectively triggers $Z \rightarrow E$ isomerization, while $E \rightarrow Z$ isomerization is triggered by UV light, enabling control over its binding affinity towards the guest 2,7-diazapyrenium ion (Scheme 112).[1724]

Tian and co-workers observed room-temperature phosphorescence emission as a result of photochemically controlled complexation of 2-hydroxy-5-((4-nitrophenyl)-diazenyl)-benzoate (**426**) in β-cyclodextrin (Scheme 113), displacing the fluorescent heavy-atom containing α-bromonaphthalene (**427**). The fluorescence of the bromonaphthalene was suppressed when complexed with the cyclodextrin but not when it was displaced by the E-isomer of the azadiene.[1725] Similarly, Wang and Wu constructed supramolecular valves from tetra-*o*-methoxy-substituted azobenzene and β-cyclodextrin to control the release of doxorubicin from nanopores of mesoporous silica nanoparticles (see section 7) using red light.[1726]

An application of a self-assembled coordination cage consisting of two square-planar-coordinated Pd^{II} ions and four photochromic dithienylethene-containing ligands was reported by Clever and co-workers.[1727] The photorelease and encapsulation of the guest, $[B_{12}F_{12}]^{2-}$, was accomplished using UV and white light, respectively. Photoactivatable metal-containing complexes[40,870] can also serve as excellent platforms for metal ion photorelease. Metal ions can induce profound biological responses, so it is desirable to control their concentrations with a high spatiotemporal resolution using photoactivatable systems. To this end, Yu and collaborators introduced the terthiazole-based molecular switch **428**, which enables photoswitchable release and uptake of Zn^{2+} ions based on a 6π-electrocyclization/cycloreversion reaction of the chromophore and excited-state intramolecular proton transfer (ESIPT; Scheme 114).[1728] Additionally, visible-light triggered switching of the G-quadruplex ligand binding mode and G-tetrad structure formation using a pyridinium-substituted dithienylethene has been demonstrated under physiologically relevant conditions.[1729]

Another notable photoswitchable system for controlled metal ion release is a bisstyrylthiophene derivative that incorporates both a π-extended photoactivatable nitrobenzyl group and a conjugated Ca^{2+} chelator (see also section 2.1).[219] This species has a large two-photon cross section (350 GM) at 775 nm. Ca^{2+} photorelease (/uptake) has also been accomplished using a photoswitchable diarylethene-containing chelator,[1730] visible-light irradiation of flavin photosensitizers in the presence of Ca^{2+}-EDTA,[1410] and two-photon excitation

Scheme 111. Examples of Photochromic Systems

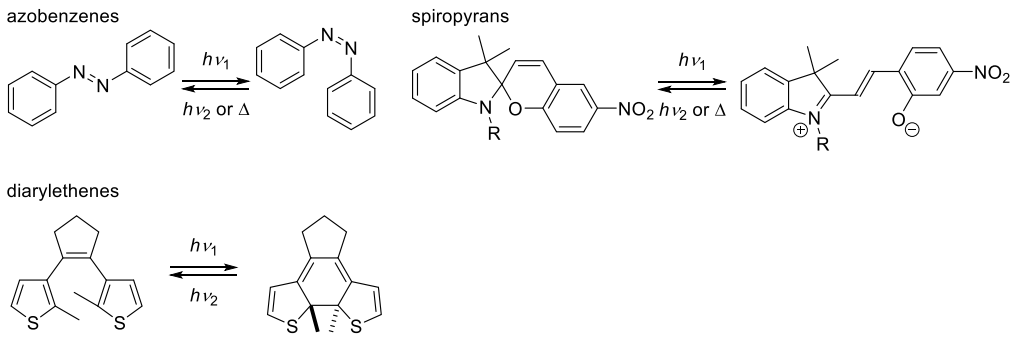

https://dx.doi.org/10.1021/acs.chemrev.0c00663
Chem. Rev. 2020, 120, 13135−13272

Scheme 112. Azobenzene Isomerization to Control Binding Affinity of a Guest[1724]

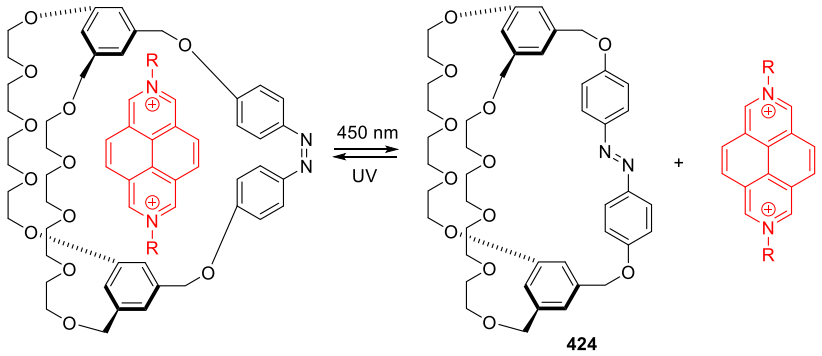

Scheme 113. Photochemically Controlled Complexation in β-Cyclodextrin[1725]

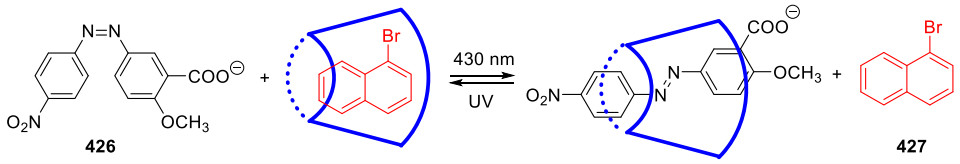

Scheme 114. Terthiazole-Based Molecular Photoswitch[1728]

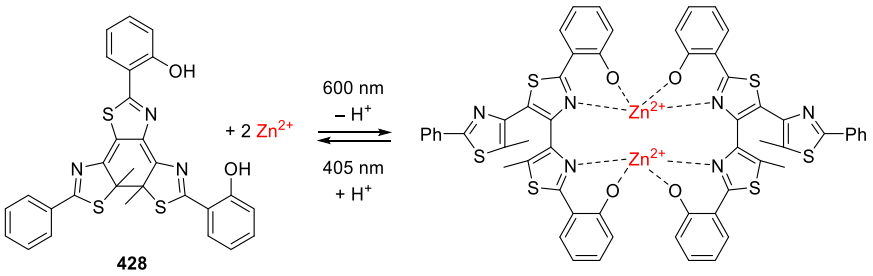

of a 5-bromo-2-nitrobenzyl-substituted ethylene glycol tetraacetic acid chelator.[188] The last example discussed here is a system that releases metal ions such as Ca^{2+}[1731] or Zn^{2+} from polymersomes, that is, bilayer vesicles that self-assemble from amphiphilic diblock copolymers.[1732] A photoresponsive polymersome system containing an ethyne-bridged bis-[(porphinato)zinc] fluorophore as a hydrophilic membrane solute and dextran in the aqueous core undergoes deformation upon irradiation at 488 nm, liberating the metal ion.[1732]

The incorporation of photoswitchable moieties into the backbones of polymer nanoparticles, micelles, polymersomes, vesicles, microgels, liposomes, mesoporous silica nanoparticles, and so on offers another way of controlling the photochemical delivery/release of cargoes encapsulated within the assembled nanocarriers.[130,1581,1707−1709,1714,1715,1733−1738] As in the supramolecular systems discussed above, photoisomerization (e.g., azobenzene) and 6π-electrocyclization of triene systems (e.g., spiropyrans and diarylethenes; Scheme 111) are commonly used mechanisms for species release from nanocarriers. This approach was exemplified by photochromic polymersomes composed of self-assembled poly(ethylene oxide) diblock copolymers containing a spiropyran-based monomer, which exhibited reversible bilayer permeability upon photoisomerization of the hydrophobic spiropyran to give the zwitterionic merocyanine upon irradiation at >450 nm; this process could be reversed by irradiation at <420 nm (Scheme 115).[1739] The authors assumed that the structure of the polymersomes is determined by multiple cooperative noncovalent interactions

Scheme 115. Photoswitching of a Spiropyran/Merocyanine Pair in Polymersome[1739]

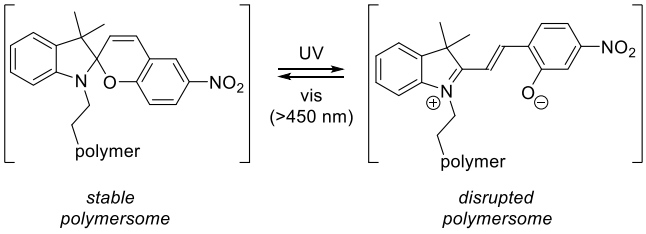

including hydrophobic, hydrogen bonding, π−π stacking, and electrostatic interactions, and that the isomerization changes the pattern of these interactions. This system was successfully used to release a nuclei-staining dye, 4′,6-diamidino-2-phenylindole, in living HeLa cells.

Similarly, photoinduced isomerization of two different donor−acceptor Stenhouse adducts upon irradiation with visible light (Scheme 116) was used to switch the permeability of polymersome by inducing the isomerization of a nonpolar triene-enol into a polar cyclopentenone within amphiphilic block copolymers containing poly(pentafluorophenyl methacrylate).[1740] The hydrophilic anticancer drug 2′-deoxy-5-fluorouridine and the DNA-intercalating dye 4′,6-diamidino-2-phenylindole were used as payloads in this system. Other photoswitchable systems have also been used for controlled delivery upon irradiation with visible or NIR light including a spiropyran−merocyanine-containing polymer,[1741] a nanocar-

https://dx.doi.org/10.1021/acs.chemrev.0c00663
Chem. Rev. 2020, 120, 13135−13272

Scheme 116. Switching of a Stenhouse Adduct within Amphiphilic Block Copolymers[1740]

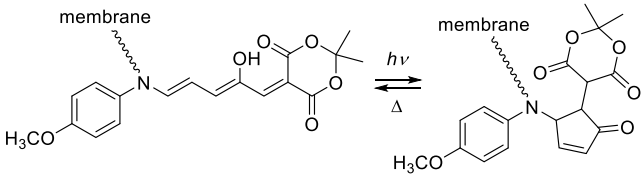

rier-based on hollow mesoporous silica (HMS) nanoparticles,[1742] polymer nanoparticles incorporating a donor–acceptor Stenhouse adduct,[1743] sulfonatocalix[4]arene with bound flavylium ions,[1744] azobenzene-containing micelles,[1745] β-cyclodextrin-grafted hyperbranched conjugated polymers,[1746] and catanionic vesicles.[1747] Additionally, the azobenzene chromophore has been used for the photochemical control of drug release from supramolecular[1748] and poly(ethylene glycol)[1749] hydrogels.

Photoisomerization-induced release of luminescent dyes and anticancer drugs from functionalized azobenzene molecules attached to the interiors of MSN pores upon irradiation at 413 nm was reported by Tamanoi, Zink, and co-workers (Figure 70).[1750] Another photoactivatable system was reported by

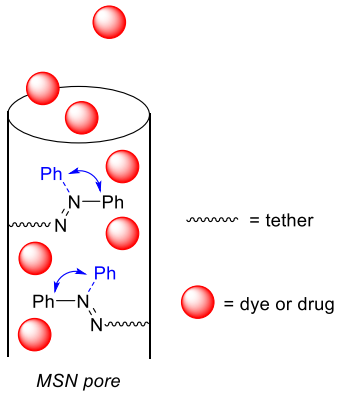

Figure 70. Azobenzene-controlled release from the pores of mesoporous silica nanoparticles.[1750]

Kneževič and co-workers,[1751] who entrapped the model dye sulforhodamine 101 inside the mesopores of mercaptopropyl-functionalized MSNs in the presence of a $Ru(bpy)_2(PPh_3)$ moiety coordinated to mercaptopropyl functional group. The dye was liberated upon irradiation at 455 nm via a ligand exchange reaction.

9. PHOTOACTIVATION AND PHOTODEACTIVATION OF DRUGS: PHOTOPHARMACOLOGY

Most of the photochemical release systems discussed in this review rely on irreversible release (uncaging) from auxiliary photochemically active/reactive chromophores that undergo various photochemical side-reactions, leading to their destruction and thus potentially to the formation of unwanted materials (Scheme 117a). These processes must be carefully considered during the design and development of new photoactivatable systems, especially in terms of their compatibility with biological systems where relevant. Despite this limitation, irreversible uncaging remains the dominant approach to photorelease in both fundamental and practical research. However, as discussed in the preceding sections, reversible release systems using (photoswitchable) photochromic moieties also exist and can be incorporated into more complex systems, where their reversible (photo)reactions such as *E*–*Z*-photoisomerization can induce changes in the binding affinity of a releasable guest upon irradiation (Scheme 117b, section 7). Active species can also be incorporated into a tether whose conformation/length changes upon irradiation to bring an attached active molecule into close proximity with a site of interest (Scheme 117c).[1752] Scheme 117d shows a different approach involving a so-called photochromic ligand that can exist in two or more different isomeric forms that are interconvertible upon irradiation, of which only one is active in a specific application. The isomerization, in this case, may also be triggered by heat (Δ) in one direction, and may thus proceed spontaneously under certain conditions. The term "photopharmacology" is used in reference to bioactive molecular systems that undergo reversible photochemical transformations that alter their pharmacokinetic or pharmacodynamic properties. This is a relatively new concept but one that has attracted considerable attention and has therefore been reviewed several times in recent years.[145,874,1752−1764]

Scheme 117. Irreversible versus Reversible Photoactivation

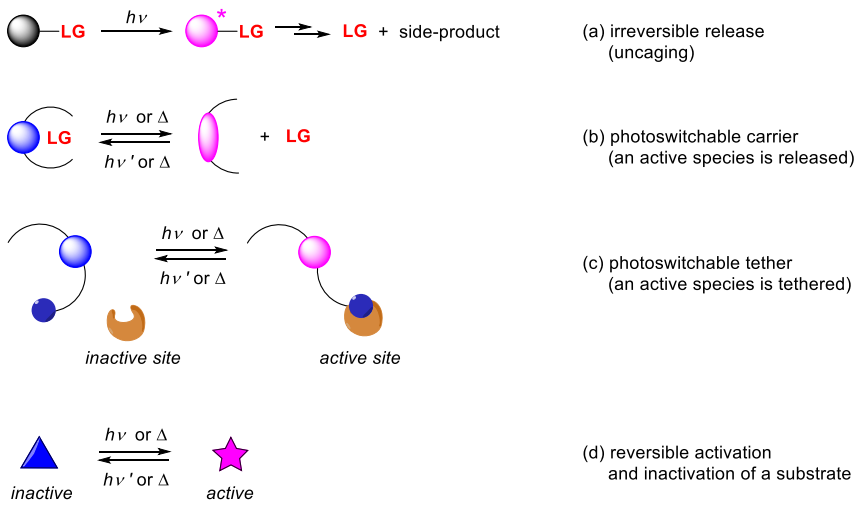

https://dx.doi.org/10.1021/acs.chemrev.0c00663
Chem. Rev. 2020, 120, 13135−13272

Consequently, we present only a few representative examples here.

Azobenzene and diarylethene photoswitches and their analogs (section 8) are the most frequently used photochromic systems in photopharmacology.[1752,1753,1758,1763,1765] Most of them are activatable by UV light in one direction and by visible light in the reverse process. Substituents attached to a photochromic group can bathochromically shift its absorption maxima such that both forward and backward photoactivation occurs in the visible part of the spectrum.

Both *E* and *Z* isomers of azobenzenes can be pharmacologically active. Trauner and co-workers introduced azobenzene derivative **429**, which is a freely diffusible photoswitchable antagonist of the α-amino-3-hydroxy-5-methyl-4-isoxazolepropionic acid (AMPA) glutamate receptor (Schemes 117 and 118).[1766] This compound is active in its stable *E*-form but considerably less active as the *Z*-isomer. Because of a significant bathochromic shift of its absorption maxima, the two isomers can be interconverted by irradiation at 460 and 600 nm, respectively.

Scheme 118. Photoswitchable Quinoxaline-2,3-dione Antagonist

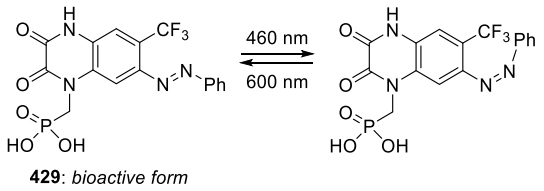

Another azobenzene-based protein ligand, **430**, was developed by Yuste, Gorostiza, and co-workers to activate the light-gated glutamate receptor LiGluR in living cells (Scheme 119; Glu = glutamate).[1767] The *E*-form of the tether is inactive, but *E*−*Z* isomerization induced by one- (>400 nm) or two-photon irradiation brings the glutamate residue at the end of the ligand chain into the vicinity of the receptor's glutamate-binding site. In the dark, the receptor is inactivated by the rapid and spontaneous reverse isomerization of the ligand.

Scheme 119. Azobenzene-Based Protein Switch

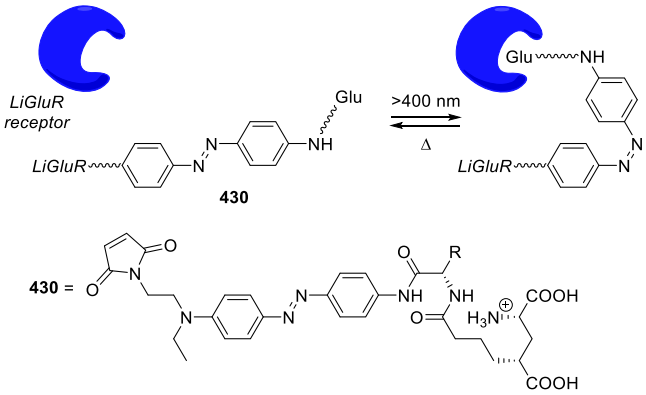

Szymanski, Feringa, and co-workers developed switchable antibacterial agents[1768] based on the azobenzene chromophore whose activity is controlled by visible-light irradiation.[1769] The *Z*-azobenzene derivative **431**, formed upon photoisomerization of the corresponding *E*-isomer at 652 nm, exhibited at least an 8-fold increase in activity (Scheme 120).

A different photoswitch based on a photochromic dithienylethene (**432**) was studied by König and co-workers who showed that the open isomer of this compound activated the dopamine D_{2S} receptor considerably more efficiently than the closed isomer (Scheme 121).[1770] Notably, the photophysical properties of these dithienylethene dopamine ligands exhibited high fatigue resistance.

Scheme 121. Photochromic Dithienylethene Derivative

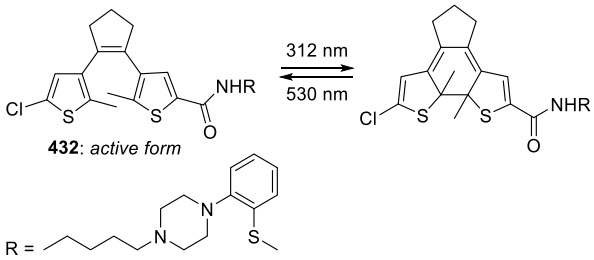

Bifunctional molecules targeting proteins for ubiquitylation by an E3 ligase complex and subsequent degradation by the proteasome (PROTACs; proteolysis targeting chimeras) are powerful tools for regulating the levels of certain cellular proteins.[1771] Photoswitchable PROTACs, or PHOTACs (photochemically targeting chimeras), that enable optical (photopharmacological) control of protein levels using azobenzene-containing photoswitches, were recently developed by Pagano and Trauner.[1772] Conceptually similar photoswitchable azobenzene-proteolysis targeting chimeras (Azo-PROTACs) were introduced by You and Jiang.[1773]

AUTHOR INFORMATION

Corresponding Authors

Roy Weinstain − *School of Plant Sciences and Food Security, Faculty of Life Sciences, Tel-Aviv University, Tel-Aviv 6997801, Israel*; orcid.org/0000-0002-1300-6802; Email: royweinstain@tauex.tau.ac.il

Scheme 120. Photoactivation of Antibacterial Azobenzene Derivative

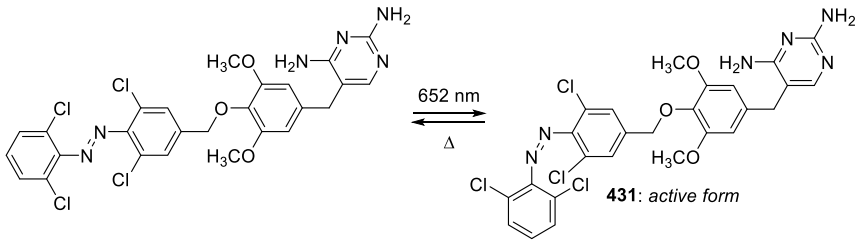

https://dx.doi.org/10.1021/acs.chemrev.0c00663
Chem. Rev. 2020, 120, 13135−13272

Petr Klán − *Department of Chemistry and RECETOX, Faculty of Science, Masaryk University, 625 00 Brno, Czech Republic;* orcid.org/0000-0001-6287-2742; Email: klan@sci.muni.cz

Authors

Tomáš Slanina − *Institute of Organic Chemistry and Biochemistry of the Czech Academy of Sciences, 166 10 Prague, Czech Republic*

Dnyaneshwar Kand − *School of Plant Sciences and Food Security, Faculty of Life Sciences, Tel-Aviv University, Tel-Aviv 6997801, Israel*

Complete contact information is available at: https://pubs.acs.org/10.1021/acs.chemrev.0c00663

Notes

The authors declare no competing financial interest.

Biographies

Roy Weinstain received his B.Sc. degree in chemistry and biology in 2005 from Tel Aviv University, Israel. He obtained his Ph.D. from the same institution in 2010 for the development of self-immolative molecular systems under the supervision of Prof. Doron Shabat. He then joined Prof. Roger Y. Tsien's group at the University of California San Diego as a post-doctoral fellow, working on the synthesis and application of fluorescent probes to study dynamic processes *in vivo*. Since 2014, he is a Senior Lecturer in the School of Plant Science and Food Security at Tel Aviv University, Israel. His research focuses on the development and implementation of chemical-biology methods to study the functions and regulation mechanisms of plant signaling molecules.

Tomáš Slanina received his M.S. degree from Masaryk University, Brno, Czech Republic in 2012. He received his Ph.D. in organic chemistry in 2015 in a joint programme between Masaryk University and the University of Regensburg, Germany, under the supervision of Prof. Petr Klán and Prof. Burkhard König. He later worked as a postdoctoral researcher in Prof. Alexander Heckel's group at Goethe University, Frankfurt am Main, Germany, and in the research group of Prof. Henrik Ottosson at Uppsala University, Sweden. He is currently a leader of the junior research group or redox photochemistry at the Institute of Organic Chemistry and Biochemistry in Prague, Czech Republic. His research interests include organic chemistry, photochemistry, physical organic chemistry, electrochemistry, time-resolved and steady-state spectroscopy, investigation of reaction mechanisms, and chemical biology.

Dnyaneshwar Kand received his B.Sc. and M.Sc. degrees in chemistry from Pune University, India. He then joined the Indian Institute of Science, Education and Research (IISER), Pune, India with Dr. Pinaki Talukdar, receiving his Ph.D. degree in organic chemistry in 2015 for the development of colorimetric and fluorescent selective thiols sensors. In 2015, he joined the group of Dr. Roy Weinstain at Tel Aviv University, Israel, as a post-doctoral fellow (and a PBC fellow), where he worked on the development of *meso*-methyl BODIPY photocages. When not doing chemistry, he enjoys playing cricket.

Petr Klán received an M.Sc. degree in organic chemistry from Masaryk University, Brno, Czech Republic in 1986. After working in the industry for five years, he stayed at Michigan State University to pursue a Ph.D. in chemistry under the tutelage of Prof. Peter J. Wagner. After receiving his Ph.D. in chemistry in 1998, he joined the faculty at Masaryk University where he is now a full professor. His current research focuses on photochemistry, mechanisms of organic reactions, kinetic flash photolysis, spectroscopy, photoremovable protecting groups, and environmental photochemistry. He co-authored the book "Photochemistry of Organic Compounds" (Wiley, 2009) with Prof. Jakob Wirz.

ACKNOWLEDGMENTS

This work was supported by the Czech Science Foundation (GA18-12477S, P.K.). We thank the CETOCOEN EXCELLENCE Teaming 2 project (supported by the Czech Ministry of Education, Youth and Sports: CZ.02.1.01/0.0/0.0/17_043/0009632 and EU H2020:857560) and the RECETOX research infrastructure (LM2018121) (P.K.). R.W. acknowledges support from the European Research Council (GAtransport) and the Binational Science Foundation (2016060). T.S. was supported by the Czech Science Foundation (GJ19-20467Y) as well as by MEYS CR (LTAIN19166). D.K. was supported in part by the Planning and Budgeting Committee (PBC) of the Israeli Council for Higher Education. The authors express their thanks to Daniel Falvey (University of Maryland), David Lawrence (University of North Carolina at Chapel Hill), Martin J. Schnermann (National Cancer Institute), Arthur Winter (Iowa State University), and Jakob Wirz (University of Basel) who read parts of the text and provided valued suggestions.

ABBREVIATIONS

λ_{max}^{abs}	absorption maximum
λ_{max}^{em}	emission maximum
λ_{irr}	irradiation wavelength
Φ_r	reaction quantum yield
Φ_Δ	quantum yield of singlet oxygen production
$\Phi_r\varepsilon(\lambda_{irr})$	uncaging cross section
σ_{TPA}	2-photon absorption cross section
δ_{unc}	2-photon uncaging cross section
1P	one-photon
1PE	1-photon excitation
2P	two-photon
2PE	2-photon excitation
4AMP	4-(aminomethyl)pyridine)
4AP	4-aminopyridine
4-pic	4-methylpyridine
AIE	aggregation-induced emission
AMPA	α-amino-3-hydroxy-5-methyl-4-isoxazole-propionic acid
ATP	adenosine triphosphate
AuNP	Au nanoparticle
BDE	bond dissociation energy
BHQ	(8-bromo-7-hydroxyquinoline-2-yl)methyl
BIST	bisstyrylthiophene
biq	2,2′-biquinoline
BODIPY	4,4-difluoro-4-bora-3a,4a-diaza-s-indacene
bpy	2,2′-bipyridyl
BRET	bioluminescence resonance energy transfer
cAMP	cyclic adenosine monophosphate
Cbl	chlorambucil
CD	carbon dot
CDNI	4-carboxymethoxy-7-nitroindolinyl
cGMP	cyclic guanosine monophosphate
cMO	caged morpholino oligonucleotide
COHb	carbonylhemoglobin
COS	carbonyl sulfide
CQD	carbon quantum dot

CRISPR	clustered regularly interspaced short palindromic repeats
CT	charge transfer
cur	curcumin
Cy5	pentamethine cyanine
Cy7	heptamethine cyanine
cyclam	1,4,8,11-tetraazacyclotetradecane
CyHQ	(8-cyano-7-hydroxyquinoline-2-yl)methyl
DANS	*E*-4-(*N*,*N*-dimethylamino)-4′-nitrostilbene
dach	1R,2R-(−)-1,2-diaminocyclohexane
DDQ	2,3-dichloro-5,6-dicyano-1,4-benzoquinone
DEA	diethylamine
DEAC	7-diethylaminocoumarin
dend.	1,4-diaminobutane dendrimer
DFT	density functional theory
DMA	dimethylacetamide
DMNB	4,5-dimethoxy-2-nitrobenzyl
DMNPB	3-(4,5-dimethoxy-2-nitrophenyl)-2-butyl
DMSO	dimethyl sulfoxide
DNA	deoxyribonucleic acid
dppn	benzo[i]dipyridophenazine
DTE	dithienylethene
EDG	electron-donating group
EDTA	ethylenediaminetetraacetic acid
EGFR	epidermal growth factor receptor
EGTA	ethylene glycol tetraacetic acid
en	ethylenediamine
ESIPT	excited-state intramolecular proton transfer
Et	ethyl
EWG	electron-withdrawing group
FBS	fetal bovine serum
Fl	9,9′-dibutyl-9*H*-fluoren-2-yl
FRET	Förster resonance energy transfer
FT-IR	Fourier transform infrared
FWHM	full-width-at-half maximum
GA_3	gibberellin A_3
GABA	γ-butyric acid
glu	glutamate
GM	Goeppert-Mayer
HBIND	H-bond-induced non-radiative decay
HBT	2-(2′-hydroxyphenyl)benzothiazole
HEPES	4-(2-hydroxyethyl)-1-piperazineethanesulfonic acid
HMO	Hückel molecular orbital
HMS	hollow mesoporous silica
HNP	harmonic nanoparticle
Hob	4-((6-hydroxyhexyl)oxy)benzonitrile)
HOMO	highest occupied molecular orbital
hydrol	hydrolysis
ICT	intramolecular charge transfer
immol	self-immolation
IP_3	inositol triphosphate
IR	infrared
ISC	intersystem crossing
L	ligand
LE	locally excited
LED	light-emitting diode
LF	ligand field
LG	leaving group
LLCT	ligand-to-ligand charge transfer
LMCT	ligand-to-metal charge transfer
LUMO	lowest unoccupied molecular orbital
Me	methyl
Me_2bpy	6,6′-dimethyl-2,2′-bipyridine
MetHb	methemoglobin
MES	2-(*N*-morpholino)ethanesulfonic acid−based buffer
MLCT	metal-to-ligand charge transfer
MMLCT	metal−metal-bond-to-ligand charge-transfer
MNPPOC	2-(3,4-methylenedioxy-6-nitrophenyl)-propoxycarbonyl
MOF	metal−organic framework
MOPS	3-(*N*-morpholino)propanesulfonic acid
MSN	mesoporous silica nanoparticle
NDBF	nitrodibenzofuran
NHS	*N*-hydroxysuccinimide
NIR	near-infrared
NO	nitric oxide
NONOate	diazeniumdiolate
NP	nanoparticle
NPEOC	1-(2-nitrophenyl)ethyloxycarbonyl
NPPOC	1-(2-nitrophenyl)propyloxycarbonyl
oNB	*o*-nitrobenzyl
PBS	phosphate buffer saline
PDT	photodynamic therapy
PEG	polyethylene glycol
PET	photoinduced electron transfer
Ph	phenyl
phen	1,10-phenanthroline
phen-CHO	phenanthrolinecarboxaldehyde
photoCORM	photoactivatable CO-releasing moiety
photoNORM	photoactivatable NO-releasing moiety
pHP	*p*-hydroxyphenacyl
PPG	photoprotecting group
py	pyridine
Py	pyrene
pydppn	(pyrid-2-yl)benzo[i]dipyridophenazine
QD	quantum dot
qmtpm	2-quinoline-*N*-(2′-methylthiophenyl)-methylenimine
RNA	ribonucleic acid
sens	sensitizer
SHG	second-harmonic generation
sol	solvent
TD-DFT	time-dependent density functional theory
TICT	twisted intramolecular charge transfer
TIP	tight ion-pair
TMG	tetramethylguanidine
TPA	two photon absorption
TPA	tris(2-pyridylmethyl)amine
TPE	tetraphenylethylene
tpy	terpyridine
TQA	tris(2-quinolinylmethyl)amine
TRIR	time-resolved ultrafast infrared spectroscopy
Tris	tris(hydroxymethyl)aminomethane
TRPV1	transient receptor potential cation channel V1
TTA	triplet−triplet annihilation
UCNP	upconversion nanoparticle
UV	ultraviolet
VPA	valproic acid
WT	wild type
z	zwitterion

REFERENCES

(1) Barltrop, J. A.; Schofield, P. Photosensitive Protecting Groups. *Tetrahedron Lett.* **1962**, *16*, 697−699.

https://dx.doi.org/10.1021/acs.chemrev.0c00663
Chem. Rev. 2020, 120, 13135−13272

(2) Barton, D. H. R.; Chow, Y. L.; Cox, A.; Kirby, G. W. Photosensitive Protection of Functional Groups. *Tetrahedron Lett.* **1962**, *23*, 1055−1057.
(3) Barton, D. H. R.; Chow, Y. L.; Cox, A.; Kirby, G. W. Photochemical Transformations. 19. Some Photosensitive Protecting Groups. *J. Chem. Soc.* **1965**, 3571−3578.
(4) Patchornik, A.; Amit, B.; Woodward, R. B. Photosensitive Protecting Groups. *J. Am. Chem. Soc.* **1970**, *92*, 6333−6335.
(5) Sheehan, J. C.; Wilson, R. M. Photolysis of Desyl Compounds. A New Photolytic Cyclization. *J. Am. Chem. Soc.* **1964**, *86*, 5277−5281.
(6) Engels, J.; Schlaeger, E. J. Synthesis, Structure, and Reactivity of Adenosine Cyclic 3′,5′-Phosphate-Benzyltriesters. *J. Med. Chem.* **1977**, *20*, 907−911.
(7) Kaplan, J. H.; Forbush, B., III; Hoffman, J. F. Rapid Photolytic Release of Adenosine 5′-Triphosphate From a Protected Analog: Utilization by the Sodium/Potassium Pump of Human Red Blood Cell Ghosts. *Biochemistry* **1978**, *17*, 1929−1935.
(8) Yang, Y. M.; Mu, J.; Xing, B. G. Photoactivated Drug Delivery and Bioimaging. *Wiley Interdiscip. Rev.-Nanomed. Nanobiotechnol.* **2017**, *9*, No. e1408.
(9) Zhou, Y.; Ye, H.; Chen, Y. B.; Zhu, R. Y.; Yin, L. C. Photoresponsive Drug/Gene Delivery Systems. *Biomacromolecules* **2018**, *19*, 1840−1857.
(10) Klán, P.; Šolomek, T.; Bochet, C. G.; Blanc, A.; Givens, R.; Rubina, M.; Popik, V.; Kostikov, A.; Wirz, J. Photoremovable Protecting Groups in Chemistry and Biology: Reaction Mechanisms and Efficacy. *Chem. Rev.* **2013**, *113*, 119−191.
(11) Šolomek, T.; Wirz, J.; Klán, P. Searching for Improved Photoreleasing Abilities of Organic Molecules. *Acc. Chem. Res.* **2015**, *48*, 3064−3072.
(12) Bort, G.; Gallavardin, T.; Ogden, D.; Dalko, P. I. From One-Photon to Two-Photon Probes: "Caged" Compounds, Actuators, and Photoswitches. *Angew. Chem., Int. Ed.* **2013**, *52*, 4526−4537.
(13) Aubert, S.; Bezagu, M.; Spivey, A. C.; Arseniyadis, S. Spatial and Temporal Control of Chemical Processes. *Nat. Rev. Chem.* **2019**, *3*, 706−722.
(14) Beauté, L.; McClenaghan, N.; Lecommandoux, S. Photo-Triggered Polymer Nanomedicines: From Molecular Mechanisms to Therapeutic Applications. *Adv. Drug Delivery Rev.* **2019**, *138*, 148−166.
(15) Wang, Y.; Kohane, D. S. External Triggering and Triggered Targeting Strategies for Drug Delivery. *Nat. Rev. Mater.* **2017**, *2*, 17020.
(16) Hansen, M. J.; Velema, W. A.; Lerch, M. M.; Szymanski, W.; Feringa, B. L. Wavelength-Selective Cleavage of Photoprotecting Groups: Strategies and Applications in Dynamic Systems. *Chem. Soc. Rev.* **2015**, *44*, 3358−3377.
(17) So, W. H.; Wong, C. T. T.; Xia, J. Peptide Photocaging: A Brief Account of the Chemistry and Biological Applications. *Chin. Chem. Lett.* **2018**, *29*, 1058−1062.
(18) Spicer, C. D.; Pashuck, E. T.; Stevens, M. M. Achieving Controlled Biomolecule−Biomaterial Conjugation. *Chem. Rev.* **2018**, *118*, 7702−7743.
(19) Brieke, C.; Rohrbach, F.; Gottschalk, A.; Mayer, G.; Heckel, A. Light-Controlled Tools. *Angew. Chem., Int. Ed.* **2012**, *51*, 8446−8476.
(20) Silva, J. M.; Silva, E.; Reis, R. L. Light-Triggered Release of Photocaged Therapeutics - Where Are We Now? *J. Controlled Release* **2019**, *298*, 154−176.
(21) Ankenbruck, N.; Courtney, T.; Naro, Y.; Deiters, A. Optochemical Control of Biological Processes in Cells and Animals. *Angew. Chem., Int. Ed.* **2018**, *57*, 2768−2798.
(22) Givens, R. S.; Rubina, M.; Wirz, J. Applications of *p*-Hydroxyphenacyl (pHP) and Coumarin-4-ylmethyl Photoremovable Protecting Groups. *Photochem. Photobiol. Sci.* **2012**, *11*, 472−488.
(23) Zhao, H.; Sterner, E. S.; Coughlin, E. B.; Theato, P. *o*-Nitrobenzyl Alcohol Derivatives: Opportunities in Polymer and Materials Science. *Macromolecules* **2012**, *45*, 1723−1736.
(24) Ellis-Davies, G. C. R. Caged Compounds: Photorelease Technology for Control of Cellular Chemistry and Physiology. *Nat. Methods* **2007**, *4*, 619−628.
(25) Shao, Q.; Xing, B. Photoactive Molecules for Applications in Molecular Imaging and Cell Biology. *Chem. Soc. Rev.* **2010**, *39*, 2835−2846.
(26) Bardhan, A.; Deiters, A. Development of Photolabile Protecting Groups and their Application to the Optochemical Control of Cell Signaling. *Curr. Opin. Struct. Biol.* **2019**, *57*, 164−175.
(27) Ellis-Davies, G. C. R. Neurobiology with Caged Calcium. *Chem. Rev.* **2008**, *108*, 1603−1613.
(28) Choi, S. K. Photocleavable Linkers: Design and Applications in Nanotechnology. *Photonanotechnology for Therapeutics and Imaging*; Choi, S. k., Ed.; Elsevier, 2020.
(29) Amatrudo, J. M.; Olson, J. P.; Agarwal, H. K.; Ellis-Davies, G. C. R. Caged Compounds for Multichromic Optical Interrogation of Neural Systems. *Eur. J. Neurosci.* **2015**, *41*, 5−16.
(30) Jakkampudi, S.; Abe, M. Caged Compounds for Two-Photon Uncaging. *Reference Module in Chemistry, Molecular Sciences and Chemical Engineering*; Elsevier, 2018.
(31) Piant, S.; Bolze, F.; Specht, A. Two-Photon Uncaging, from Neuroscience to Materials. *Opt. Mater. Express* **2016**, *6*, 1679−1691.
(32) Sankaranarayanan, J.; Muthukrishnan, S.; Gudmundsdottir, A. D. Photoremovable Protecting Groups Based on Photoenolization. *Adv. Phys. Org. Chem.* **2009**, *43*, 39−77.
(33) Bochet, C. G.; Blanc, A. Photolabile Protecting Groups in Organic Synthesis. *Handbook of Synthetic Photochemistry, Ch. 13*; Albini, A., Fagnoni, M., Eds.; Wiley: Weinheim, 2010.
(34) Kramer, R. H.; Chambers, J. J.; Trauner, D. Photochemical Tools for Remote Control of Ion Channels in Excitable Cells. *Nat. Chem. Biol.* **2005**, *1*, 360−365.
(35) Xiangming, M.; Xiaoyun, C.; Yao, F.; Qingxiang, G. Photolysis of Caged Compounds and Its Applications to Chemical Biology. *Progr. Chem.* **2008**, *20*, 2034−2044.
(36) Sjulson, L.; Miesenböck, G. Photocontrol of Neural Activity: Biophysical Mechanisms and Performance. *Chem. Rev.* **2008**, *108*, 1588−1602.
(37) Lee, H. M.; Larson, D. R.; Lawrence, D. S. Illuminating the Chemistry of Life: Design, Synthesis, and Applications of "Caged" and Related Photoresponsive Compounds. *ACS Chem. Biol.* **2009**, *4*, 409−427.
(38) Yu, H.; Li, J.; Wu, D.; Qiu, Z.; Zhang, Y. Chemistry and Biological Applications of Photo-Labile Organic Molecules. *Chem. Soc. Rev.* **2010**, *39*, 464−473.
(39) Specht, A.; Bolze, F.; Omran, Z.; Nicoud, J.-F.; Goeldner, M. Photochemical Tools to Study Dynamic Biological Processes. *HFSP J.* **2009**, *3*, 255−264.
(40) Ciesienski, K. L.; Franz, K. J. Keys for Unlocking Photolabile Metal-Containing Cages. *Angew. Chem., Int. Ed.* **2011**, *50*, 814−824.
(41) Lovell, J. F.; Liu, T. W. B.; Chen, J.; Zheng, G. Activatable Photosensitizers for Imaging and Therapy. *Chem. Rev.* **2010**, *110*, 2839−2857.
(42) Herrmann, A. Controlled Release of Volatiles Under Mild Reaction Conditions: From Nature to Everyday Products. *Angew. Chem., Int. Ed.* **2007**, *46*, 5836−5863.
(43) Herrmann, A. Using Photolabile Protecting Groups for the Controlled Release of Bioactive Volatiles. *Photochem. Photobiol. Sci.* **2012**, *11*, 446−459.
(44) Suyama, K.; Shirai, M. Photobase Generators: Recent Progress and Application Trend in Polymer Systems. *Prog. Polym. Sci.* **2009**, *34*, 194−209.
(45) Puliti, D.; Warther, D.; Orange, C.; Specht, A.; Goeldner, M. Small Photoactivatable Molecules for Controlled Fluorescence Activation in Living Cells. *Bioorg. Med. Chem.* **2011**, *19*, 1023−1029.
(46) Li, W.-H.; Zheng, G. Photoactivatable Fluorophores and Techniques for Biological Imaging Applications. *Photochem. Photobiol. Sci.* **2012**, *11*, 460−471.

(47) Fukaminato, T. Single-Molecule Fluorescence Photoswitching: Design and Synthesis of Photoswitchable Fluorescent Molecules. *J. Photochem. Photobiol., C* **2011**, *12*, 177−208.
(48) *A Special Issue of Photochem. Photobiol. Sci. on Photoremovable Protecting Groups: Developments and Applications*; Wirz, J., Ed.; Royal Society of Chemistry: Cambridge, 2012; Vol. *11*, pp 433−600.
(49) Alabugin, A. Near-IR Photochemistry for Biology: Exploiting the Optical Window of Tissue. *Photochem. Photobiol.* **2019**, *95*, 722−732.
(50) Olejniczak, J.; Carling, C. J.; Almutairi, A. Photocontrolled Release Using One-Photon Absorption of Visible or NIR Light. *J. Controlled Release* **2015**, *219*, 18−30.
(51) Martin, C. J.; Rapenne, G.; Nakashima, T.; Kawai, T. Recent Progress in Development of Photoacid Generators. *J. Photochem. Photobiol., C* **2018**, *34*, 41−51.
(52) Deiters, A. Principles and Applications of the Photochemical Control of Cellular Processes. *ChemBioChem* **2010**, *11*, 47−53.
(53) Ellis-Davies, G. C. R. Useful Caged Compounds for Cell Physiology. *Acc. Chem. Res.* **2020**, *53*, 1593−1604.
(54) Lee, M.; Rizzo, R.; Surman, F.; Zenobi-Wong, M. Guiding Lights: Tissue Bioprinting Using Photoactivated Materials. *Chem. Rev.* **2020**, *120*, 10950−11027.
(55) Dcona, M. M.; Mitra, K.; Hartman, M. C. T. Photocontrolled Activation of Small Molecule Cancer Therapeutics. *RSC Med. Chem.* **2020**, *11*, 982−1002.
(56) Zayat, L.; Filevich, O.; Baraldo, L. M.; Etchenique, R. Ruthenium Polypyridyl Phototriggers: From Beginnings to Perspectives. *Philos. Trans. R. Soc., A* **2013**, *371*, 20120330.
(57) Mari, C.; Pierroz, V.; Ferrari, S.; Gasser, G. Combination of Ru(II) Complexes and Light: New Frontiers in Cancer Therapy. *Chem. Sci.* **2015**, *6*, 2660−2686.
(58) Wang, X. H.; Wang, X. Y.; Jin, S. X.; Muhammad, N.; Guo, Z. J. Stimuli-Responsive Therapeutic Metallodrugs. *Chem. Rev.* **2019**, *119*, 1138−1192.
(59) Banerjee, S.; Chakravarty, A. R. Metal Complexes of Curcumin for Cellular Imaging, Targeting, and Photoinduced Anticancer Activity. *Acc. Chem. Res.* **2015**, *48*, 2075−2083.
(60) Chemaly, S. M. New Light on Vitamin B-12: The Adenosylcobalamin-Dependent Photoreceptor Protein CarH. *S. Afr. J. Sci.* **2016**, *112*, 39−47.
(61) Jones, A. R. The Photochemistry and Photobiology of Vitamin B-12. *Photochem. Photobiol. Sci.* **2017**, *16*, 820−834.
(62) Kumar, M.; Kozlowski, P. M. Electronic and Structural Properties of Cobalamin: Ramifications for B-12-Dependent Processes. *Coord. Chem. Rev.* **2017**, *333*, 71−81.
(63) Heilman, B.; Mascharak, P. K. Light-Triggered Nitric Oxide Delivery to Malignant Sites and Infection. *Philos. Trans. R. Soc., A* **2013**, *371*, 20120368.
(64) Padmanabhan, S.; Jost, M.; Drennan, C. L.; Elias-Arnanz, M. A New Facet of Vitamin B-12: Gene Regulation by Cobalamin-Based Photoreceptors. *Annu. Rev. Biochem.*; Kornberg, R. D., Ed.; Annual Reviews: Palo Alto, 2017; Vol. *86*.
(65) Renfrew, A. K. Transition Metal Complexes With Bioactive Ligands: Mechanisms for Selective Ligand Release and Applications for Drug Delivery. *Metallomics* **2014**, *6*, 1324−1335.
(66) Smith, N. A.; Sadler, P. J. Photoactivatable Metal Complexes: From Theory to Applications in Biotechnology and Medicine. *Philos. Trans. R. Soc., A* **2013**, *371*, 20120519.
(67) Rury, A. S.; Wiley, T. E.; Sension, R. J. Energy Cascades, Excited State Dynamics, and Photochemistry in Cob(III)alamins and Ferric Porphyrins. *Acc. Chem. Res.* **2015**, *48*, 860−867.
(68) Crespy, D.; Landfester, K.; Schubert, U. S.; Schiller, A. Potential Photoactivated Metallopharmaceuticals: From Active Molecules to Supported Drugs. *Chem. Commun.* **2010**, *46*, 6651−6662.
(69) Szacilowski, K.; Macyk, W.; Drzewiecka-Matuszek, A.; Brindell, M.; Stochel, G. Bioinorganic Photochemistry: Frontiers and Mechanisms. *Chem. Rev.* **2005**, *105*, 2647−2694.
(70) Knoll, J. D.; Albani, B. A.; Turro, C. New Ru(II) Complexes for Dual Photoreactivity: Ligand Exchange and O-1(2) Generation. *Acc. Chem. Res.* **2015**, *48*, 2280−2287.
(71) Knoll, J. D.; Turro, C. Control and Utilization of Ruthenium and Rhodium Metal Complex Excited States for Photoactivated Cancer Therapy. *Coord. Chem. Rev.* **2015**, *282*, 110−126.
(72) Li, A.; Turro, C.; Kodanko, J. J. Ru(II) Polypyridyl Polypyridyl Complexes Derived from Tetradentate Ancillary Ligands for Effective Photocaging. *Acc. Chem. Res.* **2018**, *51*, 1415−1421.
(73) Poynton, F. E.; Bright, S. A.; Blasco, S.; Williams, D. C.; Kelly, J. M.; Gunnlaugsson, T. The Development of Ruthenium(ii) Polypyridyl Complexes and Conjugates for in Vitro Cellular and in Vivo Applications. *Chem. Soc. Rev.* **2017**, *46*, 7706−7756.
(74) Knör, G. The Concept of Photochemical Enzyme Models − State of the Art. *Coord. Chem. Rev.* **2016**, *325*, 102−115.
(75) Priestman, M. A.; Lawrence, D. S. Light-Mediated Remote Control of Signaling Pathways. *Biochim. Biophys. Acta, Proteins Proteomics* **2010**, *1804*, 547−558.
(76) Bonnet, S. Shifting the Light Activation of Metallodrugs to the Red and Near-Infrared Region in Anticancer Phototherapy. *Comments Inorg. Chem.* **2015**, *35*, 179−213.
(77) Ford, P. C.; Bourassa, J.; Miranda, K.; Lee, B.; Lorkovic, I.; Boggs, S.; Kudo, S.; Laverman, L. Photochemistry of Metal Nitrosyl Complexes. Delivery of Nitric Oxide to Biological Targets. *Coord. Chem. Rev.* **1998**, *171*, 185−202.
(78) Ford, P. C. Polychromophoric Metal Complexes for Generating the Bioregulatory Agent Nitric Oxide by Single- and Two-Photon Excitation. *Acc. Chem. Res.* **2008**, *41*, 190−200.
(79) Ostrowski, A. D.; Ford, P. C. Metal Complexes as Photochemical Nitric Oxide Precursors: Potential Applications in the Treatment of Tumors. *Dalton Trans.* **2009**, 10660−10669.
(80) Slanina, T.; Sebej, P. Visible-Light-Activated photoCORMs: Rational Design of CO-Releasing Organic Molecules Absorbing in the Tissue-Transparent Window. *Photochem. Photobiol. Sci.* **2018**, *17*, 692−710.
(81) Garcia-Gallego, S.; Bernardes, G. J. L. Carbon-Monoxide-Releasing Molecules for the Delivery of Therapeutic CO In Vivo. *Angew. Chem., Int. Ed.* **2014**, *53*, 9712−9721.
(82) Wright, M. A.; Wright, J. A. PhotoCORMs: CO Release Moves into the Visible. *Dalton Trans.* **2016**, *45*, 6801−6811.
(83) Marhenke, J.; Trevino, K.; Works, C. The Chemistry, Biology and Design of Photochemical CO Releasing Molecules and the Efforts to Detect CO for Biological Applications. *Coord. Chem. Rev.* **2016**, *306*, 533−543.
(84) Kautz, A. C.; Kunz, P. C.; Janiak, C. CO-Releasing Molecule (CORM) Conjugate Systems. *Dalton Trans.* **2016**, *45*, 18045−18063.
(85) Schatzschneider, U. Novel Lead Structures and Activation Mechanisms for CO-Releasing Molecules (CORMs). *Br. J. Pharmacol.* **2015**, *172*, 1638−1650.
(86) Gonzales, M. A.; Mascharak, P. K. Photoactive Metal Carbonyl Complexes as Potential Agents for Targeted CO Delivery. *J. Inorg. Biochem.* **2014**, *133*, 127−135.
(87) Steiger, C.; Hermann, C.; Meinel, L. Localized Delivery of Carbon Monoxide. *Eur. J. Pharm. Biopharm.* **2017**, *118*, 3−12.
(88) Ismailova, A.; Kuter, D.; Bohle, D. S.; Butler, I. S. An Overview of the Potential Therapeutic Applications of CO-Releasing Molecules. *Bioinorg. Chem. Appl.* **2018**, *2018*, 8547364.
(89) Faizan, M.; Muhammad, N.; Niazi, K. U. K.; Hu, Y.; Wang, Y.; Wu, Y.; Sun, H.; Liu, R.; Dong, W.; Zhang, W.; Gao, Z. CO-Releasing Materials: An Emphasis on Therapeutic Implications, as Release and Subsequent Cytotoxicity Are the Part of Therapy. *Materials* **2019**, *12*, 1643.
(90) Yang, X.; de Caestecker, M.; Otterbein, L. E.; Wang, B. Carbon Monoxide: An Emerging Therapy for Acute Kidney Injury. *Med. Res. Rev.* **2020**, *40*, 1−31.
(91) Pinto, M. N.; Mascharak, P. K. Light-Assisted and Remote Delivery of Carbon Monoxide to Malignant Cells and Tissues: Photochemotherapy in the Spotlight. *J. Photochem. Photobiol., C* **2020**, *42*, 100341.

(92) Soboleva, T.; Berreau, L. M. 3-Hydroxyflavones and 3-Hydroxy-4-oxoquinolines as Carbon Monoxide-Releasing Molecules. *Molecules* **2019**, *24*, 1252.
(93) Rimmer, R. D.; Pierri, A. E.; Ford, P. C. Photochemically Activated Carbon Monoxide Release for Biological Targets. Toward Developing Air-Stable PhotoCORMs Labilized by Visible Light. *Coord. Chem. Rev.* **2012**, *256*, 1509−1519.
(94) Schatzschneider, U. PhotoCORMs: Light-Triggered Release of Carbon Monoxide From the Coordination Sphere of Transition Metal Complexes for Biological Applications. *Inorg. Chim. Acta* **2011**, *374*, 19−23.
(95) Kottelat, E.; Zobi, F. Visible Light-Activated PhotoCORMs. *Inorganics* **2017**, *5*, 24.
(96) Ling, K.; Men, F.; Wang, W. C.; Zhou, Y. Q.; Zhang, H. W.; Ye, D. W. Carbon Monoxide and Its Controlled Release: Therapeutic Application, Detection, and Development of Carbon Monoxide Releasing Molecules (CORMs). *J. Med. Chem.* **2018**, *61*, 2611−2635.
(97) Adach, W.; Olas, B. Carbon Monoxide and Its Donors − Their Implications for Medicine. *Future Med. Chem.* **2019**, *11*, 61−73.
(98) Ford, P. C. Metal Complex Strategies for Photo-Uncaging the Small Molecule Bioregulators Nitric Oxide and Carbon Monoxide. *Coord. Chem. Rev.* **2018**, *376*, 548−564.
(99) Dichiarante, V.; Bergamaschi, G. Photochemistry of Transition Metal Complexes (2017−2018). *Photochemistry*; The Royal Society of Chemistry, 2020; Vol. *47*.
(100) Nguyen, D.; Boyer, C. Macromolecular and Inorganic Nanomaterials Scaffolds for Carbon Monoxide Delivery: Recent Developments and Future Trends. *ACS Biomater. Sci. Eng.* **2015**, *1*, 895−913.
(101) Lee, L. C.-C.; Leung, K.-K.; Lo, K. K.-W. Recent Development of Luminescent Rhenium(I) Tricarbonyl Polypyridine Complexes as Cellular Imaging Reagents, Anticancer Drugs, and Antibacterial Agents. *Dalton Trans.* **2017**, *46*, 16357−16380.
(102) Soboleva, T.; Berreau, L. M. Tracking CO Release in Cells via the Luminescence of Donor Molecules and/or their By-Products. *Isr. J. Chem.* **2019**, *59*, 339−350.
(103) Vorobev, A. Y.; Moskalensky, A. E. Long-Wavelength Photoremovable Protecting Groups: On the Way to *in Vivo* Application. *Comput. Struct. Biotechnol. J.* **2020**, *18*, 27−34.
(104) Rong, F.; Tang, Y.; Wang, T.; Feng, T.; Song, J.; Li, P.; Huang, W. Nitric Oxide-Releasing Polymeric Materials for Antimicrobial Applications: A Review. *Antioxidants* **2019**, *8*, 556.
(105) Hotta, Y.; Kataoka, T.; Mori, T.; Kimura, K. Review of a Potential Novel Approach for Erectile Dysfunction: Light-Controllable Nitric Oxide Donors and Nanoformulations. *Sex. Med. Rev.* **2020**, *8*, 297−302.
(106) Midgley, A. C.; Wei, Y.; Li, Z.; Kong, D.; Zhao, Q. Nitric-Oxide-Releasing Biomaterial Regulation of the Stem Cell Microenvironment in Regenerative Medicine. *Adv. Mater.* **2020**, *32*, 1805818.
(107) Pierri, A. E.; Muizzi, D. A.; Ostrowski, A. D.; Ford, P. C. Photo-Controlled Release of NO and CO with Inorganic and Organometallic Complexes. *Luminescent and Photoactive Transition Metal Complexes as Biomolecular Probes and Cellular Reagents*; Lo, K. K. W., Ed.; Springer-Verlag Berlin: Berlin, 2015; Vol. *165*.
(108) Mir, J. M.; Malik, B. A.; Maurya, R. C. Nitric Oxide-Releasing Molecules at the Interface of Inorganic Chemistry and Biology: a Concise Overview. *Rev. Inorg. Chem.* **2019**, *39*, 91−112.
(109) Xiao, P.; Zhang, J.; Zhao, J.; Stenzel, M. H. Light-Induced Release of Molecules From Polymers. *Prog. Polym. Sci.* **2017**, *74*, 1−33.
(110) Nakagawa, H. Photo-Controlled Release of Small Signaling Molecules to Induce Biological Responses. *Chem. Rec.* **2018**, *18*, 1708−1716.
(111) Powell, C. R.; Dillon, K. M.; Matson, J. B. A Review of Hydrogen Sulfide (H_2S) Donors: Chemistry and Potential Therapeutic Applications. *Biochem. Pharmacol.* **2018**, *149*, 110−123.
(112) Zheng, Y.; Ji, X.; Ji, K.; Wang, B. Hydrogen Sulfide Prodrugs—A Review. *Acta Pharm. Sin. B* **2015**, *5*, 367−377.
(113) Schatzschneider, U. Photoactivated Biological Activity of Transition-Metal Complexes. *Eur. J. Inorg. Chem.* **2010**, *2010*, 1451−1467.
(114) Katz, J. S.; Burdick, J. A. Light-Responsive Biomaterials: Development and Applications. *Macromol. Biosci.* **2010**, *10*, 339−348.
(115) Givens, R. S.; Conrad, P. G. I.; Yousef, A. L.; Lee, J.-I. Photoremovable Protecting Groups; In *CRC Handbook of Organic Photochemistry and Photobiology*, 2nd ed.; CRC Press: Boca Raton, 2004.
(116) Goeldner, M.; Givens, R. S. *Dynamic Studies in Biology*; Wiley-VCH: Weinheim, Germany, 2006.
(117) Mayer, G.; Heckel, A. Biologically Active Molecules with a "Light Switch. *Angew. Chem., Int. Ed.* **2006**, *45*, 4900−4921.
(118) Pelliccioli, A. P.; Wirz, J. Photoremovable Protecting Groups: Reaction Mechanisms and Applications. *Photochem. Photobiol. Sci.* **2002**, *1*, 441−458.
(119) Cheong, W. F.; Prahl, S. A.; Welch, A. J. A Review of the Optical Properties of Biological Tissues. *IEEE J. Quantum Electron.* **1990**, *26*, 2166−2185.
(120) Tuchin, V. V. Light Scattering Study of Tissues. *Phys.-Usp.* **1997**, *40*, 495−515.
(121) Tuchin, V. V. *Tissue Optics: Light Scattering Methods and Instruments for Medical Diagnostics*; SPIE Press: Bellingham, 2015.
(122) Mang, R.; Stege, H.; Krutmann, J. Mechanisms of Phototoxic and Photoallergic Reactions; In *Contact Dermatitis*; Frosch, P. J., Menné, T., Lepoittevin, J. P., Eds.; Springer: Berlin, Heidelberg, 2006.
(123) Kim, K.; Park, H.; Lim, K.-M. Phototoxicity: Its Mechanism and Animal Alternative Test Methods. *Toxicol. Res.* **2015**, *31*, 97−104.
(124) Glickman, R. D. Ultraviolet Phototoxicity to the Retina. *Eye Contact Lens* **2011**, *37*, 196−205.
(125) Lim, Y. T.; Kim, S.; Nakayama, A.; Stott, N. E.; Bawendi, M. G.; Frangioni, J. V. Selection of Quantum Dot Wavelengths for Biomedical Assays and Imaging. *Mol. Imaging* **2003**, *2*, 50−64.
(126) Weissleder, R. A Clearer Vision for in Vivo Imaging. *Nat. Biotechnol.* **2001**, *19*, 316−317.
(127) Juzenas, P.; Juzeniene, A.; Kaalhus, O.; Iani, V.; Moan, J. Noninvasive Fluorescence Excitation Spectroscopy during Application of 5-Aminolevulinic Acid in Vivo. *Photochem. Photobiol. Sci.* **2002**, *1*, 745−748.
(128) Bashkatov, A. N.; Genina, E. A.; Kochubey, V. I.; Tuchin, V. V. Optical Properties of Human Skin, Subcutaneous and Mucous Tissues in the Wavelength Range from 400 to 2000nm. *J. Phys. D: Appl. Phys.* **2005**, *38*, 2543−2555.
(129) Ruskowitz, E. R.; DeForest, C. A. Photoresponsive Biomaterials for Targeted Drug Delivery and 4D Cell Culture. *Nat. Rev. Mater.* **2018**, *3*, 17087.
(130) Rwei, A. Y.; Wang, W.; Kohane, D. S. Photoresponsive Nanoparticles for Drug Delivery. *Nano Today* **2015**, *10*, 451−467.
(131) van Straten, D.; Mashayekhi, V.; de Bruijn, H. S.; Oliveira, S.; Robinson, D. J. Oncologic Photodynamic Therapy: Basic Principles, Current Clinical Status and Future Directions. *Cancers* **2017**, *9*, 19.
(132) dos Santos, A. F.; de Almeida, D. R. Q.; Terra, L. F.; Baptista, M. S.; Labriola, L. Photodynamic Therapy in Cancer Treatment - An Update Review. *J. Cancer Metastasis Treat.* **2019**, *5*, 25.
(133) Baskaran, R.; Lee, J.; Yang, S.-G. Clinical Development of Photodynamic Agents and Therapeutic Applications. *Biomater. Res.* **2018**, *22*, 25.
(134) Gursoy, H.; Ozcakir-Tomruk, C.; Tanalp, J.; Yılmaz, S. Photodynamic Therapy in Dentistry: A Literature Review. *Clin. Oral Investig.* **2013**, *17*, 1113−1125.
(135) Maisch, T.; Szeimies, R.-M.; Jori, G.; Abels, C. Antibacterial Photodynamic Therapy in Dermatology. *Photochem. Photobiol. Sci.* **2004**, *3*, 907−917.
(136) Klán, P.; Wirz, J. *Photochemistry of Organic Compounds: From Concepts to Practice*, 1st ed.; John Wiley & Sons Ltd.: Chichester, 2009.
(137) Bochet, C. G. Wavelength-Selective Cleavage of Photolabile Protecting Groups. *Tetrahedron Lett.* **2000**, *41*, 6341−6346.

(138) Bochet, C. G. Orthogonal Photolysis of Protecting Groups. *Angew. Chem., Int. Ed.* **2001**, *40*, 2071−2073.
(139) Kammari, L.; Šolomek, T.; Ngoy, B. P.; Heger, D.; Klán, P. Orthogonal Photocleavage of a Monochromophoric Linker. *J. Am. Chem. Soc.* **2010**, *132*, 11431−11433.
(140) Olson, J. P.; Banghart, M. R.; Sabatini, B. L.; Ellis-Davies, G. C. R. Spectral Evolution of a Photochemical Protecting Group for Orthogonal Two-Color Uncaging with Visible Light. *J. Am. Chem. Soc.* **2013**, *135*, 15948−15954.
(141) Stanton-Humphreys, M. N.; Taylor, R. D. T.; McDougall, C.; Hart, M. L.; Brown, C. T. A.; Emptage, N. J.; Conway, S. J. Wavelength-Orthogonal Photolysis of Neurotransmitters *in Vitro*. *Chem. Commun.* **2012**, *48*, 657−659.
(142) Rodrigues-Correia, A.; Weyel, X. M. M.; Heckel, A. Four Levels of Wavelength-Selective Uncaging for Oligonucleotides. *Org. Lett.* **2013**, *15*, 5500−5503.
(143) Menge, C.; Heckel, A. Coumarin-Caged dG for Improved Wavelength-Selective Uncaging of DNA. *Org. Lett.* **2011**, *13*, 4620−4623.
(144) Morihiro, K.; Kodama, T.; Mori, S.; Tsunoda, S.; Obika, S. Wavelength-Selective Light-Triggered Strand Exchange Reaction. *Org. Biomol. Chem.* **2016**, *14*, 1555−1558.
(145) Hoorens, M. W. H.; Szymanski, W. Reversible, Spatial and Temporal Control over Protein Activity Using Light. *Trends Biochem. Sci.* **2018**, *43*, 567−575.
(146) Li, J.; Kong, H.; Zhu, C.; Zhang, Y. Photo-Controllable Bioorthogonal Chemistry for Spatiotemporal Control of Bio-Targets in Living Systems. *Chem. Sci.* **2020**, *11*, 3390−3396.
(147) Protti, S.; Ravelli, D.; Fagnoni, M. Wavelength Dependence and Wavelength Selectivity in Photochemical Reactions. *Photochem. Photobiol. Sci.* **2019**, *18*, 2094−2101.
(148) Warther, D.; Gug, S.; Specht, A.; Bolze, F.; Nicoud, J. F.; Mourot, A.; Goeldner, M. Two-Photon Uncaging: New Prospects in Neuroscience and Cellular Biology. *Bioorg. Med. Chem.* **2010**, *18*, 7753−7758.
(149) Milburn, T.; Matsubara, N.; Billington, A. P.; Udgaonkar, J. B.; Walker, J. W.; Carpenter, B. K.; Webb, W. W.; Marque, J.; Denk, W. Synthesis, Photochemistry, and Biological Activity of a Caged Photolabile Acetylcholine Receptor Ligand. *Biochemistry* **1989**, *28*, 49−55.
(150) Berroy, P.; Viriot, M. L.; Carré, M. C. Photolabile Group for 5′-OH Protection of Nucleosides: Synthesis and Photodeprotection Rate. *Sens. Actuators, B* **2001**, *74*, 186−189.
(151) Bader, T. K.; Xu, F.; Hodny, M. H.; Blank, D. A.; Distefano, M. D. Methoxy-Substituted Nitrodibenzofuran-Based Protecting Group with an Improved Two-Photon Action Cross-Section for Thiol Protection in Solid Phase Peptide Synthesis. *J. Org. Chem.* **2020**, *85*, 1614−1625.
(152) Donato, L.; Mourot, A.; Davenport, C. M.; Herbivo, C.; Warther, D.; Léonard, J.; Bolze, F.; Nicoud, J.-F.; Kramer, R. H.; Goeldner, M.; Specht, A. Water-Soluble, Donor-Acceptor Biphenyl Derivatives in the 2-(*o*-Nitrophenyl)propyl Series: Highly Efficient Two-Photon Uncaging of the Neurotransmitter γ-Aminobutyric Acid at λ = 800 nm. *Angew. Chem., Int. Ed.* **2012**, *51*, 1840−1843.
(153) Boinapally, S.; Huang, B.; Abe, M.; Katan, C.; Noguchi, J.; Watanabe, S.; Kasai, H.; Xue, B.; Kobayashi, T. Caged Glutamates with π-Extended 1,2-Dihydronaphthalene Chromophore: Design, Synthesis, Two-Photon Absorption Property, and Photochemical Reactivity. *J. Org. Chem.* **2014**, *79*, 7822−7830.
(154) Barltrop, J.; Plant, P.; Schofield, P. Photosensitive Protective Groups. *Chem. Commun.* **1966**, 822−823.
(155) Corrie, J. E. T.; Barth, A.; Munasinghe, V. R. N.; Trentham, D. R.; Hutter, M. C. Photolytic Cleavage of 1-(2-Nitrophenyl)ethyl Ethers Involves Two Parallel Pathways and Product Release Is Rate-Limited by Decomposition of a Common Hemiacetal Intermediate. *J. Am. Chem. Soc.* **2003**, *125*, 8546−8554.
(156) Dunkin, I. R.; Gebicki, J.; Kiszka, M.; Sanín-Leira, D. Phototautomerism of *o*-Nitrobenzyl Compounds: *o*-Quinonoid *Aci*-Nitro Species Studied by Matrix Isolation and DFT Calculations. *J. Chem. Soc. Perk. T.* **2001**, *2*, 1414−1425.
(157) Dunkin, I. R.; Gebicki, J.; Kiszka, M.; Sanín-Leira, D. The Matrix-Isolation IR Spectrum of the *o*-Quinonoid Intermediate in the Photolysis of 2-Nitrobenzyl Methyl Ether. *Spectrochim. Acta, Part A* **1997**, *53*, 2553−2557.
(158) Il'ichev, Y. V.; Schwörer, M. A.; Wirz, J. Photochemical Reaction Mechanisms of 2-Nitrobenzyl Compounds: Methyl Ethers and Caged ATP. *J. Am. Chem. Soc.* **2004**, *126*, 4581−4595.
(159) Il'ichev, Y. V.; Wirz, J. Rearrangements of 2-Nitrobenzyl Compounds. 1. Potential Energy Surface of 2-Nitrotoluene and Its Isomers Explored with ab Initio and Density Functional Theory Methods. *J. Phys. Chem. A* **2000**, *104*, 7856−7870.
(160) Walker, J. W.; Reid, G. P.; McCray, J. A.; Trentham, D. R. Photolabile 1-(2-Nitrophenyl)ethyl Phosphate Esters of Adenine Nucleotide Analogs. Synthesis and Mechanism of Photolysis. *J. Am. Chem. Soc.* **1988**, *110*, 7170−7177.
(161) Engels, J.; Schlaeger, E. J. Synthesis, Structure, and Reactivity of Adenosine Cyclic 3′,5′-Phosphate Benzyl Triesters. *J. Med. Chem.* **1977**, *20*, 907−911.
(162) Bayley, H.; Chang, C.-Y.; Todd Miller, W.; Niblack, B.; Pan, P. Caged Peptides and Proteins by Targeted Chemical Modification. *Methods Enzymol.*; Academic Press, 1998; Vol. *291*.
(163) Aujard, I.; Benbrahim, C.; Gouget, M.; Ruel, O.; Baudin, J.-B.; Neveu, P.; Jullien, L. *o*-Nitrobenzyl Photolabile Protecting Groups with Red-Shifted Absorption: Syntheses and Uncaging Cross-Sections for One- and Two-Photon Excitation. *Chem. - Eur. J.* **2006**, *12*, 6865−6879.
(164) Kaplan, J. H.; Ellis-Davies, G. C. Photolabile Chelators for the Rapid Photorelease of Divalent Cations. *Proc. Natl. Acad. Sci. U. S. A.* **1988**, *85*, 6571−6575.
(165) Furuta, T.; Wang, S. S.; Dantzker, J. L.; Dore, T. M.; Bybee, W. J.; Callaway, E. M.; Denk, W.; Tsien, R. Y. Brominated 7-Hydroxycoumarin-4-ylmethyls: Photolabile Protecting Groups with Biologically Useful Cross-Sections for Two Photon Photolysis. *Proc. Natl. Acad. Sci. U. S. A.* **1999**, *96*, 1193−1200.
(166) Reichmanis, E.; Gooden, R.; Wilkins, C. W., Jr.; Schonhorn, H. A Study of the Photochemical Response of *o*-Nitrobenzyl Cholate Derivatives in P(MMA-MAA) Matrices. *J. Polym. Sci., Polym. Chem. Ed.* **1983**, *21*, 1075−1083.
(167) Reichmanis, E.; Smith, B. C.; Gooden, R. *o*-Nitrobenzyl Photochemistry: Solution vs. Solid-State Behavior. *J. Polym. Sci., Polym. Chem. Ed.* **1985**, *23*, 1−8.
(168) Adams, S. R.; Kao, J. P. Y.; Grynkiewicz, G.; Minta, A.; Tsien, R. Y. Biologically Useful Chelators That Release Ca2+ Upon Illumination. *J. Am. Chem. Soc.* **1988**, *110*, 3212−3220.
(169) Pease, A. C.; Solas, D.; Sullivan, E. J.; Cronin, M. T.; Holmes, C. P.; Fodor, S. P. Light-Generated Oligonucleotide Arrays for Rapid DNA Sequence Analysis. *Proc. Natl. Acad. Sci. U. S. A.* **1994**, *91*, 5022−5026.
(170) Hasan, A.; Stengele, K.-P.; Giegrich, H.; Cornwell, P.; Isham, K. R.; Sachleben, R. A.; Pfleiderer, W.; Foote, R. S. Photolabile Protecting Groups for Nucleosides: Synthesis and Photodeprotection Rates. *Tetrahedron* **1997**, *53*, 4247−4264.
(171) Wöll, D.; Walbert, S.; Stengele, K.-P.; Albert, T. J.; Richmond, T.; Norton, J.; Singer, M.; Green, R. D.; Pfleiderer, W.; Steiner, U. E. Triplet-Sensitized Photodeprotection of Oligonucleotides in Solution and on Microarray Chips. *Helv. Chim. Acta* **2004**, *87*, 28−45.
(172) Momotake, A.; Lindegger, N.; Niggli, E.; Barsotti, R. J.; Ellis-Davies, G. C. R. The Nitrodibenzofuran Chromophore: A New Caging Group for Ultra-Efficient Photolysis in Living Cells. *Nat. Methods* **2006**, *3*, 35−40.
(173) Kantevari, S.; Buskila, Y.; Ellis-Davies, G. C. R. Synthesis and Characterization of Cell-Permeant 6-Nitrodibenzofuranyl-Caged IP3. *Photochem. Photobiol. Sci.* **2012**, *11*, 508−513.
(174) Becker, Y.; Unger, E.; Fichte, M. A. H.; Gacek, D. A.; Dreuw, A.; Wachtveitl, J.; Walla, P. J.; Heckel, A. A Red-Shifted Two-Photon-Only Caging Group for Three-Dimensional Photorelease. *Chem. Sci.* **2018**, *9*, 2797−2802.

(175) Schäfer, F.; Joshi, K. B.; Fichte, M. A. H.; Mack, T.; Wachtveitl, J.; Heckel, A. Wavelength-Selective Uncaging of dA and dC Residues. *Org. Lett.* **2011**, *13*, 1450−1453.
(176) Kennedy, D. P.; Brown, D. C.; Burdette, S. C. Probing Nitrobenzhydrol Uncaging Mechanisms Using FerriCast. *Org. Lett.* **2010**, *12*, 4486−4489.
(177) Mahmoodi, M. M.; Abate-Pella, D.; Pundsack, T. J.; Palsuledesai, C. C.; Goff, P. C.; Blank, D. A.; Distefano, M. D. Nitrodibenzofuran: A One- and Two-Photon Sensitive Protecting Group That Is Superior to Brominated Hydroxycoumarin for Thiol Caging in Peptides. *J. Am. Chem. Soc.* **2016**, *138*, 5848−5859.
(178) Sõrmus, T.; Lavogina, D.; Enkvist, E.; Uri, A.; Viht, K. Efficient Photocaging of a Tight-Binding Bisubstrate Inhibitor of cAMP-Dependent Protein Kinase. *Chem. Commun.* **2019**, *55*, 11147−11150.
(179) Riguet, E.; Bochet, C. G. New Safety-Catch Photolabile Protecting Group. *Org. Lett.* **2007**, *9*, 5453−5456.
(180) Mangubat-Medina, A. E.; Trial, H. O.; Vargas, R. D.; Setegne, M. T.; Bader, T.; Distefano, M. D.; Ball, Z. T. Red-Shifted Backbone N−H Photocaging Agents. *Org. Biomol. Chem.* **2020**, *18*, 5110−5114.
(181) Bühler, S.; Lagoja, I.; Giegrich, H.; Stengele, K.-P.; Pfleiderer, W. New Types of Very Efficient Photolabile Protecting Groups Based upon the [2-(2-Nitrophenyl)propoxy]carbonyl (NPPOC) Moiety. *Helv. Chim. Acta* **2004**, *87*, 620−659.
(182) Singh, A. K.; Khade, P. K. Synthesis and Photochemical Properties of Nitro-Naphthyl Chromophore and the Corresponding Immunoglobulin Bioconjugate. *Bioconjugate Chem.* **2002**, *13*, 1286−1291.
(183) Singh, A. K.; Khade, P. K. 7-Methoxy-3-nitro-2-naphthalene-methanol—A New Phototrigger for Caging Applications. *Tetrahedron Lett.* **2011**, *52*, 4899−4902.
(184) Takaoka, K.; Tatsu, Y.; Yumoto, N.; Nakajima, T.; Shimamoto, K. Synthesis and Photoreactivity of Caged Blockers for Glutamate Transporters. *Bioorg. Med. Chem. Lett.* **2003**, *13*, 965−970.
(185) Anstaett, P.; Pierroz, V.; Ferrari, S.; Gasser, G. Two-Photon Uncageable Enzyme Inhibitors Bearing Targeting Vectors. *Photochem. Photobiol. Sci.* **2015**, *14*, 1821−1825.
(186) Liu, W.; Liang, L.; Lo, P. K.; Gou, X. J.; Sun, X. H. A Double Branched Photosensitive Prodrug: Synthesis and Characterization of Light Triggered Drug Release. *Tetrahedron Lett.* **2016**, *57*, 959−963.
(187) Abou Nakad, E.; Bolze, F.; Specht, A. *o*-Nitrobenzyl Photoremovable Groups with Fluorescence Uncaging Reporting Properties. *Org. Biomol. Chem.* **2018**, *16*, 6115−6122.
(188) Jakkampudi, S.; Abe, M.; Komori, N.; Takagi, R.; Furukawa, K.; Katan, C.; Sawada, W.; Takahashi, N.; Kasai, H. Design and Synthesis of a 4-Nitrobromobenzene Derivative Bearing an Ethylene Glycol Tetraacetic Acid Unit for a New Generation of Caged Calcium Compounds with Two-Photon Absorption Properties in the Near-IR Region and Their Application in Vivo. *ACS Omega* **2016**, *1*, 193−201.
(189) Bao, C.; Jin, M.; Li, B.; Xu, Y.; Jin, J.; Zhu, L. Long Conjugated 2-Nitrobenzyl Derivative Caged Anticancer Prodrugs with Visible Light Regulated Release: Preparation and Functionalizations. *Org. Biomol. Chem.* **2012**, *10*, 5238−5244.
(190) Jin, M.; Xu, H.; Hong, H.; Bao, C.; Pu, H.; Wan, D.; Zhu, L. Micropatterning of Polymethacrylates by Single- or Two-Photon Irradiation Using π-Conjugated *o*-Nitrobenzyl Ester Phototrigger as Side Chains. *J. Appl. Polym. Sci.* **2013**, *130*, 4099−4106.
(191) Thapaliya, E. R.; Mazza, M. M. A.; Cusido, J.; Baker, J. D.; Raymo, F. M. A Synthetic Strategy for the Structural Modification of Photoactivatable BODIPY-Oxazine Dyads. *ChemPhotoChem.* **2020**, *4*, 332−337.
(192) Dyck, R. H.; McClure, D. S. Ultraviolet Spectra of Stilbene, *p*-Monohalogen Stilbenes, and Azobenzene and the trans to cis Photoisomerization Process. *J. Chem. Phys.* **1962**, *36*, 2326−2345.
(193) Malkin, S.; Fischer, E. Temperature Dependence of Photoisomerization. Part II. Quantum Yields of cis ⇆ trans Isomerization in Azo-Compounds. *J. Phys. Chem.* **1962**, *66*, 2482−2486.
(194) Waldeck, D. H. Photoisomerization Dynamics of Stilbenes. *Chem. Rev.* **1991**, *91*, 415−436.
(195) Komori, N.; Jakkampudi, S.; Motoishi, R.; Abe, M.; Kamada, K.; Furukawa, K.; Katan, C.; Sawada, W.; Takahashi, N.; Kasai, H.; Xue, B.; Kobayashi, T. Design and Synthesis of a New Chromophore, 2-(4-Nitrophenyl)benzofuran, for Two-Photon Uncaging Using Near-IR Light. *Chem. Commun.* **2016**, *52*, 331−334.
(196) Maurits, E.; van de Graaff, M. J.; Maiorana, S.; Wander, D. P. A.; Dekker, P. M.; van der Zanden, S. Y.; Florea, B. I.; Neefjes, J. J. C.; Overkleeft, H. S.; van Kasteren, S. I. Immunoproteasome Inhibitor−Doxorubicin Conjugates Target Multiple Myeloma Cells and Release Doxorubicin upon Low-Dose Photon Irradiation. *J. Am. Chem. Soc.* **2020**, *142*, 7250−7253.
(197) Paul, A.; Jana, A.; Karthik, S.; Bera, M.; Zhao, Y.; Singh, N. D. P. Photoresponsive Real Time Monitoring Silicon Quantum Dots for Regulated Delivery of Anticancer Drugs. *J. Mater. Chem. B* **2016**, *4*, 521−528.
(198) Wang, W.; Liu, Q.; Zhan, C.; Barhoumi, A.; Yang, T.; Wylie, R. G.; Armstrong, P. A.; Kohane, D. S. Efficient Triplet−Triplet Annihilation-Based Upconversion for Nanoparticle Phototargeting. *Nano Lett.* **2015**, *15*, 6332−6338.
(199) Yan, B.; Boyer, J.-C.; Branda, N. R.; Zhao, Y. Near-Infrared Light-Triggered Dissociation of Block Copolymer Micelles Using Upconverting Nanoparticles. *J. Am. Chem. Soc.* **2011**, *133*, 19714−19717.
(200) Yan, B.; Boyer, J.-C.; Habault, D.; Branda, N. R.; Zhao, Y. Near Infrared Light Triggered Release of Biomacromolecules from Hydrogels Loaded with Upconversion Nanoparticles. *J. Am. Chem. Soc.* **2012**, *134*, 16558−16561.
(201) Zhang, Y.; Lu, G.; Yu, Y.; Zhang, H.; Gao, J.; Sun, Z.; Lu, Y.; Zou, H. NIR-Responsive Copolymer Upconversion Nanocomposites for Triggered Drug Release in Vitro and in Vivo. *ACS Applied Bio Materials* **2019**, *2*, 495−503.
(202) Yang, Y.; Liu, F.; Liu, X.; Xing, B. NIR Light Controlled Photorelease of SiRNA and Its Targeted Intracellular Delivery Based on Upconversion Nanoparticles. *Nanoscale* **2013**, *5*, 231−238.
(203) Yang, Y.; Velmurugan, B.; Liu, X.; Xing, B. NIR Photoresponsive Crosslinked Upconverting Nanocarriers Toward Selective Intracellular Drug Release. *Small* **2013**, *9*, 2937−2944.
(204) Ballister, E. R.; Aonbangkhen, C.; Mayo, A. M.; Lampson, M. A.; Chenoweth, D. M. Localized Light-Induced Protein Dimerization in Living Cells Using a Photocaged Dimerizer. *Nat. Commun.* **2014**, *5*, 5475.
(205) Koehler, M.; Lo Giudice, C.; Vogl, P.; Ebner, A.; Hinterdorfer, P.; Gruber, H. J.; Alsteens, D. Control of Ligand-Binding Specificity Using Photocleavable Linkers in AFM Force Spectroscopy. *Nano Lett.* **2020**, *20*, 4038−4042.
(206) Yu, C.; Schimelman, J.; Wang, P.; Miller, K. L.; Ma, X.; You, S.; Guan, J.; Sun, B.; Zhu, W.; Chen, S. Photopolymerizable Biomaterials and Light-Based 3D Printing Strategies for Biomedical Applications. *Chem. Rev.* **2020**, *120*, 10695−10743.
(207) Hentzen, N. B.; Mogaki, R.; Otake, S.; Okuro, K.; Aida, T. Intracellular Photoactivation of Caspase-3 by Molecular Glues for Spatiotemporal Apoptosis Induction. *J. Am. Chem. Soc.* **2020**, *142*, 8080−8084.
(208) Jedlitzke, B.; Yilmaz, Z.; Dörner, W.; Mootz, H. D. Photobodies: Light-Activatable Single-Domain Antibody Fragments. *Angew. Chem., Int. Ed.* **2020**, *59*, 1506−1510.
(209) Wexler, S.; Schayek, H.; Rajendar, K.; Tal, I.; Shani, E.; Meroz, Y.; Dobrovetsky, R.; Weinstain, R. Characterizing Gibberellin Flow in Planta Using Photocaged Gibberellins. *Chem. Sci.* **2019**, *10*, 1500−1505.
(210) Raccuglia, D.; Mueller, U. Focal Uncaging of GABA Reveals a Temporally Defined Role for Gabaergic Inhibition During Appetitive Associative Olfactory Conditioning in Honeybees. *Learn. Mem.* **2013**, *20*, 410−416.
(211) Shao, Q.; Jiang, T.; Ren, G.; Cheng, Z.; Xing, B. Photoactivable Bioluminescent Probes for Imaging Luciferase Activity. *Chem. Commun.* **2009**, 4028−4030.

(212) Shestopalov, I. A.; Sinha, S.; Chen, J. K. Light-Controlled Gene Silencing in Zebrafish Embryos. *Nat. Chem. Biol.* **2007**, *3*, 650−651.
(213) Warmutha, R.; Grell, E.; Lehn, J.-M.; Bats, J. W.; Quinkert, G. Photo-Cleavable Cryptands: Synthesis and Structure. *Helv. Chim. Acta* **1991**, *74*, 671−681.
(214) Kolarski, D.; Sugiyama, A.; Breton, G.; Rakers, C.; Ono, D.; Schulte, A.; Tama, F.; Itami, K.; Szymanski, W.; Hirota, T.; Feringa, B. L. Controlling the Circadian Clock with High Temporal Resolution through Photodosing. *J. Am. Chem. Soc.* **2019**, *141*, 15784−15791.
(215) Zhou, W.; Brown, W.; Bardhan, A.; Delaney, M.; Ilk, A. S.; Rauen, R. R.; Kahn, S. I.; Tsang, M.; Deiters, A. Spatiotemporal Control of CRISPR/Cas9 Function in Cells and Zebrafish using Light-Activated Guide RNA. *Angew. Chem., Int. Ed.* **2020**, *59*, 8998−9003.
(216) Baker, A. S.; Deiters, A. Optical Control of Protein Function through Unnatural Amino Acid Mutagenesis and Other Optogenetic Approaches. *ACS Chem. Biol.* **2014**, *9*, 1398−1407.
(217) Courtney, T.; Deiters, A. Recent Advances in the Optical Control of Protein Function through Genetic Code Expansion. *Curr. Opin. Chem. Biol.* **2018**, *46*, 99−107.
(218) Nödling, A. R.; Spear, L. A.; Williams, T. L.; Luk, L. Y. P.; Tsai, Y.-H. Using Genetically Incorporated Unnatural Amino Acids to Control Protein Functions in Mammalian Cells. *Essays Biochem.* **2019**, *63*, 237−266.
(219) Agarwal, H. K.; Janicek, R.; Chi, S.-H.; Perry, J. W.; Niggli, E.; Ellis-Davies, G. C. R. Calcium Uncaging with Visible Light. *J. Am. Chem. Soc.* **2016**, *138*, 3687−3693.
(220) Basa, P. N.; Antala, S.; Dempski, R. E.; Burdette, S. C. A Zinc(II) Photocage Based on a Decarboxylation Metal Ion Release Mechanism for Investigating Homeostasis and Biological Signaling. *Angew. Chem., Int. Ed.* **2015**, *54*, 13027−13031.
(221) Ciesienski, K. L.; Haas, K. L.; Dickens, M. G.; Tesema, Y. T.; Franz, K. J. A Photolabile Ligand for Light-Activated Release of Caged Copper. *J. Am. Chem. Soc.* **2008**, *130*, 12246−12247.
(222) Richers, M. T.; Passlick, S.; Agarwal, H.; Ellis-Davies, G. C. R. Dendrimer Conjugation Enables Multiphoton Chemical Neurophysiology Studies with an Extended π-Electron Caging Chromophore. *Angew. Chem., Int. Ed.* **2019**, *58*, 12086−12090.
(223) Shigenaga, A.; Yamamoto, J.; Sumikawa, Y.; Furuta, T.; Otaka, A. Development and Photo-Responsive Peptide Bond Cleavage Reaction of Two-Photon Near-Infrared Excitation-Responsive Peptide. *Tetrahedron Lett.* **2010**, *51*, 2868−2871.
(224) Kantevari, S.; Hoang, C. J.; Ogrodnik, J.; Egger, M.; Niggli, E.; Ellis-Davies, G. C. R. Synthesis and Two-photon Photolysis of 6-(*ortho*-Nitroveratryl)-Caged IP3 in Living Cells. *ChemBioChem* **2006**, *7*, 174−180.
(225) Neveu, P.; Aujard, I.; Benbrahim, C.; Le Saux, T.; Allemand, J.-F.; Vriz, S.; Bensimon, D.; Jullien, L. A Caged Retinoic Acid for One- and Two-Photon Excitation in Zebrafish Embryos. *Angew. Chem., Int. Ed.* **2008**, *47*, 3744−3746.
(226) Shi, D. D.; Trigo, F. F.; Semmelhack, M. F.; Wang, S. S. H. Synthesis and Biological Evaluation of Bis-CNB-GABA, a Photoactivatable Neurotransmitter with Low Receptor Interference and Chemical Two-Photon Uncaging Properties. *J. Am. Chem. Soc.* **2014**, *136*, 1976−1981.
(227) Cueto Díaz, E. J.; Picard, S.; Chevasson, V.; Daniel, J.; Hugues, V.; Mongin, O.; Genin, E.; Blanchard-Desce, M. Cooperative Dyads for Two-Photon Uncaging. *Org. Lett.* **2015**, *17*, 102−105.
(228) Cueto Diaz, E.; Picard, S.; Klausen, M.; Hugues, V.; Pagano, P.; Genin, E.; Blanchard-Desce, M. Cooperative Veratryle and Nitroindoline Cages for Two-Photon Uncaging in the NIR. *Chem. - Eur. J.* **2016**, *22*, 10848−10859.
(229) Giegrich, H.; Eisele-Bühler, S.; Hermann, C.; Kvasyuk, E.; Charubala, R.; Pfleiderer, W. New Photolabile Protecting Groups in Nucleoside and Nucleotide Chemistry—Synthesis, Cleavage Mechanisms and Applications. *Nucleosides Nucleotides* **1998**, *17*, 1987−1996.
(230) Tseng, S.-S.; Ullman, E. F. Elimination Reactions Induced by Photoenolization of *o*-Alkylbenzophenones. *J. Am. Chem. Soc.* **1976**, *98*, 541−544.
(231) Atemnkeng, W. N.; Louisiana, L. D.; Yong, P. K.; Vottero, B.; Banerjee, A. 1-[2-(2-Hydroxyalkyl)phenyl]ethanone: A New Photoremovable Protecting Group for Carboxylic Acids. *Org. Lett.* **2003**, *5*, 4469−4471.
(232) Kamdzhilov, Y.; Wirz, J. Synthesis and Reaction Mechanism of a Photoremovable Protecting Group Based on 1,4-Naphthoquinone. *Photochem. Photobiol. Sci.* **2007**, *6*, 865−872.
(233) Pirrung, M. C.; Dore, T. M.; Zhu, Y.; Rana, V. S. Sensitized Two-Photon Photochemical Deprotection. *Chem. Commun.* **2010**, *46*, 5313−5315.
(234) Sobczak, M.; Wagner, P. J. Light-Induced Decarboxylation of (*o*-Acylphenyl)acetic Acids. *Org. Lett.* **2002**, *4*, 379−382.
(235) Klán, P.; Pelliccioli, A. P.; Pospíšil, T.; Wirz, J. 2, 5-Dimethylphenacyl Esters: A Photoremovable Protecting Group for Phosphates and Sulfonic Acids. *Photochem. Photobiol. Sci.* **2002**, *1*, 920−923.
(236) Beier, M.; Hoheisel, J. D. Production by Quantitative Photolithographic Synthesis of Individually Quality Checked DNA Microarrays. *Nucleic Acids Res.* **2000**, *28*, No. e11.
(237) Pirrung, M. C.; Wang, L.; Montague-Smith, M. P. 3'-Nitrophenylpropyloxycarbonyl (NPPOC) Protecting Groups for High-Fidelity Automated 5' → 3' Photochemical DNA Synthesis. *Org. Lett.* **2001**, *3*, 1105−1108.
(238) Forsström, B.; Axnäs, B. B.; Stengele, K.-P.; Bühler, J.; Albert, T. J.; Richmond, T. A.; Hu, F. J.; Nilsson, P.; Hudson, E. P.; Rockberg, J.; Uhlen, M. Proteome-Wide Epitope Mapping of Antibodies Using Ultra-dense Peptide Arrays. *Mol. Cell. Proteomics* **2014**, *13*, 1585−1597.
(239) Hansen, L. B.; Buus, S.; Schafer-Nielsen, C. Identification and Mapping of Linear Antibody Epitopes in Human Serum Albumin Using High-Density Peptide Arrays. *PLoS One* **2013**, *8*, No. e68902.
(240) Bhushan, K. R.; DeLisi, C.; Laursen, R. A. Synthesis of Photolabile 2-(2-Nitrophenyl)propyloxycarbonyl Protected Amino Acids. *Tetrahedron Lett.* **2003**, *44*, 8585−8588.
(241) Lackey, J. G.; Mitra, D.; Somoza, M. M.; Cerrina, F.; Damha, M. J. Acetal Levulinyl Ester (ALE) Groups for 2′-Hydroxyl Protection of Ribonucleosides in the Synthesis of Oligoribonucleotides on Glass and Microarrays. *J. Am. Chem. Soc.* **2009**, *131*, 8496−8502.
(242) Wu, C.-H.; Holden, M. T.; Smith, L. M. Enzymatic Fabrication of High-Density RNA Arrays. *Angew. Chem., Int. Ed.* **2014**, *53*, 13514−13517.
(243) Franssen-Van Hal, N. L. W.; van der Putte, P.; Hellmuth, K.; Matysiak, S.; Kretschy, N.; Somoza, M. M. Optimized Light-Directed Synthesis of Aptamer Microarrays. *Anal. Chem.* **2013**, *85*, 5950−5957.
(244) Yi, H.; Maisonneuve, S.; Xie, J. Synthesis, Glycosylation and Photolysis of Photolabile 2-(2-Nitrophenyl)propyloxycarbonyl (NPPOC) Protected Glycopyranosides. *Org. Biomol. Chem.* **2009**, *7*, 3847−3854.
(245) Wu, C.-H.; Lockett, M. R.; Smith, L. M. RNA-Mediated Gene Assembly from DNA Arrays. *Angew. Chem., Int. Ed.* **2012**, *51*, 4628−4632.
(246) Specht, A.; Thomann, J.-S.; Alarcon, K.; Wittayanan, W.; Ogden, D.; Furuta, T.; Kurakawa, Y.; Goeldner, M. New Photoremovable Protecting Groups for Carboxylic Acids with High Photolytic Efficiencies at Near-UV Irradiation. Application to the Photocontrolled Release of L-Glutamate. *ChemBioChem* **2006**, *7*, 1690−1695.
(247) Salierno, M. J.; García, A. J.; del Campo, A. Photo-Activatable Surfaces for Cell Migration Assays. *Adv. Funct. Mater.* **2013**, *23*, 5974−5980.
(248) Lunzer, M.; Shi, L.; Andriotis, O. G.; Gruber, P.; Markovic, M.; Thurner, P. J.; Ossipov, D.; Liska, R.; Ovsianikov, A. A Modular Approach to Sensitized Two-Photon Patterning of Photodegradable Hydrogels. *Angew. Chem., Int. Ed.* **2018**, *57*, 15122−15127.
(249) Zhang, X.; Xi, W.; Gao, G.; Wang, X.; Stansbury, J. W.; Bowman, C. N. *o*-Nitrobenzyl-Based Photobase Generators: Efficient

Photoinitiators for Visible-Light Induced Thiol-Michael Addition Photopolymerization. *ACS Macro Lett.* **2018**, *7*, 852−857.
(250) Kretschy, N.; Holik, A.-K.; Somoza, V.; Stengele, K.-P.; Somoza, M. M. Next-Generation *o*-Nitrobenzyl Photolabile Groups for Light-Directed Chemistry and Microarray Synthesis. *Angew. Chem., Int. Ed.* **2015**, *54*, 8555−8559.
(251) Sack, M.; Hölz, K.; Holik, A.-K.; Kretschy, N.; Somoza, V.; Stengele, K.-P.; Somoza, M. M. Express Photolithographic DNA Microarray Synthesis with Optimized Chemistry and High-Efficiency Photolabile Groups. *J. Nanobiotechnol.* **2016**, *14*, 14.
(252) Wöll, D.; Smirnova, J.; Galetskaya, M.; Prykota, T.; Bühler, J.; Stengele, K.-P.; Pfleiderer, W.; Steiner, U. E. Intramolecular Sensitization of Photocleavage of the Photolabile 2-(2-Nitrophenyl)-propoxycarbonyl (NPPOC) Protecting Group: Photoproducts and Photokinetics of the Release of Nucleosides. *Chem. - Eur. J.* **2008**, *14*, 6490−6497.
(253) Wöll, D.; Smirnova, J.; Pfleiderer, W.; Steiner, U. E. Highly Efficient Photolabile Protecting Groups with Intramolecular Energy Transfer. *Angew. Chem., Int. Ed.* **2006**, *45*, 2975−2978.
(254) Gug, S.; Charon, S.; Specht, A.; Alarcon, K.; Ogden, D.; Zietz, B.; Léonard, J.; Haacke, S.; Bolze, F.; Nicoud, J.-F.; Goeldner, M. Photolabile Glutamate Protecting Group with High One- and Two-Photon Uncaging Efficiencies. *ChemBioChem* **2008**, *9*, 1303−1307.
(255) Specht, A.; Bolze, F.; Donato, L.; Herbivo, C.; Charon, S.; Warther, D.; Gug, S.; Nicoud, J.-F.; Goeldner, M. The Donor−Acceptor Biphenyl Platform: A Versatile Chromophore for the Engineering of Highly Efficient Two-Photon Sensitive Photo-removable Protecting Groups. *Photochem. Photobiol. Sci.* **2012**, *11*, 578−586.
(256) Warther, D.; Bolze, F.; Léonard, J.; Gug, S.; Specht, A.; Puliti, D.; Sun, X.-H.; Kessler, P.; Lutz, Y.; Vonesch, J.-L.; Winsor, B.; Nicoud, J.-F.; Goeldner, M. Live-Cell One- and Two-Photon Uncaging of a Far-Red Emitting Acridinone Fluorophore. *J. Am. Chem. Soc.* **2010**, *132*, 2585−2590.
(257) Schelkle, K. M.; Becht, S.; Faraji, S.; Petzoldt, M.; Müllen, K.; Buckup, T.; Dreuw, A.; Motzkus, M.; Hamburger, M. Emission Turn-On and Solubility Turn-Off in Conjugated Polymers: One- and Two-Photon-Induced Removal of Fluorescence-Quenching Solubilizing Groups. *Macromol. Rapid Commun.* **2015**, *36*, 31−37.
(258) Leonidova, A.; Anstaett, P.; Pierroz, V.; Mari, C.; Spingler, B.; Ferrari, S.; Gasser, G. Induction of Cytotoxicity through Photorelease of Aminoferrocene. *Inorg. Chem.* **2015**, *54*, 9740−9748.
(259) Farrukh, A.; Paez, J. I.; del Campo, A. 4D Biomaterials for Light-Guided Angiogenesis. *Adv. Funct. Mater.* **2019**, *29*, 1807734.
(260) García-Fernández, L.; Herbivo, C.; Arranz, V. S. M.; Warther, D.; Donato, L.; Specht, A.; del Campo, A. Dual Photosensitive Polymers with Wavelength-Selective Photoresponse. *Adv. Mater.* **2014**, *26*, 5012−5017.
(261) Carling, C.-J.; Viger, M. L.; Nguyen Huu, V. A.; Garcia, A. V.; Almutairi, A. In Vivo Visible Light-Triggered Drug Release From an Implanted Depot. *Chem. Sci.* **2015**, *6*, 335−341.
(262) Farrukh, A.; Fan, W.; Zhao, S.; Salierno, M.; Paez, J. I.; del Campo, A. Photoactivatable Adhesive Ligands for Light-Guided Neuronal Growth. *ChemBioChem* **2018**, *19*, 1271−1279.
(263) Goegan, B.; Terzi, F.; Bolze, F.; Cambridge, S.; Specht, A. Synthesis and Characterization of Photoactivatable Doxycycline Analogues Bearing Two-Photon-Sensitive Photoremovable Groups Suitable for Light-Induced Gene Expression. *ChemBioChem* **2018**, *19*, 1341−1348.
(264) Farrukh, A.; Zhao, S.; Paez, J. I.; Kavyanifar, A.; Salierno, M.; Cavalié, A.; del Campo, A. In Situ, Light-Guided Axon Growth on Biomaterials via Photoactivatable Laminin Peptidomimetic IK-(HANBP)VAV. *ACS Appl. Mater. Interfaces* **2018**, *10*, 41129−41137.
(265) Fichte, M. A. H.; Weyel, X. M. M.; Junek, S.; Schäfer, F.; Herbivo, C.; Goeldner, M.; Specht, A.; Wachtveitl, J.; Heckel, A. Three-Dimensional Control of DNA Hybridization by Orthogonal Two-Color Two-Photon Uncaging. *Angew. Chem., Int. Ed.* **2016**, *55*, 8948−8952.
(266) Herbivo, C.; Omran, Z.; Revol, J.; Javot, H.; Specht, A. Synthesis and Characterization of Cell-Permeable Caged Phosphates that Can Be Photolyzed by Visible Light or 800 nm Two-Photon Photolysis. *ChemBioChem* **2013**, *14*, 2277−2283.
(267) Gug, S.; Bolze, F.; Specht, A.; Bourgogne, C.; Goeldner, M.; Nicoud, J.-F. Molecular Engineering of Photoremovable Protecting Groups for Two-Photon Uncaging. *Angew. Chem., Int. Ed.* **2008**, *47*, 9525−9529.
(268) Schelkle, K. M.; Griesbaum, T.; Ollech, D.; Becht, S.; Buckup, T.; Hamburger, M.; Wombacher, R. Light-Induced Protein Dimerization by One- and Two-Photon Activation of Gibberellic Acid Derivatives in Living Cells. *Angew. Chem., Int. Ed.* **2015**, *54*, 2825−2829.
(269) Lin, Y.-C.; Nihongaki, Y.; Liu, T.-Y.; Razavi, S.; Sato, M.; Inoue, T. Rapidly Reversible Manipulation of Molecular Activity with Dual Chemical Dimerizers. *Angew. Chem., Int. Ed.* **2013**, *52*, 6450−6454.
(270) Miyamoto, T.; DeRose, R.; Suarez, A.; Ueno, T.; Chen, M.; Sun, T.-p.; Wolfgang, M. J.; Mukherjee, C.; Meyers, D. J.; Inoue, T. Rapid and Orthogonal Logic Gating with a Gibberellin-Induced Dimerization System. *Nat. Chem. Biol.* **2012**, *8*, 465−470.
(271) Olejniczak, J.; Sankaranarayanan, J.; Viger, M. L.; Almutairi, A. Highest Efficiency Two-Photon Degradable Copolymer for Remote Controlled Release. *ACS Macro Lett.* **2013**, *2*, 683−687.
(272) Guibourt, N. J.-B. G. *Histoire Abrégée Des Drogues Simples*; Colas, L., Ed.; Méquignon-Marvis: Paris, 1820.
(273) Guibort, N.; Jean, B.; Planchon, G. *Histoire Naturelle des Drogues Simples ou Cours D'Histoire Naturelle*; L'éCole de Pharmacie de Paris, 1869.
(274) Harborne, J. B. The Natural Coumarins: Occurrence, Chemistry and Biochemistry. *Plant, Cell Environ.* **1982**, *5*, 435−436.
(275) Givens, R. S.; Matuszewski, B. Photochemistry of Phosphate Esters: An Efficient Method for the Generation of Electrophiles. *J. Am. Chem. Soc.* **1984**, *106*, 6860−6861.
(276) Schade, B.; Hagen, V.; Schmidt, R.; Herbrich, R.; Krause, E.; Eckardt, T.; Bendig, J. Deactivation Behavior and Excited-State Properties of (Coumarin-4-yl)methyl Derivatives. 1. Photocleavage of (7-Methoxycoumarin-4-yl)methyl-Caged Acids with Fluorescence Enhancement. *J. Org. Chem.* **1999**, *64*, 9109−9117.
(277) Schmidt, R.; Geissler, D.; Hagen, V.; Bendig, J. Kinetics Study of the Photocleavage of (Coumarin-4-yl)methyl Esters. *J. Phys. Chem. A* **2005**, *109*, 5000−5004.
(278) Schmidt, R.; Geissler, D.; Hagen, V.; Bendig, J. Mechanism of Photocleavage of (Coumarin-4-yl)methyl Esters. *J. Phys. Chem. A* **2007**, *111*, 5768−5774.
(279) Givens, R.; Kotala, M. B.; Lee, J.-I. Mechanistic Overview of Phototriggers and Cage Release. *Dynamic Studies in Biology*; Goeldner, M., Givens, R., Eds., 2005.
(280) van Wilderen, L. J. G. W.; Neumann, C.; Rodrigues-Correia, A.; Kern-Michler, D.; Mielke, N.; Reinfelds, M.; Heckel, A.; Bredenbeck, J. Picosecond Activation of the DEACM Photocage Unravelled by Vis-Pump-IR-Probe Spectroscopy. *Phys. Chem. Chem. Phys.* **2017**, *19*, 6487−6496.
(281) Sarker, A. M.; Kaneko, Y.; Neckers, D. C. Photochemistry and Photophysics of Novel Photoinitiators: *N,N,N*-Tributyl-*N*-(4-methylene-7-methoxycoumarin) Ammonium Borates. *J. Photochem. Photobiol., A* **1998**, *117*, 67−74.
(282) Takano, H.; Narumi, T.; Nomura, W.; Furuta, T.; Tamamura, H. Utilization of the Heavy Atom Effect for the Development of a Photosensitive 8-Azacoumarin-Type Photolabile Protecting Group. *Org. Lett.* **2015**, *17*, 5372−5375.
(283) Senda, N.; Momotake, A.; Nishimura, Y.; Arai, T. Synthesis and Photochemical Properties of a New Water-Soluble Coumarin, Designed as a Chromophore for Highly Water-Soluble and Photolabile Protecting Group. *Bull. Chem. Soc. Jpn.* **2006**, *79*, 1753−1757.
(284) Offenbartl-Stiegert, D.; Clarke, T. M.; Bronstein, H.; Nguyen, H. P.; Howorka, S. Solvent-Dependent Photophysics of a Red-Shifted, Biocompatible Coumarin Photocage. *Org. Biomol. Chem.* **2019**, *17*, 6178−6183.

(285) Corrie, J. E. T.; Furuta, T.; Givens, R.; Yousef, A. L.; Goeldner, M. Photoremovable Protecting Groups Used for the Caging of Biomolecules. *Dynamic Studies in Biology*; Goeldner, M., Givens, R., Eds., 2005.
(286) Dore, M. T. Multiphoton Phototriggers for Exploring Cell Physiology; In *Dynamic Studies in Biology*; Goeldner, M., Givens, R., Eds., 2005.
(287) Hagen, V.; Benndorf, K.; Kaupp, U. B.; Pavlos, M. C.; Xu, H.; Toscano, P. J.; Hess, G. P.; Gillespie, C. D.; Kim, G.; Kandler, K. Control of Cellular Activity. *Dynamic Studies in Biology*; Goeldner, M., Givens, R., Eds., 2005.
(288) Loudwig, S.; Bayley, H.; Peng, L.; Goeldner, M.; Condeelis, S. J.; Lawrence, D. S. Photoregulation of Proteins. *Dynamic Studies in Biology*; Goeldner, M., Givens, R., Eds., 2005.
(289) Tatsu, Y.; Shigeri, Y.; Yumoto, N. Caged Compounds and Solid-Phase Synthesis. *Dynamic Studies in Biology*; Goeldner, M., Givens, R., Eds., 2005.
(290) Eckardt, T.; Hagen, V.; Schade, B.; Schmidt, R.; Schweitzer, C.; Bendig, J. Deactivation Behavior and Excited-State Properties of (Coumarin-4-yl)methyl Derivatives. 2. Photocleavage of Selected (Coumarin-4-yl)methyl-Caged Adenosine Cyclic 3′,5′-Monophosphates with Fluorescence Enhancement. *J. Org. Chem.* **2002**, *67*, 703−710.
(291) Fournier, L.; Aujard, I.; Le Saux, T.; Maurin, S.; Beaupierre, S.; Baudin, J.-B.; Jullien, L. Coumarinylmethyl Caging Groups with Redshifted Absorption. *Chem. - Eur. J.* **2013**, *19*, 17494−17507.
(292) Olson, J. P.; Kwon, H.-B.; Takasaki, K. T.; Chiu, C. Q.; Higley, M. J.; Sabatini, B. L.; Ellis-Davies, G. C. R. Optically Selective Two-Photon Uncaging of Glutamate at 900 nm. *J. Am. Chem. Soc.* **2013**, *135*, 5954−5957.
(293) Bao, C.; Fan, G.; Lin, Q.; Li, B.; Cheng, S.; Huang, Q.; Zhu, L. Styryl Conjugated Coumarin Caged Alcohol: Efficient Photorelease by Either One-Photon Long Wavelength or Two-Photon NIR Excitation. *Org. Lett.* **2012**, *14*, 572−575.
(294) Lin, Q.; Yang, L.; Wang, Z.; Hua, Y.; Zhang, D.; Bao, B.; Bao, C.; Gong, X.; Zhu, L. Coumarin Photocaging Groups Modified with an Electron-Rich Styryl Moiety at the 3-Position: Long-Wavelength Excitation, Rapid Photolysis, and Photobleaching. *Angew. Chem., Int. Ed.* **2018**, *57*, 3722−3726.
(295) Bojtár, M.; Kormos, A.; Kis-Petik, K.; Kellermayer, M.; Kele, P. Green-Light Activatable, Water-Soluble Red-Shifted Coumarin Photocages. *Org. Lett.* **2019**, *21*, 9410−9414.
(296) Ito, K.; Maruyama, J. Studies on Stable Diazoalkanes as Potential Fluorogenic Reagents. I. 7-Substituted 4-Diazomethylcoumarins. *Chem. Pharm. Bull.* **1983**, *31*, 3014−3023.
(297) Lopez Arbeloa, T.; Lopez Arbeloa, F.; Tapia, M. J.; Lopez Arbeloa, I. Hydrogen-Bonding Effect on the Photophysical Properties of 7-Aminocoumarin Derivatives. *J. Phys. Chem.* **1993**, *97*, 4704−4707.
(298) Rechthaler, K.; Köhler, G. Excited State Properties and Deactivation Pathways of 7-Aminocoumarins. *Chem. Phys.* **1994**, *189*, 99−116.
(299) Fabian, W. M. F.; Niederreiter, K. S.; Uray, G.; Stadlbauer, W. Substituent Effects on Absorption and Fluorescence Spectra of Carbostyrils. *J. Mol. Struct.* **1999**, *477*, 209−220.
(300) Seixas de Melo, J. S.; Becker, R. S.; Macanita, A. L. Photophysical Behavior of Coumarins as a Function of Substitution and Solvent: Experimental Evidence for the Existence of a Lowest Lying $^1\pi,\pi^*$ State. *J. Phys. Chem.* **1994**, *98*, 6054−6058.
(301) Hagen, V.; Bendig, J.; Frings, S.; Eckardt, T.; Helm, S.; Reuter, D.; Kaupp, U. B. Highly Efficient and Ultrafast Phototriggers for cAMP and cGMP by Using Long-Wavelength UV/Vis-Activation. *Angew. Chem., Int. Ed.* **2001**, *40*, 1045−1048.
(302) Donovalová, J.; Cigán, M.; Stankovičová, H.; Gašpar, J.; Danko, M.; Gáplovský, A.; Hrdlovič, P. Spectral Properties of Substituted Coumarins in Solution and Polymer Matrices. *Molecules* **2012**, *17*, 3259−3276.
(303) Fonseca, A. S.; Goncalves, M. S.; Costa, S. P. Light-Induced Cleavage of Model Phenylalanine Conjugates Based on Coumarins and Quinolones. *Amino Acids* **2010**, *39*, 699−712.
(304) Fonseca, A. S. C.; Soares, A. M. S.; Gonçalves, M. S. T.; Costa, S. P. G. Thionated Coumarins and Quinolones in the Light Triggered Release of a Model Amino Acid: Synthesis and Photolysis Studies. *Tetrahedron* **2012**, *68*, 7892−7900.
(305) Takaoka, K.; Tatsu, Y.; Yumoto, N.; Nakajima, T.; Shimamoto, K. Synthesis of Carbamate-Type Caged Derivatives of a Novel Glutamate Transporter Blocker. *Bioorg. Med. Chem.* **2004**, *12*, 3687−3694.
(306) Velema, W. A.; van der Berg, J. P.; Szymanski, W.; Driessen, A. J. M.; Feringa, B. L. Orthogonal Control of Antibacterial Activity with Light. *ACS Chem. Biol.* **2014**, *9*, 1969−1974.
(307) Velema, W. A.; van der Berg, J. P.; Szymanski, W.; Driessen, A. J. M.; Feringa, B. L. Bacterial Patterning Controlled by Light Exposure. *Org. Biomol. Chem.* **2015**, *13*, 1639−1642.
(308) Atta, S.; Jana, A.; Ananthakirshnan, R.; Narayana Dhuleep, P. S. Fluorescent Caged Compounds of 2,4-Dichlorophenoxyacetic Acid (2,4-D): Photorelease Technology for Controlled Release of 2,4-D. *J. Agric. Food Chem.* **2010**, *58*, 11844−11851.
(309) Furuta, T.; Iwamura, M. New Caged Groups: 7-Substituted Coumarinylmethyl Phosphate Esters. *Methods Enzymol.*; Academic Press, 1998; Vol. *291*.
(310) Furuta, T.; Momotake, A.; Sugimoto, M.; Hatayama, M.; Torigai, H.; Iwamura, M. Acyloxycoumarinylmethyl-Caged cAMP, the Photolabile and Membrane-Permeable Derivative of cAMP That Effectively Stimulates Pigment-Dispersion Response of Melanophores. *Biochem. Biophys. Res. Commun.* **1996**, *228*, 193−198.
(311) Yu, P.-L.; Zhang, Z.-H.; Hao, B.-X.; Zhao, Y.-J.; Zhang, L.-H.; Lee, H.-C.; Zhang, L.; Yue, J. A Novel Fluorescent Cell Membrane-permeable Caged Cyclic ADP-ribose Analogue. *J. Biol. Chem.* **2012**, *287*, 24774−24783.
(312) Luo, J.; Kong, M.; Liu, L.; Samanta, S.; Van Houten, B.; Deiters, A. Optical Control of DNA Helicase Function through Genetic Code Expansion. *ChemBioChem* **2017**, *18*, 466−469.
(313) Liu, J.; Hemphill, J.; Samanta, S.; Tsang, M.; Deiters, A. Genetic Code Expansion in Zebrafish Embryos and Its Application to Optical Control of Cell Signaling. *J. Am. Chem. Soc.* **2017**, *139*, 9100−9103.
(314) Zhou, W.; Hankinson, C. P.; Deiters, A. Optical Control of Cellular ATP Levels with a Photocaged Adenylate Kinase. *ChemBioChem* **2020**, *21*, 1832−1836.
(315) Brown, W.; Liu, J.; Tsang, M.; Deiters, A. Cell-Lineage Tracing in Zebrafish Embryos with an Expanded Genetic Code. *ChemBioChem* **2018**, *19*, 1244−1249.
(316) Courtney, T. M.; Deiters, A. Controlling Phosphate Removal with Light: The Development of Optochemical Tools to Probe Protein Phosphatase Function. *SLAS Discovery* **2020**, *25*, 957−960.
(317) Furuta, T.; Torigai, H.; Sugimoto, M.; Iwamura, M. Photochemical Properties of New Photolabile cAMP Derivatives in a Physiological Saline Solution. *J. Org. Chem.* **1995**, *60*, 3953−3956.
(318) Hagen, V.; Bendig, J.; Frings, S.; Wiesner, B.; Schade, B.; Helm, S.; Lorenz, D.; Benjamin Kaupp, U. Synthesis, Photochemistry and Application of (7-Methoxycoumarin-4-yl)methyl-Caged 8-Bromoadenosine Cyclic 3′,5′-Monophosphate and 8-Bromoguanosine Cyclic 3′,5′-Monophosphate Photolyzed in the Nanosecond Time Region. *J. Photochem. Photobiol., B* **1999**, *53*, 91−102.
(319) Fonseca, A. S. C.; Gonçalves, M. S. T.; Costa, S. P. G. Photocleavage Studies of Fluorescent Amino Acid Conjugates Bearing Different Types of Linkages. *Tetrahedron* **2007**, *63*, 1353−1359.
(320) Fernandes, M. J. G.; Gonçalves, M. S. T.; Costa, S. P. G. Comparative Study of Polyaromatic and Polyheteroaromatic Fluorescent Photocleavable Protecting Groups. *Tetrahedron* **2008**, *64*, 3032−3038.
(321) Suzuki, A. Z.; Watanabe, T.; Kawamoto, M.; Nishiyama, K.; Yamashita, H.; Ishii, M.; Iwamura, M.; Furuta, T. Coumarin-4-ylmethoxycarbonyls as Phototriggers for Alcohols and Phenols. *Org. Lett.* **2003**, *5*, 4867−4870.

(322) Furuta, T.; Hirayama, Y.; Iwamura, M. Anthraquinon-2-ylmethoxycarbonyl (Aqmoc): A New Photochemically Removable Protecting Group for Alcohols. *Org. Lett.* **2001**, *3*, 1809−1812.
(323) Atta, S.; Ikbal, M.; Boda, N.; Gauri, S. S.; Singh, N. D. P. Photoremovable Protecting Groups as Controlled-Release Device for Sex Pheromone. *Photochem. Photobiol. Sci.* **2013**, *12*, 393−403.
(324) Cürten, B.; Kullmann, P. H. M.; Bier, M. E.; Kandler, K.; Schmidt, B. F. Synthesis, Photophysical, Photochemical and Biological Properties of Caged GABA, 4-[[(2H-1-Benzopyran-2-one-7-amino-4-methoxy) carbonyl] amino] Butanoic Acid. *Photochem. Photobiol.* **2005**, *81*, 641−648.
(325) Luo, J.; Uprety, R.; Naro, Y.; Chou, C.; Nguyen, D. P.; Chin, J. W.; Deiters, A. Genetically Encoded Optochemical Probes for Simultaneous Fluorescence Reporting and Light Activation of Protein Function with Two-Photon Excitation. *J. Am. Chem. Soc.* **2014**, *136*, 15551−15558.
(326) Guardado-Alvarez, T. M.; Sudha Devi, L.; Russell, M. M.; Schwartz, B. J.; Zink, J. I. Activation of Snap-Top Capped Mesoporous Silica Nanocontainers Using Two Near-Infrared Photons. *J. Am. Chem. Soc.* **2013**, *135*, 14000−14003.
(327) Pocker, Y.; Davison, B. L.; Deits, T. L. Decarboxylation of Monosubstituted Derivatives of Carbonic Acid. Comparative Studies of Water- and Acid-Catalyzed Decarboxylation of Sodium Alkyl Carbonates in Water and Water-d_2. *J. Am. Chem. Soc.* **1978**, *100*, 3564−3567.
(328) Rossi, F. M.; Margulis, M.; Tang, C.-M.; Kao, J. P. Y. *N*-Nmoc-L-Glutamate, a New Caged Glutamate with High Chemical Stability and Low Pre-photolysis Activity. *J. Biol. Chem.* **1997**, *272*, 32933−32939.
(329) Papageorgiou, G.; Barth, A.; Corrie, J. E. T. Flash Photolytic Release of Alcohols From Photolabile Carbamates or Carbonates Is Rate-Limited by Decarboxylation of the Photoproduct. *Photochem. Photobiol. Sci.* **2005**, *4*, 216−220.
(330) Johnson, S. L.; Morrison, D. L. Kinetics and Mechanism of Decarboxylation of *N*-Arylcarbamates. Evidence for Kinetically Important Zwitterionic Carbamic Acid Species of Short Lifetime. *J. Am. Chem. Soc.* **1972**, *94*, 1323−1334.
(331) Schoenleber, R. O.; Giese, B. Photochemical Release of Amines by C, N-Bond Cleavage. *Synlett* **2003**, *2003*, 0501−0504.
(332) Shembekar, V. R.; Chen, Y.; Carpenter, B. K.; Hess, G. P. A Protecting Group for Carboxylic Acids That Can Be Photolyzed by Visible Light. *Biochemistry* **2005**, *44*, 7107−7114.
(333) Shembekar, V. R.; Chen, Y.; Carpenter, B. K.; Hess, G. P. Coumarin-Caged Glycine that Can Be Photolyzed within 3 μs by Visible Light. *Biochemistry* **2007**, *46*, 5479−5484.
(334) Hagen, V.; Frings, S.; Wiesner, B.; Helm, S.; Kaupp, U. B.; Bendig, J. [7-(Dialkylamino)coumarin-4-yl]methyl-Caged Compounds as Ultrafast and Effective Long-Wavelength Phototriggers of 8Bromo-Substituted Cyclic Nucleotides. *ChemBioChem* **2003**, *4*, 434−442.
(335) Piloto, A. M.; Costa, S. P. G.; Gonçalves, M. S. T. Wavelength-Selective Cleavage of *o*-Nitrobenzyl and Polyheteroaromatic Benzyl Protecting Groups. *Tetrahedron* **2014**, *70*, 650−657.
(336) Piloto, A. M.; Hungerford, G.; Costa, S. P. G.; Gonçalves, M. S. T. Photoinduced Release of Neurotransmitter Amino Acids from Coumarin-Fused Julolidine Ester Cages. *Eur. J. Org. Chem.* **2013**, *2013*, 7715−7723.
(337) Bassolino, G.; Nançoz, C.; Thiel, Z.; Bois, E.; Vauthey, E.; Rivera-Fuentes, P. Photolabile Coumarins with Improved Efficiency Through Azetidinyl Substitution. *Chem. Sci.* **2018**, *9*, 387−391.
(338) Chaudhuri, A.; Venkatesh, Y.; Das, J.; Behara, K. K.; Mandal, S.; Maiti, T. K.; Singh, N. D. P. Squaric Acid-Coumarin-Chlorambucil: Photoresponsive Single-Component Fluorescent Organic Nanoconjugates for Self-Monitored Therapeutics. *ACS Appl. Nano Mater.* **2018**, *1*, 6312−6319.
(339) Conceição, R.; Hungerford, G.; Costa, S. P. G.; Gonçalves, M. S. T. Photolytic Release of Bioactive Carboxylic Acids From Fused Pyran Conjugates. *Dyes Pigm.* **2018**, *148*, 368−379.
(340) Atta, S.; Ikbal, M.; Kumar, A.; Pradeep Singh, N. D. Application of Photoremovable Protecting Group for Controlled Release of Plant Growth Regulators by Sunlight. *J. Photochem. Photobiol., B* **2012**, *111*, 39−49.
(341) Geißler, D.; Kresse, W.; Wiesner, B.; Bendig, J.; Kettenmann, H.; Hagen, V. DMACM-Caged Adenosine Nucleotides: Ultrafast Phototriggers for ATP, ADP, and AMP Activated by Long-Wavelength Irradiation. *ChemBioChem* **2003**, *4*, 162−170.
(342) Bourbon, P.; Peng, Q.; Ferraudi, G.; Stauffacher, C.; Wiest, O.; Helquist, P. Development of Carbamate-Tethered Coumarins as Phototriggers for Caged Nicotinamide. *Bioorg. Med. Chem. Lett.* **2013**, *23*, 6321−6324.
(343) Herzig, L. M.; Elamri, I.; Schwalbe, H.; Wachtveitl, J. Light-Induced Antibiotic Release From a Coumarin-Caged Compound on the Ultrafast Timescale. *Phys. Chem. Chem. Phys.* **2017**, *19*, 14835−14844.
(344) Nguyen, H. P.; Stewart, S.; Kukwikila, M. N.; Jones, S. F.; Offenbartl-Stiegert, D.; Mao, S.; Balasubramanian, S.; Beck, S.; Howorka, S. A Photo-responsive Small-Molecule Approach for the Opto-epigenetic Modulation of DNA Methylation. *Angew. Chem., Int. Ed.* **2019**, *58*, 6620−6624.
(345) Wong, P. T.; Roberts, E. W.; Tang, S.; Mukherjee, J.; Cannon, J.; Nip, A. J.; Corbin, K.; Krummel, M. F.; Choi, S. K. Control of an Unusual Photo-Claisen Rearrangement in Coumarin Caged Tamoxifen through an Extended Spacer. *ACS Chem. Biol.* **2017**, *12*, 1001−1010.
(346) Zhang, X.; Xi, W.; Wang, C.; Podgórski, M.; Bowman, C. N. Visible-Light-Initiated Thiol-Michael Addition Polymerizations with Coumarin-Based Photobase Generators: Another Photoclick Reaction Strategy. *ACS Macro Lett.* **2016**, *5*, 229−233.
(347) Bourbon, P.; Peng, Q.; Ferraudi, G.; Stauffacher, C.; Wiest, O.; Helquist, P. Synthesis and Photochemical Behavior of Coumarin-Caged Cholesterol. *Bioorg. Med. Chem. Lett.* **2013**, *23*, 2162−2165.
(348) Franceschini, C.; Scrimin, P.; Prins, L. J. Light-Triggered Thiol-Exchange on Gold Nanoparticles at Low Micromolar Concentrations in Water. *Langmuir* **2014**, *30*, 13831−13836.
(349) Liu, Z.; Liu, T.; Lin, Q.; Bao, C.; Zhu, L. Photoreleasable Thiol Chemistry for Facile and Efficient Bioconjugation. *Chem. Commun.* **2014**, *50*, 1256−1258.
(350) San Miguel, V.; Bochet, C. G.; del Campo, A. Wavelength-Selective Caged Surfaces: How Many Functional Levels Are Possible? *J. Am. Chem. Soc.* **2011**, *133*, 5380−5388.
(351) Lin, W.; Long, L.; Tan, W.; Chen, B.; Yuan, L. Coumarin-Caged Rosamine Probes Based on a Unique Intramolecular Carbon−Carbon Spirocyclization. *Chem. - Eur. J.* **2010**, *16*, 3914−3917.
(352) Tang, S.; Cannon, J.; Yang, K.; Krummel, M. F.; Baker, J. R.; Choi, S. K. Spacer-Mediated Control of Coumarin Uncaging for Photocaged Thymidine. *J. Org. Chem.* **2020**, *85*, 2945−2955.
(353) Schaal, J.; Kotzur, N.; Dekowski, B.; Quilitz, J.; Klimakow, M.; Wessig, P.; Hagen, V. A Novel Photorearrangement of (Coumarin-4-yl)methylphenyl Ethers. *J. Photochem. Photobiol., A* **2009**, *208*, 171−179.
(354) Weis, S.; Shafiq, Z.; Gropeanu, R. A.; del Campo, A. Ethyl Substituted Coumarin-4-yl Derivatives as Photoremovable Protecting Groups for Amino Acids with Improved Stability for SPSS. *J. Photochem. Photobiol., A* **2012**, *241*, 52−57.
(355) Fan, L.; Lewis, R. W.; Hess, G. P.; Ganem, B. A New Synthesis of Caged GABA Compounds for Studying GABAA Receptors. *Bioorg. Med. Chem. Lett.* **2009**, *19*, 3932−3933.
(356) Yamazoe, S.; Liu, Q.; McQuade, L. E.; Deiters, A.; Chen, J. K. Sequential Gene Silencing Using Wavelength-Selective Caged Morpholino Oligonucleotides. *Angew. Chem., Int. Ed.* **2014**, *53*, 10114−10118.
(357) Seyfried, P.; Eiden, L.; Grebenovsky, N.; Mayer, G.; Heckel, A. Photo-Tethers for the (Multi-)Cyclic, Conformational Caging of Long Oligonucleotides. *Angew. Chem., Int. Ed.* **2017**, *56*, 359−363.
(358) Seyfried, P.; Heinz, M.; Pintér, G.; Klötzner, D.-P.; Becker, Y.; Bolte, M.; Jonker, H. R. A.; Stelzl, L. S.; Hummer, G.; Schwalbe, H.;

Heckel, A. Optimal Destabilization of DNA Double Strands by Single-Nucleobase Caging. *Chem. - Eur. J.* **2018**, *24*, 17568−17576.
(359) Kahlstatt, J.; Reiß, P.; Halbritter, T.; Essen, L. O.; Koert, U.; Heckel, A. A Light-Triggered Transmembrane Porin. *Chem. Commun.* **2018**, *54*, 9623−9626.
(360) Zhang, D.; Jin, S.; Piao, X.; Devaraj, N. K. Multiplexed Photoactivation of mRNA with Single-Cell Resolution. *ACS Chem. Biol.* **2020**, *15*, 1773−1779.
(361) Lin, Q.; Bao, C.; Fan, G.; Cheng, S.; Liu, H.; Liu, Z.; Zhu, L. 7-Amino Coumarin Based Fluorescent Phototriggers Coupled with Nano/Bio-Conjugated Bonds: Synthesis, Labeling and Photorelease. *J. Mater. Chem.* **2012**, *22*, 6680−6688.
(362) Dong, J.; Xun, Z.; Zeng, Y.; Yu, T.; Han, Y.; Chen, J.; Li, Y.-Y.; Yang, G.; Li, Y. A Versatile and Robust Vesicle Based on a Photocleavable Surfactant for Two-Photon-Tuned Release. *Chem. - Eur. J.* **2013**, *19*, 7931−7936.
(363) Ji, W.; Li, N.; Chen, D.; Jiao, Y.; Xu, Q.; Lu, J. A Hollow Porous Magnetic Nanocarrier for Efficient Near-Infrared Light- and pH-Controlled Drug Release. *RSC Adv.* **2014**, *4*, 51055−51061.
(364) Ji, W.; Li, N.; Chen, D.; Qi, X.; Sha, W.; Jiao, Y.; Xu, Q.; Lu, J. Coumarin-Containing Photo-Responsive Nanocomposites for NIR Light-Triggered Controlled Drug Release via a Two-Photon Process. *J. Mater. Chem. B* **2013**, *1*, 5942−5949.
(365) Zhao, L.; Peng, J.; Huang, Q.; Li, C.; Chen, M.; Sun, Y.; Lin, Q.; Zhu, L.; Li, F. Near-Infrared Photoregulated Drug Release in Living Tumor Tissue via Yolk-Shell Upconversion Nanocages. *Adv. Funct. Mater.* **2014**, *24*, 363−371.
(366) Ming, Z.; Ruan, X.; Bao, C.; Lin, Q.; Yang, Y.; Zhu, L. Micropatterned Protein for Cell Adhesion through Phototriggered Charge Change in a Polyvinylpyrrolidone Hydrogel. *Adv. Funct. Mater.* **2017**, *27*, 1606258.
(367) Kotzur, N.; Briand, B.; Beyermann, M.; Hagen, V. Wavelength-Selective Photoactivatable Protecting Groups for Thiols. *J. Am. Chem. Soc.* **2009**, *131*, 16927−16931.
(368) Hagen, V.; Dekowski, B.; Kotzur, N.; Lechler, R.; Wiesner, B.; Briand, B.; Beyermann, M. {7-[Bis(carboxymethyl)amino]coumarin-4-yl}methoxycarbonyl Derivatives for Photorelease of Carboxylic Acids, Alcohols/Phenols, Thioalcohols/Thiophenols, and Amines. *Chem. - Eur. J.* **2008**, *14*, 1621−1627.
(369) Hagen, V.; Dekowski, B.; Nache, V.; Schmidt, R.; Geißler, D.; Lorenz, D.; Eichhorst, J.; Keller, S.; Kaneko, H.; Benndorf, K.; Wiesner, B. Coumarinylmethyl Esters for Ultrafast Release of High Concentrations of Cyclic Nucleotides upon One- and Two-Photon Photolysis. *Angew. Chem., Int. Ed.* **2005**, *44*, 7887−7891.
(370) Senda, N.; Momotake, A.; Arai, T. Synthesis and Photocleavage of 7-[{Bis(carboxymethyl)amino}coumarin-4-yl]methyl-Caged Neurotransmitters. *Bull. Chem. Soc. Jpn.* **2007**, *80*, 2384−2388.
(371) Gilbert, D.; Funk, K.; Dekowski, B.; Lechler, R.; Keller, S.; Möhrlen, F.; Frings, S.; Hagen, V. Caged Capsaicins: New Tools for the Examination of TRPV1 Channels in Somatosensory Neurons. *ChemBioChem* **2007**, *8*, 89−97.
(372) Taniguchi, A.; Skwarczynski, M.; Sohma, Y.; Okada, T.; Ikeda, K.; Prakash, H.; Mukai, H.; Hayashi, Y.; Kimura, T.; Hirota, S.; Matsuzaki, K.; Kiso, Y. Controlled Production of Amyloid β Peptide from a Photo-Triggered, Water-Soluble Precursor "Click Peptide. *ChemBioChem* **2008**, *9*, 3055−3065.
(373) Priestman, M. A.; Sun, L.; Lawrence, D. S. Dual Wavelength Photoactivation of cAMP- and cGMP-Dependent Protein Kinase Signaling Pathways. *ACS Chem. Biol.* **2011**, *6*, 377−384.
(374) Peyret, A.; Ibarboure, E.; Tron, A.; Beauté, L.; Rust, R.; Sandre, O.; McClenaghan, N. D.; Lecommandoux, S. Polymersome Popping by Light-Induced Osmotic Shock under Temporal, Spatial, and Spectral Control. *Angew. Chem., Int. Ed.* **2017**, *56*, 1566−1570.
(375) Banala, S.; Arvin, M. C.; Bannon, N. M.; Jin, X.-T.; Macklin, J. J.; Wang, Y.; Peng, C.; Zhao, G.; Marshall, J. J.; Gee, K. R.; Wokosin, D. L.; Kim, V. J.; McIntosh, J. M.; Contractor, A.; Lester, H. A.; Kozorovitskiy, Y.; Drenan, R. M.; Lavis, L. D. Photoactivatable Drugs for Nicotinic Optopharmacology. *Nat. Methods* **2018**, *15*, 347−350.
(376) Noguchi, M.; Skwarczynski, M.; Prakash, H.; Hirota, S.; Kimura, T.; Hayashi, Y.; Kiso, Y. Development of Novel Water-Soluble Photocleavable Protective Group and Its Application for Design of Photoresponsive Paclitaxel Prodrugs. *Bioorg. Med. Chem.* **2008**, *16*, 5389−5397.
(377) Nadler, A.; Yushchenko, D. A.; Müller, R.; Stein, F.; Feng, S.; Mulle, C.; Carta, M.; Schultz, C. Exclusive Photorelease of Signalling Lipids at the Plasma Membrane. *Nat. Commun.* **2015**, *6*, 10056.
(378) Schuhmacher, M.; Grasskamp, A. T.; Barahtjan, P.; Wagner, N.; Lombardot, B.; Schuhmacher, J. S.; Sala, P.; Lohmann, A.; Henry, I.; Shevchenko, A.; Coskun, Ü.; Walter, A. M.; Nadler, A. Live-Cell Lipid Biochemistry Reveals a Role of Diacylglycerol Side-Chain Composition for Cellular Lipid Dynamics and Protein Affinities. *Proc. Natl. Acad. Sci. U. S. A.* **2020**, *117*, 7729.
(379) Feng, S.; Harayama, T.; Chang, D.; Hannich, J. T.; Winssinger, N.; Riezman, H. Lysosome-Targeted Photoactivation Reveals Local Sphingosine Metabolism Signatures. *Chem. Sci.* **2019**, *10*, 2253−2258.
(380) Wagner, N.; Stephan, M.; Höglinger, D.; Nadler, A. A Click Cage: Organelle-Specific Uncaging of Lipid Messengers. *Angew. Chem., Int. Ed.* **2018**, *57*, 13339−13343.
(381) Feng, S.; Harayama, T.; Montessuit, S.; David, F. P. A.; Winssinger, N.; Martinou, J.-C.; Riezman, H. Mitochondria-Specific Photoactivation to Monitor Local Sphingosine Metabolism and Function. *eLife* **2018**, *7*, No. e34555.
(382) Sarode, B. R.; Kover, K.; Friedman, S. H. Visible-Light-Activated High-Density Materials for Controlled in Vivo Insulin Release. *Mol. Pharmaceutics* **2019**, *16*, 4677−4687.
(383) Lin, Q.; Bao, C.; Yang, Y.; Liang, Q.; Zhang, D.; Cheng, S.; Zhu, L. Highly Discriminating Photorelease of Anticancer Drugs Based on Hypoxia Activatable Phototrigger Conjugated Chitosan Nanoparticles. *Adv. Mater.* **2013**, *25*, 1981−1986.
(384) Lin, Q.; Huang, Q.; Li, C.; Bao, C.; Liu, Z.; Li, F.; Zhu, L. Anticancer Drug Release from a Mesoporous Silica Based Nano-photocage Regulated by Either a One- or Two-Photon Process. *J. Am. Chem. Soc.* **2010**, *132*, 10645−10647.
(385) Liu, Z.; Lin, Q.; Sun, Y.; Liu, T.; Bao, C.; Li, F.; Zhu, L. Spatiotemporally Controllable and Cytocompatible Approach Builds 3D Cell Culture Matrix by Photo-Uncaged-Thiol Michael Addition Reaction. *Adv. Mater.* **2014**, *26*, 3912−3917.
(386) Pahattuge, T. N.; Jackson, J. M.; Digamber, R.; Wijerathne, H.; Brown, V.; Witek, M. A.; Perera, C.; Givens, R. S.; Peterson, B. R.; Soper, S. A. Visible Photorelease of Liquid Biopsy Markers Following Microfluidic Affinity-Enrichment. *Chem. Commun.* **2020**, *56*, 4098.
(387) Vuilleumier, J.; Gaulier, G.; De Matos, R.; Ortiz, D.; Menin, L.; Campargue, G.; Mas, C.; Constant, S.; Le Dantec, R.; Mugnier, Y.; Bonacina, L.; Gerber-Lemaire, S. Two-Photon-Triggered Photorelease of Caged Compounds from Multifunctional Harmonic Nanoparticles. *ACS Appl. Mater. Interfaces* **2019**, *11*, 27443−27452.
(388) Vuilleumier, J.; Gaulier, G.; De Matos, R.; Mugnier, Y.; Campargue, G.; Wolf, J.-P.; Bonacina, L.; Gerber-Lemaire, S. Photocontrolled Release of the Anticancer Drug Chlorambucil with Caged Harmonic Nanoparticles. *Helv. Chim. Acta* **2020**, *103*, No. e1900251.
(389) Gangopadhyay, M.; Singh, T.; Behara, K. K.; Karwa, S.; Ghosh, S. K.; Singh, N. D. P. Coumarin-Containing-Star-Shaped 4-Arm-Polyethylene Glycol: Targeted Fluorescent Organic Nanoparticles for Dual Treatment of Photodynamic Therapy and Chemotherapy. *Photochem. Photobiol. Sci.* **2015**, *14*, 1329−1336.
(390) Huang, Q.; Bao, C.; Ji, W.; Wang, Q.; Zhu, L. Photocleavable Coumarin Crosslinkers Based Polystyrene Microgels: Phototriggered Swelling and Release. *J. Mater. Chem.* **2012**, *22*, 18275−18282.
(391) Lin, Q.; Bao, C.; Cheng, S.; Yang, Y.; Ji, W.; Zhu, L. Target-Activated Coumarin Phototriggers Specifically Switch on Fluorescence and Photocleavage upon Bonding to Thiol-Bearing Protein. *J. Am. Chem. Soc.* **2012**, *134*, 5052−5055.
(392) Lin, Q.; Du, Z.; Yang, Y.; Fang, Q.; Bao, C.; Yang, Y.; Zhu, L. Intracellular Thiols and Photo-Illumination Sequentially Activate Doubly Locked Molecular Probes for Long-Term Cell Highlighting

and Tracking with Precise Spatial Accuracy. *Chem. - Eur. J.* **2014**, *20*, 16314−16319.
(393) Coe, B. J.; Foxon, S. P.; Harper, E. C.; Harris, J. A.; Helliwell, M.; Raftery, J.; Asselberghs, I.; Clays, K.; Franz, E.; Brunschwig, B. S.; Fitch, A. G. The Syntheses, Structures and Nonlinear Optical and Related Properties of Salts with Julolidinyl Electron Donor Groups. *Dyes Pigm.* **2009**, *82*, 171−186.
(394) Reynolds, G. A.; Drexhage, K. H. New Coumarin Dyes with Rigidized Structure for Flashlamp-Pumped Dye Lasers. *Opt. Commun.* **1975**, *13*, 222−225.
(395) Grabowski, Z. R.; Rotkiewicz, K.; Rettig, W. Structural Changes Accompanying Intramolecular Electron Transfer: Focus on Twisted Intramolecular Charge-Transfer States and Structures. *Chem. Rev.* **2003**, *103*, 3899−4032.
(396) Grimm, J. B.; English, B. P.; Chen, J.; Slaughter, J. P.; Zhang, Z.; Revyakin, A.; Patel, R.; Macklin, J. J.; Normanno, D.; Singer, R. H.; Lionnet, T.; Lavis, L. D. A General Method to Improve Fluorophores for Live-Cell and Single-Molecule Microscopy. *Nat. Methods* **2015**, *12*, 244−250.
(397) Dereka, B.; Vauthey, E. Direct Local Solvent Probing by Transient Infrared Spectroscopy Reveals the Mechanism of Hydrogen-Bond Induced Nonradiative Deactivation. *Chem. Sci.* **2017**, *8*, 5057−5066.
(398) Fita, P.; Fedoseeva, M.; Vauthey, E. Ultrafast Excited-State Dynamics of Eosin B: A Potential Probe of the Hydrogen-Bonding Properties of the Environment. *J. Phys. Chem. A* **2011**, *115*, 2465−2470.
(399) Richert, S.; Mosquera Vazquez, S.; Grzybowski, M.; Gryko, D. T.; Kyrychenko, A.; Vauthey, E. Excited-State Dynamics of an Environment-Sensitive Push−Pull Diketopyrrolopyrrole: Major Differences between the Bulk Solution Phase and the Dodecane/Water Interface. *J. Phys. Chem. B* **2014**, *118*, 9952−9963.
(400) Ramaiah, D.; Joy, A.; Chandrasekhar, N.; Eldho, N. V.; Das, S.; George, M. V. Halogenated Squaraine Dyes as Potential Photochemotherapeutic Agents. Synthesis and Study of Photophysical Properties and Quantum Efficiencies of Singlet Oxygen Generation. *Photochem. Photobiol.* **1997**, *65*, 783−790.
(401) Salice, P.; Arnbjerg, J.; Pedersen, B. W.; Toftegaard, R.; Beverina, L.; Pagani, G. A.; Ogilby, P. R. Photophysics of Squaraine Dyes: Role of Charge-Transfer in Singlet Oxygen Production and Removal. *J. Phys. Chem. A* **2010**, *114*, 2518−2525.
(402) Avirah, R. R.; Jayaram, D. T.; Adarsh, N.; Ramaiah, D. Squaraine Dyes in PDT: From Basic Design to in Vivo Demonstration. *Org. Biomol. Chem.* **2012**, *10*, 911−920.
(403) Furuta, T.; Takeuchi, H.; Isozaki, M.; Takahashi, Y.; Kanehara, M.; Sugimoto, M.; Watanabe, T.; Noguchi, K.; Dore, T. M.; Kurahashi, T.; Iwamura, M.; Tsien, R. Y. Bhc-cNMPs as either Water-Soluble or Membrane-Permeant Photoreleasable Cyclic Nucleotides for both One- and Two-Photon Excitation. *ChemBioChem* **2004**, *5*, 1119−1128.
(404) Furuta, T.; Watanabe, T.; Tanabe, S.; Sakyo, J.; Matsuba, C. Phototriggers for Nucleobases with Improved Photochemical Properties. *Org. Lett.* **2007**, *9*, 4717−4720.
(405) Loarueng, C.; Boekfa, B.; Jarussophon, S.; Pongwan, P.; Kaewchangwat, N.; Suttisintong, K.; Jarussophon, N. Theoretical and Experimental Investigation of NMR, IR and UV-Visible Spectra of Hydroxyl-Substituted-4-Chloromethylcoumarin Derivatives. *ARKIVOC* **2020**, *6*, 1−12.
(406) Jivaramonaikul, W.; Rashatasakhon, P.; Wanichwecharungruang, S. UVA Absorption and Photostability of Coumarins. *Photochem. Photobiol. Sci.* **2010**, *9*, 1120−1125.
(407) Bradley, J.; Reuter, D.; Frings, S. Facilitation of Calmodulin-Mediated Odor Adaptation by cAMP-Gated Channel Subunits. *Science* **2001**, *294*, 2176−2178.
(408) Matsumoto, M.; Solzin, J.; Helbig, A.; Hagen, V.; Ueno, S.-i.; Kawase, O.; Maruyama, Y.; Ogiso, M.; Godde, M.; Minakata, H.; Kaupp, U. B.; Hoshi, M.; Weyand, I. A Sperm-Activating Peptide Controls a cGMP-Signaling Pathway in Starfish Sperm. *Dev. Biol.* **2003**, *260*, 314−324.
(409) Geißler, D.; Antonenko, Y. N.; Schmidt, R.; Keller, S.; Krylova, O. O.; Wiesner, B.; Bendig, J.; Pohl, P.; Hagen, V. (Coumarin-4-yl)methyl Esters as Highly Efficient, Ultrafast Phototriggers for Protons and Their Application to Acidifying Membrane Surfaces. *Angew. Chem., Int. Ed.* **2005**, *44*, 1195−1198.
(410) Hagen, V.; Frings, S.; Bendig, J.; Lorenz, D.; Wiesner, B.; Kaupp, U. B. Fluorescence Spectroscopic Quantification of the Release of Cyclic Nucleotides from Photocleavable [Bis-(carboxymethoxy)coumarin-4-yl]methyl Esters inside Cells. *Angew. Chem., Int. Ed.* **2002**, *41*, 3625−3628.
(411) Chen, H.-L.; Hsu, J. C.-C.; Viet, M. H.; Li, M. S.; Hu, C.-K.; Liu, C.-H.; Luh, F. Y.; Chen, S. S.-W.; Chang, E. S.-H.; Wang, A. H.-J.; Hsu, M.-F.; Fann, W.; Chen, R. P.-Y. Studying Submicrosecond Protein Folding Kinetics Using a Photolabile Caging Strategy and Time-Resolved Photoacoustic Calorimetry. *Proteins: Struct., Funct., Genet.* **2010**, *78*, 2973−2983.
(412) Chen, E. H. L.; Lu, T. T. Y.; Hsu, J. C. C.; Tseng, Y. J.; Lim, T. S.; Chen, R. P. Y. Directly Monitor Protein Rearrangement on a Nanosecond-To-Millisecond Time-Scale. *Sci. Rep.* **2017**, *7*, 8691.
(413) Kaupp, U. B.; Solzin, J.; Hildebrand, E.; Brown, J. E.; Helbig, A.; Hagen, V.; Beyermann, M.; Pampaloni, F.; Weyand, I. The Signal Flow and Motor Response Controling Chemotaxis of Sea Urchin Sperm. *Nat. Cell Biol.* **2003**, *5*, 109−117.
(414) Bourbon, P.; Peng, Q.; Ferraudi, G.; Stauffacher, C.; Wiest, O.; Helquist, P. Synthesis, Photophysical, Photochemical, and Computational Studies of Coumarin-Labeled Nicotinamide Derivatives. *J. Org. Chem.* **2012**, *77*, 2756−2762.
(415) Shibu, E. S.; Ono, K.; Sugino, S.; Nishioka, A.; Yasuda, A.; Shigeri, Y.; Wakida, S.-i.; Sawada, M.; Biju, V. Photouncaging Nanoparticles for MRI and Fluorescence Imaging in Vitro and in Vivo. *ACS Nano* **2013**, *7*, 9851−9859.
(416) Narumi, T.; Takano, H.; Ohashi, N.; Suzuki, A.; Furuta, T.; Tamamura, H. Isostere-Based Design of 8-Azacoumarin-Type Photolabile Protecting Groups: A Hydrophilicity-Increasing Strategy for Coumarin-4-ylmethyls. *Org. Lett.* **2014**, *16*, 1184−1187.
(417) Fedoryak, O. D.; Dore, T. M. Brominated Hydroxyquinoline as a Photolabile Protecting Group with Sensitivity to Multiphoton Excitation. *Org. Lett.* **2002**, *4*, 3419−3422.
(418) Schaal, J.; Dekowski, B.; Wiesner, B.; Eichhorst, J.; Marter, K.; Vargas, C.; Keller, S.; Eremina, N.; Barth, A.; Baumann, A.; Eisenhardt, D.; Hagen, V. Coumarin-Based Octopamine Phototriggers and their Effects on an Insect Octopamine Receptor. *ChemBioChem* **2012**, *13*, 1458−1464.
(419) Goard, M.; Aakalu, G.; Fedoryak, O. D.; Quinonez, C.; St. Julien, J.; Poteet, S. J.; Schuman, E. M.; Dore, T. M. Light-Mediated Inhibition of Protein Synthesis. *Chem. Biol.* **2005**, *12*, 685−693.
(420) Robu, V. G.; Pfeiffer, E. S.; Robia, S. L.; Balijepalli, R. C.; Pi, Y.; Kamp, T. J.; Walker, J. W. Localization of Functional Endothelin Receptor Signaling Complexes in Cardiac Transverse Tubules. *J. Biol. Chem.* **2003**, *278*, 48154−48161.
(421) Nomura, W.; Narumi, T.; Ohashi, N.; Serizawa, Y.; Lewin, N. E.; Blumberg, P. M.; Furuta, T.; Tamamura, H. Synthetic Caged DAG-lactones for Photochemically Controlled Activation of Protein Kinase C. *ChemBioChem* **2011**, *12*, 535−539.
(422) Lin, W.; Lawrence, D. S. A Strategy for the Construction of Caged Diols Using a Photolabile Protecting Group. *J. Org. Chem.* **2002**, *67*, 2723−2726.
(423) Lu, M.; Fedoryak, O. D.; Moister, B. R.; Dore, T. M. Bhc-diol as a Photolabile Protecting Group for Aldehydes and Ketones. *Org. Lett.* **2003**, *5*, 2119−2122.
(424) Baron, M.; Morris, J. C.; Telitel, S.; Clément, J.-L.; Lalevée, J.; Morlet-Savary, F.; Spangenberg, A.; Malval, J.-P.; Soppera, O.; Gigmes, D.; Guillaneuf, Y. Light-Sensitive Alkoxyamines as Versatile Spatially- and Temporally- Controlled Precursors of Alkyl Radicals and Nitroxides. *J. Am. Chem. Soc.* **2018**, *140*, 3339−3344.
(425) Wosnick, J. H.; Shoichet, M. S. Three-dimensional Chemical Patterning of Transparent Hydrogels. *Chem. Mater.* **2008**, *20*, 55−60.
(426) Wylie, R. G.; Ahsan, S.; Aizawa, Y.; Maxwell, K. L.; Morshead, C. M.; Shoichet, M. S. Spatially Controlled Simultaneous Patterning

of Multiple Growth Factors in Three-Dimensional Hydrogels. *Nat. Mater.* **2011**, *10*, 799−806.
(427) Abate-Pella, D.; Zeliadt, N. A.; Ochocki, J. D.; Warmka, J. K.; Dore, T. M.; Blank, D. A.; Wattenberg, E. V.; Distefano, M. D. Photochemical Modulation of Ras-Mediated Signal Transduction Using Caged Farnesyltransferase Inhibitors: Activation by One- and Two-Photon Excitation. *ChemBioChem* **2012**, *13*, 1009−1016.
(428) Tam, R. Y.; Fisher, S. A.; Baker, A. E. G.; Shoichet, M. S. Transparent Porous Polysaccharide Cryogels Provide Biochemically Defined, Biomimetic Matrices for Tunable 3D Cell Culture. *Chem. Mater.* **2016**, *28*, 3762−3770.
(429) Fisher, S. A.; Tam, R. Y.; Fokina, A.; Mahmoodi, M. M.; Distefano, M. D.; Shoichet, M. S. Photo-Immobilized EGF Chemical Gradients Differentially Impact Breast Cancer Cell Invasion and Drug Response in Defined 3D Hydrogels. *Biomaterials* **2018**, *178*, 751−766.
(430) Mahmoodi, M. M.; Fisher, S. A.; Tam, R. Y.; Goff, P. C.; Anderson, R. B.; Wissinger, J. E.; Blank, D. A.; Shoichet, M. S.; Distefano, M. D. 6-Bromo-7-hydroxy-3-methylcoumarin (mBhc) Is an Efficient Multi-Photon Labile Protecting Group for Thiol Caging and Three-Dimensional Chemical Patterning. *Org. Biomol. Chem.* **2016**, *14*, 8289−8300.
(431) Sinha, D. K.; Neveu, P.; Gagey, N.; Aujard, I.; Benbrahim-Bouzidi, C.; Le Saux, T.; Rampon, C.; Gauron, C.; Goetz, B.; Dubruille, S.; Baaden, M.; Volovitch, M.; Bensimon, D.; Vriz, S.; Jullien, L. Photocontrol of Protein Activity in Cultured Cells and Zebrafish with One- and Two-Photon Illumination. *ChemBioChem* **2010**, *11*, 653−663.
(432) Kim, Y. A.; Ramirez, D. M. C.; Costain, W. J.; Johnston, L. J.; Bittman, R. A New Tool to Assess Ceramide Bioactivity: 6-Bromo-7-hydroxycoumarinyl-Caged Ceramide. *Chem. Commun.* **2011**, *47*, 9236−9238.
(433) Mizukami, S.; Hosoda, M.; Satake, T.; Okada, S.; Hori, Y.; Furuta, T.; Kikuchi, K. Photocontrolled Compound Release System Using Caged Antimicrobial Peptide. *J. Am. Chem. Soc.* **2010**, *132*, 9524−9525.
(434) Kawakami, T.; Cheng, H.; Hashiro, S.; Nomura, Y.; Tsukiji, S.; Furuta, T.; Nagamune, T. A Caged Phosphopeptide-Based Approach for Photochemical Activation of Kinases in Living Cells. *ChemBioChem* **2008**, *9*, 1583−1586.
(435) Perdicakis, B.; Montgomery, H. J.; Abbott, G. L.; Fishlock, D.; Lajoie, G. A.; Guillemette, J. G.; Jervis, E. Photocontrol of Nitric Oxide Production in Cell Culture Using a Caged Isoform Selective Inhibitor. *Bioorg. Med. Chem.* **2005**, *13*, 47−57.
(436) Ando, H.; Furuta, T.; Tsien, R. Y.; Okamoto, H. Photo-Mediated Gene Activation Using Caged RNA/DNA in Zebrafish Embryos. *Nat. Genet.* **2001**, *28*, 317−325.
(437) Rudd, A. K.; Devaraj, N. K. Traceless Synthesis of Ceramides in Living Cells Reveals Saturation-Dependent Apoptotic Effects. *Proc. Natl. Acad. Sci. U. S. A.* **2018**, *115*, 7485.
(438) Montgomery, H. J.; Perdicakis, B.; Fishlock, D.; Lajoie, G. A.; Jervis, E.; Guy Guillemette, J. Photo-Control of Nitric Oxide Synthase Activity Using a Caged Isoform Specific Inhibitor. *Bioorg. Med. Chem.* **2002**, *10*, 1919−1927.
(439) Feeney, M. J.; Hu, X.; Srinivasan, R.; Van, N.; Hunter, M.; Georgakoudi, I.; Thomas, S. W. UV and NIR-Responsive Layer-by-Layer Films Containing 6-Bromo-7-hydroxycoumarin Photolabile Groups. *Langmuir* **2017**, *33*, 10877−10885.
(440) de Gracia Lux, C.; Lux, J.; Collet, G.; He, S.; Chan, M.; Olejniczak, J.; Foucault-Collet, A.; Almutairi, A. Short Soluble Coumarin Crosslinkers for Light-Controlled Release of Cells and Proteins from Hydrogels. *Biomacromolecules* **2015**, *16*, 3286−3296.
(441) Owen, S. C.; Fisher, S. A.; Tam, R. Y.; Nimmo, C. M.; Shoichet, M. S. Hyaluronic Acid Click Hydrogels Emulate the Extracellular Matrix. *Langmuir* **2013**, *29*, 7393−7400.
(442) Fomina, N.; McFearin, C. L.; Sermsakdi, M.; Morachis, J. M.; Almutairi, A. Low Power, Biologically Benign NIR Light Triggers Polymer Disassembly. *Macromolecules* **2011**, *44*, 8590−8597.
(443) Rahman, N.; Purpura, K. A.; Wylie, R. G.; Zandstra, P. W.; Shoichet, M. S. The Use of Vascular Endothelial Growth Factor Functionalized Agarose to Guide Pluripotent Stem Cell Aggregates Toward Blood Progenitor Cells. *Biomaterials* **2010**, *31*, 8262−8270.
(444) Wylie, R. G.; Shoichet, M. S. Two-Photon Micropatterning of Amines within an Agarose Hydrogel. *J. Mater. Chem.* **2008**, *18*, 2716−2721.
(445) Kumar, S.; Allard, J.-F.; Morris, D.; Dory, Y. L.; Lepage, M.; Zhao, Y. Near-Infrared Light Sensitive Polypeptide Block Copolymer Micelles for Drug Delivery. *J. Mater. Chem.* **2012**, *22*, 7252−7257.
(446) Zhu, C.; Bettinger, C. J. Light-Induced Remodeling of Physically Crosslinked Hydrogels Using Near-IR Wavelengths. *J. Mater. Chem. B* **2014**, *2*, 1613−1618.
(447) Fomina, N.; McFearin, C. L.; Almutairi, A. Increasing Materials' Response to Two-Photon Nir Light via Self-Immolative Dendritic Scaffolds. *Chem. Commun.* **2012**, *48*, 9138−9140.
(448) Ikeda, M.; Tanida, T.; Yoshii, T.; Hamachi, I. Rational Molecular Design of Stimulus-Responsive Supramolecular Hydrogels Based on Dipeptides. *Adv. Mater.* **2011**, *23*, 2819−2822.
(449) Subramaniam, R.; Xiao, Y.; Li, Y.; Qian, S. Y.; Sun, W.; Mallik, S. Light-Mediated and H-Bond Facilitated Liposomal Release: The Role of Lipid Head Groups in Release Efficiency. *Tetrahedron Lett.* **2010**, *51*, 529−532.
(450) Carter Ramirez, D. M.; Pitre, S. P.; Kim, Y. A.; Bittman, R.; Johnston, L. J. Photouncaging of Ceramides Promotes Reorganization of Liquid-Ordered Domains in Supported Lipid Bilayers. *Langmuir* **2013**, *29*, 3380−3387.
(451) Yoshii, T.; Ikeda, M.; Hamachi, I. Two-Photon-Responsive Supramolecular Hydrogel for Controlling Materials Motion in Micrometer Space. *Angew. Chem., Int. Ed.* **2014**, *53*, 7264−7267.
(452) Furuta, T.; Manabe, K.; Teraoka, A.; Murakoshi, K.; Ohtsubo, A.; Suzuki, A. Design, Synthesis, and Photochemistry of Modular Caging Groups for Photoreleasable Nucleotides. *Org. Lett.* **2012**, *14*, 6182−6185.
(453) Katayama, K.; Tsukiji, S.; Furuta, T.; Nagamune, T. A Bromocoumarin-Based Linker for Synthesis of Photocleavable Peptidoconjugates with High Photosensitivity. *Chem. Commun.* **2008**, 5399−5401.
(454) Biswas, S.; Rajesh, Y.; Barman, S.; Bera, M.; Paul, A.; Mandal, M.; Pradeep Singh, N. D. A Dual-Analyte Probe: Hypoxia Activated Nitric Oxide Detection with Phototriggered Drug Release Ability. *Chem. Commun.* **2018**, *54*, 7940−7943.
(455) Tarpey, M. M.; Wink, D. A.; Grisham, M. B. Methods for Detection of Reactive Metabolites of Oxygen and Nitrogen: In Vitro and in Vivo Considerations. *Am. J. Physiol. Regul. Integr. Comp. Physiol.* **2004**, *286*, R431−R444.
(456) Zhegalova, N. G.; Gonzales, G.; Berezin, M. Y. Synthesis of Nitric Oxide Probes with Fluorescence Lifetime Sensitivity. *Org. Biomol. Chem.* **2013**, *11*, 8228−8234.
(457) Kojima, H.; Hirotani, M.; Nakatsubo, N.; Kikuchi, K.; Urano, Y.; Higuchi, T.; Hirata, Y.; Nagano, T. Bioimaging of Nitric Oxide with Fluorescent Indicators Based on the Rhodamine Chromophore. *Anal. Chem.* **2001**, *73*, 1967−1973.
(458) Christie, R. M.; Lui, C.-H. Studies of Fluorescent Dyes: Part 1. An Investigation of the Electronic Spectral Properties of Substituted Coumarins. *Dyes Pigm.* **1999**, *42*, 85−93.
(459) Gangopadhyay, M.; Mukhopadhyay, S. K.; Karthik, S.; Barman, S.; Pradeep Singh, N. D. Targeted Photoresponsive TiO_2−Coumarin Nanoconjugate for Efficient Combination Therapy in MDA-MB-231 Breast Cancer Cells: Synergic Effect of Photodynamic Therapy (PDT) and Anticancer Drug Chlorambucil. *MedChemComm* **2015**, *6*, 769−777.
(460) Hagen, V.; Kilic, F.; Schaal, J.; Dekowski, B.; Schmidt, R.; Kotzur, N. [8-[Bis(carboxymethyl)aminomethyl]-6-bromo-7-hydroxycoumarin-4-yl]methyl Moieties as Photoremovable Protecting Groups for Compounds with COOH, NH2, OH, and C=O Functions. *J. Org. Chem.* **2010**, *75*, 2790−2797.
(461) Suzuki, A. Z.; Sekine, R.; Takeda, S.; Aikawa, R.; Shiraishi, Y.; Hamaguchi, T.; Okuno, H.; Tamamura, H.; Furuta, T. A Clickable

Caging Group as a New Platform for Modular Caged Compounds with Improved Photochemical Properties. *Chem. Commun.* **2019**, *55*, 451−454.
(462) Adamczyk, M.; Cornwell, M.; Huff, J.; Rege, S.; Rao, T. V. S. Novel 7-Hydroxycoumarin Based Fluorescent Labels. *Bioorg. Med. Chem. Lett.* **1997**, *7*, 1985−1988.
(463) Suzuki, A. Z.; Shiraishi, Y.; Aoki, H.; Sasaki, H.; Watahiki, R.; Furuta, T. Design, Synthesis, and Photochemical Properties of Clickable Caged Compounds. *J. Visualized Exp.* **2019**, No. e60021.
(464) Barman, S.; Mukhopadhyay, S. K.; Gangopadhyay, M.; Biswas, S.; Dey, S.; Singh, N. D. P. Coumarin−Benzothiazole−Chlorambucil (Cou−Benz−Cbl) Conjugate: An ESIPT Based pH Sensitive Photoresponsive Drug Delivery System. *J. Mater. Chem. B* **2015**, *3*, 3490−3497.
(465) Barman, S.; Das, J.; Biswas, S.; Maiti, T. K.; Pradeep Singh, N. D. A Spiropyran−Coumarin Platform: An Environment Sensitive Photoresponsive Drug Delivery System for Efficient Cancer Therapy. *J. Mater. Chem. B* **2017**, *5*, 3940−3944.
(466) Ikegami, M.; Arai, T. Photoinduced Intramolecular Hydrogen Atom Transfer in 2-(2-Hydroxyphenyl)benzoxazole and 2-(2-Hydroxyphenyl)benzothiazole Studied by Laser Flash Photolysis. *J. Chem. Soc. Perk. T.* **2002**, *2*, 1296−1301.
(467) Zhao, J.; Ji, S.; Chen, Y.; Guo, H.; Yang, P. Excited State Intramolecular Proton Transfer (ESIPT): From Principal Photophysics to the Development of New Chromophores and Applications in Fluorescent Molecular Probes and Luminescent Materials. *Phys. Chem. Chem. Phys.* **2012**, *14*, 8803−8817.
(468) Wojtyk, J. T. C.; Wasey, A.; Xiao, N.-N.; Kazmaier, P. M.; Hoz, S.; Yu, C.; Lemieux, R. P.; Buncel, E. Elucidating the Mechanisms of Acidochromic Spiropyran-Merocyanine Interconversion. *J. Phys. Chem. A* **2007**, *111*, 2511−2516.
(469) Takano, H.; Narumi, T.; Ohashi, N.; Suzuki, A.; Furuta, T.; Nomura, W.; Tamamura, H. Development of the 8-Aza-3-bromo-7-hydroxycoumarin-4-ylmethyl Group as a New Entry of Photolabile Protecting Groups. *Tetrahedron* **2014**, *70*, 4400−4404.
(470) Klausen, M.; Dubois, V.; Clermont, G.; Tonnelé, C.; Castet, F.; Blanchard-Desce, M. Dual-Wavelength Efficient Two-Photon Photorelease of Glycine by π-Extended Dipolar Coumarins. *Chem. Sci.* **2019**, *10*, 4209−4219.
(471) Bojtár, M.; Németh, K.; Domahidy, F.; Knorr, G.; Verkman, A.; Kállay, M.; Kele, P. Conditionally Activatable Visible-Light Photocages. *J. Am. Chem. Soc.* **2020**, *142*, 15164−15171.
(472) Chitose, Y.; Abe, M.; Furukawa, K.; Katan, C. Design, Synthesis, and Reaction of π-Extended Coumarin-based New Caged Compounds with Two-photon Absorption Character in the Near-IR Region. *Chem. Lett.* **2016**, *45*, 1186−1188.
(473) Chitose, Y.; Abe, M.; Furukawa, K.; Lin, J.-Y.; Lin, T.-C.; Katan, C. Design and Synthesis of a Caged Carboxylic Acid with a Donor-π−Donor Coumarin Structure: One-photon and Two-photon Uncaging Reactions Using Visible and Near-Infrared Lights. *Org. Lett.* **2017**, *19*, 2622−2625.
(474) Balaiah, V.; Seshadri, T. R.; Venkateswarlu, V. Visible Fluorescence and Chemical Constitution of Compounds of the Benzopyrone Group. *Proc. - Indian Acad. Sci., Sect. A* **1942**, *16*, 68.
(475) Drexhage, K. H. Structure and Properties of Laser Dyes; In *Dye Lasers*; Schäfer, F. P., Ed.; Springer Berlin Heidelberg: Berlin, Heidelberg, 1990.
(476) Kuznetsova, N. y. A.; Kaliya, O. L. The Photochemistry of Coumarins. *Russ. Chem. Rev.* **1992**, *61*, 683−696.
(477) Griffiths, J.; Millar, V.; Bahra, G. S. The Influence of Chain Length and Electron Acceptor Residues in 3-Substituted 7-*N*,*N*-Diethylaminocoumarin Dyes. *Dyes Pigm.* **1995**, *28*, 327−339.
(478) Schiedel, M.-S.; Briehn, C. A.; Bäuerle, P. Single-Compound Libraries of Organic Materials: Parallel Synthesis and Screening of Fluorescent Dyes. *Angew. Chem., Int. Ed.* **2001**, *40*, 4677−4680.
(479) Schill, H.; Nizamov, S.; Bottanelli, F.; Bierwagen, J.; Belov, V. N.; Hell, S. W. 4-Trifluoromethyl-Substituted Coumarins with Large Stokes Shifts: Synthesis, Bioconjugates, and Their Use in Super-Resolution Fluorescence Microscopy. *Chem. - Eur. J.* **2013**, *19*, 16556−16565.
(480) Tang, X.-J.; Wu, Y.; Zhao, R.; Kou, X.; Dong, Z.; Zhou, W.; Zhang, Z.; Tan, W.; Fang, X. Photorelease of Pyridines Using a Metal-Free Photoremovable Protecting Group. *Angew. Chem., Int. Ed.* **2020**, *59*, 18386.
(481) Amatrudo, J. M.; Olson, J. P.; Lur, G.; Chiu, C. Q.; Higley, M. J.; Ellis-Davies, G. C. R. Wavelength-Selective One- and Two-Photon Uncaging of GABA. *ACS Chem. Neurosci.* **2014**, *5*, 64−70.
(482) Agarwal, H. K.; Zhai, S.; Surmeier, D. J.; Ellis-Davies, G. C. R. Intracellular Uncaging of cGMP with Blue Light. *ACS Chem. Neurosci.* **2017**, *8*, 2139−2144.
(483) Passlick, S.; Kramer, P. F.; Richers, M. T.; Williams, J. T.; Ellis-Davies, G. C. R. Two-Color, One-Photon Uncaging of Glutamate and GABA. *PLoS One* **2017**, *12*, No. e0187732.
(484) Richers, M. T.; Amatrudo, J. M.; Olson, J. P.; Ellis-Davies, G. C. R. Cloaked Caged Compounds: Chemical Probes for Two-Photon Optoneurobiology. *Angew. Chem., Int. Ed.* **2017**, *56*, 193−197.
(485) Matsuzaki, M.; Hayama, T.; Kasai, H.; Ellis-Davies, G. C. R. Two-Photon Uncaging of γ-Aminobutyric Acid in Intact Brain Tissue. *Nat. Chem. Biol.* **2010**, *6*, 255−257.
(486) Hiblot, J.; Yu, Q.; Sabbadini, M. D. B.; Reymond, L.; Xue, L.; Schena, A.; Sallin, O.; Hill, N.; Griss, R.; Johnsson, K. Luciferases with Tunable Emission Wavelengths. *Angew. Chem., Int. Ed.* **2017**, *56*, 14556−14560.
(487) Chang, D.; Lindberg, E.; Feng, S.; Angerani, S.; Riezman, H.; Winssinger, N. Luciferase-Induced Photouncaging: Bioluminolysis. *Angew. Chem., Int. Ed.* **2019**, *58*, 16033−16037.
(488) Belfield, K. D.; Morales, A. R.; Kang, B.-S.; Hales, J. M.; Hagan, D. J.; Van Stryland, E. W.; Chapela, V. M.; Percino, J. Synthesis, Characterization, and Optical Properties of New Two-Photon-Absorbing Fluorene Derivatives. *Chem. Mater.* **2004**, *16*, 4634−4641.
(489) Preat, J.; Jacquemin, D.; Perpète, E. A. Theoretical Investigations of the UV Spectra of Coumarin Derivatives. *Chem. Phys. Lett.* **2005**, *415*, 20−24.
(490) Tasior, M.; Kim, D.; Singha, S.; Krzeszewski, M.; Ahn, K. H.; Gryko, D. T. π-Expanded Coumarins: Synthesis, Optical Properties and Applications. *J. Mater. Chem. C* **2015**, *3*, 1421−1446.
(491) Piloto, A. M.; Rovira, D.; Costa, S. P. G.; Gonçalves, M. S. T. Oxobenzo[*f*]benzopyrans as New Fluorescent Photolabile Protecting Groups for the Carboxylic Function. *Tetrahedron* **2006**, *62*, 11955−11962.
(492) Fernandes, M. J. G.; Costa, S. P. G.; Gonçalves, M. S. T. Phototriggering of Neuroactive Amino Acids From 5,6-Benzocoumarinyl Conjugates. *Tetrahedron* **2011**, *67*, 2422−2426.
(493) Fernandes, M. J. G.; Gonçalves, M. S. T.; Costa, S. P. G. Neurotransmitter Amino Acid—Oxobenzo[*f*]benzopyran Conjugates: Synthesis and Photorelease Studies. *Tetrahedron* **2008**, *64*, 11175−11179.
(494) Soares, A. M. S.; Costa, S. P. G.; Gonçalves, M. S. T. 2-Oxo-2H-Benzo[*h*]benzopyran as a New Light Sensitive Protecting Group for Neurotransmitter Amino Acids. *Amino Acids* **2010**, *39*, 121−133.
(495) Soares, A. M. S.; Hungerford, G.; Costa, S. P. G.; Gonçalves, M. S. T. Photoactivation of Butyric Acid from 6-Aminobenzocoumarin Cages. *Eur. J. Org. Chem.* **2015**, *2015*, 5979−5986.
(496) Piloto, A. M.; Soares, A. M. S.; Hungerford, G.; Costa, S. P. G.; Gonçalves, M. S. T. Long-Wavelength Photolysis of Amino Acid 6-(Methoxy-2-oxo-2H-naphtho[1,2-b]pyran-4-yl)methyl Esters. *Eur. J. Org. Chem.* **2011**, *2011*, 5447−5451.
(497) Soares, A. M. S.; Hungerford, G.; Gonçalves, M. S. T.; Costa, S. P. G. Light Triggering of 5-Aminolevulinic Acid From Fused Coumarin Ester Cages. *New J. Chem.* **2017**, *41*, 2997−3005.
(498) Soares, A. M. S.; Hungerford, G.; Costa, S. P. G.; Gonçalves, M. S. T. Aminobenzocoumarinylmethyl Esters as Photoactive Precursors for the Release of Butyric Acid. *New J. Chem.* **2015**, *39*, 7227−7233.
(499) Sakamoto, Y.; Boinapally, S.; Katan, C.; Abe, M. Synthesis and Photochemical Reactivity of Caged Glutamates with a π-Extended

Coumarin Chromophore as a Photolabile Protecting Group. *Tetrahedron Lett.* **2013**, *54*, 7171−7174.
(500) Soares, A. M. S.; Hungerford, G.; Costa, S. P. G.; Gonçalves, M. S. T. Photoactivatable Prodrugs of Butyric Acid Based on New Coumarin Fused Oxazole Heterocycles. *Dyes Pigm.* **2017**, *137*, 91−100.
(501) Yu, J.; Shirota, Y. A New Class of High-Performance Red-Fluorescent Dyes for Organic Electroluminescent Devices, [7-Diethylamino-3-(2-thienyl)chromen-2-ylidene]-2,2-dicyanovinylamine and {10-(2-Thienyl)-2,3,6,7-tetrahydro-1H,5H-chromeno-[8,7,6-ij]quinolizin-11-ylidene}-2,2-dicyanovinylamine. *Chem. Lett.* **2002**, *31*, 984−985.
(502) Tkach, I. I.; Reznichenko, A. V.; Luk'yanets, E. A. Reaction of 4-Diethylaminosalicylaldehyde with Malononitrile. *Chem. Heterocycl. Compd.* **1992**, *28*, 872−880.
(503) Gandioso, A.; Bresolí-Obach, R.; Nin-Hill, A.; Bosch, M.; Palau, M.; Galindo, A.; Contreras, S.; Rovira, A.; Rovira, C.; Nonell, S.; Marchán, V. Redesigning the Coumarin Scaffold into Small Bright Fluorophores with Far-Red to Near-Infrared Emission and Large Stokes Shifts Useful for Cell Imaging. *J. Org. Chem.* **2018**, *83*, 1185−1195.
(504) Kirpichenok, M. A.; Gorozhankin, S. K.; Grandberg, I. I. Reactions of 7-Aminocoumarins Leading to Alkylidenebenzopyrans. *Chem. Heterocycl. Compd.* **1988**, *24*, 611−616.
(505) Maciejewski, A.; Steer, R. P. The Photophysics, Physical Photochemistry, and Related Spectroscopy of Thiocarbonyls. *Chem. Rev.* **1993**, *93*, 67−98.
(506) Steer, R. P.; Ramamurthy, V. Photophysics and Intramolecular Photochemistry of Thiones in Solution. *Acc. Chem. Res.* **1988**, *21*, 380−386.
(507) Becker, R. S.; Chakravorti, S.; Gartner, C. A.; de Graca Miguel, M. Photosensitizers: Comprehensive Photophysics/Photochemistry and Theory of Coumarins, Chromones, Their Homologues and Thione Analogues. *J. Chem. Soc., Faraday Trans.* **1993**, *89*, 1007−1019.
(508) Bhattacharyya, K.; Das, P. K.; Ramamurthy, V.; Rao, V. P. Triplet-State Photophysics and Transient Photochemistry of Cyclic Enethiones. A Laser Flash Photolysis Study. *J. Chem. Soc., Faraday Trans. 2* **1986**, *82*, 135−147.
(509) Burdzinski, G.; Buntinx, G.; Poizat, O.; Lapouge, C. Time-Resolved Resonance Raman Investigation and Ab Initio Calculations of the T1-State Structure of Thiocoumarin. *J. Mol. Struct.* **2005**, *735-736*, 115−122.
(510) Devanathan, S.; Ramamurthy, V. Photochemistry of α,β-Unsaturated Thiones: Cycloaddition of Thiocoumarin to Electron-Rich and Electron-Deficient Olefins From T1. *J. Org. Chem.* **1988**, *53*, 741−744.
(511) Fonseca, A. S. C.; Gonçalves, M. S. T.; Costa, S. P. G. Phenacyl Ester Derivatives Bearing Heterocycles as Models for Photocleavable Linkers: Synthesis and Photolysis Studies. *Tetrahedron* **2012**, *68*, 8024−8032.
(512) Chen, Z.; Sun, W.; Butt, H.-J.; Wu, S. Upconverting-Nanoparticle-Assisted Photochemistry Induced by Low-Intensity Near-Infrared Light: How Low Can We Go? *Chem. - Eur. J.* **2015**, *21*, 9165−9170.
(513) Sinha, D. K.; Neveu, P.; Gagey, N.; Aujard, I.; Le Saux, T.; Rampon, C.; Gauron, C.; Kawakami, K.; Leucht, C.; Bally-Cuif, L.; Volovitch, M.; Bensimon, D.; Jullien, L.; Vriz, S. Photoactivation of the CreERT2 Recombinase for Conditional Site-Specific Recombination with High Spatiotemporal Resolution. *Zebrafish* **2010**, *7*, 199−204.
(514) Fournier, L.; Gauron, C.; Xu, L.; Aujard, I.; Le Saux, T.; Gagey-Eilstein, N.; Maurin, S.; Dubruille, S.; Baudin, J.-B.; Bensimon, D.; Volovitch, M.; Vriz, S.; Jullien, L. A Blue-Absorbing Photolabile Protecting Group for in Vivo Chromatically Orthogonal Photoactivation. *ACS Chem. Biol.* **2013**, *8*, 1528−1536.
(515) Manna, D.; Maji, B.; Gangopadhyay, S. A.; Cox, K. J.; Zhou, Q.; Law, B. K.; Mazitschek, R.; Choudhary, A. A Singular System with Precise Dosing and Spatiotemporal Control of CRISPR-Cas9. *Angew. Chem., Int. Ed.* **2019**, *58*, 6285−6289.
(516) Piloto, A. M.; Soares, A. M. S.; Costa, S. P. G.; Gonçalves, M. S. T. Photorelease of Amino Acids From Novel Thioxobenzo[*f*]-benzopyran Ester Conjugates. *Amino Acids* **2012**, *42*, 2275−2282.
(517) Piloto, A. M.; Hungerford, G.; Sutter, J. U.; Soares, A. M. S.; Costa, S. P. G.; Gonçalves, M. S. T. Photoactivable Heterocyclic Cages in a Comparative Release Study of Butyric Acid as a Model Drug. *J. Photochem. Photobiol., A* **2015**, *299*, 44−53.
(518) Gandioso, A.; Cano, M.; Massaguer, A.; Marchán, V. A Green Light-Triggerable RGD Peptide for Photocontrolled Targeted Drug Delivery: Synthesis and Photolysis Studies. *J. Org. Chem.* **2016**, *81*, 11556−11564.
(519) Gandioso, A.; Contreras, S.; Melnyk, I.; Oliva, J.; Nonell, S.; Velasco, D.; García-Amorós, J.; Marchán, V. Development of Green/Red-Absorbing Chromophores Based on a Coumarin Scaffold That Are Useful as Caging Groups. *J. Org. Chem.* **2017**, *82*, 5398−5408.
(520) Deiters, A.; Garner, R. A.; Lusic, H.; Govan, J. M.; Dush, M.; Nascone-Yoder, N. M.; Yoder, J. A. Photocaged Morpholino Oligomers for the Light-Regulation of Gene Function in Zebrafish and Xenopus Embryos. *J. Am. Chem. Soc.* **2010**, *132*, 15644−15650.
(521) Ouyang, X.; Shestopalov, I. A.; Sinha, S.; Zheng, G.; Pitt, C. L. W.; Li, W.-H.; Olson, A. J.; Chen, J. K. Versatile Synthesis and Rational Design of Caged Morpholinos. *J. Am. Chem. Soc.* **2009**, *131*, 13255−13269.
(522) Tallafuss, A.; Gibson, D.; Morcos, P.; Li, Y.; Seredick, S.; Eisen, J.; Washbourne, P. Turning Gene Function ON and OFF Using Sense and Antisense Photo-Morpholinos in Zebrafish. *Development* **2012**, *139*, 1691−1699.
(523) Yamazoe, S.; Shestopalov, I. A.; Provost, E.; Leach, S. D.; Chen, J. K. Cyclic Caged Morpholinos: Conformationally Gated Probes of Embryonic Gene Function. *Angew. Chem., Int. Ed.* **2012**, *51*, 6908−6911.
(524) Ohta, H.; Tokumaru, K. Photolysis of Aromatic Oxime Esters. Finding of Aromatic Substitution by Diphenylmethyleneimino Radicals. *Bull. Chem. Soc. Jpn.* **1975**, *48*, 2393−2394.
(525) Qiu, W.; Li, M.; Yang, Y.; Li, Z.; Dietliker, K. Cleavable Coumarin-Based Oxime Esters with Terminal Heterocyclic Moieties: Photobleachable Initiators for Deep Photocuring Under Visible LED Light Irradiation. *Polym. Chem.* **2020**, *11*, 1356−1363.
(526) Hwu, J. R.; Tsay, S.-C.; Hong, S. C.; Leu, Y.-J.; Liu, C.-F.; Chou, S.-S. P. Oxime Esters of Anthraquinone as Photo-Induced DNA-Cleaving Agents for Single- and Double-Strand Scissions. *Tetrahedron Lett.* **2003**, *44*, 2957−2960.
(527) Hwu, J. R.; Yang, J.-R.; Tsay, S.-C.; Hsu, M.-H.; Chen, Y.-C.; Chou, S.-S. P. Photo-Induced DNA Cleavage by (Heterocyclo)-carbonyl Oxime Esters of Anthraquinone. *Tetrahedron Lett.* **2008**, *49*, 3312−3315.
(528) Fast, D. E.; Lauer, A.; Menzel, J. P.; Kelterer, A.-M.; Gescheidt, G.; Barner-Kowollik, C. Wavelength-Dependent Photochemistry of Oxime Ester Photoinitiators. *Macromolecules* **2017**, *50*, 1815−1823.
(529) Singh, A. K.; Khade, P. K. Anthracene-9-methanol—A Novel Fluorescent Phototrigger for Biomolecular Caging. *Tetrahedron Lett.* **2005**, *46*, 5563−5566.
(530) Boháčová, S.; Ludvíková, L.; Poštová Slavětínská, L.; Vaníková, Z.; Klán, P.; Hocek, M. Protected 5-(Hydroxymethyl)uracil Nucleotides Bearing Visible-Light Photocleavable Groups as Building Blocks for Polymerase Synthesis of Photocaged DNA. *Org. Biomol. Chem.* **2018**, *16*, 1527−1535.
(531) Vittorino, E.; Cicciarella, E.; Sortino, S. A "Dual-Function" Photocage Releasing Nitric Oxide and an Anthrylmethyl Cation with a Single Wavelength Light. *Chem. - Eur. J.* **2009**, *15*, 6802−6806.
(532) Hu, P.; Berning, K.; Lam, Y.-W.; Ng, I. H.-M.; Yeung, C.-C.; Lam, M. H.-W. Development of a Visible Light Triggerable Traceless Staudinger Ligation Reagent. *J. Org. Chem.* **2018**, *83*, 12998−13010.
(533) Nikitin, K.; Müller-Bunz, H.; Ortin, Y.; Muldoon, J.; McGlinchey, M. J. Restricted Rotation in 9-Phenyl-anthracenes: A Prediction Fulfilled. *Org. Lett.* **2011**, *13*, 256−259.

(534) Nazir, R.; Thorsted, B.; Balčiunas, E.; Mazur, L.; Deperasińska, I.; Samoć, M.; Brewer, J.; Farsari, M.; Gryko, D. T. π-Expanded 1,3-Diketones − Synthesis, Optical Properties and Application in Two-Photon Polymerization. *J. Mater. Chem. C* **2016**, *4*, 167−177.
(535) Shah, L.; Laughlin, S. T.; Carrico, I. S. Light-Activated Staudinger−Bertozzi Ligation within Living Animals. *J. Am. Chem. Soc.* **2016**, *138*, 5186−5189.
(536) Hu, P.; Feng, T.; Yeung, C.-C.; Koo, C.-K.; Lau, K.-C.; Lam, M. H. W. A Photo-Triggered Traceless Staudinger−Bertozzi Ligation Reaction. *Chem. - Eur. J.* **2016**, *22*, 11537−11542.
(537) Saxon, E.; Armstrong, J. I.; Bertozzi, C. R. A "Traceless" Staudinger Ligation for the Chemoselective Synthesis of Amide Bonds. *Org. Lett.* **2000**, *2*, 2141−2143.
(538) Zhuang, H.-B.; Tang, W.-J.; Yu, J.-Y.; Song, Q.-H. Acridin-9-ylmethoxycarbonyl (Amoc): A New Photochemically Removable Protecting Group for Alcohols. *Chin. J. Chem.* **2006**, *24*, 1465−1468.
(539) Jana, A.; Saha, B.; Karthik, S.; Barman, S.; Ikbal, M.; Ghosh, S. K.; Pradeep Singh, N. D. Fluorescent Photoremovable Precursor (Acridin-9-ylmethyl)ester: Synthesis, Photophysical, Photochemical and Biological Applications. *Photochem. Photobiol. Sci.* **2013**, *12*, 1041−1052.
(540) Piloto, A. M.; Hungerford, G.; Costa, S. P. G.; Gonçalves, M. S. T. Acridinyl Methyl Esters as Photoactive Precursors in the Release of Neurotransmitteramino Acids. *Photochem. Photobiol. Sci.* **2013**, *12*, 339−347.
(541) Ikbal, M.; Saha, B.; Barman, S.; Atta, S.; Banerjee, D. R.; Ghosh, S. K.; Singh, N. D. P. Benzo[a]Acridinylmethyl Esters as pH Sensitive Fluorescent Photoactive Precursors: Synthesis, Photophysical, Photochemical and Biological Applications. *Org. Biomol. Chem.* **2014**, *12*, 3459−3469.
(542) Kapuscinski, J.; Darzynkiewicz, Z. Interactions of Acridine Orange with Double Stranded Nucleic Acids. Spectral and Affinity Studies. *J. Biomol. Struct. Dyn.* **1987**, *5*, 127−143.
(543) Sayed, M.; Krishnamurthy, B.; Pal, H. Unraveling Multiple Binding Modes of Acridine Orange to DNA Using a Multi-spectroscopic Approach. *Phys. Chem. Chem. Phys.* **2016**, *18*, 24642−24653.
(544) von Tscharner, V.; Schwarz, G. Complex Formation of Acridine Orange with Single-Stranded Polyriboadenylic Acid and 5′-AMP: Cooperative Binding and Intercalation Between Bases. *Biophys. Struct. Mech.* **1979**, *5*, 75−90.
(545) Jana, A.; Atta, S.; Sarkar, S. K.; Singh, N. D. P. 1-Acetylpyrene with Dual Functions as an Environment-Sensitive Fluorophore and Fluorescent Photoremovable Protecting Group. *Tetrahedron* **2010**, *66*, 9798−9807.
(546) Furuta, T.; Torigai, H.; Osawa, T.; Iwamura, M. New Photochemically Labile Protecting Group for Phosphates. *Chem. Lett.* **1993**, *22*, 1179−1182.
(547) Fernandes, M. J. G.; Gonçalves, M. S. T.; Costa, S. P. G. Photorelease of Amino Acid Neurotransmitters From Pyrenylmethyl Ester Conjugates. *Tetrahedron* **2007**, *63*, 10133−10139.
(548) Iwamura, M.; Hodota, C.; Ishibashi, M. 1-(α-Diazobenzyl)-pyrene: A Reagent for Photolabile and Fluorescent Protection of Carboxyl Groups of Amino Acids and Peptides. *Synlett* **1991**, *1991*, 35−36.
(549) Okada, S.; Yamashita, S.; Furuta, T.; Iwamura, M. (1-Pyrenyl)methyl Carbamates for Fluorescent "Caged" Amino Acids and Peptides. *Photochem. Photobiol.* **1995**, *61*, 431−434.
(550) Pukenas, L.; Prompinit, P.; Nishitha, B.; Tate, D. J.; Singh, N. D. P.; Wälti, C.; Evans, S. D.; Bushby, R. J. Soft Ultraviolet (UV) Photopatterning and Metallization of Self-Assembled Monolayers (SAMs) Formed from the Lipoic Acid Ester of α-Hydroxy-1-acetylpyrene: The Generality of Acid-Catalyzed Removal of Thiol-on-Gold SAMs using Soft UV Light. *ACS Appl. Mater. Interfaces* **2017**, *9*, 18388−18397.
(551) Jana, A.; Saha, B.; Ikbal, M.; Ghosh, S. K.; Singh, N. D. P. 1-(Hydroxyacetyl)pyrene a New Fluorescent Phototrigger for Cell Imaging and Caging of Alcohols, Phenol and Adenosine. *Photochem. Photobiol. Sci.* **2012**, *11*, 1558−1566.
(552) Armbruster, C.; Knapp, M.; Rechthaler, K.; Schamschule, R.; Parusel, A. B. J.; Köhler, G.; Wehrmann, W. Fluorescence Properties of 1-Heptanoylpyrene: A Probe for Hydrogen Bonding in Micro-aggregates and Biological Membranes. *J. Photochem. Photobiol., A* **1999**, *125*, 29−38.
(553) Jana, A.; Ikbal, M.; Singh, N. D. P. Perylen-3-ylmethyl: Fluorescent Photoremovable Protecting Group (FPRPG) for Carboxylic Acids and Alcohols. *Tetrahedron* **2012**, *68*, 1128−1136.
(554) Zimmerman, H. E. The *Meta* Effect in Organic Photochemistry: Mechanistic and Exploratory Organic Photochemistry. *J. Am. Chem. Soc.* **1995**, *117*, 8988−8991.
(555) Zimmerman, H. E. *Meta-Ortho* Effect in Organic Photochemistry: Mechanistic and Exploratory Organic Photochemistry. *J. Phys. Chem. A* **1998**, *102*, 5616−5621.
(556) Zimmerman, H. E.; Sandel, V. R. Mechanistic Organic Photochemistry. II. Solvolytic Photochemical Reactions. *J. Am. Chem. Soc.* **1963**, *85*, 915−922.
(557) Pincock, J. A. Photochemistry of Arylmethyl Esters in Nucleophilic Solvents: Radical Pair and Ion Pair Intermediates. *Acc. Chem. Res.* **1997**, *30*, 43−49.
(558) Jana, A.; Nguyen, K. T.; Li, X.; Zhu, P.; Tan, N. S.; Ågren, H.; Zhao, Y. Perylene-Derived Single-Component Organic Nanoparticles with Tunable Emission: Efficient Anticancer Drug Carriers with Real-Time Monitoring of Drug Release. *ACS Nano* **2014**, *8*, 5939−5952.
(559) Truong, V. X.; Li, F.; Forsythe, J. S. Photolabile Hydrogels Responsive to Broad Spectrum Visible Light for Selective Cell Release. *ACS Appl. Mater. Interfaces* **2017**, *9*, 32441−32445.
(560) Truong, V. X. Break Up to Make Up: Utilization of Photocleavable Groups in Biolabeling of Hydrogel Scaffolds. *ChemPhotoChem.* **2020**, *4*, 564−570.
(561) Dong, J.; Zhang, R.; Wu, H.; Zhan, X.; Yang, H.; Zhu, S.; Wang, G. Polymer Nanoparticles for Controlled Release Stimulated by Visible Light and pH. *Macromol. Rapid Commun.* **2014**, *35*, 1255−1259.
(562) Wang, G.; Dong, J.; Yuan, T.; Zhang, J.; Wang, L.; Wang, H. Visible Light and pH Responsive Polymer-Coated Mesoporous Silica Nanohybrids for Controlled Release. *Macromol. Biosci.* **2016**, *16*, 990−994.
(563) Liu, G.; Wang, X.; Hu, J.; Zhang, G.; Liu, S. Self-Immolative Polymersomes for High-Efficiency Triggered Release and Programmed Enzymatic Reactions. *J. Am. Chem. Soc.* **2014**, *136*, 7492−7497.
(564) Kasai, H.; Oikawa, H.; Okada, S.; Nakanishi, H. Crystal Growth of Perylene Microcrystals in the Reprecipitation Method. *Bull. Chem. Soc. Jpn.* **1998**, *71*, 2597−2601.
(565) Jana, A.; Devi, K. S. P.; Maiti, T. K.; Singh, N. D. P. Perylene-3-ylmethanol: Fluorescent Organic Nanoparticles as a Single-Component Photoresponsive Nanocarrier with Real-Time Monitoring of Anticancer Drug Release. *J. Am. Chem. Soc.* **2012**, *134*, 7656−7659.
(566) Atta, S.; Bera, M.; Chattopadhyay, T.; Paul, A.; Ikbal, M.; Maiti, M. K.; Singh, N. D. P. Nano-Pesticide Formulation Based on Fluorescent Organic Photoresponsive Nanoparticles: For Controlled Release of 2,4-D and Real Time Monitoring of Morphological Changes Induced by 2,4-D in Plant Systems. *RSC Adv.* **2015**, *5*, 86990−86996.
(567) Barman, S.; Mukhopadhyay, S. K.; Behara, K. K.; Dey, S.; Singh, N. D. P. 1-Acetylpyrene−Salicylic Acid: Photoresponsive Fluorescent Organic Nanoparticles for the Regulated Release of a Natural Antimicrobial Compound, Salicylic Acid. *ACS Appl. Mater. Interfaces* **2014**, *6*, 7045−7054.
(568) Norris, S.; Warner, C. C.; Thooft, A. M.; Demirci, S. K.; Lampkin, B. J.; Miner, K.; Ellern, A.; VanVeller, B. Blue-Light Photocleavable Protecting Groups Based on Benzothiadiazole Scaffolds. *Org. Lett.* **2020**, *22*, 270−273.
(569) Perrotta, R. R.; Winter, A. H.; Falvey, D. E. Photochemical Heterolysis of 3,5-Bis(dimethylamino)benzyl Alcohols and Esters:

Generation of a Benzyl Cation with a Low-Energy Triplet State. *Org. Lett.* **2011**, *13*, 212−215.
(570) Škalamera, Đ.; Blažek Bregović, V.; Antol, I.; Bohne, C.; Basarić, N. Hydroxymethylaniline Photocages for Carboxylic Acids and Alcohols. *J. Org. Chem.* **2017**, *82*, 12554−12568.
(571) Winter, A. H.; Falvey, D. E.; Cramer, C. J.; Gherman, B. F. Benzylic Cations with Triplet Ground States: Computational Studies of Aryl Carbenium Ions, Silylenium Ions, Nitrenium Ions, and Oxenium Ions Substituted with *Meta* π Donors. *J. Am. Chem. Soc.* **2007**, *129*, 10113−10119.
(572) Reinfelds, M.; von Cosel, J.; Falahati, K.; Hamerla, C.; Slanina, T.; Burghardt, I.; Heckel, A. A New Photocage Derived from Fluorene. *Chem. - Eur. J.* **2018**, *24*, 13026−13035.
(573) Bera, M.; Maji, S.; Paul, A.; Ray, S.; Maiti, T. K.; Singh, N. D. P. A Water Soluble Light Activated Hydrogen Sulfide Donor Induced by an Excited State *meta* Effect. *Org. Biomol. Chem.* **2019**, *17*, 9059−9064.
(574) Wang, P.; Lu, W.; Devalankar, D.; Ding, Z. Photochemical Formation and Cleavage of C−N Bond. *Org. Lett.* **2015**, *17*, 170−172.
(575) Wang, P.; Lu, W.; Devalankar, D. A.; Ding, Z. Structurally Simple Benzyl-Type Photolabile Protecting Groups for Direct Release of Alcohols and Carboxylic Acids. *Org. Lett.* **2015**, *17*, 2114−2117.
(576) Wang, P.; Devalankar, D. A.; Lu, W. Photochemical Cleavage of Benzylic C−N Bond To Release Amines. *J. Org. Chem.* **2016**, *81*, 6195−6200.
(577) Freccero, M.; Fagnoni, M.; Albini, A. Homolytic vs Heterolytic Paths in the Photochemistry of Haloanilines. *J. Am. Chem. Soc.* **2003**, *125*, 13182−13190.
(578) Zhu, Y.; Pavlos, C. M.; Toscano, J. P.; Dore, T. M. 8-Bromo-7-hydroxyquinoline as a Photoremovable Protecting Group for Physiological Use: Mechanism and Scope. *J. Am. Chem. Soc.* **2006**, *128*, 4267−4276.
(579) Davis, M. J.; Kragor, C. H.; Reddie, K. G.; Wilson, H. C.; Zhu, Y.; Dore, T. M. Substituent Effects on the Sensitivity of a Quinoline Photoremovable Protecting Group to One- and Two-Photon Excitation. *J. Org. Chem.* **2009**, *74*, 1721−1729.
(580) Asad, N.; Deodato, D.; Lan, X.; Widegren, M. B.; Phillips, D. L.; Du, L.; Dore, T. M. Photochemical Activation of Tertiary Amines for Applications in Studying Cell Physiology. *J. Am. Chem. Soc.* **2017**, *139*, 12591−12600.
(581) Deodato, D.; Asad, N.; Dore, T. M. Photorearrangement of Quinoline-Protected Dialkylanilines and the Photorelease of Aniline-Containing Biological Effectors. *J. Org. Chem.* **2019**, *84*, 7342−7353.
(582) Huang, J.; Muliawan, A. P.; Ma, J.; Li, M. D.; Chiu, H. K.; Lan, X.; Deodato, D.; Phillips, D. L.; Dore, T. M. A Spectroscopic Study of the Excited State Proton Transfer Processes of (8-Bromo-7-hydroxyquinolin-2-yl)methyl-Protected Phenol in Aqueous Solutions. *Photochem. Photobiol. Sci.* **2017**, *16*, 575−584.
(583) Rea, A. C.; Vandenberg, L. N.; Ball, R. E.; Snouffer, A. A.; Hudson, A. G.; Zhu, Y.; McLain, D. E.; Johnston, L. L.; Lauderdale, J. D.; Levin, M.; Dore, T. M. Light-Activated Serotonin for Exploring Its Action in Biological Systems. *Chem. Biol.* **2013**, *20*, 1536−1546.
(584) Asad, N.; McLain, D. E.; Condon, A. F.; Gore, S.; Hampton, S. E.; Vijay, S.; Williams, J. T.; Dore, T. M. Photoactivatable Dopamine and Sulpiride to Explore the Function of Dopaminergic Neurons and Circuits. *ACS Chem. Neurosci.* **2020**, *11*, 939−951.
(585) Hennig, A.-L. K.; Deodato, D.; Asad, N.; Herbivo, C.; Dore, T. M. Two-Photon Excitable Photoremovable Protecting Groups Based on the Quinoline Scaffold for Use in Biology. *J. Org. Chem.* **2020**, *85*, 726−744.
(586) Li, Y.-M.; Shi, J.; Cai, R.; Chen, X.-Y.; Guo, Q.-X.; Liu, L. Development of New Quinoline-Based Photo-Labile Groups for Photo-Regulation of Bioactive Molecules. *Tetrahedron Lett.* **2010**, *51*, 1609−1612.
(587) Bera, M.; Maji, S.; Paul, A.; Sahoo, B. K.; Maiti, T. K.; Singh, N. D. P. Quinoline H_2S Donor Decorated Fluorescent Carbon Dots: Visible Light Responsive H_2S Nanocarriers. *J. Mater. Chem. B* **2020**, *8*, 1026−1032.
(588) Narumi, T.; Miyata, K.; Nii, A.; Sato, K.; Mase, N.; Furuta, T. 7-Hydroxy-N-Methylquinolinium Chromophore: A Photolabile Protecting Group for Blue-Light Uncaging. *Org. Lett.* **2018**, *20*, 4178−4182.
(589) Narumi, T. Creation and Application of Quinolinium-Type Caged Neurotransmitters Capable of Uncaging with Visible Light. *Yakugaku Zasshi* **2019**, *139*, 263−271.
(590) Barni, E.; Savarino, P. Quaternary Salts From 2-(Methylpyridyl or Quinolyl)benzimidazoles and Related Polymethine Dyes. *J. Heterocycl. Chem.* **1979**, *16*, 1583−1587.
(591) Sutherland, D.; Compton, C. The Absorption Spectra of some Substituted Quinolines and their Methiodides. *J. Org. Chem.* **1952**, *17*, 1257−1261.
(592) Ma, J.; Mewes, J.-M.; Harris, K. T.; Dore, T. M.; Phillips, D. L.; Dreuw, A. Unravelling the Early Photochemical Behavior of (8-Substituted-7-hydroxyquinolinyl)methyl Acetates Through Electronic Structure Theory and Ultrafast Transient Absorption Spectroscopy. *Phys. Chem. Chem. Phys.* **2017**, *19*, 1089−1096.
(593) Ma, J.; Rea, A. C.; An, H.; Ma, C.; Guan, X.; Li, M.-D.; Su, T.; Yeung, C. S.; Harris, K. T.; Zhu, Y.; Nganga, J. L.; Fedoryak, O. D.; Dore, T. M.; Phillips, D. L. Unraveling the Mechanism of the Photodeprotection Reaction of 8-Bromo- and 8-Chloro-7-hydroxyquinoline Caged Acetates. *Chem. - Eur. J.* **2012**, *18*, 6854−6865.
(594) Kohler, G.; Rechthaler, K.; Rotkiewicz, K.; Rettig, W. Formation and Stabilization of Twisted Intramolecular Charge Transfer States in Binary Mixed Solvents. *Chem. Phys.* **1996**, *207*, 85−101.
(595) Kosower, N. S.; Kosower, E. M.; Newton, G. L.; Ranney, H. M. Bimane Fluorescent Labels: Labeling of Normal Human Red Cells Under Physiological Conditions. *Proc. Natl. Acad. Sci. U. S. A.* **1979**, *76*, 3382−3386.
(596) Lavis, L. D.; Raines, R. T. Bright Ideas for Chemical Biology. *ACS Chem. Biol.* **2008**, *3*, 142−155.
(597) Taraska, J. W.; Puljung, M. C.; Zagotta, W. N. Short-Distance Probes for Protein Backbone Structure Based on Energy Transfer Between Bimane and Transition Metal Ions. *Proc. Natl. Acad. Sci. U. S. A.* **2009**, *106*, 16227−16232.
(598) Chaudhuri, A.; Venkatesh, Y.; Behara, K. K.; Singh, N. D. Bimane: A Visible Light Induced Fluorescent Photoremovable Protecting Group for the Single and Dual Release of Carboxylic and Amino Acids. *Org. Lett.* **2017**, *19*, 1598−1601.
(599) Truong, V. X.; Li, F.; Forsythe, J. S. Visible Light Activation of Nucleophilic Thiol-X Addition via Thioether Bimane Photocleavage for Polymer Cross-Linking. *Biomacromolecules* **2018**, *19*, 4277−4285.
(600) Arumugam, S.; Guo, J.; Mbua, N. E.; Friscourt, F.; Lin, N.; Nekongo, E.; Boons, G.-J.; Popik, V. V. Selective and Reversible Photochemical Derivatization of Cysteine Residues in Peptides and Proteins. *Chem. Sci.* **2014**, *5*, 1591−1598.
(601) Banerjee, A.; Falvey, D. E. Direct Photolysis of Phenacyl Protecting Groups Studied by Laser Flash Photolysis: An Excited State Hydrogen Atom Abstraction Pathway Leads to Formation of Carboxylic Acids and Acetophenone. *J. Am. Chem. Soc.* **1998**, *120*, 2965−2966.
(602) Literák, J.; Dostálová, A.; Klán, P. Chain Mechanism in the Photocleavage of Phenacyl and Pyridacyl Esters in the Presence of Hydrogen Donors. *J. Org. Chem.* **2006**, *71*, 713−723.
(603) Sheehan, J. C.; Umezawa, K. Phenacyl Photosensitive Blocking Groups. *J. Org. Chem.* **1973**, *38*, 3771−3774.
(604) Bergmark, W. R. Photolysis of α-Chloro-*o*-methylacetophenones. *J. Chem. Soc., Chem. Commun.* **1978**, 61−62.
(605) Haag, R.; Wirz, J.; Wagner, P. J. The Photoenolization of 2-Methylacetophenone and Related Compounds. *Helv. Chim. Acta* **1977**, *60*, 2595−2607.
(606) Kammari, L.; Plíštil, L.; Wirz, J.; Klán, P. 2,5-Dimethylphenacyl Carbamate: A Photoremovable Protecting Group for Amines and Amino Acids. *Photochem. Photobiol. Sci.* **2007**, *6*, 50−56.
(607) Klán, P.; Zabadal, M.; Heger, D. 2, 5-Dimethylphenacyl as a New Photoreleasable Protecting Group for Carboxylic Acids. *Org. Lett.* **2000**, *2*, 1569−1571.

(608) Literák, J.; Wirz, J.; Klán, P. 2,5-Dimethylphenacyl Carbonates: A Photoremovable Protecting Group for Alcohols and Phenols. *Photochem. Photobiol. Sci.* **2005**, *4*, 43−46.
(609) Zabadal, M.; Pelliccioli, A. P.; Klán, P.; Wirz, J. 2,5-Dimethylphenacyl Esters: A Photoremovable Protecting Group for Carboxylic Acids. *J. Phys. Chem. A* **2001**, *105*, 10329−10333.
(610) Ruzicka, R.; Zabadal, M.; Klán, P. Photolysis of Phenacyl Esters in a Two-Phase System. *Synth. Commun.* **2002**, *32*, 2581−2590.
(611) Anderson, J. C.; Reese, C. B. A Photo-Induced Rearrangement Involving Aryl Participation. *Tetrahedron Lett.* **1962**, *3*, 1−4.
(612) Givens, R. S.; Park, C.-H. *p*-Hydroxyphenacyl ATP1: A New Phototrigger. *Tetrahedron Lett.* **1996**, *37*, 6259−6262.
(613) Park, C.-H.; Givens, R. S. New Photoactivated Protecting Groups. 6. *p*-Hydroxyphenacyl: A Phototrigger for Chemical and Biochemical Probes. *J. Am. Chem. Soc.* **1997**, *119*, 2453−2463.
(614) Corrie, J. E. T.; Trentham, D. R. Synthetic, Mechanistic and Photochemical Studies of Phosphate Esters of Substituted Benzoins. *J. Chem. Soc., Perkin Trans. 1* **1992**, *1*, 2409−2417.
(615) Sheehan, J. C.; Wilson, R. M.; Oxford, A. W. Photolysis of Methoxy-Substituted Benzoin Esters. Photosensitive Protecting Group for Carboxylic Acids. *J. Am. Chem. Soc.* **1971**, *93*, 7222−7228.
(616) Shi, Y.; Corrie, J. E.; Wan, P. Mechanism of 3',5'-Dimethoxybenzoin Ester Photochemistry: Heterolytic Cleavage Intramolecularly Assisted by the Dimethoxybenzene Ring Is the Primary Photochemical Step. *J. Org. Chem.* **1997**, *62*, 8278−8279.
(617) Dong, Y.; Lam, J. W. Y.; Qin, A.; Liu, J.; Li, Z.; Tang, B. Z.; Sun, J.; Kwok, H. S. Aggregation-Induced Emissions of Tetraphenylethene Derivatives and Their Utilities as Chemical Vapor Sensors and in Organic Light-Emitting Diodes. *Appl. Phys. Lett.* **2007**, *91*, 011111.
(618) Hong, Y.; Lam, J. W. Y.; Tang, B. Z. Aggregation-Induced Emission. *Chem. Soc. Rev.* **2011**, *40*, 5361−5388.
(619) Luo, J.; Xie, Z.; Lam, J. W. Y.; Cheng, L.; Chen, H.; Qiu, C.; Kwok, H. S.; Zhan, X.; Liu, Y.; Zhu, D.; Tang, B. Z. Aggregation-Induced Emission of 1-Methyl-1,2,3,4,5-pentaphenylsilole. *Chem. Commun.* **2001**, 1740−1741.
(620) Parthiban, C.; M, P.; Vinod Kumar Reddy, L.; Sen, D.; Singh, N. D. P. Single-Component Fluorescent Organic Nanoparticles with Four-Armed Phototriggers for Chemo-Photodynamic Therapy and Cellular Imaging. *ACS Appl. Nano Mater.* **2019**, *2*, 3728−3734.
(621) Hong, Y.; Lam, J. W. Y.; Tang, B. Z. Aggregation-Induced Emission: Phenomenon, Mechanism and Applications. *Chem. Commun.* **2009**, 4332−4353.
(622) Kammath, V. B.; Šolomek, T.; Ngoy, B. P.; Heger, D.; Klán, P.; Rubina, M.; Givens, R. S. A Photo-Favorskii Ring Contraction Reaction: The Effect of Ring Size. *J. Org. Chem.* **2013**, *78*, 1718−1729.
(623) Favorskii, A. Favorskii Rearrangement. *Russ. J. Gen. Chem.* **1894**, *26*, 590.
(624) Aston, J. G.; Newkirk, J. D. α-Halo Ketones. IV. The Isomeric α-Chloroketones Derived from 3-Heptanone. *J. Am. Chem. Soc.* **1951**, *73*, 3900−3902.
(625) Bordwell, F. G.; Scamehorn, R. G.; Springer, W. R. Favorskii Rearrangements. III. Evidence for an Ionization-π-Participation Mechanism. *J. Am. Chem. Soc.* **1969**, *91*, 2087−2093.
(626) Burr, J. G.; Dewar, M. J. S. The Mechanism of the Favorski Reaction. *J. Chem. Soc.* **1954**, 1201−1203.
(627) Loftfield, R. B. On the Mechanism of the Faworskii Rearrangement of α-Halo Ketones. *J. Am. Chem. Soc.* **1950**, *72*, 632−633.
(628) Loftfield, R. B. The Alkaline Rearrangement of α-Haloketones. II. The Mechanism of the Faworskii Reaction. *J. Am. Chem. Soc.* **1951**, *73*, 4707−4714.
(629) Chiang, Y.; Kresge, A. J.; Zhu, Y. Flash Photolytic Generation and Study of *p*-Quinone Methide in Aqueous Solution. An Estimate of Rate and Equilibrium Constants for Heterolysis of the Carbon-Bromine Bond in *p*-Hydroxybenzyl Bromide. *J. Am. Chem. Soc.* **2002**, *124*, 6349−6356.
(630) Givens, R. S.; Heger, D.; Hellrung, B.; Kamdzhilov, Y.; Mac, M.; Conrad, P. G.; Cope, E.; Lee, J. I.; Mata-Segreda, J. F.; Schowen, R. L.; Wirz, J. The Photo-Favorskii Reaction of *p*-Hydroxyphenacyl Compounds Is Initiated by Water-Assisted, Adiabatic Extrusion of a Triplet Biradical. *J. Am. Chem. Soc.* **2008**, *130*, 3307−3309.
(631) Barman, S.; Mukhopadhyay, S. K.; Biswas, S.; Nandi, S.; Gangopadhyay, M.; Dey, S.; Anoop, A.; Pradeep Singh, N. D. A *p*-Hydroxyphenacyl−Benzothiazole−Chlorambucil Conjugate as a Real-Time-Monitoring Drug-Delivery System Assisted by Excited-State Intramolecular Proton Transfer. *Angew. Chem., Int. Ed.* **2016**, *55*, 4194−4198.
(632) Luo, X.; Wu, J.; Lv, T.; Lai, Y.; Zhang, H.; Lu, J.-J.; Zhang, Y.; Huang, Z. Synthesis and Evaluation of Novel O_2-Derived Diazeniumdiolates as Photochemical and Real-Time Monitoring Nitric Oxide Delivery Agents. *Org. Chem. Front.* **2017**, *4*, 2445−2449.
(633) Parthiban, C.; M, P.; L, V. K. R.; Sen, D.; S, M. S.; Singh, N. D. P. Visible-Light -Triggered Fluorescent Organic Nanoparticles for Chemo-Photodynamic Therapy with Real-Time Cellular Imaging. *ACS Appl. Nano Mater.* **2018**, *1*, 6281−6288.
(634) Hrabie, J. A.; Keefer, L. K. Chemistry of the Nitric Oxide-Releasing Diazeniumdiolate ("Nitrosohydroxylamine") Functional Group and Its Oxygen-Substituted Derivatives. *Chem. Rev.* **2002**, *102*, 1135−1154.
(635) Korman, A.; Sun, H.; Hua, B.; Yang, H.; Capilato, J. N.; Paul, R.; Panja, S.; Ha, T.; Greenberg, M. M.; Woodson, S. A. Light-Controlled Twister Ribozyme with Single-Molecule Detection Resolves RNA Function in Time and Space. *Proc. Natl. Acad. Sci. U. S. A.* **2020**, *117*, 12080−12086.
(636) Biswas, S.; Das, J.; Barman, S.; Rao Pinninti, B.; Maiti, T. K.; Singh, N. D. P. Environment Activatable Nanoprodrug: Two-Step Surveillance in the Anticancer Drug Release. *ACS Appl. Mater. Interfaces* **2017**, *9*, 28180−28184.
(637) Chang, M. C. Y.; Pralle, A.; Isacoff, E. Y.; Chang, C. J. A Selective, Cell-Permeable Optical Probe for Hydrogen Peroxide in Living Cells. *J. Am. Chem. Soc.* **2004**, *126*, 15392−15393.
(638) Kuivila, H. G.; Armour, A. G. Electrophilic Displacement Reactions. IX. Effects of Substituents on Rates of Reactions Between Hydrogen Peroxide and Benzeneboronic Acid. *J. Am. Chem. Soc.* **1957**, *79*, 5659−5662.
(639) Kuivila, H. G.; Wiles, R. A. Electrophilic Displacement Reactions. VII. Catalysis by Chelating Agents in the Reaction Between Hydrogen Peroxide and Benzeneboronic Acid. *J. Am. Chem. Soc.* **1955**, *77*, 4830−4834.
(640) Noh, J.; Kwon, B.; Han, E.; Park, M.; Yang, W.; Cho, W.; Yoo, W.; Khang, G.; Lee, D. Amplification of Oxidative Stress by a Dual Stimuli-Responsive Hybrid Drug Enhances Cancer Cell Death. *Nat. Commun.* **2015**, *6*, 6907.
(641) Ye, M.; Han, Y.; Tang, J.; Piao, Y.; Liu, X.; Zhou, Z.; Gao, J.; Rao, J.; Shen, Y. A Tumor-Specific Cascade Amplification Drug Release Nanoparticle for Overcoming Multidrug Resistance in Cancers. *Adv. Mater.* **2017**, *29*, 1702342.
(642) Major Jourden, J. L.; Cohen, S. M. Hydrogen Peroxide Activated Matrix Metalloproteinase Inhibitors: A Prodrug Approach. *Angew. Chem., Int. Ed.* **2010**, *49*, 6795−6797.
(643) Houk, A. L.; Givens, R. S.; Elles, C. G. Two-Photon Activation of p-Hydroxyphenacyl Phototriggers: Toward Spatially Controlled Release of Diethyl Phosphate and ATP. *J. Phys. Chem. B* **2016**, *120*, 3178−3186.
(644) McEvoy, A. L.; Hoi, H.; Bates, M.; Platonova, E.; Cranfill, P. J.; Baird, M. A.; Davidson, M. W.; Ewers, H.; Liphardt, J.; Campbell, R. E. mMaple: A Photoconvertible Fluorescent Protein for Use in Multiple Imaging Modalities. *PLoS One* **2012**, *7*, No. e51314.
(645) Zhang, W.; Lohman, A. W.; Zhuravlova, Y.; Lu, X.; Wiens, M. D.; Hoi, H.; Yaganoglu, S.; Mohr, M. A.; Kitova, E. N.; Klassen, J. S.; Pantazis, P.; Thompson, R. J.; Campbell, R. E. Optogenetic Control with a Photocleavable Protein, PhoCl. *Nat. Methods* **2017**, *14*, 391−394.
(646) Chattoraj, M.; King, B. A.; Bublitz, G. U.; Boxer, S. G. Ultrafast Excited State Dynamics in Green Fluorescent Protein: Multiple States and Proton Transfer. *Proc. Natl. Acad. Sci. U. S. A.* **1996**, *93*, 8362.

(647) McAnaney, T. B.; Shi, X.; Abbyad, P.; Jung, H.; Remington, S. J.; Boxer, S. G. Green Fluorescent Protein Variants as Ratiometric Dual Emission pH Sensors. 3. Temperature Dependence of Proton Transfer. *Biochemistry* **2005**, *44*, 8701−8711.
(648) Mizuno, H.; Mal, T. K.; Tong, K. I.; Ando, R.; Furuta, T.; Ikura, M.; Miyawaki, A. Photo-Induced Peptide Cleavage in the Green-to-Red Conversion of a Fluorescent Protein. *Mol. Cell* **2003**, *12*, 1051−1058.
(649) Endo, M.; Iwawaki, T.; Yoshimura, H.; Ozawa, T. Photocleavable Cadherin Inhibits Cell-to-Cell Mechanotransduction by Light. *ACS Chem. Biol.* **2019**, *14*, 2206−2214.
(650) Meador, K.; Wysoczynski, C. L.; Norris, A. J.; Aoto, J.; Bruchas, M. R.; Tucker, C. L. Achieving Tight Control of a Photoactivatable Cre Recombinase Gene Switch: New Design Strategies and Functional Characterization in Mammalian Cells and Rodent. *Nucleic Acids Res.* **2019**, *47*, No. e97.
(651) Ollech, D.; Pflästerer, T.; Shellard, A.; Zambarda, C.; Spatz, J. P.; Marcq, P.; Mayor, R.; Wombacher, R.; Cavalcanti-Adam, E. A. An Optochemical Tool for Light-Induced Dissociation of Adherens Junctions to Control Mechanical Coupling Between Cells. *Nat. Commun.* **2020**, *11*, 472.
(652) Shadish, J. A.; Strange, A. C.; DeForest, C. A. Genetically Encoded Photocleavable Linkers for Patterned Protein Release from Biomaterials. *J. Am. Chem. Soc.* **2019**, *141*, 15619−15625.
(653) Xiang, D.; Wu, X.; Cao, W.; Xue, B.; Qin, M.; Cao, Y.; Wang, W. Hydrogels With Tunable Mechanical Properties Based on Photocleavable Proteins. *Front. Chem.* **2020**, *8*, 7.
(654) Paul, A.; Biswas, A.; Sinha, S.; Shah, S. S.; Bera, M.; Mandal, M.; Singh, N. D. P. Push−Pull Stilbene: Visible Light Activated Photoremovable Protecting Group for Alcohols and Carboxylic Acids with Fluorescence Reporting Employed for Drug Delivery. *Org. Lett.* **2019**, *21*, 2968−2972.
(655) Lewis, G. N.; Magel, T. T.; Lipkin, D. The Absorption and Re-emission of Light by *cis*- and *trans*-Stilbenes and the Efficiency of their Photochemical Isomerization. *J. Am. Chem. Soc.* **1940**, *62*, 2973−2980.
(656) Moore, W. M.; Morgan, D. D.; Stermitz, F. R. The Photochemical Conversion of Stilbene to Phenanthrene. The Nature of the Intermediate. *J. Am. Chem. Soc.* **1963**, *85*, 829−830.
(657) Muszkat, K. A.; Fischer, E. Structure, Spectra, Photochemistry, and Thermal Reactions of the 4a,4b-Dihydrophenanthrenes. *J. Chem. Soc. B* **1967**, 662−678.
(658) Mallory, F. B.; Gordon, J. T.; Wood, C. S. Photochemistry of Stilbenes. II. Substituent Effects on the Rates of Phenanthrene Formation. *J. Am. Chem. Soc.* **1963**, *85*, 828−829.
(659) Lapouyade, R.; Koussini, R.; Rayez, J.-C. Photocyclisation of 1,1-Diarylethylenes; The Novel Formation of a Five-Membered Ring. *J. Chem. Soc., Chem. Commun.* **1975**, 676−677.
(660) Sargent, M. V.; Timmons, C. J. Studies in Photochemistry. Part I. The Stilbenes. *J. Chem. Soc.* **1964**, 5544−5552.
(661) Giles, R. G. F.; Sargent, M. V. Photochemical-Synthesis of Phenanthrenes from 2-Methoxystilbenes. *J. Chem. Soc., Perkin Trans. 1* **1974**, *1*, 2447−2450.
(662) Wood, C. S.; Mallory, F. B. Photochemistry of Stilbenes. IV. The Preparation of Substituted Phenanthrenes. *J. Org. Chem.* **1964**, *29*, 3373−3377.
(663) Cava, M. P.; Mitchell, M. J.; Havlicek, S. C.; Lindert, A.; Spangler, R. J. Photochemical Routes to Aporphines. New Syntheses of Nuciferine and Glaucine. *J. Org. Chem.* **1970**, *35*, 175−179.
(664) Cava, M. P.; Stern, P.; Wakisaka, K. An Improved Photochemical Aporphine Synthesis: New Syntheses of Dicentrine and Cassameridine. *Tetrahedron* **1973**, *29*, 2245−2249.
(665) Lin, C.-K.; Wang, Y.-F.; Cheng, Y.-C.; Yang, J.-S. Multisite Constrained Model of trans-4-(N, N-Dimethylamino)-4′-nitrostilbene for Structural Elucidation of Radiative and Nonradiative Excited States. *J. Phys. Chem. A* **2013**, *117*, 3158−3164.
(666) Galvan-Gonzalez, A.; Belfield, K. D.; Stegeman, G. I.; Canva, M.; Marder, S. R.; Staub, K.; Levina, G.; Twieg, R. J. Photodegradation of Selected π-Conjugated Electro-Optic Chromophores. *J. Appl. Phys.* **2003**, *94*, 756−763.
(667) Mallory, F. B.; Rudolph, M. J.; Oh, S. M. Photochemistry of Stilbenes. 8. Eliminative Photocyclization of *Ortho*-Methoxystilbenes. *J. Org. Chem.* **1989**, *54*, 4619−4626.
(668) Cuppen, T. J. H. M.; Laarhoven, W. H. Photodehydrocyclizations of Stilbene-Like Compounds. VI. Chemical Evidence of an Excited State Mechanism. *J. Am. Chem. Soc.* **1972**, *94*, 5914−5915.
(669) Mallory, F. B.; Wood, C. S.; Gordon, J. T.; Lindquist, L. C.; Savitz, M. L. Photochemistry of Stilbenes I. *J. Am. Chem. Soc.* **1962**, *84*, 4361−4362.
(670) Baxter, I.; Phillips, W. R. Reactions Between 2,5-Di-*t*-butyl-1,4-benzoquinone and Certain Primary Aliphatic Amines. *J. Chem. Soc., Perkin Trans. 1* **1973**, *1*, 268−272.
(671) Bruce, J. M. Light-Induced Reactions of Quinones. *Q. Rev., Chem. Soc.* **1967**, *21*, 405−428.
(672) El'tsov, A. V.; Studzinskii, O. P.; Grebenkina, V. M. Photoinitiation of the Reactions of Quinones. *Russ. Chem. Rev.* **1977**, *46*, 93−114.
(673) Görner, H. Photoprocesses of *p*-Benzoquinones in Aqueous Solution. *J. Phys. Chem. A* **2003**, *107*, 11587−11595.
(674) Görner, H.; von Sonntag, C. Photoprocesses of Chloro-Substituted *p*-Benzoquinones. *J. Phys. Chem. A* **2008**, *112*, 10257−10263.
(675) Ando, Y.; Suzuki, K. Photoredox Reactions of Quinones. *Chem. - Eur. J.* **2018**, *24*, 15955−15964.
(676) Amada, I.; Yamaji, M.; Tsunoda, S. i.; Shizuka, H. Laser Photolysis Studies of Electron Transfer Between Triplet Naphthoquinones and Amines. *J. Photochem. Photobiol., A* **1996**, *95*, 27−32.
(677) Görner, H. Photoreduction of 9,10-Anthraquinone Derivatives: Transient Spectroscopy and Effects of Alcohols and Amines on Reactivity in Solution. *Photochem. Photobiol.* **2003**, *77*, 171−179.
(678) Görner, H. Photoreduction of *p*-Benzoquinones: Effects of Alcohols and Amines on the Intermediates and Reactivities in Solution. *Photochem. Photobiol.* **2003**, *78*, 440−448.
(679) Jones, G.; Mouli, N.; Haney, W. A.; Bergmark, W. R. Photoreduction of Chloranil by Benzhydrol and Related Compounds. Hydrogen Atom Abstraction vs Sequential Electron-Proton Transfer via Quinone Triplet Radical Ion-Pairs. *J. Am. Chem. Soc.* **1997**, *119*, 8788−8794.
(680) Mac, M.; Wirz, J. Salt Effects on the Reactions of Radical Ion Pairs Formed by Electron Transfer Quenching of Triplet 2-Methyl-1,4-naphthoquinone by Amines. Optical Flash Photolysis and Step-Scan FTIR Investigations. *Photochem. Photobiol. Sci.* **2002**, *1*, 24−29.
(681) Wakisaka, A.; Ebbesen, T. W.; Sakuragi, H.; Tokumaru, K. Effect of Water Concentration on Photoreduction of Anthraquinone-2-sulfonate by 2-Propanol in Aqueous Acetonitrile Solution. *J. Phys. Chem.* **1987**, *91*, 6547−6551.
(682) Bruce, J. M.; Chaudhry, A.-U.-H.; Dawes, K. Light-Induced and Related Reactions of Quinones. Part X. Further Studies with Hydroxymethyl-, Vinyl-, and (2-Ethoxycarbonylethyl)-1,4-benzoquinones. *J. Chem. Soc., Perkin Trans. 1* **1974**, *1*, 288−294.
(683) Farid, S. Photolysis of *t*-Butyl-*p*-quinones: Competing 1,4- and 1,5-Dipolar Cycloadditions of the Photoproduct to Nitriles and Ketones. *J. Chem. Soc. D* **1970**, 303−304.
(684) Görner, H. Photoreactions of 2-Methyl-5-isopropyl-1,4-benzoquinone. *J. Photochem. Photobiol., A* **2004**, *165*, 215−222.
(685) Görner, H. Photoreactions of 2,5-Dibromo-3-methyl-6-isopropyl-1,4-benzoquinone. *J. Photochem. Photobiol., A* **2005**, *175*, 138−145.
(686) Orlando, C. M.; Mark, H.; Bose, A. K.; Manhas, M. S. Photoreactions: Rearrangement of Thymoquinone. *Chem. Commun.* **1966**, 714−715.
(687) Orlando, C. M.; Mark, H.; Bose, A. K.; Manhas, M. S. Photoreactions. IV. Photolysis of *tert*-Butyl-Substituted *p*-Benzoquinones. *J. Am. Chem. Soc.* **1967**, *89*, 6527−6532.
(688) Orlando, C. M.; Mark, H.; Bose, A. K.; Manhas, M. S. Photoreactions. V. Mechanism of the Photorearrangement of Alkyl-*p*-Benzoquinones. *J. Org. Chem.* **1968**, *33*, 2512−2516.

(689) Stidham, M. A.; Siedow, J. N. Photochemical Reactions of Dibromothymoquinone: Structure and Inhibitory Properties of the Photoproduct. *Photochem. Photobiol.* **1983**, *38*, 537−539.
(690) Cameron, D. W.; Giles, R. G. F. A Photochemical Rearrangement Involving Aminated Quinones. *Chem. Commun.* **1965**, 573−574.
(691) Cameron, D. W.; Giles, R. G. F. Photochemical Formation of Benzoxazoline Derivatives from Aminated Quinones. *J. Chem. Soc. C* **1968**, 1461−1464.
(692) Giles, R. G. F. The Photochemistry of an Aminated 1,4-Benzoquinone. *Tetrahedron Lett.* **1972**, *13*, 2253−2254.
(693) Maruyama, K.; Kozuka, T.; Otsuki, T. The Intramolecular Hydrogen Abstraction Reaction in the Photolysis of Aminated 1,4-Naphthoquinones. *Bull. Chem. Soc. Jpn.* **1977**, *50*, 2170−2173.
(694) Iwamoto, H. Photoinduced Intramolecular Cyclization Reaction of 3-Substituted 2-Alkenoyl-1,4-benzoquinones. *Bull. Chem. Soc. Jpn.* **1989**, *62*, 3479−3487.
(695) Iwamoto, H.; Takuwa, A. Photoinduced Intramolecular Cyclization Reaction of 2-(2-Alkenoyl)-3-isopropylthio-1,4-benzoquinones to Heterocyclic Compounds. *Bull. Chem. Soc. Jpn.* **1991**, *64*, 724−726.
(696) Kemp, D. S.; Reczek, J. New Protective Groups for Peptide Synthesis–III the Maq Ester Group Mild Reductive Cleavage of 2-Acyloxymethyleneanthraquinones. *Tetrahedron Lett.* **1977**, *18*, 1031−1034.
(697) Guo, Y.; Song, Q.; Wang, J.; Ma, J.; Zhang, X.; Phillips, D. L. Unraveling the Photodeprotection Mechanism of Anthraquinon-2-ylmethoxycarbonyl-Caged Alcohols Using Time-Resolved Spectroscopy. *J. Org. Chem.* **2018**, *83*, 13454−13462.
(698) Guo, Y.; Song, Q.; Xu, T.; Ma, J.; Phillips, D. L. The Solvent Effect on the Photodeprotection of Anthraquinone Protected Carboxylic Acid Unravelled by Time-Resolved Spectroscopic Studies. *Phys. Chem. Chem. Phys.* **2019**, *21*, 14598−14604.
(699) Ren, M.-G.; Bi, N.-M.; Mao, M.; Song, Q.-H. 2-(1′-Hydroxyethyl)-anthraquinone as a Photolabile Protecting Group for Carboxylic Acids. *J. Photochem. Photobiol., A* **2009**, *204*, 13−18.
(700) Arumugam, S.; Popik, V. V. Photochemical Generation and the Reactivity of *o*-Naphthoquinone Methides in Aqueous Solutions. *J. Am. Chem. Soc.* **2009**, *131*, 11892−11899.
(701) Arumugam, S.; Popik, V. V. Dual Reactivity of Hydroxy- and Methoxy- Substituted *o*-Quinone Methides in Aqueous Solutions: Hydration versus Tautomerization. *J. Org. Chem.* **2010**, *75*, 7338−7346.
(702) Kulikov, A.; Arumugam, S.; Popik, V. V. Photolabile Protection of Alcohols, Phenols, and Carboxylic Acids with 3-Hydroxy-2-naphthalenemethanol. *J. Org. Chem.* **2008**, *73*, 7611−7615.
(703) Yu, J.-y.; Tang, W.-J.; Wang, H.-B.; Song, Q.-H. Anthraquinon-2-ylethyl-1′,2′-diol (Aqe-Diol) as a New Photolabile Protecting Group for Aldehydes and Ketones. *J. Photochem. Photobiol., A* **2007**, *185*, 101−105.
(704) Perpète, E. A.; Lambert, C.; Wathelet, V.; Preat, J.; Jacquemin, D. Ab Initio Studies of the λ_{max} of Naphthoquinones Dyes. *Spectrochim. Acta, Part A* **2007**, *68*, 1326−1333.
(705) Russkikh, V. V. Synthesis and Efficiency of Photolysis of 2-Dialkylamino-1,4-benzoquinones and 2-Dialkylamino-1,4-anthraquinones. *Zhurnal Organicheskoi Khimii* **1995**, *31*, 380−384.
(706) Takagi, K.; Kawabe, M.; Matsuoka, M.; Kitao, T. Syntheses of Deep Coloured Aminonaphthoquinonoid Dyes. Reaction of Dichloronaphthazarins with 2-Aminobenzenethiol and Related Compounds. *Dyes Pigm.* **1985**, *6*, 177−188.
(707) Braude, E. A. Studies in Light Absorption. Part I. *p*-Benzoquinones. *J. Chem. Soc.* **1945**, 490−497.
(708) Eugster, C. H.; Bosshard, P. Abnormale Diels-Alder-Reaktionen zwischen Acylchinonen und Furanen. *Helv. Chim. Acta* **1963**, *46*, 815−851.
(709) Hammond, P. R. Substituent Effects on the Acceptor Properties of 1,4-Benzoquinone. *J. Chem. Soc.* **1964**, 471−479.
(710) Ukai, S.; Hirose, K. Reaction of Phenol Derivatives with Sulfoxides. II. A New Method of Synthesis of Monothio Derivatives of *p*-Benzoquinone. *Chem. Pharm. Bull.* **1968**, *16*, 195−201.
(711) Fabian, J.; Hartmann, H. Quinoid Dyes. *Light Absorption of Organic Colorants: Theoretical Treatment and Empirical Rules*; Fabian, J., Hartmann, H., Eds.; Springer Berlin Heidelberg: Berlin, Heidelberg, 1980.
(712) Falci, K. J.; Franck, R. W.; Smith, G. P. Approaches to Mitomycins - Photochemistry of Aminoquinones. *J. Org. Chem.* **1977**, *42*, 3317−3319.
(713) Giles, R. G. F.; Mitchell, P. R.; Roos, G. H. P.; Baxter, I. Photochemical Reaction of 2-Acetyl-3-Alkylamino-1,4-Benzoquinones - Formation of Benzoxazoles. *J. Chem. Soc., Perkin Trans. 1* **1973**, *1*, 493−496.
(714) Chen, Y. G.; Steinmetz, M. G. Photochemical Cyclization with Release of Carboxylic Acids and Phenol from Pyrrolidino-Substituted 1,4-Benzoquinones Using Visible Light. *Org. Lett.* **2005**, *7*, 3729−3732.
(715) Chen, Y. G.; Steinmetz, M. G. Photoactivation of Amino-Substituted 1,4-Benzoquinones for Release of Carboxylate and Phenolate Leaving Groups Using Visible Light. *J. Org. Chem.* **2006**, *71*, 6053−6060.
(716) Wang, X. D.; Kalow, J. A. Rapid Aqueous Photouncaging by Red Light. *Org. Lett.* **2018**, *20*, 1716−1719.
(717) Ramachandran, M. S.; Singh, U. C.; Subbaratnam, N. R.; Kelkar, V. K. Spectral Properties of Some Amino Substituted *p*-Benzoquinones. *Proc. Indian Acad. Sci., Chem. Sci.* **1979**, *88*, 155−162.
(718) Wallenfels, K.; Draber, W. Der Einfluss der Substituenten auf Elektronen- und Schwingungsspektren von Aminochinonen. *Tetrahedron* **1964**, *20*, 1889−1912.
(719) Alouane, A.; Labruère, R.; Le Saux, T.; Aujard, I.; Dubruille, S.; Schmidt, F.; Jullien, L. Light Activation for the Versatile and Accurate Kinetic Analysis of Disassembly of Self-Immolative Spacers. *Chem. - Eur. J.* **2013**, *19*, 11717−11724.
(720) Labruère, R.; Alouane, A.; Le Saux, T.; Aujard, I.; Pelupessy, P.; Gautier, A.; Dubruille, S.; Schmidt, F.; Jullien, L. Self-Immolative" Spacer for Uncaging with Fluorescence Reporting. *Angew. Chem., Int. Ed.* **2012**, *51*, 9344−9347.
(721) Schaefer, C. G.; Peters, K. S. Picosecond Dynamics of the Photoreduction of Benzophenone by Triethylamine. *J. Am. Chem. Soc.* **1980**, *102*, 7566−7567.
(722) Bruce, J. M. *The Chemistry of the Quinonoid Compounds*; Wiley and Sons: New York, 1974.
(723) Regan, C. J.; Walton, D. P.; Shafaat, O. S.; Dougherty, D. A. Mechanistic Studies of the Photoinduced Quinone Trimethyl Lock Decaging Process. *J. Am. Chem. Soc.* **2017**, *139*, 4729−4736.
(724) Ma, C.; Kwok, W. M.; Chan, W. S.; Du, Y.; Kan, J. T. W.; Toy, P. H.; Phillips, D. L. Ultrafast Time-Resolved Transient Absorption and Resonance Raman Spectroscopy Study of the Photodeprotection and Rearrangement Reactions of *p*-Hydroxyphenacyl Caged Phosphates. *J. Am. Chem. Soc.* **2006**, *128*, 2558−2570.
(725) Toteva, M. M.; Richard, J. P. The Generation and Reactions of Quinone Methides. *Adv. Phys. Org. Chem.* **2011**, *45*, 39−91.
(726) Carling, C.-J.; Olejniczak, J.; Foucault-Collet, A.; Collet, G.; Viger, M. L.; Nguyen Huu, V. A.; Duggan, B. M.; Almutairi, A. Efficient Red Light Photo-Uncaging of Active Molecules in Water Upon Assembly Into Nanoparticles. *Chem. Sci.* **2016**, *7*, 2392−2398.
(727) Walton, D. P.; Dougherty, D. A. A General Strategy for Visible-Light Decaging Based on the Quinone Trimethyl Lock. *J. Am. Chem. Soc.* **2017**, *139*, 4655−4658.
(728) Milstien, S.; Cohen, L. A. Rate Acceleration by Stereopopulation Control: Models for Enzyme Action. *Proc. Natl. Acad. Sci. U. S. A.* **1970**, *67*, 1143−1147.
(729) Milstien, S.; Cohen, L. A. Stereopopulation Control. I. Rate Enhancement in the Lactonizations of *o*-Hydroxyhydrocinnamic Acids. *J. Am. Chem. Soc.* **1972**, *94*, 9158−9165.
(730) Okoh, O. A.; Klahn, P. Trimethyl Lock: A Multifunctional Molecular Tool for Drug Delivery, Cellular Imaging, and Stimuli-Responsive Materials. *ChemBioChem* **2018**, *19*, 1668−1694.

(731) Huvelle, S.; Alouane, A.; Le Saux, T.; Jullien, L.; Schmidt, F. Syntheses and Kinetic Studies of Cyclisation-Based Self-Immolative Spacers. *Org. Biomol. Chem.* **2017**, *15*, 3435−3443.
(732) Shigenaga, A.; Morishita, K.; Yamaguchi, K.; Ding, H.; Ebisuno, K.; Sato, K.; Yamamoto, J.; Akaji, K.; Otaka, A. Development of UV-Responsive Catch-and-Release System of a Cysteine Protease Model Peptide. *Tetrahedron* **2011**, *67*, 8879−8886.
(733) Shigenaga, A.; Tsuji, D.; Nishioka, N.; Tsuda, S.; Itoh, K.; Otaka, A. Synthesis of a Stimulus-Responsive Processing Device and Its Application to a Nucleocytoplasmic Shuttle Peptide. *ChemBioChem* **2007**, *8*, 1929−1931.
(734) Barbafina, A.; Latterini, L.; Carlotti, B.; Elisei, F. Characterization of Excited States of Quinones and Identification of Their Deactivation Pathways. *J. Phys. Chem. A* **2010**, *114*, 5980−5984.
(735) Kemp, D. R.; Porter, G. Photochemistry of Methylated *p*-Benzoquinones. *Proc. R. Soc. London, A* **1971**, *326*, 117−130.
(736) Truong, V. X.; Li, F.; Ercole, F.; Forsythe, J. S. Visible-Light-Mediated Cleavage of Polymer Chains Under Physiological Conditions via Quinone Photoreduction and Trimethyl Lock. *Chem. Commun.* **2017**, *53*, 12076−12079.
(737) Rosen, B. M.; Lligadas, G.; Hahn, C.; Percec, V. Synthesis of Dendrimers Through Divergent Iterative Thio-Bromo "Click" Chemistry. *J. Polym. Sci., Part A: Polym. Chem.* **2009**, *47*, 3931−3939.
(738) Rosen, B. M.; Lligadas, G.; Hahn, C.; Percec, V. Synthesis of Dendritic Macromolecules Through Divergent Iterative Thio-Bromo "Click" Chemistry and SET-LRP. *J. Polym. Sci., Part A: Polym. Chem.* **2009**, *47*, 3940−3948.
(739) Turner, A. D.; Pizzo, S. V.; Rozakis, G.; Porter, N. A. Photoreactivation of Irreversibly Inhibited Serine Proteinases. *J. Am. Chem. Soc.* **1988**, *110*, 244−250.
(740) Turner, A. D.; Pizzo, S. V.; Rozakis, G. W.; Porter, N. A. Photochemical Activation of Acylated α-Thrombin. *J. Am. Chem. Soc.* **1987**, *109*, 1274−1275.
(741) Shiono, H.; Nohta, H.; Utsuyama, C.; Hiramatsu, M. New Method for Adding Reagents: An Application of Caged Molecules to Analytical Chemistry. *Anal. Chim. Acta* **2000**, *405*, 17−21.
(742) Norris, J. L.; Hangauer, M. J.; Porter, N. A.; Caprioli, R. M. Nonacid Cleavable Detergents Applied to MALDI Mass Spectrometry Profiling of Whole Cells. *J. Mass Spectrom.* **2005**, *40*, 1319−1326.
(743) Duan, X.-Y.; Zhai, B.-C.; Song, Q.-H. Water-Soluble *o*-Hydroxycinnamate as an Efficient Photoremovable Protecting Group of Alcohols with Fluorescence Reporting. *Photochem. Photobiol. Sci.* **2012**, *11*, 593−598.
(744) Thuring, J. W.; Li, H.; Porter, N. A. Comparative Study of the Active Site Caging of Serine Proteases: Thrombin and Factor Xa. *Biochemistry* **2002**, *41*, 2002−2013.
(745) Porter, N. A.; Bruhnke, J. D. Acyl Thrombin Photochemistry: Kinetics for Deacylation of Enzyme Cinnamate Geometric Isomers. *J. Am. Chem. Soc.* **1989**, *111*, 7616−7618.
(746) Porter, N. A.; Bruhnke, J. D. Photocoagulation of Human Plasma: Acyl Serine Proteinase Photochemistry. *Photochem. Photobiol.* **1990**, *51*, 37−43.
(747) Porter, N. A.; Bush, K. A.; Kinter, K. S. Photo-Reversible Binding of Thrombin to Avidin by Means of a Photolabile Inhibitor. *J. Photochem. Photobiol., B* **1997**, *38*, 61−69.
(748) Stoddard, B. L.; Bruhnke, J.; Porter, N.; Ringe, D.; Petsko, G. A. Structure and Activity of Two Photoreversible Cinnamates Bound to Chymotrypsin. *Biochemistry* **1990**, *29*, 4871−4879.
(749) Schelkle, K. M.; Bender, M.; Jeltsch, K.; Buckup, T.; Müllen, K.; Hamburger, M.; Bunz, U. H. F. Light-Induced Solubility Modulation of Polyfluorene To Enhance the Performance of OLEDs. *Angew. Chem., Int. Ed.* **2015**, *54*, 14545−14548.
(750) Venkatesh, Y.; Srivastava, H. K.; Bhattacharya, S.; Mehra, M.; Datta, P. K.; Bandyopadhyay, S.; Singh, N. D. P. One- and Two-Photon Uncaging: Carbazole Fused *o*-Hydroxycinnamate Platform for Dual Release of Alcohols (Same or Different) with Real-Time Monitoring. *Org. Lett.* **2018**, *20*, 2241−2244.
(751) Garrett, E. R.; Lippold, B. C.; Mielck, J. B. Kinetics and Mechanisms of Lactonization of Coumarinic Acids and Hydrolysis of Coumarins I. *J. Pharm. Sci.* **1971**, *60*, 396−405.
(752) Hershfield, R.; Schmir, G. L. Lactonization of Ring-Substituted Coumarinic Acids. Structural Effects on the Partitioning of Tetrahedral Intermediates in Esterification. *J. Am. Chem. Soc.* **1973**, *95*, 7359−7369.
(753) Hershfield, R.; Schmir, G. L. Lactonization of Coumarinic Acids. Kinetic Evidence for Three Species of the Tetrahedral Intermediate. *J. Am. Chem. Soc.* **1973**, *95*, 8032−8040.
(754) Lippold, B. C.; Garrett, E. R. Kinetics and Mechanisms of Lactonization of Coumarinic Acids and Hydrolysis of Coumarins II. *J. Pharm. Sci.* **1971**, *60*, 1019−1027.
(755) Gagey, N.; Emond, M.; Neveu, P.; Benbrahim, C.; Goetz, B.; Aujard, I.; Baudin, J.-B.; Jullien, L. Alcohol Uncaging with Fluorescence Reporting: Evaluation of *o*-Acetoxyphenyl Methyloxazolone Precursors. *Org. Lett.* **2008**, *10*, 2341−2344.
(756) Gagey, N.; Neveu, P.; Benbrahim, C.; Goetz, B.; Aujard, I.; Baudin, J.-B.; Jullien, L. Two-Photon Uncaging with Fluorescence Reporting: Evaluation of the *o*-Hydroxycinnamic Platform. *J. Am. Chem. Soc.* **2007**, *129*, 9986−9998.
(757) Paul, A.; Mengji, R.; Chandy, O. A.; Nandi, S.; Bera, M.; Jana, A.; Anoop, A.; Singh, N. D. P. ESIPT-Induced Fluorescent *o*-Hydroxycinnamate: A Self-Monitoring Phototrigger for Prompt Image-Guided Uncaging of Alcohols. *Org. Biomol. Chem.* **2017**, *15*, 8544−8552.
(758) Gagey, N.; Neveu, P.; Jullien, L. Two-Photon Uncaging with the Efficient 3,5-Dibromo-2,4-dihydroxycinnamic Caging Group. *Angew. Chem., Int. Ed.* **2007**, *46*, 2467−2469.
(759) Tremblay, M. S.; Sames, D. A New Fluorogenic Transformation: Development of an Optical Probe for Coenzyme Q. *Org. Lett.* **2005**, *7*, 2417−2420.
(760) Walton, D. P.; Dougherty, D. A. A General Strategy for Visible-Light Decaging Based on the Quinone cis-Alkenyl Lock. *Chem. Commun.* **2019**, *55*, 4965−4968.
(761) Pelliccioli, A. P.; Klán, P.; Zabadal, M.; Wirz, J. Photorelease of HCl from *o*-Methylphenacyl Chloride Proceeds through the Z-Xylylenol. *J. Am. Chem. Soc.* **2001**, *123*, 7931−7932.
(762) Chiang, Y.; Kresge, A. J.; Hellrung, B.; Schünemann, P.; Wirz, J. Flash Photolysis of 5-Methyl-1,4-naphthoquinone in Aqueous Solution: Kinetics and Mechanism of Photoenolization and of Enol Trapping. *Helv. Chim. Acta* **1997**, *80*, 1106−1121.
(763) Antony, L. A. P.; Slanina, T.; Šebej, P.; Šolomek, T.; Klán, P. Fluorescein Analogue Xanthene-9-Carboxylic Acid: A Transition-Metal-Free CO Releasing Molecule Activated by Green Light. *Org. Lett.* **2013**, *15*, 4552−4555.
(764) Štacko, P.; Šebej, P.; Veetil, A. T.; Klán, P. Carbon−Carbon Bond Cleavage in Fluorescent Pyronin Analogues Induced by Yellow Light. *Org. Lett.* **2012**, *14*, 4918−4921.
(765) Martínek, M.; Váňa, J.; Šebej, P.; Navrátil, R.; Slanina, T.; Ludvíková, L.; Roithová, J.; Klán, P. Photochemistry of a 9-Dithianyl-Pyronin Derivative: A Cornucopia of Reaction Intermediates Lead to Common Photoproducts. *ChemPlusChem* **2020**, *85*, 2230−2242.
(766) Katori, A.; Kuramochi, K.; Tsubaki, K. Oxidative Cleavage of exo-Alkylidene Xanthenes. *Tetrahedron* **2016**, *72*, 2997−3002.
(767) Dao, H. M.; Whang, C.-H.; Shankar, V. K.; Wang, Y.-H.; Khan, I. A.; Walker, L. A.; Husain, I.; Khan, S. I.; Murthy, S. N.; Jo, S. Methylene Blue as a Far-Red Light-Mediated Photocleavable Multifunctional Ligand. *Chem. Commun.* **2020**, *56*, 1673−1676.
(768) Sun, J.; Feng, F. An *S*-Alkyl Thiocarbamate-Based Biosensor for Highly Sensitive and Selective Detection of Hypochlorous Acid. *Analyst* **2018**, *143*, 4251−4255.
(769) Benstead, M.; Mehl, G. H.; Boyle, R. W. 4,4′-Difluoro-4-bora-3a,4a-diaza-s-indacenes (BODIPYs) as Components of Novel Light Active Materials. *Tetrahedron* **2011**, *67*, 3573−3601.
(770) Bessette, A.; Hanan, G. S. Design, Synthesis and Photophysical Studies of Dipyrromethene-Based Materials: Insights Into Their Applications in Organic Photovoltaic Devices. *Chem. Soc. Rev.* **2014**, *43*, 3342−3405.

(771) El-Khouly, M. E.; Fukuzumi, S.; D'Souza, F. Photosynthetic Antenna−Reaction Center Mimicry by Using Boron Dipyrromethene Sensitizers. *ChemPhysChem* **2014**, *15*, 30−47.
(772) Klfout, H.; Stewart, A.; Elkhalifa, M.; He, H. BODIPYs for Dye-Sensitized Solar Cells. *ACS Appl. Mater. Interfaces* **2017**, *9*, 39873−39889.
(773) Li, W.; Xie, Z.; Jing, X. BODIPY Photocatalyzed Oxidation of Thioanisole Under Visible Light. *Catal. Commun.* **2011**, *16*, 94−97.
(774) Boens, N.; Leen, V.; Dehaen, W. Fluorescent Indicators Based on BODIPY. *Chem. Soc. Rev.* **2012**, *41*, 1130−1172.
(775) Kamkaew, A.; Lim, S. H.; Lee, H. B.; Kiew, L. V.; Chung, L. Y.; Burgess, K. BODIPY Dyes in Photodynamic Therapy. *Chem. Soc. Rev.* **2013**, *42*, 77−88.
(776) Kowada, T.; Maeda, H.; Kikuchi, K. BODIPY-Based Probes for the Fluorescence Imaging of Biomolecules in Living Cells. *Chem. Soc. Rev.* **2015**, *44*, 4953−4972.
(777) Bertrand, B.; Passador, K.; Goze, C.; Denat, F.; Bodio, E.; Salmain, M. Metal-Based BODIPY Derivatives as Multimodal Tools for Life Sciences. *Coord. Chem. Rev.* **2018**, *358*, 108−124.
(778) Ni, Y.; Wu, J. Far-Red and Near Infrared BODIPY Dyes: Synthesis and Applications for Fluorescent pH Probes and Bio-Imaging. *Org. Biomol. Chem.* **2014**, *12*, 3774−3791.
(779) Ulrich, G.; Ziessel, R.; Harriman, A. The Chemistry of Fluorescent Bodipy Dyes: Versatility Unsurpassed. *Angew. Chem., Int. Ed.* **2008**, *47*, 1184−1201.
(780) Lu, H.; Mack, J.; Yang, Y.; Shen, Z. Structural Modification Strategies for the Rational Design of Red/Nir Region BODIPYs. *Chem. Soc. Rev.* **2014**, *43*, 4778−4823.
(781) Hinkeldey, B.; Schmitt, A.; Jung, G. Comparative Photostability Studies of BODIPY and Fluorescein Dyes by Using Fluorescence Correlation Spectroscopy. *ChemPhysChem* **2008**, *9*, 2019−2027.
(782) Singh-Rachford, T. N.; Haefele, A.; Ziessel, R.; Castellano, F. N. Boron Dipyrromethene Chromophores: Next Generation Triplet Acceptors/Annihilators for Low Power Upconversion Schemes. *J. Am. Chem. Soc.* **2008**, *130*, 16164−16165.
(783) Kollmannsberger, M.; Rurack, K.; Resch-Genger, U.; Daub, J. Ultrafast Charge Transfer in Amino-Substituted Boron Dipyrromethene Dyes and Its Inhibition by Cation Complexation: A New Design Concept for Highly Sensitive Fluorescent Probes. *J. Phys. Chem. A* **1998**, *102*, 10211−10220.
(784) Qin, W.; Baruah, M.; Stefan, A.; Van der Auweraer, M.; Boens, N. Photophysical Properties of BODIPY-Derived Hydroxyaryl Fluorescent pH Probes in Solution. *ChemPhysChem* **2005**, *6*, 2343−2351.
(785) Röhr, H.; Trieflinger, C.; Rurack, K.; Daub, J. Proton- and Redox-Controlled Switching of Photo- and Electrochemiluminescence in Thiophenyl-Substituted Boron−Dipyrromethene Dyes. *Chem. - Eur. J.* **2006**, *12*, 689−700.
(786) Sazanovich, I. V.; Kirmaier, C.; Hindin, E.; Yu, L.; Bocian, D. F.; Lindsey, J. S.; Holten, D. Structural Control of the Excited-State Dynamics of Bis(dipyrrinato)zinc Complexes: Self-Assembling Chromophores for Light-Harvesting Architectures. *J. Am. Chem. Soc.* **2004**, *126*, 2664−2665.
(787) Kee, H. L.; Kirmaier, C.; Yu, L.; Thamyongkit, P.; Youngblood, W. J.; Calder, M. E.; Ramos, L.; Noll, B. C.; Bocian, D. F.; Scheidt, W. R.; Birge, R. R.; Lindsey, J. S.; Holten, D. Structural Control of the Photodynamics of Boron-Dipyrrin Complexes. *J. Phys. Chem. B* **2005**, *109*, 20433−20443.
(788) de Wael, E. V.; Pardoen, J. A.; van Koeveringe, J. A.; Lugtenburg, J. Pyrromethene-BF_2 Complexes (4,4′-Difluoro-4-bora-3a,4a-diaza-*s*-indacenes). Synthesis and Luminescence Properties. *Recl. Trav. Chim. Pays-Bas* **1977**, *96*, 306−309.
(789) Yogo, T.; Urano, Y.; Ishitsuka, Y.; Maniwa, F.; Nagano, T. Highly Efficient and Photostable Photosensitizer Based on BODIPY Chromophore. *J. Am. Chem. Soc.* **2005**, *127*, 12162−12163.
(790) Rumyantsev, E. V.; Alyoshin, S. N.; Marfin, Y. S. Kinetic Study of BODIPY Resistance to Acids and Alkalis: Stability Ranges in Aqueous and Non-Aqueous Solutions. *Inorg. Chim. Acta* **2013**, *408*, 181−185.
(791) Yang, L.; Simionescu, R.; Lough, A.; Yan, H. Some Observations Relating to the Stability of the BODIPY Fluorophore Under Acidic and Basic Conditions. *Dyes Pigm.* **2011**, *91*, 264−267.
(792) Boens, N.; Verbelen, B.; Ortiz, M. J.; Jiao, L.; Dehaen, W. Synthesis of BODIPY Dyes Through Postfunctionalization of the Boron Dipyrromethene Core. *Coord. Chem. Rev.* **2019**, *399*, 213024.
(793) Loudet, A.; Burgess, K. BODIPY Dyes and Their Derivatives: Syntheses and Spectroscopic Properties. *Chem. Rev.* **2007**, *107*, 4891−4932.
(794) Rubinstein, N.; Liu, P.; Miller, E. W.; Weinstain, R. *meso*-Methylhydroxy BODIPY: a scaffold for photo-labile protecting groups. *Chem. Commun.* **2015**, *51*, 6369−6372.
(795) Goswami, P. P.; Syed, A.; Beck, C. L.; Albright, T. R.; Mahoney, K. M.; Unash, R.; Smith, E. A.; Winter, A. H. BODIPY-Derived Photoremovable Protecting Groups Unmasked with Green Light. *J. Am. Chem. Soc.* **2015**, *137*, 3783−3786.
(796) Albright, T. R.; Winter, A. H. A Fine Line Separates Carbocations from Diradical Ions in Donor-Unconjugated Cations. *J. Am. Chem. Soc.* **2015**, *137*, 3402−3410.
(797) Buck, A. T.; Beck, C. L.; Winter, A. H. Inverted Substrate Preferences for Photochemical Heterolysis Arise from Conical Intersection Control. *J. Am. Chem. Soc.* **2014**, *136*, 8933−8940.
(798) Slanina, T.; Shrestha, P.; Palao, E.; Kand, D.; Peterson, J. A.; Dutton, A. S.; Rubinstein, N.; Weinstain, R.; Winter, A. H.; Klán, P. In Search of the Perfect Photocage: Structure−Reactivity Relationships in meso-Methyl BODIPY Photoremovable Protecting Groups. *J. Am. Chem. Soc.* **2017**, *139*, 15168−15175.
(799) Štacko, P.; Muchovaá, L.; Vítek, L.; Klán, P. Visible to NIR Light Photoactivation of Hydrogen Sulfide for Biological Targeting. *Org. Lett.* **2018**, *20*, 4907−4911.
(800) Li, M.; Dove, A. P.; Truong, V. X. Additive-Free Green Light-Induced Ligation Using BODIPY Triggers. *Angew. Chem., Int. Ed.* **2020**, *59*, 2284−2288.
(801) Peterson, J. A.; Fischer, L. J.; Gehrmann, E. J.; Shrestha, P.; Yuan, D.; Wijesooriya, C.; Smith, E. A.; Winter, A. H. Direct Photorelease of Alcohols from Boron-Alkylated BODIPY Photocages. *J. Org. Chem.* **2020**, *85*, 5712−5717.
(802) Vohradská, N.; Sánchez-Carnerero, E. M.; Pastierik, T.; Mazal, C.; Klán, P. Controlled Photorelease of Alkynoic Acids and Their Decarboxylative Deprotection for Copper-Catalyzed Azide/Alkyne Cycloaddition. *Chem. Commun.* **2018**, *54*, 5558−5561.
(803) Blangetti, M.; Fraix, A.; Lazzarato, L.; Marini, E.; Rolando, B.; Sodano, F.; Fruttero, R.; Gasco, A.; Sortino, S. A Nonmetal-Containing Nitric Oxide Donor Activated with Single-Photon Green Light. *Chem. - Eur. J.* **2017**, *23*, 9026−9029.
(804) Liu, M.; Meng, J.; Bao, W.; Liu, S.; Wei, W.; Ma, G.; Tian, Z. Single-Chromophore-Based Therapeutic Agent Enables Green-Light-Triggered Chemotherapy and Simultaneous Photodynamic Therapy to Cancer Cells. *ACS Applied Bio Materials* **2019**, *2*, 3068−3076.
(805) Kand, D.; Pizarro, L.; Angel, I.; Avni, A.; Friedmann-Morvinski, D.; Weinstain, R. Organelle-Targeted BODIPY Photocages: Visible-Light-Mediated Subcellular Photorelease. *Angew. Chem., Int. Ed.* **2019**, *58*, 4659−4663.
(806) Toupin, N. P.; Arora, K.; Shrestha, P.; Peterson, J. A.; Fischer, L. J.; Rajagurubandara, E.; Podgorski, I.; Winter, A. H.; Kodanko, J. J. BODIPY-Caged Photoactivated Inhibitors of Cathepsin B Flip the Light Switch on Cancer Cell Apoptosis. *ACS Chem. Biol.* **2019**, *14*, 2833−2840.
(807) Peterson, J. A.; Wijesooriya, C.; Gehrmann, E. J.; Mahoney, K. M.; Goswami, P. P.; Albright, T. R.; Syed, A.; Dutton, A. S.; Smith, E. A.; Winter, A. H. Family of BODIPY Photocages Cleaved by Single Photons of Visible/Near-Infrared Light. *J. Am. Chem. Soc.* **2018**, *140*, 7343−7346.
(808) Lv, W.; Li, Y.; Li, F.; Lan, X.; Zhang, Y.; Du, L.; Zhao, Q.; Phillips, D. L.; Wang, W. Upconversion-like Photolysis of BODIPY-Based Prodrugs via a One-Photon Process. *J. Am. Chem. Soc.* **2019**, *141*, 17482−17486.

(809) Sitkowska, K.; Feringa, B. L.; Szymański, W. Green-Light-Sensitive BODIPY Photoprotecting Groups for Amines. *J. Org. Chem.* **2018**, *83*, 1819−1827.
(810) Faggi, E.; Aguilera, J.; Sáez, R.; Pujol, F.; Marquet, J.; Hernando, J.; Sebastián, R. M. Wavelength-Tunable Light-Induced Polymerization of Cyanoacrylates Using Photogenerated Amines. *Macromolecules* **2019**, *52*, 2329−2339.
(811) Kand, D.; Liu, P.; Navarro, M. X.; Fischer, L. J.; Rousso-Noori, L.; Friedmann-Morvinski, D.; Winter, A. H.; Miller, E. W.; Weinstain, R. Water-Soluble BODIPY Photocages with Tunable Cellular Localization. *J. Am. Chem. Soc.* **2020**, *142*, 4970−4974.
(812) Sitkowska, K.; Hoes, M. F.; Lerch, M.; Lameijer, L.; van der Meer, P.; Szymanski, W.; Feringa, B. L. Red − Light − Sensitive BODIPY Photoprotecting Groups for Amines and Their Biological Application in Controlling Heart Rhythm. *Chem. Commun.* **2020**, *56*, 5480.
(813) Al Anshori, J.; Slanina, T.; Palao, E.; Klán, P. The Internal Heavy-Atom Effect on 3-Phenylselanyl and 3-Phenyltellanyl BODIPY Derivatives Studied by Transient Absorption Spectroscopy. *Photochem. Photobiol. Sci.* **2016**, *15*, 250−259.
(814) Ludvíková, L.; Friš, P.; Heger, D.; Šebej, P.; Wirz, J.; Klán, P. Photochemistry of Rose Bengal in Water and Acetonitrile: A Comprehensive Kinetic Analysis. *Phys. Chem. Chem. Phys.* **2016**, *18*, 16266−16273.
(815) Shrestha, P.; Dissanayake, K. C.; Gehrmann, E. J.; Wijesooriya, C. S.; Mukhopadhyay, A.; Smith, E. A.; Winter, A. H. Efficient Far-Red/Near-IR Absorbing BODIPY Photocages by Blocking Unproductive Conical Intersections. *J. Am. Chem. Soc.* **2020**, *142*, 15505−15512.
(816) Murata, M.; Miyashita, S.; Yokoo, C.; Tamai, M.; Hanada, K.; Hatayama, K.; Towatari, T.; Nikawa, T.; Katunuma, N. Novel Epoxysuccinyl Peptides Selective Inhibitors of Cathepsin B, in Vitro. *FEBS Lett.* **1991**, *280*, 307−310.
(817) Kawatani, M.; Kamiya, M.; Takahashi, H.; Urano, Y. Factors Affecting the Uncaging Efficiency of 500 nm Light-Activatable BODIPY Caging Group. *Bioorg. Med. Chem. Lett.* **2018**, *28*, 1−5.
(818) Umeda, N.; Takahashi, H.; Kamiya, M.; Ueno, T.; Komatsu, T.; Terai, T.; Hanaoka, K.; Nagano, T.; Urano, Y. Boron Dipyrromethene As a Fluorescent Caging Group for Single-Photon Uncaging with Long-Wavelength Visible Light. *ACS Chem. Biol.* **2014**, *9*, 2242−2246.
(819) Sunahara, H.; Urano, Y.; Kojima, H.; Nagano, T. Design and Synthesis of a Library of BODIPY-Based Environmental Polarity Sensors Utilizing Photoinduced Electron-Transfer-Controlled Fluorescence ON/OFF Switching. *J. Am. Chem. Soc.* **2007**, *129*, 5597−5604.
(820) Rehm, D.; Weller, A. Kinetics of Fluorescence Quenching by Electron and H-Atom Transfer. *Isr. J. Chem.* **1970**, *8*, 259−271.
(821) Miura, T.; Urano, Y.; Tanaka, K.; Nagano, T.; Ohkubo, K.; Fukuzumi, S. Rational Design Principle for Modulating Fluorescence Properties of Fluorescein-Based Probes by Photoinduced Electron Transfer. *J. Am. Chem. Soc.* **2003**, *125*, 8666−8671.
(822) Kumari, P.; Kulkarni, A.; Sharma, A. K.; Chakrapani, H. Visible-Light Controlled Release of a Fluoroquinolone Antibiotic for Antimicrobial Photopharmacology. *ACS Omega* **2018**, *3*, 2155−2160.
(823) Sharma, A. K.; Nair, M.; Chauhan, P.; Gupta, K.; Saini, D. K.; Chakrapani, H. Visible-Light-Triggered Uncaging of Carbonyl Sulfide for Hydrogen Sulfide (H_2S) Release. *Org. Lett.* **2017**, *19*, 4822−4825.
(824) Patil, N. G.; Basutkar, N. B.; Ambade, A. V. Visible Light-Triggered Disruption of Micelles of an Amphiphilic Block Copolymer With BODIPY at the Junction. *Chem. Commun.* **2015**, *51*, 17708−17711.
(825) Dyer, R. G.; Turnbull, K. D. Hydrolytic Stabilization of Protected *p*-Hydroxybenzyl Halides Designed as Latent Quinone Methide Precursors. *J. Org. Chem.* **1999**, *64*, 7988−7995.
(826) Chauhan, P.; Bora, P.; Ravikumar, G.; Jos, S.; Chakrapani, H. Esterase Activated Carbonyl Sulfide/Hydrogen Sulfide (H_2S) Donors. *Org. Lett.* **2017**, *19*, 62−65.
(827) Schenk, S.; Kesselmeier, J.; Anders, E. How Does the Exchange of One Oxygen Atom with Sulfur Affect the Catalytic Cycle of Carbonic Anhydrase? *Chem. - Eur. J.* **2004**, *10*, 3091−3105.
(828) Steiger, A. K.; Pardue, S.; Kevil, C. G.; Pluth, M. D. Self-Immolative Thiocarbamates Provide Access to Triggered H2S Donors and Analyte Replacement Fluorescent Probes. *J. Am. Chem. Soc.* **2016**, *138*, 7256−7259.
(829) Powell, C. R.; Foster, J. C.; Okyere, B.; Theus, M. H.; Matson, J. B. Therapeutic Delivery of H_2S via COS: Small Molecule and Polymeric Donors with Benign Byproducts. *J. Am. Chem. Soc.* **2016**, *138*, 13477−13480.
(830) Olson, K. R. The Therapeutic Potential of Hydrogen Sulfide: Separating Hype From Hope. *Am. J. Physiol. Reg. I.* **2011**, *301*, R297−R312.
(831) Wijesooriya, C. S.; Peterson, J. A.; Shrestha, P.; Gehrmann, E. J.; Winter, A. H.; Smith, E. A. A Photoactivatable BODIPY Probe for Localization-Based Super-Resolution Cellular Imaging. *Angew. Chem., Int. Ed.* **2018**, *57*, 12685−12689.
(832) Li, H.; Vaughan, J. C. Switchable Fluorophores for Single-Molecule Localization Microscopy. *Chem. Rev.* **2018**, *118*, 9412−9454.
(833) Dempsey, G. T.; Vaughan, J. C.; Chen, K. H.; Bates, M.; Zhuang, X. Evaluation of Fluorophores for Optimal Performance in Localization-Based Super-Resolution Imaging. *Nat. Methods* **2011**, *8*, 1027−1036.
(834) van de Linde, S.; Löschberger, A.; Klein, T.; Heidbreder, M.; Wolter, S.; Heilemann, M.; Sauer, M. Direct Stochastic Optical Reconstruction Microscopy with Standard Fluorescent Probes. *Nat. Protoc.* **2011**, *6*, 991−1009.
(835) Zhang, Y.; Raymo, F. M. Live-Cell Imaging at the Nanoscale with Bioconjugatable and Photoactivatable Fluorophores. *Bioconjugate Chem.* **2020**, *31*, 1052−1062.
(836) Takeda, A.; Komatsu, T.; Nomura, H.; Naka, M.; Matsuki, N.; Ikegaya, Y.; Terai, T.; Ueno, T.; Hanaoka, K.; Nagano, T.; Urano, Y. Unexpected Photo-instability of 2,6-Sulfonamide-Substituted BODIPYs and Its Application to Caged GABA. *ChemBioChem* **2016**, *17*, 1233−1240.
(837) Sambath, K.; Zhao, T.; Wan, Z.; Zhang, Y. Photo-Uncaging of BODIPY Oxime Ester for Histone Deacetylases Induced Apoptosis in Tumor Cells. *Chem. Commun.* **2019**, *55*, 14162−14165.
(838) Umezawa, B.; Hoshino, O.; Sawaki, S. Organic Photochemistry. I. 3, 4-Dihydroisoquinolines from Tetrahydroisoquinoline *N*-Tosylates. *Chem. Pharm. Bull.* **1969**, *17*, 1115−1119.
(839) Hamada, T.; Nishida, A.; Matsumoto, Y.; Yonemitsu, O. Photohydrolysis of Sulfonamides via Donor-Acceptor Ion Pairs with Electron-Donating Aromatics and Its Application to the Selective Detosylation of Lysine Peptides. *J. Am. Chem. Soc.* **1980**, *102*, 3978−3980.
(840) Hamada, T.; Nishida, A.; Yonemitsu, O. Selective Removal of Electron-Accepting *p*-Toluene- and Naphthalenesulfonyl Protecting Groups for Amino Function via Photoinduced Donor Acceptor Ion Pairs With Electron-Donating Aromatics. *J. Am. Chem. Soc.* **1986**, *108*, 140−145.
(841) Hamada, T.; Nishida, A.; Yonemitsu, O. A New Amino Protecting Group Readily Removable with Near Ultraviolet Light as an Application of Electron-Transfer Photochemistry. *Tetrahedron Lett.* **1989**, *30*, 4241−4244.
(842) Papageorgiou, G.; Corrie, J. E. T. Synthetic and Photochemical Studies of *N*-Arenesulfonyl Amino Acids. *Tetrahedron* **1999**, *55*, 237−254.
(843) Boreen, A. L.; Arnold, W. A.; McNeill, K. Photochemical Fate of Sulfa Drugs in the Aquatic Environment: Sulfa Drugs Containing Five-Membered Heterocyclic Groups. *Environ. Sci. Technol.* **2004**, *38*, 3933−3940.
(844) Boreen, A. L.; Arnold, W. A.; McNeill, K. Triplet-Sensitized Photodegradation of Sulfa Drugs Containing Six-Membered Heterocyclic Groups: Identification of an SO_2 Extrusion Photoproduct. *Environ. Sci. Technol.* **2005**, *39*, 3630−3638.

(845) Weiss, B.; Dürr, H.; Haas, H. J. Photochemistry of Sulfonamides and Sulfonylureas: A Contribution to the Problem of Light-Induced Dermatoses. *Angew. Chem., Int. Ed. Engl.* **1980**, *19*, 648−650.
(846) Jones, G.; Lu, L. N.; Fu, H.; Farahat, C. W.; Oh, C.; Greenfield, S. R.; Gosztola, D. J.; Wasielewski, M. R. Intramolecular Electron Transfer across Amino Acid Spacers in the Picosecond Time Regime. Charge-Transfer Interaction through Peptide Bonds. *J. Phys. Chem. B* **1999**, *103*, 572−581.
(847) Palao, E.; Slanina, T.; Muchová, L.; Šolomek, T.; Vítek, L.; Klán, P. Transition-Metal-Free CO-Releasing BODIPY Derivatives Activatable by Visible to NIR Light as Promising Bioactive Molecules. *J. Am. Chem. Soc.* **2016**, *138*, 126−133.
(848) Fukuzumi, S. New Perspective of Electron Transfer Chemistry. *Org. Biomol. Chem.* **2003**, *1*, 609−620.
(849) Corrie, J. E. T.; Papageorgiou, G. Synthesis and Evaluation of Photolabile Sulfonamides as Potential Reagents for Rapid Photorelease of Neuroactive Amines. *J. Chem. Soc., Perkin Trans. 1* **1996**, *1*, 1583−1592.
(850) Hill, R. R.; Jeffs, G. E.; Roberts, D. R.; Wood, S. A. Photodegradation of Aryl Sulfonamides: *N*-Tosylglycine. *Chem. Commun.* **1999**, 1735−1736.
(851) Griesbeck, A. G. Photochemical Transformations of Proteinogenic and Non-Proteinogenic Amino Acids. *Chimia* **1998**, *52*, 272−283.
(852) Bucher, G.; Scaiano, J. C.; Sinta, R.; Barclay, G.; Cameron, J. Laser Flash Photolysis of Carbamates Derived from 9-Fluorenone Oxime. *J. Am. Chem. Soc.* **1995**, *117*, 3848−3855.
(853) Hwang, H.; Jang, D.-J.; Chae, K. H. Photolysis Reaction Mechanism of Dibenzophenoneoxime Hexamethylenediurethane, a New Type of Photobase Generator. *J. Photochem. Photobiol., A* **1999**, *126*, 37−42.
(854) Lalevée, J.; Allonas, X.; Fouassier, J. P.; Tachi, H.; Izumitani, A.; Shirai, M.; Tsunooka, M. Investigation of the Photochemical Properties of an Important Class of Photobase Generators: The *O*-Acyloximes. *J. Photochem. Photobiol., A* **2002**, *151*, 27−37.
(855) McCarroll, A. J.; Walton, J. C. Exploitation of Aldoxime Esters as Radical Precursors in Preparative and EPR Spectroscopic Roles. *J. Chem. Soc. Perk. T.* **2000**, *2*, 2399−2409.
(856) Chowdhury, N.; Dutta, S.; Dasgupta, S.; Singh, N. D. P.; Baidya, M.; Ghosh, S. K. Synthesis, Photophysical, Photochemical, Dna Cleavage/Binding and Cytotoxic Properties of Pyrene Oxime Ester Conjugates. *Photochem. Photobiol. Sci.* **2012**, *11*, 1239−1250.
(857) Jiang, H.; An, X.; Tong, K.; Zheng, T.; Zhang, Y.; Yu, S. Visible-Light-Promoted Iminyl-Radical Formation from Acyl Oximes: A Unified Approach to Pyridines, Quinolines, and Phenanthridines. *Angew. Chem., Int. Ed.* **2015**, *54*, 4055−4059.
(858) An, X.-D.; Yu, S. Visible-Light-Promoted and One-Pot Synthesis of Phenanthridines and Quinolines from Aldehydes and *O*-Acyl Hydroxylamine. *Org. Lett.* **2015**, *17*, 2692−2695.
(859) Matsubara, R.; Idros, U. M.; Yabuta, T.; Ma, H.; Hayashi, M.; Eda, K. Photoinduced Nitrile Formation from *O*-(Arylcarbonyl) oxime: Usage as a Photoremovable Protecting Group. *ChemPhotoChem.* **2018**, *2*, 1012−1016.
(860) *Photochemistry and Photophysics of Coordination Compounds I*; Balzani, V., Campagna, S., Eds.; Springer-Verlag: Berlin, Heidelberg, 2007.
(861) *Photochemistry and Photophysics of Coordination Compounds II*; Balzani, V., Campagna, S., Eds.; Springer-Verlag: Berlin, Heidelberg, 2007.
(862) Martins, P.; Marques, M.; Coito, L.; Pombeiro, A. J. L.; Baptista, P. V.; Fernandes, A. R. Organometallic Compounds in Cancer Therapy: Past Lessons and Future Directions. *Anti-Cancer Agents Med. Chem.* **2014**, *14*, 1199−1212.
(863) Simpson, P. V.; Desai, N. M.; Casari, I.; Massi, M.; Falasca, M. Metal-Based Antitumor Compounds: Beyond Cisplatin. *Future Med. Chem.* **2019**, *11*, 119−135.
(864) Ndagi, U.; Mhlongo, N.; Soliman, M. E. Metal Complexes in Cancer Therapy - an Update From Drug Design Perspective. *Drug Des., Dev. Ther.* **2017**, *11*, 599−616.
(865) Maity, B.; Chakravarty, A. R. Photocytotoxic Organometallic Compounds. *Indian J. Chem. A* **2012**, *51*, 69−82.
(866) Lo, K. K. W. Luminescent Rhenium(I) and Iridium(III) Polypyridine Complexes as Biological Probes, Imaging Reagents, and Photocytotoxic Agents. *Acc. Chem. Res.* **2015**, *48*, 2985−2995.
(867) Kwiatkowski, S.; Knap, B.; Przystupski, D.; Saczko, J.; Kedzierska, E.; Knap-Czop, K.; Kotlinska, J.; Michel, O.; Kotowski, K.; Kulbacka, J. Photodynamic Therapy - Mechanisms, Photosensitizers and Combinations. *Biomed. Pharmacother.* **2018**, *106*, 1098−1107.
(868) Yip, A. M. H.; Lo, K. K. W. Luminescent Rhenium(I), Ruthenium(II), and Iridium(III) Polypyridine Complexes Containing a Poly(Ethylene Glycol) Pendant or Bioorthogonal Reaction Group as Biological Probes and Photocytotoxic Agents. *Coord. Chem. Rev.* **2018**, *361*, 138−163.
(869) Imberti, C.; Zhang, P.; Huang, H.; Sadler, P. J. New Designs for Phototherapeutic Transition Metal Complexes. *Angew. Chem., Int. Ed.* **2020**, *59*, 61−73.
(870) Haas, K. L.; Franz, K. J. Application of Metal Coordination Chemistry To Explore and Manipulate Cell Biology. *Chem. Rev.* **2009**, *109*, 4921−4960.
(871) Bjelosevic, A.; Pages, B. J.; Spare, L. K.; Deo, K. M.; Ang, D. L.; Aldrich-Wright, J. R. Exposing "Bright" Metals: Promising Advances in Photoactivated Anticancer Transition Metal Complexes. *Curr. Med. Chem.* **2018**, *25*, 478−492.
(872) Bonnet, S. Why Develop Photoactivated Chemotherapy? *Dalton Trans.* **2018**, *47*, 10330−10343.
(873) Jia, P. P.; Ouyang, R. Z.; Cao, P. H.; Tong, X.; Zhou, X.; Lei, T.; Zhao, Y. F.; Guo, N.; Chang, H. Z.; Miao, Y. Q.; Zhou, S. Review: Recent Advances and Future Development of Metal Complexes as Anticancer Agents. *J. Coord. Chem.* **2017**, *70*, 2175−2201.
(874) Reessing, F.; Szymanski, W. Beyond Photodynamic Therapy: Light-Activated Cancer Chemotherapy. *Curr. Med. Chem.* **2018**, *24*, 4905−4950.
(875) Renfrew, A. K.; O'Neill, E. S.; Hambley, T. W.; New, E. J. Harnessing the Properties of Cobalt Coordination Complexes for Biological Application. *Coord. Chem. Rev.* **2018**, *375*, 221−233.
(876) Ruggiero, E.; Alonso-De Castro, S.; Habtemariam, A.; Salassa, L. The Photochemistry of Transition Metal Complexes and Its Application in Biology and Medicine. *Luminescent and Photoactive Transition Metal Complexes as Biomolecular Probes and Cellular Reagents*; Lo, K. K. W., Ed., 2015; Vol. *165*.
(877) Miller, N. A.; Wiley, T. E.; Spears, K. G.; Ruetz, M.; Kieninger, C.; Krautler, B.; Sension, R. J. Toward the Design of Photoresponsive Conditional Antivitamins B-12: A Transient Absorption Study of an Arylcobalamin and an Alkynylcobalamin. *J. Am. Chem. Soc.* **2016**, *138*, 14250−14256.
(878) Anderson, E. D.; Gorka, A. P.; Schnermann, M. J. Near-Infrared Uncaging or Photosensitizing Dictated by Oxygen Tension. *Nat. Commun.* **2016**, *7*, 13378.
(879) Zayat, L.; Salierno, M.; Etchenique, R. Ruthenium(II) Bipyridyl Complexes as Photolabile Caging Groups for Amines. *Inorg. Chem.* **2006**, *45*, 1728−1731.
(880) Lutterman, D. A.; Fu, P. K. L.; Turro, C. *cis*-$[Rh_2(\mu\text{-}O_2CCH_3)_2(CH_3CN)_6]^{2+}$ as a Photoactivated Cisplatin Analog. *J. Am. Chem. Soc.* **2006**, *128*, 738−739.
(881) Renfrew, A. K.; Bryce, N. S.; Hambley, T. Cobalt(III) Chaperone Complexes of Curcumin: Photoreduction, Cellular Accumulation and Light-Selective Toxicity towards Tumour Cells. *Chem. - Eur. J.* **2015**, *21*, 15224−15234.
(882) Hennig, H. Homogeneous Photo Catalysis by Transition Metal Complexes. *Coord. Chem. Rev.* **1999**, *182*, 101−123.
(883) Vlcek, A. The Life and Times of Excited States of Organometallic and Coordination Compounds. *Coord. Chem. Rev.* **2000**, *200*, 933−977.

(884) Vogler, A.; Kunkely, H. Charge Transfer Excitation of Organometallic Compounds - Spectroscopy and Photochemistry. *Coord. Chem. Rev.* **2004**, *248*, 273−278.
(885) Shell, T. A.; Lawrence, D. S. Vitamin B-12: A Tunable, Long Wavelength, Light-Responsive Platform for Launching Therapeutic Agents. *Acc. Chem. Res.* **2015**, *48*, 2866−2874.
(886) Kozlowski, P. M.; Garabato, B. D.; Lodowski, P.; Jaworska, M. Photolytic Properties of Cobalamins: A Theoretical Perspective. *Dalton Trans.* **2016**, *45*, 4457−4470.
(887) Barker, H. A.; Weissbach, H.; Smyth, R. D. A Coenzyme Containing Pseudovitamin B_{12}. *Proc. Natl. Acad. Sci. U. S. A.* **1958**, *44*, 1093−1097.
(888) Harris, D. A.; Stickrath, A. B.; Carroll, E. C.; Sension, R. J. Influence of Environment on the Electronic Structure of Cob(III)-alamins: Time-Resolved Absorption Studies of the S1 State Spectrum and Dynamics. *J. Am. Chem. Soc.* **2007**, *129*, 7578−7585.
(889) Subramanian, G.; Zhang, X. Y.; Kodis, G.; Kong, Q. Y.; Liu, C. M.; Chizmeshya, A.; Weierstall, U.; Spence, J. Direct Structural and Chemical Characterization of the Photolytic Intermediates of Methylcobalamin Using Time-Resolved X-ray Absorption Spectroscopy. *J. Phys. Chem. Lett.* **2018**, *9*, 1542−1546.
(890) Miller, N. A.; Deb, A.; Alonso-Mori, R.; Garabato, B. D.; Glownia, J. M.; Kiefer, L. M.; Koralek, J.; Sikorski, M.; Spears, K. G.; Wiley, T. E.; Zhu, D. L.; Kozlowski, P. M.; Kubarych, K. J.; Penner-Hahn, J. E.; Sension, R. J. Polarized XANES Monitors Femtosecond Structural Evolution of Photoexcited Vitamin B-12. *J. Am. Chem. Soc.* **2017**, *139*, 1894−1899.
(891) Miller, N. A.; Deb, A.; Alonso-Mori, R.; Glownia, J. M.; Kiefer, L. M.; Konar, A.; Michocki, L. B.; Sikorski, M.; Sofferman, D. L.; Song, S.; Toda, M. J.; Wiley, T. E.; Zhu, D. L.; Kozlowski, P. M.; Kubarych, K. J.; Penner-Hahn, J. E.; Sension, R. J. Ultrafast X-ray Absorption Near Edge Structure Reveals Ballistic Excited State Structural Dynamics. *J. Phys. Chem. A* **2018**, *122*, 4963−4971.
(892) Shiang, J. J.; Walker, L. A.; Anderson, N. A.; Cole, A. G.; Sension, R. J. Time-Resolved Spectroscopic Studies of B-12 Coenzymes: The Photolysis of Methylcobalamin Is Wavelength Dependent. *J. Phys. Chem. B* **1999**, *103*, 10532−10539.
(893) Shiang, J. J.; Cole, A. G.; Sension, R. J.; Hang, K.; Weng, Y. X.; Trommel, J. S.; Marzilli, L. G.; Lian, T. Q. Ultrafast Excited-State Dynamics in Vitamin B-12 and Related Cob(III)alamins. *J. Am. Chem. Soc.* **2006**, *128*, 801−808.
(894) Sension, R. J.; Harris, D. A.; Stickrath, A.; Cole, A. G.; Fox, C. C.; Marsh, E. N. G. Time-Resolved Measurements of the Photolysis and Recombination of Adenosylcobalamin Bound to Glutamate Mutase. *J. Phys. Chem. B* **2005**, *109*, 18146−18152.
(895) Peng, J. A.; Tang, K. C.; McLoughlin, K.; Yang, Y.; Forgach, D.; Sension, R. J. Ultrafast Excited-State Dynamics and Photolysis in Base-Off B-12 Coenzymes and Analogues: Absence of the trans-Nitrogenous Ligand Opens a Channel for Rapid Nonradiative Decay. *J. Phys. Chem. B* **2010**, *114*, 12398−12405.
(896) Wiley, T. E.; Miller, N. A.; Miller, W. R.; Sofferman, D. L.; Lodowski, P.; Toda, M. J.; Jaworska, M.; Kozlowski, P. M.; Sension, R. J. Off to the Races: Comparison of Excited State Dynamics in Vitamin B12 Derivatives Hydroxocobalamin and Aquocobalamin. *J. Phys. Chem. A* **2018**, *122*, 6693−6703.
(897) Bussandri, A. P.; Kiarie, C. W.; Van Willigen, H. Photo-induced Bond Homolysis of B_{12} Coenzymes. An FT-EPR Study. *Res. Chem. Intermed.* **2002**, *28*, 697−710.
(898) Schwartz, P. A.; Frey, P. A. 5'-Peroxyadenosine and 5'-Peroxyadenosylcobalamin as Intermediates in the Aerobic Photolysis of Adenosylcobalamin. *Biochemistry* **2007**, *46*, 7284−7292.
(899) Kruppa, A. I.; Taraban, M. B.; Leshina, T. V.; Natarajan, E.; Grissom, C. B. CIDNP in the Photolysis of Coenzyme B-12 Model Compounds Suggesting That C-CO Bond Homolysis Occurs From the Singlet State. *Inorg. Chem.* **1997**, *36*, 758−759.
(900) Padmakumar, R.; Banerjee, R. Evidence That Cobalt-Carbon Bond Homolysis Is Coupled to Hydrogen Atom Abstraction From Substrate in Methylmalonyl-CoA Mutase. *Biochemistry* **1997**, *36*, 3713−3718.
(901) Yoder, L. M.; Cole, A. G.; Walker, L. A.; Sension, R. J. Time-Resolved Spectroscopic Studies of B-12 Coenzymes: Influence of Solvent on the Photolysis of Adenosylcobalamin. *J. Phys. Chem. B* **2001**, *105*, 12180−12188.
(902) Lodowski, P.; Ciura, K.; Toda, M. J.; Jaworska, M.; Kozlowski, P. M. Photodissociation of Ethylphenylcobalamin Antivitamin B-12. *Phys. Chem. Chem. Phys.* **2017**, *19*, 30310−30315.
(903) Lodowski, P.; Jaworska, M.; Andruniow, T.; Garabato, B. D.; Kozlowski, P. M. Mechanism of Co-C Bond Photolysis in the Base-On Form of Methylcobalamin. *J. Phys. Chem. A* **2014**, *118*, 11718−11734.
(904) Lodowski, P.; Jaworska, M.; Andruniow, T.; Kumar, M.; Kozlowski, P. M. Photodissociation of Co-C Bond in Methyl- and Ethylcobalamin: An Insight from TD-DFT Calculations. *J. Phys. Chem. B* **2009**, *113*, 6898−6909.
(905) Lodowski, P.; Jaworska, M.; Garabato, B. D.; Kozowski, P. M. Mechanism of Co-C Bond Photolysis in Methylcobalamin: Influence of Axial Base. *J. Phys. Chem. A* **2015**, *119*, 3913−3928.
(906) Lodowski, P.; Toda, M. J.; Ciura, K.; Jaworska, M.; Kozlowski, P. M. Photolytic Properties of Antivitamins B-12. *Inorg. Chem.* **2018**, *57*, 7838−7850.
(907) Andruniow, T.; Lodowski, P.; Garabato, B. D.; Jaworska, M.; Kozlowski, P. M. The Role of Spin-Orbit Coupling in the Photolysis of Methylcobalamin. *J. Chem. Phys.* **2016**, *144*, 124305.
(908) Garabato, B. D.; Lodowski, P.; Jaworska, M.; Kozlowski, P. M. Mechanism of Co-C Photodissociation in Adenosylcobalamin. *Phys. Chem. Chem. Phys.* **2016**, *18*, 19070−19082.
(909) Jaworska, M.; Lodowski, P.; Andruniow, T.; Pawel, M. Photolysis of Methylcobalamin: Identification of the Relevant Excited States Involved in CO-C Bond Scission. *J. Phys. Chem. B* **2007**, *111*, 2419−2422.
(910) Kozlowski, P. M.; Kumar, M.; Piecuch, P.; Li, W.; Bauman, N. P.; Hansen, J. A.; Lodowski, P.; Jaworska, M. The Cobalt−Methyl Bond Dissociation in Methylcobalamin: New Benchmark Analysis Based on Density Functional Theory and Completely Renormalized Coupled-Cluster Calculations. *J. Chem. Theory Comput.* **2012**, *8*, 1870−1894.
(911) Mamun, A. A.; Toda, M. J.; Kozlowski, P. M. Can Photolysis of the Co-C Bond in Coenzyme B12-Dependent Enzymes Be Used to Mimic the Native Reaction? *J. Photochem. Photobiol., B* **2019**, *191*, 175−184.
(912) Mamun, A. A.; Toda, M. J.; Lodowski, P.; Jaworska, M.; Kozlowski, P. M. Mechanism of Light Induced Radical Pair Formation in Coenzyme B12-Dependent Ethanolamine Ammonia-Lyase. *ACS Catal.* **2018**, *8*, 7164−7178.
(913) Jones, A. R.; Woodward, J. R.; Scrutton, N. S. Continuous Wave Photolysis Magnetic Field Effect Investigations with Free and Protein-Bound Alkylcobalamins. *J. Am. Chem. Soc.* **2009**, *131*, 17246−17253.
(914) Jones, A. R.; Hay, S.; Woodward, J. R.; Scrutton, N. S. Magnetic Field Effect Studies Indicate Reduced Geminate Recombination of the Radical Pair in Substrate-Bound Adenosylcobalamin-Dependent Ethanolamine Ammonia Lyase. *J. Am. Chem. Soc.* **2007**, *129*, 15718−15727.
(915) Kutta, R. J.; Hardman, S. J. O.; Johannissen, L. O.; Bellina, B.; Messiha, H. L.; Ortiz-Guerrero, J. M.; Elias-Arnanz, M.; Padmanabhan, S.; Barran, P.; Scrutton, N. S.; Jones, A. R. The Photochemical Mechanism of a B-12-Dependent Photoreceptor Protein. *Nat. Commun.* **2015**, *6*, 7907.
(916) Rodgers, Z. L.; Hughes, R. M.; Doherty, L. M.; Shell, J. R.; Molesky, B. P.; Brugh, A. M.; Forbes, M. D. E.; Moran, A. M.; Lawrence, D. S. B-12-Mediated, Long Wavelength Photopolymerization of Hydrogels. *J. Am. Chem. Soc.* **2015**, *137*, 3372−3378.
(917) Rodgers, Z. L.; Shell, T. A.; Brugh, A. M.; Nowotarski, H. L.; Forbes, M. D. E.; Lawrence, D. S. Fluorophore Assisted Photolysis of Thiolato-Cob(III)alamins. *Inorg. Chem.* **2016**, *55*, 1962−1969.
(918) McCue, A. C.; Moreau, W. M.; Shell, T. A. Visible Light-Induced Radical Mediated DNA Damage. *Photochem. Photobiol.* **2018**, *94*, 545−551.

(919) Giedyk, M.; Turkowska, J.; Lepak, S.; Marculewicz, M.; Proinsias, K. O.; Gryko, D. Photoinduced Vitamin B-12-Catalysis for Deprotection of (Allyloxy)arenes. *Org. Lett.* **2017**, *19*, 2670−2673.
(920) Walker, L. A.; Jarrett, J. T.; Anderson, N. A.; Pullen, S. H.; Matthews, R. G.; Sension, R. J. Time-Resolved Spectroscopic Studies of B-12 Coenzymes, the Identification of a Metastable Cob(III)-Alamin Photoproduct in the Photolysis of Methylcobalamin. *J. Am. Chem. Soc.* **1998**, *120*, 3597−3603.
(921) Pratt, J. M. Chemistry of Vitamin B12. 2. Photochemical Reactions. *J. Chem. Soc.* **1964**, 5154−5160.
(922) Pratt, J. M.; Whitear, B. R. D. Photolysis of Methylcobalamin. *J. Chem. Soc. A* **1971**, 252−255.
(923) Chen, E.; Chance, M. R. Continuous-Wave Quantum Yields of Various Cobalamins Are Influenced by Competition Between Geminate Recombination and Cage Escape. *Biochemistry* **1993**, *32*, 1480−1487.
(924) Walker, L. A.; Shiang, J. J.; Anderson, N. A.; Pullen, S. H.; Sension, R. J. Time-Resolved Spectroscopic Studies of B12 Coenzymes: The Photolysis and Geminate Recombination of Adenosylcobalamin. *J. Am. Chem. Soc.* **1998**, *120*, 7286−7292.
(925) Endicott, J. F.; Ferraudi, G. J. Flash Photolytic Investigation of Low-Energy Homolytic Processes in Methylcobalamin. *J. Am. Chem. Soc.* **1977**, *99*, 243−245.
(926) Shell, T. A.; Lawrence, D. S. A New Trick (Hydroxyl Radical Generation) for an Old Vitamin (B-12). *J. Am. Chem. Soc.* **2011**, *133*, 2148−2150.
(927) Sension, R. J.; Cole, A. G.; Harris, A. D.; Fox, C. C.; Woodbury, N. W.; Lin, S.; Marsh, E. N. G. Photolysis and Recombination of Adenosylcobalamin Bound to Glutamate Mutase. *J. Am. Chem. Soc.* **2004**, *126*, 1598−1599.
(928) Vaid, F. H. M.; Zahid, S.; Faiyaz, A.; Qadeer, K.; Gul, W.; Anwar, Z.; Ahmad, I. Photolysis of Methylcobalamin in Aqueous Solution: A Kinetic Study. *J. Photochem. Photobiol., A* **2018**, *362*, 40−48.
(929) Ahmad, I.; Qadeer, K.; Hafeez, A.; Zahid, S.; Sheraz, M. A.; Khattak, S. U. R. Effect of Ascorbic Acid on the Photolysis of Cyanocobalamin and Aquocobalamin/Hydroxocobalamin in Aqueous Solution: A Kinetic Study. *J. Photochem. Photobiol., A* **2017**, *332*, 92−100.
(930) Shell, T. A.; Shell, J. R.; Rodgers, Z. L.; Lawrence, D. S. Tunable Visible and Near-IR Photoactivation of Light-Responsive Compounds by Using Fluorophores as Light-Capturing Antennas. *Angew. Chem., Int. Ed.* **2014**, *53*, 875−878.
(931) Priestman, M. A.; Shell, T. A.; Sun, L.; Lee, H. M.; Lawrence, D. S. Merging of Confocal and Caging Technologies: Selective Three-Color Communication with Profluorescent Reporters. *Angew. Chem., Int. Ed.* **2012**, *51*, 7684−7687.
(932) Smith, W. J.; Oien, N. P.; Hughes, R. M.; Marvin, C. M.; Rodgers, Z. L.; Lee, J.; Lawrence, D. S. Cell-Mediated Assembly of Phototherapeutics. *Angew. Chem., Int. Ed.* **2014**, *53*, 10945−10948.
(933) Hughes, R. M.; Marvin, C. M.; Rodgers, Z. L.; Ding, S.; Oien, N. P.; Smith, W. J.; Lawrence, D. S. Phototriggered Secretion of Membrane Compartmentalized Bioactive Agents. *Angew. Chem., Int. Ed.* **2016**, *55*, 16080−16083.
(934) Kainrath, S.; Stadler, M.; Reichhart, E.; Distel, M.; Janovjak, H. Green-Light-Induced Inactivation of Receptor Signaling Using Cobalamin-Binding Domains. *Angew. Chem., Int. Ed.* **2017**, *56*, 4608−4611.
(935) Chatelle, C.; Ochoa-Fernandez, R.; Engesser, R.; Schneider, N.; Beyer, H. M.; Jones, A. R.; Timmer, J.; Zurbriggen, M. D.; Weber, W. A Green-Light-Responsive System for the Control of Transgene Expression in Mammalian and Plant Cells. *ACS Synth. Biol.* **2018**, *7*, 1349−1358.
(936) Jost, M.; Fernandez-Zapata, J.; Polanco, M. C.; Ortiz-Guerrero, J. M.; Chen, P. Y. T.; Kang, G.; Padmanabhan, S.; Elias-Arnanz, M.; Drennan, C. L. Structural Basis for Gene Regulation by a B-12-Dependent Photoreceptor. *Nature* **2015**, *526*, 536−U167.
(937) Jost, M.; Simpson, J. H.; Drennan, C. L. The Transcription Factor CarH Safeguards Use of Adenosylcobalamin as a Light Sensor by Altering the Photolysis Products. *Biochemistry* **2015**, *54*, 3231−3234.
(938) Claessens, C. G.; Hahn, U.; Torres, T. Phthalocyanines: From Outstanding Electronic Properties to Emerging Applications. *Chem. Rec.* **2008**, *8*, 75−97.
(939) Doane, T. L.; Chuang, C. H.; Chomas, A.; Burda, C. Photophysics of Silicon Phthalocyanines in Aqueous Media. *ChemPhysChem* **2013**, *14*, 321−330.
(940) Moreira, L. M.; Vieira dos Santos, F.; Lyon, J. P.; Maftoum-Costa, M.; Pacheco-Soares, C.; Soares da Silva, N. Photodynamic Therapy: Porphyrins and Phthalocyanines as Photosensitizers. *Aust. J. Chem.* **2008**, *61*, 741−754.
(941) Nyokong, T. Effects of Substituents on the Photochemical and Photophysical Properties of Main Group Metal Phthalocyanines. *Coord. Chem. Rev.* **2007**, *251*, 1707−1722.
(942) Wang, K. K.-H.; Wilson, J. D.; Kenney, M. E.; Mitra, S.; Foster, T. H. Irradiation-Induced Enhancement of Pc 4 Fluorescence and Changes in Light Scattering are Potential Dosimeters for Pc 4-PDT. *Photochem. Photobiol.* **2007**, *83*, 1056−1062.
(943) Li, Z. Y.; Lieberman, M. Axial Reactivity of Soluble Silicon(IV) Phthalocyanines. *Inorg. Chem.* **2001**, *40*, 932−939.
(944) Fujitsuka, M.; Ito, O.; Konami, H. Photoexcited State Properties of Silicon Phthalocyanine Monomer, Dimer, and Trimer. *Bull. Chem. Soc. Jpn.* **2001**, *74*, 1823−1829.
(945) Maree, M. D.; Kuznetsova, N.; Nyokong, T. Silicon Octaphenoxyphthalocyanines: Photostability and Singlet Oxygen Quantum Yields. *J. Photochem. Photobiol., A* **2001**, *140*, 117−125.
(946) Allen, C. M.; Sharman, W. M.; van Lier, J. E. Current Status of Phthalocyanines in the Photodynamic Therapy of Cancer. *J. Porphyrins Phthalocyanines* **2001**, *5*, 161−169.
(947) Mitsunaga, M.; Ogawa, M.; Kosaka, N.; Rosenblum, L. T.; Choyke, P. L.; Kobayashi, H. Cancer Cell−Selective in Vivo Near Infrared Photoimmunotherapy Targeting Specific Membrane Molecules. *Nat. Med.* **2011**, *17*, 1685.
(948) Li, X.; Zheng, B.-D.; Peng, X.-H.; Li, S.-Z.; Ying, J.-W.; Zhao, Y.; Huang, J.-D.; Yoon, J. Phthalocyanines as Medicinal Photosensitizers: Developments in the Last Five Years. *Coord. Chem. Rev.* **2019**, *379*, 147−160.
(949) Oleinick, N. L.; Antunez, A. R.; Clay, M. E.; Rihter, B. D.; Kenney, M. E. New Phthalocyanine Photosensitizers for Photodynamic Therapy. *Photochem. Photobiol.* **1993**, *57*, 242−247.
(950) Maiti, B.; Manna, A. K.; McCleese, C.; Doane, T. L.; Chakrapani, S.; Burda, C.; Dunietz, B. D. Photoinduced Homolytic Bond Cleavage of the Central Si-C Bond in Porphyrin Macrocycles Is a Charge Polarization Driven Process. *J. Phys. Chem. A* **2016**, *120*, 7634−7640.
(951) Zheng, J. Y.; Konishi, K.; Aida, T. A Photoresponsive Silicon Radical Within a Porphyrin (-Cloud: Photolysis of Organo- and Nitroxysilicon Porphyrins With Visible Light. *J. Am. Chem. Soc.* **1998**, *120*, 9838−9843.
(952) Li, J.; Yang, Y.; Zhang, P.; Sounik, J. R.; Kenney, M. E. Synthesis, Properties and Drug Potential of the Photosensitive Alkyl- and Alkylsiloxy-Ligated Silicon Phthalocyanine Pc 227. *Photochem. Photobiol. Sci.* **2014**, *13*, 1690−1698.
(953) Cheng, Y.; Doane, T. L.; Chuang, C.-H.; Ziady, A.; Burda, C. Near Infrared Light-Triggered Drug Generation and Release from Gold Nanoparticle Carriers for Photodynamic Therapy. *Small* **2014**, *10*, 1799−1804.
(954) Doane, T.; Cheng, Y.; Sodhi, N.; Burda, C. NIR Photocleavage of the Si-C Bond in Axial Si-Phthalocyanines. *J. Phys. Chem. A* **2014**, *118*, 10587−10595.
(955) Rajaputra, P.; Bio, M.; Nkepang, G.; Thapa, P.; Woo, S.; You, Y. Anticancer Drug Released From Near IR-Activated Prodrug Overcomes Spatiotemporal Limits of Singlet Oxygen. *Bioorg. Med. Chem.* **2016**, *24*, 1540−1549.
(956) Bio, M.; Rajaputra, P.; Nkepang, G.; You, Y. J. Far-Red Light Activatable, Multifunctional Prodrug for Fluorescence Optical Imaging and Combinational Treatment. *J. Med. Chem.* **2014**, *57*, 3401−3409.

(957) Thapa, P.; Li, M.; Bio, M.; Rajaputra, P.; Nkepang, G.; Sun, Y.; Woo, S.; You, Y. Far-Red Light-Activatable Prodrug of Paclitaxel for the Combined Effects of Photodynamic Therapy and Site-Specific Paclitaxel Chemotherapy. *J. Med. Chem.* **2016**, *59*, 3204−3214.
(958) Anderson, E. D.; Sova, S.; Ivanic, J.; Kelly, L.; Schnermann, M. J. Defining the Conditional Basis of Silicon Phthalocyanine Near-IR Ligand Exchange. *Phys. Chem. Chem. Phys.* **2018**, *20*, 19030−19036.
(959) Sato, K.; Ando, K.; Okuyama, S.; Moriguchi, S.; Ogura, T.; Totoki, S.; Hanaoka, H.; Nagaya, T.; Kokawa, R.; Takakura, H.; Nishimura, M.; Hasegawa, Y.; Choyke, P. L.; Ogawa, M.; Kobayashi, H. Photoinduced Ligand Release from a Silicon Phthalocyanine Dye Conjugated with Monoclonal Antibodies: A Mechanism of Cancer Cell Cytotoxicity after Near-Infrared Photoimmunotherapy. *ACS Cent. Sci.* **2018**, *4*, 1559−1569.
(960) Kobayashi, H.; Choyke, P. L. Near-Infrared Photoimmunotherapy of Cancer. *Acc. Chem. Res.* **2019**, *52*, 2332−2339.
(961) Thies, S.; Sell, H.; Bornholdt, C.; Schutt, C.; Kohler, F.; Tuczek, F.; Herges, R. Light-Driven Coordination-Induced Spin-State Switching: Rational Design of Photodissociable Ligands. *Chem. - Eur. J.* **2012**, *18*, 16358−16368.
(962) Thies, S.; Sell, H.; Schütt, C.; Bornholdt, C.; Näther, C.; Tuczek, F.; Herges, R. Light-Induced Spin Change by Photodissociable External Ligands: A New Principle for Magnetic Switching of Molecules. *J. Am. Chem. Soc.* **2011**, *133*, 16243−16250.
(963) Thies, S.; Bornholdt, C.; Köhler, F.; Sönnichsen, F. D.; Näther, C.; Tuczek, F.; Herges, R. Coordination-Induced Spin Crossover (CISCO) through Axial Bonding of Substituted Pyridines to Nickel−Porphyrins: σ-Donor versus π-Acceptor Effects. *Chem. - Eur. J.* **2010**, *16*, 10074−10083.
(964) Peters, M. K.; Hamer, S.; Jakel, T.; Rohricht, F.; Sonnichsen, F. D.; von Essen, C.; Lahtinen, M.; Naether, C.; Rissanen, K.; Herges, R. Spin Switching with Triazolate-Strapped Ferrous Porphyrins. *Inorg. Chem.* **2019**, *58*, 5265−5272.
(965) Nilsson, J. R.; O'Sullivan, M. C.; Li, S.; Anderson, H. L.; Andreasson, J. A Photoswitchable Supramolecular Complex With Release-And-Report Capabilities. *Chem. Commun.* **2015**, *51*, 847−850.
(966) Juris, A.; Balzani, V.; Barigelletti, F.; Campagna, S.; Belser, P.; von Zelewsky, A. Ru(II) Polypyridine Complexes: Photophysics, Photochemistry, Eletrochemistry, and Chemiluminescence. *Coord. Chem. Rev.* **1988**, *84*, 85−277.
(967) Campagna, S.; Puntoriero, F.; Nastasi, F.; Bergamini, G.; Balzani, V. Photochemistry and Photophysics of Coordination Compounds: Ruthenium. *Photochemistry and Photophysics of Coordination Compounds I*; Balzani, V., Campagna, S., Eds.; Springer Berlin Heidelberg: Berlin, Heidelberg, 2007.
(968) Cannizzo, A.; van Mourik, F.; Gawelda, W.; Zgrablic, G.; Bressler, C.; Chergui, M. Broadband Femtosecond Fluorescence Spectroscopy of $[Ru(bpy)_3]^{2+}$. *Angew. Chem., Int. Ed.* **2006**, *45*, 3174−3176.
(969) Durham, B.; Caspar, J. V.; Nagle, J. K.; Meyer, T. J. Photochemistry of tris(2,2′-Bipyridine)ruthenium^{2+} ion. *J. Am. Chem. Soc.* **1982**, *104*, 4803−4810.
(970) Tu, Y. J.; Mazumder, S.; Endicott, J. F.; Turro, C.; Kodanko, J. J.; Schlegel, H. B. Selective Photodissociation of Acetonitrile Ligands in Ruthenium Polypyridyl Complexes Studied by Density Functional Theory. *Inorg. Chem.* **2015**, *54*, 8003−8011.
(971) Laemmel, A. C.; Collin, J. P.; Sauvage, J. P. Efficient and Selective Photochemical Labilization of a Given Bidentate Ligand in Mixed Ruthenium(II) Complexes of the $Ru(phen)_2L^{2+}$ and $Ru(bipy)_2L^{2+}$ family (L = sterically hindering chelate). *Eur. J. Inorg. Chem.* **1999**, *1999*, 383−386.
(972) Wacholtz, W. F.; Auerbach, R. A.; Schmehl, R. H. Independent Control of Charge-Transfer and Metal-Centered Excited States in Mixed-Ligand Polypyridine Ruthenium(II) Complexes via Specific Ligand Design. *Inorg. Chem.* **1986**, *25*, 227−234.
(973) Rillema, D. P.; Blanton, C. B.; Shaver, R. J.; Jackman, D. C.; Boldaji, M.; Bundy, S.; Worl, L. A.; Meyer, T. J. MLCT-dd Energy Gap in Pyridyl-Pyrimidine and Bis(Pyridine) Complexes of Ruthenium(II). *Inorg. Chem.* **1992**, *31*, 1600−1606.
(974) Allen, G. H.; White, R. P.; Rillema, D. P.; Meyer, T. J. Synthetic Control of Excited-State Properties. Tris-Chelate Complexes Containing the Ligands 2,2′-Bipyrazine, 2,2′-Bipyridine, and 2,2′-Bipyrimidine. *J. Am. Chem. Soc.* **1984**, *106*, 2613−2620.
(975) Cruz, A. J.; Kirgan, R.; Siam, K.; Heiland, P.; Rillema, D. P. Photochemical and Photophysical Properties of Ruthenium(II) bis-Bipyridine bis-Nitrile Complexes: Photolability. *Inorg. Chim. Acta* **2010**, *363*, 2496−2505.
(976) Sun, Y.; Joyce, L. E.; Dickson, N. M.; Turro, C. Efficient DNA Photocleavage by $[Ru(bpy)_2(dppn)]^{2+}$ with Visible Light. *Chem. Commun.* **2010**, *46*, 2426−2428.
(977) Li, A.; Turro, C.; Kodanko, J. J. Ru(II) Polypyridyl Complexes as Photocages for Bioactive Compounds Containing Nitriles and Aromatic Heterocycles. *Chem. Commun.* **2018**, *54*, 1280−1290.
(978) White, J. K.; Schmehl, R. H.; Turro, C. An Overview of Photosubstitution Reactions of RU(II) Imine Complexes and Their Application in Photobiology and Photodynamic Therapy. *Inorg. Chim. Acta* **2017**, *454*, 7−20.
(979) Soupart, A.; Alary, F.; Heully, J.-L.; Elliott, P. I. P.; Dixon, I. M. Recent Progress in Ligand Photorelease Reaction Mechanisms: Theoretical Insights Focusing on Ru^{II} ^{3}MC States. *Coord. Chem. Rev.* **2020**, *408*, 213184.
(980) Huisman, M.; White, J. K.; Lewalski, V. G.; Podgorski, I.; Turro, C.; Kodanko, J. J. Caging the Uncageable: Using Metal Complex Release for Photochemical Control Over Irreversible Inhibition. *Chem. Commun.* **2016**, *52*, 12590−12593.
(981) Fleming, F. F.; Yao, L. H.; Ravikumar, P. C.; Funk, L.; Shook, B. C. Nitrile-Containing Pharmaceuticals: Efficacious Roles of the Nitrile Pharmacophore. *J. Med. Chem.* **2010**, *53*, 7902−7917.
(982) Sun, W.; Thiramanas, R.; Slep, L. D.; Zeng, X. L.; Mailander, V.; Wu, S. Photoactivation of Anticancer Ru Complexes in Deep Tissue: How Deep Can We Go? *Chem. - Eur. J.* **2017**, *23*, 10832−10837.
(983) Pinnick, D. V.; Durham, B. Photosubstitution Reactions of $Ru(bpy)_2XY^{n+}$ Complexes. *Inorg. Chem.* **1984**, *23*, 1440−1445.
(984) Wacholtz, W. M.; Auerbach, R. A.; Schmehl, R. H.; Ollino, M.; Cherry, W. R. Correlation of Ligand Field Excited-State Energies With Ligand Field Strength in (Polypyridine)Ruthenium(II) Complexes. *Inorg. Chem.* **1985**, *24*, 1758−1760.
(985) Liu, Y.; Turner, D. B.; Singh, T. N.; Angeles-Boza, A. M.; Chouai, A.; Dunbar, K. R.; Turro, C. Ultrafast Ligand Exchange: Detection of a Pentacoordinate Ru(II) Intermediate and Product Formation. *J. Am. Chem. Soc.* **2009**, *131*, 26−27.
(986) Sun, Q.; Mosquera-Vazquez, S.; Suffren, Y.; Hankache, J.; Amstutz, N.; Lawson Daku, L. M.; Vauthey, E.; Hauser, A. On the Role of Ligand-Field States for the Photophysical Properties of Ruthenium(II) Polypyridyl Complexes. *Coord. Chem. Rev.* **2015**, *282-283*, 87−99.
(987) Zayat, L.; Calero, C.; Albores, P.; Baraldo, L.; Etchenique, R. A New Strategy for Neurochemical Photodelivery: Metal-Ligand Heterolytic Cleavage. *J. Am. Chem. Soc.* **2003**, *125*, 882−883.
(988) Nikolenko, V.; Yuste, R.; Zayat, L.; Baraldo, L. M.; Etchenique, R. Two-Photon Uncaging of Neurochemicals Using Inorganic Metal Complexes. *Chem. Commun.* **2005**, 1752−1754.
(989) Filevich, O.; Salierno, M.; Etchenique, R. A Caged Nicotine With Nanosecond Range Kinetics and Visible Light Sensitivity. *J. Inorg. Biochem.* **2010**, *104*, 1248−1251.
(990) Zayat, L.; Noval, M. G.; Campi, J.; Calero, C. I.; Calvo, D. J.; Etchenique, R. A New Inorganic Photolabile Protecting Group for Highly Efficient Visible Light GABA Uncaging. *ChemBioChem* **2007**, *8*, 2035−2038.
(991) Ruiu, T.; Garino, C.; Salassa, L.; Pizarro, A. M.; Nervi, C.; Gobetto, R.; Sadler, P. J. Spectroscopic and Computational Study of Ligand Photodissociation from $[Ru(dipyrido[3,2\text{-}a{:}2',3'\text{-}c]\text{-phenazine})(4\text{-aminopyridine})_4]^{2+}$. *Eur. J. Inorg. Chem.* **2010**, *2010*, 1186−1195.

(992) Salierno, M.; Fameli, C.; Etchenique, R. Caged Amino Acids for Visible-Light Photodelivery. *Eur. J. Inorg. Chem.* **2008**, *2008*, 1125−1128.
(993) Rial Verde, E. M.; Zayat, L.; Etchenique, R.; Yuste, R. Photorelease of GABA with Visible Light Using an Inorganic Caging Group. *Front. Neural Circuits* **2008**, *2*, 2.
(994) Salierno, M.; Marceca, E.; Peterka, D. S.; Yuste, R.; Etchenique, R. A Fast Ruthenium Polypyridine Cage Complex Photoreleases Glutamate With Visible or IR Light in One and Two Photon Regimes. *J. Inorg. Biochem.* **2010**, *104*, 418−422.
(995) Caraballo, R. M.; Rosi, P.; Hodak, J. H.; Baraldo, L. M. Photosubstitution of Monodentate Ligands from Ru-II-Dicarboxybipyridine Complexes. *Eur. J. Inorg. Chem.* **2017**, *2017*, 3612−3621.
(996) Battistin, F.; Balducci, G.; Wei, J. H.; Renfrew, A. K.; Alessio, E. Photolabile Ru Model Complexes with Chelating Diimine Ligands for Light-Triggered Drug Release. *Eur. J. Inorg. Chem.* **2018**, *2018*, 1469−1480.
(997) del Marmol, J.; Filevich, O.; Etchenique, R. A Ruthenium-Rhodamine Complex as an Activatable Fluorescent Probe. *Anal. Chem.* **2010**, *82*, 6259−6264.
(998) Wachter, E.; Heidary, D. K.; Howerton, B. S.; Parkin, S.; Glazer, E. C. Light-Activated Ruthenium Complexes Photobind DNA and Are Cytotoxic in the Photodynamic Therapy Window. *Chem. Commun.* **2012**, *48*, 9649−9651.
(999) Knoll, J. D.; Albani, B. A.; Durr, C. B.; Turro, C. Unusually Efficient Pyridine Photodissociation from Ru(II) Complexes with Sterically Bulky Bidentate Ancillary Ligands. *J. Phys. Chem. A* **2014**, *118*, 10603−10610.
(1000) Salassa, L.; Garino, C.; Salassa, G.; Gobetto, R.; Nervi, C. Mechanism of Ligand Photodissociation in Photoactivable Ru-$(bpy)_2L_2^{2+}$ Complexes: A Density Functional Theory Study. *J. Am. Chem. Soc.* **2008**, *130*, 9590−9597.
(1001) Salassa, L.; Garino, C.; Salassa, G.; Nervi, C.; Gobetto, R.; Lamberti, C.; Gianolio, D.; Bizzarri, R.; Sadler, P. J. Ligand-Selective Photodissociation from $Ru(bpy)(4AP)_4^{2+}$: A Spectroscopic and Computational Study. *Inorg. Chem.* **2009**, *48*, 1469−1481.
(1002) Gottle, A. J.; Alary, F.; Boggio-Pasqua, M.; Dixon, I. M.; Heully, J. L.; Bahreman, A.; Askes, S. H. C.; Bonnet, S. Pivotal Role of a Pentacoordinate (MC)-M-3 State on the Photocleavage Efficiency of a Thioether Ligand in Ruthenium(II) Complexes: A Theoretical Mechanistic Study. *Inorg. Chem.* **2016**, *55*, 4448−4456.
(1003) Loftus, L. M.; Al-Afyouni, K. F.; Rohrabaugh, T. N.; Gallucci, J. C.; Moore, C. E.; Rack, J. J.; Turro, C. Unexpected Role of Ru(II) Orbital and Spin Contribution on Photoinduced Ligand Exchange: New Mechanism To Access the Photodynamic Therapy Window. *J. Phys. Chem. C* **2019**, *123*, 10291−10299.
(1004) van Rixel, V. H. S.; Ramu, V.; Auyeung, A. B.; Beztsinna, N.; Leger, D. Y.; Lameijer, L. N.; Hilt, S. T.; Le Dévédec, S. E.; Yildiz, T.; Betancourt, T.; Gildner, M. B.; Hudnall, T. W.; Sol, V.; Liagre, B.; Kornienko, A.; Bonnet, S. Photo-Uncaging of a Microtubule-Targeted Rigidin Analogue in Hypoxic Cancer Cells and in a Xenograft Mouse Model. *J. Am. Chem. Soc.* **2019**, *141*, 18444−18454.
(1005) Loftus, L. M.; Al-Afyouni, K. F.; Turro, C. New RuII Scaffold for Photoinduced Ligand Release with Red Light in the Photodynamic Therapy (PDT) Window. *Chem. - Eur. J.* **2018**, *24*, 11550−11553.
(1006) Li, A.; White, J. K.; Arora, K.; Herroon, M. K.; Martin, P. D.; Schlegel, H. B.; Podgorski, I.; Turro, C.; Kodanko, J. J. Selective Release of Aromatic Heterocycles from Ruthenium Tris(2-pyridylmethyl)amine with Visible Light. *Inorg. Chem.* **2016**, *55*, 10−12.
(1007) Sharma, R.; Knoll, J. D.; Martin, P. D.; Podgorski, I.; Turro, C.; Kodanko, J. J. Ruthenium Tris(2-pyridylmethyl)amine as an Effective Photocaging Group for Nitriles. *Inorg. Chem.* **2014**, *53*, 3272−3274.
(1008) Arora, K.; White, J. K.; Sharma, R.; Mazumder, S.; Martin, P. D.; Schlegel, H. B.; Turro, C.; Kodanko, J. J. Effects of Methyl Substitution in Ruthenium Tris(2-pyridylmethyl)amine Photocaging Groups for Nitriles. *Inorg. Chem.* **2016**, *55*, 6968−6979.
(1009) Loftus, L. M.; Li, A.; Fillman, K. L.; Martin, P. D.; Kodanko, J. J.; Turro, C. Unusual Role of Excited State Mixing in the Enhancement of Photoinduced Ligand Exchange in Ru(II) Complexes. *J. Am. Chem. Soc.* **2017**, *139*, 18295−18306.
(1010) Bahreman, A.; Limburg, B.; Siegler, M. A.; Bouwman, E.; Bonnet, S. Spontaneous Formation in the Dark, and Visible Light-Induced Cleavage, of a Ru-S Bond in Water: A Thermodynamic and Kinetic Study. *Inorg. Chem.* **2013**, *52*, 9456−9469.
(1011) Bahreman, A.; Limburg, B.; Siegler, M. A.; Koning, R.; Koster, A. J.; Bonnet, S. Ruthenium Polypyridyl Complexes Hopping at Anionic Lipid Bilayers through a Supramolecular Bond Sensitive to Visible Light. *Chem. - Eur. J.* **2012**, *18*, 10271−10280.
(1012) Chan, H.; Ghrayche, J. B.; Wei, J. H.; Renfrew, A. K. Photolabile Ruthenium(II)-Purine Complexes: Phototoxicity, DNA Binding, and Light-Triggered Drug Release. *Eur. J. Inorg. Chem.* **2017**, *2017*, 1679−1686.
(1013) Ragazzon, G.; Bratsos, I.; Alessio, E.; Salassa, L.; Habtemariam, A.; McQuitty, R. J.; Clarkson, G. J.; Sadler, P. J. Design of Photoactivatable Metallodrugs: Selective and Rapid Light-Induced Ligand Dissociation From Half-Sandwich $[Ru([9]aneS_3)(N{-}N')(py)]^{2+}$ Complexes. *Inorg. Chim. Acta* **2012**, *393*, 230−238.
(1014) Finazzi, I.; Bratsos, I.; Gianferrara, T.; Bergamo, A.; Demitri, N.; Balducci, G.; Alessio, E. Photolabile Ru-II Half-Sandwich Complexes Suitable for Developing "Caged" Compounds: Chemical Investigation and Unexpected Dinuclear Species with Bridging Diamine Ligands. *Eur. J. Inorg. Chem.* **2013**, *2013*, 4743−4753.
(1015) Bratsos, I.; Alessio, E. The Pivotal Role of Ru-DMSO Compounds in the Discovery of Well-Behaved Precursors. *Eur. J. Inorg. Chem.* **2018**, *2018*, 2996−3013.
(1016) Respondek, T.; Garner, R. N.; Herroon, M. K.; Podgorski, I.; Turro, C.; Kodanko, J. J. Light Activation of a Cysteine Protease Inhibitor: Caging of a Peptidomimetic Nitrile with $Ru^{II}(bpy)_2$. *J. Am. Chem. Soc.* **2011**, *133*, 17164−17167.
(1017) Ramalho, S. D.; Sharma, R.; White, J. K.; Aggarwal, N.; Chalasani, A.; Sameni, M.; Moin, K.; Vieira, P. C.; Turro, C.; Kodanko, J. J.; Sloane, B. F. Imaging Sites of Inhibition of Proteolysis in Pathomimetic Human Breast Cancer Cultures by Light-Activated Ruthenium Compound. *PLoS One* **2015**, *10*, e0142527.
(1018) Herroon, M. K.; Sharma, R.; Rajagurubandara, E.; Turro, C.; Kodanko, J. J.; Podgorski, I. Photoactivated Inhibition of Cathepsin K in a 3D Tumor Model. *Biol. Chem.* **2016**, *397*, 571−582.
(1019) Lameijer, L. N.; Ernst, D.; Hopkins, S. L.; Meijer, M. S.; Askes, S. H. C.; Le Devedec, S. E.; Bonnet, S. A Red-Light-Activated Ruthenium-Caged NAMPT Inhibitor Remains Phototoxic in Hypoxic Cancer Cells. *Angew. Chem., Int. Ed.* **2017**, *56*, 11549−11553.
(1020) Zamora, A.; Denning, C. A.; Heidary, D. K.; Wachter, E.; Nease, L. A.; Ruiz, J.; Glazer, E. C. Ruthenium-Containing p450 Inhibitors for Dual Enzyme Inhibition and DNA Damage. *Dalton Trans.* **2017**, *46*, 2165−2173.
(1021) Li, A.; Yadav, R.; White, J. K.; Herroon, M. K.; Callahan, B. P.; Podgorski, I.; Turro, C.; Scott, E. E.; Kodanko, J. J. Illuminating Cytochrome P450 Binding: Ru(II)-Caged Inhibitors of CYP17A1. *Chem. Commun.* **2017**, *53*, 3673−3676.
(1022) Wei, J. H.; Renfrew, A. K. Photolabile Ruthenium Complexes to Cage and Release a Highly Cytotoxic Anticancer Agent. *J. Inorg. Biochem.* **2018**, *179*, 146−153.
(1023) Karaoun, N.; Renfrew, A. K. A Luminescent Ruthenium(II) Complex for Light-Triggered Drug Release and Live Cell Imaging. *Chem. Commun.* **2015**, *51*, 14038−14041.
(1024) Smith, N. A.; Zhang, P. Y.; Greenough, S. E.; Horbury, M. D.; Clarkson, G. J.; McFeely, D.; Habtemariam, A.; Salassa, L.; Stavros, V. G.; Dowson, C. G.; Sadler, P. J. Combatting AMR: Photoactivatable Ruthenium(II)-Isoniazid Complex Exhibits Rapid Selective Antimycobacterial Activity. *Chem. Sci.* **2017**, *8*, 395−404.
(1025) Garner, R. N.; Gallucci, J. C.; Dunbar, K. R.; Turro, C. $Ru(bpy)_2(5\text{-cyanouracil})_2^{2+}$ as a Potential Light-Activated Dual-Action Therapeutic Agent. *Inorg. Chem.* **2011**, *50*, 9213−9215.
(1026) Sgambellone, M. A.; David, A.; Garner, R. N.; Dunbar, K. R.; Turro, C. Cellular Toxicity Induced by the Photorelease of a Caged

Bioactive Molecule: Design of a Potential Dual-Action Ru(II) Complex. *J. Am. Chem. Soc.* **2013**, *135*, 11274−11282.
(1027) Mosquera, J.; Sanchez, M. I.; Mascarenas, J. L.; Vazquez, M. E. Synthetic Peptides Caged on Histidine Residues With a Bisbipyridyl Ruthenium(II) Complex That Can Be Photolyzed by Visible Light. *Chem. Commun.* **2015**, *51*, 5501−5504.
(1028) Sharma, R.; Knoll, J. D.; Ancona, N.; Martin, P. D.; Turro, C.; Kodanko, J. J. Solid-Phase Synthesis as a Platform for the Discovery of New Ruthenium Complexes for Efficient Release of Photocaged Ligands with Visible Light. *Inorg. Chem.* **2015**, *54*, 1901−1911.
(1029) Theis, S.; Iturmendi, A.; Gorsche, C.; Orthofer, M.; Lunzer, M.; Baudis, S.; Ovsianikov, A.; Liska, R.; Monkowius, U.; Teasdale, I. Metallo-Supramolecular Gels that are Photocleavable with Visible and Near-Infrared Irradiation. *Angew. Chem., Int. Ed.* **2017**, *56*, 15857−15860.
(1030) Teasdale, I.; Theis, S.; Iturmendi, A.; Strobel, M.; Hild, S.; Jacak, J.; Mayrhofer, P.; Monkowius, U. Dynamic Supramolecular Ruthenium-Based Gels Responsive to Visible/NIR Light and Heat. *Chem. - Eur. J.* **2019**, *25*, 9851−9855.
(1031) Albani, B. A.; Peña, B.; Leed, N. A.; de Paula, N. A. B. G.; Pavani, C.; Baptista, M. S.; Dunbar, K. R.; Turro, C. Marked Improvement in Photoinduced Cell Death by a New Tris-heteroleptic Complex with Dual Action: Singlet Oxygen Sensitization and Ligand Dissociation. *J. Am. Chem. Soc.* **2014**, *136*, 17095−17101.
(1032) Knoll, J. D.; Albani, B. A.; Turro, C. Excited State Investigation of a New Ru(II) Complex for Dual Reactivity With Low Energy Light. *Chem. Commun.* **2015**, *51*, 8777−8780.
(1033) Loftus, L. M.; White, J. K.; Albani, B. A.; Kohler, L.; Kodanko, J. J.; Thummel, R. P.; Dunbar, K. R.; Turro, C. New Ru-II Complex for Dual Activity: Photoinduced Ligand Release and O-1(2) Production. *Chem. - Eur. J.* **2016**, *22*, 3704−3708.
(1034) Carneiro, Z. A.; de Moraes, J. C. B.; Rodrigues, F. P.; de Lima, R. G.; Curti, C.; da Rocha, Z. N.; Paulo, M.; Bendhack, L. M.; Tedesco, A. C.; Formiga, A. L. B.; da Silva, R. S. Photocytotoxic Activity of a Nitrosyl Phthalocyanine Ruthenium Complex - A System Capable of Producing Nitric Oxide and Singlet Oxygen. *J. Inorg. Biochem.* **2011**, *105*, 1035−1043.
(1035) Burya, S. J.; Palmer, A. M.; Gallucci, J. C.; Turro, C. Photoinduced Ligand Exchange and Covalent DNA Binding by Two New Dirhodium Bis-Amidato Complexes. *Inorg. Chem.* **2012**, *51*, 11882−11890.
(1036) Chifotides, H. T.; Lutterman, D. A.; Dunbar, K. R.; Turro, C. Insight into the Photoinduced Ligand Exchange Reaction Pathway of cis- $Rh_2((-O_2CCH_3)_2(CH_3CN)_6^{2+}$ with a DNA Model Chelate. *Inorg. Chem.* **2011**, *50*, 12099−12107.
(1037) Li, Z. Y.; Burya, S. J.; Turro, C.; Dunbar, K. R. Photochemistry and DNA Photocleavage by a new Unsupported Dirhodium(II, II) Complex. *Philos. Trans. R. Soc., A* **2013**, *371*, 20120128.
(1038) Akhimie, R. N.; White, J. K.; Turro, C. Dual Photoreactivity of a New Rh_2(II, II) Complex for Biological Applications. *Inorg. Chim. Acta* **2017**, *454*, 149−154.
(1039) Bednarski, P. J.; Mackay, F. S.; Sadler, P. J. Photoactivatable Platinum Complexes. *Anti-Cancer Agents Med. Chem.* **2007**, *7*, 75−93.
(1040) Wilson, J. J.; Lippard, S. J. Synthetic Methods for the Preparation of Platinum Anticancer Complexes. *Chem. Rev.* **2014**, *114*, 4470−4495.
(1041) Farrer, N. J.; Woods, J. A.; Salassa, L.; Zhao, Y.; Robinson, K. S.; Clarkson, G.; Mackay, F. S.; Sadler, P. J. A Potent Trans-Diimine Platinum Anticancer Complex Photoactivated by Visible Light. *Angew. Chem., Int. Ed.* **2010**, *49*, 8905−8908.
(1042) Zhao, Y.; Woods, J. A.; Farrer, N. J.; Robinson, K. S.; Pracharova, J.; Kasparkova, J.; Novakova, O.; Li, H. L.; Salassa, L.; Pizarro, A. M.; Clarkson, G. J.; Song, L. J.; Brabec, V.; Sadler, P. J. Diazido Mixed-Amine Platinum(IV) Anticancer Complexes Activatable by Visible-Light Form Novel DNA Adducts. *Chem. - Eur. J.* **2013**, *19*, 9578−9591.
(1043) Zhao, Y.; Farrer, N. J.; Li, H. L.; Butler, J. S.; McQuitty, R. J.; Habtemariam, A.; Wang, F. Y.; Sadler, P. J. De Novo Generation of Singlet Oxygen and Ammine Ligands by Photoactivation of a Platinum Anticancer Complex. *Angew. Chem., Int. Ed.* **2013**, *52*, 13633−13637.
(1044) Butler, J. S.; Woods, J. A.; Farrer, N. J.; Newton, M. E.; Sadler, P. J. Tryptophan Switch for a Photoactivated Platinum Anticancer Complex. *J. Am. Chem. Soc.* **2012**, *134*, 16508−16511.
(1045) Venkatesh, V.; Mishra, N. K.; Romero-Canelón, I.; Vernooij, R. R.; Shi, H.; Coverdale, J. P. C.; Habtemariam, A.; Verma, S.; Sadler, P. J. Supramolecular Photoactivatable Anticancer Hydrogels. *J. Am. Chem. Soc.* **2017**, *139*, 5656−5659.
(1046) Yao, K.; Bertran, A.; Howarth, A.; Goicoechea, J. M.; Hare, S. M.; Rees, N. H.; Foroozandeh, M.; Bowen, A. M.; Farrer, N. J. A Visible-Light Photoactivatable di-Nuclear Pt^{IV} Triazolato Azido Complex. *Chem. Commun.* **2019**, *55*, 11287−11290.
(1047) Deng, Z.; Wang, N.; Liu, Y.; Xu, Z.; Wang, Z.; Lau, T.-C.; Zhu, G. A Photocaged, Water-Oxidizing, and Nucleolus-Targeted Pt(IV) Complex with a Distinct Anticancer Mechanism. *J. Am. Chem. Soc.* **2020**, *142*, 7803−7812.
(1048) Mitra, K.; Gautam, S.; Kondaiah, P.; Chakravarty, A. R. The cis-Diammineplatinum(II) Complex of Curcumin: A Dual Action DNA Crosslinking and Photochemotherapeutic Agent. *Angew. Chem., Int. Ed.* **2015**, *54*, 13989−13993.
(1049) Mitra, K.; Gautam, S.; Kondaiah, P.; Chakravarty, A. R. Platinum(II) Complexes of Curcumin Showing Photocytotoxicity in Visible Light. *Eur. J. Inorg. Chem.* **2017**, *2017*, 1753−1763.
(1050) Bhattacharyya, A.; Dixit, A.; Mitra, K.; Banerjee, S.; Karande, A. A.; Chakravarty, A. R. BODIPY Appended Copper(II) Complexes of Curcumin Showing Mitochondria Targeted Remarkable Photocytotoxicity in Visible Light. *MedChemComm* **2015**, *6*, 846−851.
(1051) Ramu, V.; Gautam, S.; Garai, A.; Kondaiah, P.; Chakravarty, A. R. Glucose-Appended Platinum(II)-BODIPY Conjugates for Targeted Photodynamic Therapy in Red Light. *Inorg. Chem.* **2018**, *57*, 1717−1726.
(1052) Mitra, K.; Shettar, A.; Kondaiah, P.; Chakravarty, A. R. Biotinylated Platinum(II) Ferrocenylterpyridine Complexes for Targeted Photoinduced Cytotoxicity. *Inorg. Chem.* **2016**, *55*, 5612−5622.
(1053) Mitra, K.; Lyons, C. E.; Hartman, M. C. T. A Platinum(II) Complex of Heptamethine Cyanine for Photoenhanced Cytotoxicity and Cellular Imaging in Near-IR Light. *Angew. Chem., Int. Ed.* **2018**, *57*, 10263−10267.
(1054) Downward, A. M.; Moore, E. G.; Hartshorn, R. M. Photoinduced Ligand Release in a Ruthenium(II)-Cobalt(III) Heterodinuclear Systembasic Understanding of the Lanthanide Related Upconversion Emissions. *Chem. Commun.* **2011**, *47*, 7692−7694.
(1055) Garai, A.; Pant, I.; Banerjee, S.; Banik, B.; Kondaiah, P.; Chakravarty, A. R. Photorelease and Cellular Delivery of Mitocurcumin from Its Cytotoxic Cobalt(III) Complex in Visible Light. *Inorg. Chem.* **2016**, *55*, 6027−6035.
(1056) Jana, A.; Verma, B. K.; Garai, A.; Kondaiah, P.; Chakravarty, A. R. Mitochondria Localizing High-Spin Iron Complexes of Curcumin for Photo-Induced Drug Release. *Inorg. Chim. Acta* **2018**, *483*, 571−578.
(1057) Giammanco, G. E.; Sosnofsky, C. T.; Ostrowski, A. D. Light-Responsive Iron(III)-Polysaccharide Coordination Hydrogels for Controlled Delivery. *ACS Appl. Mater. Interfaces* **2015**, *7*, 3068−3076.
(1058) Donald, J. A. Chapter 103 - Gasotransmitter Family. *Handbook of Hormones*; Takei, Y., Ando, H., Tsutsui, K., Eds.; Academic Press: San Diego, 2016.
(1059) Wareham, L. K.; Southam, H. M.; Poole, R. K. Do Nitric Oxide, Carbon Monoxide and Hydrogen Sulfide Really Qualify as 'Gasotransmitters' in Bacteria? *Biochem. Soc. Trans.* **2018**, *46*, 1107−1118.
(1060) Thorup, C.; Jones, C. L.; Gross, S. S.; Moore, L. C.; Goligorsky, M. S. Carbon Monoxide Induces Vasodilation and Nitric

Oxide Release but Suppresses Endothelial NOS. *Am. J. Physiol.-Renal* **1999**, *277*, F882−F889.
(1061) Romao, C. C.; Blattler, W. A.; Seixas, J. D.; Bernardes, G. J. L. Developing Drug Molecules for Therapy With Carbon Monoxide. *Chem. Soc. Rev.* **2012**, *41*, 3571−3583.
(1062) Queiroga, C. S. F.; Tomasi, S.; Widerøe, M.; Alves, P. M.; Vercelli, A.; Vieira, H. L. A. Preconditioning Triggered by Carbon Monoxide (CO) Provides Neuronal Protection Following Perinatal Hypoxia-Ischemia. *PLoS One* **2012**, *7*, No. e42632.
(1063) Otterbein, L. E.; Bach, F. H.; Alam, J.; Soares, M.; Tao Lu, H.; Wysk, M.; Davis, R. J.; Flavell, R. A.; Choi, A. M. K. Carbon Monoxide has Anti-Inflammatory Effects Involving the Mitogen-Activated Protein Kinase Pathway. *Nat. Med.* **2000**, *6*, 422−428.
(1064) Brandi, C.; Grimaldi, L.; Nisi, G.; Brafa, A.; Campa, A.; Calabrò, M.; Campana, M.; D'Aniello, C. The Role of Carbon Dioxide Therapy in the Treatment of Chronic Wounds. *In Vivo* **2010**, *24*, 223−226.
(1065) Schäffer, M. R.; Tantry, U.; Gross, S. S.; Wasserkrug, H. L.; Barbul, A. Nitric Oxide Regulates Wound Healing. *J. Surg. Res.* **1996**, *63*, 237−240.
(1066) Radomski, M. W.; Palmer, R. M. J.; Moncada, S. The Role of Nitric Oxide and cGMP in Platelet Adhesion to Vascular Endothelium. *Biochem. Biophys. Res. Commun.* **1987**, *148*, 1482−1489.
(1067) Garthwaite, J.; Boulton, C. L. Nitric Oxide Signaling in the Central Nervous System. *Annu. Rev. Physiol.* **1995**, *57*, 683−706.
(1068) Gullotta, F.; Masi, A. d.; Ascenzi, P. Carbon Monoxide: An Unusual Drug. *IUBMB Life* **2012**, *64*, 378−386.
(1069) Bloch, K. D.; Ichinose, F.; Roberts, J. D., Jr.; Zapol, W. M. Inhaled NO as a Therapeutic Agent. *Cardiovasc. Res.* **2007**, *75*, 339−348.
(1070) Motterlini, R.; Otterbein, L. E. The Therapeutic Potential of Carbon Monoxide. *Nat. Rev. Drug Discovery* **2010**, *9*, 728−U724.
(1071) Heinemann, S. H.; Hoshi, T.; Westerhausen, M.; Schiller, A. Carbon Monoxide - Physiology, Detection and Controlled Release. *Chem. Commun.* **2014**, *50*, 3644−3660.
(1072) Yang, X.-X.; Ke, B.-W.; Lu, W.; Wang, B.-H. CO as a Therapeutic Agent: Discovery and Delivery Forms. *Chin. J. Nat. Medicines* **2020**, *18*, 284−295.
(1073) Zhou, Y.; Yu, W.; Cao, J.; Gao, H. Harnessing Carbon Monoxide-Releasing Platforms for Cancer Therapy. *Biomaterials* **2020**, *255*, 120193.
(1074) Stucki, D.; Stahl, W. Carbon Monoxide − Beyond Toxicity? *Toxicol. Lett.* **2020**, *333*, 251−260.
(1075) Russo, M.; Štacko, P.; Nachtigallová, D.; Klán, P. Mechanisms of Orthogonal Photodecarbonylation Reactions of 3-Hydroxyflavone-Based Acid−Base Forms. *J. Org. Chem.* **2020**, *85*, 3527−3537.
(1076) Anderson, S. N.; Richards, J. M.; Esquer, H. J.; Benninghoff, A. D.; Arif, A. M.; Berreau, L. M. A Structurally-Tunable 3-Hydroxyflavone Motif for Visible Light-Induced Carbon Monoxide-Releasing Molecules (CORMs). *ChemistryOpen* **2015**, *4*, 590−594.
(1077) Ieda, N.; Hotta, Y.; Miyata, N.; Kimura, K.; Nakagawa, H. Photomanipulation of Vasodilation with a Blue-Light-Controllable Nitric Oxide Releaser. *J. Am. Chem. Soc.* **2014**, *136*, 7085−7091.
(1078) Zhang, Z.; Wu, J.; Shang, Z.; Wang, C.; Cheng, J.; Qian, X.; Xiao, Y.; Xu, Z.; Yang, Y. Photocalibrated NO Release from *N*-Nitrosated Napthalimides upon One-Photon or Two-Photon Irradiation. *Anal. Chem.* **2016**, *88*, 7274−7280.
(1079) Gonzalez, M. A.; Carrington, S. J.; Fry, N. L.; Martinez, J. L.; Mascharak, P. K. Syntheses, Structures, and Properties of New Manganese Carbonyls as Photoactive CO-Releasing Molecules: Design Strategies that Lead to CO Photolability in the Visible Region. *Inorg. Chem.* **2012**, *51*, 11930−11940.
(1080) Carrington, S. J.; Chakraborty, I.; Mascharak, P. K. Exceptionally Rapid CO Release from a Manganese(I) Tricarbonyl Complex Derived from Bis(4-chloro-phenylimino)acenaphthene upon Exposure to Visible Light. *Dalton Trans.* **2015**, *44*, 13828−13834.
(1081) Eroy-Reveles, A. A.; Leung, Y.; Beavers, C. M.; Olmstead, M. M.; Mascharak, P. K. Near-Infrared Light Activated Release of Nitric Oxide from Designed Photoactive Manganese Nitrosyls: Strategy, Design, and Potential as NO Donors. *J. Am. Chem. Soc.* **2008**, *130*, 4447−4458.
(1082) Hoffman-Luca, C. G.; Eroy-Reveles, A. A.; Alvarenga, J.; Mascharak, P. K. Syntheses, Structures, and Photochemistry of Manganese Nitrosyls Derived from Designed Schiff Base Ligands: Potential NO Donors That Can Be Activated by Near-Infrared Light. *Inorg. Chem.* **2009**, *48*, 9104−9111.
(1083) Woods, J. J.; Cao, J.; Lippert, A. R.; Wilson, J. J. Characterization and Biological Activity of a Hydrogen Sulfide-Releasing Red Light-Activated Ruthenium(II) Complex. *J. Am. Chem. Soc.* **2018**, *140*, 12383−12387.
(1084) Jimenez, R.; Kable, S. H.; Loison, J. C.; Simpson, C. J. S. M.; Adam, W.; Houston, P. L. Photodissociation Dynamics of 3-Cyclopentenone: Using the Impact Parameter Distribution as a Criterion for Concertedness. *J. Phys. Chem.* **1992**, *96*, 4188−4195.
(1085) Mondal, R.; Okhrimenko, A. N.; Shah, B. K.; Neckers, D. C. Photodecarbonylation of α-Diketones: A Mechanistic Study of Reactions Leading to Acenes. *J. Phys. Chem. B* **2008**, *112*, 11−15.
(1086) Michael, E.; Abeyrathna, N.; Patel, A. V.; Liao, Y.; Bashur, C. A. Incorporation of Photo-Carbon Monoxide Releasing Materials into Electrospun Scaffolds for Vascular Tissue Engineering. *Biomed. Mater.* **2016**, *11*, 025009.
(1087) Peng, P.; Wang, C.; Shi, Z.; Johns, V. K.; Ma, L.; Oyer, J.; Copik, A.; Igarashi, R.; Liao, Y. Visible-Light Activatable Organic CO-Releasing Molecules (PhotoCORMs) That Simultaneously Generate Fluorophores. *Org. Biomol. Chem.* **2013**, *11*, 6671−6674.
(1088) Elgattar, A.; Washington, K. S.; Talebzadeh, S.; Alwagdani, A.; Khalil, T.; Alghazwat, O.; Alshammri, S.; Pal, H.; Bashur, C.; Liao, Y. Poly(butyl Cyanoacrylate) Nanoparticle Containing an Organic PhotoCORM. *Photochem. Photobiol. Sci.* **2019**, *18*, 2666−2672.
(1089) Thapaliya, E. R.; Swaminathan, S.; Captain, B.; Raymo, F. M. Autocatalytic Fluorescence Photoactivation. *J. Am. Chem. Soc.* **2014**, *136*, 13798−13804.
(1090) Aotake, T.; Suzuki, M.; Tahara, K.; Kuzuhara, D.; Aratani, N.; Tamai, N.; Yamada, H. An Optically and Thermally Switchable Electronic Structure Based on an Anthracene−BODIPY Conjugate. *Chem. - Eur. J.* **2015**, *21*, 4966−4974.
(1091) Mondal, R.; Shah, B. K.; Neckers, D. C. Photogeneration of Heptacene in a Polymer Matrix. *J. Am. Chem. Soc.* **2006**, *128*, 9612−9613.
(1092) Mondal, R.; Adhikari, R. M.; Shah, B. K.; Neckers, D. C. Revisiting the Stability of Hexacenes. *Org. Lett.* **2007**, *9*, 2505−2508.
(1093) Gilbert, B. C.; Hodges, G. R.; Smith, J. R. L.; MacFaul, P.; Taylor, P. Photodecarboxylation of Substituted Alkylcarboxylic Acids Brought about by Visible Light and Iron(III) tetra(2-*N*-Methylpyridyl)porphyrin in Aqueous Solution. *J. Chem. Soc., Perkin Trans. 2* **1996**, *2*, 519−524.
(1094) Griffiths, H. R.; Gao, D.; Pararasa, C. Redox Regulation in Metabolic Programming and Inflammation. *Redox Biol.* **2017**, *12*, 50−57.
(1095) Banerjee, R. Redox outside the Box: Linking Extracellular Redox Remodeling with Intracellular Redox Metabolism. *J. Biol. Chem.* **2012**, *287*, 4397−4402.
(1096) Matsuura, T.; Matsushima, H.; Sakamoto, H. Photosensitized Oxygenation of 3-Hydroxyflavones. Possible Model for Biological Oxygenation. *J. Am. Chem. Soc.* **1967**, *89*, 6370−6371.
(1097) Studer, S. L.; Brewer, W. E.; Martinez, M. L.; Chou, P. T. Time-Resolved Study of the Photooxygenation of 3-Hydroxyflavone. *J. Am. Chem. Soc.* **1989**, *111*, 7643−7644.
(1098) Tournaire, C.; Croux, S.; Maurette, M.-T.; Beck, I.; Hocquaux, M.; Braun, A. M.; Oliveros, E. Antioxidant Activity of Flavonoids: Efficiency of Singlet Oxygen ($^1\Delta_g$) Quenching. *J. Photochem. Photobiol., B* **1993**, *19*, 205−215.
(1099) Protti, S.; Mezzetti, A.; Lapouge, C.; Cornard, J.-P. Photochemistry of Metal Complexes of 3-Hydroxyflavone: Towards a Better Understanding of the Influence of Solar Light on the Metal−

Soil Organic Matter Interactions. *Photochem. Photobiol. Sci.* **2008**, *7*, 109−119.
(1100) Matsuura, T.; Takemoto, T.; Nakashima, R. Photoinduced Reactions-LXXI: Photorearrangement of 3-Hydroxyflavones to 3-Aryl-3-Hydroxy-1,2-Indandiones. *Tetrahedron* **1973**, *29*, 3337−3340.
(1101) Szakács, Z.; Bojtár, M.; Drahos, L.; Hessz, D.; Kállay, M.; Vidóczy, T.; Bitter, I.; Kubinyi, M. The Kinetics and Mechanism of Photooxygenation of 4′-Diethylamino-3-hydroxyflavone. *Photochem. Photobiol. Sci.* **2016**, *15*, 219−227.
(1102) Mierziak, J.; Kostyn, K.; Kulma, A. Flavonoids as Important Molecules of Plant Interactions with the Environment. *Molecules* **2014**, *19*, 16240−16265.
(1103) Anderson, S. N.; Noble, M.; Grubel, K.; Marshall, B.; Arif, A. M.; Berreau, L. M. Influence of Supporting Ligand Microenvironment on the Aqueous Stability and Visible Light-Induced CO-Release Reactivity of Zinc Flavonolato Species. *J. Coord. Chem.* **2014**, *67*, 4061−4075.
(1104) Su, Y.; Yang, W.; Yang, X.; Zhang, R.; Zhao, J. Visible Light-Induced CO-Release Reactivity of a Series of Zn^{II}−Flavonolate Complexes. *Aust. J. Chem.* **2018**, *71*, 549−558.
(1105) Sorenson, S.; Popova, M.; Arif, A. M.; Berreau, L. M. A Bipyridine-Ligated Zinc(II) Complex with Bridging Flavonolate Ligation: Synthesis, Characterization, and Visible-Light-Induced CO Release Reactivity. *Acta Crystallogr., Sect. C: Struct. Chem.* **2017**, *73*, 703−709.
(1106) Saraf, S. L.; Fish, T. J.; Benninghoff, A. D.; Buelt, A. A.; Smith, R. C.; Berreau, L. M. Photochemical Reactivity of $Ru^{II}(\eta^6$-*p*-cymene) Flavonolato Compounds. *Organometallics* **2014**, *33*, 6341−6351.
(1107) Han, X.; Klausmeyer, K. K.; Farmer, P. J. Characterization of the Initial Intermediate Formed during Photoinduced Oxygenation of the Ruthenium(II) Bis(bipyridyl)flavonolate Complex. *Inorg. Chem.* **2016**, *55*, 7320−7322.
(1108) Han, X.; Kumar, M. R.; Hoogerbrugge, A.; Klausmeyer, K. K.; Ghimire, M. M.; Harris, L. M.; Omary, M. A.; Farmer, P. J. Mechanistic Investigations of Photoinduced Oxygenation of Ru(II) Bis-bipyridyl Flavonolate Complexes. *Inorg. Chem.* **2018**, *57*, 2416−2424.
(1109) Grubel, K.; Laughlin, B. J.; Maltais, T. R.; Smith, R. C.; Arif, A. M.; Berreau, L. M. Photochemically-Induced Dioxygenase-Type CO-Release Reactivity of Group 12 Metal Flavonolate Complexes. *Chem. Commun.* **2011**, *47*, 10431−10433.
(1110) Popova, M.; Soboleva, T.; Arif, A. M.; Berreau, L. M. Properties of a Flavonol-Based PhotoCORM in Aqueous Buffered Solutions: Influence of Metal Ions, Surfactants and Proteins on Visible Light-Induced CO Release. *RSC Adv.* **2017**, *7*, 21997−22007.
(1111) Soboleva, T.; Benninghoff, A. D.; Berreau, L. M. An H_2S-Sensing/CO-Releasing Flavonol That Operates via Logic Gates. *ChemPlusChem* **2017**, *82*, 1408−1412.
(1112) Soboleva, T.; Esquer, H. J.; Benninghoff, A. D.; Berreau, L. M. Sense and Release: A Thiol-Responsive Flavonol-Based Photonically Driven Carbon Monoxide-Releasing Molecule That Operates via a Multiple-Input AND Logic Gate. *J. Am. Chem. Soc.* **2017**, *139*, 9435−9438.
(1113) Popova, M.; Soboleva, T.; Benninghoff, A. D.; Berreau, L. M. CO Sense and Release Flavonols: Progress toward the Development of an Analyte Replacement PhotoCORM for Use in Living Cells. *ACS Omega* **2020**, *5*, 10021−10033.
(1114) Li, Y.; Shu, Y.; Liang, M.; Xie, X.; Jiao, X.; Wang, X.; Tang, B. A Two-Photon H_2O_2-Activated CO Photoreleaser. *Angew. Chem., Int. Ed.* **2018**, *57*, 12415−12519.
(1115) Cheng, J.; Zheng, B.; Cheng, S.; Zhang, G.; Hu, J. Metal-Free Carbon Monoxide-Releasing Micelles Undergo Tandem Photochemical Reactions for Cutaneous Wound Healing. *Chem. Sci.* **2020**, *11*, 4499−4507.
(1116) Zhang, M.; Cheng, J.; Huang, X.; Zhang, G.; Ding, S.; Hu, J.; Qiao, R. Photo-Degradable Micelles Capable of Releasing of Carbon Monoxide under Visible Light Irradiation. *Macromol. Rapid Commun.* **2020**, *41*, 2000323.
(1117) Soboleva, T.; Esquer, H. J.; Anderson, S. N.; Berreau, L. M.; Benninghoff, A. D. Mitochondrial-Localized Versus Cytosolic Intracellular CO-Releasing Organic PhotoCORMs: Evaluation of CO Effects Using Bioenergetics. *ACS Chem. Biol.* **2018**, *13*, 2220−2228.
(1118) Soboleva, T.; Simons, C. R.; Arcidiacono, A.; Benninghoff, A. D.; Berreau, L. M. Extracellular vs Intracellular Delivery of CO: Does It Matter for a Stable, Diffusible Gasotransmitter? *J. Med. Chem.* **2019**, *62*, 9990−9995.
(1119) Popova, M.; Soboleva, T.; Ayad, S.; Benninghoff, A. D.; Berreau, L. M. Visible-Light-Activated Quinolone Carbon-Monoxide-Releasing Molecule: Prodrug and Albumin-Assisted Delivery Enables Anticancer and Potent Anti-Inflammatory Effects. *J. Am. Chem. Soc.* **2018**, *140*, 9721−9729.
(1120) Feng, W.; Feng, S.; Feng, G. CO Release with Ratiometric Fluorescence Changes: a Promising Visible-Light-Triggered Metal-Free CO-Releasing Molecule. *Chem. Commun.* **2019**, *55*, 8987−8990.
(1121) Schwartz, B. J.; Peteanu, L. A.; Harris, C. B. Direct Observation of Fast Proton Transfer: Femtosecond Photophysics of 3-Hydroxyflavone. *J. Phys. Chem.* **1992**, *96*, 3591−3598.
(1122) Dick, B.; Ernsting, N. P. Excited-State Intramolecular Proton Transfer in 3-Hydroxylflavone Isolated in Solid Argon: Fluoroescence and Fluorescence-Excitation Spectra and Tautomer Fluorescence Rise Time. *J. Phys. Chem.* **1987**, *91*, 4261−4265.
(1123) Dávila, Y. A.; Sancho, M. I.; Almandoz, M. C.; Blanco, S. E. Solvent Effects on the Dissociation Constants of Hydroxyflavones in Organic−Water Mixtures. Determination of the Thermodynamic pKa Values by UV−Visible Spectroscopy and DFT Calculations. *J. Chem. Eng. Data* **2013**, *58*, 1706−1716.
(1124) Štacková, L.; Russo, M.; Muchová, L.; Orel, V.; Vítek, L.; Štacko, P.; Klán, P. Cyanine-Flavonol Hybrid for Near-Infrared Light-Activated Delivery of Carbon Monoxide. *Chem. - Eur. J.* **2020**, *26*, 13184−13190.
(1125) Anderson, S. N.; Larson, M. T.; Berreau, L. M. Solution or Solid − It Doesn't Matter: Visible Light-Induced CO Release Reactivity of Zinc Flavonolato Complexes. *Dalton Trans.* **2016**, *45*, 14570−14580.
(1126) An, S.-Y.; Su, Y.-Y.; Qi, X.; Zhang, R.-L.; Ma, Y.-L.; Zhao, J.-S. Photoinduced Reactivity and Cytotoxicity of a Series of Zinc(II)−Flavonolate Derivative Complexes. *Transition Met. Chem.* **2020**, *45*, 253−266.
(1127) Poloukhtine, A.; Popik, V. V. Highly Efficient Photochemical Generation of a Triple Bond: Synthesis, Properties, and Photodecarbonylation of Cyclopropenones. *J. Org. Chem.* **2003**, *68*, 7833−7840.
(1128) Urdabayev, N. K.; Poloukhtine, A.; Popik, V. V. Two-Photon Induced Photodecarbonylation Reaction of Cyclopropenones. *Chem. Commun.* **2006**, 454−456.
(1129) Wadsworth, D. H.; Donatelli, B. A. Preparation of Diarylacetylenes *via* Cyclopropenones. *Synthesis* **1981**, *1981*, 285−286.
(1130) Becker, H. D.; Andersson, K. On the Relationship between Molecular Geometry and Photochemical Properties of 1,2-Substituted 1,2-Di-9-anthrylethylenes. *J. Org. Chem.* **1987**, *52*, 5205−5213.
(1131) Kuzmanich, G.; Gard, M. N.; Garcia-Garibay, M. A. Photonic Amplification by a Singlet-State Quantum Chain Reaction in the Photodecarbonylation of Crystalline Diarylcyclopropenones. *J. Am. Chem. Soc.* **2009**, *131*, 11606−11614.
(1132) L'Abbé, G. Heterocyclic Analogues of Methylenecyclopropanes. *Angew. Chem., Int. Ed. Engl.* **1980**, *19*, 276−289.
(1133) Showalter, B. M.; Toscano, J. P. Time-Resolved IR Studies of α-Lactones. *J. Phys. Org. Chem.* **2004**, *17*, 743−748.
(1134) Mula, S.; Ray, A. K.; Banerjee, M.; Chaudhuri, T.; Dasgupta, K.; Chattopadhyay, S. Design and Development of a New Pyrromethene Dye with Improved Photostability and Lasing Efficiency: Theoretical Rationalization of Photophysical and Photochemical Properties. *J. Org. Chem.* **2008**, *73*, 2146−2154.
(1135) Costela, A.; García-Moreno, I.; Pintado-Sierra, M.; Amat-Guerri, F.; Liras, M.; Sastre, R.; Arbeloa, F. L.; Prieto, J. B.; Arbeloa, I.

L. New Laser Dye Based on the 3-Styryl Analog of the BODIPY Dye PM567. *J. Photochem. Photobiol., A* **2008**, *198*, 192−199.
(1136) Ortiz, M. J.; Garcia-Moreno, I.; Agarrabeitia, A. R.; Duran-Sampedro, G.; Costela, A.; Sastre, R.; López Arbeloa, F.; Bañuelos Prieto, J.; López Arbeloa, I. Red-Edge-Wavelength Finely-Tunable Laser Action from New BODIPY Dyes. *Phys. Chem. Chem. Phys.* **2010**, *12*, 7804−7811.
(1137) Saito, F.; Tobita, S.; Shizuka, H. Photoionization of Aniline in Aqueous Solution and its Photolysis in Cyclohexane. *J. Chem. Soc., Faraday Trans.* **1996**, *92*, 4177−4185.
(1138) Šolomek, T.; Heger, D.; Ngoy, B. P.; Givens, R. S.; Klán, P. The Pivotal Role of Oxyallyl Diradicals in Photo-Favorskii Rearrangements: Transient Spectroscopic and Computational Studies. *J. Am. Chem. Soc.* **2013**, *135*, 15209−15215.
(1139) Chakraborty, I.; Carrington, S. J.; Mascharak, P. K. Design Strategies To Improve the Sensitivity of Photoactive Metal Carbonyl Complexes (photoCORMs) to Visible Light and Their Potential as CO-Donors to Biological Targets. *Acc. Chem. Res.* **2014**, *47*, 2603−2611.
(1140) Rudolf, P.; Kanal, F.; Knorr, J.; Nagel, C.; Niesel, J.; Brixner, T.; Schatzschneider, U.; Nuernberger, P. Ultrafast Photochemistry of a Manganese-Tricarbonyl CO-Releasing Molecule (CORM) in Aqueous Solution. *J. Phys. Chem. Lett.* **2013**, *4*, 596−602.
(1141) Garino, C.; Salassa, L. The Photochemistry of Transition Metal Complexes Using Density Functional Theory. *Philos. Trans. R. Soc., A* **2013**, *371*, 20120134.
(1142) Sunderlin, L. S.; Wang, D.; Squires, R. R. Bond Strengths in First-Row-Metal Carbonyl Anions. *J. Am. Chem. Soc.* **1993**, *115*, 12060−12070.
(1143) Rimmer, R. D.; Richter, H.; Ford, P. C. A Photochemical Precursor for Carbon Monoxide Release in Aerated Aqueous Media. *Inorg. Chem.* **2010**, *49*, 1180−1185.
(1144) Motterlini, R.; Clark, J. E.; Foresti, R.; Sarathchandra, P.; Mann, B. E.; Green, C. J. Carbon Monoxide-Releasing Molecules. *Circ. Res.* **2002**, *90*, No. e17-e24.
(1145) Zhang, W.-Q.; Atkin, A. J.; Fairlamb, I. J. S.; Whitwood, A. C.; Lynam, J. M. Synthesis and Reactivity of Molybdenum Complexes Containing Functionalized Alkynyl Ligands: A Photochemically Activated CO-Releasing Molecule (PhotoCO-RM). *Organometallics* **2011**, *30*, 4643−4654.
(1146) Chakraborty, I.; Carrington, S. J.; Mascharak, P. K. Photodelivery of CO by Designed PhotoCORMs: Correlation between Absorption in the Visible Region and Metal-CO Bond Labilization in Carbonyl Complexes. *ChemMedChem* **2014**, *9*, 1266−1274.
(1147) Carrington, S. J.; Chakraborty, I.; Mascharak, P. K. Rapid CO Release from a Mn(I) Carbonyl Complex Derived from Azopyridine upon Exposure to Visible Light and Its Phototoxicity Toward Malignant Cells. *Chem. Commun.* **2013**, *49*, 11254−11256.
(1148) Jimenez, J.; Chakraborty, I.; Carrington, S. J.; Mascharak, P. K. Light-Triggered CO Delivery by a Water-Soluble and Biocompatible Manganese PhotoCORM. *Dalton Trans.* **2016**, *45*, 13204−13213.
(1149) Mansour, A. M. Green-Light-Induced PhotoCORM: Lysozyme Binding Affinity towards Mn^I and Re^I Carbonyl Complexes and Biological Activity Evaluation. *Eur. J. Inorg. Chem.* **2018**, *2018*, 4805−4811.
(1150) Kottelat, E.; Ruggi, A.; Zobi, F. Red-Light Activated PhotoCORMs of Mn(I) Species Bearing Electron Deficient 2,2′-Azopyridines. *Dalton Trans.* **2016**, *45*, 6920−6927.
(1151) Mansour, A. M.; Steiger, C.; Nagel, C.; Schatzschneider, U. Wavelength-Dependent Control of the CO Release Kinetics of Manganese(I) Tricarbonyl PhotoCORMs with Benzimidazole Coligands. *Eur. J. Inorg. Chem.* **2019**, *2019*, 4572−4581.
(1152) Atkin, A. J.; Lynam, J. M.; Moulton, B. E.; Sawle, P.; Motterlini, R.; Boyle, N. M.; Pryce, M. T.; Fairlamb, I. J. S. Modification of the Deoxy-Myoglobin/Carbonmonoxy-Myoglobin UV-vis Assay for Reliable Determination of CO-Release Rates from Organometallic Carbonyl Complexes. *Dalton Trans.* **2011**, *40*, 5755−5761.
(1153) Yempally, V.; Kyran, S. J.; Raju, R. K.; Fan, W. Y.; Brothers, E. N.; Darensbourg, D. J.; Bengali, A. A. Thermal and Photochemical Reactivity of Manganese Tricarbonyl and Tetracarbonyl Complexes with a Bulky Diazabutadiene Ligand. *Inorg. Chem.* **2014**, *53*, 4081−4088.
(1154) Kianfar, E.; Apaydin, D. H.; Knor, G. Spin-Forbidden Excitation: A New Approach for Triggering Photopharmacological Processes with Low-Intensity NIR Light. *ChemPhotoChem.* **2017**, *1*, 378−382.
(1155) Yuan, J.; Chen, R.; Tang, X.; Tao, Y.; Xu, S.; Jin, L.; Chen, C.; Zhou, X.; Zheng, C.; Huang, W. Direct Population of Triplet Excited States through Singlet−Triplet Transition for Visible-Light Excitable Organic Afterglow. *Chem. Sci.* **2019**, *10*, 5031−5038.
(1156) Mansour, A. M.; Friedrich, A. Blue-Light Induced CO Releasing Properties of Thiourea Based Manganese(I) Carbonyl Complexes. *Polyhedron* **2017**, *131*, 13−21.
(1157) Mansour, A. M.; Shehab, O. R. Reactivity of Visible-Light Induced CO Releasing Thiourea-Based Mn(I) Tricarbonyl Bromide (CORM-NS1) towards Lysozyme. *Inorg. Chim. Acta* **2018**, *480*, 159−165.
(1158) Govender, P.; Pai, S.; Schatzschneider, U.; Smith, G. S. Next Generation PhotoCORMs: Polynuclear Tricarbonylmanganese(I)-Functionalized Polypyridyl Metallodendrimers. *Inorg. Chem.* **2013**, *52*, 5470−5478.
(1159) Pierri, A. E.; Huang, P. J.; Garcia, J. V.; Stanfill, J. G.; Chui, M.; Wu, G.; Zheng, N.; Ford, P. C. A photoCORM Nanocarrier for CO Release Using NIR Light. *Chem. Commun.* **2015**, *51*, 2072−2075.
(1160) Henke, W. C.; Otolski, C. J.; Moore, W. N. G.; Elles, C. G.; Blakemore, J. D. Ultrafast Spectroscopy of $[Mn(CO)_3]$ Complexes: Tuning the Kinetics of Light-Driven CO Release and Solvent Binding. *Inorg. Chem.* **2020**, *59*, 2178−2187.
(1161) Pordel, S.; White, J. K. Impact of Mn(I) PhotoCORM Ligand Set on Photochemical Intermediate Formation During Visible Light-Activated CO Release. *Inorg. Chim. Acta* **2020**, *500*, 119206.
(1162) Kottelat, E.; Lucarini, F.; Crochet, A.; Ruggi, A.; Zobi, F. Correlation of MLCTs of Group 7 *fac*-$[M(CO)_3]^+$ Complexes (M = Mn, Re) with Bipyridine, Pyridinylpyrazine, Azopyridine, and Pyridin-2-ylmethanimine Type Ligands for Rational photoCORM Design. *Eur. J. Inorg. Chem.* **2019**, *2019*, 3758−3768.
(1163) Ruggi, A.; Zobi, F. Quantum-CORMs: Quantum Dot Sensitized CO Releasing Molecules. *Dalton Trans.* **2015**, *44*, 10928−10931.
(1164) Diring, S.; Carné-Sánchez, A.; Zhang, J.; Ikemura, S.; Kim, C.; Inaba, H.; Kitagawa, S.; Furukawa, S. Light Responsive Metal−Organic Frameworks as Controllable CO-Releasing Cell Culture Substrates. *Chem. Sci.* **2017**, *8*, 2381−2386.
(1165) Hyodo, F.; Sho, T.; Maity, B.; Fujita, K.; Tachibana, Y.; Akashi, S.; Mano, M.; Hishikawa, Y.; Matsuo, M.; Ueno, T. Photoinduced in Vivo Magnetic Resonance Imaging (MRI) with Rapid CO Release from an MnCO-Protein Needle Composite. *Chem. - Eur. J.* **2018**, *24*, 11578−11583.
(1166) Sakla, R.; Singh, A.; Kaushik, R.; Kumar, P.; Jose, D. A. Allosteric Regulation in Carbon Monoxide (CO) Release: Anion Responsive CO-Releasing Molecule (CORM) Derived from (Terpyridine)phenol Manganese Tricarbonyl Complex with Colorimetric and Fluorescence Monitoring. *Inorg. Chem.* **2019**, *58*, 10761−10768.
(1167) Jiang, Q.; Xia, Y.; Barrett, J.; Mikhailovsky, A.; Wu, G.; Wang, D.; Shi, P.; Ford, P. C. Near-Infrared and Visible Photoactivation to Uncage Carbon Monoxide from an Aqueous-Soluble PhotoCORM. *Inorg. Chem.* **2019**, *58*, 11066−11075.
(1168) Mansour, A. M.; Ragab, M. S. Spectroscopic and DFT Studies of Photoactivatable Mn(I) Tricarbonyl Complexes. *Appl. Organomet. Chem.* **2019**, *33*, No. e4944.
(1169) Carrington, S. J.; Chakraborty, I.; Bernard, J. M. L.; Mascharak, P. K. Synthesis and Characterization of a "Turn-On" photoCORM for Trackable CO Delivery to Biological Targets. *ACS Med. Chem. Lett.* **2014**, *5*, 1324−1328.

(1170) Mansour, A. M. Rapid Green and Blue Light-Induced CO Release from Bromazepam Mn(I) and Ru(II) Carbonyls: Synthesis, Density Functional Theory and Biological Activity Evaluation. *Appl. Organomet. Chem.* **2017**, *31*, No. e3564.
(1171) Musib, D.; Raza, M. K.; Martina, K.; Roy, M. Mn(I)-Based PhotoCORMs for Trackable, Visible Light-Induced CO Release and Photocytotoxicity to Cancer Cells. *Polyhedron* **2019**, *172*, 125−131.
(1172) Mede, R.; Gläser, S.; Suchland, B.; Schowtka, B.; Mandel, M.; Görls, H.; Krieck, S.; Schiller, A.; Westerhausen, M. Manganese(I)-Based CORMs with 5-Substituted 3-(2-Pyridyl)Pyrazole Ligands. *Inorganics* **2017**, *5*, 8.
(1173) Mede, R.; Hoffmann, P.; Neumann, C.; Gorls, H.; Schmitt, M.; Popp, J.; Neugebauer, U.; Westerhausen, M. Acetoxymethyl Concept for Intracellular Administration of Carbon Monoxide with $Mn(CO)_3$-Based PhotoCORMs. *Chem. - Eur. J.* **2018**, *24*, 3321−3329.
(1174) Ward, J. S.; De Palo, A.; Aucott, B. J.; Moir, J. W. B.; Lynam, J. M.; Fairlamb, I. J. S. A Biotin-Conjugated Photo-Activated CO-Releasing Molecule (BiotinCORM): Efficient CO-Release from an Avidin−BiotinCORM Protein Adduct. *Dalton Trans.* **2019**, *48*, 16233−16241.
(1175) Jimenez, J.; Chakraborty, I.; Dominguez, A.; Martinez-Gonzalez, J.; Sameera, W. M. C.; Mascharak, P. K. A Luminescent Manganese PhotoCORM for CO Delivery to Cellular Targets under the Control of Visible Light. *Inorg. Chem.* **2018**, *57*, 1766−1773.
(1176) Jimenez, J.; Pinto, M. N.; Martinez-Gonzalez, J.; Mascharak, P. K. Photo-Induced Eradication of Human Colorectal Adenocarcinoma HT-29 Cells by Carbon Monoxide (CO) Delivery from a Mn-Based Green Luminescent PhotoCORM. *Inorg. Chim. Acta* **2019**, *485*, 112−117.
(1177) Pinto, M. N.; Chakraborty, I.; Jimenez, J.; Murphy, K.; Wenger, J.; Mascharak, P. K. Therapeutic Potential of Two Visible Light Responsive Luminescent photoCORMs: Enhanced Cellular Internalization Driven by Lipophilicity. *Inorg. Chem.* **2019**, *58*, 14522−14531.
(1178) Ramu, V.; Upendar Reddy, G.; Liu, J.; Hoffmann, P.; Sollapur, R.; Wyrwa, R.; Kupfer, S.; Spielmann, C.; Bonnet, S.; Neugebauer, U.; Schiller, A. Two-Photon-Induced CO-Releasing Molecules as Molecular Logic Systems in Solution, Polymers, and Cells. *Chem. - Eur. J.* **2019**, *25*, 8453−8458.
(1179) Gandra, U. R.; Sinopoli, A.; Moncho, S.; NandaKumar, M.; Ninković, D. B.; Zarić, S. D.; Sohail, M.; Al-Meer, S.; Brothers, E. N.; Mazloum, N. A.; Al-Hashimi, M.; Bazzi, H. S. Green Light-Responsive CO-Releasing Polymeric Materials Derived from Ring-Opening Metathesis Polymerization. *ACS Appl. Mater. Interfaces* **2019**, *11*, 34376−34384.
(1180) Reddy G, U.; Liu, J.; Hoffmann, P.; Steinmetzer, J.; Görls, H.; Kupfer, S.; Askes, S. H. C.; Neugebauer, U.; Gräfe, S.; Schiller, A. Light-Responsive Paper Strips as CO-Releasing Material with a Colourimetric Response. *Chem. Sci.* **2017**, *8*, 6555−6560.
(1181) Liu, J.; Hoffmann, P.; Steinmetzer, J.; Askes, S. H. C.; Kupfer, S.; Görls, H.; Gräfe, S.; Neugebauer, U.; Gandra, U. R.; Schiller, A. Visible Light-Activated Biocompatible Photo-CORM for CO-Release with Colorimetric and Fluorometric Dual Turn-On Response. *Polyhedron* **2019**, *172*, 175−181.
(1182) Tabe, H.; Shimoi, T.; Boudes, M.; Abe, S.; Coulibaly, F.; Kitagawa, S.; Mori, H.; Ueno, T. Photoactivatable CO Release from Engineered Protein Crystals to Modulate NF-κB Activation. *Chem. Commun.* **2016**, *52*, 4545−4548.
(1183) Mansour, A. M.; Shehab, O. R. Experimental and Quantum Chemical Calculations of Novel Photoactivatable Manganese(I) Tricarbonyl Complexes. *J. Organomet. Chem.* **2016**, *822*, 91−99.
(1184) Divya, D.; Nagarajaprakash, R.; Vidhyapriya, P.; Sakthivel, N.; Manimaran, B. Single-Pot Self-Assembly of Heteroleptic Mn(I)-Based Aminoquinonato-Bridged Ester/Amide-Functionalized Dinuclear Metallastirrups: Potential Anticancer and Visible-Light-Triggered CORMs. *ACS Omega* **2019**, *4*, 12790−12802.
(1185) Ward, J. S.; Lynam, J. M.; Moir, J.; Fairlamb, I. J. S. Visible-Light-Induced CO Release from a Therapeutically Viable Tryptophan-Derived Manganese(I) Carbonyl (TryptoCORM) Exhibiting Potent Inhibition against E. coli. *Chem. - Eur. J.* **2014**, *20*, 15061−15068.
(1186) Aucott, B. J.; Eastwood, J. B.; Anders Hammarback, L.; Clark, I. P.; Sazanovich, I. V.; Towrie, M.; Fairlamb, I. J. S.; Lynam, J. M. Insight into the Mechanism of CO-Release from Trypto-CORM Using Ultra-Fast Spectroscopy and Computational Chemistry. *Dalton Trans.* **2019**, *48*, 16426−16436.
(1187) Dessent, C. E. H.; Cercola, R.; Fischer, K. C.; Sherman, S. L.; Garand, E.; Wong, N. G. K.; Hammerback, L. A.; Lynam, J. M.; Fairlamb, I. J. S. Direct Measurement of the Visible to UV Photodissociation Processes for the PhotoCORM TryptoCORM. *Chem. - Eur. J.* **2020**, *26*, 10297−10306.
(1188) Zobi, F.; Quaroni, L.; Santoro, G.; Zlateva, T.; Blacque, O.; Sarafimov, B.; Schaub, M. C.; Bogdanova, A. Y. Live-Fibroblast IR Imaging of a Cytoprotective PhotoCORM Activated with Visible Light. *J. Med. Chem.* **2013**, *56*, 6719−6731.
(1189) Mede, R.; Hoffmann, P.; Klein, M.; Görls, H.; Schmitt, M.; Neugebauer, U.; Gessner, G.; Heinemann, S. H.; Popp, J.; Westerhausen, M. A Water-Soluble $Mn(CO)_3$-Based and Non-Toxic PhotoCORM for Administration of Carbon Monoxide Inside of Cells. *Z. Anorg. Allg. Chem.* **2017**, *643*, 2057−2062.
(1190) Weiss, V. C.; Amorim, A. L.; Xavier, F. R.; Bortoluzzi, A. J.; Neves, A.; Peralta, R. A. Light Response of Three Water-Soluble MnI PhotoCORMs: Spectroscopic Features and CO Release Investigation. *J. Braz. Chem. Soc.* **2019**, *30*, 2649−2659.
(1191) Mede, R.; Klein, M.; Claus, R. A.; Krieck, S.; Quickert, S.; Görls, H.; Neugebauer, U.; Schmitt, M.; Gessner, G.; Heinemann, S. H.; Popp, J.; Bauer, M.; Westerhausen, M. CORM-EDE1: A Highly Water-Soluble and Nontoxic Manganese-Based photoCORM with a Biogenic Ligand Sphere. *Inorg. Chem.* **2016**, *55*, 104−113.
(1192) Bohlender, C.; Gläser, S.; Klein, M.; Weisser, J.; Thein, S.; Neugebauer, U.; Popp, J.; Wyrwa, R.; Schiller, A. Light-Triggered CO Release from Nanoporous Non-Wovens. *J. Mater. Chem. B* **2014**, *2*, 1454−1463.
(1193) Gläser, S.; Mede, R.; Görls, H.; Seupel, S.; Bohlender, C.; Wyrwa, R.; Schirmer, S.; Dochow, S.; Reddy, G. U.; Popp, J.; Westerhausen, M.; Schiller, A. Remote-Controlled Delivery of CO *via* Photoactive CO-Releasing Materials on a Fiber Optical Device. *Dalton Trans.* **2016**, *45*, 13222−13233.
(1194) Li, Z.; Pierri, A. E.; Huang, P. J.; Wu, G.; Iretskii, A. V.; Ford, P. C. Dinuclear PhotoCORMs: Dioxygen-Assisted Carbon Monoxide Uncaging from Long-Wavelength -Absorbing Metal-Metal-Bonded Carbonyl Complexes. *Inorg. Chem.* **2017**, *56*, 6094−6104.
(1195) Askes, S. H. C.; Reddy, G. U.; Wyrwa, R.; Bonnet, S.; Schiller, A. Red Light-Triggered CO Release from $Mn_2(CO)_{10}$ Using Triplet Sensitization in Polymer Nonwoven Fabrics. *J. Am. Chem. Soc.* **2017**, *139*, 15292−15295.
(1196) Gonzalez, M. A.; Carrington, S. J.; Chakraborty, I.; Olmstead, M. M.; Mascharak, P. K. Photoactivity of Mono- and Dicarbonyl Complexes of Ruthenium(II) Bearing an *N*,*N*,*S*-Donor Ligand: Role of Ancillary Ligands on the Capacity of CO Photorelease. *Inorg. Chem.* **2013**, *52*, 11320−11331.
(1197) Kubeil, M.; Joshi, T.; Wood, B. R.; Stephan, H. Synthesis, Structural Characterization and Photodecarbonylation Study of a Dicarbonyl Ruthenium(II)-Bisquinoline Complex. *ChemistryOpen* **2019**, *8*, 637−642.
(1198) Akatsuka, K.; Abe, R.; Takase, T.; Oyama, D. Coordination Chemistry of Ru(II) Complexes of an Asymmetric Bipyridine Analogue: Synergistic Effects of Supporting Ligand and Coordination Geometry on Reactivities. *Molecules* **2020**, *25*, 27.
(1199) Takács, J.; Soós, E.; Nagy-Magos, Z.; Markó, L.; Gervasio, G.; Hoffmann, T. Synthesis and Molecular Structure of Carbonyl Derivatives of Iron(II) Thiolates Containing Nitrogen-Donor Ligands. *Inorg. Chim. Acta* **1989**, *166*, 39−46.
(1200) Kretschmer, R.; Gessner, G.; Görls, H.; Heinemann, S. H.; Westerhausen, M. Dicarbonyl-Bis(cysteamine)iron(II): A Light Induced Carbon Monoxide Releasing Molecule Based on Iron (CORM-S1). *J. Inorg. Biochem.* **2011**, *105*, 6−9.

(1201) Poh, H. T.; Sim, B. T.; Chwee, T. S.; Leong, W. K.; Fan, W. Y. The Dithiolate-Bridged Diiron Hexacarbonyl Complex $Na_2[(\mu\text{-}SCH_2CH_2COO)Fe(CO)_3]_2$ as a Water-Soluble PhotoCORM. *Organometallics* **2014**, *33*, 959−963.
(1202) Marhenke, J.; Pierri, A. E.; Lomotan, M.; Damon, P. L.; Ford, P. C.; Works, C. Flash and Continuous Photolysis Kinetic Studies of the Iron−Iron Hydrogenase Model (μ-pdt)$[Fe(CO)_3]_2$ in Different Solvents. *Inorg. Chem.* **2011**, *50*, 11850−11852.
(1203) Nakae, T.; Hirotsu, M.; Nakajima, H. CO Release from N, C, S-Pincer Iron(III) Carbonyl Complexes Induced by Visible-to-NIR Light Irradiation: Mechanistic Insight into Effects of Axial Phosphorus Ligands. *Inorg. Chem.* **2018**, *57*, 8615−8626.
(1204) Kawatani, M.; Kamiya, M.; Takahashi, H.; Urano, Y. Factors Affecting the Ucaging Eficiency of 500nm Lght-Ativatable BODIPY Caging Group. *Bioorg. Med. Chem. Lett.* **2018**, *28*, 1−5.
(1205) Wright, M. A.; Wooldridge, T.; O'Connell, M. A.; Wright, J. A. Ferracyclic Carbonyl Complexes as Anti-inflammatory Agents. *Chem. Commun.* **2020**, *56*, 4300−4303.
(1206) Pierri, A. E.; Pallaoro, A.; Wu, G.; Ford, P. C. A Luminescent and Biocompatible PhotoCORM. *J. Am. Chem. Soc.* **2012**, *134*, 18197−18200.
(1207) Pierri, A. E.; Pallaoro, A.; Wu, G.; Ford, P. C. Correction to "A Luminescent and Biocompatible PhotoCORM. *J. Am. Chem. Soc.* **2018**, *140*, 525−525.
(1208) Rosselli, M.; Keller, R.; Dubey, R. Role of Nitric Oxide in the Biology, Physiology and Pathophysiology of Reproduction. *Hum. Reprod. Update* **1998**, *4*, 3−24.
(1209) Arnold, W. P.; Mittal, C. K.; Katsuki, S.; Murad, F. Nitric Oxide Activates Guanylate Cyclase and Increases Guanosine 3′:5′-Cyclic Monophosphate Levels in Various Tissue Preparations. *Proc. Natl. Acad. Sci. U. S. A.* **1977**, *74*, 3203−3207.
(1210) Furchgott, R. F.; Zawadzki, J. V. The Obligatory Role of Endothelial Cells in the Relaxation of Arterial Smooth Muscle by Acetylcholine. *Nature* **1980**, *288*, 373−376.
(1211) Ignarro, L. J.; Buga, G. M.; Wood, K. S.; Byrns, R. E.; Chaudhuri, G. Endothelium-Derived Relaxing Factor Produced and Released from Artery and Vein Is Nitric Oxide. *Proc. Natl. Acad. Sci. U. S. A.* **1987**, *84*, 9265−9269.
(1212) Palmer, R. M. J.; Ferrige, A. G.; Moncada, S. Nitric Oxide Release Accounts for the Biological Activity of Endothelium-Derived Relaxing Factor. *Nature* **1987**, *327*, 524−526.
(1213) Hermann, M.; Flammer, A.; Lüscher, T. F. Nitric Oxide in Hypertension. *J. Clin. Hypertens.* **2006**, *8*, 17−29.
(1214) Qiu, S.; Guo, C.; Wang, M.; Sun, Z.; Li, H.; Qian, X.; Yang, Y. Mild Dealkylative *N*-Nitrosation of *N,N*-Dialkylaniline Derivatives for Convenient Preparation of Photo-Triggered and Photo-Calibrated NO Donors. *Org. Chem. Front.* **2018**, *5*, 3206−3209.
(1215) Piech, K.; Bally, T.; Sikora, A.; Marcinek, A. Mechanistic Aspects of the Oxidative and Reductive Fragmentation of N-Nitrosoamines: A New Method for Generating Nitrenium Cations, Amide Anions, and Aminyl Radicals. *J. Am. Chem. Soc.* **2007**, *129*, 3211−3217.
(1216) He, H.; He, T.; Zhang, Z.; Xu, X.; Yang, H.; Qian, X.; Yang, Y. Ring-Restricted *N*-Nitrosated Rhodamine as a Green-Light Triggered, Orange-Emission Calibrated and Fast-Releasing Nitric Oxide Donor. *Chin. Chem. Lett.* **2018**, *29*, 1497−1499.
(1217) Yanagimoto, T.; Toyota, T.; Matsuki, N.; Makino, Y.; Uchiyama, S.; Ohwada, T. Transnitrosation of Thiols from Aliphatic *N*-Nitrosamines: *S*-Nitrosation and Indirect Generation of Nitric Oxide. *J. Am. Chem. Soc.* **2007**, *129*, 736−737.
(1218) Zhou, E. Y.; Knox, H. J.; Reinhardt, C. J.; Partipilo, G.; Nilges, M. J.; Chan, J. Near-Infrared Photoactivatable Nitric Oxide Donors with Integrated Photoacoustic Monitoring. *J. Am. Chem. Soc.* **2018**, *140*, 11686−11697.
(1219) Okuno, H.; Ieda, N.; Hotta, Y.; Kawaguchi, M.; Kimura, K.; Nakagawa, H. A Yellowish-Green-Light-Controllable Nitric Oxide Donor Based on *N*-Nitrosoaminophenol Applicable for Photo-controlled Vasodilation. *Org. Biomol. Chem.* **2017**, *15*, 2791−2796.
(1220) Ieda, N.; Oka, Y.; Yoshihara, T.; Tobita, S.; Sasamori, T.; Kawaguchi, M.; Nakagawa, H. Structure-Efficiency Relationship of Photoinduced Electron Transfer-Triggered Nitric Oxide Releasers. *Sci. Rep.* **2019**, *9*, 1430.
(1221) Ieda, N.; Hotta, Y.; Kawaguchi, M.; Kimura, K.; Nakagawa, H. *In Cellullo* and *ex Vivo* Availability of a Yellowish-Green-Light-Controllable NO Releaser. *Chem. Pharm. Bull.* **2019**, *67*, 576−579.
(1222) He, H.; Liu, Y.; Zhou, Z.; Guo, C.; Wang, H.-Y.; Wang, Z.; Wang, X.; Zhang, Z.; Wu, F.-G.; Wang, H.; Chen, D.; Yang, D.; Liang, X.; Chen, J.; Zhou, S.; Liang, X.; Qian, X.; Yang, Y. A Photo-Triggered and Photo-Calibrated Nitric Oxide Donor: Rational Design, Spectral Characterizations, and Biological Applications. *Free Radical Biol. Med.* **2018**, *123*, 1−7.
(1223) He, H.; Xia, Y.; Qi, Y.; Wang, H.-Y.; Wang, Z.; Bao, J.; Zhang, Z.; Wu, F.-G.; Wang, H.; Chen, D.; Yang, D.; Liang, X.; Chen, J.; Zhou, S.; Liang, X.; Qian, X.; Yang, Y. A Water-Soluble, Green-Light Triggered, and Photo-Calibrated Nitric Oxide Donor for Biological Applications. *Bioconjugate Chem.* **2018**, *29*, 1194−1198.
(1224) Shen, R.; Qian, Y. A Turn-on and Lysosome-Targeted Fluorescent NO Releaser in Water Media and Its Application in Living Cells and Zebrafishes. *Spectrochim. Acta, Part A* **2020**, *230*, 118024.
(1225) Shen, R.; Qian, Y. A Efficient Light-Controlled Nitric Oxide Releaser in Aqueous Solution and Its Red Fluorescence Imaging in Lysosome. *Dyes Pigm.* **2020**, *176*, 108247.
(1226) Zhang, S.; Wang, Q.; Yang, J.; Yang, X.-F.; Li, Z.; Li, H. A Photocalibrated NO Donor Based on *N*-Nitrosorhodamine 6G upon UV Irradiation. *Chin. Chem. Lett.* **2019**, *30*, 454−456.
(1227) He, H.; Ye, Z.; Xiao, Y.; Yang, W.; Qian, X.; Yang, Y. Super-Resolution Monitoring of Mitochondrial Dynamics upon Time-Gated Photo-Triggered Release of Nitric Oxide. *Anal. Chem.* **2018**, *90*, 2164−2169.
(1228) Xie, X.; Fan, J.; Liang, M.; Li, Y.; Jiao, X.; Wang, X.; Tang, B. A Two-Photon Excitable and Ratiometric Fluorogenic Nitric Oxide Photoreleaser and Its Biological Applications. *Chem. Commun.* **2017**, *53*, 11941−11944.
(1229) Saavedra, J. E.; Billiar, T. R.; Williams, D. L.; Kim, Y.-M.; Watkins, S. C.; Keefer, L. K. Targeting Nitric Oxide (NO) Delivery in Vivo. Design of a Liver-Selective NO Donor Prodrug That Blocks Tumor Necrosis Factor-α-Induced Apoptosis and Toxicity in the Liver. *J. Med. Chem.* **1997**, *40*, 1947−1954.
(1230) Kauser, N. I.; Weisel, M.; Zhong, Y.-L.; Lo, M. M.-C.; Ali, A. Calcium Dialkylamine Diazeniumdiolates: Synthesis, Stability, and Nitric Oxide Generation. *J. Org. Chem.* **2020**, *85*, 4807−4812.
(1231) Miller, M. R.; Megson, I. L. Recent Developments in Nitric Oxide Donor Drugs. *Br. J. Pharmacol.* **2007**, *151*, 305−321.
(1232) Keefer, L. K. Progress Toward Clinical Application of the Nitric Oxide−Releasing Diazeniumdiolates. *Annu. Rev. Pharmacol. Toxicol.* **2003**, *43*, 585−607.
(1233) Brilli, R. J.; Krafte-Jacobs, B.; Smith, D. J.; Roselle, D.; Passerini, D.; Vromen, A.; Moore, L.; Szabó, C.; Salzman, A. L. Intratracheal Instillation of a Novel NO/Nucleophile Adduct Selectively Reduces Pulmonary Hypertension. *J. Appl. Physiol.* **1997**, *83*, 1968−1975.
(1234) Makings, L. R.; Tsien, R. Y. Caged Nitric Oxide. Stable Organic Molecules from which Nitric Oxide can be Photoreleased. *J. Biol. Chem.* **1994**, *269*, 6282−6285.
(1235) Caruso, E. B.; Petralia, S.; Conoci, S.; Giuffrida, S.; Sortino, S. Photodelivery of Nitric Oxide from Water-Soluble Platinum Nanoparticles. *J. Am. Chem. Soc.* **2007**, *129*, 480−481.
(1236) Sharma, N.; Dhyani, A. K.; Marepally, S.; Jose, D. A. Nanoscale Lipid Vesicles Functionalized with a Nitro-Aniline Derivative for Photoinduced Nitric Oxide (NO) Delivery. *Nanoscale Adv.* **2020**, *2*, 463−469.
(1237) Vittorino, E.; Sciortino, M. T.; Siracusano, G.; Sortino, S. Light-Activated Release of Nitric Oxide with Fluorescence Reporting in Living Cells. *ChemMedChem* **2011**, *6*, 1551−1554.
(1238) Fraix, A.; Kirejev, V.; Malanga, M.; Fenyvesi, É.; Béni, S.; Ericson, M. B.; Sortino, S. A Three-Color Fluorescent Supramolecular

Nanoassembly of Phototherapeutics Activable by Two-Photon Excitation with Near-Infrared Light. *Chem. - Eur. J.* **2019**, *25*, 7091−7095.
(1239) Marino, N.; Perez-Lloret, M.; Blanco, A. R.; Venuta, A.; Quaglia, F.; Sortino, S. Photo-Antimicrobial Polymeric Films Releasing Nitric Oxide with Fluorescence Reporting under Visible Light. *J. Mater. Chem. B* **2016**, *4*, 5138−5143.
(1240) Wang, Y.; Huang, X.; Tang, Y.; Zou, J.; Wang, P.; Zhang, Y.; Si, W.; Huang, W.; Dong, X. A Light-Induced Nitric Oxide Controllable Release Nano-Platform Based on Diketopyrrolopyrrole Derivatives for pH-Responsive Photodynamic/Photothermal Synergistic Cancer Therapy. *Chem. Sci.* **2018**, *9*, 8103−8109.
(1241) Suzuki, T.; Nagae, O.; Kato, Y.; Nakagawa, H.; Fukuhara, K.; Miyata, N. Photoinduced Nitric Oxide Release from Nitrobenzene Derivatives. *J. Am. Chem. Soc.* **2005**, *127*, 11720−11726.
(1242) Hishikawa, K.; Nakagawa, H.; Furuta, T.; Fukuhara, K.; Tsumoto, H.; Suzuki, T.; Miyata, N. Photoinduced Nitric Oxide Release from a Hindered Nitrobenzene Derivative by Two-Photon Excitation. *J. Am. Chem. Soc.* **2009**, *131*, 7488−7489.
(1243) Nakagawa, H.; Hishikawa, K.; Eto, K.; Ieda, N.; Namikawa, T.; Kamada, K.; Suzuki, T.; Miyata, N.; Nabekura, J.-i. Fine Spatiotemporal Control of Nitric Oxide Release by Infrared Pulse-Laser Irradiation of a Photolabile Donor. *ACS Chem. Biol.* **2013**, *8*, 2493−2500.
(1244) Ieda, N.; Hishikawa, K.; Eto, K.; Kitamura, K.; Kawaguchi, M.; Suzuki, T.; Fukuhara, K.; Miyata, N.; Furuta, T.; Nabekura, J.; Nakagawa, H. A Double Bond-Conjugated Dimethylnitrobenzene-Type Photolabile Nitric Oxide Donor with Improved Two-Photon Cross Section. *Bioorg. Med. Chem. Lett.* **2015**, *25*, 3172−3175.
(1245) Kitamura, K.; Kawaguchi, M.; Ieda, N.; Miyata, N.; Nakagawa, H. Visible Light-Controlled Nitric Oxide Release from Hindered Nitrobenzene Derivatives for Specific Modulation of Mitochondrial Dynamics. *ACS Chem. Biol.* **2016**, *11*, 1271−1278.
(1246) Kitamura, K.; Ieda, N.; Hishikawa, K.; Suzuki, T.; Miyata, N.; Fukuhara, K.; Nakagawa, H. Visible Light-Induced Nitric Oxide Release from a Novel Nitrobenzene Derivative Cross-Conjugated with a Coumarin Fluorophore. *Bioorg. Med. Chem. Lett.* **2014**, *24*, 5660−5662.
(1247) Parisi, C.; Failla, M.; Fraix, A.; Rolando, B.; Gianquinto, E.; Spyrakis, F.; Gazzano, E.; Riganti, C.; Lazzarato, L.; Fruttero, R.; Gasco, A.; Sortino, S. Fluorescent Nitric Oxide Photodonors Based on BODIPY and Rhodamine Antennae. *Chem. - Eur. J.* **2019**, *25*, 11080−11084.
(1248) Parisi, C.; Failla, M.; Fraix, A.; Rescifina, A.; Rolando, B.; Lazzarato, L.; Cardile, V.; Graziano, A. C. E.; Fruttero, R.; Gasco, A.; Sortino, S. A Molecular Hybrid Producing Simultaneously Singlet Oxygen and Nitric Oxide by Single Photon Excitation with Green Light. *Bioorg. Chem.* **2019**, *85*, 18−22.
(1249) Butler, A. R.; Glidewell, C. Recent Chemical Studies of Sodium Nitroprusside Relevant to its Hypotensive Action. *Chem. Soc. Rev.* **1987**, *16*, 361−380.
(1250) Shishido, S. M.; de Oliveira, M. G. Photosensitivity of Aqueous Sodium Nitroprusside Solutions: Nitric Oxide Release versus Cyanide Toxicity. *Prog. React. Kinet. Mech.* **2001**, *26*, 239−261.
(1251) Feelisch, M.; Noack, E. Nitric Oxide (NO) Formation from Nitrovasodilators Occurs Independently of Hemoglobin or Non-Heme Iron. *Eur. J. Pharmacol.* **1987**, *142*, 465−469.
(1252) Holloway, L. R.; Li, L. The Preparation, Structural Characteristics, and Physical Chemical Properties of Metal-Nitrosyl Complexes. *Nitrosyl Complexes in Inorganic Chemistry, Biochemistry and Medicine II*; Mingos, D. M. P., Ed.; Springer Berlin Heidelberg: Berlin, Heidelberg, 2014.
(1253) Xiang, H.-J.; Guo, M.; Liu, J.-G. Transition-Metal Nitrosyls for Photocontrolled Nitric Oxide Delivery. *Eur. J. Inorg. Chem.* **2017**, *2017*, 1586−1595.
(1254) Ostrowski, A. D.; Absalonson, R. O.; Leo, M. A. D.; Wu, G.; Pavlovich, J. G.; Adamson, J.; Azhar, B.; Iretskii, A. V.; Megson, I. L.; Ford, P. C. Photochemistry of trans-Cr(cyclam)$(ONO)^{2+}$, a Nitric Oxide Precursor. *Inorg. Chem.* **2011**, *50*, 4453−4462.
(1255) DeRosa, F.; Bu, X.; Ford, P. C. Chromium(III) Complexes for Photochemical Nitric Oxide Generation from Coordinated Nitrite: Synthesis and Photochemistry of Macrocyclic Complexes with Pendant Chromophores, trans-$[Cr(L)(ONO)_2]BF_4$. *Inorg. Chem.* **2005**, *44*, 4157−4165.
(1256) Ostrowski, A. D.; Lin, B. F.; Tirrell, M. V.; Ford, P. C. Liposome Encapsulation of a Photochemical NO Precursor for Controlled Nitric Oxide Release and Simultaneous Fluorescence Imaging. *Mol. Pharmaceutics* **2012**, *9*, 2950−2955.
(1257) Huang, P.-J.; Garcia, J. V.; Fenwick, A.; Wu, G.; Ford, P. C. Nitric Oxide Uncaging from a Hydrophobic Chromium(III) Photo-NORM: Visible and Near-Infrared Photochemistry in Biocompatible Polymer Disks. *ACS Omega* **2019**, *4*, 9181−9187.
(1258) Burks, P. T.; Garcia, J. V.; GonzalezIrias, R.; Tillman, J. T.; Niu, M. T.; Mikhailovsky, A. A.; Zhang, J. P.; Zhang, F.; Ford, P. C. Nitric Oxide Releasing Materials Triggered by Near-Infrared Excitation Through Tissue Filters. *J. Am. Chem. Soc.* **2013**, *135*, 18145−18152.
(1259) San Miguel, V.; Alvarez, M.; Filevich, O.; Etchenique, R.; del Campo, A. Multiphoton Reactive Surfaces Using Ruthenium(II) Photocleavable Cages. *Langmuir* **2012**, *28*, 1217−1221.
(1260) Wecksler, S. R.; Mikhailovsky, A.; Korystov, D.; Ford, P. C. A Two-Photon Antenna for Photochemical Delivery of Nitric Oxide from a Water-Soluble, Dye-Derivatized Iron Nitrosyl Complex Using NIR Light. *J. Am. Chem. Soc.* **2006**, *128*, 3831−3837.
(1261) Conrado, C. L.; Wecksler, S.; Egler, C.; Magde, D.; Ford, P. C. Synthesis and Photochemical Properties of a Novel Iron-Sulfur-Nitrosyl Cluster Derivatized with the Pendant Chromophore Protoporphyrin IX. *Inorg. Chem.* **2004**, *43*, 5543−5549.
(1262) Conrado, C. L.; Bourassa, J. L.; Egler, C.; Wecksler, S.; Ford, P. C. Photochemical Investigation of Roussin's Red Salt Esters: $Fe_2(\mu\text{-}SR)_2(NO)_4$. *Inorg. Chem.* **2003**, *42*, 2288−2293.
(1263) Zheng, Q.; Bonoiu, A.; Ohulchanskyy, T. Y.; He, G. S.; Prasad, P. N. Water-Soluble Two-Photon Absorbing Nitrosyl Complex for Light-Activated Therapy through Nitric Oxide Release. *Mol. Pharmaceutics* **2008**, *5*, 389−398.
(1264) Wecksler, S. R.; Mikhailovsky, A.; Korystov, D.; Buller, F.; Kannan, R.; Tan, L.-S.; Ford, P. C. Single- and Two-Photon Properties of a Dye-Derivatized Roussin's Red Salt Ester ($Fe_2(\mu\text{-}RS)_2(NO)_4$) with a Large TPA Cross Section. *Inorg. Chem.* **2007**, *46*, 395−402.
(1265) Patra, A. K.; Afshar, R.; Olmstead, M. M.; Mascharak, P. K. The First Non-Heme Iron(III) Complex with a Ligated Carboxamido Group That Exhibits Photolability of a Bound NO Ligand. *Angew. Chem., Int. Ed.* **2002**, *41*, 2512−2515.
(1266) Patra, A. K.; Rowland, J. M.; Marlin, D. S.; Bill, E.; Olmstead, M. M.; Mascharak, P. K. Iron Nitrosyls of a Pentadentate Ligand Containing a Single Carboxamide Group: Syntheses, Structures, Electronic Properties, and Photolability of NO. *Inorg. Chem.* **2003**, *42*, 6812−6823.
(1267) Chiang, C.-K.; Chu, K.-T.; Lin, C.-C.; Xie, S.-R.; Liu, Y.-C.; Demeshko, S.; Lee, G.-H.; Meyer, F.; Tsai, M.-L.; Chiang, M.-H.; Lee, C.-M. Photoinduced NO and HNO Production from Mononuclear $\{FeNO\}_6$ Complex Bearing a Pendant Thiol. *J. Am. Chem. Soc.* **2020**, *142*, 8649−8661.
(1268) Ghosh, K.; Eroy-Reveles, A. A.; Avila, B.; Holman, T. R.; Olmstead, M. M.; Mascharak, P. K. Reactions of NO with Mn(II) and Mn(III) Centers Coordinated to Carboxamido Nitrogen: Synthesis of a Manganese Nitrosyl with Photolabile NO. *Inorg. Chem.* **2004**, *43*, 2988−2997.
(1269) Eroy-Reveles, A. A.; Leung, Y.; Mascharak, P. K. Release of Nitric Oxide From a Sol-Gel Hybrid Material Containing a Photoactive Manganese Nitrosyl Upon Illumination With Visible Light. *J. Am. Chem. Soc.* **2006**, *128*, 7166−7167.
(1270) Hitomi, Y.; Iwamoto, Y.; Kodera, M. Electronic Tuning of Nitric Oxide Release from Manganese Nitrosyl Complexes by Visible Light Irradiation: Enhancement of Nitric Oxide Release Efficiency by the Nitro-Substituted Quinoline Ligand. *Dalton Trans.* **2014**, *43*, 2161−2167.

(1271) Rose, M. J.; Mascharak, P. K. Photoactive Ruthenium Nitrosyls: Effects of Light and Potential Application as NO Donors. *Coord. Chem. Rev.* **2008**, *252*, 2093−2114.
(1272) Fry, N. L.; Mascharak, P. K. Photoactive Ruthenium Nitrosyls as NO Donors: How To Sensitize Them toward Visible Light. *Acc. Chem. Res.* **2011**, *44*, 289−298.
(1273) de Lima, R. G.; Sauaia, M. G.; Bonaventura, D.; Tedesco, A. C.; Bendhack, L. M.; da Silva, R. S. Influence of Ancillary Ligand L in the Nitric Oxide Photorelease by the $[Ru(L)(tpy)NO]^{3+}$ Complex and its Vasodilator Activity Based on visible Light Irradiation. *Inorg. Chim. Acta* **2006**, *359*, 2543−2549.
(1274) Frasconi, M.; Liu, Z.; Lei, J.; Wu, Y.; Strekalova, E.; Malin, D.; Ambrogio, M. W.; Chen, X.; Botros, Y. Y.; Cryns, V. L.; Sauvage, J.-P.; Stoddart, J. F. Photoexpulsion of Surface-Grafted Ruthenium Complexes and Subsequent Release of Cytotoxic Cargos to Cancer Cells from Mesoporous Silica Nanoparticles. *J. Am. Chem. Soc.* **2013**, *135*, 11603−11613.
(1275) Bordini, J.; Hughes, D. L.; Da Motta Neto, J. D.; Jorge da Cunha, C. Nitric Oxide Photorelease from Ruthenium Salen Complexes in Aqueous and Organic Solutions. *Inorg. Chem.* **2002**, *41*, 5410−5416.
(1276) Carlos, R. M.; Ferro, A. A.; Silva, H. A. S.; Gomes, M. G.; Borges, S. S. S.; Ford, P. C.; Tfouni, E.; Franco, D. W. Photochemical Reactions of *trans*-$[Ru(NH_3)_4L(NO)]^{3+}$ Complexes. *Inorg. Chim. Acta* **2004**, *357*, 1381−1388.
(1277) Paula, Q. A.; Batista, A. A.; Castellano, E. E.; Ellena, J. On the Lability of Dimethylsulfoxide (DMSO) Coordinated to the $\{Ru^{II}-NO^{+}\}$ Species: X-Ray Structures of *mer*-$[RuCl_3(DMSO)_2(NO)]$ and *mer*-$[RuCl_3(CD_3CN)(DMSO)(NO)]$. *J. Inorg. Biochem.* **2002**, *90*, 144−148.
(1278) Miranda, K. M.; Bu, X.; Lorković, I.; Ford, P. C. Synthesis and Structural Characterization of Several Ruthenium Porphyrin Nitrosyl Complexes. *Inorg. Chem.* **1997**, *36*, 4838−4848.
(1279) Ferreira, K. Q.; Tfouni, E. Chemical and Photochemical Properties of a Ruthenium Nitrosyl Complex with the *N*-Monosubstituted Cyclam 1-(3-Propylammonium)-1,4,8,11-Tetraazacyclotetradecane. *J. Braz. Chem. Soc.* **2010**, *21*, 1349−1358.
(1280) Oliveira, F. d. S.; Togniolo, V.; Pupo, T. T.; Tedesco, A. C.; da Silva, R. S. Nitrosyl Ruthenium Complex as Nitric Oxide Delivery Agent: Synthesis, Characterization and Photochemical Properties. *Inorg. Chem. Commun.* **2004**, *7*, 160−164.
(1281) Sauaia, M. G.; de Lima, R. G.; Tedesco, A. C.; da Silva, R. S. Photoinduced NO Release by Visible Light Irradiation from Pyrazine-Bridged Nitrosyl Ruthenium Complexes. *J. Am. Chem. Soc.* **2003**, *125*, 14718−14719.
(1282) Marquele-Oliveira, F.; de Almeida Santana, D. C.; Taveira, S. F.; Vermeulen, D. M.; Moraes de Oliveira, A. R.; da Silva, R. S.; Lopez, R. F. V. Development of Nitrosyl Ruthenium Complex-Loaded Lipid Carriers for Topical Administration: Improvement in Skin Stability and in Nitric Oxide Release by Visible Light Irradiation. *J. Pharm. Biomed. Anal.* **2010**, *53*, 843−851.
(1283) Works, C. F.; Jocher, C. J.; Bart, G. D.; Bu, X.; Ford, P. C. Photochemical Nitric Oxide Precursors: Synthesis, Photochemistry, and Ligand Substitution Kinetics of Ruthenium Salen Nitrosyl and Ruthenium Salophen Nitrosyl Complexes. *Inorg. Chem.* **2002**, *41*, 3728−3739.
(1284) Tfouni, E.; Krieger, M.; McGarvey, B. R.; Franco, D. W. Structure, Chemical and Photochemical Reactivity and Biological Activity of Some Ruthenium Amine Nitrosyl Complexes. *Coord. Chem. Rev.* **2003**, *236*, 57−69.
(1285) Lorković, I. M.; Miranda, K. M.; Lee, B.; Bernhard, S.; Schoonover, J. R.; Ford, P. C. Flash Photolysis Studies of the Ruthenium(II) Porphyrins Ru(P)(NO)(ONO). Multiple Pathways Involving Reactions of Intermediates with Nitric Oxide. *J. Am. Chem. Soc.* **1998**, *120*, 11674−11683.
(1286) Vorobyev, V.; Budkina, D. S.; Tarnovsky, A. N. Femtosecond Excited-State Dynamics and Nitric Oxide Photorelease in a Prototypical Ruthenium Nitrosyl Complex. *J. Phys. Chem. Lett.* **2020**, *11*, 4639−4643.
(1287) Oliveira, F. d. S.; Ferreira, K. Q.; Bonaventura, D.; Bendhack, L. M.; Tedesco, A. C.; Machado, S. d. P.; Tfouni, E.; Silva, R. S. d. The Macrocyclic Effect and Vasodilation Response Based on the Photoinduced Nitric Oxide Release from *trans*-$[RuCl(tetraazamacrocycle)NO]^{2+}$. *J. Inorg. Biochem.* **2007**, *101*, 313−320.
(1288) Bordini, J.; Ford, P. C.; Tfouni, E. Photochemical Release of Nitric Oxide from a Regenerable, Sol-Gel Encapsulated Ru−Salen−Nitrosyl Complex. *Chem. Commun.* **2005**, 4169−4171.
(1289) Fry, N. L.; Heilman, B. J.; Mascharak, P. K. Dye-Tethered Ruthenium Nitrosyls Containing Planar Dicarboxamide Tetradentate N4 Ligands: Effects of In-Plane Ligand Twist on NO Photolability. *Inorg. Chem.* **2011**, *50*, 317−324.
(1290) Patra, A. K.; Rose, M. J.; Murphy, K. A.; Olmstead, M. M.; Mascharak, P. K. Photolabile Ruthenium Nitrosyls with Planar Dicarboxamide Tetradentate N4 Ligands: Effects of In-Plane and Axial Ligand Strength on NO Release. *Inorg. Chem.* **2004**, *43*, 4487−4495.
(1291) Kumar, R.; Kumar, S.; Bala, M.; Ratnam, A.; Singh, U. P.; Ghosh, K. Unprecedented Oxidation of Aldimine to Carboxamido Function During Reactivity Studies on Ruthenium Complex with Acidified Nitrite Solution: Synthesis of Ruthenium Nitrosyl Complex Having $\{RuNO\}^6$ Moiety and Photorelease of Coordinated NO. *J. Organomet. Chem.* **2018**, *863*, 77−83.
(1292) Rose, M. J.; Olmstead, M. M.; Mascharak, P. K. Photoactive Ruthenium Nitrosyls Derived from Quinoline- and Pyridine-Based Ligands: Accelerated Photorelease of NO Due to Quinoline Ligation. *Polyhedron* **2007**, *26*, 4713−4718.
(1293) Bukhanko, V.; Lacroix, P. G.; Sasaki, I.; Tassé, M.; Mallet-Ladeira, S.; Voitenko, Z.; Malfant, I. Mechanism and Oxidation State Involved in the Nitric Oxide (NO) Photorelease in a Terpyridine-Bipyridine-Based Ruthenium Nitrosyl Complex. *Inorg. Chim. Acta* **2018**, *482*, 195−205.
(1294) Amabilino, S.; Tasse, M.; Lacroix, P. G.; Mallet-Ladeira, S.; Pimienta, V.; Akl, J.; Sasaki, I.; Malfant, I. Photorelease of Nitric Oxide (NO) on Ruthenium Nitrosyl Complexes with Phenyl Substituted Terpyridines. *New J. Chem.* **2017**, *41*, 7371−7383.
(1295) Roose, M.; Sasaki, I.; Bukhanko, V.; Mallet-Ladeira, S.; Barba-Barba, R. M.; Ramos-Ortiz, G.; Enriquez-Cabrera, A.; Farfán, N.; Lacroix, P. G.; Malfant, I. Nitric Oxide Photo-Release from a Ruthenium Nitrosyl Complex with a 4,4′-Bisfluorenyl-2,2′-Bipyridine Ligand. *Polyhedron* **2018**, *151*, 100−111.
(1296) Enriquez-Cabrera, A.; Lacroix, P. G.; Sasaki, I.; Mallet-Ladeira, S.; Farfán, N.; Barba-Barba, R. M.; Ramos-Ortiz, G.; Malfant, I. Comparison of Carbazole and Fluorene Donating Effects on the Two-Photon Absorption and Nitric Oxide Photorelease Capabilities of a Ruthenium−Nitrosyl Complex. *Eur. J. Inorg. Chem.* **2018**, *2018*, 531−543.
(1297) Roose, M.; Tassé, M.; Lacroix, P. G.; Malfant, I. Nitric Oxide (NO) Photo-Release in a Series of Ruthenium−Nitrosyl Complexes: New Experimental Insights in the Search for a Comprehensive Mechanism. *New J. Chem.* **2019**, *43*, 755−767.
(1298) Sasaki, I.; Amabilino, S.; Mallet-Ladeira, S.; Tassé, M.; Sournia-Saquet, A.; Lacroix, P. G.; Malfant, I. Further Studies on the Photoreactivities of Ruthenium−Nitrosyl Complexes with Terpyridyl Ligands. *New J. Chem.* **2019**, *43*, 11241−11250.
(1299) Xiang, H.-J.; An, L.; Tang, W.-W.; Yang, S.-P.; Liu, J.-G. Photo-Controlled Targeted Intracellular Delivery of Both Nitric Oxide and Singlet Oxygen Using a Fluorescence-Trackable Ruthenium Nitrosyl Functional Nanoplatform. *Chem. Commun.* **2015**, *51*, 2555−2558.
(1300) Xiang, H.-J.; Deng, Q.; An, L.; Guo, M.; Yang, S.-P.; Liu, J.-G. Tumor Cell Specific and Lysosome-Targeted Delivery of Nitric Oxide for Enhanced Photodynamic Therapy Triggered by 808 nm Near-Infrared Light. *Chem. Commun.* **2016**, *52*, 148−151.
(1301) Giri, B.; Kumbhakar, S.; Kalai Selvan, K.; Muley, A.; Maji, S. Formation, Reactivity, Photorelease, and Scavenging of NO in Ruthenium Nitrosyl Complexes. *Inorg. Chim. Acta* **2020**, *502*, 119360.
(1302) De Candia, A. G.; Marcolongo, J. P.; Etchenique, R.; Slep, L. D. Widely Differing Photochemical Behavior in Related Octahedral

(Ru-NO)$_6$ Compounds: Intramolecular Redox Isomerism of the Excited State Controlling the Photodelivery of NO. *Inorg. Chem.* **2010**, *49*, 6925−6930.
(1303) Carneiro, Z. A.; Biazzotto, J. C.; Alexiou, A. D. P.; Nikolaou, S. Nitric Oxide Photorelease from a Trinuclear Ruthenium Nitrosyl Complex and its *in Vitro* Cytotoxicity Against Melanoma Cells. *J. Inorg. Biochem.* **2014**, *134*, 36−38.
(1304) Shin, S.; Choe, J.; Park, Y.; Jeong, D.; Song, H.; You, Y.; Seo, D.; Cho, J. Artificial Control of Cell Signaling Using a Photocleavable Cobalt(III)−Nitrosyl Complex. *Angew. Chem., Int. Ed.* **2019**, *58*, 10126−10131.
(1305) Ford, P. C. Photochemical Delivery of Nitric Oxide. *Nitric Oxide* **2013**, *34*, 56−64.
(1306) Fraix, A.; Sortino, S. Combination of PDT Photosensitizers with NO Photodononors. *Photochem. Photobiol. Sci.* **2018**, *17*, 1709−1727.
(1307) Neuman, D.; Ostrowski, A. D.; Absalonson, R. O.; Strouse, G. F.; Ford, P. C. Photosensitized NO Release from Water-Soluble Nanoparticle Assemblies. *J. Am. Chem. Soc.* **2007**, *129*, 4146−4147.
(1308) Rose, M. J.; Fry, N. L.; Marlow, R.; Hinck, L.; Mascharak, P. K. Sensitization of Ruthenium Nitrosyls to Visible Light via Direct Coordination of the Dye Resorufin: Trackable NO Donors for Light-Triggered NO Delivery to Cellular Targets. *J. Am. Chem. Soc.* **2008**, *130*, 8834−8846.
(1309) Rose, M. J.; Mascharak, P. K. Photosensitization of Ruthenium Nitrosyls to Red Light with an Isoelectronic Series of Heavy-Atom Chromophores: Experimental and Density Functional Theory Studies on the Effects of O-, S- and Se-Substituted Coordinated Dyes. *Inorg. Chem.* **2009**, *48*, 6904−6917.
(1310) Fry, N. L.; Wei, J.; Mascharak, P. K. Triggered Dye Release via Photodissociation of Nitric Oxide from Designed Ruthenium Nitrosyls: Turn-ON Fluorescence Signaling of Nitric Oxide Delivery. *Inorg. Chem.* **2011**, *50*, 9045−9052.
(1311) Rose, M. J.; Mascharak, P. K. A Photosensitive $\{Ru-NO\}^6$ Nitrosyl Bearing Dansyl Chromophore: Novel NO Donor with a Fluorometric On/Off Switch. *Chem. Commun.* **2008**, 3933−3935.
(1312) Becker, T.; Kupfer, S.; Wolfram, M.; Görls, H.; Schubert, U. S.; Anslyn, E. V.; Dietzek, B.; Gräfe, S.; Schiller, A. Sensitization of NO-Releasing Ruthenium Complexes to Visible Light. *Chem. - Eur. J.* **2015**, *21*, 15554−15563.
(1313) Wecksler, S. R.; Hutchinson, J.; Ford, P. C. Toward Development of Water Soluble Dye Derivatized Nitrosyl Compounds for Photochemical Delivery of NO. *Inorg. Chem.* **2006**, *45*, 1192−1200.
(1314) Levy, E. S.; Morales, D. P.; Garcia, J. V.; Reich, N. O.; Ford, P. C. Near-IR Mediated Intracellular Uncaging of NO from Cell Targeted Hollow Gold Nanoparticles. *Chem. Commun.* **2015**, *51*, 17692−17695.
(1315) Li, Y.-H.; Guo, M.; Shi, S.-W.; Zhang, Q.-L.; Yang, S.-P.; Liu, J.-G. A Ruthenium-Nitrosyl-Functionalized Nanoplatform for the Targeting of Liver Cancer Cells and NIR-Light-Controlled Delivery of Nitric Oxide Combined with Photothermal Therapy. *J. Mater. Chem. B* **2017**, *5*, 7831−7838.
(1316) Guo, M.; Xiang, H.-J.; Wang, Y.; Zhang, Q.-L.; An, L.; Yang, S.-P.; Ma, Y.; Wang, Y.; Liu, J.-G. Ruthenium Nitrosyl Functionalized Graphene Quantum Dots as an Efficient Nanoplatform for NIR-Light-Controlled and Mitochondria-Targeted Delivery of Nitric Oxide Combined with Photothermal Therapy. *Chem. Commun.* **2017**, *53*, 3253−3256.
(1317) Yu, Y.-T.; Shi, S.-W.; Wang, Y.; Zhang, Q.-L.; Gao, S.-H.; Yang, S.-P.; Liu, J.-G. A Ruthenium Nitrosyl-Functionalized Magnetic Nanoplatform with Near-Infrared Light-Controlled Nitric Oxide Delivery and Photothermal Effect for Enhanced Antitumor and Antibacterial Therapy. *ACS Appl. Mater. Interfaces* **2020**, *12*, 312−321.
(1318) Deng, Q.; Xiang, H.-J.; Tang, W.-W.; An, L.; Yang, S.-P.; Zhang, Q.-L.; Liu, J.-G. Ruthenium Nitrosyl Grafted Carbon Dots as a Fluorescence-Trackable Nanoplatform for Visible Light-Controlled Nitric Oxide Release and Targeted Intracellular Delivery. *J. Inorg. Biochem.* **2016**, *165*, 152−158.
(1319) Shi, S.-W.; Li, Y.-H.; Zhang, Q.-L.; Yang, S.-P.; Liu, J.-G. Targeted and NIR Light-Controlled Delivery of Nitric Oxide Combined with a Platinum(IV) Prodrug for Enhanced Anticancer Therapy. *J. Mater. Chem. B* **2019**, *7*, 1867−1874.
(1320) Neuman, D.; Ostrowski, A. D.; Mikhailovsky, A. A.; Absalonson, R. O.; Strouse, G. F.; Ford, P. C. Quantum Dot Fluorescence Quenching Pathways with Cr(III) Complexes. Photosensitized NO Production from *trans*-Cr(cyclam)$(ONO)^{2+}$. *J. Am. Chem. Soc.* **2008**, *130*, 168−175.
(1321) Tan, L.; Wan, A.; Zhu, X.; Li, H. Nitric Oxide Release Triggered by Two-Photon Excited Photoluminescence of Engineered Nanomaterials. *Chem. Commun.* **2014**, *50*, 5725−5728.
(1322) Tan, L.; Wan, A.; Zhu, X.; Li, H. Visible Light-Triggered Nitric Oxide Release from Near-Infrared Fluorescent Nanospheric Vehicles. *Analyst* **2014**, *139*, 3398−3406.
(1323) Heilman, B. J.; St. John, J.; Oliver, S. R. J.; Mascharak, P. K. Light-Triggered Eradication of Acinetobacter baumannii by Means of NO Delivery from a Porous Material with an Entrapped Metal Nitrosyl. *J. Am. Chem. Soc.* **2012**, *134*, 11573−11582.
(1324) Chen, G.; Qiu, H.; Prasad, P. N.; Chen, X. Upconversion Nanoparticles: Design, Nanochemistry, and Applications in Theranostics. *Chem. Rev.* **2014**, *114*, 5161−5214.
(1325) Liu, Y.; Tu, D.; Zhu, H.; Chen, X. Lanthanide-Doped Luminescent Nanoprobes: Controlled Synthesis, Optical Spectroscopy, and Bioapplications. *Chem. Soc. Rev.* **2013**, *42*, 6924−6958.
(1326) Mase, J. D.; Razgoniaev, A. O.; Tschirhart, M. K.; Ostrowski, A. D. Light-Controlled Release of Nitric Oxide from Solid Polymer Composite Materials using Visible and Near Infra-Red Light. *Photochem. Photobiol. Sci.* **2015**, *14*, 775−785.
(1327) Welbes, L. L.; Borovik, A. S. Confinement of Metal Complexes within Porous Hosts: Development of Functional Materials for Gas Binding and Catalysis. *Acc. Chem. Res.* **2005**, *38*, 765−774.
(1328) Halpenny, G. M.; Olmstead, M. M.; Mascharak, P. K. Incorporation of a Designed Ruthenium Nitrosyl in PolyHEMA Hydrogel and Light-Activated Delivery of NO to Myoglobin. *Inorg. Chem.* **2007**, *46*, 6601−6606.
(1329) Robbins, M. E.; Schoenfisch, M. H. Surface-Localized Release of Nitric Oxide via Sol-Gel Chemistry. *J. Am. Chem. Soc.* **2003**, *125*, 6068−6069.
(1330) Heilman, B. J.; Halpenny, G. M.; Mascharak, P. K. Synthesis, Characterization, and Light-Controlled Antibiotic Application of a Composite Material Derived from Polyurethane and Silica Xerogel with Embedded Photoactive Manganese Nitrosyl. *J. Biomed. Mater. Res., Part B* **2011**, *99B*, 328−337.
(1331) Duan, Y.; Wang, Y.; Li, X.; Zhang, G.; Zhang, G.; Hu, J. Light-Triggered Nitric Oxide (NO) Release From Photoresponsive Polymersomes for Corneal Wound Healing. *Chem. Sci.* **2020**, *11*, 186−194.
(1332) Nocito, G.; Petralia, S.; Malanga, M.; Béni, S.; Calabrese, G.; Parenti, R.; Conoci, S.; Sortino, S. Biofriendly Route to Near-Infrared-Active Gold Nanotriangles and Nanoflowers through Nitric Oxide Photorelease for Photothermal Applications. *ACS Appl. Nano Mater.* **2019**, *2*, 7916−7923.
(1333) Chen, Z.; Thiramanas, R.; Schwendy, M.; Xie, C.; Parekh, S. H.; Mailänder, V.; Wu, S. Upconversion Nanocarriers Encapsulated with Photoactivatable Ru Complexes for Near-Infrared Light-Regulated Enzyme Activity. *Small* **2017**, *13*, 1700997.
(1334) Diring, S.; Wang, D. O.; Kim, C.; Kondo, M.; Chen, Y.; Kitagawa, S.; Kamei, K.-i.; Furukawa, S. Localized Cell Stimulation by Nitric Oxide Using a Photoactive Porous Coordination Polymer Platform. *Nat. Commun.* **2013**, *4*, 2684.
(1335) Kabil, O.; Banerjee, R. Enzymology of H_2S Biogenesis, Decay and Signaling. *Antioxid. Redox Signaling* **2014**, *20*, 770−782.
(1336) Wallace, J. L.; Wang, R. Hydrogen Sulfide-Based Therapeutics: Exploiting a Unique but Ubiquitous Gasotransmitter. *Nat. Rev. Drug Discovery* **2015**, *14*, 329−345.

(1337) Lefer, D. J. A New Gaseous Signaling Molecule Emerges: Cardioprotective Role of Hydrogen Sulfide. *Proc. Natl. Acad. Sci. U. S. A.* **2007**, *104*, 17907−17908.
(1338) Polhemus, D. J.; Lefer, D. J. Emergence of Hydrogen Sulfide as an Endogenous Gaseous Signaling Molecule in Cardiovascular Disease. *Circ. Res.* **2014**, *114*, 730−737.
(1339) Kang, J.; Li, Z.; Organ, C. L.; Park, C.-M.; Yang, C.-t.; Pacheco, A.; Wang, D.; Lefer, D. J.; Xian, M. pH-Controlled Hydrogen Sulfide Release for Myocardial Ischemia-Reperfusion Injury. *J. Am. Chem. Soc.* **2016**, *138*, 6336−6339.
(1340) Benavides, G. A.; Squadrito, G. L.; Mills, R. W.; Patel, H. D.; Isbell, T. S.; Patel, R. P.; Darley-Usmar, V. M.; Doeller, J. E.; Kraus, D. W. Hydrogen Sulfide Mediates the Vasoactivity of Garlic. *Proc. Natl. Acad. Sci. U. S. A.* **2007**, *104*, 17977−17982.
(1341) Li, H.; Yao, Y.; Shi, H.; Lei, Y.; Huang, Y.; Wang, K.; He, X.; Liu, J. A Near-Infrared Light-Responsive Nanocomposite for Photothermal Release of H_2S and Suppression of Cell Viability. *J. Mater. Chem. B* **2019**, *7*, 5992−5997.
(1342) Huang, Y.; Li, H.; He, X.; Yang, X.; Li, L.; Liu, S.; Zou, Z.; Wang, K.; Liu, J. Near-Infrared Photothermal Release of Hydrogen Sulfide from Nanocomposite Hydrogels for Anti-Inflammation Applications. *Chin. Chem. Lett.* **2020**, *31*, 787−791.
(1343) Levinn, C. M.; Cerda, M. M.; Pluth, M. D. Development and Application of Carbonyl Sulfide-Based Donors for H2S Delivery. *Acc. Chem. Res.* **2019**, *52*, 2723−2731.
(1344) Devarie-Baez, N. O.; Bagdon, P. E.; Peng, B.; Zhao, Y.; Park, C.-M.; Xian, M. Light-Induced Hydrogen Sulfide Release from "Caged" gem-Dithiols. *Org. Lett.* **2013**, *15*, 2786−2789.
(1345) Fukushima, N.; Ieda, N.; Sasakura, K.; Nagano, T.; Hanaoka, K.; Suzuki, T.; Miyata, N.; Nakagawa, H. Synthesis of a Photocontrollable Hydrogen Sulfide Donor Using Ketoprofenate Photocages. *Chem. Commun.* **2014**, *50*, 587−589.
(1346) Fukushima, N.; Ieda, N.; Kawaguchi, M.; Sasakura, K.; Nagano, T.; Hanaoka, K.; Miyata, N.; Nakagawa, H. Development of Photo-Controllable Hydrogen Sulfide Donor Applicable in Live Cells. *Bioorg. Med. Chem. Lett.* **2015**, *25*, 175−178.
(1347) Fox, M. A.; Triebel, C. A. A New Pathway for Cleavage of Some Phenacyl and Styryl Thioethers. *J. Org. Chem.* **1983**, *48*, 835−840.
(1348) Xiao, Z.; Bonnard, T.; Shakouri-Motlagh, A.; Wylie, R. A. L.; Collins, J.; White, J.; Heath, D. E.; Hagemeyer, C. E.; Connal, L. A. Triggered and Tunable Hydrogen Sulfide Release from Photogenerated Thiobenzaldehydes. *Chem. - Eur. J.* **2017**, *23*, 11294−11300.
(1349) Tron, A.; Peyret, A.; Thevenot, J.; Bofinger, R.; Lecommandoux, S.; McClenaghan, N. D. A Prototype Reversible Polymersome-Stabilized H_2S Photoejector Operating under Pseudo-physiological Conditions. *Org. Biomol. Chem.* **2016**, *14*, 6394−6397.
(1350) Chen, W.; Chen, M.; Zang, Q.; Wang, L.; Tang, F.; Han, Y.; Yang, C.; Deng, L.; Liu, Y.-N. NIR Light Controlled Release of Caged Hydrogen Sulfide Based on Upconversion Nanoparticles. *Chem. Commun.* **2015**, *51*, 9193−9196.
(1351) Chaudhuri, A.; Venkatesh, Y.; Das, J.; Gangopadhyay, M.; Maiti, T. K.; Singh, N. D. P. One- and Two-Photon-Activated Cysteine Persulfide Donors for Biological Targeting. *J. Org. Chem.* **2019**, *84*, 11441−11449.
(1352) Supuran, C. T.; Scozzafava, A. Carbonic Anhydrases as Targets for Medicinal Chemistry. *Bioorg. Med. Chem.* **2007**, *15*, 4336−4350.
(1353) Zhao, Y.; Bolton, S. G.; Pluth, M. D. Light-Activated COS/H_2S Donation from Photocaged Thiocarbamates. *Org. Lett.* **2017**, *19*, 2278−2281.
(1354) Parthiban, C.; M, P.; Reddy, L. V. K.; Sen, D.; Samuel S, M.; Singh, N. D. P. Tetraphenylethylene Conjugated *p*-Hydroxyphenacyl: Fluorescent Organic Nanoparticles for the Release of Hydrogen Sulfide under Visible Light with Real-Time Cellular Imaging. *Org. Biomol. Chem.* **2018**, *16*, 7903−7909.
(1355) Venkatesh, Y.; Das, J.; Chaudhuri, A.; Karmakar, A.; Maiti, T. K.; Singh, N. D. P. Light Triggered Uncaging of Hydrogen Sulfide (H_2S) with Real-Time Monitoring. *Chem. Commun.* **2018**, *54*, 3106−3109.
(1356) Chaudhuri, A.; Venkatesh, Y.; Jena, B. C.; Behara, K. K.; Mandal, M.; Singh, N. D. P. Real-Time Monitoring of a Photoactivated Hydrogen Persulfide Donor for Biological Entities. *Org. Biomol. Chem.* **2019**, *17*, 8800−8805.
(1357) Yi, S. Y.; Moon, Y. K.; Kim, S.; Kim, S.; Park, G.; Kim, J. J.; You, Y. Visible Light-Driven Photogeneration of Hydrogen Sulfide. *Chem. Commun.* **2017**, *53*, 11830−11833.
(1358) Li, L.; Whiteman, M.; Guan, Y. Y.; Neo, K. L.; Cheng, Y.; Lee, S. W.; Zhao, Y.; Baskar, R.; Tan, C.-H.; Moore, P. K. Characterization of a Novel, Water-Soluble Hydrogen Sulfide-Releasing Molecule (GYY4137). *Circulation* **2008**, *117*, 2351−2360.
(1359) Alexander, B. E.; Coles, S. J.; Fox, B. C.; Khan, T. F.; Maliszewski, J.; Perry, A.; Pitak, M. B.; Whiteman, M.; Wood, M. E. Investigating the Generation of Hydrogen Sulfide from the Phosphonamidodithioate Slow-Release Donor GYY4137. *MedChemComm* **2015**, *6*, 1649−1655.
(1360) DeMartino, A. W.; Zigler, D. F.; Fukuto, J. M.; Ford, P. C. Carbon Disulfide. Just Toxic or Also Bioregulatory and/or Therapeutic? *Chem. Soc. Rev.* **2017**, *46*, 21−39.
(1361) Bernt, C. M.; Burks, P. T.; DeMartino, A. W.; Pierri, A. E.; Levy, E. S.; Zigler, D. F.; Ford, P. C. Photocatalytic Carbon Disulfide Production via Charge Transfer Quenching of Quantum Dots. *J. Am. Chem. Soc.* **2014**, *136*, 2192−2195.
(1362) Zivic, N.; Kuroishi, P. K.; Dumur, F.; Gigmes, D.; Dove, A. P.; Sardon, H. Recent Advances and Challenges in the Design of Organic Photoacid and Photobase Generators for Polymerizations. *Angew. Chem., Int. Ed.* **2019**, *58*, 10410−10422.
(1363) Sun, X.; Jin, M.; Wu, X.; Pan, H.; Wan, D.; Pu, H. Bis-Substituted Thiophene-Containing Oxime Sulfonates Photoacid Generators for Cationic Polymerization Under UV−Visible LED Irradiation. *J. Polym. Sci., Part A: Polym. Chem.* **2018**, *56*, 776−782.
(1364) Sambath, K.; Wan, Z.; Wang, Q.; Chen, H.; Zhang, Y. BODIPY-Based Photoacid Generators for Light-Induced Cationic Polymerization. *Org. Lett.* **2020**, *22*, 1208−1212.
(1365) Fu, C.; Xu, J.; Boyer, C. Photoacid-Mediated Ring Opening Polymerization Driven by Visible Light. *Chem. Commun.* **2016**, *52*, 7126−7129.
(1366) Hayes, C. O.; Bell, W. K.; Cassidy, B. R.; Willson, C. G. Synthesis and Characterization of a Two Stage, Nonlinear Photobase Generator. *J. Org. Chem.* **2015**, *80*, 7530−7535.
(1367) Kaye, W. Near-Infrared Spectroscopy: I. Spectral Identification and Analytical Applications. *Spectrochim. Acta* **1954**, *6*, 257.
(1368) Pansare, V. J.; Hejazi, S.; Faenza, W. J.; Prud'homme, R. K. Review of Long-Wavelength Optical and NIR Imaging Materials: Contrast Agents, Fluorophores, and Multifunctional Nano Carriers. *Chem. Mater.* **2012**, *24*, 812−827.
(1369) Pawlicki, M.; Collins, H. A.; Denning, R. G.; Anderson, H. L. Two-Photon Absorption and the Design of Two-Photon Dyes. *Angew. Chem., Int. Ed.* **2009**, *48*, 3244−3266.
(1370) Klausen, M.; Dubois, V.; Verlhac, J.-B.; Blanchard-Desce, M. Tandem Systems for Two-Photon Uncaging of Bioactive Molecules. *ChemPlusChem* **2019**, *84*, 589−598.
(1371) Speiser, S. Photophysics and Mechanisms of Intramolecular Electronic Energy Transfer in Bichromophoric Molecular Systems: Solution and Supersonic Jet Studies. *Chem. Rev.* **1996**, *96*, 1953−1976.
(1372) Dietliker, K.; Broillet, S.; Hellrung, B.; Rzadek, P.; Rist, G.; Wirz, J.; Neshchadin, D.; Gescheidt, G. Photophysical Investigations on Photoinitiators with Covalently Linked Thioxanthone Sensitizer Moieties. *Helv. Chim. Acta* **2006**, *89*, 2211−2225.
(1373) Wagner, P. J.; Klán, P. Intramolecular Triplet Energy Transfer in Flexible Molecules: Electronic, Dynamic, and Structural Aspects. *J. Am. Chem. Soc.* **1999**, *121*, 9626−9635.
(1374) Falvey, D. E.; Sundararajan, C. Photoremovable Protecting Groups Based on Electron Transfer Chemistry. *Photochem. Photobiol. Sci.* **2004**, *3*, 831−838.

(1375) Houmam, A. Electron Transfer Initiated Reactions: Bond Formation and Bond Dissociation. *Chem. Rev.* **2008**, *108*, 2180−2237.
(1376) Dougherty, T. J.; Gomer, C. J.; Henderson, B. W.; Jori, G.; Kessel, D.; Korbelik, M.; Moan, J.; Peng, Q. Photodynamic Therapy. *JNCI-J. Natl. Cancer Inst.* **1998**, *90*, 889−905.
(1377) DeRosa, M. C.; Crutchley, R. J. Photosensitized Singlet Oxygen and Its Applications. *Coord. Chem. Rev.* **2002**, *233*, 351−371.
(1378) Detty, M. R.; Gibson, S. L.; Wagner, S. J. Current Clinical and Preclinical Photosensitizers for Use in Photodynamic Therapy. *J. Med. Chem.* **2004**, *47*, 3897−3915.
(1379) Ormond, A. B.; Freeman, H. S. Dye Sensitizers for Photodynamic Therapy. *Materials* **2013**, *6*, 817−840.
(1380) Klán, P.; Wagner, P. J. Intramolecular Triplet Energy Transfer in Bichromophores With Long Flexible Tethers. *J. Am. Chem. Soc.* **1998**, *120*, 2198−2199.
(1381) Vrbka, L.; Klán, P.; Kříž, Z.; Koča, J.; Wagner, P. J. Computer Modeling and Simulations on Flexible Bifunctional Systems: Intramolecular Energy Transfer Implications. *J. Phys. Chem. A* **2003**, *107*, 3404−3413.
(1382) Papageorgiou, G.; Corrie, J. E. T. Optimised Synthesis and Photochemistry of Antenna-Sensitised 1-Acyl-7-Nitroindolines. *Tetrahedron* **2005**, *61*, 609−616.
(1383) Papageorgiou, G.; Lukeman, M.; Wan, P.; Corrie, J. E. T. An Antenna Triplet Sensitiser for 1-Acyl-7-Nitroindolines Improves the Efficiency of Carboxylic Acid Photorelease. *Photochem. Photobiol. Sci.* **2004**, *3*, 366−373.
(1384) Papageorgiou, G.; Ogden, D.; Corrie, J. E. T. An Antenna-Sensitized Nitroindoline Precursor to Enable Photorelease of l-Glutamate in High Concentrations. *J. Org. Chem.* **2004**, *69*, 7228−7233.
(1385) Papageorgiou, G.; Ogden, D.; Corrie, J. E. T. An Antenna-Sensitised 1-Acyl-7-Nitroindoline That Has Good Solubility Properties in the Presence of Calcium Ions and Is Suitable for Use as a Caged L-Glutamate in Neuroscience. *Photochem. Photobiol. Sci.* **2008**, *7*, 423−432.
(1386) Wöll, D.; Laimgruber, S.; Galetskaya, M.; Smirnova, J.; Pfleiderer, W.; Heinz, B.; Gilch, P.; Steiner, U. E. On the Mechanism of Intramolecular Sensitization of Photocleavage of the 2-(2-Nitrophenyl)propoxycarbonyl (NPPOC) Protecting Group. *J. Am. Chem. Soc.* **2007**, *129*, 12148−12158.
(1387) Röthlingshöfer, M.; Gorska, K.; Winssinger, N. Nucleic Acid-Templated Energy Transfer Leading to a Photorelease Reaction and its Application to a System Displaying a Nonlinear Response. *J. Am. Chem. Soc.* **2011**, *133*, 18110−18113.
(1388) Ndzeidze, G. N.; Li, L.; Steinmetz, M. G. Reversible Triplet Excitation Transfer in a Trimethylene-Linked Thioxanthone and Benzothiophene-2-Carboxanilide that Photochemically Expels Leaving Group Anions. *J. Org. Chem.* **2018**, *83*, 8995−9007.
(1389) Lv, W.; Wang, W. One-Photon Upconversion-Like Photolysis: A New Strategy to Achieve Long-Wavelength Light-Excitable Photolysis. *Synlett* **2020**, *31*, 1129−1134.
(1390) Rehm, D.; Weller, A. Kinetik und Mechanismus der Elektronübertragung bei der Fluoreszenzlöschung in Acetonitril. *Berich. Bunsen. Gesell.* **1969**, *73*, 834−839.
(1391) Hoffmann, N. Efficient Photochemical Electron Transfer Sensitization of Homogeneous Organic Reactions. *J. Photochem. Photobiol., C* **2008**, *9*, 43−60.
(1392) Romero, N. A.; Nicewicz, D. A. Organic Photoredox Catalysis. *Chem. Rev.* **2016**, *116*, 10075−10166.
(1393) Banerjee, A.; Falvey, D. E. Protecting Groups That Can Be Removed through Photochemical Electron Transfer: Mechanistic and Product Studies on Photosensitized Release of Carboxylates from Phenacyl Esters. *J. Org. Chem.* **1997**, *62*, 6245−6251.
(1394) Lee, K.; Falvey, D. E. Photochemically Removable Protecting Groups Based on Covalently Linked Electron Donor-Acceptor Systems. *J. Am. Chem. Soc.* **2000**, *122*, 9361−9366.
(1395) Banerjee, A.; Lee, K.; Falvey, D. E. Photoreleasable Protecting Groups Based on Electron Transfer Chemistry. Donor Sensitized Release of Phenacyl Groups From Alcohols, Phosphates and Diacids. *Tetrahedron* **1999**, *55*, 12699−12710.
(1396) Sundararajan, C.; Falvey, D. E. Photorelease of Carboxylic and Amino Acids From *N*-Methyl-4-Picolinium Esters by Mediated Electron Transfer. *Photochem. Photobiol. Sci.* **2006**, *5*, 116−121.
(1397) Sundararajan, C.; Falvey, D. E. Photolytic Release of Carboxylic Acids Using Linked Donor-Acceptor Molecules: Direct versus Mediated Photoinduced Electron Transfer to *N*-Alkyl-4-picolinium Esters. *Org. Lett.* **2005**, *7*, 2631−2634.
(1398) Zeppuhar, A. N.; Hill-Byrne, K.; Falvey, D. E. Mechanism of the Photorelease of Alcohols From the 9-Phenyl-9-Tritylone Protecting Group. *Photochem. Photobiol. Sci.* **2019**, *18*, 1990−1995.
(1399) Banerjee, A.; Lee, K.; Yu, Q.; Fang, A. G.; Falvey, D. E. Protecting Group Release Through Photoinduced Electron Transfer: Wavelength Control Through Sensitized Irradiation. *Tetrahedron Lett.* **1998**, *39*, 4635−4638.
(1400) Speckmeier, E.; Zeitler, K. Desyl and Phenacyl as Versatile, Photocatalytically Cleavable Protecting Groups: A Classic Approach in a Different (Visible) Light. *ACS Catal.* **2017**, *7*, 6821−6826.
(1401) Sundararajan, C.; Falvey, D. E. Photorelease of Carboxylic Acids, Amino Acids, and Phosphates from N-Alkylpicolinium Esters Using Photosensitization by High Wavelength Laser Dyes. *J. Am. Chem. Soc.* **2005**, *127*, 8000−8001.
(1402) Borak, J. B.; Falvey, D. E. A New Photolabile Protecting Group for Release of Carboxylic Acids by Visible-Light-Induced Direct and Mediated Electron Transfer. *J. Org. Chem.* **2009**, *74*, 3894−3899.
(1403) Borak, J. B.; Falvey, D. E. Ketocoumarin Dyes as Electron Mediators for Visible Light Induced Carboxylate Photorelease. *Photochem. Photobiol. Sci.* **2010**, *9*, 854−860.
(1404) Kunsberg, D. J.; Kipping, A. H.; Falvey, D. E. Visible Light Photorelease of Carboxylic Acids via Charge-Transfer Excitation of *N*-Methylpyridinium Iodide Esters. *Org. Lett.* **2015**, *17*, 3454−3457.
(1405) Thum, M. D.; Falvey, D. E. Photoreleasable Protecting Groups Triggered by Sequential Two-Photon Absorption of Visible Light: Release of Carboxylic Acids from a Linked Anthraquinone-N-Alkylpicolinium Ester Molecule. *J. Phys. Chem. A* **2018**, *122*, 3204−3210.
(1406) Edson, J. B.; Spencer, L. P.; Boncella, J. M. Photorelease of Primary Aliphatic and Aromatic Amines by Visible-Light-Induced Electron Transfer. *Org. Lett.* **2011**, *13*, 6156−6159.
(1407) Yu, Y.; Kang, X.; Yang, X.; Yuan, L.; Feng, W.; Cui, S. Surface Charge Inversion of Self-Assembled Monolayers by Visible Light Irradiation: Cargo Loading and Release by Photoreactions. *Chem. Commun.* **2013**, *49*, 3431−3433.
(1408) Ciuciu, A. I.; Korzycka, K. A.; Lewis, W. J. M.; Bennett, P. M.; Anderson, H. L.; Flamigni, L. Model Dyads for 2PA Uncaging of a Protecting Group via Photoinduced Electron Transfer. *Phys. Chem. Chem. Phys.* **2015**, *17*, 6554−6564.
(1409) Denning, D. M.; Pedowitz, N. J.; Thum, M. D.; Falvey, D. E. Uncaging Alcohols Using UV or Visible Light Photoinduced Electron Transfer to 9-Phenyl-9-tritylone Ethers. *Org. Lett.* **2015**, *17*, 5986−5989.
(1410) Heymann, R. R.; Thum, M. D.; Hardee, A. L.; Falvey, D. E. Visible Light Initiated Release of Calcium Ions Through Photochemical Electron Transfer Reactions. *Photochem. Photobiol. Sci.* **2017**, *16*, 1003−1008.
(1411) Wang, H.; Li, W.-G.; Zeng, K.; Wu, Y.-J.; Zhang, Y.; Xu, T.-L.; Chen, Y. Photocatalysis Enables Visible-Light Uncaging of Bioactive Molecules in Live Cells. *Angew. Chem., Int. Ed.* **2019**, *58*, 561−565.
(1412) Gorska, K.; Manicardi, A.; Barluenga, S.; Winssinger, N. DNA-Templated Release of Functional Molecules With an Azide-Reduction-Triggered Immolative Linker. *Chem. Commun.* **2011**, *47*, 4364−4366.
(1413) Rothlingshofer, M.; Gorska, K.; Winssinger, N. Nucleic Acid Templated Uncaging of Fluorophores Using Ru-Catalyzed Photoreduction with Visible Light. *Org. Lett.* **2012**, *14*, 482−485.

(1414) Dariva, C. G.; Coelho, J. F. J.; Serra, A. C. Near Infrared Light-Triggered Nanoparticles Using Singlet Oxygen Photocleavage for Drug Delivery Systems. *J. Controlled Release* **2019**, *294*, 337−354.
(1415) Shim, G.; Ko, S.; Kim, D.; Le, Q.-V.; Park, G. T.; Lee, J.; Kwon, T.; Choi, H.-G.; Kim, Y. B.; Oh, Y.-K. Light-Switchable Systems for Remotely Controlled Drug Delivery. *J. Controlled Release* **2017**, *267*, 67−79.
(1416) Zamadar, M.; Ghosh, G.; Mahendran, A.; Minnis, M.; Kruft, B. I.; Ghogare, A.; Aebisher, D.; Greer, A. Photosensitizer Drug Delivery via an Optical Fiber. *J. Am. Chem. Soc.* **2011**, *133*, 7882−7891.
(1417) Ghosh, G.; Belh, S. J.; Chiemezie, C.; Walalawela, N.; Ghogare, A. A.; Vignoni, M.; Thomas, A. H.; McFarland, S. A.; Greer, E. M.; Greer, A. *S, S*-Chiral Linker Induced U Shape with a Syn-facial Sensitizer and Photocleavable Ethene Group. *Photochem. Photobiol.* **2019**, *95*, 293−305.
(1418) Anderson, V. C.; Thompson, D. H. Triggered Release of Hydrophilic Agents From Plasmologen Liposomes Using Visible Light or Acid. *Biochim. Biophys. Acta, Biomembr.* **1992**, *1109*, 33−42.
(1419) Murthy, R. S.; Bio, M.; You, Y. Low Energy Light-Triggered Oxidative Cleavage of Olefins. *Tetrahedron Lett.* **2009**, *50*, 1041−1044.
(1420) Baugh, S. D. P.; Yang, Z.; Leung, D. K.; Wilson, D. M.; Breslow, R. Cyclodextrin Dimers as Cleavable Carriers of Photodynamic Sensitizers. *J. Am. Chem. Soc.* **2001**, *123*, 12488−12494.
(1421) Ruebner, A.; Yang, Z.; Leung, D.; Breslow, R. A Cyclodextrin Dimer With a Photocleavable Linker as a Possible Carrier for the Photosensitizer in Photodynamic Tumor Therapy. *Proc. Natl. Acad. Sci. U. S. A.* **1999**, *96*, 14692−14693.
(1422) Jiang, M. Y.; Dolphin, D. Site-Specific Prodrug Release Using Visible Light. *J. Am. Chem. Soc.* **2008**, *130*, 4236−4237.
(1423) Liu, J.; Yang, G.; Zhu, W.; Dong, Z.; Yang, Y.; Chao, Y.; Liu, Z. Light-Controlled Drug Release From Singlet-Oxygen Sensitive Nanoscale Coordination Polymers Enabling Cancer Combination Therapy. *Biomaterials* **2017**, *146*, 40−48.
(1424) Wang, H.; Han, R.-l.; Yang, L.-m.; Shi, J.-h.; Liu, Z.-j.; Hu, Y.; Wang, Y.; Liu, S.-j.; Gan, Y. Design and Synthesis of Core−Shell−Shell Upconversion Nanoparticles for NIR-Induced Drug Release, Photodynamic Therapy, and Cell Imaging. *ACS Appl. Mater. Interfaces* **2016**, *8*, 4416−4423.
(1425) Chai, S.; Guo, Y.; Zhang, Z.; Chai, Z.; Ma, Y.; Qi, L. Cyclodextrin-Gated Mesoporous Silica Nanoparticles as Drug Carriers for Red Light-Induced Drug Release. *Nanotechnology* **2017**, *28*, 145101.
(1426) Yang, G.; Sun, X.; Liu, J.; Feng, L.; Liu, Z. Light-Responsive, Singlet-Oxygen-Triggered On-Demand Drug Release from Photosensitizer-Doped Mesoporous Silica Nanorods for Cancer Combination Therapy. *Adv. Funct. Mater.* **2016**, *26*, 4722−4732.
(1427) Ghosh, G.; Minnis, M.; Ghogare, A. A.; Abramova, I.; Cengel, K. A.; Busch, T. M.; Greer, A. Photoactive Fluoropolymer Surfaces That Release Sensitizer Drug Molecules. *J. Phys. Chem. B* **2015**, *119*, 4155−4164.
(1428) Li, J.; Huang, J.; Lyu, Y.; Huang, J.; Jiang, Y.; Xie, C.; Pu, K. Photoactivatable Organic Semiconducting Pro-Nanoenzymes. *J. Am. Chem. Soc.* **2019**, *141*, 4073−4079.
(1429) Bartusik, D.; Aebisher, D.; Ghosh, G.; Minnis, M.; Greer, A. Fluorine End-Capped Optical Fibers for Photosensitizer Release and Singlet Oxygen Production. *J. Org. Chem.* **2012**, *77*, 4557−4565.
(1430) Lee, J.; Park, J.; Singha, K.; Kim, W. J. Mesoporous Silica Nanoparticle Facilitated Drug Release Through Cascade Photosensitizer Activation and Cleavage of Singlet Oxygen Sensitive Linker. *Chem. Commun.* **2013**, *49*, 1545−1547.
(1431) Dinache, A.; Smarandache, A.; Simon, A.; Nastasa, V.; Tozar, T.; Pascu, A.; Enescu, M.; Khatyr, A.; Sima, F.; Pascu, M. L.; Staicu, A. Photosensitized Cleavage of Some Olefins as Potential Linkers to Be Used in Drug Delivery. *Appl. Surf. Sci.* **2017**, *417*, 136−142.
(1432) Saravanakumar, G.; Lee, J.; Kim, J.; Kim, W. J. Visible Light-Induced Singlet Oxygen-Mediated Intracellular Disassembly of Polymeric Micelles Co-loaded With a Photosensitizer and an Anticancer Drug for Enhanced Photodynamic Therapy. *Chem. Commun.* **2015**, *51*, 9995−9998.
(1433) Thapa, P.; Li, M.; Karki, R.; Bio, M.; Rajaputra, P.; Nkepang, G.; Woo, S.; You, Y. Folate-PEG Conjugates of a Far-Red Light-Activatable Paclitaxel Prodrug to Improve Selectivity toward Folate Receptor-Positive Cancer Cells. *ACS Omega* **2017**, *2*, 6349−6360.
(1434) Nkepang, G.; Bio, M.; Rajaputra, P.; Awuah, S. G.; You, Y. Folate Receptor-Mediated Enhanced and Specific Delivery of Far-Red Light-Activatable Prodrugs of Combretastatin A-4 to FR-Positive Tumor. *Bioconjugate Chem.* **2014**, *25*, 2175−2188.
(1435) Bio, M.; Rajaputra, P.; Nkepang, G.; You, Y. Far-Red Light Activatable, Multifunctional Prodrug for Fluorescence Optical Imaging and Combinational Treatment. *J. Med. Chem.* **2014**, *57*, 3401−3409.
(1436) Bio, M.; Nkepang, G.; You, Y. Click and Photo-Unclick Chemistry of Aminoacrylate for Visible Light-Triggered Drug Release. *Chem. Commun.* **2012**, *48*, 6517−6519.
(1437) Hossion, A. M. L.; Bio, M.; Nkepang, G.; Awuah, S. G.; You, Y. Visible Light Controlled Release of Anticancer Drug through Double Activation of Prodrug. *ACS Med. Chem. Lett.* **2013**, *4*, 124−127.
(1438) Yavlovich, A.; Smith, B.; Gupta, K.; Blumenthal, R.; Puri, A. Light-Sensitive Lipid-Based Nanoparticles for Drug Delivery: Design Principles and Future Considerations for Biological Applications. *Mol. Membr. Biol.* **2010**, *27*, 364−381.
(1439) Chitgupi, U.; Shao, S.; Carter, K. A.; Huang, W.-C.; Lovell, J. F. Multicolor Liposome Mixtures for Selective and Selectable Cargo Release. *Nano Lett.* **2018**, *18*, 1331−1336.
(1440) Carter, K. A.; Shao, S.; Hoopes, M. I.; Luo, D.; Ahsan, B.; Grigoryants, V. M.; Song, W.; Huang, H.; Zhang, G.; Pandey, R. K.; Geng, J.; Pfeifer, B. A.; Scholes, C. P.; Ortega, J.; Karttunen, M.; Lovell, J. F. Porphyrin−Phospholipid Liposomes Permeabilized by Near-Infrared Light. *Nat. Commun.* **2014**, *5*, 3546.
(1441) Miranda, D.; Carter, K.; Luo, D.; Shao, S.; Geng, J.; Li, C.; Chitgupi, U.; Turowski, S. G.; Li, N.; Atilla-Gokcumen, G. E.; Spernyak, J. A.; Lovell, J. F. Multifunctional Liposomes for Image-Guided Intratumoral Chemo-Phototherapy. *Adv. Healthcare Mater.* **2017**, *6*, 1700253.
(1442) Luo, D.; Geng, J.; Li, N.; Carter, K. A.; Shao, S.; Atilla-Gokcumen, G. E.; Lovell, J. F. Vessel-Targeted Chemophototherapy with Cationic Porphyrin-Phospholipid Liposomes. *Mol. Cancer Ther.* **2017**, *16*, 2452−2461.
(1443) Luo, D.; Carter, K. A.; Razi, A.; Geng, J.; Shao, S.; Giraldo, D.; Sunar, U.; Ortega, J.; Lovell, J. F. Doxorubicin Encapsulated in Stealth Liposomes Conferred With Light-Triggered Drug Release. *Biomaterials* **2016**, *75*, 193−202.
(1444) Carter, K. A.; Wang, S.; Geng, J.; Luo, D.; Shao, S.; Lovell, J. F. Metal Chelation Modulates Phototherapeutic Properties of Mitoxantrone-Loaded Porphyrin−Phospholipid Liposomes. *Mol. Pharmaceutics* **2016**, *13*, 420−427.
(1445) Peng, P.-C.; Hong, R.-L.; Tsai, Y.-J.; Li, P.-T.; Tsai, T.; Chen, C.-T. Dual-Effect Liposomes Encapsulated With Doxorubicin and Chlorin e6 Augment the Therapeutic Effect of Tumor Treatment. *Lasers Surg. Med.* **2015**, *47*, 77−87.
(1446) Luo, D.; Li, N.; Carter, K. A.; Lin, C.; Geng, J.; Shao, S.; Huang, W.-C.; Qin, Y.; Atilla-Gokcumen, G. E.; Lovell, J. F. Rapid Light-Triggered Drug Release in Liposomes Containing Small Amounts of Unsaturated and Porphyrin−Phospholipids. *Small* **2016**, *12*, 3039−3047.
(1447) Meyer, A.; Mokhir, A. RNA Interference Controlled by Light of Variable Wavelength. *Angew. Chem., Int. Ed.* **2014**, *53*, 12840−12843.
(1448) Brega, V.; Scaletti, F.; Zhang, X.; Wang, L.-S.; Li, P.; Xu, Q.; Rotello, V. M.; Thomas, S. W. Polymer Amphiphiles for Photoregulated Anticancer Drug Delivery. *ACS Appl. Mater. Interfaces* **2019**, *11*, 2814−2820.
(1449) Lyu, Y.; He, S.; Li, J.; Jiang, Y.; Sun, H.; Miao, Y.; Pu, K. A Photolabile Semiconducting Polymer Nanotransducer for Near-

Infrared Regulation of CRISPR/Cas9 Gene Editing. *Angew. Chem., Int. Ed.* **2019**, *58*, 18197−18201.
(1450) Xu, X.; Zeng, Z.; Huang, Z.; Sun, Y.; Huang, Y.; Chen, J.; Ye, J.; Yang, H.; Yang, C.; Zhao, C. Near-Infrared Light-Triggered Degradable Hyaluronic Acid Hydrogel for On-Demand Drug Release and Combined Chemo-Photodynamic Therapy. *Carbohydr. Polym.* **2020**, *229*, 115394.
(1451) Wang, C.; Huang, B.; Yang, G.; Ouyang, Y.; Tian, J.; Zhang, W. NIR-Triggered Multifunctional and Degradable Nanoplatform Based on an ROS-Sensitive Block Copolymer for Imaging-Guided Chemo-Phototherapy. *Biomacromolecules* **2019**, *20*, 4218−4229.
(1452) Wilson, D. S.; Dalmasso, G.; Wang, L.; Sitaraman, S. V.; Merlin, D.; Murthy, N. Orally Delivered Thioketal Nanoparticles Loaded with TNF-α−siRNA Target Inflammation and Inhibit Gene Expression in the Intestines. *Nat. Mater.* **2010**, *9*, 923−928.
(1453) Shim, M. S.; Xia, Y. A Reactive Oxygen Species (ROS)-Responsive Polymer for Safe, Efficient, and Targeted Gene Delivery in Cancer Cells. *Angew. Chem., Int. Ed.* **2013**, *52*, 6926−6929.
(1454) Yuan, Y.; Liu, J.; Liu, B. Conjugated-Polyelectrolyte-Based Polyprodrug: Targeted and Image-Guided Photodynamic and Chemotherapy with On-Demand Drug Release upon Irradiation with a Single Light Source. *Angew. Chem., Int. Ed.* **2014**, *53*, 7163−7168.
(1455) Liu, L.-H.; Qiu, W.-X.; Li, B.; Zhang, C.; Sun, L.-F.; Wan, S.-S.; Rong, L.; Zhang, X.-Z. A Red Light Activatable Multifunctional Prodrug for Image-Guided Photodynamic Therapy and Cascaded Chemotherapy. *Adv. Funct. Mater.* **2016**, *26*, 6257−6269.
(1456) Pei, Q.; Hu, X.; Zheng, X.; Liu, S.; Li, Y.; Jing, X.; Xie, Z. Light-Activatable Red Blood Cell Membrane-Camouflaged Dimeric Prodrug Nanoparticles for Synergistic Photodynamic/Chemotherapy. *ACS Nano* **2018**, *12*, 1630−1641.
(1457) Seah, G. L.; Yu, J. H.; Yang, M. Y.; Kim, W. J.; Kim, J.-H.; Park, K.; Cho, J.-W.; Kim, J. S.; Nam, Y. S. Low-Power and Low-Drug-Dose Photodynamic Chemotherapy via the Breakdown of Tumor-Targeted Micelles by Reactive Oxygen Species. *J. Controlled Release* **2018**, *286*, 240−253.
(1458) Sun, C.-Y.; Zhang, B.-B.; Zhou, J.-Y. Light-Activated Drug Release from a Hyaluronic Acid Targeted Nanoconjugate for Cancer Therapy. *J. Mater. Chem. B* **2019**, *7*, 4843−4853.
(1459) Yue, C.; Zhang, C.; Alfranca, G.; Yang, Y.; Jiang, X.; Yang, Y.; Pan, F.; Fuente, J. M. d. l.; Cui, D. Near-Infrared Light Triggered ROS-activated Theranostic Platform based on Ce6-CPT-UCNPs for Simultaneous Fluorescence Imaging and Chemo-Photodynamic Combined Therapy. *Theranostics* **2016**, *6*, 456−469.
(1460) Wang, X.; Meng, G.; Zhang, S.; Liu, X. A Reactive $^1O_2$ -Responsive Combined Treatment System of Photodynamic and Chemotherapy for Cancer. *Sci. Rep.* **2016**, *6*, 29911.
(1461) Li, J.; Wei, K.; Zuo, S.; Xu, Y.; Zha, Z.; Ke, W.; Chen, H.; Ge, Z. Light-Triggered Clustered Vesicles with Self-Supplied Oxygen and Tissue Penetrability for Photodynamic Therapy against Hypoxic Tumor. *Adv. Funct. Mater.* **2017**, *27*, 1702108.
(1462) Phua, S. Z. F.; Xue, C.; Lim, W. Q.; Yang, G.; Chen, H.; Zhang, Y.; Wijaya, C. F.; Luo, Z.; Zhao, Y. Light-Responsive Prodrug-Based Supramolecular Nanosystems for Site-Specific Combination Therapy of Cancer. *Chem. Mater.* **2019**, *31*, 3349−3358.
(1463) Li, Y.; Wang, S.; Huang, Y.; Chen, Y.; Wu, W.; Liu, Y.; Zhang, J.; Feng, Y.; Jiang, X.; Gou, M. Light-Activated Drug Release From Prodrug Nanoassemblies by Structure Destruction. *Chem. Commun.* **2019**, *55*, 13128−13131.
(1464) Li, X.; Gao, M.; Xin, K.; Zhang, L.; Ding, D.; Kong, D.; Wang, Z.; Shi, Y.; Kiessling, F.; Lammers, T.; Cheng, J.; Zhao, Y. Singlet Oxygen-Responsive Micelles for Enhanced Photodynamic Therapy. *J. Controlled Release* **2017**, *260*, 12−21.
(1465) Watanabe, K.; Terao, N.; Kii, I.; Nakagawa, R.; Niwa, T.; Hosoya, T. Indolizines Enabling Rapid Uncaging of Alcohols and Carboxylic Acids by Red Light-Induced Photooxidation. *Org. Lett.* **2020**, *22*, 5434−5438.
(1466) Nunes, E. D.; Villela, A. D.; Basso, L. A.; Teixeira, E. H.; Andrade, A. L.; Vasconcelos, M. A.; do Nascimento Neto, L. G.; Gondim, A. C. S.; Diógenes, I. C. N.; Romo, A. I. B.; Nascimento, O. R.; Zampieri, D.; Paulo, T. F.; de Carvalho, I. M. M.; de França Lopes, L. G.; Sousa, E. H. S. Light-Induced Disruption of an Acyl Hydrazone Link as a Novel Strategy for Drug Release and Activation: Isoniazid as a Proof-of-Concept Case. *Inorg. Chem. Front.* **2020**, *7*, 859−870.
(1467) Xu, H.; Cao, W.; Zhang, X. Selenium-Containing Polymers: Promising Biomaterials for Controlled Release and Enzyme Mimics. *Acc. Chem. Res.* **2013**, *46*, 1647−1658.
(1468) Cao, W.; Li, Y.; Yi, Y.; Ji, S.; Zeng, L.; Sun, Z.; Xu, H. Coordination-Responsive Selenium-Containing Polymer Micelles for Controlled Drug Release. *Chem. Sci.* **2012**, *3*, 3403−3408.
(1469) Deepagan, V. G.; Kwon, S.; You, D. G.; Nguyen, V. Q.; Um, W.; Ko, H.; Lee, H.; Jo, D.-G.; Kang, Y. M.; Park, J. H. In situ Diselenide-Crosslinked Polymeric Micelles for ROS-Mediated Anticancer Drug Delivery. *Biomaterials* **2016**, *103*, 56−66.
(1470) Han, P.; Ma, N.; Ren, H.; Xu, H.; Li, Z.; Wang, Z.; Zhang, X. Oxidation-Responsive Micelles Based on a Selenium-Containing Polymeric Superamphiphile. *Langmuir* **2010**, *26*, 14414−14418.
(1471) Ma, N.; Li, Y.; Ren, H.; Xu, H.; Li, Z.; Zhang, X. Selenium-Containing Block Copolymers and Their Oxidation-Responsive Aggregates. *Polym. Chem.* **2010**, *1*, 1609−1614.
(1472) Zhou, W.; Wang, L.; Li, F.; Zhang, W.; Huang, W.; Huo, F.; Xu, H. Selenium-Containing Polymer@Metal-Organic Frameworks Nanocomposites as an Efficient Multiresponsive Drug Delivery System. *Adv. Funct. Mater.* **2017**, *27*, 1605465.
(1473) Ren, H.; Wu, Y.; Ma, N.; Xu, H.; Zhang, X. Side-Chain Selenium-Containing Amphiphilic Block Copolymers: Redox-Controlled Self-Assembly and Disassembly. *Soft Matter* **2012**, *8*, 1460−1466.
(1474) Zhai, S.; Hu, X.; Hu, Y.; Wu, B.; Xing, D. Visible Light-Induced Crosslinking and Physiological Stabilization of Diselenide-Rich Nanoparticles for Redox-Responsive Drug Release and Combination Chemotherapy. *Biomaterials* **2017**, *121*, 41−54.
(1475) Han, P.; Li, S.; Cao, W.; Li, Y.; Sun, Z.; Wang, Z.; Xu, H. Red Light Responsive Diselenide-Containing Block Copolymer Micelles. *J. Mater. Chem. B* **2013**, *1*, 740−743.
(1476) Ren, H.; Wu, Y.; Li, Y.; Cao, W.; Sun, Z.; Xu, H.; Zhang, X. Visible-Light-Induced Disruption of Diselenide-Containing Layer-by-Layer Films: Toward Combination of Chemotherapy and Photodynamic Therapy. *Small* **2013**, *9*, 3981−3986.
(1477) Sun, C.; Ji, S.; Li, F.; Xu, H. Diselenide-Containing Hyperbranched Polymer with Light-Induced Cytotoxicity. *ACS Appl. Mater. Interfaces* **2017**, *9*, 12924−12929.
(1478) Fang, R.; Xu, H.; Cao, W.; Yang, L.; Zhang, X. Reactive Oxygen Species (ROS)-Responsive Tellurium-Containing Hyperbranched Polymer. *Polym. Chem.* **2015**, *6*, 2817−2821.
(1479) Cao, W.; Wang, L.; Xu, H. Selenium/Tellurium Containing Polymer Materials in Nanobiotechnology. *Nano Today* **2015**, *10*, 717−736.
(1480) Li, F.; Li, T.; Cao, W.; Wang, L.; Xu, H. Near-Infrared Light Stimuli-Responsive Synergistic Therapy Nanoplatforms Based on the Coordination of Tellurium-Containing Block Polymer and Cisplatin for Cancer Treatment. *Biomaterials* **2017**, *133*, 208−218.
(1481) Ratanatawanate, C.; Chyao, A.; Balkus, K. J. *S*-Nitrosocysteine-Decorated PbS QDs/TiO_2 Nanotubes for Enhanced Production of Singlet Oxygen. *J. Am. Chem. Soc.* **2011**, *133*, 3492−3497.
(1482) Tang, J.; Robichaux, M. A.; Wu, K.-L.; Pei, J.; Nguyen, N. T.; Zhou, Y.; Wensel, T. G.; Xiao, H. Single-Atom Fluorescence Switch: A General Approach toward Visible-Light-Activated Dyes for Biological Imaging. *J. Am. Chem. Soc.* **2019**, *141*, 14699−14706.
(1483) Sun, W.; Parowatkin, M.; Steffen, W.; Butt, H.-J.; Mailänder, V.; Wu, S. Ruthenium-Containing Block Copolymer Assemblies: Red-Light-Responsive Metallopolymers with Tunable Nanostructures for Enhanced Cellular Uptake and Anticancer Phototherapy. *Adv. Healthcare Mater.* **2016**, *5*, 467−473.
(1484) Kachkovskii, A. D. The Nature of Electronic Transitions in Linear Conjugated Systems. *Russ. Chem. Rev.* **1997**, *66*, 647−664.

(1485) Bricks, J. L.; Kachkovskii, A. D.; Slominskii, Y. L.; Gerasov, A. O.; Popov, S. V. Molecular Design of Near Infrared Polymethine Dyes: A Review. *Dyes Pigm.* **2015**, *121*, 238−255.
(1486) Frangioni, J. V. In Vivo Near-Infrared Fluorescence Imaging. *Curr. Opin. Chem. Biol.* **2003**, *7*, 626−634.
(1487) Luo, S.; Zhang, E.; Su, Y.; Cheng, T.; Shi, C. A Review of Nir Dyes in Cancer Targeting and Imaging. *Biomaterials* **2011**, *32*, 7127−7138.
(1488) Shi, C.; Wu, J. B.; Pan, D. Review on Near-Infrared Heptamethine Cyanine Dyes as Theranostic Agents for Tumor Imaging, Targeting, and Photodynamic Therapy. *J. Biomed. Opt.* **2016**, *21*, 50901.
(1489) Alander, J. T.; Kaartinen, I.; Laakso, A.; Patila, T.; Spillmann, T.; Tuchin, V. V.; Venermo, M.; Valisuo, P. A Review of Indocyanine Green Fluorescent Imaging in Surgery. *Int. J. Biomed. Imaging* **2012**, *2012*, 940585.
(1490) Reinhart, M. B.; Huntington, C. R.; Blair, L. J.; Heniford, B. T.; Augenstein, V. A. Indocyanine Green: Historical Context, Current Applications, and Future Considerations. *Surg. Innov.* **2016**, *23*, 166−175.
(1491) Gorka, A. P.; Yamamoto, T.; Zhu, J.; Schnermann, M. J. Cyanine Photocages Enable Spatial Control of Inducible Cre-Mediated Recombination. *ChemBioChem* **2018**, *19*, 1239−1243.
(1492) Feng, Q.; Tong, R. Anticancer Nanoparticulate Polymer-Drug Conjugate. *Bioeng. Transl. Med.* **2016**, *1*, 277−296.
(1493) Kowalik, L.; Chen, J. K. Illuminating Developmental Biology Through Photochemistry. *Nat. Chem. Biol.* **2017**, *13*, 587−598.
(1494) Gorka, A. P.; Nani, R. R.; Schnermann, M. J. Cyanine Polyene Reactivity: Scope and Biomedical Applications. *Org. Biomol. Chem.* **2015**, *13*, 7584−7598.
(1495) Zheng, Q.; Juette, M. F.; Jockusch, S.; Wasserman, M. R.; Zhou, Z.; Altman, R. B.; Blanchard, S. C. Ultra-Stable Organic Fluorophores for Single-Molecule Research. *Chem. Soc. Rev.* **2014**, *43*, 1044−1056.
(1496) Byers, G. W.; Gross, S.; Henrichs, P. M. Direct and Sensitized Photooxidation of Cyanine Dyes. *Photochem. Photobiol.* **1976**, *23*, 37−43.
(1497) Chen, P.; Li, J.; Qian, Z.; Zheng, D.; Okasaki, T.; Hayami, M. Study on the Photooxidation of a Near-Infrared-Absorbing Benzothiazolone Cyanine Dye. *Dyes Pigm.* **1998**, *37*, 213−222.
(1498) Chen, X.; Peng, X.; Cui, A.; Wang, B.; Wang, L.; Zhang, R. Photostabilities of Novel Heptamethine 3*H*-Indolenine Cyanine Dyes with Different *N*-Substituents. *J. Photochem. Photobiol., A* **2006**, *181*, 79−85.
(1499) Engel, E.; Schraml, R.; Maisch, T.; Kobuch, K.; Koenig, B.; Szeimies, R. M.; Hillenkamp, J.; Baumler, W.; Vasold, R. Light-Induced Decomposition of Indocyanine Green. *Invest. Ophthalmol. Visual Sci.* **2008**, *49*, 1777−1783.
(1500) Henary, M.; Mojzych, M. Stability and Reactivity of Polymethine Dyes in Solution. *Heterocyclic Polymethine Dyes: Synthesis, Properties and Applications*; Strekowski, L., Ed.; Springer Berlin Heidelberg: Berlin, Heidelberg, 2008.
(1501) Lepaja, S.; Strub, H.; Lougnot, D. J. Photophysical Study of a Series of Cyanines. 3. The Direct Photo-Oxidation Reaction. *Z. Naturforsch., A: Phys. Sci.* **1983**, *38*, 56−60.
(1502) Renikuntla, B. R.; Rose, H. C.; Eldo, J.; Waggoner, A. S.; Armitage, B. A. Improved Photostability and Fluorescence Properties Through Polyfluorination of a Cyanine Dye. *Org. Lett.* **2004**, *6*, 909−912.
(1503) Samanta, A.; Vendrell, M.; Das, R.; Chang, Y.-T. Development of Photostable Near-Infrared Cyanine Dyes. *Chem. Commun.* **2010**, *46*, 7406−7408.
(1504) Toutchkine, A.; Kraynov, V.; Hahn, K. Solvent-Sensitive Dyes to Report Protein Conformational Changes in Living Cells. *J. Am. Chem. Soc.* **2003**, *125*, 4132−4145.
(1505) Toutchkine, A.; Nguyen, D. V.; Hahn, K. M. Merocyanine Dyes with Improved Photostability. *Org. Lett.* **2007**, *9*, 2775−2777.
(1506) Patel, N. J.; Manivannan, E.; Joshi, P.; Ohulchanskyy, T. J.; Nani, R. R.; Schnermann, M. J.; Pandey, R. K. Impact of Substituents in Tumor Uptake and Fluorescence Imaging Ability of Near-Infrared Cyanine-like Dyes. *Photochem. Photobiol.* **2015**, *91*, 1219−1230.
(1507) Fouassier, J. P.; Lougnot, D. J.; Faure, J. Transient Absorptions in a Polymethine Laser Dye. *Chem. Phys. Lett.* **1975**, *35*, 189−194.
(1508) Kuzmin, V. A.; Tatikolov, A. S.; Borisevich, Y. E. Charge-Transfer Complexing in Course of Triplet-State Quenching of Carbo-Cyanine Dyes by Nitroxyl Radical. *Chem. Phys. Lett.* **1978**, *53*, 52−55.
(1509) Delaey, E.; van Laar, F.; De Vos, D.; Kamuhabwa, A.; Jacobs, P.; de Witte, P. A Comparative Study of the Photosensitizing Characteristics of Some Cyanine Dyes. *J. Photochem. Photobiol., B* **2000**, *55*, 27−36.
(1510) Redmond, R. W.; Gamlin, J. N. A Compilation of Singlet Oxygen Yields From Biologically Relevant Molecules. *Photochem. Photobiol.* **1999**, *70*, 391−475.
(1511) Franck, B.; Schneider, U. Photooxidation Products of Merocyanine 540 Formed Under Preactivation Conditions for Tumor Therapy. *Photochem. Photobiol.* **1992**, *56*, 271−276.
(1512) Gorka, A. P.; Nani, R. R.; Zhu, J.; Mackem, S.; Schnermann, M. J. A Near-IR Uncaging Strategy Based on Cyanine Photochemistry. *J. Am. Chem. Soc.* **2014**, *136*, 14153−14159.
(1513) Nani, R. R.; Kelley, J. A.; Ivanic, J.; Schnermann, M. J. Reactive Species Involved in the Regioselective Photooxidation of Heptamethine Cyanines. *Chem. Sci.* **2015**, *6*, 6556−6563.
(1514) Yamamoto, T.; Caldwell, D. R.; Gandioso, A.; Schnermann, M. J. A Cyanine Photooxidation/β-Elimination Sequence Enables Near-Infrared Uncaging of Aryl Amine Payloads. *Photochem. Photobiol.* **2019**, *95*, 951−958.
(1515) Yang, S.; Tian, H.; Xiao, H.; Shang, X.; Gong, X.; Yao, S.; Chen, K. Photodegradation of Cyanine and Merocyanine Dyes. *Dyes Pigm.* **2001**, *49*, 93−101.
(1516) Altman, R. B.; Zheng, Q.; Zhou, Z.; Terry, D. S.; Warren, J. D.; Blanchard, S. C. Enhanced Photostability of Cyanine Fluorophores Across the Visible Spectrum. *Nat. Methods* **2012**, *9*, 428−429.
(1517) van der Velde, J. H. M.; Oelerich, J.; Huang, J.; Smit, J. H.; Hiermaier, M.; Ploetz, E.; Herrmann, A.; Roelfes, G.; Cordes, T. The Power of Two: Covalent Coupling of Photostabilizers for Fluorescence Applications. *J. Phys. Chem. Lett.* **2014**, *5*, 3792−3798.
(1518) van der Velde, J. H. M.; Ploetz, E.; Hiermaier, M.; Oelerich, J.; de Vries, J. W.; Roelfes, G.; Cordes, T. Mechanism of Intramolecular Photostabilization in Self-Healing Cyanine Fluorophores. *ChemPhysChem* **2013**, *14*, 4084−4093.
(1519) Widengren, J.; Chmyrov, A.; Eggeling, C.; Löfdahl, P.-Å.; Seidel, C. A. M. Strategies to Improve Photostabilities in Ultrasensitive Fluorescence Spectroscopy. *J. Phys. Chem. A* **2007**, *111*, 429−440.
(1520) Zheng, Q.; Jockusch, S.; Zhou, Z.; Blanchard, S. C. The Contribution of Reactive Oxygen Species to the Photobleaching of Organic Fluorophores. *Photochem. Photobiol.* **2014**, *90*, 448−454.
(1521) Wu, X.; Zhu, W. Stability Enhancement of Fluorophores for Lighting Up Practical Application in Bioimaging. *Chem. Soc. Rev.* **2015**, *44*, 4179−4184.
(1522) Oushiki, D.; Kojima, H.; Terai, T.; Arita, M.; Hanaoka, K.; Urano, Y.; Nagano, T. Development and Application of a Near-Infrared Fluorescence Probe for Oxidative Stress Based on Differential Reactivity of Linked Cyanine Dyes. *J. Am. Chem. Soc.* **2010**, *132*, 2795−2801.
(1523) Sun, M.; Yu, H.; Zhu, H.; Ma, F.; Zhang, S.; Huang, D.; Wang, S. Oxidative Cleavage-Based Near-Infrared Fluorescent Probe for Hypochlorous Acid Detection and Myeloperoxidase Activity Evaluation. *Anal. Chem.* **2014**, *86*, 671−677.
(1524) Nani, R. R.; Gorka, A. P.; Nagaya, T.; Yamamoto, T.; Ivanic, J.; Kobayashi, H.; Schnermann, M. J. In Vivo Activation of Duocarmycin-Antibody Conjugates by Near-Infrared Light. *ACS Cent. Sci.* **2017**, *3*, 329−337.
(1525) Nani, R. R.; Gorka, A. P.; Nagaya, T.; Kobayashi, H.; Schnermann, M. J. Near-IR Light-Mediated Cleavage of Antibody-

Drug Conjugates Using Cyanine Photocages. *Angew. Chem., Int. Ed.* **2015**, *54*, 13635−13638.
(1526) Reynolds, G. A.; Drexhage, K. H. Stable Heptamethine Pyrylium Dyes That Absorb in the Infrared. *J. Org. Chem.* **1977**, *42*, 885−888.
(1527) Slominskii, Y. L.; Radchenko, I.; Tolmachev, A. Polymethine Dyes with Hydrocarbon Bridges. Effect of Substituents in the Chromophore on the Color of Tricarbocyanines. *Zhurnal. Organicheskoi Khimii* **1979**, *10*, 400−407.
(1528) Strekowski, L.; Lipowska, M.; Patonay, G. Substitution-Reactions of a Nucleofugal Group in Heptamethine Cyanine Dyes - Synthesis of an Isothiocyanato Derivative for Labeling of Proteins with a Near-Infrared Chromophore. *J. Org. Chem.* **1992**, *57*, 4578−4580.
(1529) Lim, S. Y.; Hong, K. H.; Kim, D. I.; Kwon, H.; Kim, H. J. Tunable Heptamethine-Azo Dye Conjugate as an Nir Fluorescent Probe for the Selective Detection of Mitochondrial Glutathione Over Cysteine and Homocysteine. *J. Am. Chem. Soc.* **2014**, *136*, 7018−7025.
(1530) Zaheer, A.; Wheat, T. E.; Frangioni, J. V. IRDye78 Conjugates for Near-Infrared Fluorescence Imaging. *Mol. Imaging* **2002**, *1*, 354−364.
(1531) Nani, R. R.; Shaum, J. B.; Gorka, A. P.; Schnermann, M. J. Electrophile-Integrating Smiles Rearrangement Provides Previously Inaccessible C4′-*O*-Alkyl Heptamethine Cyanine fluorophores. *Org. Lett.* **2015**, *17*, 302−305.
(1532) Saari, W. S.; Schwering, J. E.; Lyle, P. A.; Smith, S. J.; Engelhardt, E. L. Cyclization-Activated Prodrugs - Basic Carbamates of 4-Hydroxyanisole. *J. Med. Chem.* **1990**, *33*, 97−101.
(1533) Dal Corso, A.; Borlandelli, V.; Corno, C.; Perego, P.; Belvisi, L.; Pignataro, L.; Gennari, C. Fast Cyclization of a Proline-Derived Self-Immolative Spacer Improves the Efficacy of Carbamate Prodrugs. *Angew. Chem., Int. Ed.* **2020**, *59*, 4176−4181.
(1534) Guo, Z.; Ma, Y.; Liu, Y.; Yan, C.; Shi, P.; Tian, H.; Zhu, W.-H. Photocaged Prodrug Under NIR Light-Triggering with Dual-Channel Fluorescence: In Vivo Real-Time Tracking for Precise Drug Delivery. *Sci. China: Chem.* **2018**, *61*, 1293−1300.
(1535) Mujumdar, R. B.; Ernst, L. A.; Mujumdar, S. R.; Lewis, C. J.; Waggoner, A. S. Cyanine Dye Labeling Reagents - Sulfoindocyanine Succinimidyl Esters. *Bioconjugate Chem.* **1993**, *4*, 105−111.
(1536) Levitz, A.; Marmarchi, F.; Henary, M. Introduction of Various Substitutions to the Methine Bridge of Heptamethine Cyanine Dyes via Substituted Dianil Linkers. *Photochem. Photobiol. Sci.* **2018**, *17*, 1409−1416.
(1537) Mojzych, M.; Henary, M. Synthesis of Cyanine Dyes. *Heterocyclic Polymethine Dyes: Synthesis, Properties and Applications*; Strekowski, L., Ed.; Springer Berlin Heidelberg: Berlin, Heidelberg, 2008.
(1538) Štacková, L.; Štacko, P.; Klán, P. Approach to a Substituted Heptamethine Cyanine Chain by the Ring Opening of Zincke Salts. *J. Am. Chem. Soc.* **2019**, *141*, 7155−7162.
(1539) Hilderbrand, S. A.; Kelly, K. A.; Weissleder, R.; Tung, C.-H. Monofunctional Near-Infrared Fluorochromes for Imaging Applications. *Bioconjugate Chem.* **2005**, *16*, 1275−1281.
(1540) Lee, H.; Mason, J. C.; Achilefu, S. Heptamethine Cyanine Dyes with a Robust C-C Bond at the Central Position of the Chromophore. *J. Org. Chem.* **2006**, *71*, 7862−7865.
(1541) Mahajan, S. S.; Deu, E.; Lauterwasser, E. M.; Leyva, M. J.; Ellman, J. A.; Bogyo, M.; Renslo, A. R. A Fragmenting Hybrid Approach for Targeted Delivery of Multiple Therapeutic Agents to the Malaria Parasite. *ChemMedChem* **2011**, *6*, 415−419.
(1542) Santi, D. V.; Schneider, E. L.; Reid, R.; Robinson, L.; Ashley, G. W. Predictable and Tunable Half-Life Extension of Therapeutic Agents by Controlled Chemical Release From Macromolecular Conjugates. *Proc. Natl. Acad. Sci. U. S. A.* **2012**, *109*, 6211−6216.
(1543) Spangler, B.; Morgan, C. W.; Fontaine, S. D.; Vander Wal, M. N.; Chang, C. J.; Wells, J. A.; Renslo, A. R. A Reactivity-Based Probe of the Intracellular Labile Ferrous Iron Pool. *Nat. Chem. Biol.* **2016**, *12*, 680.
(1544) Tu, J.; Xu, M.; Parvez, S.; Peterson, R. T.; Franzini, R. M. Bioorthogonal Removal of 3-Isocyanopropyl Groups Enables the Controlled Release of Fluorophores and Drugs in Vivo. *J. Am. Chem. Soc.* **2018**, *140*, 8410−8414.
(1545) Luciano, M. P.; Nourian, S.; Gorka, A. P.; Nani, R. R.; Nagaya, T.; Kobayashi, H.; Schnermann, M. J. A Near-Infrared Light-Mediated Cleavable Linker Strategy Using the Heptamethine Cyanine Chromophore. *Methods Enzymol.*; Academic Press, 2020.
(1546) Johnson, S. L.; Morrison, D. L. Kinetics and Mechanism of Decarboxylation of *N*-Arylcarbamates - Evidence for Kinetically Important Zwitterionic Carbamic Acid Species of Short Lifetime. *J. Am. Chem. Soc.* **1972**, *94*, 1323−1334.
(1547) Conceição, S. D.; Ferreira, P. D.; Ferreira, F. V. L. Photochemistry and Cytotoxicity Evaluation of Heptamethinecyanine Near Infrared (NIR) Dyes. *Int. J. Mol. Sci.* **2013**, *14*, 18557−18571.
(1548) Morales, M.-C.; Freire, V.; Asumendi, A.; Araiz, J.; Herrera, I.; Castiella, G.; Corcóstegui, I.; Corcóstegui, G. Comparative Effects of Six Intraocular Vital Dyes on Retinal Pigment Epithelial Cells. *Invest. Ophthalmol. Visual Sci.* **2010**, *51*, 6018−6029.
(1549) Yang, X.; Shi, C.; Tong, R.; Qian, W.; Zhau, H. E.; Wang, R.; Zhu, G.; Cheng, J.; Yang, V. W.; Cheng, T.; Henary, M.; Strekowski, L.; Chung, L. W. K. Near IR Heptamethine Cyanine Dye−Mediated Cancer Imaging. *Clin. Cancer Res.* **2010**, *16*, 2833.
(1550) Beck, A.; Goetsch, L.; Dumontet, C.; Corvaïa, N. Strategies and Challenges for the Next Generation of Antibody−Drug Conjugates. *Nat. Rev. Drug Discovery* **2017**, *16*, 315.
(1551) Birrer, M. J.; Moore, K. N.; Betella, I.; Bates, R. C. Antibody-Drug Conjugate-Based Therapeutics: State of the Science. *J. Natl. Cancer Inst.* **2019**, *111*, 538−549.
(1552) Nagaya, T.; Gorka, A. P.; Nani, R. R.; Okuyama, S.; Ogata, F.; Maruoka, Y.; Choyke, P. L.; Schnermann, M. J.; Kobayashi, H. Molecularly Targeted Cancer Combination Therapy with Near-Infrared Photoimmunotherapy and Near-Infrared Photorelease with Duocarmycin-Antibody Conjugate. *Mol. Cancer Ther.* **2018**, *17*, 661−670.
(1553) Cao, G.; Wang, Y. *Nanostructures and Nanomaterials*, 2nd ed.; World Scientific Publishing Company, 2010.
(1554) Doane, T. L.; Burda, C. The Unique Role of Nanoparticles in Nanomedicine: Imaging, Drug Delivery and Therapy. *Chem. Soc. Rev.* **2012**, *41*, 2885−2911.
(1555) Li, Y.; Zhang, Y.; Wang, W. Phototriggered Targeting of Nanocarriers for Drug Delivery. *Nano Res.* **2018**, *11*, 5424−5438.
(1556) Karimi, M.; Zangabad, P. S.; Baghaee-Ravari, S.; Ghazadeh, M.; Mirshekari, H.; Hamblin, M. R. Smart Nanostructures for Cargo Delivery: Uncaging and Activating by Light. *J. Am. Chem. Soc.* **2017**, *139*, 4584−4610.
(1557) Lai, W.-F.; Rogach, A. L.; Wong, W.-T. Molecular Design of Upconversion Nanoparticles for Gene Delivery. *Chem. Sci.* **2017**, *8*, 7339−7358.
(1558) Xiong, Q.; Lim, Y.; Li, D.; Pu, K.; Liang, L.; Duan, H. Photoactive Nanocarriers for Controlled Delivery. *Adv. Funct. Mater.* **2020**, *30*, 1903896.
(1559) Alvarez-Lorenzo, C.; Bromberg, L.; Concheiro, A. Light-Sensitive Intelligent Drug Delivery Systems. *Photochem. Photobiol.* **2009**, *85*, 848−860.
(1560) Bansal, A.; Zhang, Y. Photocontrolled Nanoparticle Delivery Systems for Biomedical Applications. *Acc. Chem. Res.* **2014**, *47*, 3052−3060.
(1561) Hou, Y.; Zhou, Z.; Huang, K.; Yang, H.; Han, G. Long Wavelength Light Activated Prodrug Conjugates for Biomedical Applications. *ChemPhotoChem.* **2018**, *2*, 1005−1011.
(1562) De Jong, W. H.; Borm, P. J. A. Drug Delivery and Nanoparticles: Applications and Hazards. *Int. J. Nanomed.* **2008**, *3*, 133−149.
(1563) Zhao, W.; Zhao, Y.; Wang, Q.; Liu, T.; Sun, J.; Zhang, R. Remote Light-Responsive Nanocarriers for Controlled Drug Delivery: Advances and Perspectives. *Small* **2019**, *15*, 1903060.
(1564) Singh, R.; Lillard, J. W. Nanoparticle-Based Targeted Drug Delivery. *Exp. Mol. Pathol.* **2009**, *86*, 215−223.

(1565) Farokhi, M.; Mottaghitalab, F.; Saeb, M. R.; Thomas, S. Functionalized Theranostic Nanocarriers With Bio-Inspired Polydopamine for Tumor Imaging and Chemo-Photothermal Therapy. *J. Controlled Release* **2019**, *309*, 203−219.
(1566) He, L.; Liu, Y.; Lau, J.; Fan, W.; Li, Q.; Zhang, C.; Huang, P.; Chen, X. Recent Progress in Nanoscale Metal-Organic Frameworks for Drug Release and Cancer Therapy. *Nanomedicine* **2019**, *14*, 1343−1365.
(1567) Zheng, F.; Xiong, W.; Sun, S.; Zhang, P.; Zhu Jun, J. Recent Advances in Drug Release Monitoring. *Nanophotonics* **2019**, *8*, 391−413.
(1568) Denkova, A. G.; de Kruijff, R. M.; Serra-Crespo, P. Nanocarrier-Mediated Photochemotherapy and Photoradiotherapy. *Adv. Healthcare Mater.* **2018**, *7*, 1701211.
(1569) Xu, Y.; Shan, Y.; Cong, H.; Shen, Y.; Yu, B. Advanced Carbon-Based Nanoplatforms Combining Drug Delivery and Thermal Therapy for Cancer Treatment. *Curr. Pharm. Des.* **2019**, *24*, 4060−4076.
(1570) Sagar, V.; Nair, M. Near-Infrared Biophotonics-Based Nanodrug Release Systems and Their Potential Application for Neuro-Disorders. *Expert Opin. Drug Delivery* **2018**, *15*, 137−152.
(1571) Obaid, G.; Broekgaarden, M.; Bulin, A.-L.; Huang, H.-C.; Kuriakose, J.; Liu, J.; Hasan, T. Photonanomedicine: A Convergence of Photodynamic Therapy and Nanotechnology. *Nanoscale* **2016**, *8*, 12471−12503.
(1572) Blum, A. P.; Kammeyer, J. K.; Rush, A. M.; Callmann, C. E.; Hahn, M. E.; Gianneschi, N. C. Stimuli-Responsive Nanomaterials for Biomedical Applications. *J. Am. Chem. Soc.* **2015**, *137*, 2140−2154.
(1573) Rahoui, N.; Jiang, B.; Taloub, N.; Huang, Y. D. Spatio-Temporal Control Strategy of Drug Delivery Systems Based Nano Structures. *J. Controlled Release* **2017**, *255*, 176−201.
(1574) Liu, Q.; Zhan, C.; Kohane, D. S. Phototriggered Drug Delivery Using Inorganic Nanomaterials. *Bioconjugate Chem.* **2017**, *28*, 98−104.
(1575) Li, L.; Scheiger, J. M.; Levkin, P. A. Design and Applications of Photoresponsive Hydrogels. *Adv. Mater.* **2019**, *31*, 1807333.
(1576) Ding, C. D.; Tong, L.; Feng, J.; Fu, J. J. Recent Advances in Stimuli-Responsive Release Function Drug Delivery Systems for Tumor Treatment. *Molecules* **2016**, *21*, 1715.
(1577) Raza, A.; Hayat, U.; Rasheed, T.; Bilal, M.; Iqbal, H. M. N. Smart" Materials-Based Near-Infrared Light-Responsive Drug Delivery Systems for Cancer Treatment: A Review. *J. Mater. Res. Technol.* **2019**, *8*, 1497−1509.
(1578) Yu, Z.; Chan, W. K.; Tan, T. T. Y. Neodymium-Sensitized Nanoconstructs for Near-Infrared Enabled Photomedicine. *Small* **2020**, *16*, 1905265.
(1579) Mohamed, M. S.; Veeranarayanan, S.; Maekawa, T.; Kumar, D. S. External Stimulus Responsive Inorganic Nanomaterials for Cancer Theranostics. *Adv. Drug Delivery Rev.* **2019**, *138*, 18−40.
(1580) Guo, M.; Song, H.; Li, K.; Ma, M.; Liu, Y.; Fu, Q.; He, Z. A New Approach to Developing Diagnostics and Therapeutics: Aggregation-Induced Emission-Based Fluorescence Turn-on. *Med. Res. Rev.* **2020**, *40*, 27−53.
(1581) Swaminathan, S.; Garcia-Amoros, J.; Fraix, A.; Kandoth, N.; Sortino, S.; Raymo, F. M. Photoresponsive Polymer Nanocarriers With Multifunctional Cargo. *Chem. Soc. Rev.* **2014**, *43*, 4167−4178.
(1582) Tan, P.; Jiang, Y.; Liu, X.-Q.; Sun, L.-B. Making Porous Materials Respond to Visible Light. *ACS Energy Lett.* **2019**, *4*, 2656−2667.
(1583) Wells, C. M.; Harris, M.; Choi, L.; Murali, V. P.; Guerra, F. D.; Jennings, J. A. Stimuli-Responsive Drug Release from Smart Polymers. *J. Funct. Biomater.* **2019**, *10*, 34.
(1584) Mehtani, D.; Seth, A.; Sharma, P.; Maheshwari, N.; Kapoor, D.; Shrivastava, S. K.; Tekade, R. K. Biomaterials for Sustained and Controlled Delivery of Small Drug Molecules. *Biomaterials and Bionanotechnology*; Tekade, R. K., Ed.; Academic Press, 2019.
(1585) Li, J.; Pu, K. Semiconducting Polymer Nanomaterials as Near-Infrared Photoactivatable Protherapeutics for Cancer. *Acc. Chem. Res.* **2020**, *53*, 752−762.
(1586) Panwar, N.; Soehartono, A. M.; Chan, K. K.; Zeng, S.; Xu, G.; Qu, J.; Coquet, P.; Yong, K.-T.; Chen, X. Nanocarbons for Biology and Medicine: Sensing, Imaging, and Drug Delivery. *Chem. Rev.* **2019**, *119*, 9559−9656.
(1587) Tartakovskii, A. *Quantum Dots: Optics, Electron Transport and Future Applications*; Cambridge University Press: Cambridge, 2012.
(1588) Wang, Y.; Hu, A. Carbon Quantum Dots: Synthesis, Properties and Applications. *J. Mater. Chem. C* **2014**, *2*, 6921−6939.
(1589) Chinnathambi, S.; Chen, S.; Ganesan, S.; Hanagata, N. Silicon Quantum Dots for Biological Applications. *Adv. Healthcare Mater.* **2014**, *3*, 10−29.
(1590) Sansalone, L.; Tang, S.; Zhang, Y.; Thapaliya, E. R.; Raymo, F. M.; Garcia-Amorós, J. Semiconductor Quantum Dots with Photoresponsive Ligands. *Top. Curr. Chem.* **2016**, *374*, 73.
(1591) Michalet, X.; Pinaud, F. F.; Bentolila, L. A.; Tsay, J. M.; Doose, S.; Li, J. J.; Sundaresan, G.; Wu, A. M.; Gambhir, S. S.; Weiss, S. Quantum Dots for Live Cells, in Vivo Imaging, and Diagnostics. *Science* **2005**, *307*, 538−544.
(1592) Burks, P. T.; Ford, P. C. Quantum Dot Photosensitizers. Interactions With Transition Metal Centers. *Dalton Trans.* **2012**, *41*, 13030−13042.
(1593) Burks, P. T.; Ostrowski, A. D.; Mikhailovsky, A. A.; Chan, E. M.; Wagenknecht, P. S.; Ford, P. C. Quantum Dot Photoluminescence Quenching by Cr(III) Complexes. Photosensitized Reactions and Evidence for a FRET Mechanism. *J. Am. Chem. Soc.* **2012**, *134*, 13266−13275.
(1594) Fowley, C.; McHale, A. P.; McCaughan, B.; Fraix, A.; Sortino, S.; Callan, J. F. Carbon Quantum Dot−NO Photoreleaser Nanohybrids for Two-Photon Phototherapy of Hypoxic Tumors-photochemistry of Metal Nitrosyl Complexes. Delivery of Nitric Oxide to Biological Targets. *Chem. Commun.* **2015**, *51*, 81−84.
(1595) Karthik, S.; Saha, B.; Ghosh, S. K.; Pradeep Singh, N. D. Photoresponsive Quinoline Tethered Fluorescent Carbon Dots for Regulated Anticancer Drug Delivery. *Chem. Commun.* **2013**, *49*, 10471−10473.
(1596) Liu, Z.; Lin, Q.; Huang, Q.; Liu, H.; Bao, C.; Zhang, W.; Zhong, X.; Zhu, L. Semiconductor Quantum Dots Photosensitizing Release of Anticancer Drug. *Chem. Commun.* **2011**, *47*, 1482−1484.
(1597) Franco, L. P.; Cicillini, S. A.; Biazzotto, J. C.; Schiavon, M. A.; Mikhailovsky, A.; Burks, P.; Garcia, J.; Ford, P. C.; Silva, R. S. d. Photoreactivity of a Quantum Dot−Ruthenium Nitrosyl Conjugate. *J. Phys. Chem. A* **2014**, *118*, 12184−12191.
(1598) Wijtmans, M.; Rosenthal, S. J.; Zwanenburg, B.; Porter, N. A. Visible Light Excitation of CdSe Nanocrystals Triggers the Release of Coumarin from Cinnamate Surface Ligands. *J. Am. Chem. Soc.* **2006**, *128*, 11720−11726.
(1599) Han, G.; Mokari, T.; Ajo-Franklin, C.; Cohen, B. E. Caged Quantum Dots. *J. Am. Chem. Soc.* **2008**, *130*, 15811−15813.
(1600) Impellizzeri, S.; McCaughan, B.; Callan, J. F.; Raymo, F. M. Photoinduced Enhancement in the Luminescence of Hydrophilic Quantum Dots Coated with Photocleavable Ligands. *J. Am. Chem. Soc.* **2012**, *134*, 2276−2283.
(1601) Miesch, C.; Emrick, T. Photo-Sensitive Ligands on Nanoparticles for Achieving Triggered Emulsion Inversion. *J. Colloid Interface Sci.* **2014**, *425*, 152−158.
(1602) Ye, C.; Zhou, L.; Wang, X.; Liang, Z. Photon Upconversion: From Two-Photon Absorption (TPA) to Triplet−Triplet Annihilation (TTA). *Phys. Chem. Chem. Phys.* **2016**, *18*, 10818−10835.
(1603) Bonacina, L. Nonlinear Nanomedecine: Harmonic Nanoparticles toward Targeted Diagnosis and Therapy. *Mol. Pharmaceutics* **2013**, *10*, 783−792.
(1604) Dong, H.; Sun, L.-D.; Yan, C.-H. Basic Understanding of the Lanthanide Related Upconversion Emissions. *Nanoscale* **2013**, *5*, 5703−5714.
(1605) Zhou, J.; Liu, Q.; Feng, W.; Sun, Y.; Li, F. Upconversion Luminescent Materials: Advances and Applications. *Chem. Rev.* **2015**, *115*, 395−465.

(1606) Jafari, M.; Rezvanpour, A. Upconversion Nano-Particles From Synthesis to Cancer Treatment: A Review. *Adv. Powder Technol.* **2019**, *30*, 1731−1753.
(1607) Auzel, F. Upconversion and Anti-Stokes Processes with f and d Ions in Solids. *Chem. Rev.* **2004**, *104*, 139−174.
(1608) Gulzar, A.; Xu, J.; Yang, P.; He, F.; Xu, L. Upconversion Processes: Versatile Biological Applications and Biosafety. *Nanoscale* **2017**, *9*, 12248−12282.
(1609) Lingeshwar Reddy, K.; Balaji, R.; Kumar, A.; Krishnan, V. Lanthanide Doped Near Infrared Active Upconversion Nanophosphors: Fundamental Concepts, Synthesis Strategies, and Technological Applications. *Small* **2018**, *14*, 1801304.
(1610) Lin, M.; Gao, Y.; Hornicek, F.; Xu, F.; Lu, T. J.; Amiji, M.; Duan, Z. Near-Infrared Light Activated Delivery Platform for Cancer Therapy. *Adv. Colloid Interface Sci.* **2015**, *226*, 123−137.
(1611) Cho, H. J.; Chung, M.; Shim, M. S. Engineered Photo-Responsive Materials for Near-Infrared-Triggered Drug Delivery. *J. Ind. Eng. Chem.* **2015**, *31*, 15−25.
(1612) Yang, G. B.; Liu, J. J.; Wu, Y. F.; Feng, L. Z.; Liu, Z. Near-Infrared-Light Responsive Nanoscale Drug Delivery Systems for Cancer Treatment. *Coord. Chem. Rev.* **2016**, *320*, 100−117.
(1613) Li, K.; Hong, E.; Wang, B.; Wang, Z.; Zhang, L.; Hu, R.; Wang, B. Advances in the Application of Upconversion Nanoparticles for Detecting and Treating Cancers. *Photodiagn. Photodyn. Ther.* **2019**, *25*, 177−192.
(1614) Bagheri, A.; Arandiyan, H.; Boyer, C.; Lim, M. Lanthanide-Doped Upconversion Nanoparticles: Emerging Intelligent Light-Activated Drug Delivery Systems. *Adv. Sci.* **2016**, *3*, 1500437.
(1615) González-Béjar, M.; Francés-Soriano, L.; Pérez-Prieto, J. Upconversion Nanoparticles for Bioimaging and Regenerative Medicine. *Front. Bioeng. Biotechnol.* **2016**, *4*, 47.
(1616) Sun, L.; Wei, R.; Feng, J.; Zhang, H. Tailored Lanthanide-Doped Upconversion Nanoparticles and Their Promising Bioapplication Prospects. *Coord. Chem. Rev.* **2018**, *364*, 10−32.
(1617) Fan, W.; Bu, W.; Shi, J. On The Latest Three-Stage Development of Nanomedicines based on Upconversion Nanoparticles. *Adv. Mater.* **2016**, *28*, 3987−4011.
(1618) Yang, D.; Ma, P. a.; Hou, Z.; Cheng, Z.; Li, C.; Lin, J. Current Advances in Lanthanide Ion (Ln^{3+})-Based Upconversion Nanomaterials for Drug Delivery. *Chem. Soc. Rev.* **2015**, *44*, 1416−1448.
(1619) Carling, C.-J.; Nourmohammadian, F.; Boyer, J.-C.; Branda, N. R. Remote-Control Photorelease of Caged Compounds Using Near-Infrared Light and Upconverting Nanoparticles. *Angew. Chem., Int. Ed.* **2010**, *49*, 3782−3785.
(1620) Wang, Z.; Thang, D. C.; Han, Q.; Zhao, X.; Xie, X.; Wang, Z.; Lin, J.; Xing, B. Near-Infrared Photocontrolled Therapeutic Release via Upconversion Nanocomposites. *J. Controlled Release* **2020**, *324*, 104−123.
(1621) Li, H.; Wang, X.; Huang, D. X.; Chen, G. Y. Recent Advances of Lanthanide-Doped Upconversion Nanoparticles for Biological Applications. *Nanotechnology* **2020**, *31*, 29.
(1622) Jayakumar, M. K. G.; Idris, N. M.; Zhang, Y. Remote Activation of Biomolecules in Deep Tissues Using Near-Infrared-to-UV Upconversion Nanotransducers. *Proc. Natl. Acad. Sci. U. S. A.* **2012**, *109*, 8483−8488.
(1623) Michael Dcona, M.; Yu, Q.; Capobianco, J. A.; Hartman, M. C. T. Near Infrared Light Mediated Release of Doxorubicin Using Upconversion Nanoparticles. *Chem. Commun.* **2015**, *51*, 8477−8479.
(1624) Fedoryshin, L. L.; Tavares, A. J.; Petryayeva, E.; Doughan, S.; Krull, U. J. Near-Infrared-Triggered Anticancer Drug Release from Upconverting Nanoparticles. *ACS Appl. Mater. Interfaces* **2014**, *6*, 13600−13606.
(1625) Chen, G.; Jaskula-Sztul, R.; Esquibel, C. R.; Lou, I.; Zheng, Q.; Dammalapati, A.; Harrison, A.; Eliceiri, K. W.; Tang, W.; Chen, H.; Gong, S. Neuroendocrine Tumor-Targeted Upconversion Nanoparticle-Based Micelles for Simultaneous NIR-Controlled Combination Chemotherapy and Photodynamic Therapy, and Fluorescence Imaging. *Adv. Funct. Mater.* **2017**, *27*, 1604671.
(1626) Yang, Y.; Shao, Q.; Deng, R.; Wang, C.; Teng, X.; Cheng, K.; Cheng, Z.; Huang, L.; Liu, Z.; Liu, X.; Xing, B. In Vitro and In Vivo Uncaging and Bioluminescence Imaging by Using Photocaged Upconversion Nanoparticles. *Angew. Chem., Int. Ed.* **2012**, *51*, 3125−3129.
(1627) Chien, Y.-H.; Chou, Y.-L.; Wang, S.-W.; Hung, S.-T.; Liau, M.-C.; Chao, Y.-J.; Su, C.-H.; Yeh, C.-S. Near-Infrared Light Photocontrolled Targeting, Bioimaging, and Chemotherapy with Caged Upconversion Nanoparticles in Vitro and in Vivo. *ACS Nano* **2013**, *7*, 8516−8528.
(1628) Li, J.; Leung, C. W. T.; Wong, D. S. H.; Xu, J.; Li, R.; Zhao, Y.; Yung, C. Y. Y.; Zhao, E.; Tang, B. Z.; Bian, L. Photocontrolled SiRNA Delivery and Biomarker-Triggered Luminogens of Aggregation-Induced Emission by Up-Conversion $NaYF_4$:Yb_3+Tm_3+@SiO_2 Nanoparticles for Inducing and Monitoring Stem-Cell Differentiation. *ACS Appl. Mater. Interfaces* **2019**, *11*, 22074−22084.
(1629) Pan, Y.; Yang, J.; Luan, X.; Liu, X.; Li, X.; Yang, J.; Huang, T.; Sun, L.; Wang, Y.; Lin, Y.; Song, Y. Near-Infrared Upconversion-Activated CRISPR-Cas9 System: A Remote-Controlled Gene Editing Platform. *Sci. Adv.* **2019**, *5*, No. eaav7199.
(1630) Kang, H.; Zhang, K.; Pan, Q.; Lin, S.; Wong, D. S. H.; Li, J.; Lee, W. Y.-W.; Yang, B.; Han, F.; Li, G.; Li, B.; Bian, L. Remote Control of Intracellular Calcium Using Upconversion Nanotransducers Regulates Stem Cell Differentiation In Vivo. *Adv. Funct. Mater.* **2018**, *28*, 1802642.
(1631) Xiang, J.; Tong, X.; Shi, F.; Yan, Q.; Yu, B.; Zhao, Y. Near-Infrared Light-Triggered Drug Release From UV-Responsive Diblock Copolymer-Coated Upconversion Nanoparticles With High Monodispersity. *J. Mater. Chem. B* **2018**, *6*, 3531−3540.
(1632) Li, J.; Lee, W. Y.-W.; Wu, T.; Xu, J.; Zhang, K.; Hong Wong, D. S.; Li, R.; Li, G.; Bian, L. Near-Infrared Light-Triggered Release of Small Molecules for Controlled Differentiation and Long-Term Tracking of Stem Cells in Vivo Using Upconversion Nanoparticles. *Biomaterials* **2016**, *110*, 1−10.
(1633) Wong, P. T.; Chen, D.; Tang, S.; Yanik, S.; Payne, M.; Mukherjee, J.; Coulter, A.; Tang, K.; Tao, K.; Sun, K.; Baker, J. R., Jr.; Choi, S. K. Modular Integration of Upconverting Nanocrystal−Dendrimer Composites for Folate Receptor-Specific NIR Imaging and Light-Triggered Drug Release. *Small* **2015**, *11*, 6078−6090.
(1634) Liu, G.; Liu, N.; Zhou, L.; Su, Y.; Dong, C.-M. NIR-Responsive Polypeptide Copolymer Upconversion Composite Nanoparticles for Triggered Drug Release and Enhanced Cytotoxicity. *Polym. Chem.* **2015**, *6*, 4030−4039.
(1635) Yuan, Y.; Min, Y.; Hu, Q.; Xing, B.; Liu, B. NIR Photoregulated Chemo- and Photodynamic Cancer Therapy Based on Conjugated Polyelectrolyte−Drug Conjugate Encapsulated Upconversion Nanoparticles. *Nanoscale* **2014**, *6*, 11259−11272.
(1636) Liu, G.; Zhou, L.; Su, Y.; Dong, C.-M. An NIR-Responsive and Sugar-Targeted Polypeptide Composite Nanomedicine for Intracellular Cancer Therapy. *Chem. Commun.* **2014**, *50*, 12538−12541.
(1637) Zhang, Y.; Ren, K.; Zhang, X.; Chao, Z.; Yang, Y.; Ye, D.; Dai, Z.; Liu, Y.; Ju, H. Photo-Tearable Tape Close-Wrapped Upconversion Nanocapsules for Near-Infrared Modulated Efficient Sirna Delivery and Therapy. *Biomaterials* **2018**, *163*, 55−66.
(1638) Wong, P. T.; Tang, S.; Cannon, J.; Chen, D.; Sun, R.; Lee, J.; Phan, J.; Tao, K.; Sun, K.; Chen, B.; Baker, J. R.; Choi, S. K. Photocontrolled Release of Doxorubicin Conjugated through a Thioacetal Photocage in Folate-Targeted Nanodelivery Systems. *Bioconjugate Chem.* **2017**, *28*, 3016−3028.
(1639) Zhao, H.; Hu, W.; Ma, H.; Jiang, R.; Tang, Y.; Ji, Y.; Lu, X.; Hou, B.; Deng, W.; Huang, W.; Fan, Q. Photo-Induced Charge-Variable Conjugated Polyelectrolyte Brushes Encapsulating Upconversion Nanoparticles for Promoted siRNA Release and Collaborative Photodynamic Therapy under NIR Light Irradiation. *Adv. Funct. Mater.* **2017**, *27*, 1702592.
(1640) Liu, J.; Bu, W.; Pan, L.; Shi, J. NIR-Triggered Anticancer Drug Delivery by Upconverting Nanoparticles with Integrated

Azobenzene-Modified Mesoporous Silica. *Angew. Chem., Int. Ed.* **2013**, *52*, 4375−4379.
(1641) Jayakumar, M. K. G.; Bansal, A.; Huang, K.; Yao, R.; Li, B. N.; Zhang, Y. Near-Infrared-Light-Based Nano-Platform Boosts Endosomal Escape and Controls Gene Knockdown in Vivo. *ACS Nano* **2014**, *8*, 4848−4858.
(1642) Liu, Z.; Shi, J.; Wang, Y.; Gan, Y.; Wan, P. Facile Preparation of Pyrenemethyl Ester-Based Nanovalve on Mesoporous Silica Coated Upconversion Nanoparticle for NIR Light-Triggered Drug Release With Potential Monitoring Capability. *Colloids Surf., A* **2019**, *568*, 436−444.
(1643) Li, H.; Lei, W.; Wu, J.; Li, S.; Zhou, G.; Liu, D.; Yang, X.; Wang, S.; Li, Z.; Zhang, J. An Upconverting Nanotheranostic Agent Activated by Hypoxia Combined With NIR Irradiation for Selective Hypoxia Imaging and Tumour Therapy. *J. Mater. Chem. B* **2018**, *6*, 2747−2757.
(1644) Ruggiero, E.; Habtemariam, A.; Yate, L.; Mareque-Rivas, J. C.; Salassa, L. Near Infrared Photolysis of a Ru Polypyridyl Complex by Upconverting Nanoparticles. *Chem. Commun.* **2014**, *50*, 1715−1718.
(1645) Dai, Y.; Bi, H.; Deng, X.; Li, C.; He, F.; Ma, P. a.; Yang, P.; Lin, J. 808 nm Near-Infrared Light Controlled Dual-Drug Release and Cancer Therapy in Vivo by Upconversion Mesoporous Silica Nanostructures. *J. Mater. Chem. B* **2017**, *5*, 2086−2095.
(1646) Dai, Y.; Xiao, H.; Liu, J.; Yuan, Q.; Ma, P. a.; Yang, D.; Li, C.; Cheng, Z.; Hou, Z.; Yang, P.; Lin, J. In Vivo Multimodality Imaging and Cancer Therapy by Near-Infrared Light-Triggered trans-Platinum Pro-Drug-Conjugated Upconverison Nanoparticles. *J. Am. Chem. Soc.* **2013**, *135*, 18920−18929.
(1647) Xu, Z.; Wu, Z.; Sun, J.; Gui, R. Glutathione Capped Mn^{2+}-Doped ZnSe Quantum Dots-Photodonors Nanocomposites for Two-Photon Excited Fluorescence-Induced Nitric Oxide Release. *Mater. Chem. Phys.* **2015**, *162*, 286−290.
(1648) Chen, Y.; Hao, Y.; Huang, Y.; Wu, W.; Liu, X.; Li, Y.; Gou, M.; Qian, Z. An Injectable, Near-Infrared Light-Responsive Click Cross-Linked Azobenzene Hydrogel for Breast Cancer Chemotherapy. *J. Biomed. Nanotechnol.* **2019**, *15*, 1923−1936.
(1649) Yao, C.; Wang, P.; Li, X.; Hu, X.; Hou, J.; Wang, L.; Zhang, F. Near-Infrared-Triggered Azobenzene-Liposome/Upconversion Nanoparticle Hybrid Vesicles for Remotely Controlled Drug Delivery to Overcome Cancer Multidrug Resistance. *Adv. Mater.* **2016**, *28*, 9341−9348.
(1650) Zhang, Z.; Jayakumar, M. K. G.; Zheng, X.; Shikha, S.; Zhang, Y.; Bansal, A.; Poon, D. J. J.; Chu, P. L.; Yeo, E. L. L.; Chua, M. L. K.; Chee, S. K.; Zhang, Y. Upconversion Superballs for Programmable Photoactivation of Therapeutics. *Nat. Commun.* **2019**, *10*, 4586.
(1651) Chen, S.; Gao, Y.; Cao, Z.; Wu, B.; Wang, L.; Wang, H.; Dang, Z.; Wang, G. Nanocomposites of Spiropyran-Functionalized Polymers and Upconversion Nanoparticles for Controlled Release Stimulated by Near-Infrared Light and pH. *Macromolecules* **2016**, *49*, 7490−7496.
(1652) Yang, Z. Z.; Sun, Z. R.; Ren, Y.; Chen, X.; Zhang, W.; Zhu, X. H.; Mao, Z. W.; Shen, J. L.; Nie, S. N. Advances in Nanomaterials for Use in Photothermal and Photodynamic Therapeutics. *Mol. Med. Rep.* **2019**, *20*, 5−15.
(1653) Xu, J. W.; Yao, K.; Xu, Z. K. Nanomaterials With a Photothermal Effect for Antibacterial Activities: An Overview. *Nanoscale* **2019**, *11*, 8680−8691.
(1654) Guerrero, A. R.; Hassan, N.; Escobar, C. A.; Albericio, F.; Kogan, M. J.; Araya, E. Gold Nanoparticles for Photothermally Controlled Drug Release. *Nanomedicine* **2014**, *9*, 2023−2039.
(1655) Liao, H.; Nehl, C. L.; Hafner, J. H. Biomedical Applications of Plasmon Resonant Metal Nanoparticles. *Nanomedicine* **2006**, *1*, 201−208.
(1656) Cobley, C. M.; Au, L.; Chen, J. Y.; Xia, Y. N. Targeting Gold Nanocages to Cancer Cells for Photothermal Destruction and Drug Delivery. *Expert Opin. Drug Delivery* **2010**, *7*, 577−587.
(1657) Yavuz, M. S.; Cheng, Y.; Chen, J.; Cobley, C. M.; Zhang, Q.; Rycenga, M.; Xie, J.; Kim, C.; Song, K. H.; Schwartz, A. G.; Wang, L. V.; Xia, Y. Gold Nanocages Covered by Smart Polymers for Controlled Release With Near-Infrared Light. *Nat. Mater.* **2009**, *8*, 935−939.
(1658) Borak, J. B.; López-Sola, S.; Falvey, D. E. Photorelease of Carboxylic Acids Mediated by Visible-Light-Absorbing Gold-Nanoparticles. *Org. Lett.* **2008**, *10*, 457−460.
(1659) Bergamini, L.; Voliani, V.; Cappello, V.; Nifosì, R.; Corni, S. Non-Linear Optical Response by Functionalized Gold Nanospheres: Identifying Design Principles to Maximize the Molecular Photorelease. *Nanoscale* **2015**, *7*, 13345−13357.
(1660) Song, J.; Pu, L.; Zhou, J.; Duan, B.; Duan, H. Biodegradable Theranostic Plasmonic Vesicles of Amphiphilic Gold Nanorods. *ACS Nano* **2013**, *7*, 9947−9960.
(1661) Voliani, V.; Ricci, F.; Signore, G.; Nifosì, R.; Luin, S.; Beltram, F. Multiphoton Molecular Photorelease in Click-Chemistry-Functionalized Gold Nanoparticles. *Small* **2011**, *7*, 3271−3275.
(1662) Agarwal, A.; Mackey, M. A.; El-Sayed, M. A.; Bellamkonda, R. V. Remote Triggered Release of Doxorubicin in Tumors by Synergistic Application of Thermosensitive Liposomes and Gold Nanorods. *ACS Nano* **2011**, *5*, 4919−4926.
(1663) Li, M.; Yan, H.; Teh, C.; Korzh, V.; Zhao, Y. NIR-Triggered Drug Release From Switchable Rotaxane-Functionalized Silica-Covered Au Nanorods. *Chem. Commun.* **2014**, *50*, 9745−9748.
(1664) Luo, G.; Chen, W.; Jia, H.; Sun, Y.; Cheng, H.; Zhuo, R.; Zhang, X. An Indicator-Guided Photo-Controlled Drug Delivery System Based on Mesoporous Silica/Gold Nanocomposites. *Nano Res.* **2015**, *8*, 1893−1905.
(1665) Cai, H.; Shen, T.; Kirillov, A. M.; Zhang, Y.; Shan, C.; Li, X.; Liu, W.; Tang, Y. Self-Assembled Upconversion Nanoparticle Clusters for NIR-controlled Drug Release and Synergistic Therapy after Conjugation with Gold Nanoparticles. *Inorg. Chem.* **2017**, *56*, 5295−5304.
(1666) Zandberg, W. F.; Bakhtiari, A. B. S.; Erno, Z.; Hsiao, D.; Gates, B. D.; Claydon, T.; Branda, N. R. Photothermal Release of Small Molecules From Gold Nanoparticles in Live Cells. *Nanomedicine* **2012**, *8*, 908−915.
(1667) Basuki, J. S.; Qie, F.; Mulet, X.; Suryadinata, R.; Vashi, A. V.; Peng, Y. Y.; Li, L.; Hao, X.; Tan, T.; Hughes, T. C. Photo-Modulated Therapeutic Protein Release from a Hydrogel Depot Using Visible Light. *Angew. Chem.* **2017**, *129*, 986−991.
(1668) You, J.; Shao, R.; Wei, X.; Gupta, S.; Li, C. Near-Infrared Light Triggers Release of Paclitaxel from Biodegradable Microspheres: Photothermal Effect and Enhanced Antitumor Activity. *Small* **2010**, *6*, 1022−1031.
(1669) Ju, E.; Li, Z.; Liu, Z.; Ren, J.; Qu, X. Near-Infrared Light-Triggered Drug-Delivery Vehicle for Mitochondria-Targeted Chemo-Photothermal Therapy. *ACS Appl. Mater. Interfaces* **2014**, *6*, 4364−4370.
(1670) Yang, X.; Liu, Z.; Li, Z.; Pu, F.; Ren, J.; Qu, X. Near-Infrared-Controlled, Targeted Hydrophobic Drug-Delivery System for Synergistic Cancer Therapy. *Chem. - Eur. J.* **2013**, *19*, 10388−10394.
(1671) Han, S.; Samanta, A.; Xie, X.; Huang, L.; Peng, J.; Park, S. J.; Teh, D. B. L.; Choi, Y.; Chang, Y.-T.; All, A. H.; Yang, Y.; Xing, B.; Liu, X. Gold and Hairpin DNA Functionalization of Upconversion Nanocrystals for Imaging and In Vivo Drug Delivery. *Adv. Mater.* **2017**, *29*, 1700244.
(1672) Xiong, H.; Li, X.; Kang, P.; Perish, J.; Neuhaus, F.; Ploski, J. E.; Kroener, S.; Ogunyankin, M. O.; Shin, J. E.; Zasadzinski, J. A.; Wang, H.; Slesinger, P. A.; Zumbuehl, A.; Qin, Z. Near-Infrared Light Triggered-Release in Deep Brain Regions Using Ultra-photosensitive Nanovesicles. *Angew. Chem., Int. Ed.* **2020**, *59*, 8608−8615.
(1673) Zhu, H.; Deng, J.; Yang, Y.; Li, Y.; Shi, J.; Zhao, J.; Deng, Y.; Chen, X.; Yang, W. Cobalt Nanowire-Based Multifunctional Platform for Targeted Chemo-Photothermal Synergistic Cancer Therapy. *Colloids Surf., B* **2019**, *180*, 401−410.
(1674) Li, N.; Wen, X.; Liu, J.; Wang, B.; Zhan, Q.; He, S. Yb^{3+}-Enhanced UCNP@SiO_2 Nanocomposites for Consecutive Imaging,

Photothermal-Controlled Drug Delivery and Cancer Therapy. *Opt. Mater. Express* **2016**, *6*, 1161−1171.
(1675) Zhou, M.; Liu, S.; Jiang, Y.; Ma, H.; Shi, M.; Wang, Q.; Zhong, W.; Liao, W.; Xing, M. M. Q. Doxorubicin-Loaded Single Wall Nanotube Thermo-Sensitive Hydrogel for Gastric Cancer Chemo-Photothermal Therapy. *Adv. Funct. Mater.* **2015**, *25*, 4730−4739.
(1676) Liu, B.; Chen, C.; Wang, R.; Dong, S.; Li, J.; Zhang, G.; Cai, D.; Zhai, S.; Wu, Z. Near-Infrared Light-Responsively Controlled-Release Herbicide Using Biochar as a Photothermal Agent. *ACS Sustainable Chem. Eng.* **2019**, *7*, 14924−14932.
(1677) Viger, M. L.; Sheng, W.; Doré, K.; Alhasan, A. H.; Carling, C.-J.; Lux, J.; de Gracia Lux, C.; Grossman, M.; Malinow, R.; Almutairi, A. Near-Infrared-Induced Heating of Confined Water in Polymeric Particles for Efficient Payload Release. *ACS Nano* **2014**, *8*, 4815−4826.
(1678) Ercole, F.; Davis, T. P.; Evans, R. A. Photo-Responsive Systems and Biomaterials: Photochromic Polymers, Light-Triggered Self-Assembly, Surface Modification, Fluorescence Modulation and Beyond. *Polym. Chem.* **2010**, *1*, 37−54.
(1679) Gohy, J.-F.; Zhao, Y. Photo-Responsive Block Copolymer Micelles: Design and Behavior. *Chem. Soc. Rev.* **2013**, *42*, 7117−7129.
(1680) Grimm, O.; Wendler, F.; Schacher, F. H. Micellization of Photo-Responsive Block Copolymers. *Polymers* **2017**, *9*, 396.
(1681) Lino, M. M.; Ferreira, L. Light-Triggerable Formulations for the Intracellular Controlled Release of Biomolecules. *Drug Discovery Today* **2018**, *23*, 1062−1070.
(1682) Linsley, C. S.; Wu, B. M. Recent Advances in Light-Responsive On-Demand Drug- Delivery Systems. *Ther. Delivery* **2017**, *8*, 89−107.
(1683) Zeng, X. L.; Zhou, X. C.; Wu, S. Red and Near-Infrared Light-Cleavable Polymers. *Macromol. Rapid Commun.* **2018**, *39*, 1800034.
(1684) Fomina, N.; Sankaranarayanan, J.; Almutairi, A. Photochemical Mechanisms of Light-Triggered Release From Nanocarriers. *Adv. Drug Delivery Rev.* **2012**, *64*, 1005−1020.
(1685) Yan, Q.; Han, D.; Zhao, Y. Main-Chain Photoresponsive Polymers With Controlled Location of Light-Cleavable Units: From Synthetic Strategies to Structural Engineering. *Polym. Chem.* **2013**, *4*, 5026−5037.
(1686) Dai, Y.; Chen, X.; Zhang, X. Recent Advances in Stimuli-Responsive Polymeric Micelles via Click Chemistry. *Polym. Chem.* **2019**, *10*, 34−44.
(1687) Liu, G.; Liu, W.; Dong, C.-M. UV- and NIR-Responsive Polymeric Nanomedicines for On-Demand Drug Delivery. *Polym. Chem.* **2013**, *4*, 3431−3443.
(1688) Tong, R.; Kohane, D. S. Shedding Light on Nanomedicine. *WIREs Nanomed. Nanobi.* **2012**, *4*, 638−662.
(1689) Boase, N. R. B. Shining a Light on Bioorthogonal Photochemistry for Polymer Science. *Macromol. Rapid Commun.* **2020**, *41*, 2000305.
(1690) Griffin, D. R.; Kasko, A. M. Photoselective Delivery of Model Therapeutics from Hydrogels. *ACS Macro Lett.* **2012**, *1*, 1330−1334.
(1691) Barhoumi, A.; Liu, Q.; Kohane, D. S. Ultraviolet Light-Mediated Drug Delivery: Principles, Applications, and Challenges. *J. Controlled Release* **2015**, *219*, 31−42.
(1692) Zhao, H.; Hou, B.; Tang, Y.; Hu, W.; Yin, C.; Ji, Y.; Lu, X.; Fan, Q.; Huang, W. *o*-Nitrobenzyl-Alt-(Phenylethynyl)Benzene Copolymer-Based Nanoaggregates With Highly Efficient Two-Photon-Triggered Degradable Properties via a FRET Process. *Polym. Chem.* **2016**, *7*, 3117−3125.
(1693) Peng, K.; Tomatsu, I.; van den Broek, B.; Cui, C.; Korobko, A. V.; van Noort, J.; Meijer, A. H.; Spaink, H. P.; Kros, A. Dextran Based Photodegradable Hydrogels Formed via a Michael Addition. *Soft Matter* **2011**, *7*, 4881−4887.
(1694) Cao, J.; Huang, S.; Chen, Y.; Li, S.; Li, X.; Deng, D.; Qian, Z.; Tang, L.; Gu, Y. Near-Infrared Light-Triggered Micelles for Fast Controlled Drug Release in Deep Tissue. *Biomaterials* **2013**, *34*, 6272−6283.
(1695) de Gracia Lux, C.; McFearin, C. L.; Joshi-Barr, S.; Sankaranarayanan, J.; Fomina, N.; Almutairi, A. Single UV or Near IR Triggering Event Leads to Polymer Degradation into Small Molecules. *ACS Macro Lett.* **2012**, *1*, 922−926.
(1696) Li, L.; Wu, Y.; Du, F.-S.; Li, Z.-C. Modular Synthesis of Photodegradable Polymers With Different Sensitive Wavelengths As UV/NIR Responsive Nanocarriers. *J. Polym. Sci., Part A: Polym. Chem.* **2019**, *57*, 334−341.
(1697) Kehrloesser, D.; Behrendt, P. J.; Hampp, N. Two-Photon Absorption Triggered Drug Delivery From a Polymer for Intraocular Lenses in Presence of an UV-Absorber. *J. Photochem. Photobiol., A* **2012**, *248*, 8−14.
(1698) Babin, J.; Pelletier, M.; Lepage, M.; Allard, J.-F.; Morris, D.; Zhao, Y. A New Two-Photon-Sensitive Block Copolymer Nanocarrier. *Angew. Chem., Int. Ed.* **2009**, *48*, 3329−3332.
(1699) Hang, C.; Zou, Y.; Zhong, Y.; Zhong, Z.; Meng, F. NIR and UV-Responsive Degradable Hyaluronic Acid Nanogels for CD44-Targeted and Remotely Triggered Intracellular Doxorubicin Delivery. *Colloids Surf., B* **2017**, *158*, 547−555.
(1700) Goodwin, A. P.; Mynar, J. L.; Ma, Y.; Fleming, G. R.; Fréchet, J. M. J. Synthetic Micelle Sensitive to IR Light via a Two-Photon Process. *J. Am. Chem. Soc.* **2005**, *127*, 9952−9953.
(1701) Mynar, J. L.; Goodwin, A. P.; Cohen, J. A.; Ma, Y.; Fleming, G. R.; Fréchet, J. M. J. Two-Photon Degradable Supramolecular Assemblies of Linear-Dendritic Copolymers. *Chem. Commun.* **2007**, 2081−2082.
(1702) Liu, G.-Y.; Chen, C.-J.; Li, D.-D.; Wang, S.-S.; Ji, J. Near-Infrared Light-Sensitive Micelles for Enhanced Intracellular Drug Delivery. *J. Mater. Chem.* **2012**, *22*, 16865−16871.
(1703) Yuan, Y.; Wang, Z.; Cai, P.; Liu, J.; Liao, L.-D.; Hong, M.; Chen, X.; Thakor, N.; Liu, B. Conjugated Polymer and Drug Co-encapsulated Nanoparticles for Chemo- and Photo-Thermal Combination Therapy With Two-Photon Regulated Fast Drug Release. *Nanoscale* **2015**, *7*, 3067−3076.
(1704) Sun, L.; Ma, X.; Dong, C.-M.; Zhu, B.; Zhu, X. NIR-Responsive and Lectin-Binding Doxorubicin-Loaded Nanomedicine from Janus-Type Dendritic PAMAM Amphiphiles. *Biomacromolecules* **2012**, *13*, 3581−3591.
(1705) Sun, L.; Yang, Y.; Dong, C.-M.; Wei, Y. Two-Photon-Sensitive and Sugar-Targeted Nanocarriers from Degradable and Dendritic Amphiphiles. *Small* **2011**, *7*, 401−406.
(1706) Sun, W.; Li, S.; Häupler, B.; Liu, J.; Jin, S.; Steffen, W.; Schubert, U. S.; Butt, H.-J.; Liang, X.-J.; Wu, S. An Amphiphilic Ruthenium Polymetallodrug for Combined Photodynamic Therapy and Photochemotherapy In Vivo. *Adv. Mater.* **2017**, *29*, 1603702.
(1707) Zhao, T.; Chen, L.; Li, Q.; Li, X. Near-Infrared Light Triggered Drug Release From Mesoporous Silica Nanoparticles. *J. Mater. Chem. B* **2018**, *6*, 7112−7121.
(1708) Chen, F.; Hableel, G.; Zhao, E. R.; Jokerst, J. V. Multifunctional Nanomedicine With Silica: Role of Silica in Nanoparticles for Theranostic, Imaging, and Drug Monitoring. *J. Colloid Interface Sci.* **2018**, *521*, 261−279.
(1709) Bayir, S.; Barras, A.; Boukherroub, R.; Szunerits, S.; Raehm, L.; Richeter, S.; Durand, J.-O. Mesoporous Silica Nanoparticles in Recent Photodynamic Therapy Applications. *Photochem. Photobiol. Sci.* **2018**, *17*, 1651−1674.
(1710) Croissant, J. G.; Zink, J. I.; Raehm, L.; Durand, J.-O. Two-Photon-Excited Silica and Organosilica Nanoparticles for Spatiotemporal Cancer Treatment. *Adv. Healthcare Mater.* **2018**, *7*, 1701248.
(1711) Hernández-Montoto, A.; Gorbe, M.; Llopis-Lorente, A.; Terrés, J. M.; Montes, R.; Cao-Milán, R.; Díaz de Greñu, B.; Alfonso, M.; Orzaez, M.; Marcos, M. D.; Martínez-Máñez, R.; Sancenón, F. A NIR Light-Triggered Drug Delivery System Using Core−Shell Gold Nanostars−Mesoporous Silica Nanoparticles Based on Multiphoton Absorption Photo-Dissociation of 2-Nitrobenzyl PEG. *Chem. Commun.* **2019**, *55*, 9039−9042.
(1712) Qu, D. H.; Wang, Q. C.; Zhang, Q. W.; Ma, X.; Tian, H. Photoresponsive Host-Guest Functional Systems. *Chem. Rev.* **2015**, *115*, 7543−7588.

(1713) Bleger, D.; Hecht, S. Visible-Light-Activated Molecular Switches. *Angew. Chem., Int. Ed.* **2015**, *54*, 11338−11349.
(1714) Wang, D.; Zhao, W.; Wei, Q.; Zhao, C.; Zheng, Y. Photoswitchable Azobenzene/Cyclodextrin Host-Guest Complexes: From UV- to Visible/Near-IR-Light-Responsive Systems. *ChemPhotoChem.* **2018**, *2*, 403−415.
(1715) Yao, X.; Li, T.; Wang, J.; Ma, X.; Tian, H. Recent Progress in Photoswitchable Supramolecular Self-Assembling Systems. *Adv. Opt. Mater.* **2016**, *4*, 1322−1349.
(1716) Lee, S.; Flood, A. H. Photoresponsive Receptors for Binding and Releasing Anions. *J. Phys. Org. Chem.* **2013**, *26*, 79−86.
(1717) Kim, T. Y.; Vasdev, R. A. S.; Preston, D.; Crowley, J. D. Strategies for Reversible Guest Uptake and Release from Metallosupramolecular Architectures. *Chem. - Eur. J.* **2018**, *24*, 14878−14890.
(1718) Diaz-Moscoso, A.; Ballester, P. Light-Responsive Molecular Containers. *Chem. Commun.* **2017**, *53*, 4635−4652.
(1719) Ramamurthy, V. Photochemistry within a Water-Soluble Organic Capsule. *Acc. Chem. Res.* **2015**, *48*, 2904−2917.
(1720) Abendroth, J. M.; Bushuyev, O. S.; Weiss, P. S.; Barrett, C. J. Controlling Motion at the Nanoscale: Rise of the Molecular Machines. *ACS Nano* **2015**, *9*, 7746−7768.
(1721) Marturano, V.; Cerruti, P.; Giamberini, M.; Tylkowski, B.; Ambrogi, V. Light-Responsive Polymer Micro- and Nano-Capsules. *Polymers* **2017**, *9*, 8.
(1722) Moncelsi, G.; Ballester, P. Photoswitchable Host-Guest Systems Incorporating Hemithioindigo and Spiropyran Units. *ChemPhotoChem.* **2019**, *3*, 304−317.
(1723) Ueno, A.; Yoshimura, H.; Saka, R.; Osa, T. Photocontrol of Binding Ability of Capped Cyclodextrin. *J. Am. Chem. Soc.* **1979**, *101*, 2779−2780.
(1724) Liu, M.; Yan, X.; Hu, M.; Chen, X.; Zhang, M.; Zheng, B.; Hu, X.; Shao, S.; Huang, F. Photoresponsive Host-Guest Systems Based on a New Azobenzene-Containing Crytpand. *Org. Lett.* **2010**, *12*, 2558−2561.
(1725) Ma, X.; Cao, J.; Wang, Q.; Tian, H. Photocontrolled Reversible Room Temperature Phosphorescence (RTP) Encoding β-Cyclodextrin Pseudorotaxane. *Chem. Commun.* **2011**, *47*, 3559−3561.
(1726) Wang, D.; Wu, S. Red-Light-Responsive Supramolecular Valves for Photocontrolled Drug Release from Mesoporous Nanoparticles. *Langmuir* **2016**, *32*, 632−636.
(1727) Han, M. X.; Michel, R.; He, B.; Chen, Y. S.; Stalke, D.; John, M.; Clever, G. H. Light-Triggered Guest Uptake and Release by a Photochromic Coordination Cage. *Angew. Chem., Int. Ed.* **2013**, *52*, 1319−1323.
(1728) Guerin, J.; Leaustic, A.; Berthet, J.; Metivier, R.; Guillot, R.; Delbaere, S.; Nakatani, K.; Yu, P. Light-Controlled Release and Uptake of Zinc Ions in Solution by a Photochromic Terthiazole-Based Ligand. *Chem. - Asian J.* **2017**, *12*, 853−859.
(1729) O'Hagan, M. P.; Ramos-Soriano, J.; Haldar, S.; Sheikh, S.; Morales, J. C.; Mulholland, A. J.; Galan, M. C. Visible-Light Photoswitching of Ligand Binding Mode Suggests G-Quadruplex DNA as a Target for Photopharmacology. *Chem. Commun.* **2020**, *56*, 5186−5189.
(1730) Dozova, N.; Pousse, G.; Barnych, B.; Mallet, J.-M.; Cossy, J.; Valeur, B.; Plaza, P. A Novel Diarylethene-Based Photoswitchable Chelator for Reversible Release and Capture of Ca^{2+} in Aqueous Media. *J. Photochem. Photobiol., A* **2018**, *360*, 181−187.
(1731) Ma, G. L.; Wen, S. F.; He, L.; Huang, Y.; Wang, Y. J.; Zhou, Y. B. Optogenetic Toolkit for Precise Control of Calcium Signaling. *Cell Calcium* **2017**, *64*, 36−46.
(1732) Griepenburg, J. C.; Sood, N.; Vargo, K. B.; Williams, D.; Rawson, J.; Therien, M. J.; Hammer, D. A.; Dmochowski, I. J. Caging Metal Ions with Visible Light-Responsive Nanopolymersomes. *Langmuir* **2015**, *31*, 799−807.
(1733) Jia, S.; Fong, W.-K.; Graham, B.; Boyd, B. J. Photoswitchable Molecules in Long-Wavelength Light-Responsive Drug Delivery: From Molecular Design to Applications. *Chem. Mater.* **2018**, *30*, 2873−2887.
(1734) Huang, L.; Han, G. Near Infrared Boron Dipyrromethene Nanoparticles for Optotheranostics. *Small Methods* **2018**, *2*, 1700370.
(1735) Basílio, N.; García-Río, L. Photoswitchable Vesicles. *Curr. Opin. Colloid Interface Sci.* **2017**, *32*, 29−38.
(1736) Gautier, A.; Gauron, C.; Volovitch, M.; Bensimon, D.; Jullien, L.; Vriz, S. How to Control Proteins with Light in Living Systems. *Nat. Chem. Biol.* **2014**, *10*, 533−541.
(1737) Kataoka, K.; Harada, A.; Nagasaki, Y. Block Copolymer Micelles for Drug Delivery: Design, Characterization and Biological Significance. *Adv. Drug Delivery Rev.* **2001**, *47*, 113−131.
(1738) Puri, A. Phototriggerable Liposomes: Current Research and Future Perspectives. *Pharmaceutics* **2014**, *6*, 1−25.
(1739) Wang, X.; Hu, J.; Liu, G.; Tian, J.; Wang, H.; Gong, M.; Liu, S. Reversibly Switching Bilayer Permeability and Release Modules of Photochromic Polymersomes Stabilized by Cooperative Noncovalent Interactions. *J. Am. Chem. Soc.* **2015**, *137*, 15262−15275.
(1740) Rifaie-Graham, O.; Ulrich, S.; Galensowske, N. F. B.; Balog, S.; Chami, M.; Rentsch, D.; Hemmer, J. R.; Read de Alaniz, J.; Boesel, L. F.; Bruns, N. Wavelength-Selective Light-Responsive DASA-Functionalized Polymersome Nanoreactors. *J. Am. Chem. Soc.* **2018**, *140*, 8027−8036.
(1741) Wang, Z.; Johns, V. K.; Liao, Y. Controlled Release of Fragrant Molecules with Visible Light. *Chem. - Eur. J.* **2014**, *20*, 14637−14640.
(1742) Xing, Q.; Li, N.; Chen, D.; Sha, W.; Jiao, Y.; Qi, X.; Xu, Q.; Lu, J. Light-Responsive Amphiphilic Copolymer Coated Nanoparticles as Nanocarriers and Real-Time Monitors for Controlled Drug Release. *J. Mater. Chem. B* **2014**, *2*, 1182−1189.
(1743) Senthilkumar, T.; Zhou, L.; Gu, Q.; Liu, L.; Lv, F.; Wang, S. Conjugated Polymer Nanoparticles with Appended Photo-Responsive Units for Controlled Drug Delivery, Release, and Imaging. *Angew. Chem., Int. Ed.* **2018**, *57*, 13114−13119.
(1744) Romero, M. A.; Mateus, P.; Matos, B.; Acuña, Á.; García-Río, L.; Arteaga, J. F.; Pischel, U.; Basílio, N. Binding of Flavylium Ions to Sulfonatocalix[4]arene and Implication in the Photorelease of Biologically Relevant Guests in Water. *J. Org. Chem.* **2019**, *84*, 10852−10859.
(1745) Hu, X.-Y.; Jia, K.; Cao, Y.; Li, Y.; Qin, S.; Zhou, F.; Lin, C.; Zhang, D.; Wang, L. Dual Photo- and pH-Responsive Supramolecular Nanocarriers Based on Water-Soluble Pillar[6]arene and Different Azobenzene Derivatives for Intracellular Anticancer Drug Delivery. *Chem. - Eur. J.* **2015**, *21*, 1208−1220.
(1746) Huang, Y.; Shen, L.; Guo, D.; Yasen, W.; Wu, Y.; Su, Y.; Chen, D.; Qiu, F.; Yan, D.; Zhu, X. A NIR-Triggered Gatekeeper of Supramolecular Conjugated Unimicelles With Two-Photon Absorption for Controlled Drug Release. *Chem. Commun.* **2019**, *55*, 6735−6738.
(1747) Liu, Y.-C.; Le Ny, A.-L. M.; Schmidt, J.; Talmon, Y.; Chmelka, B. F.; Lee, C. T. Photo-Assisted Gene Delivery Using Light-Responsive Catanionic Vesicles. *Langmuir* **2009**, *25*, 5713−5724.
(1748) Pianowski, Z. L.; Karcher, J.; Schneider, K. Photoresponsive Self-Healing Supramolecular Hydrogels for Light-Induced Release of Dna and Doxorubicin. *Chem. Commun.* **2016**, *52*, 3143−3146.
(1749) Nehls, E. M.; Rosales, A. M.; Anseth, K. S. Enhanced User-Control of Small Molecule Drug Release From a Poly(Ethylene Glycol) Hydrogel via Azobenzene/Cyclodextrin Complex Tethers. *J. Mater. Chem. B* **2016**, *4*, 1035−1039.
(1750) Lu, J.; Choi, E.; Tamanoi, F.; Zink, J. I. Light-Activated Nanoimpeller-Controlled Drug Release in Cancer Cells. *Small* **2008**, *4*, 421−426.
(1751) Knežević, N. Ž.; Trewyn, B. G.; Lin, V. S. Y. Functionalized Mesoporous Silica Nanoparticle-Based Visible Light Responsive Controlled Release Delivery System. *Chem. Commun.* **2011**, *47*, 2817−2819.
(1752) Hull, K.; Morstein, J.; Trauner, D. In Vivo Photopharmacology. *Chem. Rev.* **2018**, *118*, 10710−10747.
(1753) Velema, W. A.; Szymanski, W.; Feringa, B. L. Photopharmacology: Beyond Proof of Principle. *J. Am. Chem. Soc.* **2014**, *136*, 2178−2191.

(1754) Arrue, L.; Ratjen, L. Internal Targeting and External Control: Phototriggered Targeting in Nanomedicine. *ChemMedChem* **2017**, *12*, 1908−1916.
(1755) Bregestovski, P.; Maleeval, G. Photopharmacology: Mini Review by Example of Potassium Channels Modulation by Light. *Zh. Vyssh. Nerv. Deyat.* **2017**, *67*, 41−52.
(1756) Lubbe, A. S.; Szymanski, W.; Feringa, B. L. Recent Developments in Reversible Photoregulation of Oligonucleotide Structure and Function. *Chem. Soc. Rev.* **2017**, *46*, 1052−1079.
(1757) Dong, M. X.; Babalhavaeji, A.; Samanta, S.; Beharry, A. A.; Woolley, G. A. Red-Shifting Azobenzene Photoswitches for in Vivo Use. *Acc. Chem. Res.* **2015**, *48*, 2662−2670.
(1758) Broichhagen, J.; Frank, J. A.; Trauner, D. A Roadmap to Success in Photopharmacology. *Acc. Chem. Res.* **2015**, *48*, 1947−1960.
(1759) Meisel, P.; Jahrig, D.; Jahrig, K. What Is Photopharmacology, and What Can It Do? *Pharmazie* **1980**, *35*, 377−388.
(1760) Albert, L.; Vazquez, O. Photoswitchable Peptides for Spatiotemporal Control of Biological Functions. *Chem. Commun.* **2019**, *55*, 10192−10213.
(1761) Curcic, S.; Tiapko, O.; Groschner, K. Photopharmacology and Opto-Chemogenetics of Trpc Channels-Some Therapeutic Visions. *Pharmacol. Ther.* **2019**, *200*, 13−26.
(1762) Morstein, J.; Trauner, D. New Players in Phototherapy: Photopharmacology and Bio-Integrated Optoelectronics. *Curr. Opin. Chem. Biol.* **2019**, *50*, 145−151.
(1763) Szymański, W.; Beierle, J. M.; Kistemaker, H. A. V.; Velema, W. A.; Feringa, B. L. Reversible Photocontrol of Biological Systems by the Incorporation of Molecular Photoswitches. *Chem. Rev.* **2013**, *113*, 6114−6178.
(1764) Fuchter, M. J. On the Promise of Photopharmacology Using Photoswitches: A Medicinal Chemist's Perspective. *J. Med. Chem.* **2020**, *63*, 11436−11447.
(1765) Mafy, N. N.; Matsuo, K.; Hiruma, S.; Uehara, R.; Tamaoki, N. Photoswitchable CENP-E Inhibitor Enabling the Dynamic Control of Chromosome Movement and Mitotic Progression. *J. Am. Chem. Soc.* **2020**, *142*, 1763−1767.
(1766) Barber, D. M.; Liu, S.-A.; Gottschling, K.; Sumser, M.; Hollmann, M.; Trauner, D. Optical Control of AMPA Receptors Using a Photoswitchable Quinoxaline-2,3-dione Antagonist. *Chem. Sci.* **2017**, *8*, 611−615.
(1767) Izquierdo-Serra, M.; Gascón-Moya, M.; Hirtz, J. J.; Pittolo, S.; Poskanzer, K. E.; Ferrer, È.; Alibés, R.; Busqué, F.; Yuste, R.; Hernando, J.; Gorostiza, P. Two-Photon Neuronal and Astrocytic Stimulation with Azobenzene-Based Photoswitches. *J. Am. Chem. Soc.* **2014**, *136*, 8693−8701.
(1768) Velema, W. A.; van der Berg, J. P.; Hansen, M. J.; Szymanski, W.; Driessen, A. J. M.; Feringa, B. L. Optical Control of Antibacterial Activity. *Nat. Chem.* **2013**, *5*, 924−928.
(1769) Wegener, M.; Hansen, M. J.; Driessen, A. J. M.; Szymanski, W.; Feringa, B. L. Photocontrol of Antibacterial Activity: Shifting from UV to Red Light Activation. *J. Am. Chem. Soc.* **2017**, *139*, 17979−17986.
(1770) Lachmann, D.; Studte, C.; Männel, B.; Hübner, H.; Gmeiner, P.; König, B. Photochromic Dopamine Receptor Ligands Based on Dithienylethenes and Fulgides. *Chem. - Eur. J.* **2017**, *23*, 13423−13434.
(1771) Skaar, J. R.; Pagan, J. K.; Pagano, M. SCF Ubiquitin Ligase-Targeted Therapies. *Nat. Rev. Drug Discovery* **2014**, *13*, 889−903.
(1772) Reynders, M.; Matsuura, B. S.; Bérouti, M.; Simoneschi, D.; Marzio, A.; Pagano, M.; Trauner, D. PHOTACs Enable Optical Control of Protein Degradation. *Sci. Adv.* **2020**, *6*, No. eaay5064.
(1773) Jin, Y.-H.; Lu, M.-C.; Wang, Y.; Shan, W.-X.; Wang, X.-Y.; You, Q.-D.; Jiang, Z.-Y. Azo-PROTAC: Novel Light-Controlled Small-Molecule Tool for Protein Knockdown. *J. Med. Chem.* **2020**, *63*, 4644−4654.

https://dx.doi.org/10.1021/acs.chemrev.0c00663
Chem. Rev. 2020, 120, 13135−13272